

PhD Thesis

The effects of heatwave-related stressors on gametogenesis and pathogenesis in two model molluscs from Aotearoa, New Zealand.



Joanna Copedo

**The effects of heatwave-related stressors on
gametogenesis and pathogenesis in two model
molluscs from Aotearoa, New Zealand.**

Joanna S. Copedo

A thesis submitted to Auckland University of Technology in fulfilment of the
requirements for the degree of Doctor of Philosophy (PhD)

2025

Faculty of Health and Environmental Sciences
School of Science
Auckland University of Technology (AUT)

Supervisor: Professor. Andrea C. Alfaro
Co-Supervisor 1: Dr. Stephen C. Webb
Co-Supervisor 2: Dr. Norman L. C. Ragg
AUT admin lead: Professor. Lindsey White

“You can’t use up creativity. The more you use, the more you have”.

- **Maya Angelou**

Abstract

Elevated temperature challenges associated to changing climate are a risk to many marine molluscs. As average sea temperatures rise, marine heatwaves (MHW) are also likely to increase in frequency and intensity. The temperature elevations are also associated with increased frequency of extreme events such as storms and floods, which can have consequences on the local marine ecosystems. The Green-lipped mussel (GLM) (Greenshell™ mussel), *Perna canaliculus* (Gmelin 1791), and the Blackfoot pāua *Haliotis iris* (Gmelin 1791) are endemic marine molluscs in New Zealand. Both species play a key role in the marine environment, hold cultural value and support fisheries and aquaculture industries. The changing climate is impacting both species in terms of growth, reproduction, pathogen dynamics and survival and this trend is likely to worsen. This thesis aims to explore the environment/host/pathogen interactions in relation to changing climate in the selected molluscan study species, and their shared parasite *Perkinsus olseni*. Investigations aimed to identify pathologies and pathogens associated with host, phenology, vulnerability, and disease susceptibility. More broadly, to provide insights into deleterious processes and their detection methods that are applicable to the species studied and to molluscs in general. A forensic histopathology approach with supporting techniques was used to identify the microscopic changes at the tissue level. Field monitoring and laboratory scenarios were conducted to explore findings and attempt to extrapolate to real-world scenarios.

Positive temperature anomalies of up to 3°C and summer temperatures above 22°C were regularly detected in one of the field survey sites (Chapter 2), with the others regularly above 16°C. Tissue conditions of *H. iris* and green-lipped mussels indicated physiological and reproductive stress associated to temperature, as well as several conditions correlating to pathogen presence. The gametogenesis cycle appeared to be prolonged for the green-lipped mussel (Chapter 2) and *H. iris* (Chapter 4), with both potentially using oocyte atresia (nutrient resorption from developing eggs) as a resource for maintaining condition. Ceroid was elevated in the slower-growing population of *H. iris* and may allude to advanced physiological age and increased vulnerability under a changing climate (Chapter 3 and 4). In the lab scenarios elevated temperature and prolonged exposure time resulted in an increase in the number of focal ceroid aggregations, haemocytosis, a decrease in energy reserve cells (glycogen) and a decline in reproductive condition (Chapter 5). Flood events, in addition to impacting our low-lying research facility, were also observed to impact reproductive condition by causing the mussels in the system to spawn (Chapter 6). Finally, under controlled challenge conditions and in the absence of thermal stress, the parasite *Perkinsus olseni* was still able to outcompete the host (Green-lipped mussel) immune response and continue to develop within the tissues (Chapter 7). The findings demonstrate that fine-scale tissue-level research can provide useful information on many levels, can be applied to other molluscan species, and highlight the importance of monitoring marine health. Finally, continued integration of field and laboratory research is critical in elucidating the effects of external and internal stressors on molluscs to provide early detection of non-infectious and infectious diseases.

TABLE OF CONTENTS

Abstract	i
Table of Contents	ii
List of Tables	viii
List of Figures	xi
List of Appendices	xix
Attestation of authorship	xx
Co-author contribution	xx
Acknowledgements	xxiv
Section 1. General introduction	1
Preamble	2
Chapter 1. Introduction	0
1.1. A changing marine environment	0
1.1.1. <i>Global climate change</i>	0
1.1.2. <i>Marine heatwaves</i>	2
1.1.3. <i>Increasing storm events and precipitation</i>	2
1.1.4. <i>Impact of global warming on marine ecosystems</i>	3
1.2. Marine organisms in a changing world	4
1.2.1. <i>Physiological tolerance and stress</i>	4
1.2.2. <i>Molluscs: Gastropods and bivalves</i>	7
1.2.3. <i>Gastropod and bivalve reproduction</i>	8
1.2.4. <i>Gametogenesis: spermatogonia and oogonia</i>	10
1.2.5. <i>Oocyte atresia</i>	11
1.3. Influence of pathogens	12
1.3.1. <i>A complex interactome inducing disease</i>	12
1.3.2. <i>Marine mortality events</i>	14
1.3.3. <i>A causative pathogen: Perkinsus species</i>	14
1.3.4. <i>Defence against a pathogen: molluscan immunity</i>	15
1.4. Ecological context	17
1.4.1. <i>New Zealand climate</i>	17
1.4.2. <i>Selected species 1: Perna canaliculus</i>	18
1.4.3. <i>Selected species 2: Haliotis iris</i>	19
1.4.4. <i>The pathogen of focus: Perkinsus olseni</i>	20
1.5. Techniques	20
1.5.1. <i>Histopathology as a core technique</i>	20
1.5.2. <i>Integration of complementary techniques</i>	22
1.6. Significance of this research	22
1.7. Research objectives	23
1.8. Thesis structure	24

Section 2. Influence of the marine environment on bivalves and gastropods: Explorative field studies on <i>Perna canaliculus</i> and <i>Haliotis iris</i>	26
Section 2. Preamble	27
Chapter 2. The interacting influence of season and recurrent marine heatwaves upon gametogenesis and parasite burden in the green-lipped mussel <i>Perna canaliculus</i>.	28
2.1. Introduction	28
2.2. Methods	30
2.2.1. <i>Environmental monitoring: estimation of SST</i>	30
2.2.2. <i>Sampling location and collection</i>	31
2.2.3. <i>Histopathology</i>	31
2.2.4. <i>Molecular diagnostics</i>	33
2.2.5. <i>Bioinformatics</i>	34
2.2.6. <i>Statistical analyses</i>	35
2.3. Results	35
2.3.1. <i>Environmental temperature</i>	35
2.3.2. <i>Perna canaliculus tissue conditions</i>	36
2.3.3. <i>Perna canaliculus reproductive condition and atresia</i>	39
2.3.4. <i>Pathogen and parasites</i>	41
2.3.5. <i>Epidemiological triad: environment: host: pathogens</i>	44
2.4. Discussion	46
2.5. Conclusion	51
Chapter 3. Histopathological investigation of four populations of abalone (<i>Haliotis iris</i>) exhibiting divergent growth performance: Part A	52
3.1. Introduction	52
3.2. Methods:	54
3.2.1. <i>Sampling locations and animal collection</i>	54
3.2.2. <i>Histopathological preparation</i>	55
3.2.3. <i>Statistical analyses:</i>	60
3.3. Results	60
3.3.1. <i>Midgut: algal quality scoring</i>	61
3.3.2. <i>Tissue anomalies</i>	62
3.3.3. <i>Gill</i>	62
3.3.4. <i>Right kidney</i>	63
3.4. Discussion:	65
3.4.1. <i>Nutrition</i>	65
3.4.2. <i>Ceroid granules</i>	67
3.4.3. <i>Kidney crystals</i>	68
3.4.4. <i>Pathogen detection</i>	69
3.4.5. <i>Additional factors and implications</i>	69
3.4.6. <i>Conclusions:</i>	70

Chapter 4. Elucidating divergent growth performance and climate vulnerability in abalone (<i>Haliotis iris</i>): Part B	72
4.1. Introduction	72
4.2. Methods	75
4.2.1. <i>Environmental monitoring: estimation of SST for Chatham Islands</i>	75
4.2.2. <i>Sampling location and animal collection</i>	75
4.2.3. <i>Histopathology</i>	76
4.2.4. <i>General tissue alterations</i>	77
4.2.5. <i>Reproductive staging and egg viability</i>	78
4.2.6. <i>Pathogens and parasites</i>	78
4.2.7. <i>DNA isolation, PCR and metabarcoding sequencing</i>	79
4.2.8. <i>Bioinformatics</i>	80
4.2.9. <i>Statistical analysis</i>	80
4.3. Results	81
4.3.1. <i>Temperature profile</i>	81
4.3.2. <i>Morphometric parameters</i>	82
4.3.3. <i>Tissue alterations</i>	83
4.3.4. <i>Reproductive status and atresia</i>	85
4.3.5. <i>Pathogens and parasites</i>	87
4.3.5.1. <i>Histological assessment</i>	87
4.3.5.2. <i>Molecular identification of parasites</i>	88
4.4. Discussion	90
4.4.1. <i>Nutritional stress and an ageing population</i>	90
4.4.2. <i>Site-specific reproductive condition and atresia</i>	92
4.4.3. <i>Pathogens</i>	94
4.4.4. <i>Contributing factors to slow growth and future vulnerabilities</i>	95
4.4.5. <i>Conclusions</i>	96
Section 3. Exploration of thermal stress and food deprivation: laboratory scenarios	98
Section 3. Preamble	99
Chapter 5. Histopathological changes in the green-lipped mussel, <i>Perna canaliculus</i>, in response to chronic thermal stress	100
5.1. Introduction	100
5.2. Methods	102
5.2.1. <i>Experimental design</i>	102
5.2.2. <i>Water quality sampling</i>	103
5.2.3. <i>Histopathology</i>	103
5.2.3.1. <i>Tissue Analysis</i>	105
5.2.3.2. <i>Gill and digestive gland scoring</i>	105
5.2.3.3. <i>Mantle and connective tissue scoring</i>	105

5.2.3.4.	<i>Immunohistochemical detection of HSP70 in gill and gonad: A preliminary investigation</i>	106
5.2.3.5.	<i>Reproductive staging</i>	106
5.2.3.6.	<i>Pathogens</i>	110
5.2.4.	<i>Statistical analysis</i>	110
5.3.	Results	111
5.3.1.	<i>Water quality and survival</i>	111
5.3.2.	<i>Tissue condition</i>	111
5.3.2.1.	<i>Gill and digestive gland architecture</i>	111
5.3.2.2.	<i>Mantle and connective tissue</i>	112
5.3.2.3.	<i>Immunohistochemical exploration of HSP70 in gill and gonad: A preliminary investigation</i>	115
5.3.3.	<i>Reproductive tissue</i>	117
5.3.4.	<i>Pathogens</i>	119
5.4.	Discussion	120
5.4.1.	<i>Impacts on survival and growth</i>	121
5.4.2.	<i>Tissue abnormalities</i>	121
5.4.3.	<i>Pathogen prevalence and influence on the host</i>	122
5.4.4.	<i>Reproductive condition</i>	124
5.4.5.	<i>Research implications</i>	126
5.4.6.	<i>Conclusions</i>	127
Chapter 6. Implications of flooding events for the green-lipped mussels (<i>Perna canaliculus</i>): An Aquatic health perspective: Part A		128
6.1.	Introduction	128
6.2.	Methods	130
6.2.2.	<i>Tissue sampling</i>	131
6.3.	Results	132
6.3.1.	<i>Temperature and survival</i>	132
6.3.2.	<i>Reproductive condition</i>	133
6.3.3.	<i>Tissue conditions</i>	134
6.4.	Discussion	137
6.4.1.	<i>Histological observations</i>	138
6.4.2.	<i>Implications of salinity stress and contamination from flooding</i>	140
6.4.3.	<i>Perspective: implications for research facilities, research outcomes and the utility of serendipitous findings.</i>	141
6.4.4.	<i>Conclusion</i>	142
Chapter 6. Thermal stress and food limitation in adult mussel (<i>Perna canaliculus</i>) Part B.		143
6.5.	Introduction	143
6.6.	Methods	144
6.6.1.	<i>Experimental set up</i>	144

6.6.2.	<i>Elaboration of experimental food treatments</i>	145
6.6.3.	<i>Physiological measurements</i>	145
6.6.4.	<i>General physiology</i>	146
6.6.5.	<i>Condition index</i>	146
6.6.6.	<i>Histology</i>	147
6.6.7.	<i>Cryo histology: preliminary investigation</i>	147
6.6.8.	<i>Biochemistry</i>	148
6.6.9.	<i>Statistical analysis</i>	148
6.7.	Results	149
6.7.1.	<i>Water quality parameters</i>	149
6.7.2.	<i>Physiology under stress</i>	150
6.7.3.	<i>Pathological findings</i>	153
6.8.	Discussion	157
6.9.	Conclusion	159
Section 4. Disease progression of <i>Perkinsus olseni</i> in <i>Perna canaliculus</i>: A laboratory study		160
Section 4. Preamble		161
Chapter 7. Disease progression of <i>Perkinsus olseni</i> in adult, green-lipped mussels, <i>Perna canaliculus</i>		162
7.1.	Introduction	162
7.2.	Methods	164
7.2.1.	<i>Naturally, infected mussel population and <i>Perkinsus</i> collection</i>	164
7.2.2.	<i>Experimentally infected mussels</i>	165
7.2.2.1.	<i>Experimental setup</i>	165
7.2.2.2.	<i>Pathogen source and infection</i>	166
7.2.3.	<i>Sampling</i>	166
7.2.4.	<i>Standard H&E tissue analysis</i>	167
7.2.5.	<i>Fluorescence in situ hybridisation (F-ISH)</i>	171
7.2.6.	<i>Standard H&E and Fluorescence in situ hybridisation (F-ISH) comparison</i>	172
7.2.7.	<i>Statistical analysis</i>	172
7.3.	Results	173
7.3.1.	<i>Perkinsosis in naturally infected mussels</i>	173
7.3.2.	<i>Perkinsosis in experimentally infected mussels</i>	176
7.4.	Discussion	179
7.4.1.	<i>Conclusion</i>	183
Section 5. General discussion		185
Chapter 8. General Discussion		186
8.1.	Discussion	186
8.1.1.	<i>Overview</i>	186
8.1.2.	<i>Effects of the environmental stressors on molluscs</i>	187

8.1.3.	<i>Host: pathogen interactions and coevolution.</i>	190
8.1.4.	<i>A complex interactome: environment: host: pathogen.</i>	193
8.1.5.	<i>Risks to wild and industry populations</i>	196
8.1.6.	<i>Guardianship versus utility in a changing world.</i>	197
8.1.7.	<i>Logistical issues, unforeseen circumstances, limitations, and biases</i>	198
8.1.8.	<i>Future research avenues and recommendations</i>	200
8.1.9.	<i>Conclusion</i>	203
References		205
Appendix		236
9.1.	Appendix: Research outputs	236
9.1.1.	<i>Peer reviewed published papers.</i>	236
9.1.2.	<i>Peer reviewed co-authored papers (During PhD program)</i>	236
9.1.3.	<i>Book chapters</i>	237
9.1.4.	<i>Conference poster presentations</i>	237
9.1.5.	<i>Conference oral presentations</i>	237
9.2.	Appendix: unique outputs	238
9.3.	Appendix: supplementary tables.	240

LIST OF TABLES

Table 2.1 The mean mussel length (L (mm)) ± SD, sample size, F:M sex ratio and percent prevalence data for 11 general tissue conditions are presented, including gill haemocytosis (Gill HE), gill ceroid (Gill BC), focal haemocytosis (F HE), mantle haemocyte infiltration (M HE), mantle ceroid (M BC), digestive gland haemocyte infiltration (DG HE), gastrointestinal epithelium diapodosis (GI d), gastrointestinal epithelium disruption from APX transitioning through (GI ED), kidney haemocyte infiltration (K HE), tissue atrophy ((Not including the DG) T Atro), digestive gland atrophy (DG Atro), and high apoptosis of haemocytes (Apop), NR: No record: no samples provided.....	38
Table 2.2 The semi-quantitative grade, range and percent of atresic oocytes in a subset (n=87) of females where the range is the percent of atresic oocyte through visual microscopic estimates. The count is the number of females within the grade that underwent the image counting process to acquire the mean percentage.....	41
Table 2.3 Sequencing results from gene blasting compiled bioinformatics of the 18S PCR of the 2 PCR positive FFPE mussel samples with the top three potential features for the multinucleate parasite. The top 1 to 2 closest species and the last common ancestor was recorded.....	44
Table 2.4 Linear model results showing interactions (indicated by *) and statistical results (significant results at p -values < 0.05). Shows the interactions for each of the key models.....	46
Table 3.1 Morphometric and physiological data whereby size range is the min and max shell length. Additional values report the mean ± SD. Weight in g (W), Shell length in mm (SL), Shell width in mm (SW), Shell height in mm (SH) shell length to shell height ratio (SL:SH), Percent population reproductively active (% RA) and the female: male sex ratio (F:M).....	60
Table 3.2 Summary of semi-quantitative tissue assessments (mean ± SD). Ceroid material in the gut sub-epithelium reflects the relative quantity (0 – 3) of ceroid material in the connective tissue adjacent to the gut epithelium. ‘Coverage’ (criterion 1) provides an indication of the proportion of digestive tubules (DG) showing detachment (score 1 – 4 corresponding to 0 – 100% occurrence), while ‘extent’ (criterion 2) considers the mean extent to which tubules have detached (0 – 4 corresponds to no detachment and whole tubule has detached, respectively). The subjective ‘DG quality’ (criterion 3) classifies the overall quality of the tubules. Ceroid score in DG reflects the relative quantity in the interstitial spaces.....	62
Table 4.1 Sampling numbers and time course of <i>H. iris</i> sampling for the Chatham Islands. The first timepoint (13/03/2020) has previously been analysed (Copedo et al., 2024) (Chapter 3) and is included as a reference for comparison.....	76
Table 4.2 Generalised reproductive gonad staging descriptions of <i>Haliotis iris</i>	78
Table 4.3 Morphometric and sex ratio data for the adults (n=60) and sub-adults (n=54) at site 1 (Ascots) and the adults (n=60) and sub-adults (n=60) at site 2 (Owenga Harbour). Data are reported as mean ± standard deviations. The L:H ratio is the length to height ratio and sex ratio is M:F or male to female. Letters indicate statistical differences between site and life stages ($p < 0.05$). For the sex ratio the asterisk (*) indicates significantly different values when compared with a typical 1:1 sex ratio; $p \leq 0.05$ and two asterisks (**) $p \leq 0.001$	83
Table 4.4 Data for 14 general pathological findings and tissue alterations are presented, including a semi quantitative food score, ciliate (<i>Scyphidia</i> - like) prevalence, ciliate intensity (int), gill alterations (e.g., epithelial atrophy or cilia loss), gill protein score (Gill P), haemocytosis (He), ceroid prevalence, ceroid score of the: right kidney (CK), digestive gland (CDG) and sub epithelial layer of the gastrointestinal tract (CSG), detachment of digestive gland tubule from basement membrane (DG	

gaping), interstitial space between the digestive tubules (DG IS), kidney stones (KS) and haplosporidian-like parasite (Hap) (Copedo et al., 2024), % percent prevalence, * only 1 sample, NR: Not recorded/ no samples provided.....	84
Table 4.5 Statistical analysis of the pathological findings and general tissue alterations observed through histology in table. 4.4. Text in bold indicate statistically significant values $p < 0.05$	85
Table 4.6 Mean (\pm SD) percent of atresic (non-viable) oocytes in females that were graded as spent, ripe or late developing. NR = not recorded, empty spaces = no samples available.	87
Table 4.7 Gene sequence results from gene blasting the 18S amplicon sequence variants, of particular interest, of the 3 samples of abalone kidney tissue. The top 2 to 3 closest species were recorded for each of the 3 selected features and the last common ancestor was recorded.	89
Table 5.1 Sampling numbers and collection months for each of the temperature treatments over the 15 months (July 2018 – Sept 2019). A fixation issue at month 3 resulted in a lack of individuals for the histology assessment. Thus, month 3 is represented graphically but was not included in the statistical analysis. Month 2B was the initial sampling, where all mussels were at 17°C, prior to raising the mussels to the desired temperature achieved by month 3 (None available (NA)). At month 15B there were no mussels left in the 24C treatment to sample (NA).....	104
Table 5.2 Semi-quantitative scoring of level of ceroid material and focal haemocytosis from least severe (1) to most severe (4). Criteria are similar to the grading scale of Carella et al., (2015) and Bignell et al. (2008) and specific illustrations are located in the results section.....	105
Table 5.3 Semi-quantitative scoring of level of storage cell material (glycogen) and gut subepithelial thickening from least severe (1) to most severe (3). A score of 3 for storage cell coverage indicates glycogen rich mantle tissue whereas a score of 1 for the gut is indicative of healthy gut performance, with low numbers of haemocytes around the gut epithelial layer.....	106
Table 5.4 Histological criteria of seven stages and the associated gonad index score for the reproductive condition of green-lipped mussels.	108
Table 5.5 Two parasites, APX and <i>Perkinsus olseni</i> , were scored using a 0 – 5 grading scale, where 0 indicated no parasites were observed and 5 is a severe level of parasites was observed.....	110
Table 5.6 Water quality parameters (mean \pm standard error (SE)) measured throughout the experiment for further details see Ericson et al., (2023).	111
Table 5.7 Heatmap of the semi-quantitative levels of ceroid material, focal haemocytosis, mantle storage cell coverage and the thickness of the subepithelial layer of the gut. Sampling month 3 had fixation issues and, as such, only had an $n = 1$ at 17 °C and $n = 3$ at 21°C; no samples were available for the 24 °C treatment. Sampling months 4 to 15 had $n = 8$ at 17°C, $n = 8$ at 21 °C and $n = 8$ at 24 °C for each sampling month (Table. 5.1). Where no data were collected, cells are blacked out....	113
Table 5.8 Total population percentage prevalence (%) of parasites found in the green-lipped mussels during the experiment. APX and <i>P. olseni</i> are excluded from this table and discussed in further detail below (17°C ($n=142$), 21°C ($n=129$) and 24°C ($n=104$)).	119
Table 5.9 Population prevalence (%) of APX and <i>P. olseni</i> during 15 months of sampling at three temperatures 17°C, 21 °C and 24 °C (sample numbers available in Table. 5.1)	120
Table 6.1 The percent prevalence of common tissue conditions and parasites observed in the green-lipped mussels during the 3-month period of sampling around the August 2022 flood: Base	

(Baseline), M1 (Month 1) and M2 (Month 2). The ambient (Amb) temperature samples represent mussels collected from the field (source farm) within a 5 to 10-day period after laboratory sampling. Tissue conditions include Ceroid, infiltration of haemocytes in the gill epithelium (Gill infil), and the gastrointestinal tract epithelial layer (GIT infil), digestive gland necrosis (DG nec), digestive gland wall atrophy (DG atr). Common parasites include *Endozoicomonas*-like organisms in the gastrointestinal tract and DG epithelium (GI ELO), intracellular bacterial cysts in the gills and mantle tissue (BA cyst), gill ciliates (CI), parasitic copepods in gastrointestinal tract lumen or mantle (CO), *Microsporidium rapuae*, APX in mantle and interstitial connective tissue (APX), and APX transitioning through the gastrointestinal tract wall to the luminal space (APX GI).136

Table 6.2 Trend of tissue conditions based on prevalence data presented in table. 6.1 whereby the increase in a condition (response variable) in relation to the environmental factor (explanatory variable) is indicated by an arrow up (↑), no change is indicated by a dash (-), and a decrease by arrow down (↓, not observed herein).137

Table 6.3 Mean (± SD) water quality parameters throughout the trial period for the external seawater (SW) ponds, High food and Low food treatment for dissolved oxygen, salinity (ppt) and pH.149

Table 6.4 Mean (± SD) Chl- *a* ± of in-flow, algae consumed (in-flow minus out- flow), chl-*a* mussel/day, amount and the chl- *a* reading converted to algal cells (n=50).149

Table 6.5 Mean (± SD) length and weight data for each treatment at each sampling timepoint. Collection date is indicated by month with approximately 30 days between collections.151

Table 6.6 Statistical results from length, weight and condition index (CI_{Adapted}) data using a GLM. A *p* value < 0.05 was considered statistically significant and is indicated by the bold text.151

Table 6.7 Mean (± SD) condition index (CI_{Adapted}) for each treatment for each sampling time point. Collection date is indicated by month with approximately 30 days between collections.152

Table 6.8 Percent prevalence of tissue pathology and parasites detected in green-lipped mussels during the experiment. The ambient (Amb) temperature samples represent mussels collected from the field (source farm). Tissue conditions include mean score of glycogen storage cell density in the mantle and digestive gland tubules (**G-S cell**) (Copedo et al., 2023), digestive gland necrosis (**DG nec**), digestive gland wall atrophy (**DG atr**), infiltration of haemocytes in the gill epithelium (**Gill HE**), and **Ceroid**. Common parasites include intracellular bacterial cysts and *Endozoicomonas*-like organisms (ELOs) in the gills (**BA cyst**), gill ciliates, *Pseudomyicola* sp. (**Copepods**), *Microsporidium rapuae*, *Paravortex*, APX in mantle and interstitial connective tissue (**APX**), and APX transitioning through the gastrointestinal tract wall to the luminal space (**APX GI**), and ELOs in the gastrointestinal tract and DG epithelium (**GI ELO**).155

Table 7.1 Total number of *Perna canaliculus* sampled in each treatment at each timepoint.167

Table 7.2 Proposed histopathological scoring of *Perkinsus olseni* including number of tissues affected (Fig. 1), haemocyte aggregation, and development of lesions, as well as encapsulated *P. olseni* cells and systemic presence. The score is the sum of the individual score in each column. The minimum score is 2 and must consist of detection of 1 *P. olseni* cell in 1 tissue type. A score of 20 is the maximum value and indicates a severe impact. A score of 10 is moderate and 15 is high. Values between 2 and 20 can be created by a combination of these scores. For example, a score of 15 could be created by the combination 5, 5, 5, 0 (very high cell number, 5 tissues, diffuse haemocytosis, but no pustule). Note* pustule descriptions are hypothetical, and based on clam and abalone species (Handler, 2022). Systemic free cells have been observed in green-lipped mussels in a thermal challenge trial Chapter 5.170

LIST OF FIGURES

- Figure 1.1 Infographic showing impacts of the changing climate variables (temperature, increasing precipitation, sedimentation, and decreasing salinity) on the marine ecosystems and shellfish farms. Image credit: Infographic designed by Revell Design, commissioned by the Cawthron Institute for the Greenshell Mussel (GSM) adaptation planning pathways workshop 2023. Reproduced with permission from the authors: James Butler and Jess Ericson.....1
- Figure 1.2 Generalised depiction of the marine heatwave model indicating categories and standardised thresholds that determine the difference between a heat spike (left) and a heatwave (right) with increasing sea surface temperature (°C). The contours represent typical climatological temperature. Image adapted from Hobday et al. (2016).2
- Figure 1.3 Generalised image of Shelford’s law of tolerance and adapted from the thermal tolerance range model from Portner and Farrell (2008) and Sokolova et al. (2012). The solid line indicates a single stressor scenario using temperature as an example. The dashed lines and arrows indicate hypothetical deviations away from the typical single factor bell curve range. For example, skewed to the left, or right, could be the bell curve for salinity overlapping the curve for temperature, or adaptation to a chronic stressor and shifting thresholds. The dashed and dotted line is an example of the influence of multi-stressor and/or moderate to extreme intensity exposure to a stressor. The optimal band may then become narrower and therefore there is a higher chance of crossing into the stressed category. The optimum is range of maximum physiological fitness and beyond the critical section is the lethal range.5
- Figure 1.4 Generalised depiction of the multi-stressor model derived and adapted from Gunderson et al. (2016) predicting physiological stress responses from 3 potential stressors. The numbers (1-4) represent the hypothetical temporal pattern with the expected consequence (Gunderson et al., 2016). Pattern 4 has been further adapted to include an additional hypothetical option depending on: a) 2 initial stressors prior to a third or b) a first initial stressor followed by 2 co-occurring in a similar time frame. Examples of stressors could include Stressor 1: thermal stress, Stressor 2: Reproductive maturation, Stressor 3: pathogen invasion/occurrence.....7
- Figure 1.5 Simplified oogenesis and spermatogenesis cycle for gastropods and bivalves within the gonad tissue adapted from Galtsoff (1964) and Costa (2018a). **a)** female with developing oocytes. Undifferentiated (resting) cells develop into early oocytes attached to follicle wall with a clear cytoplasm (c), nucleus (N) and nucleolus (n). As the oocytes develop the attached section becomes stalk-like (s), the stalk thins as the oocyte grows and matures. Once ripe and mature (m) the oocyte detaches from wall and starts to round up. The jelly coat (j) is a common feature in gastropod (g) oocytes; it is not present in bivalves (b). The gonad will empty during spawning and residual oocytes will typically become atresic (ao) and be cleared by phagocytosis or reabsorbed (see below). Atresic oocytes are characterised by their jigsaw-like shape, detachment of cytoplasm from the cell wall, unusual staining breakdown of the cell membrane. **b)** developing male where undifferentiated cells develop into spermatogonia and further in sequence into spermatocytes (Sc), spermatids (St) and mature spermatozoa (Sz). Residual sperm after spawning will also be cleared by phagocytosis.....10
- Figure 1.6 The three key factors influencing disease outbreaks: the changing environment, the host condition, and the associated pathogens (based on Burge et al. (2014)). The arrow into the marine environment section indicates added stressors from a changing climate which exacerbates conditions.13
- Figure 1.7 A generic *Perkinsus* spp. life cycle derived from Goggin and Lester (1995) and Soudant et al. (2013). The vegetative stage typically occurs inside the host and the proliferative stage outside the host.15

Figure 1.8 Biological levels from molecular through to ecosystem and the range, or link, that molecular biology, cell biology, physiology and ecology can extend through to at each level. Histopathology sits centrally on the continuum from ‘ecologically relevant but increased confounding factors’ through to ‘mechanistic with high specificity’. Image adapted from Costa, (2018b).21

Figure 1.9 Graphic representation of the layout of this thesis. The layout is defined by the complexity of the environmental conditions followed by field and laboratory components. The tapering triangular shape reflects the big picture field studies down to specific host- pathogen interactions.24

Figure 2.1 Coarse daily multi-sensor sea surface temperature (SST) for the Coromandel region (latitude 37.03°S, longitude 175.35°E) between Jan 2017 and Mar 2021. The dashed line represents the 22 °C threshold of sub-optimal temperatures, whereby physiological conditions and reproduction are impacted with prolonged exposure to >22 °C (Ericson et al., 2023; Venter et al., 2023; Benjamin et al., 2024). The sampling period is highlighted by the shaded area. Source: IMOS36

Figure 2.2 Visual representation of the NZ and Chatham Island area showing average sea surface temperature (SST) anomalies for the month of December for the years a) 2017, b) 2018, c) 2019 and d) 2020. December 2017 appears to be the warmest followed by 2018 and 2019. Coromandel and sampling location (arrow), e) SST anomaly timeseries showing degrees above the climatological baseline from December 2016 to December 2023 for the Coromandel region near the sample site (latitude 37.03°S, longitude 175.35°E).37

Figure 2.3 Mean gametogenesis index score of mussels identified as female and male for each month (secondary y-axis). A score of 0 indicates a resting or spent population and a score of three indicates the population is in the mature or ripe phase. Maximum sea surface temperature values (dots) for each of the four years (2017 to 2020) (primary y-axis). Southern hemisphere seasons are indicated by shaded areas, summer (Dec. to Feb., red), Autumn (Mar. to May, yellow), Winter (Jun. to Aug., blue), and Spring (Sep. to Nov., green).....39

Figure 2.4 Percent gametogenesis stages showing annual reproductive cycle of green-lipped mussel from April 2018 to May 2021 (n = 570). The mean (solid line), maximum (dash) and minimum (dash and dot) sea surface temperature (SST) for each month is displayed for visual representation.40

Figure 2.5 Percent prevalence (coloured grid), and total number (primary y-axis), of parasites and pathogens observed in adult green-lipped mussels (H&E histological slides) collected from April 2018 to May 2021. The average (solid line), maximum (dash) and minimum (dash and dot) sea surface temperature (SST) for each month during the sampling period is displayed for ease of visual representation (secondary y-axis). Apicomplexan- X (APX), rod bacteria in digestive gland connective tissue and mantle (BA Rod), rickettsia-like bacteria across tissue types was fine and shadowy in appearance (BA T3 – Gen), bacterial cocci cysts (rounded) in the gill (BA T1), *Endozoicomonas*-like organisms (BA T2) in the gill and the gastrointestinal tract epithelium (GI), *Microsporidium rapuae*, *Perkinsus olseni*, copepods in the gastrointestinal tract luminal space, hydroid polyps in the pallial cavity, *Bucephalus* sp. and multinucleate cells/bodies (multinuc cells).42

Figure 2.6 Two of the parasites detected in adult green-lipped mussels within this study during late 2020 and early 2021; a) hydroid polyps attached to external surface of mantle in the pallial cavity; and b) Sporocysts of *Bucephalus* sp. containing cercariae in mantle, and the new multinucleate parasite or bodies (arrows) detected in green-lipped mussel kidney and heart tissue; c) kidney tissue with high number of parasites transitioning through the kidney epithelial layer (Ke) with no associated immune response; d) kidney tissue depicting the immune response around the kidney epithelial (Ke) and kidney lumen (Kl) (scale = 50µm); e) oil immersion showing the plasmodia of the haplosporidian-like parasite (arrows) transitioning through the kidney epithelial layer (scale =

20µm) and; f) cluster of multinucleate plasmodia detected near the heart tissue (H) (scale = 20µm).	43
Figure 2.7 Kendall's rank correlation matrix of the tissue conditions, parasites and pathogens detected in green-lipped mussels during three years of sampling. Positive correlations are indicated green (> 0) and negative correlations in brown (< 0). Significant differences with a p value of < 0.05 are indicated by an asterisk (*). Strong significant differences < 0.005 are indicated by multiple asterisks (***).	45
Figure 2.8 Predicted relationship of the maximum temperature and the mean sum of parasite species across each gametogenesis maturation stage (score 0 – 3) derived from the linear model.....	46
Figure 3.1 Generalised map of Chatham Island (43°52'49.7" S 176°32'02.6" W) depicting the four selected 'stunted' or 'fast-growing' sites selected for sampling. Site 1: Ascots (44°00'56" S 176°23'12" W); Site 2: Owenga harbour (44°01'28" S 176°21'56" W); Site 3: Durham (44°00'24" S 176°40'54" W) and Site 4: Wharekauri Harbour (43°42'18" S 176°35'04" W).	55
Figure 3.2 General anatomy depiction of New Zealand abalone (<i>Haliotis iris</i>). Rectangular windows show approximate location of the histology sections, which were chosen to maximise chances of acquiring all tissue types, including midgut, digestive gland, left and right gill, gonad, left and right kidney, hypobranchial gland, nervous tissue, and muscle.	56
Figure 3.3 Photomicrographs of the crop/stomach region of <i>Haliotis iris</i> . a) Grade 5: 'Old', where algal material has broken down to fine particles of grey-coloured debris (arrow). b) Grade 1: 'Fresh', where structure of the algae is still largely intact and cells still visible (arrow).	57
Figure 3.4 Mid-gut sub-epithelium from a) slow-growing individual (site 2: Owenga harbour) showing the high level (score 3) of ceroid material presence, and b) fast-growing individual (site 1: Ascots) showing minimal ceroid material (score 1). Examples of fine ceroid granules (Arrow) and ceroid aggregate (Arrowhead) are marked.....	57
Figure 3.5 Scoring criteria to quantify the severity of the alterations in the digestive gland tubules of <i>Haliotis iris</i> . a) Normal digestive gland tissue whereby none of the digestive tubules are showing signs of gaping and all are tightly packed (Score 0). b) Digestive gland tissue showing signs of gaping away from basement membrane (Score 3) and poor-quality tubules (DG quality score 3) displaying changes to basophilic cells and increased staining affinity, developing space in interstitial space and increased haemocytes (arrow). Digestive tubule lumen (L), digestive cells (dc) and basophilic cells (arrowhead) of the digestive tubule epithelial layer are indicated. c) Zoom of digestive gland (a) showing connection of the epithelium to the basement membrane. Section shows pink/purple-toned basophilic cells (arrowhead), a light scattering of ceroid granules (star) in basophilic cells. d) Zoom of image b showing separation of epithelium from the basement membrane creating a void (arrow), compression of the basophilic pyramidal cells and an increase in ceroid material in both the basophilic cells and interstitial tissue.....	58
Figure 3.6 Example photomicrograph (Frame size: 1857 x 3308µm) of <i>Haliotis iris</i> gill, <i>Sphenophyra</i> -like ciliates with dense nuclei are shown (black arrows) between the gill filaments. 59	
Figure 3.7 Food score (Mean ± SE) 1 being 100% Fresh (intact) food visible and 5 being 100% old (degraded/digested) food (Adults: site 1. Ascots n=9, site 2. Owenga n=9, site 3. Durham n=7, site 4. Wharekauri n=10; Sub-adults: site 1. Ascots n=10, site 2. Owenga n=9, site 3. Durham n=10, site 4. Wharekauri n=10). Significant differences (p < 0.05) among groups are shown with lower case letters above bars.....	61

Figure 3.8 Histology wax block of an example individual with “older” food and almost empty mid-gut tract. a) histology block sample photographed at ~5x magnification (dissection microscope), indicating a gut lumen filled with sediment (arrow); inset is the corresponding histology slide stained with H&E. b) Enlarged image of gut tract showing sediment particles.....	61
Figure 3.9 Number of ciliates per 1 mm ² of abalone gill transverse section (Mean ± SE) from four sites around the Chatham Island (Adults: site 1. Ascots n=10, site 2. Owenga n=9, site 3. Durham n=10, site 4. Wharekauri n=10; Sub-adults: site 1. Ascots n=10, site 2. Owenga n=10, site 3. Durham n=8, site 4. Wharekauri n=9). Inset: Enlarged image of a group of 4 ciliates (Arrow).	63
Figure 3.10 Population percent prevalence (%) (n=10) for the presence/absence of a) haplosporidian-like parasite and b) kidney crystals in the right kidney tissue of <i>H. iris</i> from four sites around the Chatham Island (Adults: site 1. Ascots n=10, site 2. Owenga n=10, site 3. Durham n=11, site 4. Wharekauri n=10; Sub-adults: site 1. Ascots n=10, site 2. Owenga n=10, site 3. Durham n=10, site 4. Wharekauri n=10). Letters indicate significant differences between sites and life stages ($p < 0.05$).	63
Figure 3.11 Crystals in an H&E-stained right kidney section from an adult abalone, viewed under a) bright-field kidney crystals (arrows), b) using a crossed polar filter to observe differences in the inclusions and the anisotropic affect from the birefringent properties c) kidney concretion embedded in the right kidney epithelial (Rke) layer H&E under oil immersion e) oil immersion image of kidney concretion with polarised filter. Right kidney tubule (arrowhead), kidney lumen (Rkl), kidney epithilium (Rke) and mucous cells (m).	64
Figure 3.12 Multicellular haplosporidian-like parasite (Arrowhead) cluster in the lumen of right kidney (RkL) of <i>H. iris</i> . Right kidney epithelium (Rke) and haplosporidian-like sporocyst (arrow).	65
Figure 4.1 General anatomical depiction of New Zealand abalone (<i>Haliotis iris</i>) by Copedo et al. (2024) (Chapter 3). Location of the histology sections, indicated by rectangular windows, were chosen to maximise likelihood of acquiring all tissue types, including gastrointestinal tract, digestive gland, gill, left and right kidney, hypobranchial gland, nervous tissue, muscle and gonad.	77
Figure 4.2 Course daily sea surface temperature (SST) (Left axis; blue dots) from a single location approximately 4 km from Site 1 (Ascots) and Site 2 (Owenga Harbour) (latitude 43.99°S, longitude 176.34°W). Data source: (JPL, 2015). Monthly SST anomaly timeseries from December 2016 to December 2023 (Right axis; orange line). The SST anomaly timeseries shows degrees above the climatological baseline covering the 1985-1990 plus 1993 period.....	81
Figure 4.3 Visual representation of the average sea surface temperature (SST) anomaly data for the month of December for the years 2020, 2021, 2022 and 2023 around New Zealand (NZ) and the Chatham Islands (arrow). SST anomaly data sourced from NOAA Coral Reef Watch (https://coralreefwatch.noaa.gov) (Liu et al., 2014).	82
Figure 4.4 Frequency of reproductive staging of <i>H. iris</i> from 2 sites (Site 1: Ascots and Site 2: Owenga) on the Chatham Islands over multiple timepoints between March 2020 and April 2021 for a) adult abalone and b) sub-adults.....	86
Figure 4.5 Representative images of the reproductive staging of female <i>H. iris</i> showing a) late-stage gonad development of oocytes, b) ripe stage gonad with mature oocytes, c) spent stage with degrading/ atresia oocytes and atresic debris, and d) atresic oocytes (ao) of a ripe stage female indicating potential pre-spawning atresia, jelly membrane of the oocytes (*) and atresic oocyte showing detachment from the membrane (arrow).	86

Figure 4.6 Photomicrographs of the parasites observed in *H. iris* samples a) gross observation of the ciliates attached to the gills (arrows) inset: enlargement of ciliate attached to gill filament, b) ciliates observed in histology stained with H and E, c) the haplosporidian-like multinucleate plasmodia (arrow) located in the lumen of the right kidney was observed to have refractive spore-like structure H&E, d) the plasmodia in the lumen of the right kidney stained using ZN, e) PAS-D and f) PAS. Plasmodia are indicated with arrows.....88

Figure 4.7 The PCR Gel results for a) 18s primers using different dilutions of DNA extraction from sample 1: a1) pure, a2) 1/10 concentration, a3) 1/100, a4) 1/1000, and sample 2: a5) pure, a6) 1/10, a7) 1/100, a8) 1/1000, and a9) neg control, b) PCR gel results using NZAH-F4 and NZAH-R1 primers on 1/100 diluted samples b1) sample 1, b2) sample 2, b3) sample 3, b4) sample 4 b5) GBlock, positive control at approximately 1100 base pairs, and b8) neg control, b6, b7, and b9 are empty slots.89

Figure 5.1 Green-lipped mussel (*Perna canaliculus*) general anatomy depiction. Rectangular window indicates the location of the 5 mm histology section. This section was selected to maximise chances of acquiring all tissue types, including midgut, digestive gland, gill, gonad (mantle) and muscle. 104

Figure 5.2 Female gonad stained with H&E indicating stages of oocytes immature (I), mature (M), atresic (A) within the follicles (f) and glycogen rich mantle storage cell (Sc).....109

Figure 5.3 General alterations to digestive gland tissues at trial start and trial end A) normal digestive gland at trial initiation (graded as 0) B) altered digestive gland after 14 months at 24 °C with expanded intracellular spaces (graded as 2). *Perna canaliculus* gill prior to acclimation to the temperature treatments C) Healthy gill filaments (graded as 0) and D) Gill filaments after 14 months with alterations to the gill architecture and no loss of cilia as described in section 2.3.1.1. (graded as 2). Scale = 50µm.112

Figure 5.4 Ceroid level and the focal haemocytosis level 3. a) Severe level (score 3) of ceroid material, multiple accumulations observed (arrowhead) b) Severe level (score 3) of focal haemocytosis with multiple patches throughout the mantle tissue.113

Figure 5.5 Mantle storage cell coverage and the subepithelial extent or thickness of green-lipped mussels. a) Mantle tissue with a score of 0 no glycogen cells (granules) observed higher levels of haemocytes and connective tissue visible. b) Mantle tissue with a score of 2 with some patches of no storage cell tissue. c) Zoomed in mantle tissue of image a, only connective and some musculature tissue, with no visible glycogen granules. d) Zoomed in mantle tissue of image b showing densely packed storage cells e) Subepithelial layer of the intestine score of 1, low level of haemocytes surrounding the epithelial layer of the intestine f) Subepithelial anomalous thick layer (score of 3) around the intestine extending into the digestive tubule region, indicating increased number of haemocytes surrounding the intestine Black line indicating subepithelial layer.....114

Figure 5.6 Preliminary investigations show the presence of HSP70 in gill and gonad tissue determined by immunohistochemistry. a) gill tissue in 17 °C temperature at month 2 prior to the temperature elevation. Images b, c and d correspond to mussels that had been exposed for 1 month at 17, 21 and 24°C, respectively. Male reproductive follicle HSP70 (magenta) detected to be associated to spermatogonia and spermatocytes, green is the mature sperm cell at 2 temperatures 1-month post-temperature increase e) 17 °C and f) 21°C. Female reproductive follicle at 2 temperatures 1-month post-temperature increase g) 17 °C and h) 21 °C with increased atresic oocytes (A). Magenta (arrow) is the HSP70, and green (arrowhead) is the nuclear material. Images A - D Scale bar= 100µm, Images E – H Scale bar= 50µm.116

Figure 5.7 Gonad condition (proportion of sampled individuals in each development stage and overall gonad index) over 14 months exposure to a) 17°C, b) 21 °C and c) 24°C. No data were collected at month 3 or 15B for 24°C.	117
Figure 5.8 Female reproductive tissue (mantle) showing: a) anomalous dilated post-spawning follicle (f), b) dilated follicles with high levels of atresic debris, c) female mantle tissue with low levels of storage cell (glycogen (Sc)), regressing and atrophying follicles (Arrow) and focal haemocytosis (Fh) from a female in the 24 °C treatment, d) full follicles with high level of atresic oocytes (A), residual oocytes (R), and phagocytosis (Ph) within the follicle.	118
Figure 5.9 Representative microphotographs of a) APX at a score of level 2: a group of 6 APX zoites within the mantle tissue no ceroid material or haemocytosis associated, and b) <i>P. olsenii</i> indicating level 3 displays different stages of the lifecycle trophozoite signet ring (arrow) and the rosette-like (arrowhead). <i>P. olsenii</i> cells detectable across mantle and connective tissue of multiple tissues occasionally associated with haemocytosis.	119
Figure 6.1 Time series of temperature between July 22nd and 13th Sept 2022. Sampling time points are indicated by the red circles: July 2022 is the baseline sampling when mussels arrived on site. The flood occurred on 17th Aug 2022 (second circle). The flood section indicates length of time (5 days) where site access was prohibited. The opportunistic post-flood collection occurred at the site access resumption point (third circle). A post-flood recovery of approximately 3½ weeks was used to monitor survival prior to final sampling (month 2, circle four). The designation “cool” is the treatment destined to be 17°C and “warm” indicates 22°C	132
Figure 6.2 Example histology micrographs of gonad follicles in <i>Perna canaliculus</i> a) Male in ripe condition with follicles containing mature sperm cells b) Male partially spawned, c) Female spawning base on missing ripe oocytes (arrow) and atresic spent follicles (*), however many developing oocytes are still attached to the wall (arrow head) and d) female spent with small follicles and most follicles containing atresic (degenerating) oocytes.....	133
Figure 6.3 Visual representation of the reproduction condition and gametogenesis frequency stages for the mussels from the field and the laboratory experiment. The temperature treatments are grouped by the target experimental temperatures, feed treatment and sample month. For sample size per treatment see Table 6.1.	134
Figure 6.4 Histological micrographs of example conditions detected in adult <i>Perna canaliculus</i> , a) gill epithelium with increased haemocyte infiltration b) and c) Cluster of haemocytes, sediment, and ceroid transitioning through the gastrointestinal tract epithelium, digestive gland tubules with some displaying atrophy (arrow), e) Gill intracellular bacteria-like cells (arrow), f) ELO and shadowy to fine bacterium in the secondary duct of the digestive gland, considered as part of the gastrointestinal tract within the text and table. 6.1, g) large cluster of APX transitioning through the gastrointestinal tract epithelium.	135
Figure 6.5 Representative images of gonad condition whereby a) is a mussel with no condition and scored as a 0 (arrow), whereas b) is gaining condition and was given a score of 8 out 10 (arrow).	147
Figure 6.6 Cryosectioning and staining process completed at the Malaghan Institute; a) embedding mussel mantle tissue in OCT (optimal cutting temperature) compound in the mould. b) and c) freezing mould and tissue sample in Gentle Jane. d) Sectioning the frozen sample in a cryostat to acquire 3-5µm frozen sections. e) frozen section mounted on to the slide, f) OCT compound rinsed off the slide, the tissue on the slide was fixed in a paraformaldehyde solution (4%) and rinsed off with RO water, g) glass around the tissue sample was dried then a border was drawn around the section. The tissue was the stained using DAPI (4',6-diamidino-2-phenylindole) and Nile Red; once	

stained and rinsed the slide was mounted with a DPX Solvet containing; distyrene, a plasticizer, and xylene) cover slip medium and a coverslip, h) once samples were completed, they were examined using a confocal microscope.	148
Figure 6.7 Raw temperature data of the experiment between July and December 2022. The warm (nominal 22°C) treatment temperature is in yellow and cool (nominal 17°C) treatment in dark blue. The heat pump temperature spikes occurred between November 15 th and 25 th	150
Figure 6.8 Raw temperature of the reference field population with loggers set at 1 meter and 5 meters. Data were logged every 30min. There is considerable overlap of the temperatures where they are the same.	150
Figure 6.9 Final condition index (CI) using the a) commercial and b) biological equations of 40 mussels for each treatment (\pm standard deviation).	152
Figure 6.10 Visual grading of gonad condition for each sampling timepoint and treatment.	153
Figure 6.11 Digestive gland tubules in green-lipped mussels in a) a mussel sampled at the initial baseline, tubules have thick epithelial walls and a typical star or cross shape lumen, and b) digestive gland at final time point of a mussel in the 22°C low food treatment with sparse tubules with atrophy (thinning and attenuation of walls).	153
Figure 6.12 Copepod detected in green-lipped mussels a) histology micrograph stained with H&E and b) image of live specimen on a ruler.	154
Figure 6.13 Frequency of gametogenesis stages for each sampling timepoint at each temperature (17 or 22°C) and each food level treatment (low or high).	156
Figure 6.14 Confocal microscope imaging of the green-lipped mussels female gonad tissue showing a) lipid droplets (Red) in a ripening female and, b) Atresic oocytes in a spent female – green (autofluorescence of tissue) in colour with sparse lipid droplets. Nucei in both stained with DAPI (blue).	156
Figure 6.15 Kaplan Meyer probability curve for the 4 experimental groups. Statistical differences indicated by a and b $p = <0.05$	157
Figure 7.1 Typical, green-lipped mussel transverse histological section (~130mm ²). <i>P. olsenii</i> cells detected were recorded and allocated to the following tissues: (a) mantle, where gonad was likely to develop, (b) digestive gland tissue (DG) including the interstitial space between tubules, (c) haemal space (connective tissue) between DG and foot muscle, (d) gastrointestinal tract including the subepithelial layer and the surrounding interstitial tissue gill, (e) muscle, (f) either foot or adductor (if available in section), and (g) palp	168
Figure 7.2 <i>Perkinsus olsenii</i> life stages encountered in the injected trophozoite culture in green-lipped mussels a) small rosette stage engulfed by a haemocyte, b) small rosette cells dividing and developing into small immature trophozoites, c) large well-developed trophozoite. The <i>P. olsenii</i> life stages of the naturally infected, green-lipped mussels d) small rosette with early division and 3 trophozoites nearby, e) large cluster of rosette stage cells encapsulated by haemocytes and small early developing trophozoites, a second cluster to the right with slightly larger trophozoites and f) large well-developed trophozoite. <i>P. olsenii</i> cells indicated by arrows.	174
Figure 7.3 Histological (hematoxylin and eosin) micrographs of transverse tissue sections of green-lipped mussels 33 days post-injection, a) mussel with infiltration of haemocytes between the muscle fibres as a result of injection and external to adductor muscle between kidney tissue and gill (yellow	

arrow), b) high number of focal haemocyte aggregations associated to mantle, digestive gland, the gastrointestinal tract and the interstitial space between digestive gland and muscle, c) enlarged view of one of the focal aggregations with ceroid (white arrow) and multiplying *P. olsenii* cells, at 66 dpi, d) a naturally infected mussel from the broodstock holding system with *P. olsenii* trophozoite (white arrowhead) and rosette stage (yellow pointed arrowhead) cells associated with large aggregation of haemocytes. Comparison of the same microphotograph of an aggregation of haemocytes associated with *P. olsenii* stained with, e) Fluorescence *in situ* hybridisation, nuclei of haemocytes are green (blue arrow) and *P. olsenii* positive cells are magenta (white arrowhead), autofluorescence (yellow: white arrow) is likely to be phagocytosis, and f) traditional H&E staining, detectable *P. olsenii* cells (arrow).....175

Figure 7.4 *Perkinsus olsenii* cells per mm² detected in each tissue type of the mussels that were *P. olsenii* positive. *Perkinsus olsenii* cells were counted 33 days post injection (dpi) (Blue/Black) adductor (n = 6), DG (n = 5), Gastrointestinal tract (GI) (n = 2), Interstitial (n = 2), Mantle (n = 4), and 60 dpi (Yellow) adductor n = 1, DG n = 9, GI n = 5, Interstitial n = 10, Mantle n = 6). The outliers on the digestive gland (DG), interstitial and mantle are from one individual mussel.....177

Figure 7.5 Histological (hematoxylin and eosin) micrographs of transverse tissue sections of green-lipped mussel mantle tissue two months post *P. olsenii* injection (60dpi), a) very high diffuse haemocyte aggregations in the mantle on the shell edge (L) potentially disrupting the epithelial layer (ep), b) oil immersion 1000x view of the disrupted epithelium with *P. olsenii* cells identified external to the epithelial layer (yellow arrowhead) and within the epithelial layer (white arrowhead).....178

Figure 7.6 The weighted histopathological score (Table. 7.1) for the *P. olsenii* injected mussels at 33 days post injection (dpi) (n = 8) and 66 dpi (n = 16) and naturally *P. olsenii* infected mussels detected and collected November 2021 (n = 5) and December 2021 (n=8). The middle line of each box indicates the median.....178

Figure 7.7 Image analysis and quantification of a) total cell number detected within the focal haemocyte aggregation, and b) the number of *P. olsenii* cells within the focal haemocyte aggregation.179

Figure 8.1 A generalised and simplified depiction of the complex nature of the host pathogen environment interactome. Changing climate can either be a stressor for the host or the pathogen, or both. Under optimal conditions the host and pathogen can either compete thereby driving co-evolution or remain in a state of coexistence. However, if the host becomes stressed either by the environment, by its own physiology (e.g. reproduction) or by the pathogen infecting the host this will drive disease. The severity of the infectious disease will be in theory moderated by the competing interactions of the environment and/or the pathogen, and the ability of the host to defend against both. In conditions which are optimal for the host and suboptimal for the pathogen disease is not likely to progress and the pathogen may be eliminated.194

Figure 8.2 General depiction of optimum and tolerance ranges of green-lipped mussels (Copedo et al., 2023; Ericson et al., 2023; Venter et al., 2023), *H. iris* (Searle et al., 2006; Nguyen et al., 2023), and *P. olsenii* (Delisle et al., 2025) based on current knowledge/ information. Shade area (in colour yellow to red) is the region where a potential synergistic stress effect and physiological stress may increase. *Perkinsus olsenii* may induce a shift in the critical region at a lower temperature (green dotted line). The white section indicates the hypothetical region where the host immune response could maintain defence even with the parasite (*P. olsenii*) present.195

LIST OF APPENDICES

Appendix 1. Research outputs.

Appendix 2. Establishment of the Oceania Aquatic Histopathology Network as founder.

Appendix 3. Promo for the NZOAC conference as a chair and co-chair of the organising committee.

Appendix 4. Supplementary tables.

ATTESTATION OF AUTHORSHIP

I hereby declare that this submission is my own work and that, to the best of my knowledge and belief, it contains no material previously published or written by another person (except where explicitly defined in the acknowledgements), nor used artificial intelligence tools or generative artificial intelligence tools (unless it is clearly stated, and referenced, along with the purpose of use), nor material which to a substantial extent has been submitted for the award of any other degree or diploma of a university or other institution of higher learning.

Joanna Stacey Copedo

CO-AUTHOR CONTRIBUTION

Co-authored chapters within this thesis have been weighted (% time) to provide an author contribution score for each research output. I have provided to the best of my ability representative scores and hereby approve and declare my role in each of the outputs and provide consent publication as part of the PhD. Whereby contribution is allocated by 1. Experimental design, 2. Sample analysis, 3. Data processing, 4. Writing original, and 5. Review and editing.

Chapter Number:	Chapter 2	
Manuscript Title:	Influence of the changing climate on gametogenesis and pathogen diversity in the bivalve, <i>Perna canaliculus</i> .	
Publication Status:	Unpublished/Ready for submission for Publication	
Reference if published:		
AUTHOR SURNAME: (order as per manuscript)	CONTRIBUTION (contribution list above)	
Joanna S Copedo	81%	1, 2, 3, 4, 5
Steve C Webb	3.0%	1, 4, 5
Lizenn Delisle	3.0%	1, 5
Paula Casanovas	4.0%	1, 4, 5
Ben Knight	2.0%	1, 5
Jess Ericson	1.0%	5
Olivier Laroche	1.0%	2, 5
Leonie Venter	1.0%	1, 5
Norman L. C Ragg	2.0%	5
Andrea C Alfaro	2.0%	1, 5

Chapter Number:	Chapter 3	
Manuscript Title:	Histopathological investigation of four populations of abalone (<i>Haliotis iris</i>) exhibiting divergent growth performance.	
Publication Status:	Accepted for Publication	
Reference if published:	Copedo, J. S., Webb, S. C., Ragg, N. L. C., Venter, L., Alfaro, A. C., 2023. Histopathological investigation of four populations of abalone (<i>Haliotis iris</i>) exhibiting divergent growth performance. Journal of Invertebrate Pathology. DOI: 10.1016/j.jip.2023.108042	
AUTHOR SURNAME: (order as per manuscript)	CONTRIBUTION	
Joanna S Copedo	85%	1, 2, 3, 4, 5
Steve C Webb	4.5%	1, 4, 5
Norman L. C Ragg	3.5%	1, 5
Leonie Venter	3.5%	1, 5
Andrea C Alfaro	3.5%	1, 5

Chapter Number:	Chapter 4	
Manuscript Title:	Elucidating divergent growth and climate vulnerability in 2 populations of <i>Haliotis iris</i> .	
Publication Status:	Accepted for Publication	
Reference if published:	Copedo, J. S., Webb, S. C., Delisle, L., Knight, B., Ragg, N. L. C., Laroche, O., Venter, L., Alfaro, A. C., 2025. Elucidating divergent growth and climate vulnerability in abalone (<i>Haliotis iris</i>): A multi-year snapshot. Marine Environmental Research. 107090, DOI: 10.1016/j.marenvres.2025.107090	
AUTHOR SURNAME: (order as per manuscript)	CONTRIBUTION	
Joanna S Copedo	84%	1, 2, 3, 4, 5
Steve C Webb	4.0%	1, 4, 5
Lizenn Delisle	3.0%	2, 3, 4, 5
Ben Knight	2.5%	3, 5
Norman L. C Ragg	2.0%	1, 5
Olivier Laroche	2.0%	2, 5
Leonie Venter	1.5%	1, 5
Andrea C Alfaro	1.5%	1, 5

Chapter Number:	Chapter 5	
Manuscript Title:	Histopathological changes in the greenshell mussel, <i>Perna canaliculus</i> , in response to chronic thermal stress.	
Publication Status:	Accepted for Publication	
Reference if published:	Copedo JS, Webb SC, Ragg NLC, Ericson JA, Venter L, Schmidt AJ, Delorme NJ, Alfaro AC. Histopathological changes in the greenshell mussel, <i>Perna canaliculus</i> , in response to chronic thermal stress. Journal of Thermal Biology. 2023 DOI:10.1016/j.jtherbio.2023.103699.	
AUTHOR SURNAME: (order as per manuscript)	CONTRIBUTION	
Joanna S Copedo	85%	1, 2, 3, 4, 5
Steve C Webb	3.5%	1, 4, 5
Norman L. C Ragg	1.5%	1, 5
Jess A. Ericson	2.0%	1, 5
Leonie Venter	2.0%	1, 5
Alfonso Schmidt	2.0%	2, 3, 4, 5
Natali J. Delorme	2.0%	4, 5
Andrea C Alfaro	1.5%	1, 5

Chapter Number:	Chapter 6	
Manuscript Title:	Implications of flooding events for the green-lipped mussels (<i>Perna canaliculus</i>): An Aquatic health perspective	
Publication Status:	Accepted for Publication	
Reference if published:	Copedo, J. S., Webb, S. C., Ragg, N. L. C., Alfaro, A. C., 2025. Implications of flooding events for the green-lipped mussels (<i>Perna canaliculus</i>): An Aquatic health perspective New Zealand Journal of Marine and Freshwater Research. DOI: 10.1080/00288330.2025.2474570.	
AUTHOR SURNAME: (order as per manuscript)	CONTRIBUTION (May copy from the guidelines above)	
Joanna S Copedo	92%	1, 2, 3, 4, 5
Steve C Webb	4.0%	1, 4, 5
Norman L. C Ragg	2.0%	1, 5
Andrea C Alfaro	2.0%	1, 5

Chapter Number:	Chapter 7	
Manuscript Title:	Progression of <i>Perkinsus olseni</i> in the green-lipped mussel (<i>Perna canaliculus</i>)	
Publication Status:	Unpublished/Ready for submission for Publication	
Reference if published:		
AUTHOR SURNAME: (order as per manuscript)	CONTRIBUTION	
Joanna S Copedo	81%	1, 2, 3, 4, 5
Alfonso Schmidt	7%	1, 2, 3, 4, 5
Steve C Webb	1%	4, 5
Natali J Delorme	1%	5
Norman L. C Ragg	1%	5
Kate S Hutson	1%	5
Chaya Bandaranayake	1%	2, 5
Lizenn Delisle	7%	1, 2, 3, 4, 5

STUDENT, SUPERVISOR AND CO-AUTHOR APPROVALS

By signing you are confirming that the co-author contributions stated in the table(s) above are accurate.

Student Name	Joanna Copedo	Signature	Date	23/04/2025
Supervisor Name	Andrea C Alfaro	Signature	Date	27/11/2024
Supervisor Name	Stephen C Webb	Signature	Date	24/04/2025
Supervisor Name	Norman L. C Ragg	Signature	Date	28/04/2025
Co-Author	Jessica Ericson	Signature	Date	26/11/2024
Co-Author	Natali J Delorme	Signature	Date	22/11/2024
Co-Author	Lizenn Delisle	Signature	Date	28/11/2024
Co-Author	Alfonso Schmidt	Signature	Date	07/04/2025
Co-Author	Paula Casanovas	Signature	Date	24/04/2025
Co-Author	Ben Knight	Signature	Date	22/11/2024
Co-Author	Leonie Venter	Signature	Date	27/11/2024
Co-Author	Olivier Laroche	Signature	Date	25/11/2024
Co-Author	Kate Hutson	Signature	Date	30/04/2025
Co-Author	Chaya Bandaranayake	Signature	Date	23/04/2024

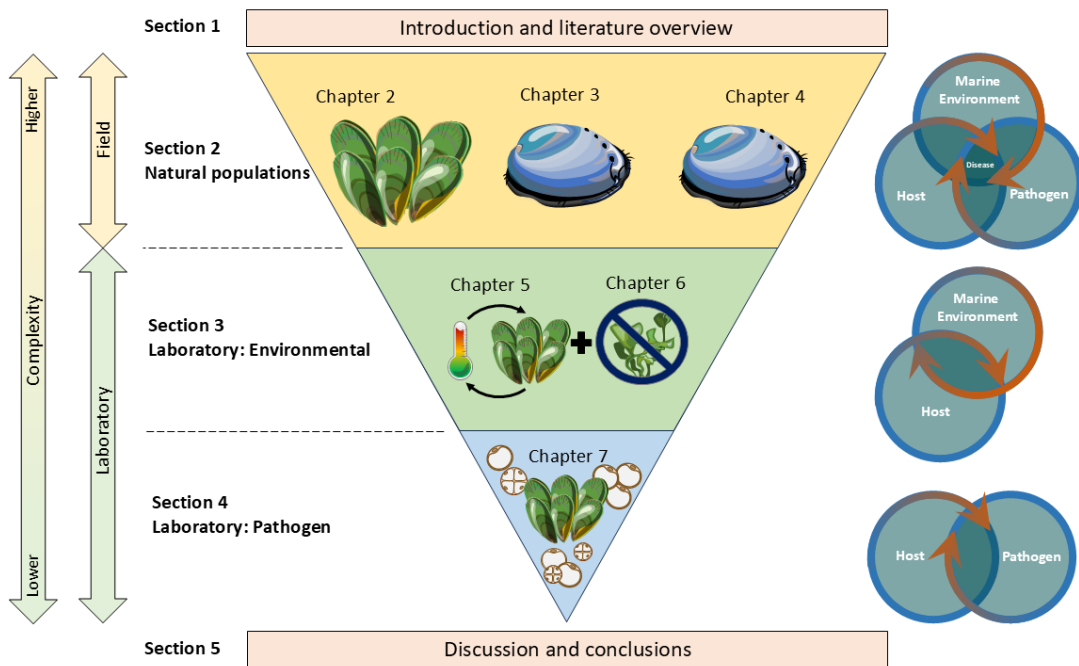
ACKNOWLEDGEMENTS

First, I would like to express my deepest gratitude to Steve Webb, Norman Ragg and Andrea Alfaro, who have been my amazing supervisors during these past few years. I am incredibly grateful for the opportunity you gave me, and all the effort that was involved in developing my career. Thank you for your patience, your guidance, your time, and your support it has been greatly appreciated. Thank you also to Linsey White for stepping in at the end. I am incredibly grateful to my amazing coaches/friends Lizenn Delisle, Natali Delorme, Jessica Ericson, and Leo Zamora. Your advice and critique of each of the chapters has taken this thesis to a level to be proud of (In my opinion). Your knowledge and expertise have been a gift which has made me a better and more diverse scientist.

There are also several other people who contributed to my development, thank you, Kate Hutson, Seumas Walker, Patrick Cahill, Serean Adams, Kevin Heasman for your support of the PhD. Thank you to Leonie Venter for your support on the manuscripts and supplying the early samples, Alfonso Schmidt for the amazing bioimaging training and collaboration, Brian Jones for answering additional pathology questions, Paula Casanova for all your statistics mentoring, Ben Knight for your knowledge on the satellite data, and Rob Bell for IT support. Olivier Laroche, Jacob Thomson-Liang, Chaya Bandaranayake, and Jonathan Banks thank you for your knowledge regarding the molecular work. I have learnt a lot from all of you. There are many scientists and technicians who helped with the practical input and operations, in addition to their intellectual input and encouragement over these past few years. There are too many to name, but you all know who you are – thank you for your dedication. Thank you to Rodney Roberts and Tom McCown for your reviews, comments and discussions on the manuscripts it was greatly appreciated. Thank you SpatNZ and the Coromandel farmer for providing the GreenshellTM mussels, and Dive Chathams, Nick Cameron (PAUMAC4), and Jeremy Cooper for providing the Paua. Thank you to the Hugh Green Technology Centre, Bioimaging Core, Malaghan Institute of Medical Research, through Alfonso Schmidt. Thank you, Anastasija Zaiko, at SeQuench for the metabarcoding sequencing and Medlab Central, Palmerston North, and Awanui Veterinary Histology for their assistance with histology processing. Importantly, thank you Cawthron Institute for this opportunity and providing funding through the Aquaculture Health Strategies to Maximise Productivity and Security programme (CAWX1707), Cawthron's Shellfish Aquaculture Research Platform (CAWX1801) and the Endeavour Emerging Aquatic Diseases: a novel diagnostic pipeline and management framework (CAWX2207). To Cawthron and the Aquaculture Biotechnology Research Group at the Auckland University of technology thank you.

To my wonderful partner Stefan Miller thank you for your support. Your strength, love and encouragement have been a source of comfort and motivation. I am grateful for your patience and understanding even during the challenging moments. I am thankful to have you beside me. Finally, dear reader thank you for seeking this thesis out. I hope you enjoy reading it and it offers you some insights.

SECTION 1. GENERAL INTRODUCTION



In this section:

Section 1: Preamble

Chapter 1: Introduction and literature overview.

Preamble

The green-lipped mussel (GLM), *Perna canaliculus* (Gmelin 1791), also known locally as Greenshell™ mussel (GSM), and the Blackfoot pāua *Haliotis iris* (Gmelin 1791) are two endemic marine molluscs in New Zealand, and both are ecologically and culturally valuable species. In addition to their key role in the marine environment they also hold cultural value and support fisheries and aquaculture industries. The green-lipped mussel is one of 3 established aquaculture species which also include the chinook salmon (*Oncorhynchus tshawytscha*) and the Pacific oyster (*Crassostrea gigas*). Pāua is an upcoming aquaculture species with two land-based facilities currently established. The changing climate and anthropogenic pressures are impacting these two species in terms of growth, reproduction, and survival (Doney et al., 2012b). Although these are not the only valuable molluscs in NZ the accessibility of them allows us to provide key information that may eventually drive other research in the future. Furthermore, the ability to access both field and aquaculture animals allows us to investigate the responses of some of the pressures under different scenarios. This thereby allowing us to fill key knowledge gaps such as the impact of thermal stress on tissue condition, changing pathogen presence, the effect of abiotic and biotic stressors on various other biological aspects such as reproduction. In addition, provides increased understanding of changes that are implicated, and potentially associated to mass mortality events.

Chapter 1 “Introduction and combined literature overview” introduces a wide literature overview of a changing marine environment resulting from climate change, heatwaves and impacts of increased precipitation. The chapter then considers the target organisms in the changing world, which includes an examination of typical physiological performance and response to stress. A more in-depth introduction is then developed, with a focus on gastropods and bivalves, examining their reproduction and gametogenesis, as well as oocyte atresia, leading into an introduction of molluscan pathogens and immune response to complete the environment-host-pathogen epidemiological Venn diagram. The New Zealand context is then provided, and the species that were selected for this thesis and why. All of which provides extensive background for subsequent chapters. Finally, the chapter concludes by considering the potential significance of this work, the research objectives, and the overall thesis layout.

CHAPTER 1. INTRODUCTION

May be published as a modified version.

1.1. A changing marine environment*1.1.1. Global climate change*

The global climate is an interconnected system of atmosphere, land and sea, driven by natural processes such as, but not limited to, earth's orbit and ocean currents, and regulated by naturally occurring greenhouse gases (Le Treut et al., 2006; Alley et al., 2007; Houghton, 2009; Venegas et al., 2023). The increase in greenhouse gases, and aerosols, from anthropogenic sources such as fossil fuels, deforestation and industrial processes is modifying the natural level of such gas production (Houghton et al., 1990; Gruber et al., 2019; Venegas et al., 2023). Carbon dioxide (CO₂) is the most frequently discussed gas affected by anthropogenic sources and is considered as the predominant gas, along with aerosols, likely to further influence climate change (Allen and Ingram, 2002). Accumulation of CO₂ leads to a gradual increase in atmospheric temperature hence the term 'global warming' (Alley et al., 2007; Pachauri and Meyer, 2014; Venegas et al., 2023).

The oceans are a primary component of the climate system as they cover approximately 71% of the earth's surface and play a fundamental role in carbon and thermal absorption and exchange (Rhein et al., 2013; Venegas et al., 2023). The absorption of this atmospheric heat increases the temperature of the oceans, altering the chemistry and impacting the structure and function of marine ecosystems (Moore et al., 2006a; Venegas et al., 2023) (Fig. 1.1.). As the oceans continue to warm there has also been an increase in the frequency of discrete, localised periods of anomalous temperature elevation termed 'marine heatwaves' (Hobday et al., 2016; Oliver et al., 2018; Venegas et al., 2023).

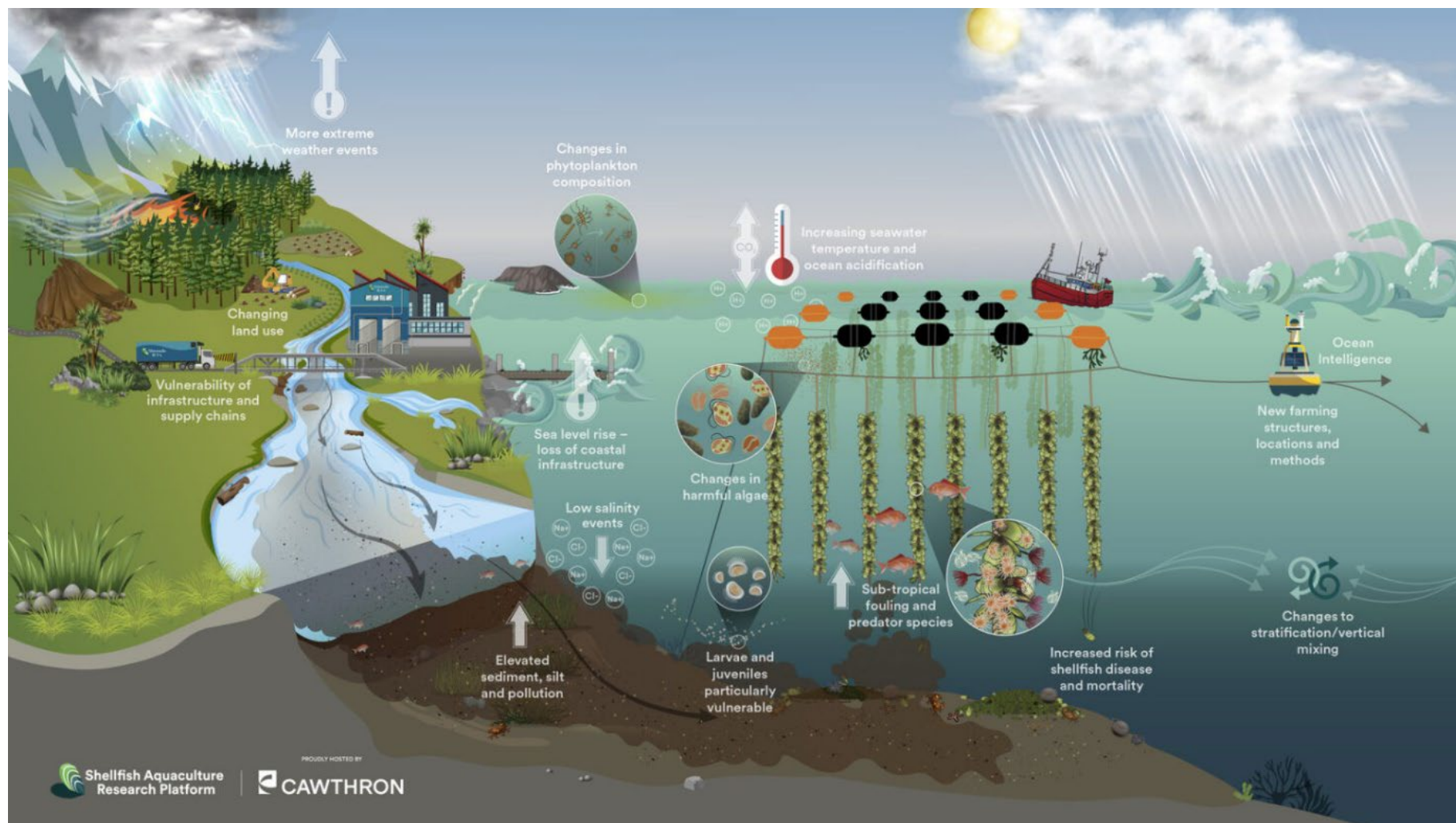


Figure 1.1 Infographic showing impacts of the changing climate variables (temperature, increasing precipitation, sedimentation, and decreasing salinity) on the marine ecosystems and shellfish farms. Image credit: Infographic designed by Revell Design, commissioned by the Cawthron Institute for the Greenshell Mussel (GSM) adaptation planning pathways workshop 2023. Reproduced with permission from the authors: James Butler and Jess Ericson.

1.1.2. Marine heatwaves

Marine heatwaves (MHW) are a result of various atmospheric and oceanic processes at both spatial and temporal scales (Hobday et al., 2016; Salinger et al., 2019). These processes include the El Niño Southern Oscillation, and therefore the El Niño and La Niña cycles, as well as localised heat fluxes (Heidemann and Ribbe, 2019; Salinger et al., 2019). Concurrent to atmospheric definitions of heatwaves, according to Perkins and Alexander (2013), Hobday et al. (2016) determined that MHWs should be defined based on day-specific (e.g. 3-5 consecutive days) and 90th percentile temperature criteria (Fig. 1.2.).

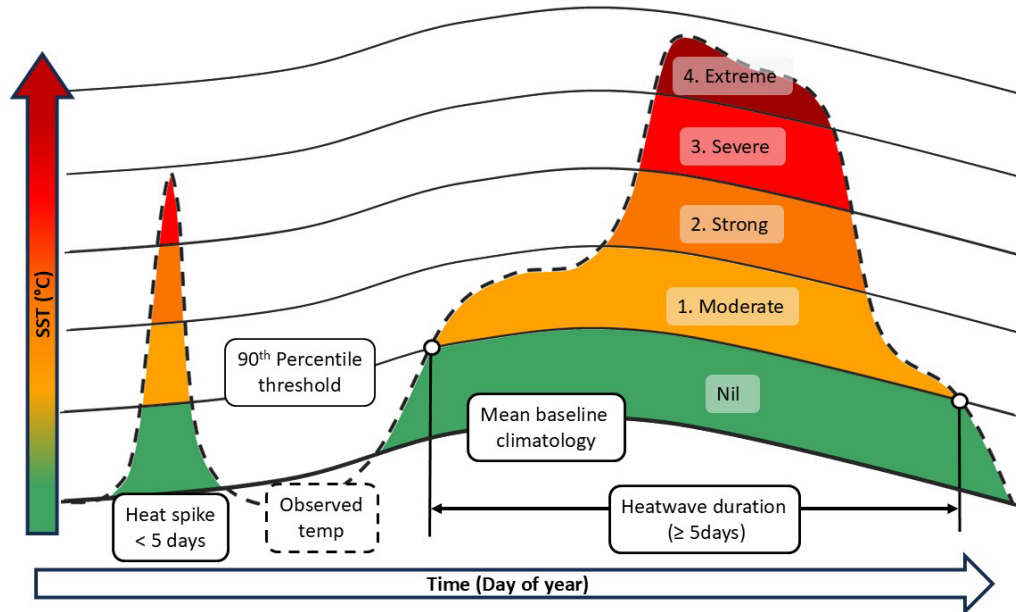


Figure 1.2 Generalised depiction of the marine heatwave model indicating categories and standardised thresholds that determine the difference between a heat spike (left) and a heatwave (right) with increasing sea surface temperature (°C). The contours represent typical climatological temperature. Image adapted from Hobday et al. (2016).

This definition allows for detection of heatwave events throughout the year and therefore includes both winter and summer periods (Hobday et al., 2016). Hobday et al. (2016) suggested that the criteria to define a MHW includes at least 5 consecutive days above the 90th percentile temperature range of the baseline climatology, and anything shorter is defined as a heat-spike (Fig. 1.2.). These MHW events, both summer and winter, pose a high risk to ecosystems and the organisms within them (Smale et al., 2019; Venegas et al., 2023). However, with the elevation of temperature and increased frequency of MHWs there has also been an increased frequency of extreme storm events and floods. Storm events and flooding increase sedimentation, which can have direct and indirect consequences on the local coastal marine ecosystems (Houghton et al., 2001; Petes et al., 2007; Filgueira et al., 2016; Hobday et al., 2016; Smale et al., 2019; Venegas et al., 2023).

1.1.3. Increasing storm events and precipitation

Precipitation is also a key component of climate processes. As the climate changes and global warming progresses, the alterations to precipitation patterns are resulting in the increase in extreme

weather events. The impact of increasing precipitation events is related to their frequency, intensity, and duration (Houghton et al., 2001; Trenberth, 2011; Hartmann and Pendergrass, 2014; Hettiarachchi et al., 2018). The increase in the intensity and duration of precipitation is likely to also increase the risk of not only suspended sediment loading but also flood events in surrounding areas (Jacobs et al., 2000; Hettiarachchi et al., 2018). In typical precipitation events increased rainfall can result in "predictable seasonal flooding events" which can have positive impacts and benefits on various ecosystems, such as recharging wetlands, rejuvenating soil and creating wildlife habitats (Poff, 2002; Talbot et al., 2018). Extreme rainfall events with increased intensity and duration can result in flooding which have negative effects and can threaten the organisms and the environment they inhabit (Poff, 2002; Talbot et al., 2018; Roussel et al., 2020).

In urban regions with ill-equipped infrastructure, flood events can result in an extensive amount of damaged and cause anthropogenic contamination, e.g. sewage or industrial discharge, to enter the waterways and river systems (Euripidou and Murray, 2004; Booij, 2005; Talbot et al., 2018). In addition, land use changes related to agriculture and forestry are also resulting in increasing runoff which is impacting the coastal system (e.g., Doney et al., 2012a; Swales et al., 2021; Hawks et al., 2022). The flood water and runoff enter the marine (coastal) system increasing sediment loading and reducing the salinity of the seawater (e.g., Doney et al., 2012a; Swales et al., 2021; Hawks et al., 2022; Rothig et al., 2023). Sediment deposition can result in the rapid deterioration of fitness of a species in coastal habitats by; 1) smothering, which reduces, for example, light, and oxygen; 2) perturbation of feeding; 3) abrasion, which can impact the soft tissues of organisms, or; 4) physical alterations, which can result in the loss of settlement substrata (e.g., Gibson and Atkinson, 2003; Milliman and Mei-e, 2021). Along with sedimentation and warming, salinity reduction from flood waters and runoff also has the capacity to alter the behaviour, osmotic stress, and net survival of various marine organisms (e.g., Rothig et al., 2023).

1.1.4. Impact of global warming on marine ecosystems

Coastal marine ecosystems, from rocky reefs to mangrove forests, provide critical natural services including nursery grounds, water filtration, as well as supporting fisheries and aquaculture (e.g., Burge et al., 2014). However, anthropogenic climate change is impacting the oceans and the organisms inhabiting these ecosystems. The changing climate is influencing the oceans globally. The associated decline in biodiversity of marine organisms is well reported (e.g., Salinger et al., 2020b; Behrens et al., 2022; Santana-Falcón and Séférian, 2022; Venegas et al., 2023). For many of these species their biological response and projections of future vulnerability to changing climate are largely neglected. However, what is known is that one of the consequences is the contraction, or expansion, of the suitability of marine habitats of certain species. In addition, species that are adaptable will take advantage and those that are susceptible, such as narrow-range (stenothermal) ectotherms are likely to face extinction (Doney et al., 2012a; Venegas et al., 2023). The role of climate change on the marine environment has been clearly demonstrated over the past decade through climate modelling (Houghton et al., 2001; Petes et al., 2007; Filgueira et al., 2016; Smale et

al., 2019; Venegas et al., 2023). Impacts predicted by climate models have predicted a 15-37% loss of species by the year 2050 (Thomas et al., 2004; Mooney et al., 2009). Future research on species responses to various climate and environmental stressors, both short-term and long-term, is crucial for providing information on outcomes and consequences to inform management decisions (Froehlich et al., 2022). Ongoing and increasing excursions outside of the optimal performance range is likely to lead to various biological consequences and changes in geographic distributions for many species (e.g., Sunday et al., 2015).

1.2. Marine organisms in a changing world

1.2.1. Physiological tolerance and stress

The natural environment plays a fundamental role in the development and survival of any given species (Gunderson et al., 2016). Environmental (abiotic) conditions fluctuate naturally through time in all environments, including seasonal variations. In addition, there are also biotic conditions, such as reproduction cycles and pathogen occurrence (discussed in sections 1.2.3 and 1.3.1) that are energy-demanding and can influence stress responses. This is due to homeostasis requiring energy demanding processes and maintaining it therefore exacts a cost (Webb, 1999). Occasionally, natural environmental conditions will pass homeostasis-coping thresholds, inducing physiological and cellular stress in an organism. Physiological stress tolerance requires a fine balance between cellular response, cell integrity and homeostatic conditions (Trump et al., 1997; Manduzio et al., 2005; Fulda et al., 2010; Carella, 2015). The fine balance is a result of the equilibrium of net cell growth versus net cell death. Exposure to cell stress past a certain threshold, beyond which restoration of homeostasis is no longer possible, induces a cascade of cell death pathways (e.g., Fulda et al., 2010).

The definitions of stress, stressor and challenges are mostly dependent on the perspective of the discipline and the biological level (e.g., physiology or ecology and organisms or population, respectively). Stress is typically the change in an organism, population, or ecosystem where fitness declines and the changes become deleterious. Stress in theory could also be a cause that moves the organism along the tolerance/ intolerance continuum in response to intrinsic or extrinsic processes (Webb, 1999). Through this thesis stress is the physiological response, or deleterious consequence, of exposure to a 'stressor' (causal variable) (e.g., Koolhaas et al., 2011; Esposito et al., 2022). Greater knowledge of responses and adaptive capability is required to understand the ability of marine invertebrates to survive stressors associated with warming conditions because of climate change (Solan and Whiteley, 2016).

Marine environmental stressors such as increasing temperature, turbidity, decreasing salinity and pH, are common and heterogeneous with no environment being stress free (Webb, 1999; Di Lorenzo and Mantua, 2016; Carrier-Belleau et al., 2021). Temperature, for example, is a crucial environmental factor and one of the strongest drivers for processes such as growth, metabolic rate, reproduction, immune response, and survival (Portner, 2002; Angilletta Jr and Angilletta, 2009; Filgueira et al., 2016; Dunphy et al., 2018). The thermal tolerance, or optimal functioning range, of an organism is

the range in which fitness (physiological performance) is maximised, and an organism experiences the least amount of stress (Fig. 1.3.) (Portner, 2002). The thresholds of the optimum range are typically where the aerobic metabolism of an organism is disrupted and it can no longer maintain energetic homeostasis (Portner and Farrell, 2008; Kooijman and Kooijman, 2010; Delorme, 2017; Booth, 2018; Steeves et al., 2018). Furthermore, at the optimum range, ATP production from aerobic metabolism is high and energy remains after basal maintenance, both cellular (e.g. protein turnover), and organismal (e.g. respiration and circulation). The surplus energy from aerobic metabolism allows for energy investment into growth, reproduction and storage to buffer future conditions (i.e. seasonal patterns in food levels) (Portner and Farrell, 2008; Kooijman and Kooijman, 2010; Sokolova et al., 2012; Delorme, 2017; Booth, 2018; Steeves et al., 2018). The stress range (termed *pejus*) is where aerobic scope is lower because of the maintenance costs being higher. Maintenance typically is the priority, when compared to growth and reproduction, due to the increase in energy demand relating to stress protection and repair of damaged cells. Growth and reproduction are typically reduced and can cease if there is no available energy after maintenance. Following stress there is a critical range (*pessimum*) where energy availability (aerobic scope) is critically low and aerobic metabolism is impaired, anaerobic metabolism is usually engaged to cover basal maintenance. Finally, the lethal range follows the critical range where survival is at stake (Portner and Farrell, 2008; Kooijman and Kooijman, 2010; Delorme, 2017; Booth, 2018; Steeves et al., 2018) (Fig. 1.3.).

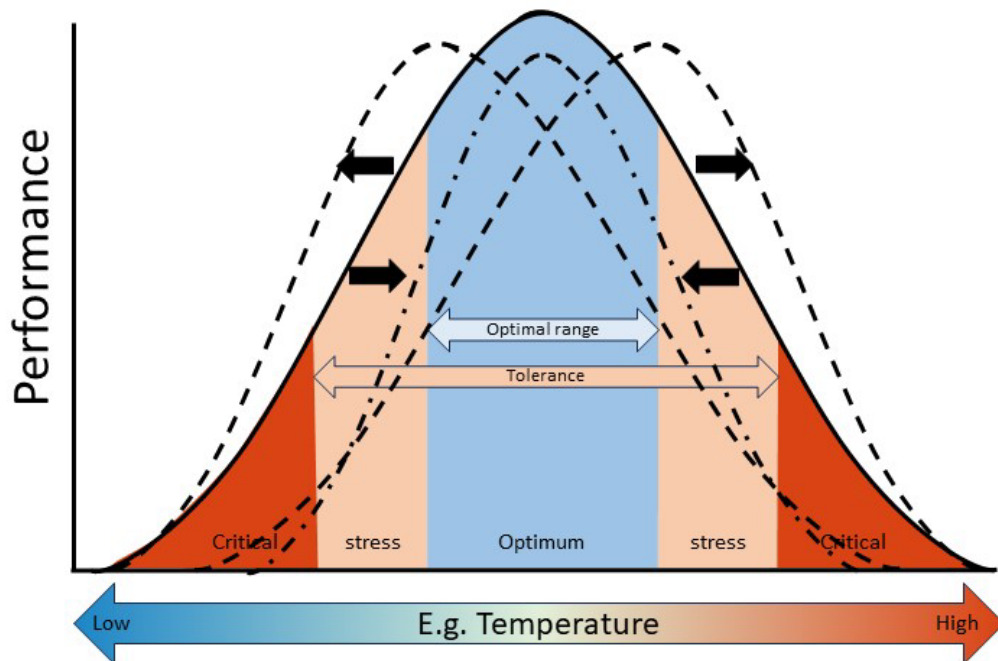


Figure 1.3 Generalised image of Shelford's law of tolerance and adapted from the thermal tolerance range model from Portner and Farrell (2008) and Sokolova et al. (2012). The solid line indicates a single stressor scenario using temperature as an example. The dashed lines and arrows indicate hypothetical deviations away from the typical single factor bell curve range. For example, skewed to the left, or right, could be the bell curve for salinity overlapping the curve for temperature, or adaptation to a chronic stressor and shifting thresholds. The dashed and dotted line is an example of

the influence of multi-stressor and/or moderate to extreme intensity exposure to a stressor. The optimal band may then become narrower and therefore there is a higher chance of crossing into the stressed category. The optimum is range of maximum physiological fitness and beyond the critical section is the lethal range.

Models such as the tolerance range above (Fig. 1.3.) typically only incorporate a single factor for simplicity. However, the tolerance range model is not fixed and can be influenced by both abiotic and biotic factors and their interactions (Sokolova et al., 2012). This complexity of the models also increases with host pathogen interactions. The optimum range can also shift, or expand and contract, for a variety of reasons including organism adaptation, acclimation, season, life stage and size (Sokolova et al., 2012) (Fig. 1.3.). Although these models are complex and typically there is not a “single best” model for understanding the energy status derived from the tolerance range and additive models can provide insights into the complex, multifactorial and interactive relationships between stressors (Sokolova et al., 2012).

The multifarious interactive relationship of stressors can also phase in and out temporally (Sokolova et al., 2012; Todgham and Stillman, 2013; Gunderson et al., 2016). The temporal pattern can lead to what is known as additive, synergistic and/ or antagonistic interactions which further affect physiological fitness (Todgham and Stillman, 2013; Gunderson et al., 2016). The terms synergistic and antagonistic are frequently used to describe the combined effects of multiple stressors. Synergistic is more than the sum of the effects of the additive individual stressors while antagonistic is less than the sum (Hay, 1996; Folt et al., 1999; Webb, 1999). In terms of physiological performance, if stressors are additive, the impact on the physiology is likely to be smaller compared to synergistic models, particularly when there is a temporal difference in exposure to each stressor (Todgham and Stillman, 2013; Gunderson et al., 2016) (Fig. 1.4.). For example, organisms that already have suboptimal fitness because of an abiotic stressor (e.g., stressor 1) suffer more from biotic stressors (e.g., stressor 2), which indicates a synergistic interaction (Temporal pattern 3 and 4) (Gunderson et al., 2016) (Fig. 1.4.). How organisms respond to stressors, particularly those in relation to changing climate is dependent on the timing, intensity, and duration of exposure, which can vary widely (Gunderson et al., 2016; Carrier-Belleau et al., 2021). Identifying these interactions is critical to informing management decisions regarding the local ecological system (Gunderson et al., 2016; Carrier-Belleau et al., 2021).

In terms of the changing climate, marine organisms are already inhabiting areas which are increasingly impacted (Todgham and Stillman, 2013; Venegas et al., 2023). The decline in aerobic scope in relation to thermal tolerance for marine ectotherms is well reported (e.g., Portner and Farrell, 2008; Sokolova et al., 2012; Delorme, 2017). Furthermore, there are likely to be species ‘winners and losers’ depending on their capability to reproduce and survive. The losers are those species that have a lower thermal tolerance whereby reproduction, habitat range and survival are disproportionately affected by rising temperatures (Doney et al., 2012a; Venegas et al., 2023).

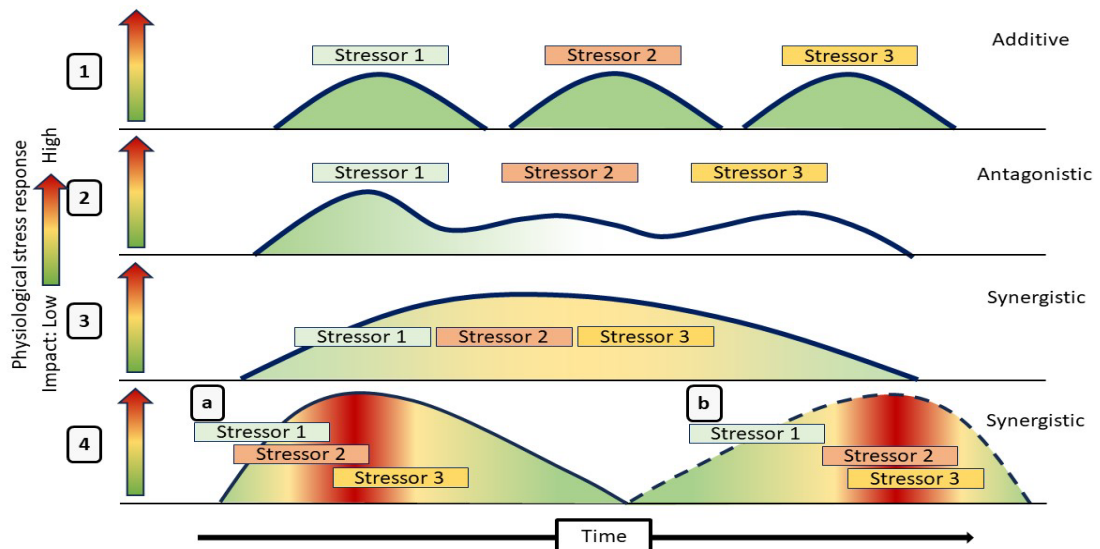


Figure 1.4 Generalised depiction of the multi-stressor model derived and adapted from Gunderson et al. (2016) predicting physiological stress responses from 3 potential stressors. The numbers (1-4) represent the hypothetical temporal pattern with the expected consequence (Gunderson et al., 2016). Pattern 4 has been further adapted to include an additional hypothetical option depending on: a) 2 initial stressors prior to a third or b) a first initial stressor followed by 2 co-occurring in a similar time frame. Examples of stressors could include Stressor 1: thermal stress, Stressor 2: Reproductive maturation, Stressor 3: pathogen invasion/occurrence.

If reproduction and survival are dependent on a narrow range of temperatures then these are the species where abundance and spatial distribution decline, and therefore risk extinction (Venegas et al., 2023). Additional stressors are likely to further impact the survival of various species across different life stages and alter invasive species interactions (Todgham and Stillman, 2013; Malagoli et al., 2023). Benthic marine species such as molluscs often have limited ability to move and avoid stressful environments. They are exposed to direct and indirect stressors in their natural ecosystem and are therefore considered ‘logical’ models to assess stressor effects (Borja et al., 2000; Carrier-Belleau et al., 2021).

1.2.2. Molluscs: Gastropods and bivalves

The Phylum Mollusca contains almost 80,000 species (Eckelbarger and Hodgson, 2021; Esposito et al., 2022), of which approximately 90% of these are benthic (Pandian, 2018). Among the four main classes (of seven recognised) the most species rich are the Gastropoda and Bivalvia (Gosling, 2008; Eckelbarger and Hodgson, 2021; Esposito et al., 2022). The majority of both phyla are marine (Pandian, 2018). Most molluscs consist of a soft body protected with a hard shell. For marine molluscs, the shells are typically calcareous and aragonitic in nature (Pandian, 2018; Eckelbarger and Hodgson, 2021; Esposito et al., 2022). The soft body of molluscs in generalised terms consists of a foot, visceral mass, gills, and mantle. The foot is used for locomotion and is typically reduced or absent in sedentary species. The visceral mass contains the organs such as the stomach, digestive glands, kidney, and heart. The mantle consists of tissue with a specialised epithelium for shell growth

and, in bivalves, the mantle can function as reproductive tissue (gonad). Lastly, the mantle cavity provides spaces for the gills for respiration (Gosling, 2008).

In marine gastropods the shell is typically reduced and consists of a single, asymmetric spiral. The foot is prominent and used for locomotion. A buccal mass which contains a radula with chitinous teeth which they can use to triturate food, e.g. macro algae (Barnes, 1987; Healy, 2001). In bivalves the foot is reduced, and the shells are typically bilaterally symmetrical, they have a hinge which encases the soft tissues (Barnes, 1987; Healy, 2001). Rather than requiring a buccal mass, bivalves feed using ctenidial filtration with support from siphons and palps. Typically, bivalves will feed on microalgae and diatoms. Digestion of food for both classes is similar (Barnes, 1987; Healy, 2001). The food is drawn into the stomach by a mucous and crystalline style ribbon from the style sac. Extracellular digestion is initiated in the stomach, for gastropods this occurs in the crop as well, then intracellular digestion takes place in the digestive glands. Excretion occurs in the kidney, or kidneys for gastropods, and the reproductive tissue develops near to the digestive glands (Barnes, 1987; Healy, 2001).

Most marine gastropods and bivalves are benthic and cover a wide range of habitats from rocky shores to mud and sand, and estuaries as well as tropical, temperate and polar environments. As a result of the wide distribution, individual populations can be exposed to varying conditions, including regional atmospheric differences (Barnes, 1987; Healy, 2001). Molluscs are directly and indirectly affected by abiotic factors. Marine molluscs have been reported to display wide variations in phenotypic parameters such as growth in response to various extrinsic and intrinsic drivers, including temperature, nutrition and habitat differences (Trussell, 1996; Steffani and Branch, 2003; Saunders et al., 2009a; Ren et al., 2019; Saulsbury et al., 2019). Therefore, exposure to various short-term and long-term stressors outside the molluscs' optimum tolerance range will ultimately impact them and traits, such as survival, growth, and reproduction (e.g. Petes et al., 2007; Delorme et al., 2021b). In addition, long-term environmental impacts are expected to be more detrimental and lead to impacts in reproductive timing and effort and therefore a decline in recruitment to the next generation (Philippart et al., 2003; Filgueira et al., 2016; Steeves et al., 2018).

1.2.3. Gastropod and bivalve reproduction

Marine gastropods and bivalves are typically gonochoric (dioecious) with fertilisation generally occurring in the surrounding water (Pandian, 2018). Hermaphroditic individuals are occasionally observed in gonochoric species (Pandian, 2018). For gastropods, the gonad develops as a single organ surrounding the digestive gland, with gametes being discharged through a gonoduct. For bivalves, the gonad is typically paired and diffuse across the mantle lobe developing a complex network of follicles (Seed, 1969; Eckelbarger and Hodgson, 2021). In both classes, the reproductive cycle is generally considered as the activation of gametogenesis in the gonad and spawning through to gonad regression. The reproductive process also tends to be seasonal (Bayne et al., 1982; Bignell et al., 2008), and strongly correlated to nutrient storage, as well as environmental factors including

temperature and food availability (Gabbot, 1975; Bayne, 1976; Pérez et al., 2013). The storage of the energy substrates for aerobic metabolism is considered to be dependent on reproductive development (Benomar et al., 2010), with many types of somatic cells storing nutrients destined for gamete development. Energy is stored in these somatic cells as glycogen, lipids and proteins that can then be mobilised by the follicle cells for reproductive activities (Benomar et al., 2010; Hassan et al., 2018; Eckelbarger and Hodgson, 2021).

The success of any organism, i.e. the continuation of the lineage, will ultimately depend on the surplus metabolic energy and the available nutrients for successful gamete development and fertilisation (Eckelbarger and Hodgson, 2021). The nutritional support for gamete development is primarily provided by the ovary or follicle cells, from the energy stored in the 'vesicular connective tissue (VCT)' and in some species specialised 'adipogranular (ADG) tissue', 'adipose' or 'Leydig' (glycogen laden) cells (Andrews, 1974; Pipe, 1987; Eckelbarger and Hodgson, 2021). The variety and range of these cells as well as energetic strategy has been considered as a mechanism to ensure that the required nutrients are available for gametogenesis (Eckelbarger and Hodgson, 2021).

Glycogen is an essential component in supplying energy and metabolites for gametogenesis in molluscs (e.g. Gabbot, 1975; Bayne et al., 1982; Brokordt et al., 2019). It is the main carbohydrate and is typically stored in large amounts in VCT during the growing season, before reproduction (Eckelbarger and Hodgson, 2021). It is representative of the overall nutritional condition of the organism (Uzaki et al., 2003; Ke and Li, 2013). Investigations of glycogen storage and mobilization for reproduction in bivalves have largely focussed on the blue mussel (*M. edulis*) with other species being neglected (Brokordt et al., 2019).

Lipids have a higher caloric content and represent an important energy reserve (Ke and Li, 2013). Females are likely to have higher concentrations of lipids (e.g., triacylglycerols) due to the accumulation of reserves required for oocyte development (Darriba et al., 2005; Ke and Li, 2013). Proteins, on the other hand, are considered as major structural material for the mantle and gonad during development. Proteins have also been hypothesised as a potential source of reserve energy supporting the end of gametogenesis (Berthelin et al., 2000; Gabbott and Bayne, 2009; Ke and Li, 2013). Both protein and lipids have been shown to be good indicators for oocyte quality and therefore larval viability (Massapina et al., 1999; Le Pennec et al., 2001; Fukazawa et al., 2005; Ke and Li, 2013).

Several investigations have examined the biochemical properties of different tissues in marine bivalves during gametogenesis and have shown variation in energy sources. For example, for blue mussels (*Mytilus edulis*) oocytes accumulate glucids from specialised tissue, conversely proteins from the adductor muscle are sequestered in scallop (*Pecten maximus*) oogenesis (de Zwaan and Zandee, 1972; Galap et al., 1997; Hasani et al., 2023).

As a result of the high energy requirements for gametogenesis, different energy metabolism strategies can be employed. Two strategies have been considered according to Bayne (1976), these are opportunistic or conservative (Hassan et al., 2018). Opportunistic are those that obtain and store energy prior to gametogenesis, and conservative relies on feeding during gametogenesis. Most molluscan species, particularly those in temperate regions, are thought to employ the conservative strategy (e.g. Karray et al., 2015; Hassan et al., 2018). The strategy and the amount of energy stored, and allocated, to reproduction determines the overall reproductive pattern (Galap et al., 1997; Gabbott and Bayne, 2009; Vitt and Caldwell, 2014).

1.2.4. Gametogenesis: spermatogonia and oogonia

Gametogenesis (spermatogenesis and oogenesis) is the cell division and differentiation process germ cells (gametocytes) undergo in order to form gametes (Hassan et al., 2018). Spermatogonia and oogonia bud off the follicular epithelium (wall). Both sexes are indistinguishable in the very early stages of development (Seed, 1969). In general, both spermatogonia and oogonia undergo meiosis to produce the spermatocytes and primary oocytes followed by a second division. Spermatocytes will divide and develop into spermatids and then mature spermatozoa. While the early secondary oocytes remain attached to the wall by a stalk which reduces in size until yolk develops and the oocytes start to mature (Seed, 1969; Costa, 2018a; Eckelbarger and Hodgson, 2021). Once the oocyte has matured it will detach from the follicle wall. A jelly coat also develops on gastropod oocytes which is not present in bivalves (Eckelbarger and Hodgson, 2021) (Fig. 1.5.).

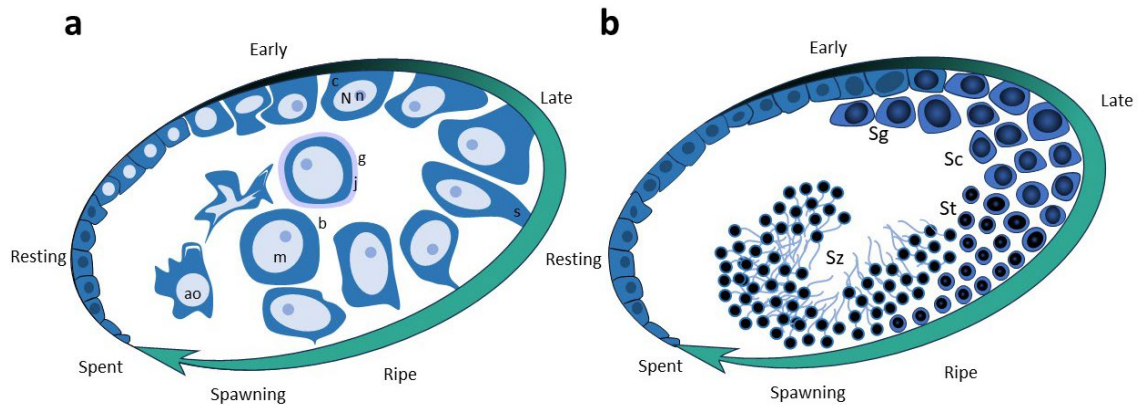


Figure 1.5 Simplified oogenesis and spermatogenesis cycle for gastropods and bivalves within the gonad tissue adapted from Galtsoff (1964) and Costa (2018a). **a)** female with developing oocytes. Undifferentiated (resting) cells develop into early oocytes attached to follicle wall with a clear cytoplasm (c), nucleus (N) and nucleolus (n). As the oocytes develop the attached section becomes stalk-like (s), the stalk thins as the oocyte grows and matures. Once ripe and mature (m) the oocyte detaches from wall and starts to round up. The jelly coat (j) is a common feature in gastropod (g) oocytes; it is not present in bivalves (b). The gonad will empty during spawning and residual oocytes will typically become atresic (ao) and be cleared by phagocytosis or reabsorbed (see below). Atresic oocytes are characterised by their jigsaw-like shape, detachment of cytoplasm from the cell wall, unusual staining breakdown of the cell membrane. **b)** developing male where undifferentiated cells develop into spermatogonia and further in sequence into spermatocytes (Sc), spermatids (St) and mature spermatozoa (Sz). Residual sperm after spawning will also be cleared by phagocytosis.

Several assessment techniques have been devised because of the impact of reproduction on various aspects of the organism and the population. Simple techniques include dry tissue weights, condition indices, oocyte size and more complex techniques including histological examination. Histological quantification of the gametogenesis cycle has resulted in the development of various staging criteria and appears to be the most common technique applied (Seed, 1969; Kennedy, 1977; Alfaro et al., 2001; Buchanan, 2001; Vélez-Arellano et al., 2015; Shin et al., 2020). Criteria are typically split into 5 or more stages for bivalves, depending on species. The general descriptions are 1) Resting; 2) Early; 3) late; 4) Ripe; 5) Spawning; and 6) Spent (e.g., Seed, 1969; Kennedy, 1977; Alfaro et al., 2001; Buchanan, 2001; Vélez-Arellano et al., 2015; Shin et al., 2020). Complexity and number of stages devised depends on the species (Costa, 2018a), as well as the interpretation of the researcher. Although these methods can be highly subjective and result in semi-quantitative models, they are still useful, particularly with the ongoing development of image analysis techniques (e.g. Beninger, 1987; Thompson et al., 2014).

These techniques are key to quantifying the response of reproductive tissue to an extrinsic stressor. For instance, environmental temperature can positively or negatively influence reproductive cues. Timing of reproduction can be modulated and induced by altering the temperature. Negative temperature effects in the marine environment can include detrimental effects such as asynchronicity of spawning, reduced fertilisation and a decline in recruitment success (Philippart et al., 2003; Petes et al., 2007). Furthermore, one response to increased stress may be the release of gametes to the water column and this in turn leads to reduced larval survivorship or no fertilisation at all due to detrimental water conditions for the early life stages (Philippart et al., 2003). The reproductive cycle can also be inhibited by environmental stressors, particularly those that are near sublethal and fall into the stress or critical tolerance range. This is due to the reallocation of energy from gamete production to defence and repair mechanisms (e.g. Michalek-Wagner and Willis, 2001; Petes et al., 2007). Conversely, rather than release through premature spawning, the gametes could be sacrificed through the process of atresia and therefore reabsorbed.

1.2.5. Oocyte atresia

Most bivalves cannot spawn all their oocytes on completion of the reproductive period. Gametes (oocytes) that remain post-spawning are termed ‘residual’ or ‘relict,’ which degenerate and are resorbed in the gonad by macrophages or recycled by follicle cells (Le Pennec et al., 1991; Beninger and Le Pennec, 2016; Eckelbarger and Hodgson, 2021). The term ‘atresia’ was taken from vertebrate studies, meaning follicular degradation. It is a term that is progressively emerging to designate oocyte degradation and the autolysis of normal oocytes. The process of destruction and resorption is common and considered a normal process post-spawning under optimal conditions (Beninger and Le Pennec, 2016). The same process prior to spawning and during development, typically termed ‘pre-spawning atresia,’ in relation to increasing stressors is of particular interest to the research field (Beninger and Le Pennec, 2016). Atresia in molluscs (e.g. bivalves) has only rarely been mentioned

in the literature until recently (Beninger and Le Pennec, 2016). It has been characterised by histological and cytological changes and can appear to have a range of abnormal formations in the oocyte (i.e. lobular, irregular shape, shrunken, pronounced staining, granular cytoplasm or cytoplasmic retraction followed by lysing of the membrane (Beninger, 2017; Chérel and Beninger, 2017).

Three types of processes causing atresia to have been proposed; 1. 'Residual' whereby remaining oocytes post-spawning degenerate; 2. 'Ecological' whereby the atresia during development is a response to unfavourable conditions; and 3. 'Physiological' whereby regulatory mechanisms govern the number of oocytes developing (Motavkine and Varaksine, 1983 cited in; Beninger, 2017). Recognition and quantification of atresia is essential for the proper interpretation of reproductive processes. Failure to identify and incorporate atresia will ultimately lead to biased estimates of fecundity, reproductive effort and recruitment (Beninger, 2017). Extensive oocyte atresia in relation to prolonged warming has been observed already in *Mytilus galloprovincialis* by (Marigomez et al., 2017). The prolonged warming was also noted to impair reproduction. Gonad resorption may provide an additional energy source to cope with the extra metabolic demand resulting from environmental stressors (Fearman and Moltschaniwskyj, 2010; Marigomez et al., 2017). Therefore, detailed knowledge of the species-specific reproductive biology, gametogenesis, atresia and pathogen presence is key to the management of mollusc populations in a changing environment (Beninger, 2017).

1.3. Influence of pathogens

1.3.1. A complex interactome inducing disease.

The environment contains a wide range of pathogens (causative harmful agents, e.g., Burge et al. (2014)) and parasites including viruses, bacteria, fungi, protozoa and metazoa, which may cause diseases and stimulate the immune system. Disease, in this case, is the result of cell injury and is indicative of an "endpoint" when adaptive response fails to accommodate the stress (biological, physical or chemical) (Carella, 2015). Traditionally, disease has been considered as a 'one pathogen / one disease' system and associated to one host, one pathogen, one environment and therefore one disease (Burge et al., 2014; Guo et al., 2015; Guo and Ford, 2016b) (Fig. 1.6). This relationship is highly vulnerable to environmental changes, with disease outbreaks ensuing (Burge et al., 2014). Recently, there has been a move towards a more holistic, realistic, and ecological view of a complex interactome. The interactome model incorporates a suite of abiotic and biotic factors that interact and participate in the disease process and is potentially a more predictive approach (Koch, 2018; King et al., 2019).

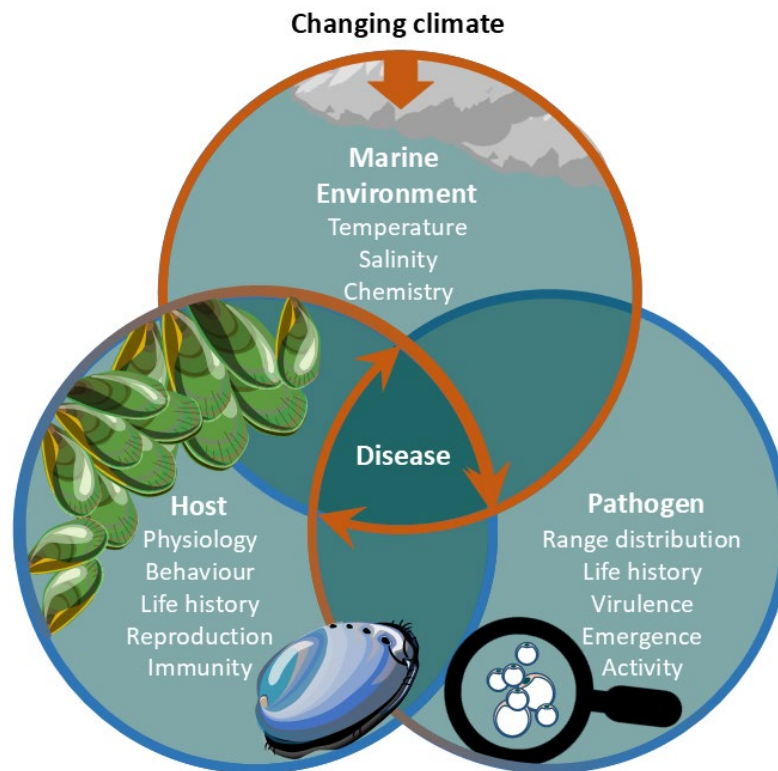


Figure 1.6 The three key factors influencing disease outbreaks: the changing environment, the host condition, and the associated pathogens (based on Burge et al. (2014)). The arrow into the marine environment section indicates added stressors from a changing climate which exacerbates conditions.

Infectious diseases (caused by transmissible agents) are considered as important drivers in an ecosystem and can influence trophic interactions, community and biotic structures, and host distribution (Burge et al., 2014). It is well established that diseases have seasonal and geographical ranges, but how climate change may alter these distributions, and the host-pathogen interaction remains relatively under studied (Harvell et al., 2002; de La Rocque et al., 2008; Burge et al., 2014). As previously mentioned, temperature is often a major trigger influencing both host and pathogen, impacting growth, reproduction, and health of molluscs, as well as being linked to changes in disease expression studied (e.g., Harvell et al., 2002; Bignell et al., 2008; de La Rocque et al., 2008; Burge et al., 2014). However, it also isn't the only stressor that can influence pathogen resistance, virulence, and pathogenicity (Burge et al., 2014).

The influence of diseases is well known in molluscs of economic value worldwide (Burge et al., 2014; Guo and Ford, 2016b; Lynch et al., 2022). Infectious diseases in commercially harvested molluscs such as oysters, mussels and abalone can devastate wild populations and primary industries (Fisheries and aquaculture) (Burge et al., 2014; Guo and Ford, 2016b). Molluscs are vulnerable to a range of viruses, bacteria, haplosporidians, microsporidians and microparasites (Lynch et al., 2022). For example, parasitic aetiological agents (parasitic disease) such as *Steinhausia mytilovum* and bucephalids are known to inhibit gonad maturation and *Marteilia* sp. and haplosporidians displace digestive epithelium (Bignell et al., 2008). Furthermore, MSX and dermo disease (Villalba et al., 2004) and caused by pathogens and initially detected in affected commercially grown oysters. The

causative agent for MSX is the parasite *Haplosporidium nelsoni* and for dermo it is *Perkinsus marinus*. Both of which can cause mortality and in both the prevalence and intensity is influenced by changing temperature and salinity (Burge et al., 2014).

Conversely, increasing temperature can also be beneficial for an organism and used as a management tool to increase survival rates. This is seen in *Crassostrea gigas* (Recently named as: *Magallana gigas*) where mortality outbreaks are often associated with the *Ostreid herpesvirus* (OsHV-1). Delisle et al. (2018) observed that by increasing the temperature to 29 °C in *C. gigas*, susceptibility to the virus declined. This is because temperature must favour the replication stage of the pathogen to elicit development and disease (Chu et al., 2003; Carella, 2015). Disease, as a result of pathogen emergence, remains relatively under-studied (Froehlich et al., 2022). Therefore, knowledge regarding both the host and the pathogen's response to a stressor can be crucial for disease management. However, research and investment has gone into selective breeding programmes, vaccination programmes and therapeutants for disease resistance (Naylor et al., 2021), in response to mortality events.

1.3.2. Marine mortality events

Marine heatwaves and associated pathogen-related mortality events have been affecting several molluscan species worldwide (Harvell et al., 2002; Smale et al., 2019). Summer mortalities are a consequence of the complex interaction of environment-host-pathogen relationships and are typically associated with summer marine heatwaves. Mortalities during the summer season can arise from factors correlated with elevated temperature, including low dissolved oxygen levels, greater host oxygen demand, depressed immunity, reproductive state and pathogen presence (e.g., bacteria), which lead to disease and eventual mortality (Gagnaire et al., 2007; Rahman et al., 2019). Summer mortalities have impacted several molluscan populations and aquaculture industries worldwide with several environmental stressors, such as elevated temperature, hyposalinity and pathogens (e.g., *Perkinsus marinus*) being identified as correlating causal factors (Harvell et al., 1999; Garrabou et al., 2009; Rubio-Portillo et al., 2016).

Responses to pathogens can vary between species, and populations within species. For example, in the early 2000s, Berthelin et al. (2000) noted that summer mortalities in oysters (*C. gigas*) coincided with high nutrient levels, higher temperatures and reproductive ripeness (e.g., Perdue et al., 1981). Increases in mortalities also coincide with infection of OsHV-1 (Petton et al., 2021). As such, further research is required to determine the effects of climate change on pathogen emergence, virulence and distribution, as well as the immune response and reproductive cycle (Froehlich et al., 2022).

1.3.3. A causative pathogen: *Perkinsus* species

Perkinsus spp. is a World Organisation for Animal Health (WOAH) notifiable protozoan parasite and, due to the impact it has on the host species, interactions have been extensively studied. There are currently seven known species of *Perkinsus* across the globe, primarily infecting bivalves. One species, *P. olseni*, is also known to infect the Haliotid gastropods (Villalba et al., 2004; Soudant et

al., 2013; Carella et al., 2018; Lane et al., 2023). *Perkinsus marinus* is known to cause disease-associated mortalities, with severity correlated to environmental conditions which also impact host physiology (Villalba et al., 2004; de Montaudouin et al., 2010; Soudant et al., 2013). Lipids are required as an energy source for development, typically acquired from the host (Soudant et al., 2013). The life cycle of *Perkinsus* consists of four life stages: trophozoites, hypnospores, zoosporangia and zoospores (Fig. 1.7.).

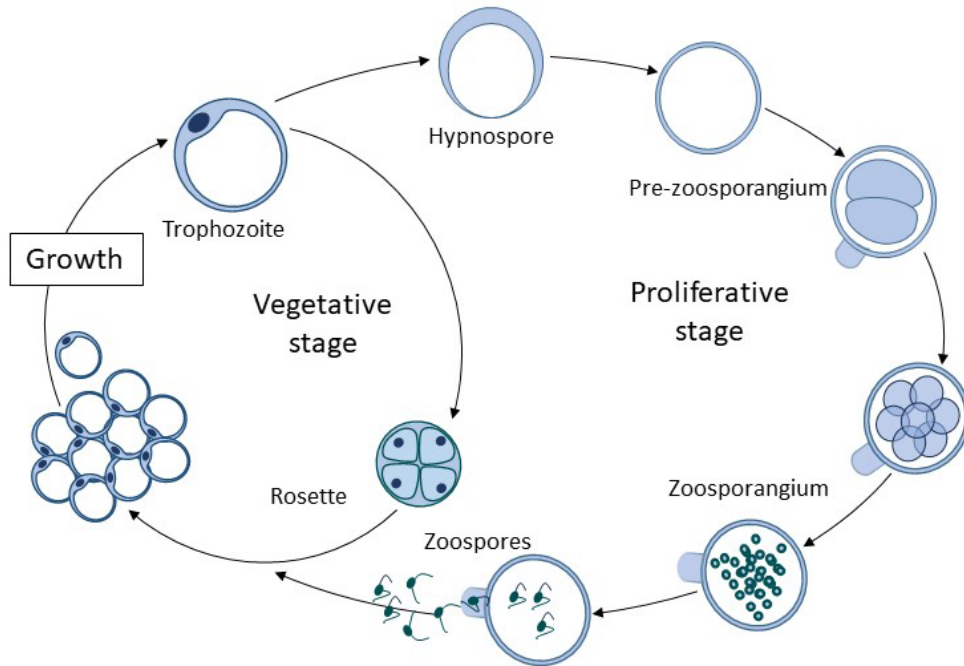


Figure 1.7 A generic *Perkinsus* spp. life cycle derived from Goggin and Lester (1995) and Soudant et al. (2013). The vegetative stage typically occurs inside the host and the proliferative stage outside the host.

Perkinsus spp. initiates a host response whereby haemocytes infiltrate the infected region. As discussed in section 1.3.4, the immune response has a humoral and cell mediated process to defend against these pathogens (Soudant et al., 2013). The ability of *Perkinsus* species to evade the host response means it can keep proliferating within the host (Soudant et al., 2013). The parasite presence can increase the immune response to the point of pustules being detectable with in, and on the surface of, the host tissue. These lesions will then burst, releasing cells into the seawater allowing transmission to the next host (Goggin and Lester, 1995; Villalba et al., 2004; Lane et al., 2023). In addition to the lesions, severe infections of *Perkinsus* can result in reduced host growth and inhibition of reproduction as energy is diverted towards immune defence. Furthermore, the fate of the host infected with *Perkinsus* spp. is regulated by host defence, host physiology and parasite virulence in addition to environmental factors such as temperature and pollutants (Villalba et al., 2004; Soudant et al., 2013; Gignoux-Wolfsohn et al., 2021).

1.3.4. Defence against a pathogen: molluscan immunity.

The first line in defence to a stressor or pathogen for any marine mollusc are the external barriers e.g., shell and mucosal layer (Rolton and Ragg, 2020). When a pathogen is detected past these

defences, the immune response and a cascade of processes is initiated to defend and repair the host tissue. Immune defence to a pathogen or disease is an energy-demanding process. Defence against a pathogen or tissue repair will, in part, be determined by the capacity of the immune response (Brokordt et al., 2019). For instance, high water temperature can influence haemocyte abundance, number, phagocytic ability, viability and membrane permeability which weakens the immune defence capability (de la Ballina et al., 2022). Molluscs have an innate immune system, rather than adaptive immunity, consisting of cell-mediated (e.g., phagocytosis) and humoral immune systems (e.g., lysosomal activity) (Brokordt et al., 2019; Rahman et al., 2019; de la Ballina et al., 2020). Molluscs also have an open circulatory system which allows haemocytes to migrate to other tissues and organs (Beninger and Le Pennec, 2016; Brokordt et al., 2019; de la Ballina et al., 2022). Additionally, no haematopoietic organ has been identified, and the process of haematopoiesis (haemocyte production) remains unclear. However, haemocytes, as the only circulating cells, play a key role in several physiological functions, including nutrient storage, tissue repair and immune responses (Rebelo Mde et al., 2013; Beninger and Le Pennec, 2016; Brokordt et al., 2019; de la Ballina et al., 2022).

The haemocytes in molluscs have been classified into two groups hyalinocytes, which are considered to be involved in wound healing, and the typically more abundant granulocytes, which are considered as key in the role of defence (e.g., Mitta et al., 2000; Soudant et al., 2013; Rahman et al., 2019; de la Ballina et al., 2020; Rolton and Ragg, 2020). In various species a variety of subpopulations of haemocytes (based on staining affinity) have also been identified, for example, blast-like cells (Rolton and Ragg, 2020; de la Ballina et al., 2022). The number and abundance of each haemocyte type is dependent on a variety of factors including species, size, maturity, food availability, season and temperature. *Perna canaliculus*, for instance, typically have a greater number of hyalinocytes (Rolton and Ragg, 2020; de la Ballina et al., 2022). The ability to counteract various environmental stressors and infections is determined by mediation of these haemocytes.

In immune defence, there are several available mechanisms including: phagocytosis, haemocytosis (including focal infiltration, granulomas and granulocytomas), and encapsulation, and programmed cell death processes such as apoptosis and autophagy (Carella, 2015; Azizan et al., 2023). Phagocytosis is considered as the key mechanism for pathogen elimination. Foreign particles such as pathogens are engulfed by the cell and broken down. This process and the build-up of phagocytic debris are also impacted by internal and external stressors (Bouallegui, 2019; Azizan et al., 2023). Although granulocytes typically have a higher capacity for phagocytosis both haemocyte types can internalise and remove foreign bodies (Gosling, 2015a; de la Ballina et al., 2022).

Haemocytosis is the infiltration and aggregation of haemocytes, focal (granulomas) and diffuse, to a region for repair or defence (e.g., Allam and Raftos, 2015; Carella, 2015; Azizan et al., 2023). There are several histotypes based on morphology including focal accumulation, development of a nodule or granuloma, a large inflammatory response (de la Ballina et al., 2022), and encapsulation responses.

Although the process of infiltrative haemocytosis, or haemocyte aggregation, can be non-specific they do indicate general immune response and tissue injury (Carella, 2015; de la Ballina et al., 2022). The nodular type occurs as a cluster with a centre of degenerating haemocytes (Carella, 2015). Haemocytes enclose the particle or pathogen and employ several extracellular abilities to destroy it (e.g., Soudant et al., 2013; Allam and Raftos, 2015; Carella, 2015; de la Ballina et al., 2022; Azizan et al., 2023). Encapsulation occurs if particles are too large for phagocytosis, by creating a capsule around the parasite (trophozoite) whereby recruited haemocytes secrete polypeptides (Carella, 2015). Lysosomal enzyme production is enlisted to assist in containment and destruction (Montes et al., 1997; Carella, 2015). For parasites such as *Perkinsus* spp. phagocytosis and encapsulation are commonly observed processes (Chagot et al., 1987; Villalba et al., 2004; Carella, 2015).

Following immune response and injury from disease haemocytes undergo regressive changes and programmed cell death. Apoptosis, autophagy, and necrosis are three types of cell death processes, the latter being accidental in nature (Kroemer et al., 2009; Carella, 2015). Apoptosis is the most basic and fundamental process in the homeostasis of the immune system. It is typically characterised by cell wrinkling, chromatin condensation, membrane blebbing and lesions on cell membrane termed apoptotic bodies (Sokolova, 2009; Carella, 2015). In contrast to apoptosis, autophagy occurs without condensation of the chromatin and appears as cytoplasm vacuolisation (Kroemer et al., 2009; Carella, 2015). Autophagy is an intracellular process that is employed as a second layer of defence to eliminate damaged or redundant cellular structures. It is crucial to maintain homeostasis and has been shown to be important for mobilising stored nutrients and defence against oxidative damage (Balbi et al., 2018; Kalachev and Yurchenko, 2019). Furthermore, although critical to tissue maintenance when the normal processes of autophagy are compromised autophagic cell death will be triggered (Moore et al., 2006b; Carella, 2015). Finally, necrosis, which is considered as “accidental” cell death is characterised by the swelling of cells and rupturing of the cell membrane (Carella, 2015). Typically, the damage to the cell membrane results in the release of other inflammatory molecules resulting in haemocyte infiltration and inflammation (Golstein and Kroemer, 2007; Carella, 2015).

1.4. Ecological context

1.4.1. New Zealand climate.

Due to its biogeographic isolation, wide temperature range and coastal diversity, New Zealand is an ideal location to understand the impacts of climate change (Costello et al., 2010; Montie et al., 2023). As a result of global warming, marine heatwave days in NZ are predicted to increase a further 0.3 to 0.9 days per year (Salinger et al., 2019). Unprecedented summer heatwaves have already been detected and reported in New Zealand in 2017/2018 (Salinger et al., 2019) and 2022 (Bell et al., 2023). Sea surface temperatures (SSTs) during the austral summers reached 3-4 °C above climatological averages. These extreme temperatures have significant effects on marine biology and fisheries (Reid et al., 2015). Heatwaves have been attributed to a reduction in habitat-forming seaweeds and shifts in community structure (Wernberg et al., 2013), as well as mass mortalities. For

example, in the NZ heatwave of 2017/2018 Thomsen et al. (2019) observed a localised loss in the bull kelp (*Durvillea* sp.) canopy in relation to both temperature stress and disease. The loss in bull kelp canopy was followed by a recruitment and replacement by *Undaria pinnatifida* (Thomsen et al., 2019). These kelps are an important foundation in terms of community structure and provide ecosystem services to important species, including abalone such as *Haliotis iris* (Taylor and Schiel, 2003; Schiel et al., 2018; Thomsen et al., 2019). Additionally, in NZ there has been growing recognition of other events, including extreme storm events, resulting in increased sedimentation and reduced salinity from flooding events.

Currently worldwide there are 65 molluscan species (mostly bivalves) in aquaculture (Tacon, 2020; Naylor et al., 2021). The NZ aquaculture industry consists of three established species: the Pacific oyster (*Crassostrea gigas*) the green-lipped mussel (*Perna canaliculus*) and chinook salmon (*Oncorhynchus tshawytscha*) producing ~1805 tons, ~97462 tons, and 14180 tons p.a., respectively, totalling \$NZ673 million (Stenton-Dozey et al., 2020). Several other species have been investigated for their potential inclusion in the aquaculture industry e.g., Black-foot abalone (*Haliotis iris*, 'pāua') (Alfaro et al., 2014; Stenton-Dozey et al., 2020). Abalone, such as *H. iris*, are highly valued species for recreational and commercial fisheries (Naylor et al., 2021).

Most aquaculture systems are reliant to some extent on ambient conditions (Reid et al., 2019a). Depending on which taxa are grown (e.g., seaweed, molluscs, finfish), climate change may have positive or negative influences (Reid et al., 2019a). Warming could provide initial positive benefits, including increased growth rates, if nutrition is not limited, resulting in increased productivity. Conversely, further temperature rises may have adverse effects and negate the initial positive effects in the industry (Reid et al., 2015; Froehlich et al., 2022). The green-lipped mussel and the *H. iris* are both endemic to New Zealand and unlike the Pacific oyster, which is introduced, cannot tolerate extreme temperatures. Both species, green-lipped mussel and *H. iris*, are also ecologically and commercially significant (e.g., Jeffs et al., 1999; Alfaro et al., 2001; Venter et al., 2022). The dependence of the aquaculture industry on green-lipped mussel production has prompted the need for ongoing studies on its biology and ecophysiology (Stenton-Dozey et al., 2020). Additionally, *H. iris* research is being driven by concern of the current fishery stock numbers and the decrease in the catches associated with a lack of growth to legal size.

1.4.2. Selected species 1: *Perna canaliculus*

The green-lipped mussel, *Perna canaliculus*, (commercially Greenshell™) is endemic to New Zealand waters and is common, particularly in the central and northern regions (Jeffs et al., 1999). They are gonochoric broadcast spawners with gonadal development and gametogenesis occurring throughout the year. Most of the spawning events occur in late summer and late winter, but some individuals can shed gametes throughout the year and thereby maintain their spawning condition (Jeffs et al., 1999; Buchanan, 2001; Petes et al., 2007). Knowledge about the reproductive condition and health of green-lipped mussels is crucial for the industry. Knowing the natural patterns of the

spawning cycle allows the industry to predict the best times for broodstock collection and for harvesting. Improving knowledge around egg quality and pre-spawning atresia through histopathology analysis could provide answers to production inconsistencies, such as periodic reduction in hatchery D larvae yields (Beninger, (2017).

In terms of pathogens and parasites for green-lipped mussels, current research indicates presence of *Vibrio* spp., *Bucephalus*, *Microsporidium rapuae*, apicomplexan X, *Tergestia agnostomi*, rickettsia-like organisms and Endozoicomonas-like organisms, various copepods and ciliates, and *Perkinsus olseni* (Hine and Diggles, 2002; Suong et al., 2018; Castinel et al., 2019; Webb and Duncan, 2019; Muznebin et al., 2022a; Copedo et al., 2023). Furthermore, diseases are relatively uncommon in green-lipped mussels (Castinel et al., 2019) and as such they are considered as resilient when compared to *C. gigas*. However, *C. gigas* was also considered as resilient to disease prior to emergence of Ostreid herpesvirus type 1 (OsHV-1) in 2010 infection and mortalities ensued (Castinel et al., 2019). It is likely that with climate change and co-habitation with blue mussels and exotic *Perna* spp., the green-lipped mussel is likely to be vulnerable to new and emerging diseases in the future (Castinel et al., 2014). With the changing environment several questions arise: is spawning still predicable and how will the temperature impact health and reproduction? What is the expected susceptibility towards pathogens such as *P. olseni*? Will new pathogens take the opportunity to invade, and could there be a change in the intensity and prevalence of current pathogens? For further information and discussion regarding these questions please refer to Chapters 2, 5, 6 and 7.

1.4.3. Selected species 2: *Haliotis iris*

New Zealand's black-footed abalone, pāua, *Haliotis iris* is also an important wild fishery and aquaculture species and commonly found in rocky areas of the coastline. They are considered sedentary due to their small home range but will move if local conditions become less hospitable. In Australian abalone, shell proportions vary with habitat. Abalone with shorter, higher, and wider shells commonly occupy sheltered sites, whereas lower, broader animals are more typical in high flow environments where drag reduction could be critical for adhesion (Breen and Adkins 1982; Shepherd and Hearn 1983; McShane and Naylor 1995; Wells and Mulvay 1995; Saunders et al. 2009b). Abalone display large variations in growth phenotypes resulting in the appearance of stunted individuals with higher, shorter shells. For NZ it has been suggested that slow growth and stunting in some *H. iris* at certain sites is a response to receiving less food due to algae drift compared to high flow areas (Day and Fleming 1992; McShane and Naylor 1995, Saunders et al. 2009a).

Depletion of *H. iris* stocks was also reported in 2023 by fishers. These reports were followed by concern around the sustainability and the future impacts of changing weather patterns on the populations. Fisheries catch quotas, both commercial and recreational, have been reduced in some regions of NZ in order to support *H. iris* population growth (MPI, 2023b). Understanding not only the effects of climate change, but also the cause of slower growth/ stunting of some populations will allow for development of strategies to ensure sustainability and future survival of the species (Van

Nguyen et al., 2023). In addition to understanding the effects of climate change, identifying and recording the pathogens and parasites present as well as reproductive condition in wild stock is key for early detection of potential future threats to the population. There are several pathogens of interest in relation to *Haliotis* spp. which can cause mortalities including viruses that cause withering syndrome and ganglioneuritis, *Vibrio* spp. Haplosporidians, and *Perkinsus* spp.; these, among others, are reported in detail in Grandiosa (2019) and Handler (2022). The most common parasites and pathogens reported in NZ *H. iris* is the *Vibrio* spp., a haplosporidian-like parasite (closely related to *Urosporidium*) (Diggles et al., 2002; Reece and Stokes, 2003), and *Perkinsus olseni* (Diggles and Oliver, 2005; Muznebin et al., 2021; Handler, 2022).

1.4.4. The pathogen of focus: *Perkinsus olseni*

Perkinsus olseni is common to both *H. iris* and green-lipped mussels in NZ. However, for green-lipped mussels it is a relatively new appearance, identified in 2014 (Hine and Diggles, 2002; McDonald, 2014; Muznebin et al., 2022a; Lane et al., 2023). *Perkinsus olseni* is a WOAHP notifiable protozoan parasite (Hine and Diggles, 2002; Muznebin et al., 2022a; Lane et al., 2023). In NZ *P. olseni*, despite affecting several species, has yet to be associated with mortalities and clinical disease (Hine and Diggles, 2002; Lane et al., 2023). Appearance and development of *P. olseni* in green-lipped mussels and *H. iris* is typically associated with warmer water and has also been observed to be undergoing range extension (Lane et al., 2023). Initial observations of *P. olseni* are typically observed in routine histopathology and Ray's fluid thioglycolate medium (RFTM) culture assay. Confirmation of the pathogen is obtained through PCR and *in situ* hybridisation (Muznebin et al., 2022a; Lane et al., 2023). Unlike *H. iris*, in green-lipped mussel *P. olseni* presents differently, large trophozoites (>20µm) and haemocyte encapsulation are typically not observed (Muznebin et al., 2022a; Lane et al., 2023). *Perkinsus olseni* cells in green-lipped mussel are also smaller, very few cells aggregating and no external lesions (Muznebin et al., 2022a; Lane et al., 2023). For further introduction to *P. olseni* please refer to Chapter 7.

1.5. Techniques

1.5.1. Histopathology as a core technique

Histopathology is an essential tool for the investigation and characterisation of tissues under stress (Bignell et al., 2008; Costa, 2018b). Histology is the intermediate point between molecular changes in cells, tissues and organs and biological responses in an individual or population (Costa, 2018b). It also provides a direct opportunity to observe deviations away from normality within the tissues and provides a key component in the integrated understanding of biological status (Costa, 2018b) (Fig. 1.9.).

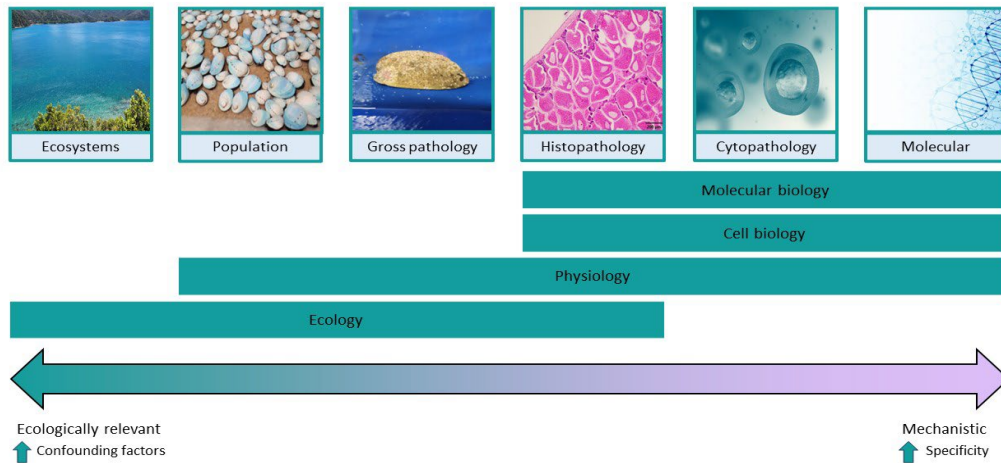


Figure 1.8 Biological levels from molecular through to ecosystem and the range, or link, that molecular biology, cell biology, physiology and ecology can extend through to at each level. Histopathology sits centrally on the continuum from ‘ecologically relevant but increased confounding factors’ through to ‘mechanistic with high specificity’. Image adapted from Costa, (2018b).

For aquatic species, histopathology is relatively new (1970s) when compared to other fields and often used as a complementary technique. However, it has seen increasing application in the aquatic fields and is a key tool in several fields, including toxicological studies and disease diagnostics (Costa, 2018b; Meyerholz and Beck, 2018). While histology provides a large amount of information it is, however, time consuming and requires extensive practical experience and professional training (Aranguren and Figueras, 2016; Costa, 2018b). To overcome these disadvantages, molecular techniques are rapidly developing, and in some cases are used without prior histological analysis (Aranguren and Figueras, 2016). For example, PCR, although widely used, can only indicate the presence of a chosen infectious agent; it cannot confirm if it is causing pathology (Aranguren and Figueras, 2016). Therefore, histopathology is key to the identification of new parasites and diseases in host species (Kent et al., 2013; Aranguren and Figueras, 2016).

Semi-quantitative scoring or grading methods are often used to derive data from histology samples as it is inexpensive and no software or additional hardware is required (Meyerholz and Beck, 2018). Three fundamental characteristics in semi-quantitative analysis which should be exhibited: “it should be: 1) definable, 2) reproducible and 3) produce meaningful results” (Crissman et al., 2004; Gibson-Corley et al., 2013). Awareness is then required for the collection, scoring and data analysis methods. For example, a lack of masking (blind examination) of samples can in some cases create a bias towards a treatment, care is required to assess the samples objectively and score them appropriately. The number of categories within the ordinal scale can range from 3 up to 10 or more, depending on the system: too few results in a loss of sensitivity but too many results in a loss in reproducibility; 4-5 has been considered as the optimal level for detectability and repeatability (Shackelford et al., 2002; Gibson-Corley et al., 2013). It is important to select statistical tests more suited for ordinal data. Since such data do not meet assumptions of normality or heterogeneity of variance, non-parametric

tests may be more appropriate (Gibson-Corley et al., 2013). The most common tests used were the Mann Whitney and the chi-squared tests, however these are also limited depending on the data and must be applied only where appropriate Gibson-Corley et al. (2013) provides a range of resources which are recommend prior to analysis.

1.5.2. Integration of complementary techniques

Traditional histology involves fixation of a tissue, followed by paraffin embedding, cutting a 3-5um section then placing it on the slide, deparaffination and rehydration then staining. Hematoxylin and Eosin are the most versatile and common stains, however, there are many other stains and techniques that can be used (Costa, 2018b). Other more advanced histology techniques include *in-situ* hybridisation (ISH), or fluorescence *in-situ* hybridisation (FISH), and immunohistochemistry (IHC). ISH and FISH require the use of caspases, or mRNA probes, to induce a reaction in a cell. *In-situ* hybridisation is commonly used to provide visual proof of cells of interest (Costa, 2018b), as well as pathogen detection, e.g. *P. olsenii* in green-lipped mussels (Muznebin et al., 2022a). Immunohistochemistry allows for specific staining using antibodies, either through brightfield or fluorescence microscopy. For example, IHC probes can be used to determine location of heat-shock protein, a family of heat-inducible proteins typically expressed under stress (Feder and Hofmann, 1999; Hu et al., 2022). However, other techniques can be used to complement and provide support for findings. For molecular analysis, metabarcoding and PCR can be used to provide more specific pathogen detection and cellular responses. DNA metabarcoding of a tissue or water samples can enable bulk identification of species present by amplifying and sequencing DNA fragments. One limitation to metabarcoding is that it requires previous identification and gene banking of pathogens in order to process the data (Elbrecht et al., 2017; Steyaert et al., 2020). PCR is considered as a critical standard in diagnostic techniques. Although time-consuming it can amplify targeted DNA, thereby allowing for pathogen specificity (e.g., Yang and Rothman, 2004; Zhu et al., 2020).

Complementary physiological techniques can also be used to provide information such as growth rates, condition indices for reproductive condition estimates, suspended microalgal cell counting for food consumption, respirometry (oxygen consumption) for metabolic rate (e.g., Bayne et al., 1977; Delorme et al., 2020a) and LT50 acute studies for survival-based heat sensitivity screening (e.g., Delorme et al., 2020a).

1.6. Significance of this research

Environmental challenges and climate change is at the forefront of most discussions. Environment-host-pathogen based research is crucial to securing shellfish species and shellfish industries for future generations. Consequently, attention is being drawn to the rapidly expanding aquaculture sector in regard to its vulnerability (Froehlich et al., 2022). There are several papers that review global climate risks to various aquaculture sectors (e.g. Reid et al., 2019a; Froehlich et al., 2022). A key gap in knowledge identified by Froehlich et al. (2022) was around adaptation, resilience and the response of populations and regions to climate-based stressors. Assessment of reproductive condition using

histology techniques has been described for green-lipped mussels and *H. iris* in the late 1990s and early 2000s. Neither of these have been well studied under environmental stressor trials although there have been acute stressor trials (e.g., Delorme et al., 2021b; Ericson et al., 2023; Venter et al., 2023). The significance of pre-spawning atresia in relation to stressors is also limited, this research aims to fill the gap and provide additional knowledge through histological techniques. By researching both the bivalve, green-lipped mussels, and the gastropod *H. iris* it will allow observations to the similarities and differences to infer generalities within these molluscan classes. Overall, the work will advance the current knowledge with the intention of using and developing different techniques. This work could provide important knowledge to support decision-making and understand the future impact of the changing marine environment on molluscan species. In addition to improving diagnostics, this study will develop identification methods for deleterious conditions so that optimal management methods may be applied in the aquaculture industry.

1.7. Research objectives

This thesis explores environment-host-pathogen interactions in relation to heatwave related stressors as it affects the two molluscan study species, green-lipped mussels and *H. iris*, and their shared parasite *P. olseni*. The project adopts a forensic histopathology approach to identify subtle, microscopic changes at the tissue level. Investigations aim to identify pathologies and pathogens associated with host, phenology, vulnerability, and disease susceptibility. This study, it is hoped, will give insights into deleterious processes and their detection methods that are applicable to the species studied and to molluscs in general. This knowledge will help inform management of molluscan disease and further the understanding of climate change effects on wild and cultured shellfish. The following introduction details relevant topics and expected outcomes.

Three generic questions will be addressed:

1. What is the tissue-level impacts of marine heatwave-related stressors and are organismic changes indicative of these stressors?
2. What are the implications for reproductive performance and is there evidence for resource recycling from reproductive tissues under stress?
3. Do opportunistic pathogens take advantage of the host stress and exacerbate environmental effects?

By studying the targeted species in naturally heatwave-challenged populations and simplified laboratory simulations, the following specific questions will be addressed:

- a. What is the current health and reproductive status of key molluscs (Green-lipped mussels and *H. iris*) in a naturally heatwave challenged environment and how are further summer heatwaves likely to impact them? (Chapter 2, 3, and 4).

b. How does prolonged exposure to benign and elevated temperatures affect the tissue physiology of green-lipped mussels? (Chapter 5)

c. Do these sub-optimal factors cause energy to be reallocated from reproductive effort to growth, immune response and/or defence? How does the gametogenesis process change and is energy allocation between oocytes and somatic tissue fluid? (Chapter 6)

d. What is the disease progression of *P. olseni* in green-lipped mussel and what are the technical barriers to undertaking this type of research? (Chapter 7)

1.8. Thesis structure

To answer the objectives of this thesis three field research collections and three experiments were conducted. The results for each experiment will be, or have been, published in peer-reviewed journals, and are presented as 6 chapters (Chapters 2-7) across 3 sections (Fig. 1.9.).

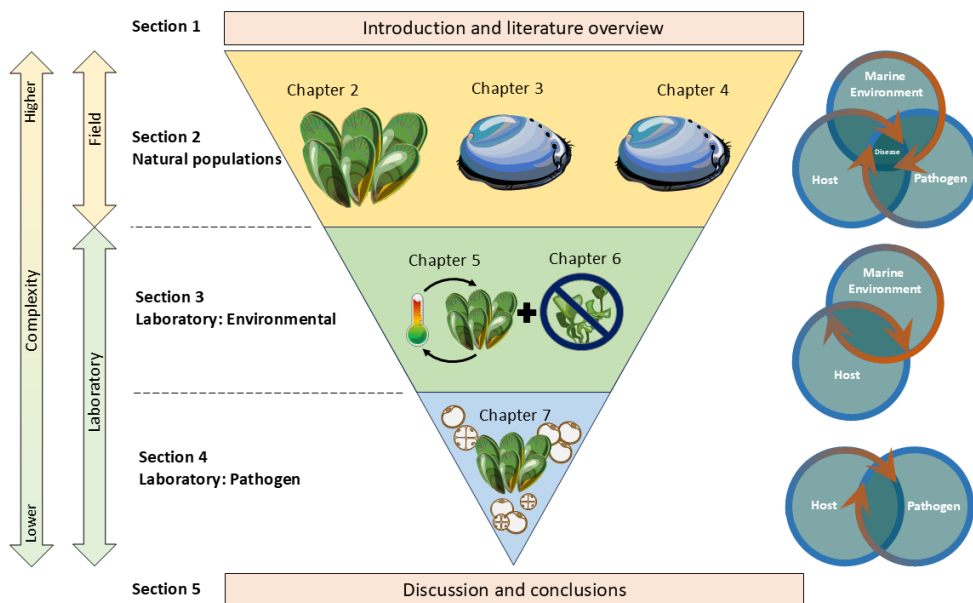


Figure 1.9 Graphic representation of the layout of this thesis. The layout is defined by the complexity of the environmental conditions followed by field and laboratory components. The tapering triangular shape reflects the big picture field studies down to specific host- pathogen interactions.

- Section 1: General introduction and literature overview (Chapter 1)
- Section 2: Influence of the natural environment on the bivalve, green-lipped mussels and the gastropod, *H. iris*, and their parasites through field surveillance (Chapter 2, 3 and 4)
- Section 3: Influence of single and multiple stressors on green-lipped mussels (Chapter 5 and 6)
- Section 4: Disease progression of *P. olseni* in green-lipped mussels (Chapter 7)
- Section 5: Discussion and Conclusion (Chapter 8)

The sections are ordered in decreasing complexity of aspects of the environment-host-pathogen interactions studied from natural populations to a single pathogen (Fig. 1.9.).

Section 1 is introductory including a *raison d'être* for the work, an overview of relevant literature and research in the New Zealand context. Topics covered in subsequent sections are accompanied by up-to-date specific literature reviews as part of their respective introductions.

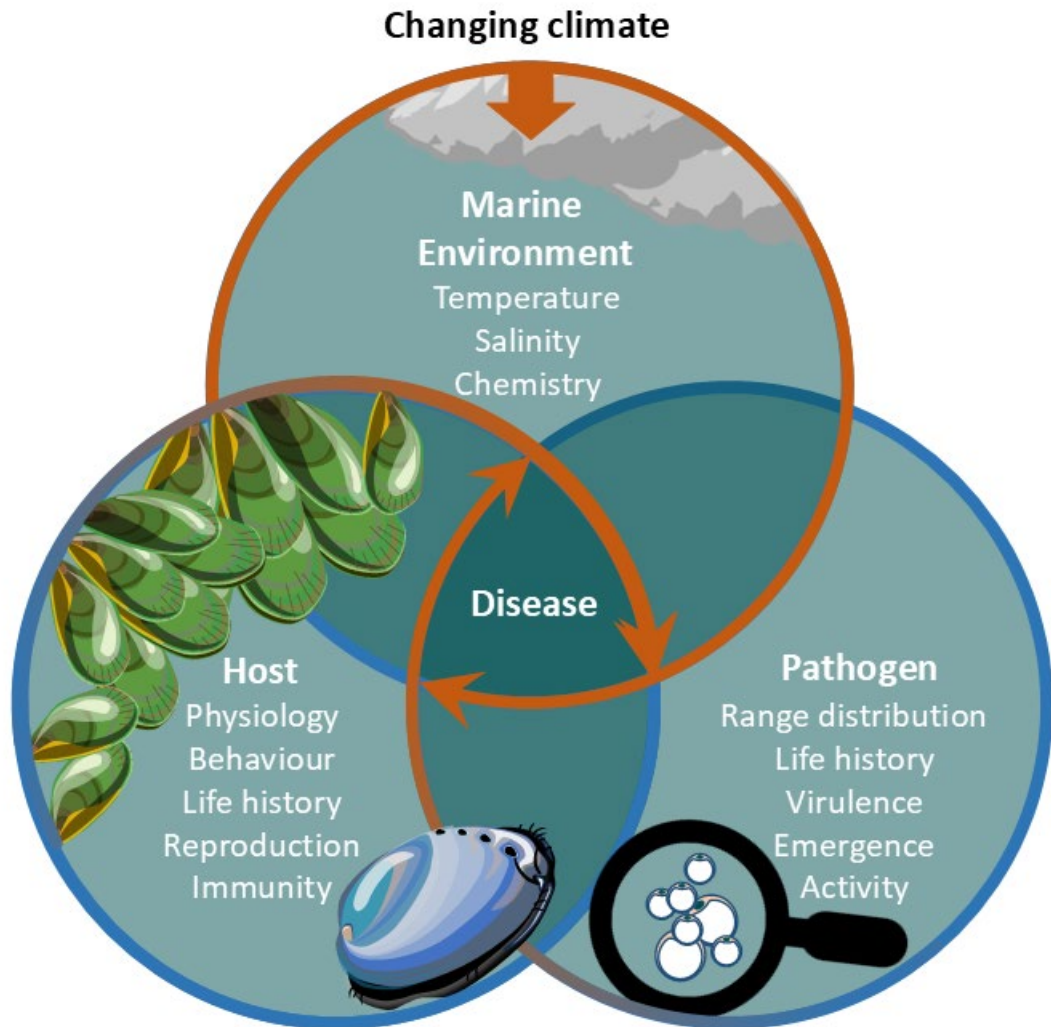
Section 2 describes field studies on green-lipped mussels and *H. iris*. Complex environmental interactions, including heatwaves, weather conditions, seasonal changes and multiple pests and pathogens are studied for both mollusc species. Three-year monthly surveillance of a green-lipped mussels farm allowed for development of an up-to-date gametogenesis cycle on an annual basis as well as for charting changing pathogen loads and species (Chapter 2; Manuscript ready for submission). Collection of the *H. iris* in comparison to green-lipped mussels is more difficult due to fishing techniques (i.e. diving) and funding is limited, as such, experiments in following sections were conducted only on green-lipped mussels. Investigations of *H. iris* provided information to support potential surveillance studies which are required to further understand growth divergence and potential impacts of heatwaves on tissue condition, pathogens, and reproduction (Chapter 3 and 4; both published in their entirety to The Journal of Invertebrate Pathology and Marine Environmental Research, respectively).

Section 3 delves deeper into tissue alterations and reproductive condition by using green-lipped mussels. A 15-month single factor (i.e. temperature) experiment with samples collected each month was conducted to observe the differences between green-lipped mussels exposed to 3 temperatures (17°C, 21°C and 24°C) (Chapter 5; Published in its entirety to Thermal Biology). To gain a better understanding of oocyte atresia detected in the 15-month thermal experiment, a 6-month multi-stressor experiment was conducted looking at 2 temperatures (17°C and 22°C) and low and high food scenarios. This experiment (and Chapter) was split due to the impact of a flood that resulted in the evacuation of the research facility. The first part looks at the effect of the flood exposure on the unfed and fed treatment of green-lipped mussels (Chapter 6a; published in its entirety to New Zealand Journal of Marine and Freshwater Research) followed by the re-initiation of the conditioning experiment (Chapter 6b).

Section 4 looks at the host-pathogen components of the interactome of the common parasite, *P. olseni*, in green-lipped mussel. Green-lipped mussel adults were exposed to the parasite under controlled environmental conditions (20°C) to understand disease progression prior to developing multi-stressor experiments (Chapter 7; Ready for submission).

Section 5 comprises of a general discussion and conclusion which addresses not only the generic and specific questions but also a discussion on different conditions between both species, assessment of future risks in future climate change scenarios, host pathogen co evolution and guardianship of the marine organisms (Chapter 8).

SECTION 2. INFLUENCE OF THE MARINE ENVIRONMENT ON BIVALVES AND GASTROPODS:
EXPLORATIVE FIELD STUDIES ON *PERNA CANALICULUS* AND *HALIOTIS IRIS*



In this section:

Section 2: Preamble

Chapter 2: Interacting influence of changing environment on parasite assemblage and reproductive potential of a marine heatwave-affected population of mussels.

Chapter 3: Histopathological investigation of four populations of abalone (*Haliotis iris*) exhibiting divergent growth performance: Part A

Chapter 4: Elucidating divergent growth performance and climate vulnerability in abalone (*Haliotis iris*): Part B

Section 2. Preamble

As with the global climate, New Zealand, with its wide temperature range and coastal diversity is being impacted by changing climate. The biogeographic isolation of NZ makes it an ideal location to understand the impacts of climate change on its molluscs. Unprecedented summer heatwaves have already been detected and reported in NZ. Heatwaves been attributed to alterations to reproductive patterns and pathogen presence.

The green-lipped mussel and the abalone *Haliotis iris* are both endemic to NZ. Unlike the Pacific oyster, which is introduced, they cannot tolerate extreme temperatures. Both species, green-lipped mussels and *H. iris*, are also ecologically and commercially significant. The changing climate, increasing temperatures and the dependence of the aquaculture industry on green-lipped mussels' production has prompted the need for ongoing studies on its biology. Additionally, *H. iris* research is being driven by concern for the current fishery stock numbers, potentially driven by low recruitment, and the decrease in the catches associated with a lack of growth to legal size. The green-lipped mussel and *H. iris* within this research originate from commercial stocks, aquaculture grow-out and fisheries respectively. Both species are located in coastal regions affected by changing climate and warming sea water temperatures. Surveys were conducted to track year to year changes.

Knowledge about the reproductive condition and health of green-lipped mussels and *H. iris* is crucial for the industry. Understanding the natural patterns of the spawning cycle allows the industry to predict the best times for broodstock collection and for harvesting. Furthermore, understanding the cause of slower growth/ stunting of some populations will allow for development of strategies to ensure sustainability and future survival of the species. As such this section aims to understand the influence of the natural environment on green-lipped mussels, tissue condition, reproductive condition, and pathogen presence. In addition, there is an emphasis upon observing the natural level and variation of oocyte atresia and elucidating effects of thermal stress and growth performance. Chapter 2 "Interacting influence of changing environment on parasite assemblage and reproductive potential of a marine heatwave-affected population of mussels" provides an in-depth histological assessment of green-lipped mussels during a three-year monitoring programme after a major heatwave event whereby mortalities were observed. Chapter 3 "Histopathological investigation of four populations of abalone (*Haliotis iris*) exhibiting divergent growth performance" and Chapter 4 "Elucidating divergent growth performance and climate vulnerability in abalone (*Haliotis iris*)" provide in-depth histological assessments to initially elucidate growth performance differences then expand into a snapshot sampling over 3 years to explore the impact of potential heatwaves on reproductive condition and pathogens as with the green-lipped mussel.

CHAPTER 2. THE INTERACTING INFLUENCE OF SEASON AND RECURRENT MARINE
HEATWAVES UPON GAMETOGENESIS AND PARASITE BURDEN IN THE GREEN-LIPPED
MUSSEL *PERNA CANALICULUS*.

To be submitted for publication

Abstract

Analysis of satellite data from the Integrated Marine Observing System demonstrates that the Coromandel region (Firth of Thames, New Zealand) now experiences regular marine heatwaves with temperature anomalies of up to 3°C. Marine bivalves occupying the shallow subtidal zone are likely to become increasingly vulnerable to rising sea surface temperatures; hence field studies of sentinel species impacted by periodic heatwave events provides essential baseline health and natural variability data, while gauging the longer-term impacts of a changing climate. This work specifically assessed histopathological changes in reproductive condition, health and parasite presence in a population of the keystone mussel *Perna canaliculus* during a three-year sampling programme (2018 to 2021). A period that serendipitously coincided with the onset of significant summer marine heatwaves. Histopathological analysis of tissue conditions indicated physiological stress after the 2017 summer marine heatwave and several conditions correlated to pathogen presence. The gametogenesis cycle showed a prolonged spawning period during 2018/2019 and full spawn during 2020/2021, with 40-60% of oocytes showing signs of atresia (resorption), regardless of gametogenesis stage. Based on the gametogenesis pattern reproduction is likely to continue to be negatively impacted because of increasing number of days spent above 22 °C. During early-stage gametogenesis, parasite number was positively correlated with temperature and subsequently becomes negatively correlated when mussels are ripe. Eleven pathogens were detected histologically over the survey period, with a change in diversity over time. Three parasites of concern included hydroids attached to the mantle in the pallial cavity, *Endozoicomonas*-like organisms detected in the gastrointestinal tract epithelium and an unfamiliar, potentially novel, multinucleate stage parasite. The unfamiliar parasite was tentatively placed in the Apicomplexa group using non-targeted metabarcoding techniques and subsequent bioinformatics.

2.1. Introduction

Natural populations of marine invertebrates, such as mussels, are under threat from a changing climate, intensified commercialisation and recreational exploitation. The impact of warming waters on the growth and reproduction is well documented (e.g., Harvell et al., 2002; Lane et al., 2023; Petes et al., 2007). Rising sea temperatures, marine heatwaves and unusual weather patterns also increase invertebrate susceptibility to disease (Carella et al., 2018; Coates and Söderhäll, 2021). Diseases of marine invertebrates are typically governed by complex and poorly understood host-pathogen interactions which are highly influenced by environmental change (Burge et al., 2014; Guo and Ford,

2016; Guo et al., 2015). Therefore, the changing climate and associated emerging diseases may have major consequences for, not only the organisms themselves in the natural environment, but the aquaculture and fisheries industries they support (Castinel et al., 2019; Harvell et al., 1999).

Globally, aquaculture production is projected to rise to at least 32% by the year 2030 (Lane et al., 2023), as these industries are recognised as valuable low carbon food sources (Halpern et al., 2022). It is clear, though, that plans for expansion, intensification, and introduction of new species in aquaculture production, current and new geographic regions, are becoming increasingly constrained by health conditions and diseases associated with a changing climate (Castinel et al., 2019; Petes et al., 2007). For instance, prolonged exposure to suboptimal environmental conditions can inhibit reproduction reducing larval output (e.g., Chérel and Beninger, 2017; Michalek-Wagner and Willis, 2001; Petes et al., 2007).

Surveillance programmes are essential for assessing health status and enable early identification and management of emerging pathological problems (Jones, 2016; Webb and Duncan, 2019). Occurrences of pathologies, symbionts, parasites and infectious diseases may exhibit seasonal patterns which can be influenced by a changing climate (de La Rocque et al., 2008; Harvell et al., 2002). It is also well known that anomalous temperatures can have an impact on the proliferation, virulence and distribution of existing and emerging pathogens in bivalves (de La Rocque et al., 2008). Health and disease monitoring typically relies on histopathology as it is an effective tool for identifying of novel pathogens and elucidating host – pathogen interactions (Aranguren and Figueras, 2016; Kent et al., 2013; Webb and Duncan, 2019). Histopathological analysis can also provide insights into effects of exposure to environmental stressors on a range of degenerative tissue conditions and changes in reproductive cycle thereby enhancing management preparedness (Benito et al., 2022; Bignell et al., 2008; Costa, 2018; Webb and Duncan, 2019).

New Zealand (NZ) is an ideal location to understand the impacts of the changing climate on marine invertebrates due to its coastal diversity and wide seawater temperature range (Costello et al., 2010; Montie et al., 2023). Following global trends, above-average sea surface temperatures (SSTs) have also been observed in NZ, with future increases in marine heatwave frequency predicted (Montie et al., 2023). In the past decade two austral summers in NZ have reached 3-4 °C above climatological averages, indicating anomalous heatwaves. One of these heatwave events occurred in 2017/18 (Salinger et al., 2019), and another in 2022/23 (Bell et al., 2023), causing localised extinction of *Durvillea* spp. in southeastern, NZ, and local sponges in Fiordland, NZ, respectively (Montie et al., 2023). Northern NZ is also regularly experiencing maximum SSTs of 26°C during the summer period (Delorme et al., 2024). These extreme temperatures have significant effects on marine biology, aquaculture and fisheries activities (Reid et al., 2015).

The green-lipped mussel, *Perna canaliculus* (Gmelin, 1791), is one such species at risk under most climate change scenarios (Ericson et al., 2023; Venter et al., 2023). This bivalve is endemic to NZ

and not only plays a vital role in the natural environment as an ecosystem engineer, but is one of three established aquaculture species farmed around the country (e.g., Alfaro et al., 2001; Castinel et al., 2019; Ericson et al., 2023; Jeffs et al., 1999; Lane et al., 2023; Stenton-Dozey et al., 2020; Venter et al., 2023). They are dioecious spawners with gonadal development occurring annually. Spawning events typically occur during the late summer and winter; however, depending on the population, some individuals can maintain their spawning condition (Buchanan, 2001; Jeffs et al., 1999; Petes et al., 2007). Previously, histological examination of the reproductive cycle and gametogenesis (process of reproductive cell division and differentiation) for green-lipped mussels has been documented by Alfaro et al. (2001), Buchanan (2001) and Copedo et al. (2023), the latter as part of a chronic thermal challenge laboratory study. Despite these studies there is a lack of annual histological gonad staging reports for green-lipped mussels naturally exposed to the changing climate over the past decade.

Green-lipped mussels, in contrast with many other species of mollusc worldwide, have relatively few reported diseases (Castinel et al., 2019; Lane et al., 2023). Pathogens and parasites associated with green-lipped mussels include bacteria such as *Vibrio* and *Photobacterium* sp. (Azizan et al., 2024; Ericson et al., 2022; Kesarcodi-Watson et al., 2009) and IMCs (intracellular microcolonies) (e.g., rickettsia-like organisms and *Endozoicomonas*-like organisms) (Cano et al., 2020), *Microsporidium rapuae* (Jones, 1975), apicomplexan X (Suong et al., 2018), digeneans (*Tergestia agnostomi* and *Bucephalus* sp.), various crustaceans (including pea crabs, and copepods, e.g. *Lichomolgus uncus* n. sp. and *Pseudomyicola* sp.) (Jones, 1976; Webb and Duncan, 2019), ciliates and *Perkinsus olseni* (Castinel et al., 2019; Copedo et al., 2023; Hine and Diggles, 2002; Muznebin et al., 2022; Suong et al., 2018; Webb and Duncan, 2019). Further research and monitoring of a valuable species, such as the green-lipped mussel, is key to futureproofing and managing sustainability of the natural populations and the industry it supports in the face of seasonal challenges.

This research therefore primarily employed histopathological techniques and, where required, complementary techniques such as remote satellite data for temperature, and metabarcoding and PCR for parasite detection. Adult, green-lipped mussels were collected from a reference population of mussels maintained on a marine farm in Coromandel, NZ, during a three-year monitoring programme (2018 to 2021) with the aim of identifying host-pathogen associations and vulnerabilities, and alterations to gametogenesis in a multifactorial environment known to experience marine heat waves and mussel mortality events.

2.2. Methods *Environmental monitoring: estimation of SST*

Due to the impracticality of deploying temperature sensors at the survey site, the sea surface temperature (SST) for the, Firth of Thames, Coromandel region (latitude 37.03°S, longitude 175.35°E), NZ, was determined remotely through satellite data acquisition. Daily multi-sensor daytime SST data (Govekar et al., 2022) was acquired between January 2017 and June 2024 from the integrated marine observing system at a spatial resolution of 2 km using the following data portal: <https://portal.aodn.org.au/search> (Proctor et al., 2010). It is worth noting that these large spatial

resolutions may conceal local variations in temperature, particularly low-wave action, tidally dominated estuarine regions such as the Firth of Thames (Boehnert et al., 2020).

The sea surface temperature (SST) anomaly timeseries (v3.1) at a 5 km spatial resolution for the period December 2016 and December 2023 was sourced from NOAA Coral Reef Watch (<https://coralreefwatch.noaa.gov>), using a baseline period of 1985-1990 plus 1993 to calculate anomalies (Liu et al., 2014; Skirving et al., 2020). December was selected for visual representation and yearly comparison of the SST anomalies for the mainland NZ and Chatham Islands region for the years 2017, 2018, 2019 and 2020, as it showed the greatest differences in SST anomalies among years. The mean baseline was set at zero and the SST anomalies (°C) referenced above or below the mean.

2.2.2. *Sampling location and collection*

The source population of adult, green-lipped mussels was established on near-shore sub-surface long-lines used for commercial mussel farming in Whakatūwai, Firth of Thames, NZ (37° S, 175° E). Standard NZ aquaculture practices were used to establish the population by seeding juveniles sourced from 90 Mile Beach (Northland, NZ) onto suspended polypropylene rope and allowing approximately 12 – 18 months for growth. Monthly collections of the adults were attempted between April 2018 and May 2021 (Muznebin et al., 2022); occasionally collections were missed due to logistics and unforeseen circumstances (Table 1). Therefore only 26 months of data were collected and analysed. At each collection event 20 - 30 adult mussels were randomly sampled. During the study period a total of 570 mussels (Length: Mean 94mm, Min.: 59mm, Max.: 121mm) were collected and sampled. The mussels were emersed (<2h total), chilled and transported alive to the Auckland University of Technology (AUT), Auckland, NZ, for assessment. On arrival the mussels were measured (shell length, ±1 mm) before histological preparation.

2.2.3. *Histopathology*

The tissues of each green-lipped mussel were removed carefully and intact from the shell and sectioned as per Howard (2004) and Copedo et al. (2023). A 5mm tissue steak was acquired to maximise chances of sectioning mantle, gill, digestive gland, gastro-intestinal tract, and muscle. Each of the steaks was placed into histological cassettes and immediately fixed in 4% formalin solution (1:9 v/v, 37% formaldehyde: 0.35µm filtered seawater). After 48 hours, the samples were then transferred to a 70% ethanol solution for further histological processing (Howard, 2004). The fixed samples underwent routine processing for histological analysis followed by hematoxylin and eosin staining (H&E) (Howard, 2004). Due to the poor sample quality, September 2018 histology results were omitted from the data set.

2.2.3.1. *General tissue alterations*

The prepared histological slides were observed under a light microscope (Olympus BX40), at magnifications of x40 to x1000. Twelve tissue-specific conditions were scored as present or absent across available tissues including mantle, gill, digestive gland, gastro-intestinal tract, kidney, heart,

and muscle. These conditions included: 1) presence of focal haemocytosis as well as haemocyte infiltration (characterised as not focal or diffuse in nature); 2) ceroid deposition; 3) gastrointestinal tract diapedesis; 4) disruption in the gastrointestinal tract architecture as parasites pass through; 5) atrophy (Cuevas et al., 2015); and 6) elevated presence of apoptotic cells (Azizan et al., 2023; Elmore et al., 2016). In addition to the presence/absence data collected above, two conditions were selected and graded using four subjective semi-quantitative criteria, each graded from the least (1) to most (3) accumulation; 1) intensity of ceroid observed across available tissues (Copedo et al., 2023); and 2) density of storage cell material in the mantle (Copedo et al., 2023).

The sex of each green-lipped mussel was recorded visually once shucked, then again through histological assessment (365 of the 570 were identifiable microscopically). A binary true/false score was then also allocated to each mussel for correct visual allocation of sex visually confirmed by histology. The sex ratio was determined using the histology results by the number of males detected divided by the number of females. Mussels where sex could not be identified were excluded from the sex ratio analysis.

2.2.3.2. *Reproduction and atresia*

The gonad development was scored using a scheme adapted from Kennedy (1977), Alfaro et al. (2001) and Buchanan (2001), and used in Copedo et al., (2023), whereby gametogenesis stages were characterised as resting, early development, late development, ripe or mature, spawning, spent or redeveloping. The proportion of individuals at each stage, at each month, was plotted for visual representation. Each stage was allocated a score of 0 (resting or spent), 1 (early), 2 (late or spawning), or 3 (ripe mature) to generate a gonadal index (GIn), after King et al. (2009), Buchanan (2001), Alfaro et al. (2001) and Copedo et al. (2023), and the average GIn score calculated for each sampling event.

To determine the intensity and impact of atresia (oocytes with cytoplasmic discolouration, irregular jigsaw shape, as well as retraction and detachment of the cytoplasm from the membrane (Beninger, 2017; Copedo et al., 2023)), two methods were employed. The first method was a semi-quantitative assessment based on the allocation of atresic and normal oocytes in the follicles across the mantle/gonad tissue, with a scale ranging from 0 to 5:

- 0: no atresia observed
- 1: 0% to 20% of the oocytes were observed as atresic
- 2: 20% to 40%
- 3: 40% to 60%
- 4: 60% to 80%
- 5: 80% to 100%

Note: If atresia of the oocytes was greater than 80% then the gametogenesis stage of the mussel was scored as spent.

The second method was designed to corroborate the graded scale, whereby atresic and normal oocytes for a subset of females ($n = 87$) were counted to produce a single percent value for each mussel. Three micrograph images per individual female were taken using the 20x objective of an Olympus BX53 compound microscope and cellSens™ software [cellSens Standard 3.1 (build 21199)] Oocytes in each image were counted as atresic or normal as per Chérel and Beninger (2017) but not identified or categorised as mature or immature. The three counts were then averaged and recorded to produce a single value for each egg-bearing mussel. The percent of oocytes displaying atresia was then recorded and compared with the scale.

2.2.3.3. *Pathogens and parasites*

Parasites within the 570 green-lipped mussel samples were observed histologically using a light microscope (Olympus BX40), at magnifications of x40 to x1000, then recorded as present/absent and presented as percent of population prevalence. The whole section was screened at lower magnifications (e.g. x20 and x40), and areas of interest were explored using an oil immersion x1000 lens. The numbers of pathogens or parasites observed in each mussel were also scored to record species diversity, and the sum of species identified during each sample event was recorded. A multinucleate parasite detected in the kidney tissue was also initially recorded as present/absent then subjected to further analysis as below. Upon detection of the multinucleate parasite, 25 of the parasites in 5 mussels ($n=5$ per mussel) were measured in length (longest dimension) and width to the nearest 0.01 μm using cellSens™ software (Olympus cellSens Standard 3.1 [build 21199] on an Olympus BX53 compound microscope). The number of nuclei of the premeasured parasites was also counted. Based on the detection of the multinucleate parasite in the histological assessment three of the associated paraffin blocks were selected for molecular analysis as described in the next section.

2.2.4. *Molecular diagnostics*

DNA purification, PCR and metabarcoding were used to investigate and diagnosis the newly identified multinucleate parasite. Six histology wax blocks were selected, three were identified to be positive for the parasite and three identified to be negative according to the histological analysis. Five 5 μm sections of tissue from the wax blocks were cut using a rotary microtome and placed into an Eppendorf tube for deparaffinisation and DNA extraction as per manufacturing kit methodologies (Quick-DNA™ FFPE Miniprep kit, Zymo Research, Ngai Diagnostics). A negative control which contained no green-lipped mussel tissue was also included and subjected to the same process. The deparaffinisation was followed by tissue digestion and DNA elution. Extracted DNA was stored at -20°C for further processing. DNA purity and concentration were measured using a Nanophotometer® (Implen GmbH, Munich, Germany).

A PCR assay using the generic primers Perk ITS750/Perk ITS 85 (Casas et al., 2002) was performed to rule out *Perkinsus* spp. in the six selected samples. Each of the reactions was carried out in 20 μl of final volume using 1 μl of 10 mM each primer, 10 μl MiFy mix (Bioline, Meridian Bioscience), 6 μl sterile water and 2 μl DNA (1/10). A negative control containing the PCR mixture but without the

target, and a positive control using a DNA extracted from a pure *in vitro* *Perkinsus olseni* culture was also included. PCR thermocycling was completed on a Eppendorf Mastercycler (nexus gradient) using the following profile: 1 cycle of 95°C for 1 minute and 40 cycles of 95°C for 15s, 55°C for 30s and 72°C for 60s followed by an additional 10 min step at 72°C then hold at 4°C (Casas et al., 2002) The size of final PCR product was assessed by electrophoresis.

In the untargeted approach, 18S rRNA eukaryotic primers Uni18SF and Uni18SR by Zhan et al. (2013), primarily targeting micro-eukaryotes were used. Each 18S PCR reaction included 1µl of 10 mM each primer, 25µl MiFy mix (Bioline, Meridian Bioscience), 3 µl DNA (1/10), and 20 µl sterile water. A negative control was also carried out in duplicate with the PCR mixture and without the target. The reaction was incubated for 2 min at 95°C, followed by 40 cycles of 15 s at 94°C for the denaturing step, a 15 s annealing step at 52°C, a 15 s extension step at 72°C and a final extension step of 5 min at 72°C. The 18S PCR products were purified using the NucleospinGel and PCR Clean-up kit (Macherey-Nagel, Germany), following the manufacturer methodologies and sent for paired-end sequencing on an Illumina MiSeq platform (Sequench, Nelson, NZ). One sample of the three positive samples was removed due to the poor-quality PCR amplification result.

2.2.5. Bioinformatics

Sequencing data in the format of FASTQ files were demultiplexed and primers removed using CUTADAPT (version 4.2; Martin (2011)). This required a minimum overlap of fifteen bp and no insertion or deletion. To remove low-quality calls, sequences were truncated on their 3' end at 225 bp and 216 bp for 18S, for the forward and reverse sequences, respectively. Sequences were quality filtered and denoised using the default parameters of the DADA2 R package (version 1.26; (Callahan et al., 2016)) and merged using a minimum overlap of 10 bp. Potential chimeric sequences were removed using the 'consensus' option of DADA2, where sequences found to be chimeric in a majority of samples are discarded.

As per Copedo et al. (2025a) (Chapter 3) a combination of approaches and databases was used to assign the taxonomy in order to increase resolution and maintain assignation confidence. The 18S data were assigned with the RDP Naïve Bayesian Classifier algorithm (Wang et al., 2007) applied on the reference database SILVA (version 132; Quast et al. (2013)), and blastn and megablast (Camacho et al., 2009) on the GenBank nucleotide database (Benson et al., 2008) using the default values of the 'blastn_taxo_assignment' function of the biohelper R package (Laroche, 2024). The taxonomic assignments from each of the approaches were combined using the taxo_merge function of biohelper, which first normalizes taxonomy using the NCBI curated taxonomic database (Schoch et al., 2020). If there is consensus (>50%) across assigned ranks among the different approaches, the highest taxonomic resolution among them is used. If not, the last common ancestor (with > 50% consensus) is assigned.

The top three amplicon sequence variants (ASVs) of interest among the 18S data were selected for deeper exploration, and geneblasted using Blastn (NCBI, <https://blast.ncbi.nlm.nih.gov/Blast.cgi>).

Results were recorded in Table. 2.3, including accession number, identity, the E- value, query cover, closest species, and the last common ancestor.

2.2.6. *Statistical analyses*

For analysing the relationship between temperature and the different mussel characteristics we first summarised the data by month. A one-way ANOVA was used to compare length (mm) between the months. Sex ratio within each month and total combined was used to produce a final value which was calculated using a chi-squared test and a binomial test. No statistical analyses were performed on the prevalence of the tissue conditions within each month. However, the tissue data were used in the correlation matrix analysis as described below.

The monthly maximum, minimum and mean sea surface temperature were calculated. The monthly mean gonadal index (GIn) value, and the monthly mean number of parasite species was then also calculated. Linear models were fitted to explore the relationship between these variables of the summarised data, with mean gonadal index or the total number of parasite species as response variables, and temperature as the explanatory variable. We also tested if there was an interaction effect of temperature and GIn, parasite richness or sex in each model. A linear model was used to examine the relationship between the semi-quantitative atresia grade and date.

The effect of temperature on a given variable could be affected by autocorrelation or could show a delayed pattern in biological systems. We tested if the results of the above models changed if we introduced a temporal autocorrelation term to the models (corAR1 type of autocorrelation with a generalised least square model, (Pinheiro and Bates, 2023)). For testing a lag effect of temperature, we performed the linear models with GIn or parasite mean richness as the response variable, and lag temperature as the explanatory variable. Temperature was lagged for 1 to 18 months. Furthermore, a linear model was also constructed to observe the mean number of parasites in response to GIn and temperature.

Finally, we tested the correlation between all tissue alteration variables (including gametogenesis variables) and the presence of pathogens or parasites. For this, we calculated Kendall's rank correlation coefficient (τ values) among the variables describing tissue alterations for females and males separately. Kendall rank correlation is a non-parametric method appropriate when the data do not fit a normal distribution (Abdi, 2007). All statistical analyses were conducted using R version 4.4.0 (R Core Team, 2024).

2.3. Results

2.3.1. *Environmental temperature*

The sea surface temperature (SST) from the Australian Integrated Marine Observing System (IMOS) near the survey site showed that temperatures reached a maximum of 25.1 °C during the summer period (Jan. 2018) prior to initiation of sampling in April 2018. Summer SSTs within the sampling period exceeded 22 °C and from early January 2018 were above 23 °C for 30 days or more. Maximum

SSTs of 23.8 °C and 22.8 °C were also recorded for 2018/19 and 2019/20, respectively. After the sampling period maximum SSTs were 24.7 °C (Feb. 2022) and 24.6 °C (Jan. 2024) (Fig. 2.1).

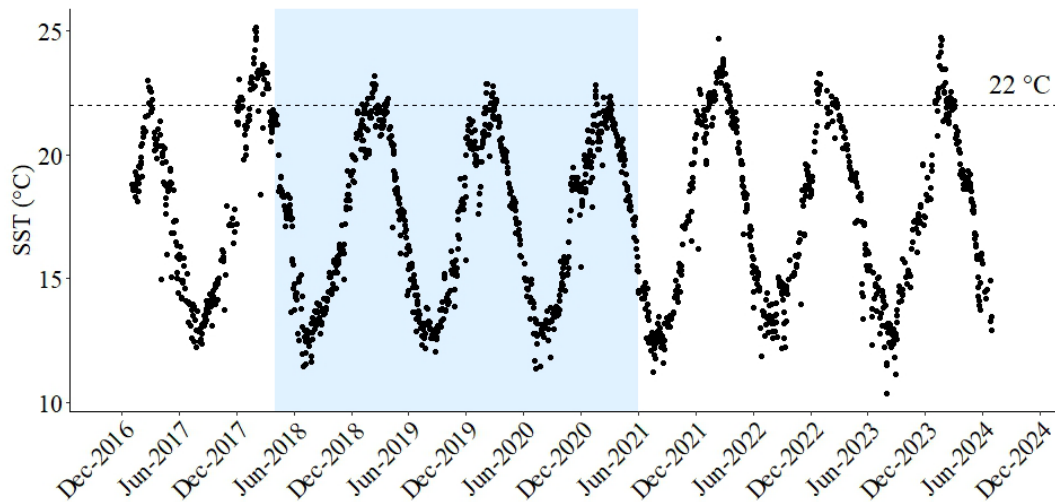


Figure 2.1 Coarse daily multi-sensor sea surface temperature (SST) for the Coromandel region (latitude 37.03°S, longitude 175.35°E) between Jan 2017 and Mar 2021. The dashed line represents the 22 °C threshold of sub-optimal temperatures, whereby physiological conditions and reproduction are impacted with prolonged exposure to >22 °C (Ericson et al., 2023; Venter et al., 2023; Benjamin et al., 2024). The sampling period is highlighted by the shaded area. Source: IMOS

The SST anomaly data indicated regular long anomalous heatwave events with the most extreme being the summers of 2017/2018, and 2021/2022, with 2023/2024 trending in a similar pattern. During the sampling period, April 2018 to May 2021, SST anomalies during the summer were still reaching 2 °C above the climatological baseline (1985-1990 plus 1993 (Liu et al., 2014)). The visual representations of December show the yearly variation in the SST anomalies for NZ. Images show that NZ generally, including Coromandel area, regularly experiences SST anomalies with localised hotspots (Fig. 2.2).

2.3.2. *Perna canaliculus* tissue conditions

The shell length of the mussels was different between each sampling date ($F_{(23, 482)} = 8.17, p < 0.001$). The sex ratios across each month were also statistically significant different ($X^2_{26} = 43.05, p = 0.019$) (Table. 2.1.). Furthermore, when the month combined total of the sex is explored there were 215 males versus 150 females detected of the 570 mussels, resulting in a statistically significant bias towards a male dominated population ($p < 0.001$). Although data is not recorded herein, approximately 19% of the samples based on visual gross assessment had a misidentified sex when confirmed histologically. This misidentification is likely due to either their early development stage, whereby when the mussels building glycogen energy reserves prior to gametogenesis appear white (similar to male), or female oocytes are lacking colour.

Typical tissue conditions such as ceroid, haemocytosis and gastrointestinal tract diapedesis were also detected within this study, however all were low in intensity and therefore no quantitative analysis

was performed. The presence of ceroid (a typical by-product of phagocytosis) was observed frequently in the green-lipped mussels and generally associated with APX. Focal haemocytosis appeared to be most prevalent in May 2019 and January 2021 (affecting 100% of individuals). Aggregations of haemocytes were also detected in the gills of 100% of the mussels on six occasions through the sampling programme. Gut diapedesis appeared more prevalent from October 2018 through to June 2019, along with the presence of digestive gland atrophy and atypically high presence of apoptotic haemocytes. Lastly, the gastrointestinal tract disruption co-occurring with APX implies that APX is regularly transitioning through the epithelium (Table. 2.1).

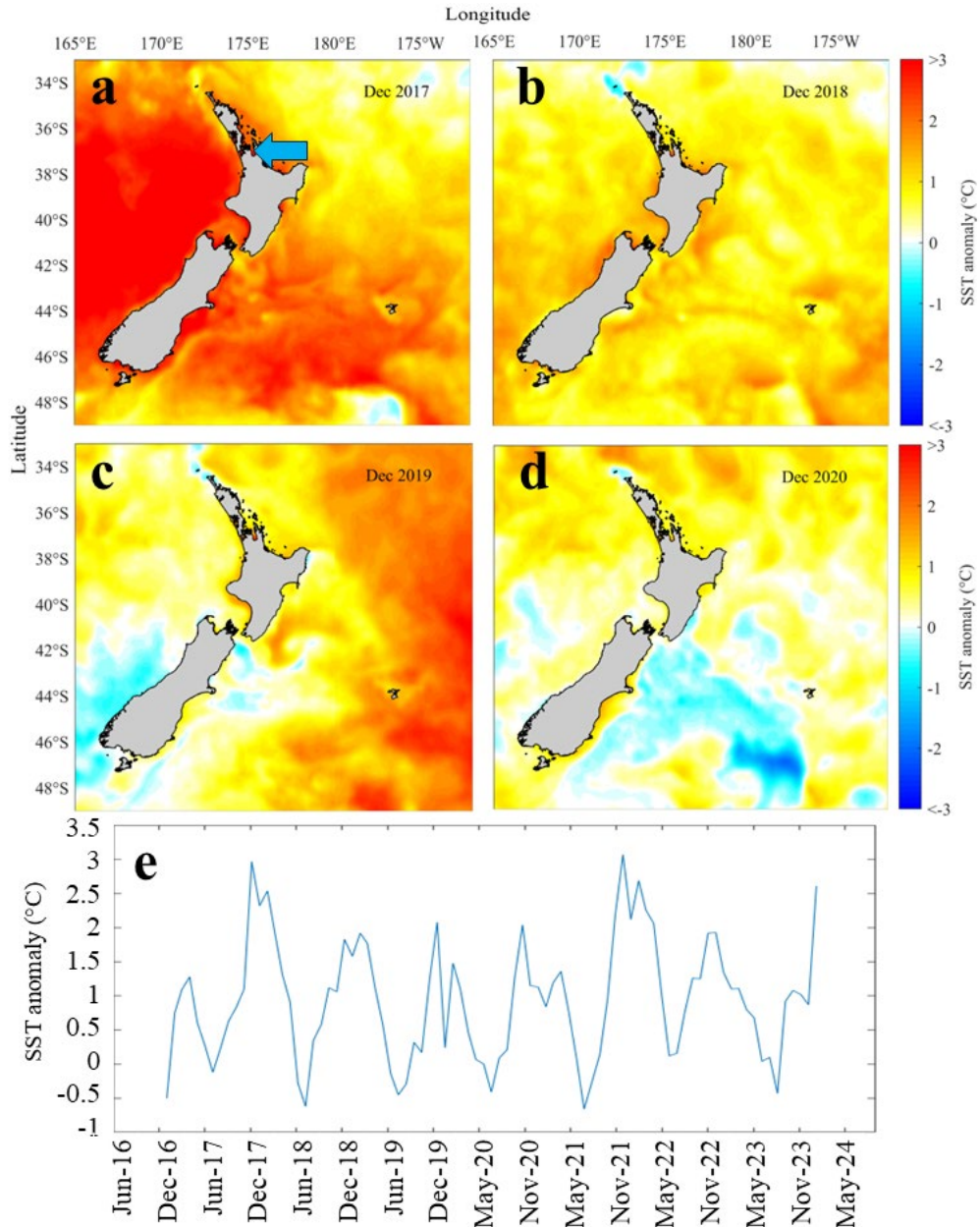


Figure 2.2 Visual representation of the NZ and Chatham Island area showing average sea surface temperature (SST) anomalies for the month of December for the years a) 2017, b) 2018, c) 2019 and d) 2020. December 2017 appears to be the warmest followed by 2018 and 2019. Coromandel and sampling location (arrow), e) SST anomaly timeseries showing degrees above the climatological baseline from December 2016 to December 2023 for the Coromandel region near the sample site (latitude 37.03°S, longitude 175.35°E).

Table 2.1 The mean mussel length (L (mm)) \pm SD, sample size, F:M sex ratio and percent prevalence data for 11 general tissue conditions are presented, including gill haemocytosis (Gill HE), gill ceroid (Gill BC), focal haemocytosis (F HE), mantle haemocyte infiltration (M HE), mantle ceroid (M BC), digestive gland haemocyte infiltration (DG HE), gastrointestinal epithelium diapedesis (GI d), gastrointestinal epithelium disruption from APX transitioning through (GI ED), kidney haemocyte infiltration (K HE), tissue atrophy ((Not including the DG) T Atro), digestive gland atrophy (DG Atro), and high apoptosis of haemocytes (Apop), NR: No record: no samples provided.

	L (mm) \pm SD	n	Sex ratio	Gill HE	Gill BC	F HE	M HE	M BC	DG HE	GI d	GI ED	K HE	T Atro	DG Atro	Apop
Apr-18	NR	20	0.8	69	0	18	56	31	87	67	0	0	94	94	0
Jul-18	97.1 \pm 5.5	20	1.9	56	0	5	85	75	5	25	0	0	0	20	0
Oct-18	106.9 \pm 7.4	20	1.5	100	10	0	0	100	0	100	0	NR	100	100	0
Nov-18	95.5 \pm 14.7	20	0.5	60	5	0	15	80	0	100	5	0	100	100	100
Jan-19	93.1 \pm 8.7	20	1.2	100	60	5	5	100	0	95	0	0	100	100	75
Feb-19	92.9 \pm 10.5	20	0.9	100	0	25	10	100	10	100	20	0	100	100	100
Mar-19	92.8 \pm 8.1	20	1.0	0	0	5	5	40	0	10	20	NR	0	0	0
May-19	93.8 \pm 7.7	20	1.6	33	0	100	94	39	100	94	44	0	0	0	0
Jun-19	94.9 \pm 7.5	20	1.2	100	0	20	20	100	0	100	55	0	0	95	100
Jul-19	86.7 \pm 5.8	20	0.4	70	35	0	5	100	0	65	25	0	0	5	0
Aug-19	97.2 \pm 8.8	20	1.2	80	40	40	65	100	30	89	5	0	20	20	30
Oct-19	89.4 \pm 9.8	20	1.6	45	5	10	10	80	10	70	30	0	5	35	0
Nov-19	95.8 \pm 6.3	20	2.0	20	5	30	40	100	0	85	35	0	0	0	0
Dec-19	91.3 \pm 7.1	20	1.4	20	0	20	20	100	0	5	30	0	0	0	0
Feb-20	101.3 \pm 7	20	0.5	5	0	35	25	20	5	25	30	0	0	0	0
Mar-20	88.1 \pm 7.4	20	1.9	100	0	40	45	100	5	0	15	0	0	0	0
May-20	86.6 \pm 7.3	20	2.3	100	0	20	20	100	0	0	70	0	0	0	0
Jul-20	97.1 \pm 5.1	20	1.0	40	0	5	5	95	0	25	10	0	0	0	0
Sep-20	105.6 \pm 6.3	20	1.9	10	0	10	0	100	10	35	0	0	0	0	0
Oct-20	94.8 \pm 8.1	20	3.8	50	55	50	50	90	65	55	10	0	0	0	0
Nov-20	91.1 \pm 6.6	20	2.8	60	40	40	40	100	15	70	15	11	0	5	0
Dec-20	91 \pm 9.3	30	1.8	20	0	73	63	100	60	60	7	20	30	40	3
Jan-21	92.5 \pm 7.3	20	0.5	60	0	100	95	40	30	20	5	15	15	50	0
Feb-21	91.1 \pm 7.4	30	4.0	10	0	47	30	67	13	19	7	5	0	0	0
Mar-21	97.1 \pm 5.5	30	1.9	40	70	40	33	90	3	10	10	19	13	0	3
May-21	106.9 \pm 7.4	20	0.5	30	75	45	45	100	20	25	0	10	5	0	15

2.3.3. *Perna canaliculus* reproductive condition and atresia

When the gametogenesis score data is pooled into months irrespective of year a “typical” pattern of development is observed for females from October to April followed by inconsistent development. For the males, early development is the same as the females. Furthermore, the population of mussels appear to be in condition through the year (Fig. 2.3).

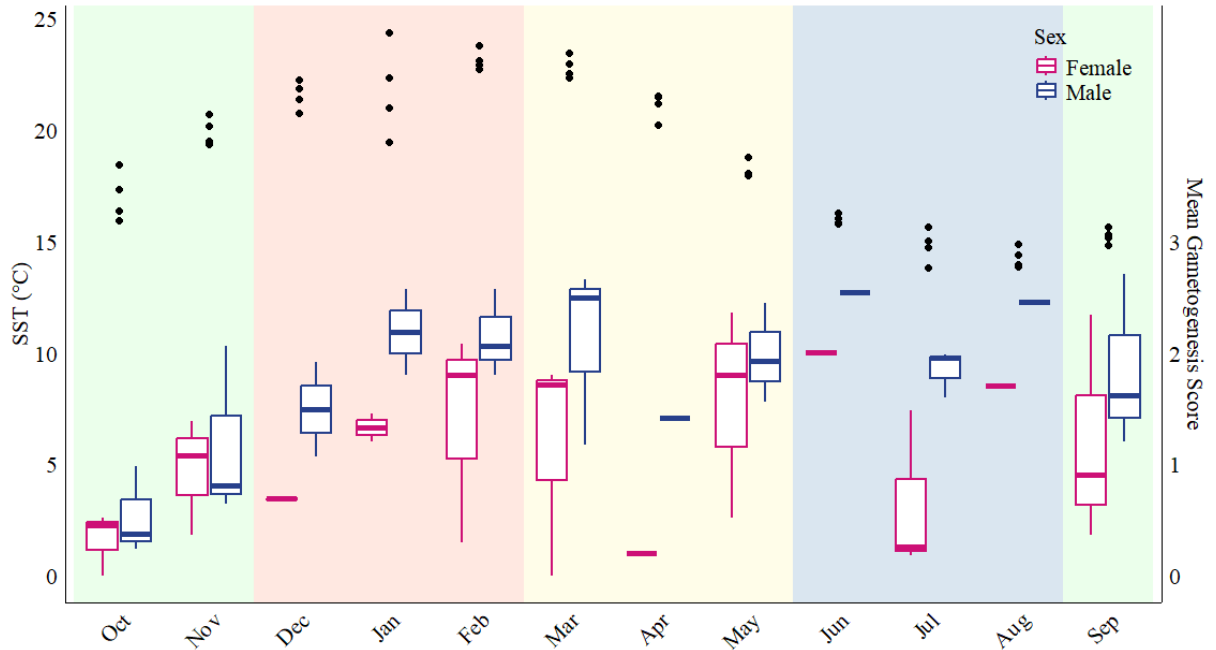


Figure 2.3 Mean gametogenesis index score of mussels identified as female and male for each month (secondary y-axis). A score of 0 indicates a resting or spent population and a score of three indicates the population is in the mature or ripe phase. Maximum sea surface temperature values (dots) for each of the four years (2017 to 2020) (primary y-axis). Southern hemisphere seasons are indicated by shaded areas, summer (Dec. to Feb., red), Autumn (Mar. to May, yellow), Winter (Jun. to Aug., blue), and Spring (Sep. to Nov., green).

When the gametogenesis pattern is separated into months and years the patterns can be compared across successive years. The reproductive condition shows an initial unexpected pattern in the distribution of gametogenesis stages during the early stages, with a more typical pattern (complete spawn then new development) detected from November 2020 (Fig. 2.4). As a result of the inconsistent pattern of gametogenesis no statistical differences were detected between the mean gametogenesis index (GI) and maximum temperature ($t = -0.37_{(46)}, p = >0.05$), minimum temperature ($t = -0.099_{(46)}, p = >0.05$), and mean temperature ($t = -0.22_{(46)}, p = >0.05$). When applying a time lag effect of temperature to the gametogenesis index, we observed two periods where the prior temperature was predicted to impact gametogenesis; these were at 8 months ($p = <0.001$) and 9 months ($p = <0.001$) prior. However, the R^2 values indicated that the model accounted for only 11.6% and 11.1% of the variance, respectively.

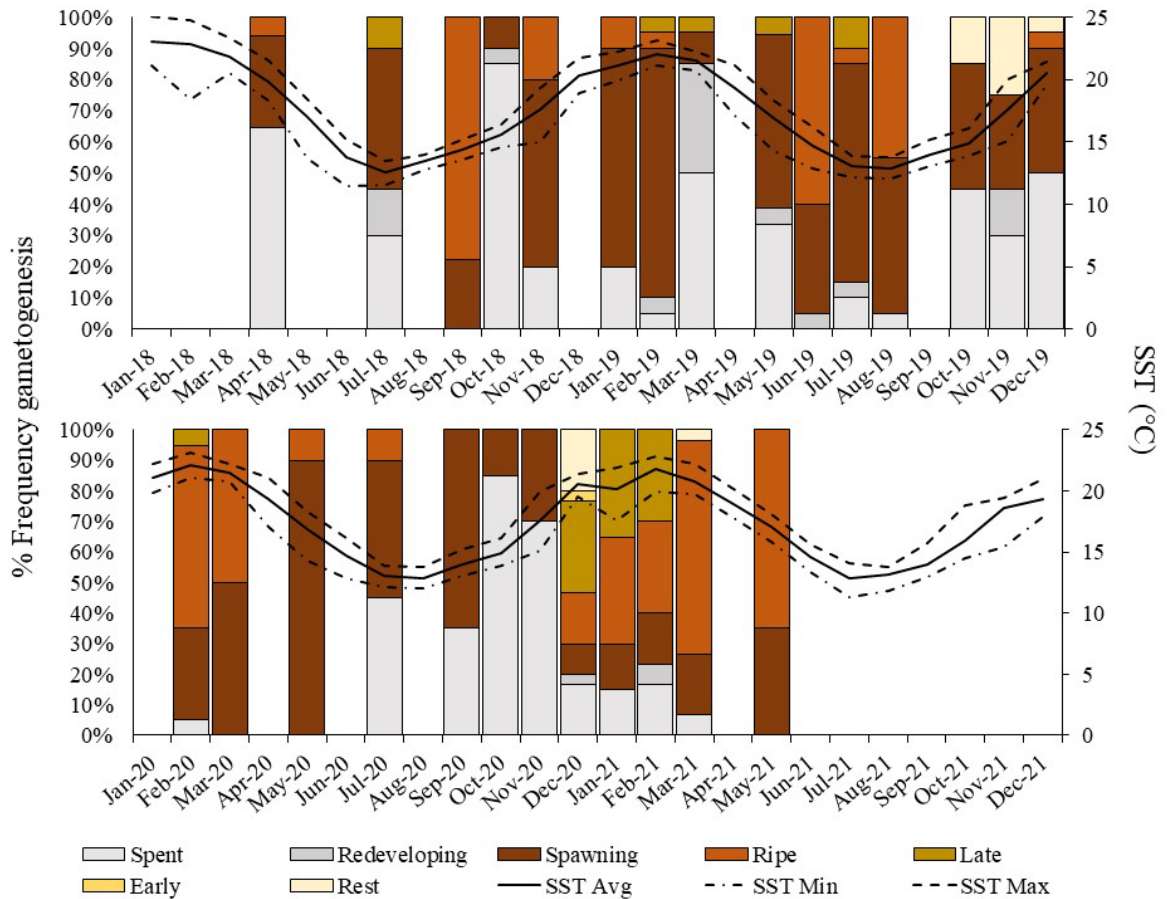


Figure 2.4 Percent gametogenesis stages showing annual reproductive cycle of green-lipped mussel from April 2018 to May 2021 (n = 570). The mean (solid line), maximum (dash) and minimum (dash and dot) sea surface temperature (SST) for each month is displayed for visual representation.

The estimated coverage (mean) of the gonadal follicles within the mantle tissue was also considered. The months where follicle coverage of the mantle was above 50% occurred between November 2018 to January 2019, May to June and August 2019. For the subsequent years, follicle coverage above 50% occurred from February 2020 to July 2020 and January 2021 to May 2021. Visual estimates of atresic oocytes vs. well-developed oocytes within the gonadal follicles using the grading criteria was also repeatable (Table. 2.2). The atresia appeared to affect the counts and therefore the percent coverage due to the occasional localisation of atresia in the follicles in one area of the mantle tissue resulting in a minimum or maximum value being outside of the allocated range.

The number of atresic oocytes counted in the female adult green-lipped mussels was of interest as only four females had a grade of 1. This indicates that atresia was relatively high even across each gametogenesis stage. The mean atresia grade at each stage was Rest: 3.7; Early: 3; Late: 2.5; Ripe: 3; Spawning: 2.9; Spent: 4.5; and Redeveloping: 2.5. No differences were detected in the atresia grade over time ($t = 0.947_{(568)}, p = 0.5$).

Table 2.2 The semi-quantitative grade, range and percent of atresic oocytes in a subset (n=87) of females where the range is the percent of atresic oocyte through visual microscopic estimates. The count is the number of females within the grade that underwent the image counting process to acquire the mean percentage.

Grade	Range atresia (%)	Count	Percent atresic oocytes		
			Mean \pm St Dev	Min	Max
1	>0 to 20	4	17.1 \pm 7.3	11.8	27.8
2	>20 to 40	15	30.8 \pm 7.5	20.0	45.3
3	>40 to 60	26	46.7 \pm 13.3	18.9	79.6
4	>60 to 80	18	70.5 \pm 9.9	52.1	89.2
5	>80 to 100	24	96.8 \pm 6.3	80.3	100.0

2.3.4. Pathogen and parasites

The 12 pathologies detected in the green-lipped mussels showed a change in prevalence and diversity over time. When reported as discrete months the prevalence appeared to increase in a more random pattern rather than with season and temperature (Fig. 2.5). Maximum temperature ($t=0.3_{(44)}, p>0.05$), minimum temperature ($t=0.4_{(44)}, p>0.05$), and mean temperature ($t=-0.34_{(44)}, p>0.05$) had no impact on the number of parasites. August 2019 was the month which had the highest number of pathogens detected. APX was at 100% prevalence. The type 1 bacteria were detected in 35% of the mussels. An *Endozoicomonas* – like organism (Bacteria type 2) was occasionally observed in the gills however it was also regularly detected in the epithelial layer of the gastrointestinal tract (tentatively assumed to be the same species). Furthermore, within August 2019 the population prevalence of *Perkinsus olseni* was observed to be 25%. The hydroid polyps (Fig. 2.5 and 2.6a) were regularly detected from July 2019 and an unidentified multinucleate parasite (Fig. 2.5 and 2.6 c - d) emerged in December 2019.

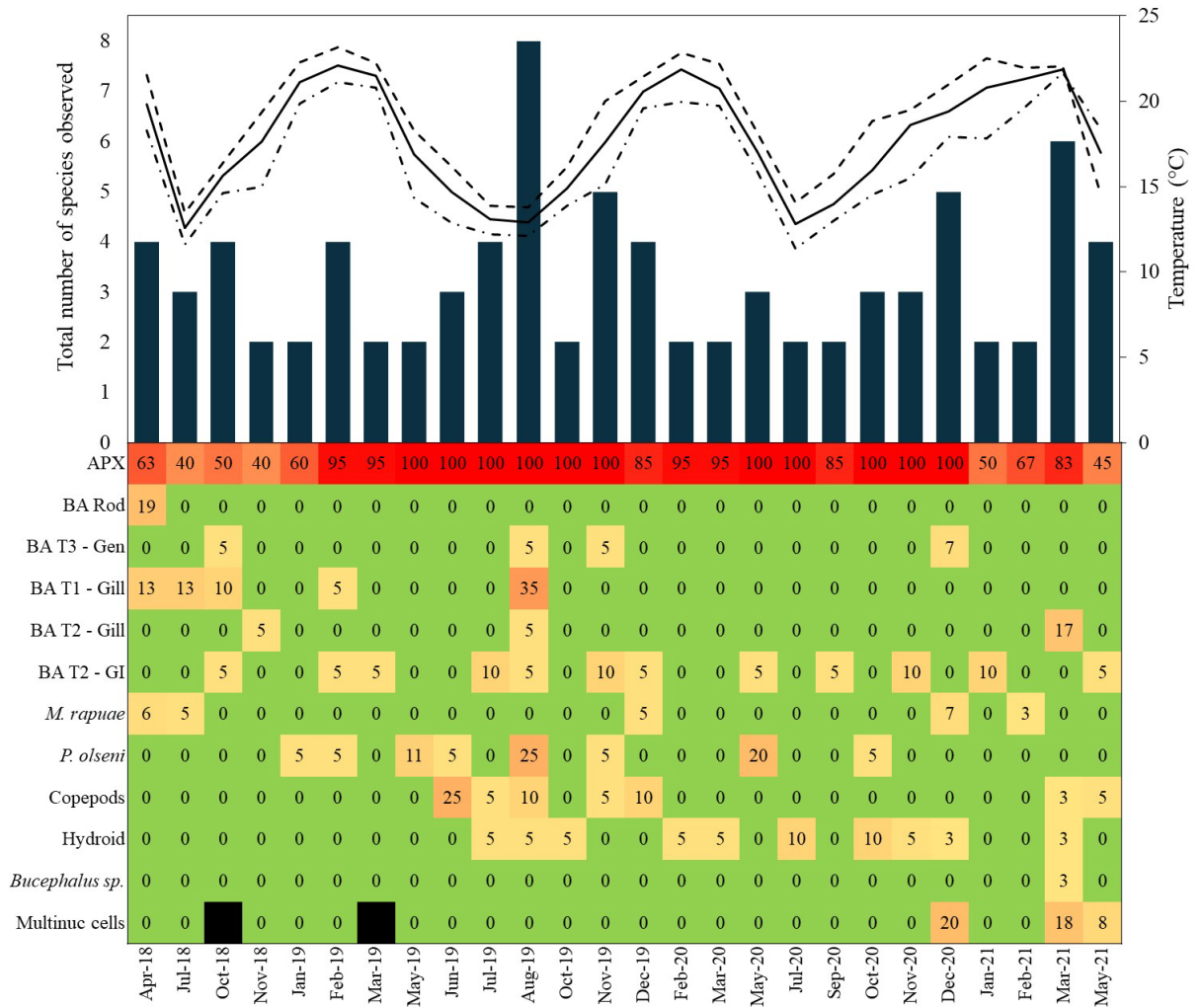


Figure 2.5 Percent prevalence (coloured grid), and total number (primary y-axis), of parasites and pathogens observed in adult green-lipped mussels (H&E histological slides) collected from April 2018 to May 2021. The average (solid line), maximum (dash) and minimum (dash and dot) sea surface temperature (SST) for each month during the sampling period is displayed for ease of visual representation (secondary y-axis). Apicomplexan- X (APX), rod bacteria in digestive gland connective tissue and mantle (BA Rod), rickettsia-like bacteria across tissue types was fine and shadowy in appearance (BA T3 – Gen), bacterial cocci cysts (rounded) in the gill (BA T1), *Endozoicomonas*-like organisms (BA T2) in the gill and the gastrointestinal tract epithelium (GI), *Microsporidium rapuae*, *Perkinsus olseni*, copepods in the gastrointestinal tract luminal space, hydroid polyps in the pallial cavity, *Bucephalus sp.* and multinucleate cells/bodies (multinuc cells).

Multinucleate bodies of an unknown parasite were observed in 6 of 570 mussels. However, kidney tissue was detected only in 142 mussels, giving a total population prevalence (percent) of 4.2%, thereby potentially underestimating the incidence of this parasite. Multinucleate bodies of the parasite were detected in the kidney tissue and associated with the heart tissue, but only occasionally associated with an infiltration of haemocytes. The multinucleate bodies ranged in length from 7.3 μm to 10.7 μm , width from 5.4 μm to 9.3 μm and had a range of nuclei numbers from 1 to 8 with the nuclei diameter = 1.96 μm \pm 0.21 μm (Mean \pm SD) (Fig. 2.6 c - d).

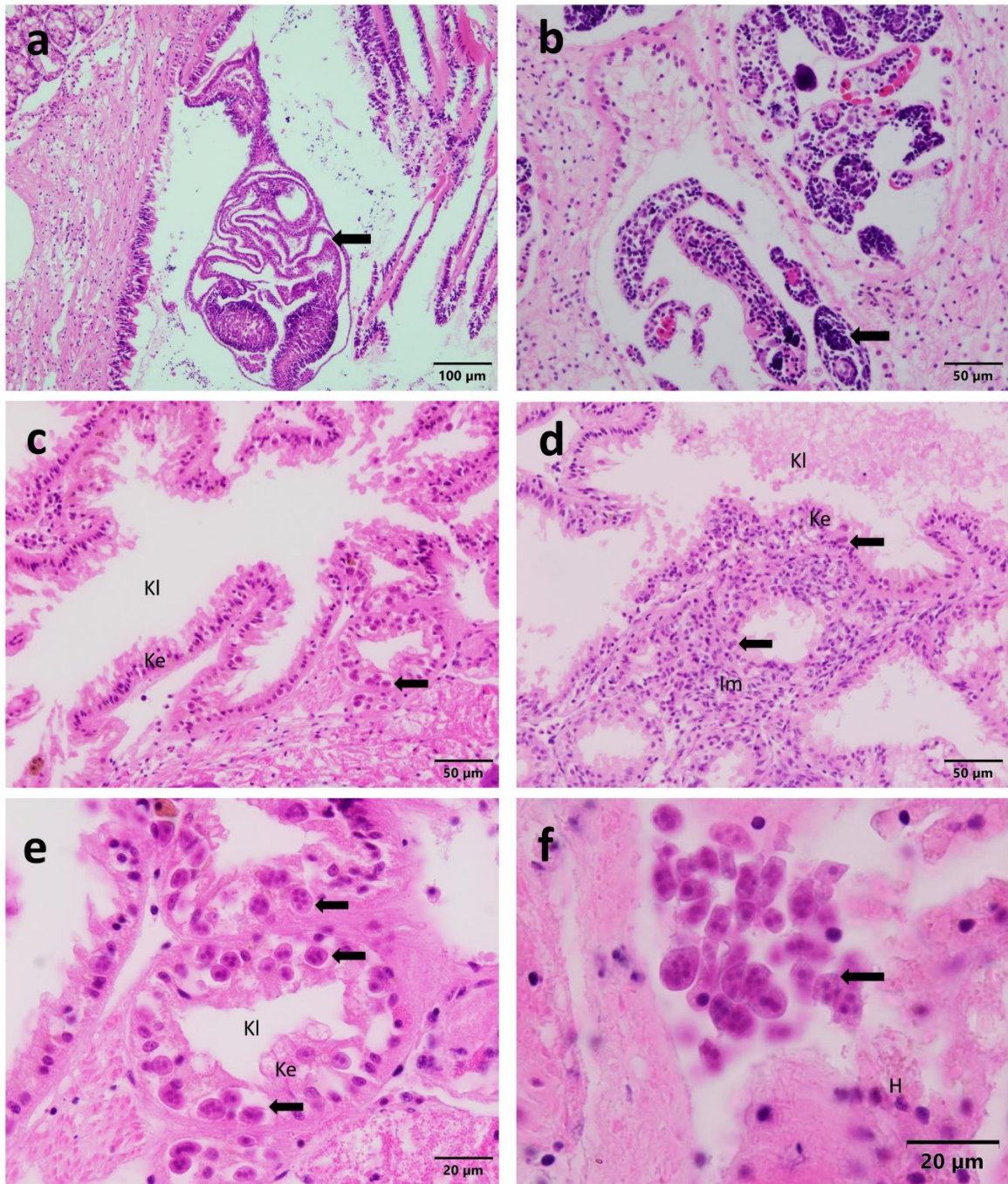


Figure 2.6 Two of the parasites detected in adult green-lipped mussels within this study during late 2020 and early 2021; a) hydroid polyps attached to external surface of mantle in the pallial cavity; and b) Sporocysts of *Bucephalus* sp. containing cercariae in mantle, and the new multinucleate parasite or bodies (arrows) detected in green-lipped mussel kidney and heart tissue; c) kidney tissue with high number of parasites transitioning through the kidney epithelial layer (Ke) with no associated immune response; d) kidney tissue depicting the immune response around the kidney epithelial (Ke) and kidney lumen (Kl) (scale = 50 μm); e) oil immersion showing the plasmodia of the haplosporidian-like parasite (arrows) transitioning through the kidney epithelial layer (scale = 20 μm) and; f) cluster of multinucleate plasmodia detected near the heart tissue (H) (scale = 20 μm).

The six selected samples were negative for *Perkinsus* spp. using the Perk ITS750/Perk ITS 85 generic primers. The 18S PCR was positive on two of the three histology samples selected which contained the unidentified parasite. From the metabarcoding approach the sequenced data contained a total of

131,090 reads. After data processing (i.e. filtering, paired-end merging, and removal of chimeric sequences) a total of 174 ASVs and 25,019 reads remained, an average of 12,509 per sample. Due to the nature of the samples (histology block), several groups were detected, including other pathogens in other tissues. Apicomplexa was the last common ancestor of the four main features (Table. 2.3).

Table 2.3 Sequencing results from gene blasting compiled bioinformatics of the 18S PCR of the 2 PCR positive FFPE mussel samples with the top three potential features for the multinucleate parasite. The top 1 to 2 closest species and the last common ancestor was recorded.

Feature ID	Accession number	Identity	E-Value	Query coverage	Closest species	Last common ancestor	Relative abundance
6f373dbe6cbc 5bcd6e50fa56 da154f77	MH375329.1	80%	2.00E-72	100%	<i>Cryptosporidium</i> sp.	<i>Apicomplexa</i>	5.1%
	MN493109.1	80%	2.00E-71	100%	<i>Theileria</i> sp.		
b5f996ff0a3d bccf46555b68 775554c1	MH532205.1	100%	0.00E+0	100%	uncultured bacterium clone OTU_8557	<i>Apicomplexa</i>	0.4%
	MW829618.1	80%	9.00E-71	97%	<i>Theileria</i> sp.		
ff198bffb3367 2bc2207a0238 fe9e23f	EF024723.1	88%	7.00E-72	100%	Heterocapsaceae	<i>Apicomplexa</i>	2.3%

2.3.5. Epidemiological triad: environment: host: pathogens

Kendall's rank correlation detected several negative and positive associations (Fig. 2.7). Some were expected such as focal haemocytosis aggregations of haemocytes in the mantle, digestive gland and kidney. Focal haemocytosis was also positively correlated with *P. olseni*. Ceroid in the mantle showed a weak positive correlation to gastrointestinal tract diapedesis and digestive gland haemocytosis and a strong positive correlation with APX. Tissue conditions such as general tissue atrophy, digestive gland atrophy and gastrointestinal tract diapedesis were also correlated to elevated apoptosis. Elevated apoptosis was also positively associated with the presence of *P. olseni*. Interestingly the undescribed multinucleate cell parasite was associated with haemocytosis in the kidney as well as a bacterium in the gill. The presence of hydroids was also associated with the *Endozoicomonas*-like organism in the gills.

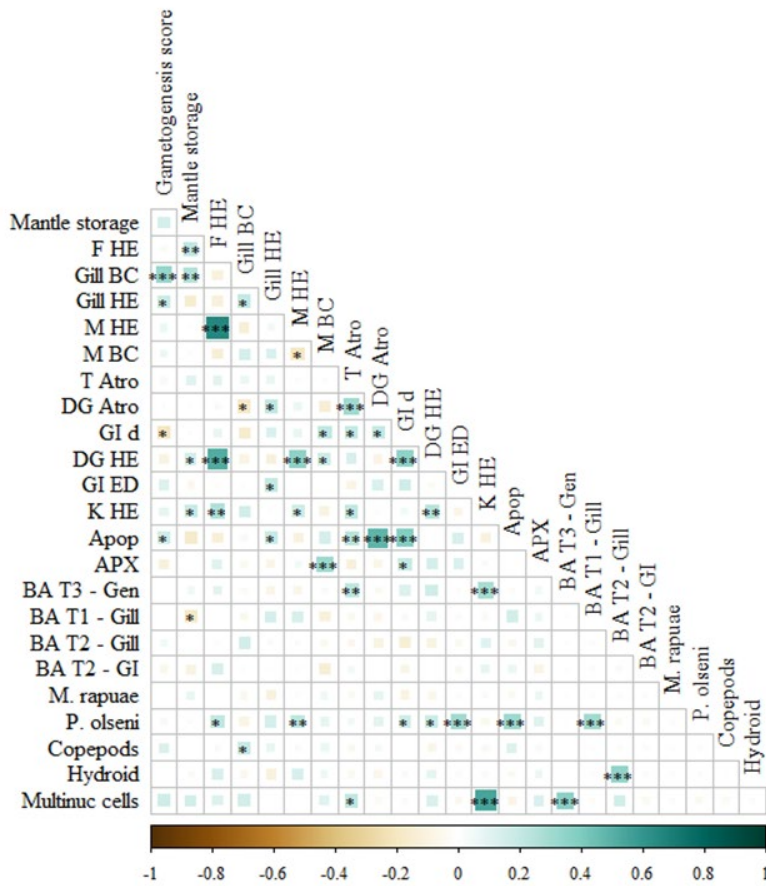


Figure 2.7 Kendall's rank correlation matrix of the tissue conditions, parasites and pathogens detected in green-lipped mussels during three years of sampling. Positive correlations are indicated green (> 0) and negative correlations in brown (< 0). Significant differences with a p value of < 0.05 are indicated by an asterisk (*). Strong significant differences < 0.005 are indicated by multiple asterisks (***)

The relationship between maximum temperature and mean parasite sum between gametogenesis ranks showed interesting patterns at the lower gonad maturation scores. There was a positive relationship with the number of parasite species detected increasing with temperature. Conversely, at the 'ripe' stage (score 3), the relationship appeared negative with a reduction in parasite numbers with increasing temperature (Fig. 2.8). Therefore, there was a statistically significant interaction between mean parasite sum, gametogenesis score and both mean and maximum temperature when mean parasite sum was considered as the response variable (Table. 2.4).

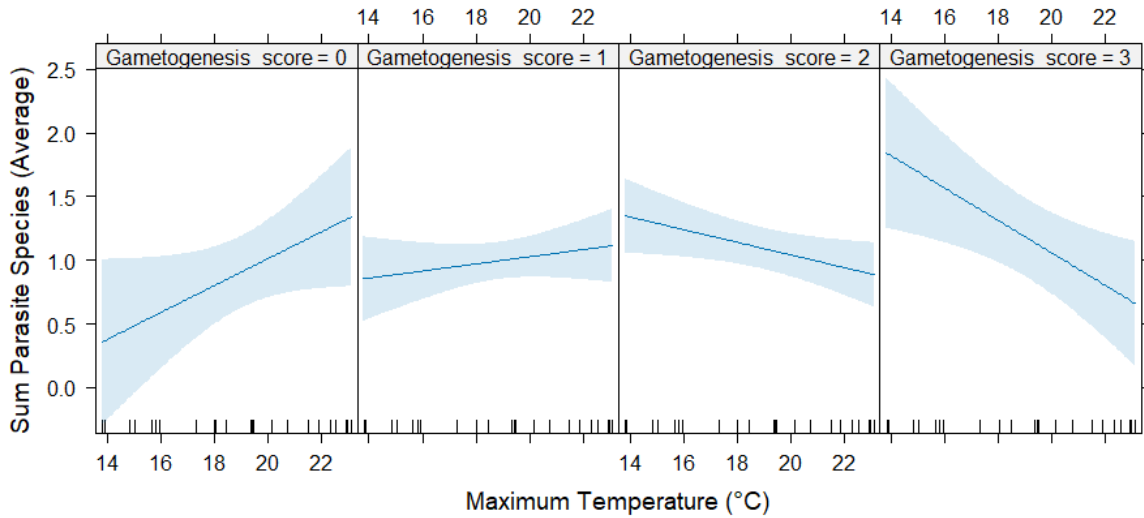


Figure 2.8 Predicted relationship of the maximum temperature and the mean sum of parasite species across each gametogenesis maturation stage (score 0 – 3) derived from the linear model.

Table 2.4 Linear model results showing interactions (indicated by *) and statistical results (significant results at p -values < 0.05). Shows the interactions for each of the key models

Response variable	Model (GLS)	Result	P value
Mean parasite sum	~ Mean gametogenesis * maximum temperature	Significant interaction	0.019
Mean parasite sum	~ Mean gametogenesis * minimum temperature	Not significant	0.07
Mean parasite sum	~ Mean gametogenesis * mean temperature	Significant interaction	0.033
Mean gametogenesis	~ Maximum temperature * mean parasite sum + date	Not significant	0.096
Mean gametogenesis	~ Maximum temperature + date	Not significant	0.882
Mean gametogenesis	~ Mean parasite sum + date	Not significant	0.202
Mean parasite sum	~ Maximum temperature * mean gametogenesis + date	Significant interaction	0.009
Mean parasite sum	~ Maximum temperature + date	Not significant	0.25
Mean parasite sum	~ Mean gametogenesis + date	Not significant	0.731

2.4. Discussion

This study presents a comprehensive 3-year assessment of green-lipped mussels health, reproduction and parasite presence sourced from a population established in the Coromandel region in NZ. Coarse satellite data indicated that temperatures during summer are frequently above 22°C for this region. Temperature anomalies are also regular occurrences, with summer marine heatwaves being detected in 2017/18 (Salinger et al., 2019), 21/22 (Montie et al., 2023), and 23/24. Reproduction appeared to be impacted by the heatwave in the summer of 2017/2018, with the gametogenesis cycle breaking down. This breakdown is based on the consistent appearance of ripe, spawning and redeveloping mussels, and the high level of atresia. The expected reproductive cycle patterns re-appeared after 2019 with a full spawn and resting phase late 2020.

Tissue pathology indicated that stress or immune defence also appeared to be more prevalent after the initial heatwave in 2017/2018, indicating poor health of the mussel population. Some of the tissue pathologies were also positively correlated to the gametogenesis stage and pathogens and parasites such as *P. olsenii*. There were several parasites and pathogens detected in the green-lipped mussels, which changed in diversity over time. An unfamiliar, potentially novel, multinucleate stage parasite was detected and tentatively placed in the Apicomplexa group. This multinucleate parasite was detected in December 2020 and again in 2021 and will require further investigation. Furthermore, pathogens and parasites such as *Endozoicomonas*-like organisms, hydroid polyps and *P. olsenii* were also regularly detected. Interestingly, the presence of parasites and pathogens appear less correlated to season. The lack of correlation could be related to the age of the mussels or unfavourable conditions for the parasites. Finally, during early reproductive development, parasite number appears positively correlated with temperature and subsequently becomes negatively correlated when mussels are ripe.

Sea surface temperatures are currently reaching maxima $\geq 25^{\circ}\text{C}$ around the NZ coastline (Delorme et al., 2024). This includes the Coromandel region, as presented in the current study. These warm temperatures ($25 - 26^{\circ}\text{C}$) approach critical thermal tolerance limits for green-lipped mussels (Benjamin et al., 2024; Ericson et al., 2023) and therefore increase the risk of summer mortality syndrome. Furthermore, it is now established that prolonged exposure above 22°C impacts reproduction and physiological condition (Benjamin et al., 2024; Copedo et al., 2023; Ericson et al., 2023). The trends in tissue pathology presented appeared higher in prevalence after the 2017/2018 anomalous summer marine heatwave. For example, the presence of higher-than-normal levels of haemocyte apoptosis and digestive gland tubule atrophy in green-lipped mussels appeared more prevalent in the year 2018, likely related to poor health associated to the preceding summer marine heatwave. Laboratory studies such as those by Delorme et al. (2021), Venter et al. (2023), and Ericson et al. (2023) are consistent with these pathologies, reflected as altered condition, shifts to anaerobic metabolism, alterations to haemocyte response (both increasing number and increasing apoptosis) when maintained at high temperatures $\sim 24^{\circ}\text{C}$. In addition to the tissue pathology, the presence of rod bacteria within the tissues indicates poor health post-heatwave of several mussels, also described by Muznebin et al. (2024).

It is well known that temperature influences molluscan immune defence, growth and survival (Angilletta Jr, 2009; Dunphy et al., 2018; Filgueira et al., 2016; Portner, 2002), with temperature playing a key role in reproductive cycling and synchronicity (Petes et al., 2007; Philippart et al., 2003), and pathogen emergence (e.g., Bignell et al., 2008; Burge et al., 2014; de La Rocque et al., 2008; Harvell et al., 2002; Lane et al., 2023). However, although temperature was a focus in the current study, it is not the only factor influencing the marine environment. The marine environment is inherently complex and multifactorial in nature, particularly at a local scale. For instance, the reference mussel population sampled in the current study is located in the Coromandel region, more

specifically the Firth of Thames. The Firth of Thames is a shallow, tidally dominated embayment with low wave action which is fed by the Waihou and Piako rivers (Boehnert et al., 2020). The land in this region has been considerably deforested for urbanisation, construction and agricultural activities (Boehnert et al., 2020; McLeod et al., 2014). Therefore, the mussels are likely to be exposed to large quantities of sediment, nutrients, urban contaminants (heavy metals, fertilizers etc), and other riverine inputs in addition to the thermal stress, seawater quality changes and food quality and quantity alterations (Fraser et al., 2021). The region also, historically, consisted of extensive mussel beds which supported a thriving marine ecosystem. However, the exploitation of the mussel beds resulted in a depletion of the natural population and a decline in benthic ecosystem health (Paul, 2012). Furthermore, there are now more than 100 mussel farms supplying approximately a third of the harvest in NZ to address the shortfall in supply (Paul, 2012). Based on the increasing frequency of warming waters, and fluctuating terrestrial influence, the mussel farms and the natural populations in Firth of Thames region are at further risk of physiological stress (Paul, 2012).

The changing environmental conditions impact reproduction and the complex environment- host-pathogen interactions. There was an interaction between the gametogenesis stage, parasite presence and maximum temperature, with parasite species numbers increasing with temperature. Both reproduction and immune responses are energy hungry processes and have typically evolved for optimisation rather than maximisation, therefore both are constrained, and trade-offs are often required (Brokordt et al., 2019). Reproduction, although impacted by sub-optimal environmental conditions, can also represent a confounding physiological stressor, particularly during spawning (Benito et al., 2022; Cuevas et al., 2015; Wendling and Wegner, 2013). For instance, in oysters and scallops' immune parameters decrease after spawning (Brokordt et al., 2019; Wendling and Wegner, 2013).

In the current study a prolonged period of ripe condition, trickle spawning, and redevelopment was observed during 2018 and 2019. After this period, the reproductive pattern was observed to be more cyclic and annual. This trickle spawning could be a strategy to minimise the energetic trade-off between reproduction and immune responses. Additionally, it is worth noting that full reproductive ripening of mussels in sub-optimal environments (such as warming waters and low quality and quantity of food), is only accomplished by a small number within the population (Bayne, 1976). Prolonged reproductive periods in green-lipped mussels are also common and have been observed by Alfaro et al. (2001) in the North Island of NZ. This differed from the two spawning periods (Spring and Autumn) observed in the South Island, NZ (Buchanan, 2001). This highlights the potential local differences between the mussel populations. The reproductive cycle, and therefore gametogenesis is regulated by exogenous factors, including temperature and food availability, presumably in conjunction with endogenous endocrine influence (e.g., Bayne and Thompson, 1970; Giese and Pearse, 1974; MacDonald and Thompson, 1986; Oyarzún et al., 2016; Thorarinsdóttir and Gunnarsson, 2003). Abrupt temperature, salinity or food changes, such as those occurring during the

spring and autumn, trigger spawning events and oocyte atresia in many bivalves (e.g., Alfaro et al., 2001; Hawkins and Bayne, 1985; Hooker and Creese, 1995).

Most bivalves cannot spawn all of their oocytes and remaining oocytes are generally reabsorbed or recycled by follicle cells, typically characterised by oocyte atresia (Beninger and Le Pennec, 2016; Eckelbarger and Hodgson, 2021; Le Pennec et al., 1991). Additionally, bivalves can reabsorb oocytes and undergo “pre-spawning atresia” which occurs in earlier stages of gametogenesis under suboptimal conditions. This has been observed in the cockle *Cerastoderma edule*, whereby throughout gametogenesis approximately 30% of the oocyte volume was atresic and considered non-viable (Chérel and Beninger, 2019). In the current study the percent coverage of atresic oocytes was also relatively high and up to 40-60%, even in females considered as ‘late’ or ‘ripe’. This could be due to continuous gametogenic activity, which is also reflected in the prolonged ripe and spawning phases. The high intensity of atresia also highlights a potential overestimation of fecundity as observed in other species (Chérel and Beninger, 2019). Further research is required to characterise oocyte atresia and elucidate whether the observed is typical or a result of sub-optimal conditions and the pathogen/parasite presence.

No substantial tissue pathologies were detected. Although minor haemocytosis, tissue atrophy and diapedesis were occasionally associated with *P. olseni*. Interestingly, the prevalence of *P. olseni* was lower than expected, based on previous research by Muznebin et al. (2022), with results similar to Lane et al. (2023). These differences could be influenced by the relative sensitivity of the techniques used. In Muznebin et al. (2022), in-situ hybridisation staining techniques were used which allows for easier detection of low presence compared with traditional hematoxylin and eosin (H&E). Targeted *P. olseni* specific PCR of all the samples, fresh and formalin fixed, would likely provide a more accurate population prevalence. Therefore, sampling for, targeted and non-targeted, PCR and histology are recommended for future investigations.

Several other pathogens and parasites were also detected in the histology and the bioinformatic analysis, which are of interest for future research. Firstly, the *Endozoicomonas*-like organism (Bacteria type 2, ‘ELO’) detected in the gills and the gastrointestinal tract epithelium, which has previously been reported in the gills of the pipi (*Paphies australis*) by Bennion et al. (2021) and Howells et al. (2021). In the current study there was no host response, and it appeared to be present regardless of season. Interestingly, although ELOs have occasionally been associated with mortality events in pipis it has been suggested by Bennion et al. (2021) and Li et al. (2022) that they potentially participate in antimicrobial production which could play a role in gastrointestinal health.

Secondly, the hydroid polyps which were attached to the mantle in the pallial cavity. Hydroid polyps have been detected in pipis and tentatively identified as *Eugymnanthea* sp. by Howells et al. (2021). Reports of *Eugymnanthea* sp. and *Eutmima* sp. have also occurred in several regions including Japan,

Taiwan and the Mediterranean in bivalves such as *Mytilus* sp. and *Mizuhopecten* sp., with varying impacts on the host (Baba et al., 2007; Kubota, 1992; Piraino et al., 1994).

Thirdly, the unknown parasite detected in the kidney and heart tissue, was tentatively placed in the Apicomplexa family using metabarcoding techniques. In a review of pathogens and parasites detected using histology in green-lipped mussels between 2007 and 2017, Webb and Duncan (2019) did not describe this pathogen, suggesting this may be a novel species.

Finally, the DNA sequencing and metabarcoding detected *Cryptosporidium* sp. and *Theileria* sp., both of which are parasitic to cattle. These parasites weren't specifically sought or detected histologically. *Cryptosporidium* sp. is a widespread protozoan parasite in NZ which is commonly detected during flood events (Garcia-R and Hayman, 2023). This detection could represent freshwater contamination and increased sedimentation from the riverine inputs and could be exacerbated in the presence of other stressors, such as increasing temperature. Furthermore, reduced salinity (25-35ppt) has also been considered as optimal for *P. olsenii* zoosporulation (La Peyre et al., 2006). The combination of warming waters and reduced salinity could represent a significant risk to the proliferation and increasing prevalence of *P. olsenii* in green-lipped mussels.

Interestingly, in the current study the pattern of parasite presence appeared to be less well defined across time, even though they are known to exhibit seasonal patterns in other bivalve species (Burge et al., 2014; de La Rocque et al., 2008; Harvell et al., 2002). The lack of seasonal pattern is most likely related to the complex interactions of reproductive condition, the health of the mussels, and the environmental conditions. Reproductive stage and maximum temperature did have a positive influence on the number of parasites detected, however, there appeared to be no patterns observed in response to season. Baseline sampling data for green-lipped mussels and its parasites is limited and should be made a key priority to enable prediction of pathology trends (Lane et al., 2020).

The typical hypothesis is that rising seawater temperatures will enhance pathogen and parasite population densities due to the ability to complete their lifecycle more rapidly (Costello et al., 2021; Löhmus and Björklund, 2015; Marcogliese, 2001; Masanja et al., 2024). The sub-optimal environment will then reduce the host health, making them more vulnerable to infection. Conversely, there are other parasites that may reach their thermal optima. For instance, some hydrozoan medusas are observed to show greater production in warmer waters, while others displayed population declines (Purcell, 2005). Interestingly, the prevalence of the hydroid *Eugymnanthea* sp. in other bivalve populations has previously been reported as higher in dense bivalve populations in confined locations, yet no impact on reproductive condition has been observed (Mladineo et al., 2012). Furthermore, growing mussels typically accumulate more parasites as they age (Coen and Bishop, 2015; Sorensen and Minchella, 2001); however, the mussels in the current study were relatively young, approximately 12 to 18 months old, and may be healthy enough to defend against the parasites. It may also be that these seasonal patterns occur only in older mussels. Continued

investigation is required to elucidate this lack of seasonal variation, particularly when parasites such as *P. olsenii* are known to thrive in warmer waters (Villalba et al., 2004). Furthermore, disentangling the effect of multiple stressors on host pathogen interactions is critical in understanding future impacts on key species (Reid et al., 2019; Riebesell and Gattuso, 2014). It should also be noted that most studies such as this one occur in populations associated to aquaculture activities, due to the relative ease with which sampling can be standardised. As such the natural populations are largely ignored unless there is a large-scale mortality event. Therefore, impacts to reproductive condition and parasite presence in wild populations may go unnoticed and understudied (Lane et al., 2020), or even be misinterpreted.

2.5. Conclusion

With sea surface temperatures reaching 25°C green-lipped mussels are at risk under future warming scenarios in the Northern region of NZ. It was observed that poor health and reproductive condition in the reference population were impacted by the initial 2017/18 summer marine heatwave. The present study is the first long-term histological gonad staging report for green-lipped mussels naturally exposed to the changing NZ coastal climate of recent years. Reproduction was impacted and is likely to continue to be impacted due to the increasing number of days spent above 22 °C. Continued monitoring of the reproductive condition, and the effect multiple stressors has on it, is essential to the future success (survival) of commercial, green-lipped mussel populations. Similarly, although green-lipped mussels experience very few diseases in comparison to other mussels worldwide, this may change particularly with reports of parasites and pathogens such as the hydroids and the multinucleate kidney parasite. The present study therefore underlines the critical role of histological monitoring in the early detection of emerging conditions and pathogens that could impact mussel populations.

CHAPTER 3. HISTOPATHOLOGICAL INVESTIGATION OF FOUR POPULATIONS OF ABALONE
(*HALIOTIS IRIS*) EXHIBITING DIVERGENT GROWTH PERFORMANCE: PART A

Published in its entirety in Journal of Invertebrate Pathology:

Copedo, J. S., Webb, S. C., Ragg, N. L. C., Venter, L., Alfaro, A. C., (2023). *Histopathological investigation of four populations of abalone (Haliotis iris) exhibiting divergent growth performance. Journal of Invertebrate Pathology. Vol, 202. <https://doi.org/10.1016/j.jip.2023.108042>*

Abstract

The black-foot abalone (pāua), *Haliotis iris*, is a unique and valuable species to New Zealand with cultural importance for Māori. Abalone are marine gastropods that can display a high level of phenotypic variation, including slow-growing or ‘stunted’ variants. This investigation focused on identifying factors that are associated with growth performance, with particular interest in the slow-growing variants. Tissue alterations in *H. iris* were examined using histopathological techniques, in relation to growth performance, contrasting populations classified by commercial harvesters as ‘stunted’ (i.e., slow growing) and ‘non-stunted’ (i.e., fast-growing) from four sites around the Chatham Islands (New Zealand). Ten adults and 10 sub-adults were collected from each of the four sites and prepared for histological assessment of condition, tissue alterations, presence of food and presence of parasites. The gut epithelium connective tissue, digestive gland, gill lamellae and right kidney tissues all displayed signs of structural differences between the slow-growing and fast-growing populations. Overall, several factors appear to be correlated to growth performance. The individuals from slow-growing populations were observed to have more degraded macroalgal fragments in the midgut, increased numbers of ceroid granules in multiple tissues, as well as increased prevalence of birefringent mineral crystals and haplosporidian-like parasites in the right kidney. The histopathological approaches presented here complement anecdotal field observations of reduced seaweed availability and increased sand incursion at slow-growing sites, while providing an insight into the health of individual abalone and sub-populations. The approaches described here will ultimately help elucidate the drivers behind variable growth performance which, in turn, supports fisheries management decisions and future surveillance programs.

3.1. Introduction

The New Zealand (NZ) black-foot abalone, *Haliotis iris* (Gmelin, 1791), locally known as pāua, is one of three haliotid species commonly found around the NZ rocky shores at depths of approximately 15 metres, typically between 0.5 and 7 metres (Poore, 1973; McShane et al., 1994). Since the early 1990s, *H. iris* has been gaining a foothold as a key aquaculture species and is still an important wild fisheries species for NZ.

Abalone have a mostly sedentary lifestyle and feed on various attached and drifting seaweed (Poore, 1972; Allen et al., 2006). Due to this limited mobility, they are exposed to several environmental stresses, and their diet is dependent on local supply and hydrographic processes, such as tidal currents (Poore, 1972; Allen et al., 2006; Laferriere, 2016; Morash and Alter, 2016). They occupy varied habitats that can be considered optimal or sub-optimal. Correspondingly, *H. iris* can show a large variation in morphology and growth phenotypes (Saunders et al., 2008; Saunders et al., 2009b), which may reflect the presence of slow-growing or ‘stunted’ populations (Naylor and Andrew, 2004; Naylor et al., 2007; Saunders et al., 2008; Saunders et al., 2009a; Laferriere, 2016).

Stunted populations show chronic slow growth, which results in reduced size-at-age when compared with ‘normal’ growing populations (Wells and Mulvay, 1995; Saunders et al., 2008). Growth suppression can be most apparent in the shell profile, or the shell length: height ratio, resulting in relatively high and wide individuals compared to their non-stunted conspecifics (Saunders et al., 2009a). The changes in shell morphology are likely to reflect diminished longitudinal calcite layer growth, while accretion of the inner nacreous layer continues. There are specific areas along the North and South Islands of NZ where abalone populations do not reach the minimum legal fishing size limit of 125 mm shell length; these are generically referred to as ‘stunted’ populations (McShane et al. 1994, Naylor et al. 2006). This phenomenon has been observed in a number of mollusc species, including mussels (e.g., *Mytilus galloprovincialis*, Hine, 1997), oysters (e.g., *Crassostrea gigas*, Hine, 1997; Kang et al., 2010), the land snail, *Patera appressa* (Martin and Bergey, 2013), the abalone, *Haliotis rubra* (Saunders et al., 2008) and *H. iris* (McShane and Naylor, 1995; Saunders et al., 2009b), as a result of complex environmental interactions. ‘Stunted’ abalone occur around NZ and can typically be found in sheltered areas protected from wave action, which typically have low flow, reduced complexity in terms of substrate topography (Laferriere, 2016), and low seaweed abundance (Saunders et al., 2009b). In sheltered areas with low wave action, sediment will also accumulate (Schiel et al., 2006). Non-stunted *H. iris* can generally be found in areas with higher wave action, increased food and topographic complexity, where drift seaweed may collect (Saunders et al., 2009b; Laferriere, 2016).

The complex relationship of extrinsic and intrinsic drivers affects the growth rate of marine molluscs (Ren et al., 2019; Saulsbury et al., 2019). The range of these factors is diverse and not only includes the quality and the quantity of food, but also water quality parameters, such as temperature, water velocity, salinity, and pH (Diggles et al., 2002; Searle et al., 2006; Bergström and Lindegarth, 2016), as well as reproductive state, immune response and parasite association (Diggles et al., 2002; Morash and Alter, 2016; Wu et al., 2018). Variations between these factors are likely to result in morphometric variation within a species (Ren et al., 2019). The two most well-studied predictors of growth rate are food availability and temperature (Saulsbury et al., 2019). Sedentary marine invertebrates have been reported to display high variations in morphology associated with responses to environmental stresses (Trussell, 1996; Steffani and Branch, 2003; Saunders et al., 2009b). Coastal

ecosystems are often highly impacted by increasing environmental stresses underpinned by climate change (Halpern et al., 2008; Lima and Wetthey, 2012). Global sea surface temperature trajectories indicate that most coastlines are experiencing less frequent cold days and a significant increase in marine heatwaves (Halpern et al., 2008; Lima and Wetthey, 2012). These environmental stresses not only drive habitat alterations but may result in episodes of mass mortalities of invertebrates and could have enduring negative impacts on populations (Soon and Ransangan, 2019).

The Chatham Islands (43°53'S, 176°31'W) lie in an oceanic convergence zone, influenced by both colder southern water and warmer northern water, having predominantly a temperate climate (Wilcox, 2007). The islands (commercial area PAU4) support the largest abalone fishery in NZ. Both 'stunted' (slow growing) and 'non-stunted' (fast-growing) populations around the Island within the commercial fishery have been observed by divers and fisheries managers and there is a growing concern for the future performance of local *H. iris* populations. Additionally, the reduced growth to minimum legal catch size results in light catches and dense population numbers. Therefore, it is crucial to understand the causes of divergent growth performance in wild populations of *H. iris*, especially with regards to the complex abalone-environment interactions and potential role of pathogens. In the current study, histopathological tools were used to compare tissue alterations on four populations of abalone to investigate tissue-level responses and potential ecological causes of the observed variation in growth performance.

3.2. Methods:

3.2.1. Sampling locations and animal collection

The Chatham Islands are located approximately 800km east of New Zealand's South Island. Four geographically distinct sites were selected based on the growth performance differences among resident abalone populations established by monitoring within the commercial fishery (Fig. 3.1).

Sites were characterised based on direct observations, growth performance and commercial abalone harvest performance (historic data and personal communications: Pāua Industry Council Ltd)

Site 1 (Ascots) supports an abalone population of 'fast-growing' individuals that readily reach the legal fishing size of 125 mm and are therefore fished more often. The site was characterised as having spaces of bare rock and sand with a high density and diversity of seaweed, with dominant resident species, including green (e.g., *Ulva lactuca*, *Chaetomorpha coliformis*), brown (e.g., *Zonaria turneriana*, *Cystophora scalaris*) and red (e.g., *Gigartina clavulatum*) macrophytes, with an abundant supply of mixed drift algae (unpublished observations, March 2020).

Site 2 (Owenga harbour) had a dense abalone population of 'stunted' individuals, with very few reaching the legal catch size. The habitat was characterised as having extensive bare rock and sandy areas with low seaweed diversity and density, the dominant species being the chlorophyte *Ulva lactuca* and phaeophytes (e.g., *C. scalaris*).

Site 3 (Durham) was considered to have ‘stunted’ growth performance. The site had areas of bare rock and gravel. Seaweed density and diversity was intermediary between sites 1 and 2, dominated by phaeophytes (e.g., *C. scalaris*) and chlorophytes (e.g., *U. lactuca*, drift and attached)

Site 4 (Wharekauri harbour) was considered ‘fast-growing’. The site was characterised by extensive bare rock. The dominant seaweed species being the brown kelp *Durvillaea chathamensis* with representatives of other phaeophytes (e.g., *C. scalaris*) and chlorophytes (e.g., *U. lactuca*).

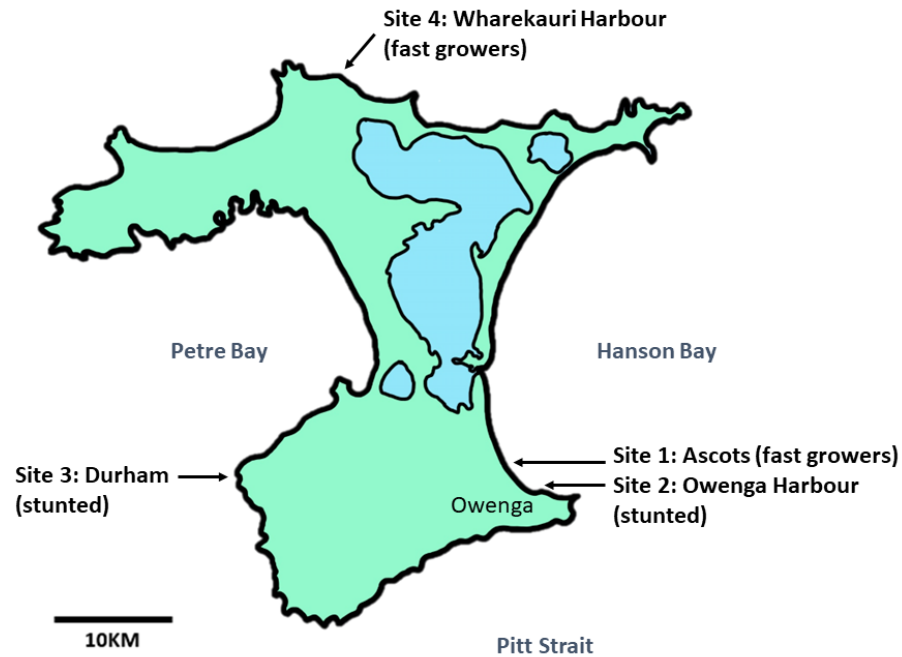


Figure 3.1 Generalised map of Chatham Island (43°52'49.7" S 176°32'02.6" W) depicting the four selected ‘stunted’ or ‘fast-growing’ sites selected for sampling. Site 1: Ascots (44°00'56" S 176°23'12" W); Site 2: Owenga harbour (44°01'28" S 176°21'56" W); Site 3: Durham (44°00'24" S 176°40'54" W) and Site 4: Wharekauri Harbour (43°42'18" S 176°35'04" W).

A total of 10 adults (pāua identified to be >110 mm, >250 g live mass) and 10 sub-adults (Pāua identified to be <110 mm, <250 g) were randomly collected by divers from each of the four sites in sets of 10 over 3 days for surveillance. The adult and sub-adult groups are termed as life stage throughout the thesis. Individuals were measured to the nearest 0.1 mm for shell length (SL) and weighed to the nearest 0.1 g (W), followed by retrospective measurements of shell width (SW), shell height (SH) and calculation of the SL: SH ratio before sampling and histological preparation. Sampling per individual occurred within 15 min. Additionally, the sex of each individual pāua was recorded and confirmed using histological techniques, and both percent population reproductively active and the F:M sex ratio was reported.

3.2.2. Histopathological preparation

Tissue was removed from the shell to expose the organs and the viscera dissected and sectioned as shown in Figure 3.2. The sectioned samples (midgut, digestive gland, left and right gill, left and right

kidney) were carefully placed into histological cassettes and fixed in a 4% formalin solution (1:9 v/v, 37% Formaldehyde:0.35µm filtered seawater) for 48 hours before being transferred into 70% ethanol for processing (Howard, 2004). Samples were dehydrated, cleared, and embedded in paraffin wax, sectioned (3-5µm) using a microtome and stained using routine hematoxylin and eosin (H&E).

A range of tissues were examined under a compound light microscope (Olympus BX40) at magnifications from x40 to x1000, including midgut, digestive gland, gills, gonad, kidneys, hypobranchial gland, nervous tissue, and muscle. Semi-quantitative scales were devised and used to grade deviations from normality for the midgut, digestive gland, gill, and right kidney (see below sections 2.2.1. to 2.2.4.).

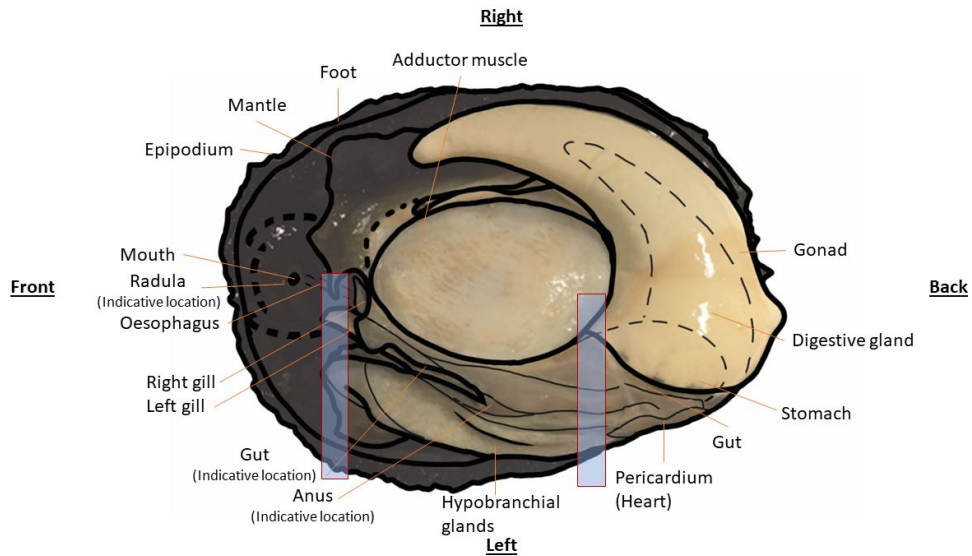


Figure 3.2 General anatomy depiction of New Zealand abalone (*Haliotis iris*). Rectangular windows show approximate location of the histology sections, which were chosen to maximise chances of acquiring all tissue types, including midgut, digestive gland, left and right gill, gonad, left and right kidney, hypobranchial gland, nervous tissue, and muscle.

Initial surveillance revealed tissue anomalies between the 'stunted' and fast-growing populations. The anomalies were observed in the stomach/crop (in relation to algae condition), digestive gland, gill, and right kidney and these tissues were therefore targeted for this investigation.

3.2.2.1. Midgut: Food scoring and subepithelial analysis

Gut contents were scored semi-quantitatively across the samples of the posterior section of midgut. Only food items that were clearly inside the crop/stomach region were scored using a subjective criterion on a grade scale from 1 to 5. Grade 1 = 100% Fresh, Grade 2 = 75% Fresh: 25% Old, Grade 3 = 50% Fresh: 50% Old, Grade 4 = 25% Fresh: 75% Old, Grade 5 = 100% Old. 'Fresh' algae fragments were large and retained cellular structure (Fig. 3.3a), 'Old' algae describes a mixture of fine debris and degraded algae cellular structure (Fig. 3.3b)

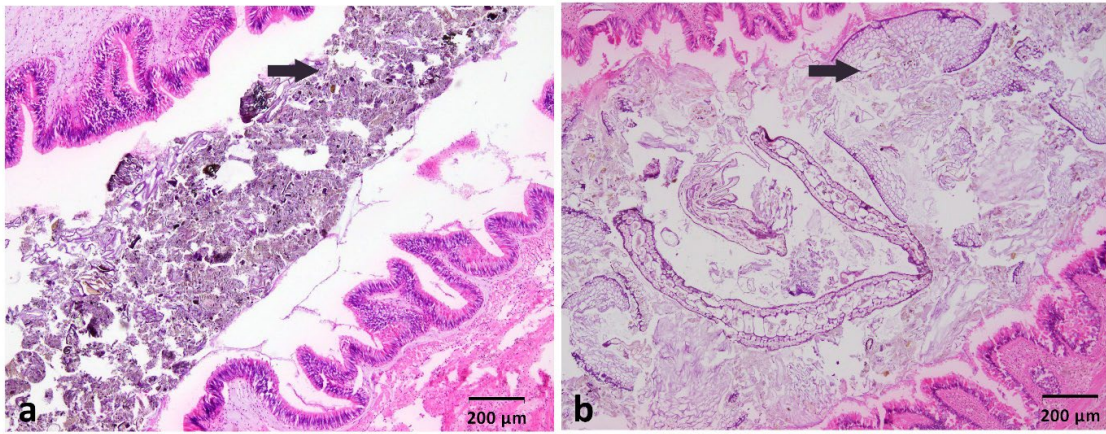


Figure 3.3 Photomicrographs of the crop/stomach region of *Haliotis iris*. a) Grade 5: ‘Old’, where algal material has broken down to fine particles of grey-coloured debris (arrow). b) Grade 1: ‘Fresh’, where structure of the algae is still largely intact and cells still visible (arrow).

The presence of ceroid granules (a brown oxidised lipid material) was scored semi-quantitatively based on level of accumulation within the interstitial tissue of the gastrointestinal tract, digestive gland, and kidney. Histopathological alterations (i.e. ceroid granules) were categorised as described by Costa et al. (2013) and Muznebin et al. (2022a) with minor modifications. In brief, ceroid granules were categorised by level of severity 0: None observed, 1: Mild (light or occasional scattering), 2: Moderate (light scattering with occasional focal dense patches) and 3: High, (dense, diffuse, and frequent patches) (Fig. 3.4).

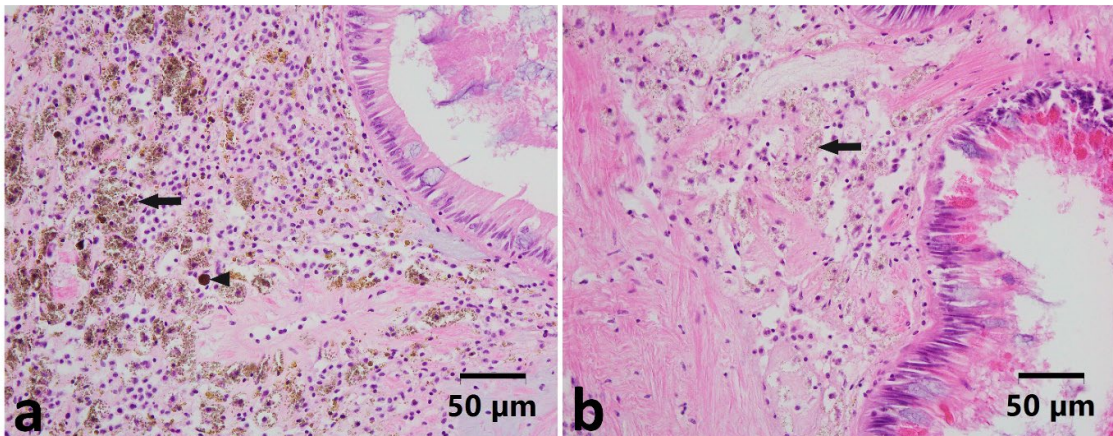


Figure 3.4 Mid-gut sub-epithelium from a) slow-growing individual (site 2: Owenga harbour) showing the high level (score 3) of ceroid material presence, and b) fast-growing individual (site 1: Ascots) showing minimal ceroid material (score 1). Examples of fine ceroid granules (Arrow) and ceroid aggregate (Arrowhead) are marked.

3.2.2.2. Digestive gland scoring

Criteria were developed to semi-quantitatively score the severity of the alteration in the digestive gland tubules, refining a general alteration scoring system proposed by Knowles et al. (2014), Fraga et al. (2022) and Perez-Cebrecos et al. (2022):

Criterion 1: The proportion of tubules (coverage) with separation of digestive epithelium from the basement membrane. Score of 0 = No spaces seen (Fig. 3.5a), Score of 1 = Less than 25% of epithelial cells had spaces, Score of 2 = Between 25 and 50%, Score of 3 = Between 50 and 75%, Score of 4 = More than 75% were shown to have spaces.

Criterion 2: A gauge of the extent of separation on each tubule (extent): Score of 0 = No spaces, Score of 1 = Less than 25% of the tubule is retracting, Score of 2 = Between 25 and 50% tubule retraction, Score of 3 = Between 50 and 75% tubule retraction, Score of 4 = More than 75% of the tubule was shown to have retracted away from connective tissue (Fig. 3.5b).

Criterion 3: The quality of the digestive tubule (termed ‘DG quality’) was determined by the following factors: 1. alteration of the basophilic pyramidal cells (Shumway and Parsons, 2011; Cuevas et al., 2015), as well as 2. the staining affinity of these cells, 3. lumen shape, 4. increased number of ceroid granules within the tubule wall, 5. level of haemocytes near connective tissue and 6. presence of oedema in interstitial spaces. A score of 0: apparent normality (Fig. 3.5a), 1: minor alterations to tissue architecture, 2: 1/2 of the tissue architecture impacted and/or displayed 2 - 4 of the 6 factors above, 3: 3/4 of tissue affected and 4 to 6 of the factors above observed, 4: whole tissue structure affected and 4-6 of the factors observed was applied (Fig. 3.5).

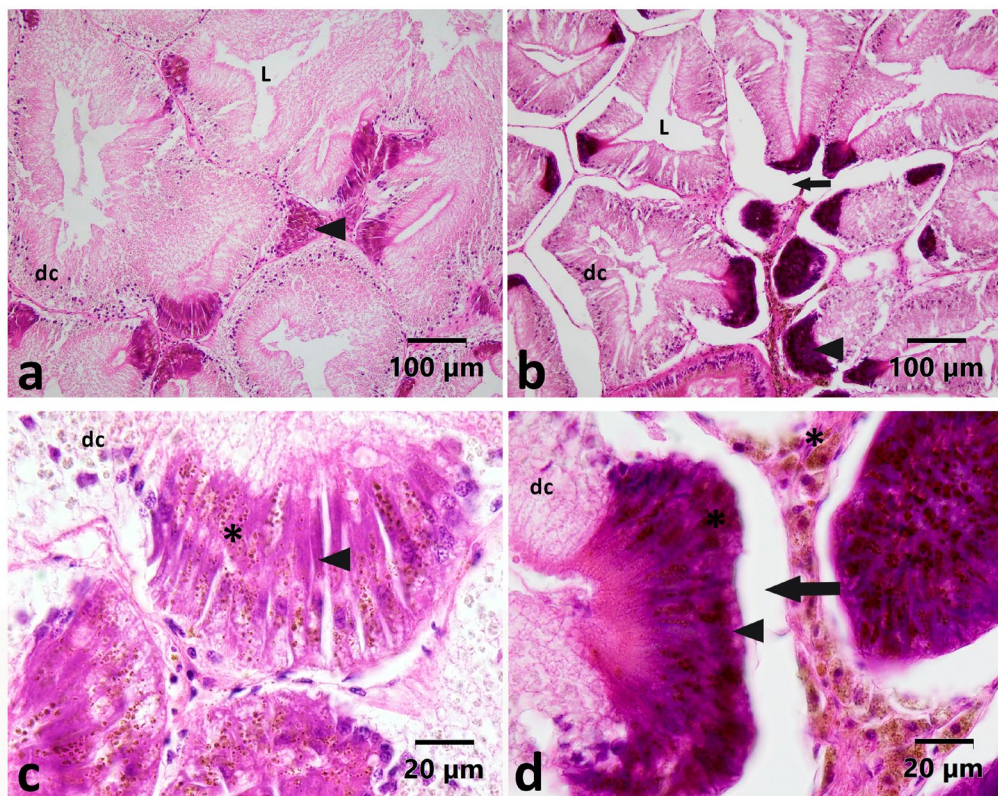


Figure 3.5 Scoring criteria to quantify the severity of the alterations in the digestive gland tubules of *Haliotis iris*. a) Normal digestive gland tissue whereby none of the digestive tubules are showing signs of gaping and all are tightly packed (Score 0). b) Digestive gland tissue showing signs of gaping away from basement membrane (Score 3) and poor-quality tubules (DG quality score 3) displaying changes to basophilic cells and increased staining affinity, developing space in interstitial space and increased haemocytes (arrow). Digestive tubule lumen (L), digestive cells (dc) and basophilic cells (arrowhead) of the digestive tubule epithelial layer are indicated. c) Zoom of digestive gland (a)

showing connection of the epithelium to the basement membrane. Section shows pink/purple-toned basophilic cells (arrowhead), a light scattering of ceroid granules (star) in basophilic cells. d) Zoom of image b showing separation of epithelium from the basement membrane creating a void (arrow), compression of the basophilic pyramidal cells and an increase in ceroid material in both the basophilic cells and interstitial tissue.

3.2.2.3. Gill

The gills were screened for pathogens and abnormalities. The number of ciliates per frame was counted to characterise the alterations observed in gill tissue. An 1857 x 3308 μm frame at 40x magnification was selected as the optimal area to include the full lamella length (Fig. 3.6). The counts were then converted to a standardised value per 1mm² of lamella cross-sectional area. This approach represents a refinement of standard surveying performed at 200x magnification. To validate the use of the larger frame size, five individuals were randomly selected for further analysis. Ciliates in five random sections of gill at 200x were counted and averaged. It was observed that the mean of 5 smaller frames leads to greater variation in the estimated number per mm² due to non-homogenous focal presence of the ciliates, indicating that a single large frame introduced less risk of bias.

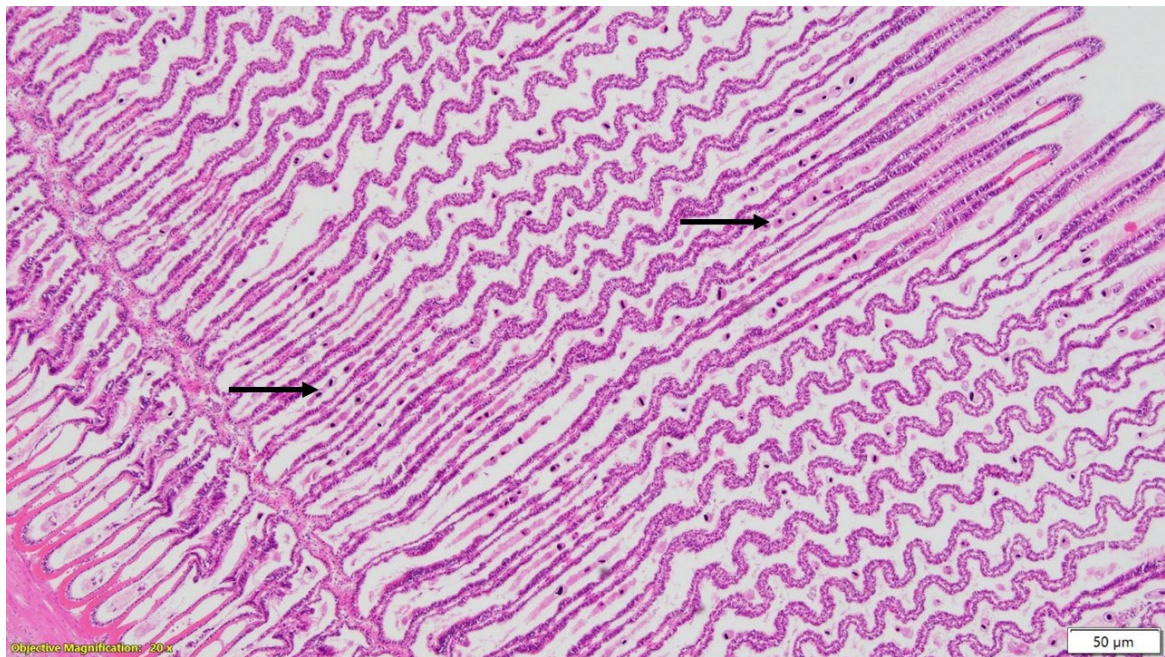


Figure 3.6 Example photomicrograph (Frame size: 1857 x 3308 μm) of *Haliotis iris* gill, *Sphenophyra*-like ciliates with dense nuclei are shown (black arrows) between the gill filaments.

3.2.2.4. Right kidney

Presence/absence of haplosporidian-like parasites and kidney crystals were recorded and expressed as percentage prevalence for each sample population. Initial detection of the kidney crystals was performed using cross polarisation of the light source to highlight birefringent properties. For photograph imaging only one of the polarising filters was required. This application allowed for the clearer detection of the birefringent properties of the kidney crystals. By further reducing the camera

exposure to $-2/3$ this balanced the brightness of the reflective light and facilitated the detection of very small crystals that were not otherwise noticeable at the magnifications applied here.

3.2.3. Statistical analyses:

Data were checked for normality and heterogeneity of variance using the Shapiro-Wilks and Levene's tests, respectively. Site and life stage were used as factors in the models used. Most of the semi-quantitative data including parameters of the midgut and digestive gland data were treated as non-parametric. Ordinal Logistic Regression (OLR) models and linear models were used to detect differences, performed using the MASS package (Venables and Ripley, 2002). A general linear model (GLM) was used to analyse the ciliate numbers as well as morphometric data. The ciliate data were log-transformed to meet the assumption of homogeneity of variance. Post-hoc pairwise analysis was performed using the package emmeans (Lenth, 2021), followed by p value adjustment using Tukey method to avoid cumulative type I error. For prevalence data (i.e., presence/ absence) of kidney crystals or haplosporidian-like parasites, GLM using binomial data were used to detect differences. As a result of the "perfect" separation between responses, a ridge penalizer was used to add a 'ridge prior' to the estimates to increase sensibility of the parameter estimates (Cule and Frankowski, 2021). Un-transformed data were used for the graphs. R version 4.0.3 (R Core Team, 2024) was used for statistical analysis.

3.3. Results

There were statistically significant interactive effects between site and life stage in weight ($\chi^2_{(3)} = 94.16, p = <0.001$) (Table. S1), shell length ($\chi^2_{(3)} = 39.55, p = <0.001$) (Table. S2), shell width ($\chi^2_{(3)} = 9.43, p = 0.024$) (Table. S3), shell height ($\chi^2_{(3)} = 10.81, p = 0.013$) (Table. S4), and no statistical interaction effects between site and life stage on shell length: shell height ratio ($\chi^2_{(3)} = 6.18, p = 0.103$).

However, for the shell length: shell height ratio both site and life stage were individually affected (Site: $\chi^2_{(3)} = 18.66, p = <0.001$, and life stage: $\chi^2_{(1)} = 14.09, p = <0.001$). Ascotts and Durham had lower height to shell ratio when compared to Owenga and Wharekauri ($p = <0.0028$ and $p = <0.001$, $p = <0.0091$ and $p = <0.001$, respectively) (Table. 3.1).

Table 3.1 Morphometric and physiological data whereby size range is the min and max shell length. Additional values report the mean \pm SD. Weight in g (W), Shell length in mm (SL), Shell width in mm (SW), Shell height in mm (SH) shell length to shell height ratio (SL:SH), Percent population reproductively active (% RA) and the female: male sex ratio (F:M)

		Size	W (\pm SD)	SL (\pm SD)	SW (\pm SD)	SH (\pm SD)	SL:SH (\pm SD)	% RA	F:M
Adult	Ascots	121 - 138	440 \pm 41	131 \pm 4.4	99 \pm 4	46 \pm 2.6	2.9 \pm 0.2	100	0.3
	Owenga	110 - 122	228 \pm 25	117 \pm 4.0	89 \pm 5.9	37 \pm 3.6	3.2 \pm 0.3	100	0.7
	Durham	126 - 147	461 \pm 36	131 \pm 5.9	97 \pm 5.9	45 \pm 2.8	2.9 \pm 0.3	100	4
	Wharekauri	136 - 149	526 \pm 62	143 \pm 5.2	107 \pm 7.6	40 \pm 3.5	3.6 \pm 0.4	100	2.3
Sub-adult	Ascots	69 - 93	77 \pm 20	80 \pm 6.3	61 \pm 4.2	23 \pm 2.3	3.5 \pm 0.3	50	0.3
	Owenga	78 - 88	92 \pm 14	85 \pm 3.1	60 \pm 4.5	21 \pm 2.5	4.2 \pm 0.6	50	4
	Durham	77 - 101	120 \pm 42	90 \pm 7.4	65 \pm 6	26 \pm 4.8	3.6 \pm 0.4	60	0.5
	Wharekauri	82 - 102	118 \pm 28	92 \pm 7.0	69 \pm 3.7	23 \pm 1.6	4.0 \pm 0.3	50	1.5

3.3.1. *Midgut: algal quality scoring*

There were significant site-specific differences whereby the combined life stages (adult and sub adult groups) at faster growing sites appeared to have fresher (more intact) food in the gut when compared to the ‘stunted’ sites ($\chi^2 = 50.56, p < 0.001$) (Fig. 3.7) (Table. S5). There was no significant site and life stage interaction ($\chi^2_{(3)} = 1.08, p = 0.78$) and no life stage differences ($\chi^2_{(1)} = 0.69, p = 0.4$). Additionally, sand particles were observed in the wax blocks of some individuals (Fig. 3.8).

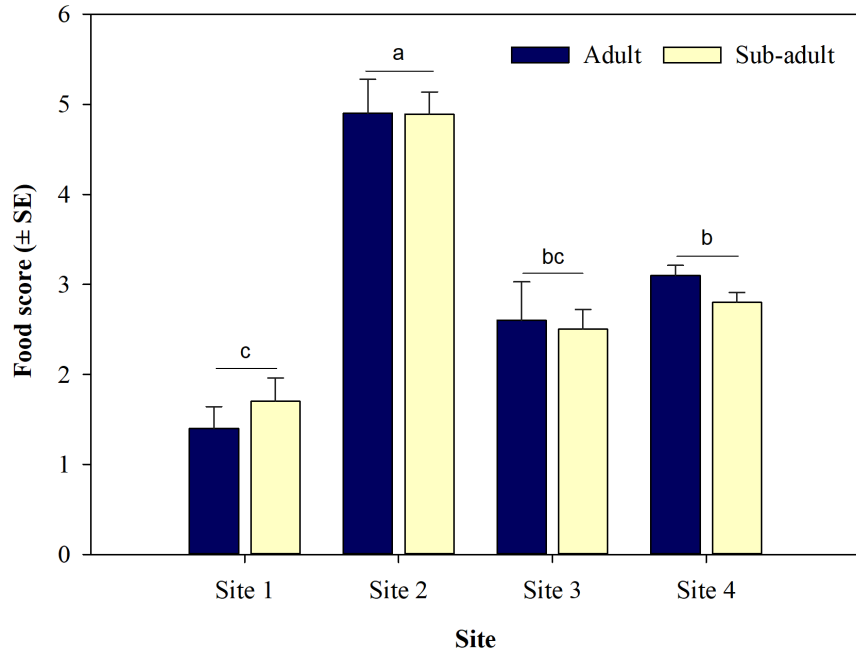


Figure 3.7 Food score (Mean \pm SE) 1 being 100% Fresh (intact) food visible and 5 being 100% old (degraded/digested) food (Adults: site 1. Ascots n=9, site 2. Owenga n=9, site 3. Durham n=7, site 4. Wharekauri n=10; Sub-adults: site 1. Ascots n=10, site 2. Owenga n=9, site 3. Durham n=10, site 4. Wharekauri n=10). Significant differences ($p < 0.05$) among groups are shown with lower case letters above bars.

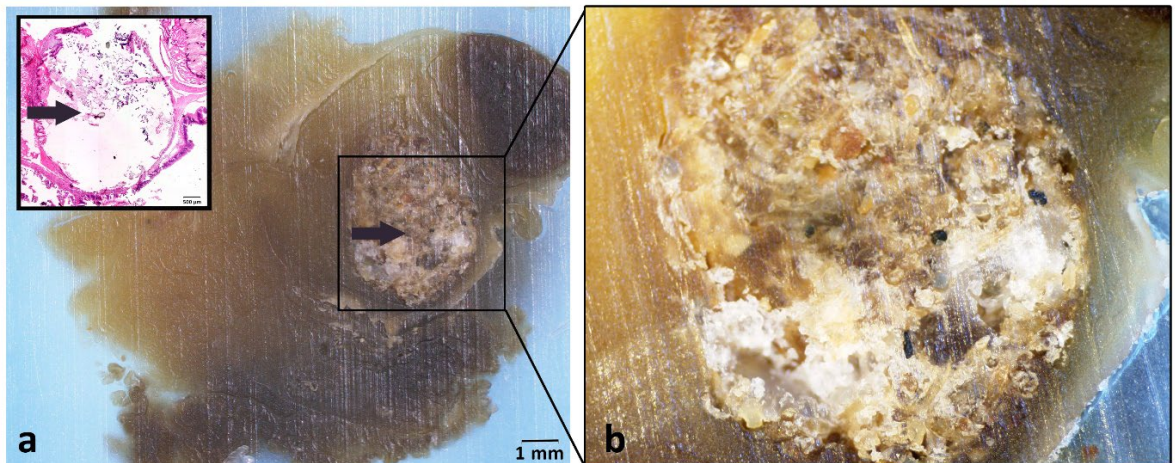


Figure 3.8 Histology wax block of an example individual with “older” food and almost empty mid-gut tract. a) histology block sample photographed at $\sim 5x$ magnification (dissection microscope), indicating a gut lumen filled with sediment (arrow); inset is the corresponding histology slide stained with H&E. b) Enlarged image of gut tract showing sediment particles.

3.3.2. Tissue anomalies

There were no significant site and life stage interactions in the number of ceroid granules (ceroid score) observed in gut epithelium connective tissue ($\chi^2_{(3)} = 0, p = 1.0$). There was no life stage difference ($\chi^2_{(1)} = 0, p = 0.98$). However, there was a site-specific difference ($\chi^2_{(3)} = 51.56, p = <0.001$) (Table. 2). The adults at sites 1 and 4 had lower scores when compared with the adults at site 2 and site 3 (Table. S6) It was also noted that the ceroid levels within the connective tissue was also perceptibly higher than in individuals collected from site 2. There were no site and life stage interactions in the proportion of digestive gland tubules detaching (coverage) from the basement membrane creating voids ($\chi^2_{(3)} = 3.69, p = 0.3$). There was however a site-specific difference ($\chi^2_{(3)} = 9.93, p = 0.019$) (Table. S7). There was a significant site and life stage interaction in the mean extent of the void around each of the tubules ($\chi^2_{(3)} = 9.05, p = 0.029$) (Table. S8). The adults at site 1 had lower scores when compared with the adults at site 2 and site 3 ($p = 0.0006$ and $p = 0.04$ respectively) (Table. 3.2). There were no differences in the digestive gland quality between the sites ($\chi^2_{(3)} = 0.697, p = 0.87$). There was a significant site and life stage interaction in the number of ceroid granules within the digestive gland connective tissues ($\chi^2_{(3)} = 20.72, p = <0.001$) (Table. 3.2) (Table. S9).

Table 3.2 Summary of semi-quantitative tissue assessments (mean \pm SD). Ceroid material in the gut sub-epithelium reflects the relative quantity (0 – 3) of ceroid material in the connective tissue adjacent to the gut epithelium. ‘Coverage’ (criterion 1) provides an indication of the proportion of digestive tubules (DG) showing detachment (score 1 – 4 corresponding to 0 – 100% occurrence), while ‘extent’ (criterion 2) considers the mean extent to which tubules have detached (0 – 4 corresponds to no detachment and whole tubule has detached, respectively). The subjective ‘DG quality’ (criterion 3) classifies the overall quality of the tubules. Ceroid score in DG reflects the relative quantity in the interstitial spaces.

		Adults				Sub-adults			
		Site 1. Ascots	Site 2. Owenga	Site 3. Durham	Site 4. Wharekauri	Site 1. Ascots	Site 2. Owenga	Site 3. Durham	Site 4. Wharekauri
Mid-gut epithelium	Ceroid score	1.0 \pm 0.0	3.0 \pm 0.0	2.7 \pm 0.5	1.0 \pm 0.0	1.0 \pm 0.0	1.4 \pm 0.5	1.0 \pm 0.0	1.0 \pm 0.5
	Coverage	0.8 \pm 0.4	2.2 \pm 0.7	2 \pm 0.9	1.6 \pm 1.8	1.3 \pm 1.2	1.4 \pm 1.1	1.5 \pm 0.7	1.0 \pm 0.7
Digestive gland	Extent	0.8 \pm 0.4	2.6 \pm 0.7	2 \pm 0.8	1.6 \pm 1.5	1.1 \pm 0.7	1.2 \pm 0.8	1.5 \pm 0.8	0.9 \pm 0.6
	DG quality	1.5 \pm 0.8	2.75 \pm 1.3	2.5 \pm 0.9	2.8 \pm 1.0	1.4 \pm 1.0	1.5 \pm 1.2	2 \pm 0.7	2.0 \pm 0.8
	Ceroid score	2.0 \pm 0.8	3 \pm 0.0	1.8 \pm 0.9	1 \pm 0.0	1.9 \pm 0.6	2.1 \pm 0.6	1.8 \pm 0.5	1.6 \pm 0.5

3.3.3. Gill

Ciliates (Protozoa, Ciliophora) were commonly found between the lamellae of the gill. The ciliates were identified to be ectocommensal *Sphenophyra*-like ciliates (Diggles and Oliver, 2005; Muznebin et al., 2021) by the macronucleus, which is densely basophilic. Ciliates were detected at all sites.

There was no interaction between site and life stage ($f_{(68,3)}=1.3, p=0.28$), and no life stage difference ($F_{(68,1)}=0.1, p=0.7$) but there was a site-specific difference ($F_{(68,3)}=3.98, p=0.011$) (Table. S10) (Fig. 3.9).

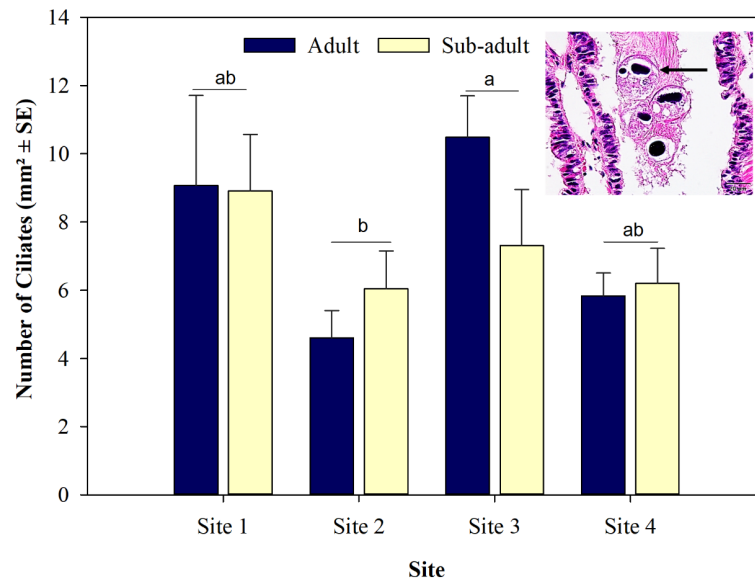


Figure 3.9 Number of ciliates per 1 mm² of abalone gill transverse section (Mean ± SE) from four sites around the Chatham Island (Adults: site 1. Ascots n=10, site 2. Owenga n=9, site 3. Durham n=10, site 4. Wharekauri n=10; Sub-adults: site 1. Ascots n=10, site 2. Owenga n=10, site 3. Durham n=8, site 4. Wharekauri n=9). Inset: Enlarged image of a group of 4 ciliates (Arrow).

3.3.4. Right kidney

Kidney crystals of a crystalline structure were found to occur with a higher prevalence at site 2 ($t=2.852, p=0.004$) and site 3 ($t=3.830, p<0.001$) when compared to the site 1 (Fig. 3.10). There was a significant difference between adults and sub-adults in the prevalence of kidney crystals ($t=-2.977, p=0.002$). The larger crystals reaching between 50 - 60µm. (Fig. 3.11a-c).

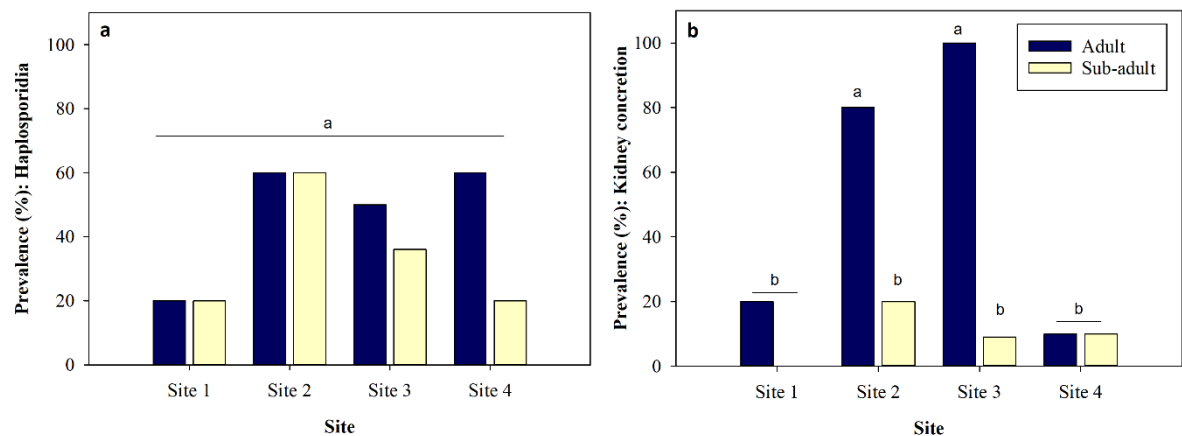


Figure 3.10 Population percent prevalence (%) (n=10) for the presence/absence of a) haplosporidian-like parasite and b) kidney crystals in the right kidney tissue of *H. iris* from four sites around the Chatham Island (Adults: site 1. Ascots n=10, site 2. Owenga n=10, site 3. Durham n=11, site 4. Wharekauri n=10; Sub-adults: site 1. Ascots n=10, site 2. Owenga n=10, site 3. Durham n=10, site 4. Wharekauri n=10). Letters indicate significant differences between sites and life stages ($p < 0.05$).

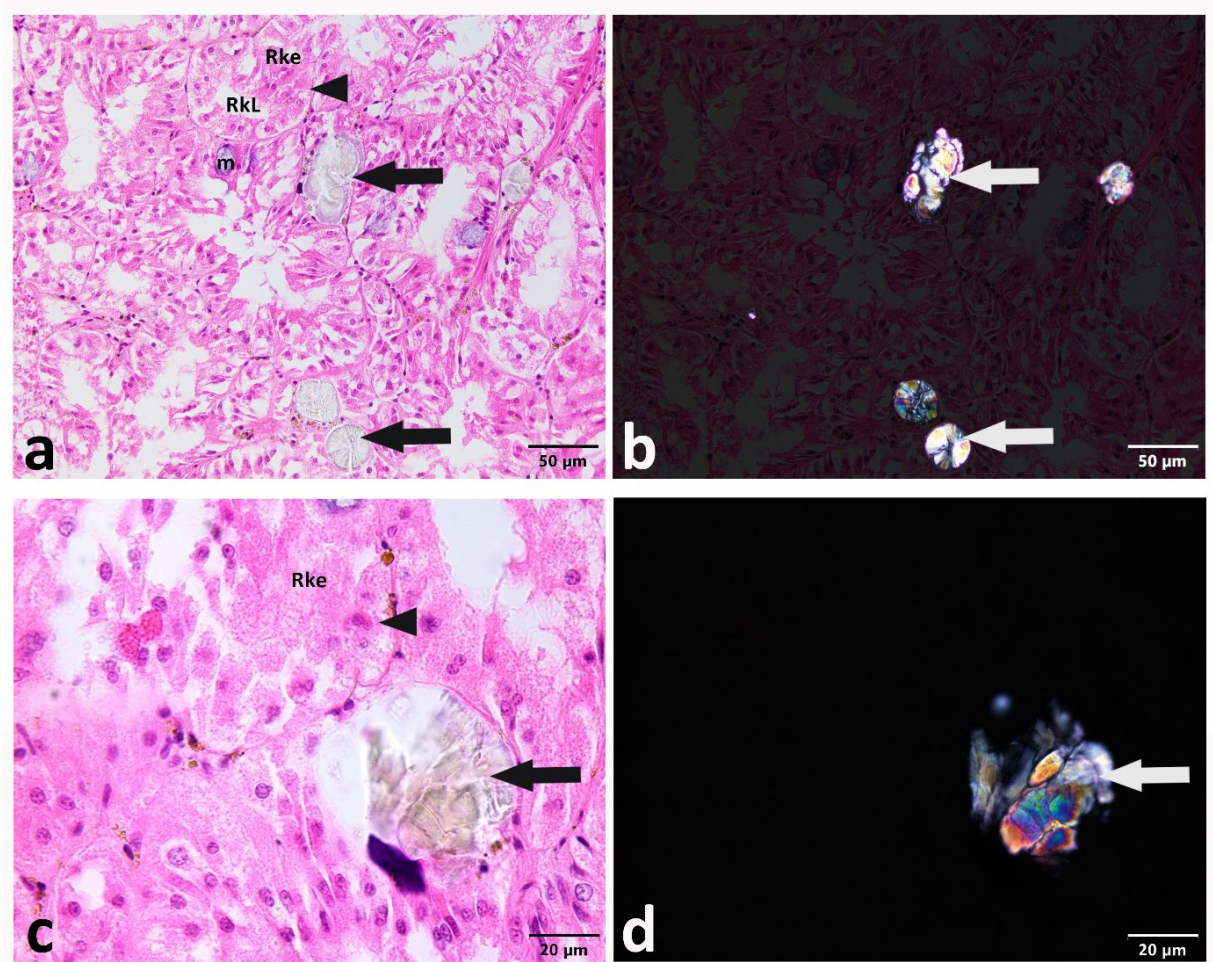


Figure 3.11 Crystals in an H&E-stained right kidney section from an adult abalone, viewed under a) bright-field kidney crystals (arrows), b) using a crossed polar filter to observe differences in the inclusions and the anisotropic affect from the birefringent properties c) kidney concretion embedded in the right kidney epithelial (Rke) layer H&E under oil immersion e) oil immersion image of kidney concretion with polarised filter. Right kidney tubule (arrowhead), kidney lumen (Rkl), kidney epithilium (Rke) and mucous cells (m).

A haplosporidian-like parasite was observed in the right kidney of *H. iris* (Fig. 3.12) collected from all four sites. There was a population prevalence of 60% in the adults at site 2 and 4 and only 20% and 10% at site 1 and site 4, respectively. Additionally, the sub-adults at site 2 also had a population prevalence of 60% for haplosporidian-like parasite detection (Fig. 3.10); however, the low sensitivity of the binomial GLM analysis required for this data format failed to detect significant differences.

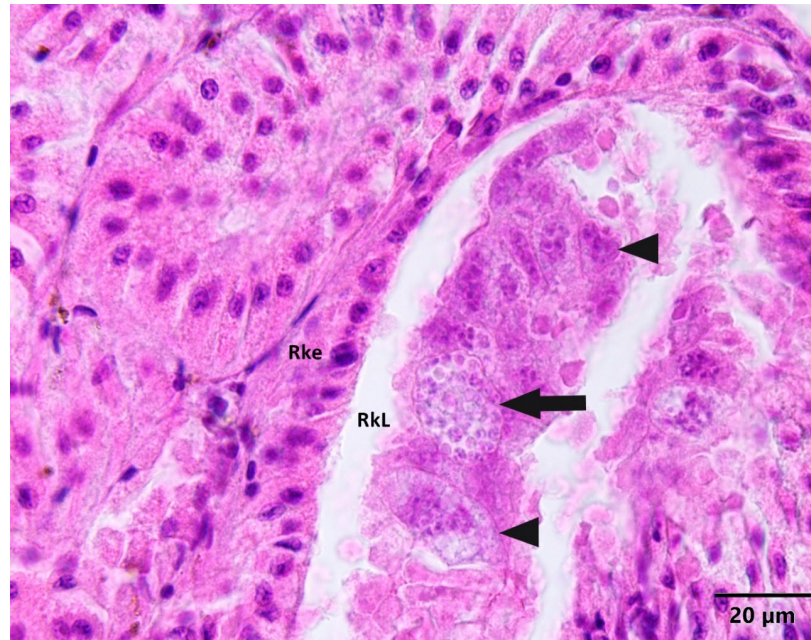


Figure 3.12 Multicellular haplosporidian-like parasite (Arrowhead) cluster in the lumen of right kidney (RkL) of *H. iris*. Right kidney epithelium (Rke) and haplosporidian-like sporocyst (arrow).

3.4. Discussion:

Attributed site-specific growth performance appears to be correlated with alterations found in the midgut (algal structure), digestive glands, and right kidney of *H. iris*. From the histopathological investigations, there are several factors that could potentially affect the growth of the abalone. The differences in macroalgal integrity ('food score') observed in the stomach and crop lumen may reflect variability in the food quality, accessibility, and digestibility, indicating a potential nutritional effect. The presence of a high quantity of sediment particles, particularly in relation to the algal food particles, could indicate reduced nutritional intake and the ingestion of excess toxins or minerals. Additionally, the accumulation of ceroid material in the connective tissue, as along with the crystals found in the right kidney suggests that there may be either site-specific water quality issues, prior pathogen incursion or advanced age. Furthermore, the appearance of kidney crystals and a haplosporidian-like parasite could be impairing kidney function and negatively impacting physiological performance.

3.4.1. Nutrition

Abalone from the Ascots and Owenga sites were found to have differences in the integrity of macroalgal food found in the stomach/crop region. This suggests that either food supply was limiting, and therefore old food tended to persist in the gut, or the food available was tougher and less digestible and therefore remained in the gut for a longer period of time (Day and Cook, 1995; Britz et al., 1996). Additionally, they were preferentially selecting algae depending on availability. At site 1 (Ascots), *H. iris* has access to a diverse assemblage of green, red, and brown seaweed types (unpublished observations) and do not appear to be food limited in terms of quality or quantity. Conversely, the macroalgal assemblage available to the 'stunted' population at site 2 (Owenga) is limited to approximately 8 species of seaweed. Abalone growth is known to improve when

individuals feed on a variety of macroalgal species compared to single species (Stuart and Brown, 1994; Mai et al., 1995; Viera et al., 2011), particularly if that species is of limited nutritional value. The decrease in topographic complexity at site 2 is also likely to reduce the availability of drift seaweed, further limiting food availability. Poore (1972) correspondingly found that a limited supply of drift weed led to slower abalone growth. Additionally, phaeophytes, which were common at site 2, contain phlorotannin's which can potentially reduce digestibility and damage the intestinal tract walls (Day and Cook, 1995). No anomalies in the intestinal tract, other than algal quality, were initially observed at the start of this investigation. Therefore, it is likely that the potential consumption of phaeophytes that contain phlorotannin's was limited.

During initial sample preparation (Personal communication), it was also noted that brown and green macroalgal fragments were apparent in the guts of 'stunted' *H. iris* at site 2 (Owenga), where the Chlorophytes *Ulva lactuca* and *Codium fragile* were noted to be abundant. It is likely that the green and red alga types are preferable. This selection is supported by Foale and Day (1992) and Day and Cook (1995) and whereby it is suggested that NZ abalone have evolved preferences to red and green seaweeds and only consume phaeophytes when preferred foods are absent. Previous studies investigating the consumption of red and brown seaweeds suggest that soft (non-calcareous) red seaweeds (Rhodophyta) were generally noted to have a higher energetic and nutritional value and often considered to be more attractive and palatable to abalone, subsequently supporting faster growth (Poore, 1973; Britton et al., 2020). It therefore seems reasonable to suggest the availability of Rhodophytes at favourable growth sites, notably Ascots, could substantially explain the improved growth performance of abalone and the greens (e.g., *Ulva* sp.) may not provide the required nutritional components to support faster growth.

Ulva lactuca was observed to be among the most abundant macrophytes at three sites (site 1: Ascots, site 2: Owenga and site 3: Durham) with *Durvillea chathamensis* being the most abundant at site 4: Wharekauri. Kelp species such as *D. chathamensis* and *D. antarctica* have been previously described as being the most abundant at many of the locations around the Chatham Islands (Schiel et al., 1995). Wilcox (2007) gives a general overview of past kelp assemblages. Interestingly, *D. chathamensis* and *Grateloupia proliferus* were previously the most dominant with *U. lactuca* occupying the deeper section of the subtidal zone in Owenga (Wilcox, 2007). This suggests that the assemblage has changed over time, with opportunistic *U. lactuca* replacing the *D. chathamensis* in the upper range and may reflect environmental changes, such as increasing sedimentation (Schiel et al., 2006) and temperature fluctuations (Thomsen et al., 2019). Although the thallus of the *U. lactuca* is soft and palatable to *H. iris*, it is generally regarded as a poor food source as it has a low food conversion ratio and typically results in poor growth rates (Stuart and Brown, 1994). Other sedentary marine invertebrates have been observed to display a high degree of phenotypic plasticity associated with their response to an environmental stressor (Trussell, 1996; Steffani and Branch, 2003; Saunders et al., 2009b). For example, Saunders et al. (2009b) found that when they translocated *H. rubra* (black-

lipped abalone) to a site where the reef topography and algal assemblage supported faster growth, slow-growing, or 'stunted' abalone showed improved compensatory growth rates.

Additionally, the presence of sediment particles found in the gut lumen of the wax-embedded tissue of individual *H. iris* is also of interest. This suggests that the *H. iris* is consuming large quantities of sediment when feeding which is likely to have significant nutritional impacts. Ingestion of small amounts of sand and detritus is common and seen in other abalone species (Harris et al., 1998). Further analysis of the types of algae that the *H. iris* is consuming as well as the amount of sand compared to the algae ingested would be beneficial and supplementary to the present study. Care also needs to be taken in relation to sample quality and interpretation, with such high levels of sand typically being lost during histological sectioning, leaving voids in the lumen, introducing a risk of misinterpretation of tissues e.g., the intestinal tract.

3.4.2. Ceroid granules

The accumulation of ceroid material was observed in greater numbers in the connective tissue of the gut, digestive gland, and right kidney in the 'stunted' Owenga *H. iris* population. Ceroid or lipofuscin-like cells are pigmented brown to yellow waxy aggregates formed as a consequence of oxidative stress (Carella, 2015; Webb and Duncan, 2019). Traditionally, lipofuscin accumulation has been associated with age-dependent pigments e.g., in clams (Lomovasky et al., 2002), whereas ceroid pigments have been associated with pathological conditions (Zaroogian and Yevich, 1993; Seehafer and Pearce, 2006; Jung et al., 2007b). Pathological conditions include immune response to pathogens (Zaroogian and Yevich, 1993), contaminant degradation and detoxification, e.g. mussels (Carella, 2015; Shaw et al., 2019), and metals accumulation, e.g. oysters (Apeti et al., 2014). Ceroid material has been previously correlated with metals, including cadmium, copper, iron, mercury, and zinc, in mussels, clams and oysters (Thomson et al., 1985; Zaroogian and Yevich, 1993; Marigomez et al., 2002).

The proliferation of ceroid observed in the stunted individuals in the present study could be associated with either: an advancement in age (e.g., physiological vs chronological age) (e.g., Basova et al., 2012), as 'stunted' individuals are generally older than their fast-growing neighbours, or the accumulation of metals derived from consumption of contaminated seaweed or sediments, thus presenting in the gut, digestive glands, and right kidney as the sites of absorption and excretion. Conversely, the proliferation could be a result of excessive oxidative stress and disease from pathological conditions associated with sub-optimal conditions and summer marine heatwaves, or another unknown factor. Additional research is required to elucidate the production and function of the different manifestations of ceroid granules observed and their connection to different processes (Webb and Duncan, 2019). Additionally, further investigation is required to unravel the site-specific influence of aging, pathogens, and environmental perturbations upon ceroid and/ or lipofuscin accumulation in abalone and, determine the differences between ceroid and lipofuscin pigments in *H. iris*.

3.4.3. *Kidney crystals*

The appearance of crystalline crystals, or ‘spherites,’ similar to human kidney stones, in the right kidney of *H. iris* potentially provides additional clues to environmental perturbations and diet inefficiencies. The prevalence of crystals was high in the adults from the nominally slow-growing sites at Owenga and Durham. The appearance of the crystals was that of a harden and shattered crystalline structure with an anisotropic affect and therefore referred to here as a ‘kidney crystal.’ Kidney crystals of different sizes and morphology may occur during environmental stress, resulting from contaminated water, temperature stress, salinity and/or anoxia, such as in the bivalves *Argopecten irradians* and *Mercenaria mercenaria* (Doyle et al., 1978; Carmichael et al., 1979; Mauri and Orlando, 1982; Klobucar et al., 2001), as well as nutritional and reproductive stress (Klobucar et al., 2001). Previously Doyle et al. (1978) note that kidney crystals could develop in various textures and colours, from dark brown and black to ochre and beige, with a diameter of up to 250µm in *M. mercenaria* and are most associated with phosphorite formation, particularly mineralised magnesium/ calcium Mg/Ca as phosphate and carbonate. Calcium phosphate mineralisation has been observed in kidney of the cephalopod *Nautilus pompilius* and reported as whitlockite uroliths. The uroliths were initially considered as potential storage for Ca ions to be mobilised during septal formation (Crick et al., 2009). There are several examples of the development of crystals in response to toxins, e.g. pentachlorophenol (PCP) in the snail *Planorbarius corneus* (Klobucar et al., 2001) and cadmium exposure in *A. irradians*, with the possibility that the development is a mechanism for removing excess toxins. However, it should be noted that these were previously described as yellow to brown in colour, in contrast to the clear crystals observed herein (Carmichael et al., 1979; Carmichael and Fowler, 1981). Concretion granules of up to 20µm in diameter have been described in scallops, *Pecten maximus*, with the increase in size thought to reflect the longer residence time in the tissue, (Marigomez et al., 2002).

The kidney crystals found in this study are reminiscent of calcium oxalate crystals found in vertebrate kidney stone disease (nephrolithiasis) with similarities in colour, clarity and texture when stained with H&E and similar anisotropic properties under polarised light (Cossey et al., 2020; Geraghty et al., 2020). Possible causes of vertebrate kidney stone disease include hyperoxaluria, high oxalate diets, thiamine/ pyridoxine deficiencies, excessive dieting, and alterations in interstitial flora (Geraghty et al., 2020). Therefore, there is a possibility that the limited food access and ingestion of sediments in the *H. iris* is causing these crystals. Furthermore, calcium carbonate polymorph crystals: calcite, aragonite and vaterite, are common birefringent minerals used in molluscan shell development, the latter associated with shell repair and pearling (Spann et al., 2010; Checa, 2018). There are several potential constituents of such crystals in molluscs including, magnesium oxalate, calcium oxalate and calcium phosphate (the latter as whitlockite, brushite, and hydroxyapatite) (Tiffany et al., 1980; Crick et al., 2009). In mammal nephrolithiasis calcite and vaterite have been shown to promote calcium oxalate crystallisation (Geider et al., 1996). Further research is required

to determine what the composition of the crystals is, as well as the causes and consequences for *H. iris*.

3.4.4. Pathogen detection

Ectocommensal *Sphenophyra*-like ciliates (Diggles and Oliver, 2005) were recorded in most of the individuals collected. Ciliates are commonly found in close association with many marine molluscs and attachment to the gill filaments is generally superficial (Bower et al., 1994; Bower, 2006). No signs of effect were evident on the gill epithelium, nor was there evidence of the immunological response or haemocytosis observed in this study as opposed to affected tissues in the geoduck (*Panopea abbreviate*) by Vázquez et al. (2015). It is worth noting that ciliates may become pathological at higher intensities, restricting water flow over the gill filaments and reducing host respiration rates (Vázquez et al., 2015).

The prevalence of a haplosporidian-like parasite species in the ‘stunted’ population could be a contributing factor to the slower host growth. This haplosporidian-like parasite shows similarity to the novel haplosporidian identified by Diggles et al. (2002) and Hine et al. (2002) in farmed *H. iris* in New Zealand during a mortality event in 2000 and 2001. Both Hine et al. (2002) and Diggles et al. (2002) suggested that the appearance of the haplosporidian parasite could be associated with poor growth and condition, although it remains unclear whether the pathogen represents a cause or effect. Diggles et al. (2002) suggested that the appearance of larger parasite cells within the right kidney, when compared with other infected tissues, could potentially be due to low intensity levels and is perhaps representative of natural infection level in wild populations. Haplosporidian parasites are considered to be “of concern” to aquatic animal industries worldwide (Arzul and Carnegie, 2015). The haplosporidian group includes three well-known species that cause epizootic disease in oysters; *Haplosporidium nelsoni*, *Bonamia ostreae* and *Bonamia exitiosa* (Hill et al., 2014; Arzul and Carnegie, 2015; Hine, 2020) and also includes *Urosporidium* sp. (Le et al., 2015) (Arzul and Carnegie, 2015). Very little is known about the haplosporidian species found in *H. iris*, other than the fact that in high levels it can be associated with mortalities in juveniles, and DNA sequencing places it close to *Urosporidium* (Reece and Stokes, 2003). Further research is required to robustly identify this haplosporidian – *Urosporidium*, as well as clarifying its current host-interactions, before considering the future implications under the influence of climate change.

3.4.5. Additional factors and implications

There are two effects yet to be addressed. The sections in some cases displayed minor to moderate distortion, potentially due to sand or sediments in the guts of the abalone. The changes in the digestive tubules, including shrinkage of the epithelial tissue away from the basal membrane, and the compression and increased staining affinity of the basophilic cells. Similar shrinkage and the detachment effect has been indicated previously in the crustacean *Nephrops norvegicus* as a result of starvation (Karapanagiotidis et al., 2015). However, due to the lack of proteinous material in the voids, a fixation affect cannot yet be ruled out (Wolf et al., 2015; Webb, 2020). This effect warrants

further investigation to distinguish fixative artefacts from the influence of environmental toxicity and nutrition, as well as establishing why some individuals are more affected by the process than others.

Histopathology is an essential and powerful tool for diagnosing stressors in various environments and providing general assessment of an individual's health (Hooper et al., 2014; Costa, 2018b). It is not without its limitations and misinterpretation can arise from sampling and fixation issues, preparation artefacts and variable observer expertise. Knowledge of the fine-scale changes seen through histological techniques is required to fully understand the effects of a stressor on the individual, particularly the subtle effects of heat, feeding, nutrition and diseases (Hooper et al., 2014). There are very few studies that define a clear baseline range for the variability in tissue structure between individuals under 'real-world' conditions (Costa et al., 2013; Damodaran, 2020); this shortfall should be addressed in future studies.

The designation of the 'stunted' and 'non-stunted' *H. iris* populations was based on both anecdotal observations from the industry experience and descriptions by McShane et al. (1994) and Naylor et al. (2006). The morphometric values such as weight and length broadly supported the 'stunted' vs fast-growing classification in the adults, however the length to height ratio showed no differences. If feasible, a larger sample size may have increased statistical power to detect biological differences. Ideally, if the variability had been known an *a priori* power analysis would support the experimental design by determining the appropriate sample size to provide further confidence in the findings. Nutrition is hypothesised to be the key driver due to direct observation of habitat and seaweed assemblage and is a potential factor for growth performance. It is worth investigating further not only the analysis of gut contents but the timing of analysis. Gut contents can be biased towards less digestible alga and timing of analysis is key to correct interpretation due to the ingestion and evacuation rates of food consumption (Foale and Day, 1992; Day and Cook, 1995). There are also additional potential contributing factors that could be driving the divergence in growth performance for example local increases in sedimentation, temperature, and pathogens.

3.4.6. Conclusions:

The histopathological assessment broadly supported the growth performance differences between the 'stunted' and 'non-stunted' populations. The differences in the algal quality, the level of ceroid material found in multiple tissues, the appearance of kidney crystals and the appearance of a haplosporidian-like parasite are potential causative agents of the reduced growth performance. This investigation provided an opportunity to gain valuable insight into the current tissue condition of a small number of individual *H. iris* populations around the Chatham Islands. Greater sampling numbers and timepoints will ultimately help elucidate the drivers behind variable growth performance and potential sensitivity to climate change. Not only is further sampling and surveillance required to gain a better understanding, but further research is needed to clarify the causes of the effects identified in this study, especially with regards to the extent to which food

availability, digestibility, pathogen loads, and environmental conditions contribute to growth performance of *H. iris*.

CHAPTER 4. ELUCIDATING DIVERGENT GROWTH PERFORMANCE AND CLIMATE
VULNERABILITY IN ABALONE (*HALIOTIS IRIS*): PART B

Published in its entirety in Marine Environmental Research:

Copedo, J. S., Webb, S. C., Delisle, L., Knight, B., Ragg, N. L. C., Laroche, O., Venter, L., Alfaro, A. C., 2025. Elucidating divergent growth and climate vulnerability in abalone (*Haliotis iris*): A multi-year snapshot. *Marine Environmental Research*. 107090,

<https://doi.org/10.1016/j.marenvres.2025.107090>.

Abstract

Many abalone populations worldwide are in decline because of changing climate and fishing pressure. In New Zealand (NZ) *Haliotis iris* is the largest and most abundant of the endemic abalone species. This species displays high levels of phenotypic variation with slow-growing populations having an impact on their commercial utilisation. The present study incorporates targeted histopathological approaches to characterise tissue-level factors in abalone from NZ's principal fishing region. Adult (n= 60) and sub-adult (n = 56) *H. iris* were collected from two Chatham Island sites that display differential growth rates; sampling was repeated on six occasions over three years. Through histology the slower-growing adult population was observed to have an elevated ceroid score, higher prevalence of kidney stones and increased prevalence of a plasmodia stage of haplosporidian-like parasites in the right kidney, when compared with the faster-growing and sub-adult populations. Furthermore, the faster-growing adult population appeared to be retaining mature oocytes over the predicted spawning season with higher-than-expected atresia (oocyte degeneration). Factors implicated in growth performance between the two populations include site, environment, parasites, pathology, reproduction, ceroid deposition and previously reported nutritional status. The 18S PCR and metabarcoding on the right kidney tissue were negative for haplosporidian/*Urosporidium* previously reported in *H. iris*, with metabarcoding results detecting an apicomplexan ancestral group. The reproductive, somatic and parasite findings from the current study provides critical information on abalone physiological condition which allows facilitation of early detection of conditions that may impact the sustainability and management of *H. iris* stocks in NZ under a changing climate. For instance, changes to reproductive condition may reduce oocyte quality and quantity thereby reducing recruitment to the next generation.

4.1. Introduction

Abalone are ecologically important coastal marine gastropods from the Haliotidae family and are globally widespread (Geiger, 1999). Many abalone populations are in decline, with several nearing biological extinction (Gnanalingam et al., 2021). These declines are often attributed to over-fishing, habitat degradation, and disease (Cook, 2014; Van Nguyen et al., 2023). Additionally, the coastal ecosystems which abalone inhabit are often highly impacted by environmental alterations influenced

by climate change (Halpern et al., 2008; Lima and Wethey, 2012). The influence of climate change and corresponding decline in biodiversity of marine organisms within coastal ecosystems is well known and reported (e.g., Salinger et al., 2020b; Behrens et al., 2022; Santana-Falcón and Séférian, 2022). Habitat alterations due to climate change have enduring impacts on various invertebrate populations and community resilience, resulting in shifts in ecological structure (Lotze et al., 2006; Subritzky, 2013; Soon and Ransangan, 2019; Montie et al., 2023).

Globally, anomalous events of prolonged above-average warm water have increased in frequency and intensity. These prolonged warming events have been termed marine heatwaves (MHWs) (e.g., Houghton et al., 2001; Petes et al., 2007; Smale et al., 2019; Salinger et al., 2020b; Copedo et al., 2023; Montie et al., 2023). MHWs can directly affect abalone as well as indirectly through influencing food supply and habitat (Rogers-Bennett et al., 2010). Although temperature is one of the key factors affecting aquatic organisms, other covarying environmental stressors, including increasing sedimentation and increased extreme weather events, also need to be considered (Rogers-Bennett et al., 2010; Nguyen et al., 2021).

Abalone populations are well known to display high morphological variability in growth, whereby the maximum size and growth rate vary both geographically and temporally. These large-scale variations can result in the appearance of slow-growing phenotypes (commonly termed as ‘stunted’) within the population (Schiel, 1993; Trussell, 1996; Steffani and Branch, 2003; Naylor et al., 2006; Saunders et al., 2009b; Subritzky, 2013; Copedo et al., 2024) (Chapter 3). Slow-growing variants are common in many species of abalone, including *Haliotis rubra* (Saunders et al., 2008) and *Haliotis iris* (McShane et al., 1994), as well as several other molluscan species, such as *Mytilus galloprovincialis* (Hine, 1997), with stunted variants occurring with a smaller maximum size with shorter, wider and higher shells when compared to the fast-growing - typical growth conspecifics (McShane et al., 1994; Saunders et al., 2009b; Van Nguyen et al., 2023). The growth rate of many molluscs responds to a complex relationship between endogenous and exogenous factors. Some of these contributing factors are population density, feed availability, water chemistry, reef topography, hydrodynamics of the microhabitat, pathogen load and immune response (Diggle et al., 2002; Searle et al., 2006; Morash and Alter, 2016; Ren et al., 2019; Saulsbury et al., 2019). For example, a low energy hydrodynamic habitat could result in higher recruitment of larvae in the area versus a higher energy habitat where larvae can drift further, which impacts the population density and food availability (Ragg, 2023). In addition, warming waters and reduced kelp diversity, in association with climate change, have been observed to correlate with slower than normal growth in abalone (Saunders et al., 2009b; Rogers-Bennett et al., 2010).

Locally known as pāua, *H. iris* (Blackfoot abalone; Gmelin, 1791) is the largest and most abundant of the abalone species endemic to New Zealand (NZ) (Sainsbury, 2010; Gnanalingam et al., 2021). *Haliotis iris* is not only culturally significant but is also an ecosystem engineer, is prized by the recreational fishery, and supports a significant commercial fishing industry (Subritzky, 2013;

Gnanalingam et al., 2021; MPI, 2023a; Pāua Industry Council, 2023). Although harvesting is nationally managed using QMAs (quota management areas), *H. iris* is still vulnerable to overfishing, due to a few factors including its slow growth, aggregation behaviour, and reproductive biology. This results in challenges in setting an appropriate minimum legal harvest size based on regional pāua growth rate differences, and changing environmental challenges e.g., habitat disturbance and climate change (Houghton et al., 2001; Gordon and Cook, 2004; Gnanalingam et al., 2021; Van Nguyen et al., 2023).

Slow growing (or stunted) *H. iris* populations, which typically do not reach the minimum legal catch size of 125 mm shell length have been observed in several areas of the NZ coastline (McShane et al. 1994, Naylor et al. 2006). These populations are typically found in sheltered areas with low food availability and low wave action (Saunders et al., 2009b; Laferriere, 2016). The complex interactions of factors influencing growth can lead to additional challenges in the management of *H. iris* populations. Depletion of *H. iris* stocks in the central to southern region of the North Island of NZ (QMA 'PAU2'), in 2023 was reported by customary and recreational fishers. These reports raised resource managers' concerns around the sustainability of these stocks and the impacts of increasing extreme weather patterns, which led to the reduction of the recreation catch limit for pāua collections (MPI, 2023b). Commercially, stakeholders generally report a sustainable commercial fishery. Industry management is formalised by annual operating plans outlining management tools to support the pāua populations. QMAs are divided into micro regions (statistical areas) whereby harvest catch and minimum harvest size are applied at fine scales, taking into consideration the growth rate, length at maturity and habitat type, in order to support and enhance the fishery. Further understanding the cause of differential growth among abalone populations will allow for more targeted management strategies, thereby further supporting the objectives outlined in the plan and ensuring further sustainability (Van Nguyen et al., 2023). Although determining the impacts of environmental change is often complicated by the confounding influence of fishing pressures, understanding the effects of environmental stress on abalone biology is also key for managing populations (Morash and Alter, 2016; Roussel et al., 2020).

The Chatham Islands are located about 800 km off the coast of NZ and comprise of an archipelago of approximately 10 islands, the two largest are the main Chatham Island and Pitt Island. The main Chatham Island supports a large *H. iris* fishery. The minimum legal size of 125 mm has historically created localised areas of low and high fishing effort as a result of slower- and fast-growing populations. In addition to proposing harvest guidelines, the Chatham Island pāua management area committee (PauaMAC4) actively promotes research to identify new management strategies to support population growth (Venter et al., 2022; Van Nguyen et al., 2023). Additionally, the Chatham Islands are biogeographically isolated, and hence experience minimal local anthropogenic influence, but are vulnerable to global climate change, being situated in a warming region with an increasing

number of MHW days (Montie et al., 2023). Abalone from the Chatham Islands therefore represent a rare case study opportunity of proactive fishery management in a changing ocean.

A histopathological approach was taken to investigate contributing factors to differential growth between two populations on the main Chatham Island. The populations are exposed to a range of different conditions i.e., physical environment (e.g. wave exposure), and nutrition (e.g. influence of food quality and quantity), which are further described in Venter et al. (2022), Van Nguyen et al. (2023) and Copedo et al. (2024) (Chapter 3). Collections of *H. iris* at both sites were extended over three years to provide an indication of variability over time, particularly in response to summer marine heatwaves of varying intensity. This study ensured repeated population sampling aimed at exploring the relationship between tissue health, pathogen burden, perceived growth performance and potential vulnerability during summer heatwave events. Results and inferences strive to inform directions for further work and management options for *H. iris* exposed to different environmental conditions, nutrient deficiencies, and pathological findings.

4.2. Methods

4.2.1. Environmental monitoring: estimation of SST for Chatham Islands

While the geographic isolation of the sample locations made *in situ* environmental monitoring impractical, the principal driving variable of sea surface temperature (SST) was determined remotely through satellite. SST data were acquired using daily satellite information from Group for High Resolution Sea Surface Temperature (GHRSSST) MUR L4 product (Chin et al., 2017) and the following data portal:

<https://oceanlab3.rsmas.miami.edu/erddap/griddap/jplMURSST41.html>. Due to the coarse resolution of the satellite, SST was estimated about 4 km away (latitude 43.99°S, longitude 176.34°W) from both sampling sites (sites 1 and 2) although considered as representative. Sea surface temperature anomaly data were sourced from NOAA Coral Reef Watch (<https://coralreefwatch.noaa.gov>) using a 1985-1990 plus 1993 climatological baseline period to calculate anomalies (Liu et al., 2014). The month of December was selected for visual representation of the SST anomalies for the New Zealand and Chatham Islands region for the years 2020, 2021, 2022 and 2023 for comparison, whereby zero is the baseline average and SST anomalies are the degrees Celsius above or below the average.

4.2.2. Sampling location and animal collection

Two sites were selected around the Chatham Islands, New Zealand, based on performance differences of resident abalone (historic data and personal communications: Pāua Industry Council Ltd) as well as initial sampling and screening assessment (Venter et al., 2022; Van Nguyen et al., 2023). Site 1: Ascots (44°00'56" S 176°23'12" W) supports a population of *H. iris* identified as faster-growing, while site 2: Owenga (44°01'28" S 176°21'56" W) supports a population of slow-growing *H. iris* (Venter et al., 2022; Van Nguyen et al., 2023).

Ten adult (125.5 mm \pm 6.8 mm shell length) and 10 sub-adult (92 mm \pm 10.4 mm) *H. iris* were randomly collected, and identified as belonging in one of the two groups, by a research diver using SCUBA from each of the two sites at each designated timepoint (Table. 4.1). Adults were classified as those above 110 mm and sub-adults between 60 mm and 110 mm at both sites (Copedo et al., 2024) (Chapter 3). Sample preparation during the first collection event (March 2020) was completed on site on the day of collection (Copedo et al., 2024) (Chapter 3). For subsequent samples, individual *H. iris* were transported alive (6°C humid air) to Auckland University of Technology (AUT), Auckland, New Zealand.

The animals collected were weighed to the nearest 0.01 g, followed by measurements of shell length, width, and height (nearest 0.01 mm) before histological preparation. Additionally, the sex of each individual animal was recorded if identifiable (based on the colour of the gonad which was white/cream in males and green in females) and confirmed using histological techniques. Unidentifiable sexes were only detected in the sub-adults (13 of the 114). The sex ratio was determined as the proportion of males among the sex-verified individuals.

Table 4.1 Sampling numbers and time course of *H. iris* sampling for the Chatham Islands. The first timepoint (13/03/2020) has previously been analysed (Copedo et al., 2024) (Chapter 3) and is included as a reference for comparison.

	Site 1: Ascots		Site 2: Owenga		Reference
	Adults	Sub-adult	Adults	Sub-adult	
13 March 2020	10	10	10	10	(Copedo et al., 2024)
26 November 2020	10	10	10	10	
04 March 2021	10	10	10	10	
02 April 2021	10	10	10	10	
15 May 2021	10	10	10	10	
07 April 2022	10	4	10	10	

4.2.3. Histopathology

Abalone were shucked using a blunt shucking blade to detach soft tissues from the shell. The viscera was transversally sectioned in three positions, as per Copedo et al. (2024) (Chapter 3) and Poore (1973) to acquire three, 5 mm histology cuts to maximise chances of sectioning crop / stomach, digestive gland, gill, gonad, left and right kidney (determined histologically by organ architecture (Handler, 2022)), adductor muscle and heart (Fig. 4.1).

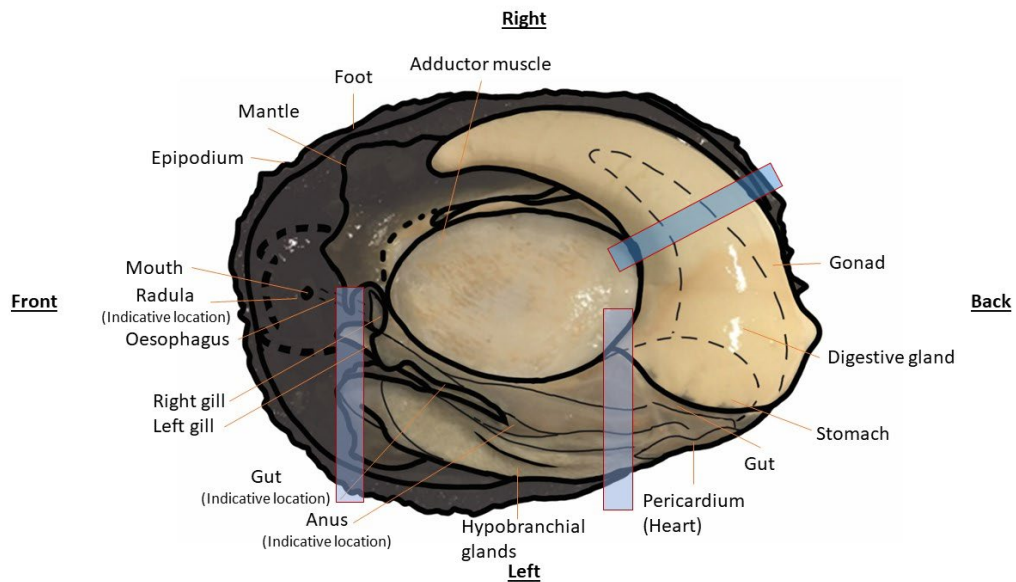


Figure 4.1 General anatomical depiction of New Zealand abalone (*Haliotis iris*) by Copedo et al. (2024) (Chapter 3). Location of the histology sections, indicated by rectangular windows, were chosen to maximise likelihood of acquiring all tissue types, including gastrointestinal tract, digestive gland, gill, left and right kidney, hypobranchial gland, nervous tissue, muscle and gonad.

The sections were placed into histological cassettes and immediately fixed in 4% formalin in 1 µm filtered seawater for 48 hours. Following fixation, the samples were transferred to 70% ethanol. Samples were sectioned and stained with haematoxylin and eosin (H&E) at either the histopathology department of Medlab Central (Palmerston North, NZ), or Awanui Veterinary (Formerly: Gribbles, Christchurch, NZ). Additional stains, such as Ziehl-Neelsen (ZN) for haplosporidians (Diggles et al., 2002), Periodic acid/Schiff (PAS) and Periodic acid/Schiff- Diastase (PAS-D) for polysaccharides were also used on selected samples (Howard, 2004; Carella et al., 2018). An additional small section of right kidney tissue was also collected and stored in 100% ethanol for further molecular analysis.

4.2.4. General tissue alterations

Histology preparations were observed by light microscopy using an Olympus BX35 at magnifications of x40 to x1000. Eleven tissue-specific alterations were scored as presence/absence or semi-quantitatively, as described below, in relation to site and timepoint. Semi-quantitative assessment included the following: ceroid material deposition (brown pigmented oxidised lipid material) in connective tissue of right kidney, digestive gland and surrounding intestinal tract, as well as kidney stones (Copedo et al., 2024) (Chapter 3), haemocytosis, digestive gland atrophy, organ/tissue inflammation, gill epithelial atrophy or cilia loss (Perez-Cebrecos et al., 2022), gill protein level (Hooper et al., 2014), as described previously by Knowles et al. (2014), whereby 0: Absent, 1: Mild or minor changes to the tissue structure, 2: Moderate, $\frac{1}{2}$ of the organ disrupted, 3: High, up to $\frac{3}{4}$ of the tissue disrupted and 4. Severe, marked disruption and majority of tissue structure affected. The macroalgal quality within the stomach cavity was scored semi-quantitatively on a scale of 1 to 5 whereby 1 was 100% fresh with larger pieces of algae and 5 was 100% old, whereby algae

were degraded/digested to mostly fine particles, as previously described by Copedo et al. (2024) (Chapter 3).

4.2.5. Reproductive staging and egg viability

Female and male gonad development was categorised and graded using a generalised scheme adapted from Vélez-Arellano et al. (2015) and Shin et al. (2020), as described in Table. 4.2:

Table 4.2 Generalised reproductive gonad staging descriptions of *Haliotis iris*.

Gonad stage	Grade	Description
Resting	0	Early inactive stage where sex is generally unidentifiable
Early	1	Early inactive with mostly primordial or previtellogenic cells; sex determination is possible
Late	2	Gonad/ follicles are developing vitellogenic (formation of yolk protein) oocytes and spermatogonia, the appearance of mature well-developed oocytes and sperm cells. Many primordial/ previtellogenic cells observed
Ripe	3	Gonad at full maturity with very few previtellogenic cells in female and mostly large, well developed oval oocytes with a thick jelly membrane and, in males, dense, numerous mature sperm cells
Spawning	1	Loss of mature cells due to the spawning process
Spent	0	Degenerating stage whereby the follicle is observed to have atresic oocytes and/ or reabsorption of gametes through the process of phagocytosis
Redeveloping	1	Evidence of recent release of gametes but still has developing previtellogenic and vitellogenic cells

The proportion of individuals presenting gonads at each stage of development was plotted for visual representation (Fig. 4.5). An average maturation score was calculated as the number of individuals at each stage identified as the grade. For each of the females detected, further analysis was done to quantify pre-spawning atresia. Atresic oocytes were determined as those that were degrading and being reabsorbed. Identification included: cytoplasmic discolouration and darker staining giving a necrotic appearance, irregular jigsaw shape, as well as retraction and detachment from the jelly membrane. Three microphotographs were taken of the gonad of each female using cellsens imaging software (Olympus cellsens 3.1 [build 21,199]). The objective of an Olympus BX53 was set at x20, and three images of the gonad were randomly collected. For each image, the number of viable developing or vitellogenic and non-viable (atresic) oocytes were counted and recorded. The method proposed by Beninger (2017) was used to derive a percentage of atresia per individual egg-bearing pāua that had been graded as developing or mature (late or ripe). Spent females were included for visual representation but not included in the pre-spawning atresia analysis.

4.2.6. Pathogens and parasites

Parasites observed within the *H. iris* were identified histologically and recorded as present/absent. Additionally, ciliates previously identified through histology were freshly observed by dissecting a 10 mm section of live gill tissue and examining it using an Olympus dissecting microscope. The plasmodia of a haplosporidian-like parasite in the right kidney tissue previously described by Diggles

et al. (2002) and detected by Copedo et al. (2024) (Chapter 3) was also initially recorded by presence/absence but was subjected to further analysis and further histological staining, as described in Section 2.3. Upon detection of the plasmodia in the right kidney, the length of 35 plasmodia was measured (longest point) to $\pm 0.01 \mu\text{m}$ across three individual abalone ($n = 15$, $n = 10$, $n = 10$). The nuclei of five of the pre-measured plasmodia per individual *H. iris* were counted. Further to the measurements and counts of the plasmodia, individual abalone with plasmodia detected were analysed for parasite intensity. Once visual detection occurred using the x40 objective, a count was initiated followed by counts in an additional 24 randomly selected fields using cellSens™ software (Olympus cellsens Standard 3.1 [build 21199] on an Olympus BX53 compound microscope). The first count on initial detection was also included in the analysis because of the focal clustering of larger numbers of the plasmodia in few kidney tubules. Removal of these counts from several individuals resulted in a score of 0. The 25 counts were then averaged to provide a relative intensity score per individual abalone. Six of the corresponding ethanol fixed right kidney samples with a range of plasmodia intensities were selected for targeted molecular identification using PCR and metabarcoding methods see Section 4.2.7.

4.2.7. DNA isolation, PCR and metabarcoding sequencing

Molecular analysis was used to corroborate the putative diagnosis of haplosporidian infection, using primers for previously observed *H. iris* haplosporidians (Reece and Stokes, 2003) and generic eDNA primers to detect alternative pathogens. DNA was extracted and purified from approximately 20-25mg of the ethanol preserved right kidney tissue for each of 6 haplosporidian-like parasite infected *H. iris* individuals using a DNeasy Blood and Tissue kit (Qiagen, Hilden, Germany) according to the manufacturing protocols. As a result of PCR inhibition regularly associated with mollusc native DNA (Adema, 2021), a preliminary PCR was performed on a cascade dilution of 0x, 10x, 100x and 1000x of the DNA extracted using 18S rRNA eukaryotic primers Uni18SF and Uni18SR by (Zhan et al., 2013) to identify the optimal dilution factor required for the samples. Following this first assessment, the 10x dilution was selected and used to perform PCR (Fig. 7a). Two methods of PCR were conducted: a targeted approach using the primers 16S-A/ NZAH-R1 and 16S-B/ NZAH-F4 following methods from Reece and Stokes (2003), designed for the Haplosporidian/ Urosporidium parasite in previous publications and a non-targeted PCR using the 18S rRNA eukaryotic primers Uni18SF and Uni18SR by (Zhan et al., 2013), primarily targeting micro-eukaryotes.

For the targeted method, each PCR reaction included 1 μl of 10 mM of each primer, 10 μl MiFy mix (Bioline, Meridian Bioscience), 2 μl DNA (1/10), 7 μl sterile water. For each PCR run, a negative control (RNA/DNA-free water; Life Technologies), and one positive control (Gblock (DNA fragment), diluted 1/10,000) were carried out, PCR thermocycling was completed on an Eppendorf Mastercycler (nexus gradient) using the following profile: 1 cycle of 94°C for 4 min, then 35 cycles of 53°C for NZAH-F4 + 16S-B, or 59°C for 16S-A + NZAH-R1 for 30 s, 72°C for 1.5 min and a final extension 72°C for 5 min (Reece and Stokes, 2003). The size of final PCR product was assessed by electrophoresis.

In the non-targeted approach, each 18S PCR reaction included 1 µl of 10 mM each primer, 25 µl MiFy mix (Bioline, Meridian Bioscience), 3 µl DNA (1/10), 20 µl sterile water, a negative control was carried out in duplicate with the PCR mixture without the target. The total volume of the PCR reactions was 50 µl. The following profile was used: 95°C for 2 min, 40 cycles of 94°C for 15 s, 52°C for 15 s and an extension step at 72°C for 15 s. The 18S PCR positive samples then went through the clean-up method using the NucleospinGel and PCR Clean-up kit (Macherey-Nagel, Germany) and sent for paired-end sequencing on an Illumina MiSeq platform (Sequençh, Nelson, NZ).

4.2.8. *Bioinformatics*

The FASTQ files, containing the sequence data, were demultiplexed and primers removed using CUTADAPT (version 4.2; Martin (2011)), requiring a minimum overlap of 15 bp and no insertion or deletion. To remove low-quality calls, sequences were truncated on their 3' end at 215 bp and 190 bp for 16S, and at 225 bp and 216 bp for 18S, for the forward and reverse sequences, respectively. Sequences were subsequently quality filtered and denoised using the default parameters of the DADA2 R package (version 1.26; (Callahan et al., 2016)) and merged using a minimum overlap of 10 bp. Potential chimeric sequences were removed using the 'consensus' option of DADA2, where sequences found to be chimeric in a majority of samples are discarded.

Taxonomy was assigned using a combination of approaches and databases to increase taxonomic resolution while maintaining confidence in the assignments. Specifically, 18S data were assigned with the RDP Naïve Bayesian Classifier algorithm (Wang et al., 2007) applied on the SILVA reference database (version 132; Quast et al. (2013)) and with blastn and megablast (Camacho et al., 2009) on the GenBank nucleotide database (Benson et al., 2008) using the default values of the 'blastn_taxo_assignment' function of the biohelper R package (Laroche, 2024). Taxonomic assignments from each approach were then combined using the taxo_merge function of biohelper, which first normalizes taxonomy using the NCBI curated taxonomic database (Schoch et al., 2020), and, if there is consensus (>50%) across assigned ranks among the different approaches, uses the highest taxonomic resolution among them. Otherwise, it assigns taxonomy to the last common ancestor among the majority (>50%) of the approaches.

The top potential parasite amplicon sequence variants (ASVs) were selected for deeper exploration. Their sequences were blasted using Blastn (NCBI, <https://blast.ncbi.nlm.nih.gov/Blast.cgi>), the top 2 to 3 results within in each of the ASVs were collated and the accession number recorded in a table (Table. 4.6). The relative abundance was then determined for each feature based on the number of hits divided by the total number detected.

4.2.9. *Statistical analysis*

Statistical analyses were conducted with the R studio interface Build 375 (RStudio Team, 2021) using R version 4.4.0 (R Core Team, 2024). For the morphometric and sex ratio data the 13/03/2020

reference timepoint as cited in Copedo et al. (2024) (Chapter 3) was also included in the statistical analysis. The morphometric data were combined for all timepoints and analysed using a general linear model using the *car*, *emmeans* (Lenth, 2021), and *ordinal* package. Additionally, the sex ratio data for each timepoint were combined and only site and life stage were considered using chi squared tests. Histological data were analysed using site and date as explanatory factors. Analysis of the semi-quantitative data were performed using a polynomial ordinal linear regression model using the *MASS* package (Venables and Ripley, 2002). Binomial general linear models were performed on prevalence data *MCMCglmm* package (Hadfield, 2010). A p value < 0.05 was considered statistically significant. Additionally, for the semi-quantitative data three statistical models were created: 1) site*sample date, 2) site*sample date + life stage (adult vs sub-adult), and 3) site+sample date, the model with the lowest AIC (model, but not AIC (Akaike Information Criterion) value, reported in results) was selected as the model used in the analysis. Gonad scoring was performed using a generalised linear model followed by ANOVA with a type two sums sq and *emmeans* for post hoc comparison (Lenth, 2021)

4.3. Results

4.3.1. Temperature profile

Temperature data from the GHRSSST approximately 4 km from site 1 and site 2 indicated temperature offshore to be maximum 17.0 °C and minimum 10.6 °C, during the sampling period between March 2020 and April 2022. However, during the summer 2018 and 2019 SSTs reached 18.2 °C and 17.6 °C, respectively. Sea surface temperature (SST) anomaly data indicated regular occurrences above the 1985-1990 plus 1993 baseline temperature, indicating frequent marine heatwave events (Fig. 4.2).

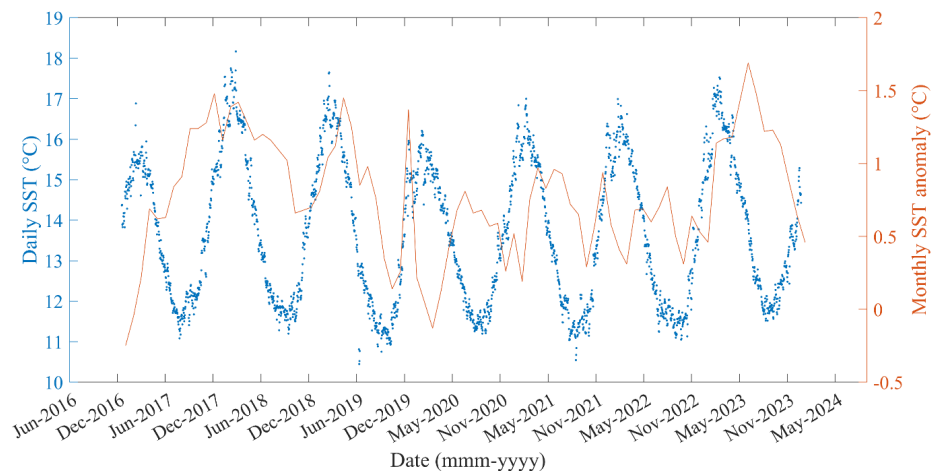


Figure 4.2 Course daily sea surface temperature (SST) (Left axis; blue dots) from a single location approximately 4 km from Site 1 (Ascots) and Site 2 (Owenga Harbour) (latitude 43.99°S, longitude 176.34°W). Data source: (JPL, 2015). Monthly SST anomaly timeseries from December 2016 to December 2023 (Right axis; orange line). The SST anomaly timeseries shows degrees above the climatological baseline covering the 1985-1990 plus 1993 period

Based on the timeseries data in Fig. 4.2. the average anomaly data for December was selected for visual representation for 2020, 2021, 2022 and 2023 (Fig. 4.3). December 2021 visually appears to be the warmest of the four time periods based on the SST anomaly gradient.

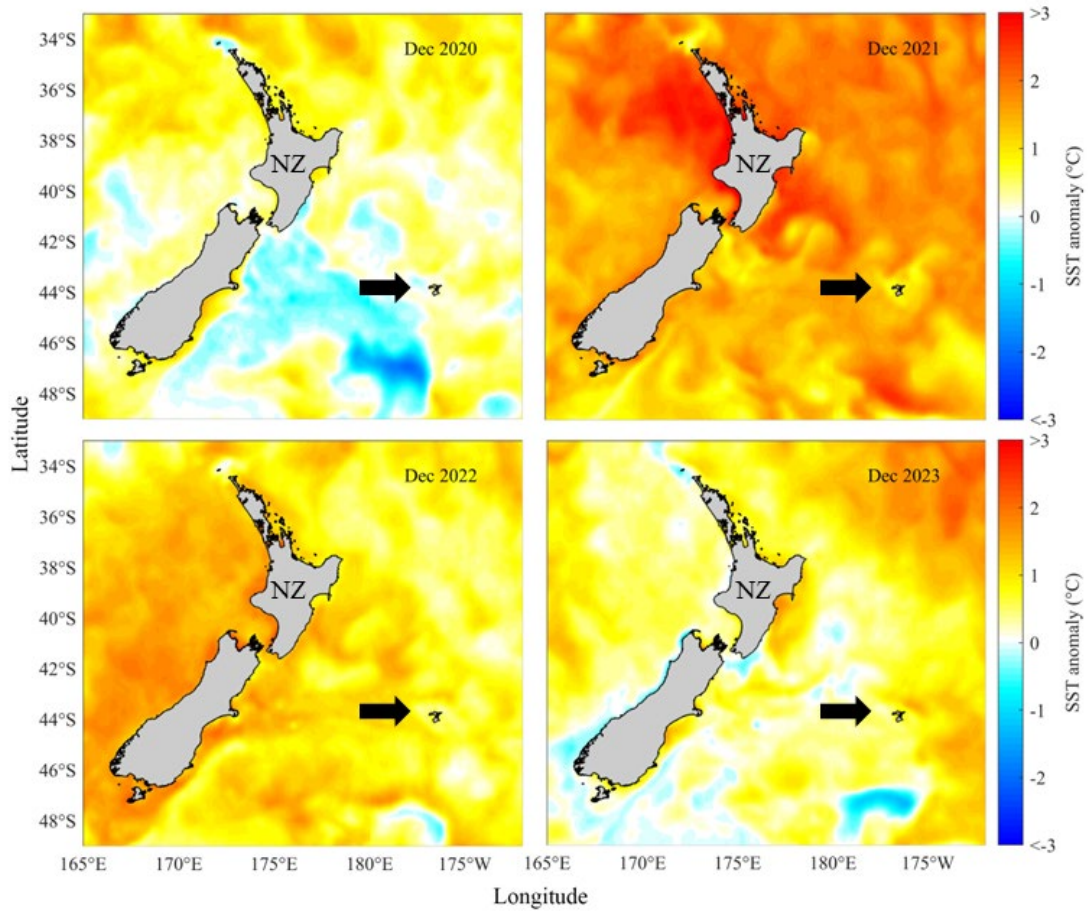


Figure 4.3 Visual representation of the average sea surface temperature (SST) anomaly data for the month of December for the years 2020, 2021, 2022 and 2023 around New Zealand (NZ) and the Chatham Islands (arrow). SST anomaly data sourced from NOAA Coral Reef Watch (<https://coralreefwatch.noaa.gov>) (Liu et al., 2014).

4.3.2. Morphometric parameters

The morphometric data indicated a significant difference in the whole animal wet weight between site 1 (Ascots) and 2 (Owenga) (Site x Life stage: $\chi^2_{(1)} = 31.4$, $p = < 0.001$), with adults at site 1 being heavier than those at site 2 ($t = 8.2$, $p = < 0.001$). Interactions were found between site and life stage for shell length measures (Site x Life stage: $\chi^2_{(1)} = 11.9$, $p = < 0.001$), whereby the sub-adults at site 2 were recorded to be slightly longer than those at site 1 ($t = 2.2$, $p = 0.03$). There was no difference in shell width or shell height between *H. iris* at site 1 and site 2 (Site: $\chi^2_{(1)} = 0.1$, $p = 0.78$ and Site: $\chi^2_{(1)} = 0.09$, $p = 0.75$, respectively) (Table. 3). Therefore, there was no differences in the L:H ratio between the 2 sites (Site: $\chi^2_{(1)} = 1.08$, $p = 0.3$). In terms of the sex ratio, the combined adult (n=60) and sub-adult (n=54) data for site 1 indicated a weak significance difference with sex deviating from the 1:1 ratio towards a female dominated population ($\chi^2_{(1)} = 3.7$, $p = 0.054$) whereas site 2 (adult (n=60) and sub-adult (n=60)) was not significantly different from the 1:1 sex ratio ($\chi^2_{(1)} = 2.3$, $p = 0.13$). However, when considering the adults only for both populations there appeared to be

significant deviations whereby site 1 was female dominated and site 2 male dominated ($\chi^2_{(1)} = 5.4$, $p = 0.02$ and $\chi^2_{(1)} = 8.3$, $p = 0.004$, respectively) (Table. 4.3).

Table 4.3 Morphometric and sex ratio data for the adults (n=60) and sub-adults (n=54) at site 1 (Ascots) and the adults (n=60) and sub-adults (n=60) at site 2 (Owenga Harbour). Data are reported as mean \pm standard deviations. The L:H ratio is the length to height ratio and sex ratio is M:F or male to female. Letters indicate statistical differences between site and life stages ($p < 0.05$). For the sex ratio the asterisk (*) indicates significantly different values when compared with a typical 1:1 sex ratio; $p \leq 0.05$ and two asterisks (**) $p \leq 0.001$.

		Weight (g)	Length (mm)	Width (mm)	Height (mm)	L: H ratio	Sex ratio M:F
Site 1.	Adult	390.7 \pm 59.2 a	127.0 \pm 7.2 c	88.4 \pm 10.8	36.7 \pm 8.7	3.7 \pm 1.2	0.54 *
Ascots	Sub-adult	117.4 \pm 57.1 c	87.7 \pm 13.5 b	67.0 \pm 9.7	23.1 \pm 5.1	3.9 \pm 0.6	0.95
Site 2.	Adult	320.6 \pm 39.3 b	123.6 \pm 6.6 c	91.7 \pm 4.9	34.9 \pm 6.7	4.3 \pm 5.1	2.22 **
Owenga	Sub-adult	118.3 \pm 28.8 c	92.2 \pm 6.8 a	71.1 \pm 12.9	24.1 \pm 6.3	4.0 \pm 0.9	0.79

4.3.3. Tissue alterations

The population prevalence for eight of the indices, along with additional semi-quantitative scores is recorded in Table. 4.4. No significant deleterious alterations were detected in the soft tissues. There were significant interactions between the two sites and the collection dates in some tissue conditions (Table 4.4). Prevalences and scores varied between the two locations and sampling timepoints for example elevated ceroid accumulation around the right kidney, digestive gland and sub epithelium of the gastrointestinal tract was detected (Table. 4.4 and 4.5). While there was an interaction of location and sample date with the presence of older food detected within the crop/stomach region, no differences were seen between life stages (Table. 4.4 and 4.5). For the prevalence of presence of spaces in the interstitial tissue of the digestive gland and kidney stone presence there was no interaction between location and sample date. Differences were also detected in the prevalence of kidney stones, with prevalence regularly above 40% at site 2 and above 20% at site 1 while prevalence in the sub-adults was between 0 and 40% (Table. 4.4 and 4.5).

Table 4.4 Data for 14 general pathological findings and tissue alterations are presented, including a semi quantitative food score, ciliate (*Scyphidia*- like) prevalence, ciliate intensity (int), gill alterations (e.g., epithelial atrophy or cilia loss), gill protein score (Gill P), haemocytosis (He), ceroid prevalence, ceroid score of the: right kidney (CK), digestive gland (CDG) and sub epithelial layer of the gastrointestinal tract (CSG), detachment of digestive gland tubule from basement membrane (DG gaping), interstitial space between the digestive tubules (DG IS), kidney stones (KS) and haplosporidian-like parasite (Hap) (Copedo et al., 2024), % percent prevalence, * only 1 sample, NR: Not recorded/ no samples provided.

Life stage	Site	Collection date	Food score	Ciliate (%)	Ciliate int	Gill alt (%)	Gill P	He (%)	Ceroid (%)	CK	CDG	CSG	DG gaping (%)	DG IS (%)	KS (%)	Hap (%)	
Adults	Site 1: Ascots	Mar-20	1.4	100	2.3	0	0.6	0	100	1.0	2.0	1.0	13	20	20	20	
		Nov-20	2.8	100	1.4	0	2.9	0	100	0.1	1.6	1.6	89	0	90	20	
		Mar-21	2.8	100	1.4	0	1.8	0	100	1.0	1.3	0.4	100	0	50	10	
		Apr-21	2.8	100	2.3	0	2.2	0	100	0.5	1.8	1.1	100	0	25	0	
		May-21	2.6	100	1.6	0	1.5	0	100	0.8	2.0	1.4	44	0	44	78	
		Apr-22	2.9	100	1.8	0	3.0	0	100	1.0	1.0	2.0	0	0	40	20	
	Site 2: Owenga	Mar-20	4.9	100	1.8	0	0.7	0	100	3.0	3.0	3.0	100	0	80	60	
		Nov-20	3.1	100	1.9	0	1.8	0	100	0.9	2.3	3.0	67	0	89	50	
		Mar-21	3.5	100	1.6	0	2.2	0	100	1.5	2.0	2.6	100	20	70	60	
		Apr-21	3.7	100	2.2	0	2.6	0	100	2.0	2.1	2.9	88	0	100*	100*	
		May-21	3.9	100	1.3	0	1.9	0	100	1.0	2.3	2.9	80	0	71	75	
		Apr-22	3.5	100	1.3	0	2.3	0	100	1.8	2.1	2.9	13	0	40	50	
		Site 1: Ascots	Mar-20	1.7	100	2.2	0	0.0	0	100	1.0	1.9	1.0	50	0	0	20
			Nov-20	3.1	100	1.5	0	1.7	0	100	0.0	2.1	1.1	40	10	20	50
Mar-21	2.9		100	1.0	0	1.4	0	100	0.2	1.0	0.0	100	0	10	0		
Apr-21	2.7		100	2.5	0	2.2	0	100	0.0	1.5	0.0	100	0	0	10		
May-21	NR		NR	NR	NR	NR	NR	NR	NR	NR	NR	NR	NR	NR	NR	NR	
Apr-22	3.5		100	2.3	0	3.3	0	100	0.0	1.0	1.0	0	0	0	0		
Sub-adult	Site 1: Ascots	Mar-20	4.9	100	2.0	0	1.1	0	100	1.4	2.1	1.4	70	0	20	60	
		Nov-20	3.8	100	1.9	0	1.1	0	100	0.0	2.3	2.0	100	20	40	40	
		Mar-21	3.3	100	1.3	0	1.9	0	100	0.4	1.6	1.3	90	0	10	70	
	Site 2: Owenga	Apr-21	4.1	100	1.6	0	2.0	0	100	0.8	1.8	2.2	100	0	0	67	
		May-21	3.4	100	1.1	0	2.2	0	100	0.2	1.7	1.2	70	0	0	50	
		Apr-22	3.9	100	1.2	0	2.7	0	100	1.5	1.4	2.3	0	0	30	40	

Table 4.5 Statistical analysis of the pathological findings and general tissue alterations observed through histology in table. 4.4. Text in bold indicate statistically significant values $p < 0.05$.

Scoring method	Alteration	Statistical method	χ^2	df	p value
Prevalence	Ciliates	Location * sample date	0	5	1
		Life stage	0	5	>0.05
	Gill alterations	Location * sample date	0	5	1
		Life stage	0	5	>0.05
	Haemocytosis	Location * sample date	0	5	1
		Life stage	0	5	>0.05
	Ceroid	Location * sample date	0	5	1
		Life stage	0	5	>0.05
	DG gaping	Location * sample date	0	5	1
		Life stage	0	5	>0.05
	DG spacing	Location * sample date	3.06	5	0.69
		Life stage	6.5	5	0.01
	Kidney stones	Location*sample date	5.02	5	0.41
		Location	52.09	1	0.001
		Life stage	52.09	1	0.001
Haplo-like parasite	Location * sample date	16.85	5	0.005	
Semi-quantitative	Food score	Location * sample date	84.67	5	0.001
		Life stage	2.38	1	0.12
	Ciliate intensity	Location * sample date	17.86	5	0.003
		Life stage	1.37	1	0.24
	gill protein score	Location * sample date	20.05	5	0.001
		Life stage	2.31	1	0.13
	Ceroid kidney	Location * sample date	20.75	5	0.001
		Life stage	57.26	1	0.001
	Ceroid DG	Location * sample date	12.59	5	0.028
		Life stage	18.78	1	0.001
	Ceroid SG	Location * sample date	26.52	5	0.001
		Life stage	100.81	1	0.001

4.3.4. Reproductive status and atresia

The gonad tissue from most of the adult *H. iris* were observed to be in the ripe stage, with large mature oocytes. The adults at Ascots appeared to be in the ripe stage from November 2020 to May 2021, while adults at Owenga were developing in November 2020 and ripe from March through to May 2021. This resulted in a significant interaction in site and date for the mean gonad scoring (Location* sample date: $\chi^2_{(5)} = 11.64$, $p = 0.04$). The sub-adults were observed to spent and early developing gonad which also resulted in a difference between life stages ($\chi^2_{(1)} = 26.99$, $p = <0.001$) (Fig. 4.4).

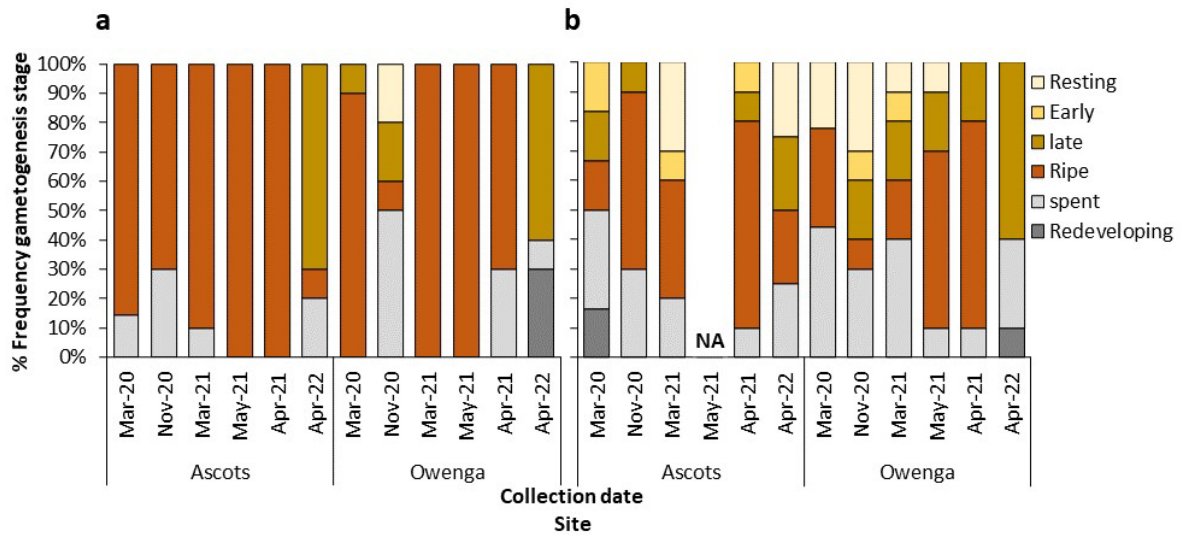


Figure 4.4 Frequency of reproductive staging of *H. iris* from 2 sites (Site 1: Ascots and Site 2: Owenga) on the Chatham Islands over multiple timepoints between March 2020 and April 2021 for a) adult abalone and b) sub-adults.

Atresic oocytes were detected through histological analysis (Fig. 4.5). The number of atresic oocytes counted in the female adults of *H. iris* was of interest and percentage of affected oocytes was relatively high. There were significant interactions in site and date for the mean of the pre-spawning atresia ($F_{(4, 179)} = 4.22, p = 0.0027$) and no differences between life stages ($F_{(1, 179)} = 0.4, p = 0.53$). The percentage of atresic oocytes was highest at site 1 (Ascots) in adults sampled in November 2020 (74%) and in the sub-adults in March 2021 (85%) (Table. 4.6).

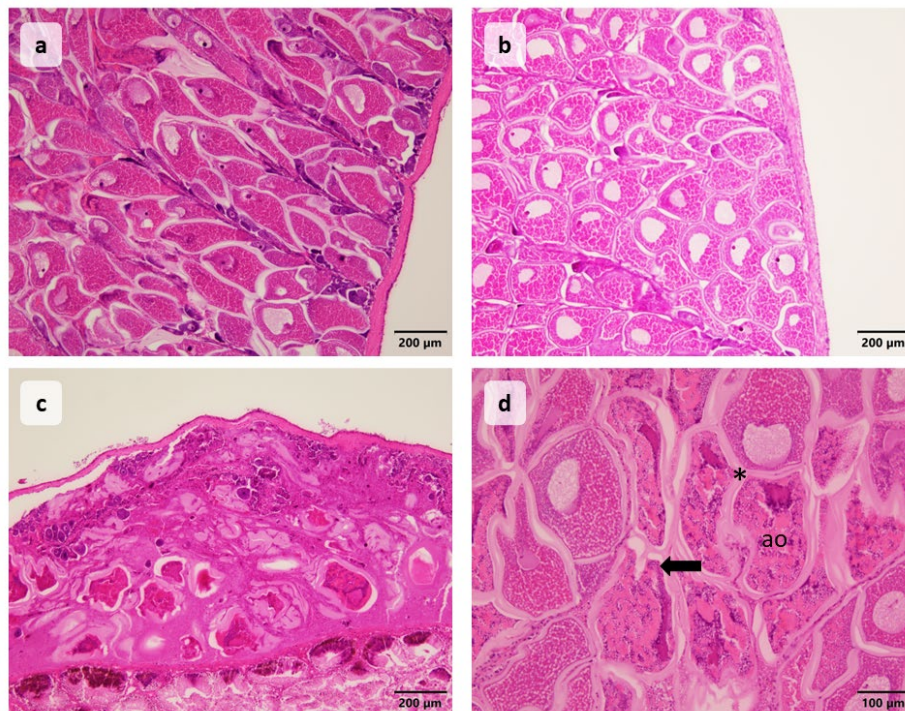


Figure 4.5 Representative images of the reproductive staging of female *H. iris* showing a) late-stage gonad development of oocytes, b) ripe stage gonad with mature oocytes, c) spent stage with degrading/ atresia oocytes and atresic debris, and d) atresic oocytes (ao) of a ripe stage female

indicating potential pre-spawning atresia, jelly membrane of the oocytes (*) and atresic oocyte showing detachment from the membrane (arrow).

Table 4.6 Mean (\pm SD) percent of atresic (non-viable) oocytes in females that were graded as spent, ripe or late developing. NR = not recorded, empty spaces = no samples available.

		Ascots					Owenga						
		Mar-20	Nov-20	Mar-21	Apr-21	May-21	Apr-22	Mar-20	Nov-20	Mar-21	Apr-21	May-21	Apr-22
Adults	Spent	90 \pm 0	89 \pm 8	98 \pm 0			95 \pm 0		100 \pm 0		96 \pm 1		80 \pm 0
	Ripe	39 \pm 13	74 \pm 12	55 \pm 17	65 \pm 13	30 \pm 16	47 \pm 0	59 \pm 8		21 \pm 4	49 \pm 9	49 \pm 16	
	Late						59 \pm 17						
Sub-adults	Spent	92 \pm 8	96 \pm 5	100 \pm 0	91 \pm 0	NR	100 \pm 0	93 \pm 12	100 \pm 0	98 \pm 2	100 \pm 0	100 \pm 0	93 \pm 10
	Ripe			85 \pm 11	61 \pm 20	NR	38 \pm 0	19 \pm 0		47 \pm 0	49 \pm 24	16 \pm 0	
	Late	25 \pm 0				NR				68 \pm 12	12 \pm 1		

4.3.5. Pathogens and parasites

4.3.5.1. Histological assessment

Two parasite types were observed in association with *H. iris*. *Scyphidia*-like ciliates (Diggles and Oliver, 2005) and a haplosporidian-like parasite. *Scyphidia*-like ciliates were observed at 100% prevalence in both populations at each time point (Table. 4.4) and were easily identifiable under a dissecting microscope (Fig. 4.6 a and b). There was a significant interaction in the presence of the haplosporidian-like parasite between site and collection date (Tables. 4.4 and 4.5). Differences between the collection dates in 2021 were apparent at site 1 for March/April and May ($p = 0.03$ and $p = 0.034$, respectively) (Table. 4.4).

Multinucleate plasmodia of the haplosporidian-like parasite were observed only in the right kidney tissue of several individual pāua (Fig. 4.6 c-d). The mean plasmodia length was 14 μm and ranged from 4.91 μm to 22.37 μm , width from 5.39 μm to 9.28 μm ($n=35$) and each plasmodium was observed to have between 5 and 8 nuclei ($n=15$). The relative intensity (mean number) of the plasmodia within the right kidney of *H. iris* were as follows: during March, April, and May adults at site 1: 2.32 ($n=1$), 0 ($n=0$), 1.16 \pm 1.19 ($n=7$) and site 2: 1.1 \pm 1.1 ($n=5$), 5.8 ($n=1$), and 2.85 \pm 2.1 ($n=6$), respectively. For Sub-adults at site 1: 0, 0.08 ($n=1$), and 0 and sub-adults at site 2: 1.76 \pm 1.25 ($n=4$), 1.03 \pm 0.5 ($n=4$), 1.31 \pm 1.2 ($n=5$), respectively. No differences were observed between date and site ($f_{(28,2)}=0.63$, $p=0.54$) and site and life stage ($f_{(30,2)}=0.01$, $p=0.91$). Plasmodia were detected using ZN, PAS and PAS-D stains with H&E being the most effective stain for detection overall (Fig. 4.6 c, d, e, f). In contrast to Diggles et al. (2002) ZN staining indicated that the plasmodia were not acid-fast. The PAS and PAS-D indicated presence of glycogen-like material within the plasmodia bodies. Overall, right kidney tissue appeared to be in good condition, and no haemocyte proliferation was detected.

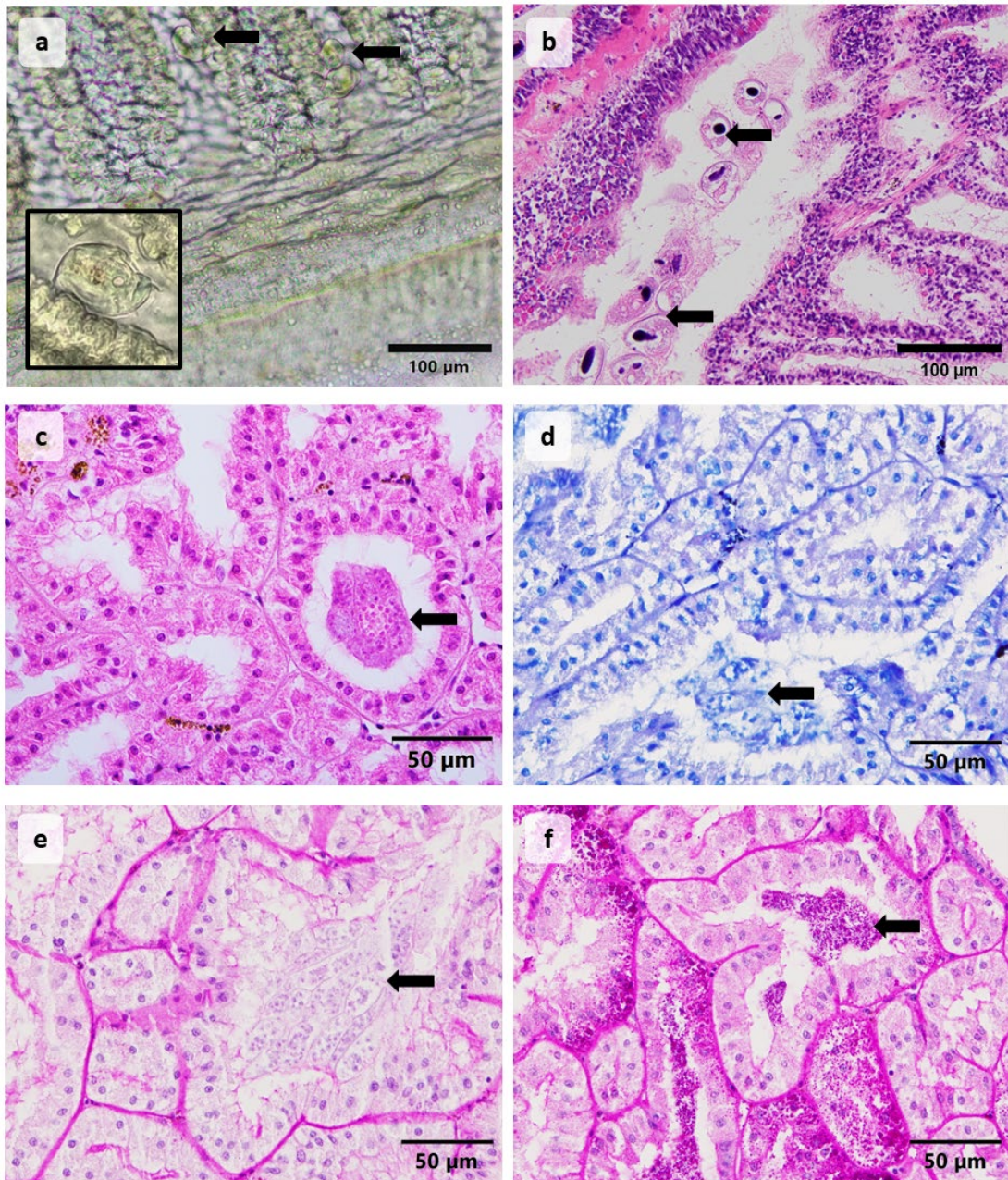


Figure 4.6 Photomicrographs of the parasites observed in *H. iris* samples a) gross observation of the ciliates attached to the gills (arrows) inset: enlargement of ciliate attached to gill filament, b) ciliates observed in histology stained with H and E, c) the haplosporidian-like multinucleate plasmodia (arrow) located in the lumen of the right kidney was observed to have refractive spore-like structure H&E, d) the plasmodia in the lumen of the right kidney stained using ZN, e) PAS-D and f) PAS. Plasmodia are indicated with arrows.

4.3.5.2. Molecular identification of parasites

Two molecular approaches were performed to further identify the haplosporidian-like cells: a PCR targeting the SSU rRNA gene sequence of the haplosporidian-like parasite from NZ *H. iris* (Reece and Stokes, 2003) and metabarcoding.

The PCR analysis performed on the right kidney tissue shows negative results for the haplosporidian-like parasite (Diggle et al., 2002; Reece and Stokes, 2003) except for the positive control (Gblock, Fig. 4.7), suggesting the observation of a different/new parasite in this study.

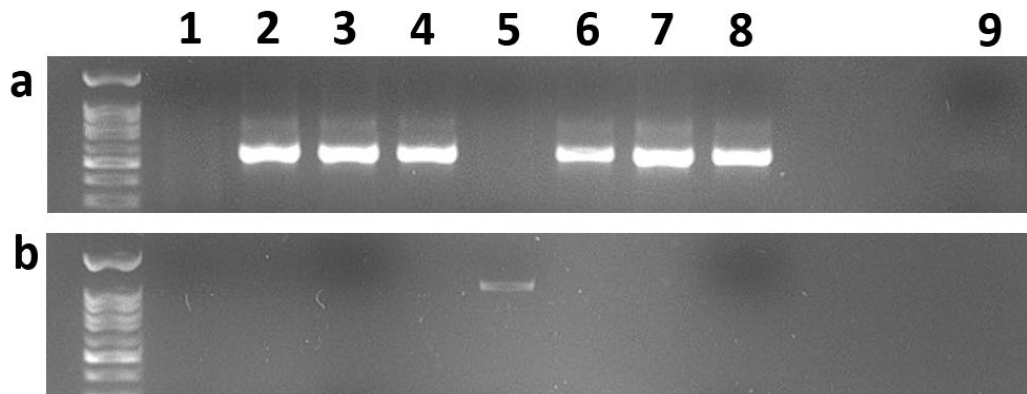


Figure 4.7 The PCR Gel results for a) 18s primers using different dilutions of DNA extraction from sample 1: a1) pure, a2) 1/10 concentration, a3) 1/100, a4) 1/1000, and sample 2: a5) pure, a6) 1/10, a7) 1/100, a8) 1/1000, and a9) neg control, b) PCR gel results using NZAH-F4 and NZAH-R1 primers on 1/100 diluted samples b1) sample 1, b2) sample 2, b3) sample 3, b4) sample 4 b5) GBlock, positive control at approximately 1100 base pairs, and b8) neg control, b6, b7, and b9 are empty slots.

A total of 65,431 reads were obtained from the sequenced data. After quality filtering, denoising, paired-end merging and removal of potential chimeric sequences, a total of 100 ASVs and 45,946 reads remained, with a mean of 15,315 reads / sample.

The three main groups detected based on the last common ancestor were Apicomplexa, Sessilida and Haptoria (Table. 4.7). No hits were detected for the previously identified Urosporidium/haplosporidian-like parasite.

Table 4.7 Gene sequence results from gene blasting the 18S amplicon sequence variants, of particular interest, of the 3 samples of abalone kidney tissue. The top 2 to 3 closest species were recorded for each of the 3 selected features and the last common ancestor was recorded.

Feature ID	Accession number	Identity	E-Value	Query coverage	Closest species	Last common ancestor	Relative abundance
6f373dbe6c bc5bcd6e50 fa56da154f 77	MH375329.1	79.86%	2.00E-72	100%	<i>Cryptosporidium</i> sp.	<i>Apicomplexa</i>	0.1%
0d2c9b021 4a245445ba e15860cab5 201	MN493109.1	80.10%	2.00E-72	100%	<i>Theileria</i> sp.		
	KP698209.1	95.85%	0	100%	<i>Scyphidia ubiquita</i>	<i>Sessilida</i>	53.7%
	KP698210.1	93.66%	4.00E-169	100%	<i>Mantoscaphidia branchi</i>		
	ON157280.1	91.55%	8.00E-156	100%	<i>Vorticella</i> sp.		
6e9fcd2b0c 6e21db389e 738de2591c 7d	KY355505.1	98.86%	8.00E-175	100%	Uncultured eukaryote	<i>Haptoria</i>	44.9%
	LN870157.1	96.59%	2.00E-161	100%	<i>Haptoria</i> sp.		
	OR042381.1	96.58%	7.00E-161	100%	<i>Pseudoamphileptu s apomacrostroma</i>		

4.4. Discussion

The histological information presented in the current study adds critical seasonal and inter-year dimensions to an initial investigation by Copedo et al. (2024) (Chapter 3) and provides further information on the site-specific differences between two *H. iris* populations from the main Chatham Island. Marked differences were noted in the *H. iris* tissues between the two sites; however, these differentials varied in significance over time. For example, elevation of ciliate numbers occurred in March 2020 and April 2021 when compared to November 2020 and March 2021 indicating potential seasonal and annual variations. More consistently, tissue condition observations made during the March 2021 collection support those reported by Copedo et al. (2024) (Chapter 3) in similar-sized individuals sampled in the same month. The increased temporal resolution in the present study confers greater confidence in the detection of pathological findings and tissue alterations including ceroid accumulation, kidney stones, ciliates, and haplosporidian-like plasmodia being associated with slower growth. These combined observations emphasised the health and performance differences between the sites. Food integrity, as an indicator of quality, in the gastrointestinal tract was similar between both populations post-transport to the laboratory. However, based on site characterisations *H. iris* from Ascots had more available algae than Owenga. Although, site differences can only be tentatively inferred as availability, diversity and quality of algal species may change over time. *Haliotis iris* from the Owenga site also had increased prevalences of kidney stones, haplosporidian-like parasites in the gut, and elevated ceroid. In addition, this population showed evidence of spawning events and a lower proportion of atresic oocytes when compared with the second site.

4.4.1. Nutritional stress and an ageing population.

Proportionally wider shells of the slower growing site (site 2, Owenga) were apparent within this study, lengths were similar between the two sites providing an opportunity for ‘same size’ comparison. It is likely that depleted nutrition contributes substantially to the slow growth due to dietary limitations, as mentioned previously by Bayne (2004), Venter et al. (2022), Van Nguyen et al. (2023) and Copedo et al. (2024) (Chapter 3). This is supported by Van Nguyen et al. (2023) who found that slower growing *H. iris* from the Chatham Islands, including Owenga, had lower levels of several key organic acids (including some essential fatty and amino acids) circulating in the haemolymph. However, this influence is closely followed in importance by physiological alterations from external and internal stressors (Bayne, 2004). For example, increased sedimentation also impacts nutrient absorption and respiration, which can affect tissue and shell growth (Poore, 1973; Schiel et al., 2006; Saunders et al., 2009b; Laferriere, 2016). Additionally, increased population density has been observed to correlate with slower growth and the degree of reproductive development in *H. laevigata* (McAvaney et al., 2004).

Based on the results from Copedo et al. (2024) (Chapter 3) and A. C. Alfaro (unpublished observations), it appears that algae at site 1 are more abundant, palatable, and easier to digest, with consequently higher consumption. Access to a diverse range of macroalgal species is also known to

improve abalone growth (Stuart and Brown, 1994; Mai et al., 1995; Viera et al., 2011). It should, however, be noted that the algal architecture within the stomach/crop region was decayed in samples from both sites post 24–48-hour transport, which is consistent with digestion time (Day and Cook, 1995; Britz et al., 1996). It is therefore likely that reduced nutritional quality and quantity of food available (reduced energy availability) to the slower-growing population is limiting growth, while exacerbating other tissue conditions such as ceroid-lipofuscin accumulation. The inferences based on gut content are therefore tentative and would benefit from further *in situ* assessments.

Ceroid and lipofuscin both present as pigmented brown to yellow waxy aggregates and both are by-products of oxidative stress and typically termed as ‘ceroid-lipofuscin’ due to the similarities (Carella, 2015; Miller and Zachary, 2017; Webb and Duncan, 2019; Copedo et al., 2024). Lipofuscin is typically associated with age as a ‘wear and tear’ pigment in vertebrates where the yellow/brown pigments accumulate as cellular debris, from the lysosomes, in the cytoplasm as part of a normal cellular process. Although similar to lipofuscin, ceroid pigments are considered to be associated with pathological conditions (Dolman and MacLeod, 1981; Zaroogian and Yevich, 1993; Seehafer and Pearce, 2006; Jung et al., 2007b; Miller and Zachary, 2017). Lipofuscin and ceroid can also increase accumulation of lipid peroxidation as a result of their ability to facilitate their own production (Jung et al., 2007a). The lysosomes within the cell may not be able to digest all the pigment, resulting in the accumulation outside of the cell (Dolman and MacLeod, 1981). The build-up of both lipofuscin and ceroid pigments impairs tissue function and can correlate with impacted growth (Hole et al., 1995). As a result of the similarities between ceroid and lipofuscin and the difficulty of separating the two, the term ‘ceroid’ will be used generically henceforth.

Incidence of elevated ceroid material within the interstitial tissues of the *H. iris*, was observed to be higher in the adults at the slower growing site (site 2, Owenga) based on the statistical interaction, reflecting a pattern previously observed by Copedo et al. (2024) (Chapter 3). The increased level of ceroid in the slower-growing population indicates a potential cumulative tissue maintenance cost (Terman and Brunk, 1998). The increase in ceroid, whether from poor nutrition, potential thermal stress from heatwaves or self-driven production is also likely to impact growth by reallocating energy away from growth for general tissue and cellular maintenance (Portner and Farrell, 2008; Kooijman and Kooijman, 2010; Sokolova et al., 2012; Delorme, 2017; Booth, 2018; Steeves et al., 2018). If the habitat with the slower growing population is warmer, then accumulation of oxidative damage is to be expected, exacerbating the formation of ceroid production (Marigomez et al., 2002; Carella, 2015; Shaw et al., 2019; Webb and Duncan, 2019). Finally, if, ceroid production is constant with age and aging is a “progressive loss of physiological integrity,” based on the statement by Cohen (2018), then the build-up of ceroid would impair tissue function. Therefore, the slower growing population displays not only a reduced scope for growth because of cellular destabilisation but also accelerated senescence (age). Although *H. iris* were not aged during this study (e.g., by counting shell growth rings), based on the ceroid differences between the adults and subadults, and the differences between

the slower and faster growing populations, as well as the biased sex ratios, and parasite accumulation, there is evidence to suggest that the adults in the slower growing population are older than their faster growing counterparts. However, future investigations should include aging techniques to confirm these findings. Comparisons of physiological age (loose measure of physiological fitness) versus the chronological age (absolute lifespan) (Philipp et al., 2005) between the two populations would definitively confirm the ‘slower growing’ characterisation. Typically, physiological age and chronological age are positively correlated, however they may not be linear. Furthermore, based on minimum legal catch sizes it is also possible that there is an accumulation of older abalone in the slower growing population which never grow large enough to be removed by fishing activity.

In terms of the sex ratios, the adult populations from the slower-growing site were male dominated when compared to the fast-growing, female dominated, site. This result is consistent with the observations of Poore (1973), who suggested that older populations of *H. iris* trended towards male dominance. This is also supported by Leonart (1992), who observed a male dominated population in *H. laevigata* and attributed it to the females being fished first due to their larger size. However, it is also likely that due to the suboptimal habitat and the energetic investment required to produce oocytes, female mortality could be higher in the slower growing population resulting in a bias towards male survival. Although the slow-growing population histologically appears to have conditions, such as the ceroid and kidney stones, which would influence metabolic maintenance of the tissues, as well as the nutrient deprivation from limited food access and, potential exposure to suboptimal temperatures, they are still reproductively active. Based on these factors (diet, temperature, reproduction), it could be suggested that they have adapted to ‘life in the slow lane’ (Clarke, 1988; Philipp et al., 2005).

4.4.2. *Site-specific reproductive condition and atresia*

The reproductive stages encountered and elevation of oocyte atresia in the adults is of particular interest. Gametogenesis was observed in the November 2020 snapshot, but the ripe gametes appeared to be retained up until May 2021. If these observations represent stasis within the gonad, it becomes unclear when/if spawning occurred in 2021. Additionally, developing gametes were observed in November 2020 at the Owenga site (site 2), which may suggest a previous spawning event (Autumn) and local population differences in each bay. Poore (1973) also observed differences in gametogenesis staging between two sites in NZ, whereby at one of the site’s spent gonads were very rarely observed whereas all were spent post-spawning at the other site. The results of the present study also support Poore’s (1973) original statement regarding the unreliability of making generalisations regarding spawning season when samples are only collected for one year. Although the present study provides only a snapshot of the gametogenesis cycle, the data suggest variability in timing of the spawning season each year. There is variation in spawning magnitude and timing, the broad trends described by Poore (1973) and Wilson and Schiel (1995) suggested development of gametes leading up to the November 2020 sampling could be expected, following the Autumn spawning. This would theoretically be followed by ripening, then spawning associated with the

February and March 2021, and potentially April 2021 sample events, depending on localised variability. Few studies on *H. iris* in NZ have focused on the histological staging of reproductive development over multiple seasons. This is particularly so with respect to localised populations and changing climate, but such knowledge gaps indicate profitable future directions for research. A further area for investigation would be the assessment of gametogenesis patterns and differential oocyte quality between populations across multiple years to build on the data and provide greater confidence in interpretation.

There is generally high variation in the spawning season of haliotids with some species maintaining condition for months and others such as *H. iris* having discrete spawning seasons (e.g., Webber and Giese, 1969; Poore, 1973; Wilson and Schiel, 1995). Additionally, spawning failure is common, Poore (1973) and Sainsbury (2010) both reported years where there was no spawning detected, for example 1969 and 1974, respectively. According to Poore (1973), temperature alone could not explain spawning failure in 1969, due to a successful site having a similar temperature profile. Gonad production is an energy demanding process that can impact behaviour and growth rate: during the winter period shell growth slows and correlates with the production of gonad (Poore, 1973), highlighting the value in exploring energy balance as a means to interpret variability in reproductive performance. Furthermore, controlled experiments are required to assess the relationship between reproductive performance, temperature and nutrition.

In addition to the unusual reproductive staging results, there was also an increase in appearance of pre-spawning atresia (oocyte resorption) in the adults. The increase in atresia is potentially indicative of a delayed spawning and a sub-optimal environment (Beninger, 2017; Chérel and Beninger, 2017). The percent of atresic oocytes was observed to be higher in the faster growing population and could potentially support the hypothesis that atresia is removing older oocytes, to favour development of the younger oocytes, rather than over-investing in a single spawning event. Atresia is known to be a reabsorption strategy of energy recycling during adverse conditions, such as thermal stress (Beninger, 2017; Chérel and Beninger, 2017). It has been observed in several mollusc species including, clams, mussels, and oysters (Steele and Mulcahy, 1999; Pérez et al., 2013; Chérel and Beninger, 2017; Copedo et al., 2023). In a previous study (Wilson and Schiel, 1995), resorption of oocytes in *H. iris* was also noted during the lead up to spawning, as well as during recovery post-spawning, indicating removal of mature oocytes. Also, for *Haliotis discus hannai* it was found that oocyte quality improved, in terms of lipid and protein content, after the first spawning and post reabsorption, resulting in more consistent survival of the larvae (Fukazawa et al., 2005).

Although Poore (1973) could not attribute temperature to the spawning failure, temperature does influence the reproductive cycle of many species of *Haliotis* and can potentially alter reproductive phenology (Poore, 1972; Wilson and Schiel, 1995; Kim et al., 2016). It is also known that spawning events occur after a change in temperature and typically occur as water temperature starts to decline (Poore, 1972; Wilson and Schiel, 1995; Kim et al., 2016). Disruptions associated with ocean

warming, e.g. temperature, habitat alteration and food availability, can also impact reproductive condition and therefore spawning (Moss, 1998). The present study therefore highlights the need for ongoing multi-year sampling to build a reliable gametogenesis map for *H. iris* particularly regarding the changing climate. Additionally, further research confirming scope for growth and impact of temperature is required to resolve questions such as, whether the fine-scale genetic variability underpins the site-specific growth patterns, whether there is a greater benefit of being larger or smaller under stress whether temperature will impact spawning cues, and how the occurrence of pathogens further impacts growth and reproduction.

4.4.3. Pathogens

The detection of 2 groups of ciliates, the first being *Sessilida* and the second *Haptoria* in the metabarcoding analysis was expected as there was a high number attached to the gills of the *H. iris* and 100% prevalence in both populations. Numerous species of ciliates also live in association with aquatic molluscs (Bower, 2006). Previous studies on *H. iris* have detected ciliates on the gills and determined them to be either *Sphenophyra*-like or *Scyphidia*-like (Diggles et al., 2002; Muznebin et al., 2021; Copedo et al., 2024). The high DNA metabarcoding identity score of the groups indicates that the ciliates detected on the gills are likely to be *Scyphidia* sp.

The detection of the haplosporidian-like plasmodia within the right kidney tissue of adult *H. iris* were initially of concern due to the >50% population prevalence in the adults of site 2, and >40% prevalence in the sub-adult population of site 2, as well as a similar occurrence associated with a mortality event in juvenile *H. iris* reported by Diggles et al. (2002), Hine et al. (2002) and Reece and Stokes (2003). However, unlike the above studies, within the current study no other plasmodial parasites were observed in other tissues histologically. Based on results of Copedo et al. (2024) (Chapter 3), the right kidney tissue was targeted within the present study to investigate the parasite and provide more taxonomic information. It was found using targeted and non-targeted (metabarcoding) PCR techniques that the parasite in the right kidney within this study was different from previously identified by Diggles et al. (2002) and Reece and Stokes (2003). The current parasite within the *H. iris* was only detected in the right kidney lumen of both life stages (adult and sub-adult) and no immune response or mortalities were associated with it. Furthermore, in contrast to the parasite detected within this study the juveniles in Diggles et al. (2002), Hine et al. (2002) and Reece and Stokes (2003) presented with a plasmodia stage of a novel parasite in most tissue types (e.g. gill and epipodium etc.). Diggles et al. (2002) also reported the haplosporidian-like plasmodia in the right kidney of adult *H. iris* and suggested the low numbers and prevalence could be representative of a natural infection, and thus adults could potentially be asymptomatic carriers. Whereby, the question remained whether the parasite detected within this study is the same species previously described and observed or whether they were a coincidental occurrence. In addition, based on Diggles et al. (2002) study, the parasites were associated with poorer host growth, with results from Reece and Stokes (2003) placing it closer in the phylogenetic tree to *Urosporidium*. Little is known about the

haplosporidian-like (*Urosporidium*) parasite found in *H. iris* by Diggles et al. (2002) and Hine et al. (2002) or the host-pathogen interaction particularly regarding climate change.

The metabarcoding analysis also identified the presence of apicomplexans (*Cryptosporidium* and *Theileria* sp.). *Theileria* sp. and *Cryptosporidium*'s are protozoan parasites of mammalian species. *Cryptosporidium*'s are typically found in cattle faecal matter which can contaminate shellfish, particularly if the waters are polluted by anthropogenic discharge (e.g. livestock faeces during rain events) (Srisuphanunt et al., 2009; Srisuphanunt et al., 2023). *Cryptosporidium*-like cells have previously been observed adhered to the mucosa layer of the intestine in abalone (Handlering et al., 2002), so detection is expected in the *H. iris*. Detection, of *Cryptosporidium* in the kidney tubules is likely incidental and represents contamination from the main gut section (Handlering et al., 2002). However, *Cryptosporidium* is also a member of the apicomplexan group (Rajapandi, 2020), along with Eimeriidae, which causes renal coccidiosis in several molluscan species (Chong, 2022a). Due to the low identity value of the Apicomplexa group, the limited genetic data of NZ parasites (Thomas et al., 2022), small sample number, and the possibility of low-quality DNA or degradation, the haplosporidian-like parasite could not be identified further. Based on the molecular results it is hypothesised that the parasite belongs to the apicomplexan group rather than the ciliate or haplosporidian/ *Urosporidium* group, but further molecular research is required for species specificity. Additional research is required to confirm and validate the parasites detected in the kidney tissue of Chatham Island *H. iris*. Regardless of parasite specificity based on previous pathogen research on emergence and spread, such as *Perkinsus olseni*, a protistan parasite (Muznebin et al., 2021; Lane et al., 2023), the information presented provides a potential early warning of a parasite that may impact the *H. iris* in the future.

4.4.4. Contributing factors to slow growth and future vulnerabilities

The lack of amino acids observed previously in algal food (Van Nguyen et al., 2023) and the limited and poor algal quality inferred in this study implicates inadequate nutrition as a key influence on slow growth. Although ceroid deposition in the tissues was unlikely to be the initial cause of the slow growth, once it reaches an intensity where it propagates it is likely to have cumulative impacts on the energy budget. Furthermore, the *H. iris* from both sites showed signs of gametogenesis, presence of kidney stones (right kidney), and parasites which represent additional energetic demands on the *H. iris* because of energy reallocation and immune defence. Due to these additional energetic demands the energy available for growth is likely limited, resulting in slower growth.

The Chatham Islands sit in a marine heatwave hotspot, which regularly experiences anomalous sea surface temperatures and extended MHW days (Montie et al., 2023). Although approximate maximum temperatures during the sampling period remained below 17 °C there were strong sea surface temperatures anomalies observed during this period. In addition, the previous two summers showed temperatures reaching ~18 °C. Elevated temperature can interact and exacerbate the conditions discussed above, and impact the overall metabolic scope, thus further reducing available

energy. In a study by Nguyen et al. (2023), it was found that with prolonged periods (weeks) of temperature above 18°C *H. iris* could not reduce their energy expenditure, resulting in energy demand exceeding supply, leading to a vulnerability to thermal stress during the summer period. However, it is also likely that local adaptation of *H. iris* to cooler temperatures in the Chatham Islands mean that lower thermal tolerance is possible. Furthermore, increasing sea temperatures due to climate change are likely to impact local seaweed abundance and diversity. It is well known that marine heatwaves threaten marine biodiversity resulting in impacts on kelp forests, resulting in compromised future food sources for *H. iris* (Rogers-Bennett and Catton, 2019; Thomsen et al., 2019; Rogers-Bennett et al., 2021; Nguyen et al., 2023). The food supply, temperature, and parasite presence observed within the current study, as well as other research (Morash and Alter, 2016; Venter et al., 2022; Nguyen et al., 2023; Van Nguyen et al., 2023), indicate that *H. iris* populations are likely to be vulnerable to climate change phenomena, notably marine heatwaves. In addition, research by Nguyen et al. (2023) and Aalto et al. (2020) also indicate that the adult life stage is likely the most vulnerable to future environmental stressors.

4.4.5. Conclusions

This histological investigation provides key information about the factors contributing to slow/stunted growth in NZ abalone. The following factors were implicated: site, environment, parasites, pathology, reproduction, as well as nutrition as previously described in Copedo et al. (2024) (Chapter 3), exacerbated by a likely vulnerability to increased temperature. pathological findings observed (e.g. ceroid) were primarily detected in the adult populations which could indicate that growth differentials start to occur once the individuals reach maturity. If ceroid is an indicator of age and production is constant, then even without chronologically aging the shells, its presence supports the anecdotal observations of growth differences. The current study highlights several dynamic parameters following on from the initial March 2020 investigation to further elucidate population differences. Further information on the gametogenesis cycle over multiple years, spawning failure, and recruitment of new juveniles of *H. iris* are critical, not only in a changing climate but also under the additive pressure of fishing. In addition, further monitoring of the gametogenesis cycle will also provide key knowledge in understanding growth phenology and energy allocation. In parallel to the monitoring of growth and reproduction, a means of assessing age across a large size range and quantifying ceroid deposition would also be beneficial in determining the relationship between chronological and physiological age. Finally, pathogens present a potential threat; the parasite observed in the right kidney tissue in wild *H. iris* deserves particular attention, noting that it could also provide a potential early warning of future health problems. Such possibilities could be assessed if there is greater knowledge of host/parasite interactions under the influence of climate change. Further work should include the impact that this parasite may have on the population in the future and the implications for fisheries management.

Improving knowledge on the following: seasonal and annual variation in seaweed diversity, gametogenesis and oocyte quality of the *H. iris* thermal stress, energetic budget, and initial cause of

ceroid deposition (e.g. age or stress) would provide beneficial information to support other management strategies already being implemented by fishing industry. These factors and pathological findings, as discussed above, are also likely to increase the vulnerability with increasing pressure during summer heatwaves. Due to changing climate, increasing abnormal weather patterns, high morphological variation, alternations to reproduction, and the depletion of *H. iris* populations, the concern around sustainability of the *H. iris* fishery in NZ is warranted. However, collaborative partnerships between researchers, such as the current study, and the pāua industry (in this case PauaMAC4 and the Pāua Industry Council), provide unique opportunities for developing new management strategies to ensure future growth of pāua populations.

SECTION 3. EXPLORATION OF THERMAL STRESS AND FOOD DEPRIVATION: LABORATORY SCENARIOS

In this section:

Section 3: Preamble

Chapter 5: Histopathological changes in the green-lipped mussel, *Perna canaliculus*, in response to chronic thermal stress.

Chapter 6a: Climate hazards, research, and green-lipped mussels (*Perna canaliculus*): From unexpected flooding to opportunistic research in an aquaculture facility: Part A

Chapter 6b: Impact of temperature and diet on adult mussel (*Perna canaliculus*) gametogenesis and immune defence: Part B

Section 3. Preamble

To make inferences in the overall health, including reproduction, growth and pathogen presence a combination of field-based studies and laboratory experiments is required. Chapter 5 “Histopathological changes in the greenshell mussel, *Perna canaliculus*” was the first chapter completed using histopathology techniques, and it became the hypothesis-driving manuscript which gave direction to the thesis story and the techniques used. Laboratory experiments are key in understanding the effects of a stressor on an organism. With climate change exacerbating temperature, a temperature trial was critical in determining the effects of mussel health, reproduction and pathogen presence. However, even laboratory experiments can be complex and incur their own issues. The high level of oocyte atresia and the unexpected appearance of *Perkinsus olseni* detected in the green-lipped mussel gave rise to the next two chapters. Within this current section, leading on from the 15-month thermal challenge trial was an additional broodstock conditioning trial with both temperature and food deprivation as stressors. The initial aim was to provide more insight into the oocyte atresia and whether the same techniques could be applied to the *H. iris*.

The second experiment, Chapter 6, was well underway when a 1 in 100-year flood resulted in the evacuation of the aquaculture facility. As such Chapter 6 is split into two parts: Part A “Implications of flooding events for the green-lipped mussels (*Perna canaliculus*): An Aquatic health perspective” and Part B “Thermal stress and food deprivation in adult mussel (*Perna canaliculus*)”. Once the flood waters receded and staff were able to access the site a quick decision was made to do a sampling to see what impact the flood had on the mussels. The flood did cause most of the ripe mussels to spawn and as such a redirection for the experiment was required. The flood did have some impact on the mussels, however there were no mortalities during the recovery period and as such the experiment was continued. Unfortunately, a second incident occurred whereby the heat pumps failed on several occasions within a week. These failures resulted in mortality of a high number of mussels in the experiment and we were unable to acquire the results to answer the initial questions regarding oocyte atresia. However, the experience and collaborative relationships gained still provide value which can be applied to future experiments. Furthermore, the flood event and the heat pump failures resulted in our inability to conduct the experiment on the *H. iris* and therefore provided more scope for the *P. olseni* work described in section 4.

CHAPTER 5. HISTOPATHOLOGICAL CHANGES IN THE GREEN-LIPPED MUSSEL, *PERNA CANALICULUS*, IN RESPONSE TO CHRONIC THERMAL STRESS.

Published in its entirety in Journal of Thermal Biology:

Copedo, J. S., Webb, S. C., Ragg, N. L. C., Ericson, J. A., Venter, L., Schmidt, A. J., Delorme, N. J., Alfaro, A. C., (2023). *Histopathological Changes in the Greenshell Mussel, Perna canaliculus, in Response to Chronic Thermal Stress. Journal of Thermal Biology. Vol, 117. DOI: <https://doi.org/10.1016/j.jtherbio.2023.103699>*

Abstract

Climate change associated temperature challenges pose a serious threat to the marine environment. Elevations in average sea surface temperatures are occurring and increasing frequency of marine heatwaves resulting in mortalities of organisms are being reported. In recent years, marine farmers have reported summer mass mortality events of the New Zealand green-lipped mussel, *Perna canaliculus*, during the summer months; however, the etiological agents have yet to be determined. To elucidate the role of thermal stress, adult, green-lipped mussels were exposed to three chronic temperature treatments: a benign control of 17 °C and stressful elevations of 21 °C and 24 °C. Eight mussels per treatment were collected each month throughout a 14-month challenge period to identify and investigate histopathological differences among green-lipped mussel populations exposed to the three temperatures. Histopathology revealed several significant deleterious alterations to tissue structure associated with elevated temperature and exposure time. As temperature increased and exposure time progressed there was an increase in the number of focal lipofuscin-ceroid aggregations. Concurrently there was an increase in focal haemocytosis and an increase in the thickness of the sub-epithelial layer of the intestinal tract. Additionally, there was a reduction in energy reserve cell (glycogen) coverage in the mantle. Prolonged exposure, irrespective of temperature, impacted gametogenesis, which was effectively arrested. Furthermore, increased levels of the heat shock protein 70 kDa (HSP 70) were seen in gill and gonad from thermally challenged mussels. The occurrence of the parasite *Perkinsus olseni* at month 5 in the 24 °C treatment, and month 7 at 21 °C was unexpected and may have exacerbated the fore-mentioned tissue conditions. Prolonged exposure to stable thermal conditions therefore appears to impact green-lipped mussels, tissues with implications for broodstock captivity. Mussels experiencing elevated temperatures of 21 and 24 °C demonstrated more rapid pathological signs. This research provides further insight into the complex host-pathogen-environment interactions for green-lipped mussels in response to prolonged elevated temperature.

5.1. Introduction

Climate observations have demonstrated the role of climate change on global environmental stressors for more than a decade (Thomas et al., 2004; Mooney et al., 2009). Oceanic environmental challenges as a result of climate change include wider fluctuations in pH, salinity and temperature (Boyd et al.,

2014). Not only are elevated average sea temperatures expected (Houghton et al., 2001), but marine heatwaves (MHW) are likely to increase in frequency, particularly in coastal regions (Lubchenco et al., 1993; Houghton et al., 2001; Petes et al., 2007; Filgueira et al., 2016; Smale et al., 2019). Ocean temperatures have already increased by an average of 1.5 °C over the past century and will continue rising (Hobday et al., 2016; Tuckett et al., 2017). Marine heatwaves are of particular interest due to correlations between elevated temperature and mass die-offs of marine organisms during the summer period, loosely termed “summer mortalities” (Salinger et al., 2020a). Heatwave-related mortalities have impacted several molluscan populations and aquaculture industries worldwide, with several environmental stressors, including high temperature and pathogens (e.g., *Perkinsus marinus*) being identified as causal agents (Harvell et al., 1999; Garrabou et al., 2009; Rubio-Portillo et al., 2016).

New Zealand’s coastal waters host a rich and diverse ecosystem, which is greatly impacted by temperature elevations (Stenton-Dozey et al., 2020; Behrens et al., 2022). In addition to long-term warming of NZ’s coastal waters, there has been a rise in MHW frequency (Oliver et al., 2017; Salinger et al., 2019; Sutton and Bowen, 2019; Behrens et al., 2022). An unprecedented MHW in the austral summer of 2017/2018 resulted in a mass mortality event of bull kelp (*Durvillea* spp.) in the South Island of NZ (Thomsen et al., 2019; Salinger et al., 2020b). As a result of increasing frequency of MHW events, it is likely that sea surface temperature (SST) will exceed thermal optima for local species, resulting in increased detrimental thermal exposure for many marine organisms. Elevated temperatures can significantly affect processes such as, metabolism, reproduction, immune response, and growth (Portner, 2002; Angilletta Jr and Angilletta, 2009; Filgueira et al., 2016; Dunphy et al., 2018). Survival of thermal stress requires a fine balance between cellular response, cell integrity and homeostatic capacity. Furthermore, stress compromises the immune system resulting in disease susceptibility (Trump et al., 1997; Manduzio et al., 2005; Fulda et al., 2010; Carella, 2015; Delorme et al., 2021b). When an animal is exposed to sublethal stressors such as increased temperature, reproduction can also be inhibited as energy is reallocated to defence and tissue repair (Michalek-Wagner and Willis, 2001; Petes et al., 2007). In addition, timing of reproduction can be disrupted and result in asynchronicity of spawning and decreased fertilization (Walther et al., 2002; Philippart et al., 2003; Petes et al., 2007). Response to these increasing heatwave events is, therefore, likely to lead to various biological consequences and may even alter phenology and species ranges (Parmesan and Yohe, 2003; Petes et al., 2007; Seuront et al., 2019; Delorme et al., 2021b).

The green-lipped mussel, *Perna canaliculus* (Gmelin 1791), is endemic to NZ (Jeffs et al., 1999; Alfaro et al., 2001) naturally inhabiting a wide range of temperatures and salinities (Jeffs et al., 1999). It is not only an ecologically and culturally valuable species, but green-lipped mussel farming is considered the cornerstone of the aquaculture industry in NZ (Dawber et al., 2004; Stenton-Dozey et al., 2020). Unlike more mobile species such as fish, mussels have a limited capacity to relocate when conditions, such as increasing seawater temperatures, become unfavourable. Due to this sedentary lifestyle mussels, such as the green-lipped mussel, have developed effective strategies to minimise

the impact when exposed to short term environmental stressors (e.g. de la Ballina et al., 2022). Key strategies include the ability to close their shells thereby reducing contact to the soft tissues, and physiological adaptations such as the development of an effective immune system (e.g. Gosling, 2008; Chong, 2022b; de la Ballina et al., 2022). The importance of the green-lipped mussel has prompted various research projects in relation to thermal stress (e.g. Ren and Ross, 2005; Ren et al., 2020; Stenton-Dozey et al., 2020). Effects of acute thermal stressors on green-lipped mussels have previously been studied to some extent (e.g. Dunphy et al., 2013; Dunphy et al., 2015; Dunphy et al., 2018; Delorme et al., 2020a; Delorme et al., 2021b); however, very few studies have focused on the effects of prolonged thermal stress (Ericson et al., 2023). Previous works include recent metabolomic research on green-lipped mussels during a summer heatwave event and acute, and chronic, heat exposure studies. These have found signs of stress and disruptions to metabolic pathways relating to, for example, energy metabolism and oxidative stress (Li et al., 2020; Nguyen and Alfaro, 2020; Delorme et al., 2021b; Ericson et al., 2023). Metabolomic assessments provide a snapshot of the biological response at the time of sampling (Alfaro and Young, 2018), in contrast histology can give insights into cumulative effects on tissues that may develop over time (Costa, 2018b). Consequently, this method may provide further insights into the effects of prolonged thermal stress and marine heatwave exposure at the tissue level of green-lipped mussels in NZ as these are largely unknown, as are the etiological agents of thermally mediated mortalities.

Histopathology is an essential tool in the presumptive diagnosis of diseases and mortality investigations as part of health surveillance (Hooper et al., 2014; Knowles et al., 2014; Costa, 2018b). It is a bench-mark screening method that can provide a phenotypic anchor point for specific data as it provides tissue-level measures of general, reproductive, and metabolic condition as well as pathogen detection (Bignell et al., 2008; Zannella et al., 2017). In the present study, histopathology, and immunohistochemistry (IHC) were used to elucidate alterations in green-lipped mussel tissues, as well as presence and prevalence of pathogens, when exposed to prolonged thermal stress. Temperatures were selected based on a summer ambient (17 °C SST), present-day high summer temperatures (21 °C high summer SST), and a projected high according to a +2.5 °C predicted increase (24 °C projected summer SST by the year 2100) (Law et al., 2017; Ericson et al., 2023).

Identifying alterations to green-lipped mussel tissue condition and constitution in response to increasing and prolonged temperature exposure is essential for understanding the effects of stressors on the tissue structure and architecture. This research aims to improve our ability to detect changes in response thermal stress and its correlation with tissue condition and parasite presence, thereby providing insights into potential impacts and implications under future climate stress scenarios.

5.2. Methods

5.2.1. *Experimental design*

Adult, green-lipped mussels (80 – 120 mm shell length, n=1215) were transported from a farm in the Pelorus Sound, Marlborough, New Zealand to laboratories at the Cawthron Aquaculture Park,

Nelson, in May 2018. The mussels were weighed (± 1 g), shell length measured (± 1 mm) and engraved with identification numbers (Dremel 3000 rotary tool with a 1.6mm round diamond tip). The mussels were then distributed to nine well aerated 100 L tanks ($n = 135$ per tank) designed for broodstock holding. After 6 weeks of acclimation to the current ambient seawater ($16\text{ }^{\circ}\text{C} \pm 2\text{ }^{\circ}\text{C}$), the temperature was increased approximately 0.25° and $1.8\text{ }^{\circ}\text{C}/\text{day}$ over two weeks depending on temperature treatment until the tanks reached the desired temperatures: ‘benign’ 17°C , and elevated $21\text{ }^{\circ}\text{C}$ and 24°C , with three replicate tanks per temperature (see Figure 1 in Ericson et al. (2023) for the temperature trajectory for each treatment). The control temperature was maintained in three primary header tanks using a heat pump set to 17°C , while the $21\text{ }^{\circ}\text{C}$ and $24\text{ }^{\circ}\text{C}$ treatment temperatures were obtained by heating the control temperature using titanium and glass submersible heaters.

Mussels were continuously fed bloomed algae pond seawater throughout the trial supplemented with a 50:50 combination of monocultured *Tisochrysis lutea* (formerly *Isochrysis galbana*) and *Chaetoceros calcitrans* (250L/ day) for a full description of feed and water conditions see Ericson et al. (2023). Green-lipped mussel individuals were weighed (g) and measured (mm) after 2-, 5-, and 10-months exposure. Mortalities were reported daily and immediately removed from the system. The shell lengths of dead animals were measured and recorded to provide an indication of growth to mortality. Weighing was not performed due to loss of tissue mass through rapid decay. This rapid decay also prevented harvest of dead specimens for histopathology.

5.2.2. *Water quality sampling*

Seawater flows ($2.5 \pm 0.5\text{L}/\text{min}$) were measured twice weekly and adjusted as required. Water quality parameters (dissolved oxygen, temperature, pH and chlorophyll-*a*) were measured throughout the trial and reported within Ericson et al. (2023).

5.2.3. *Histopathology*

Eight green-lipped mussels per temperature treatment (17°C , $21\text{ }^{\circ}\text{C}$ and 24°C) were randomly collected across replicate tanks each month and prepared for histopathological assessment. An additional 10 mussels per temperature, were collected at 4 time points throughout the trial (labelled as month and letter B in Table. 5.1).

Table 5.1 Sampling numbers and collection months for each of the temperature treatments over the 15 months (July 2018 – Sept 2019). A fixation issue at month 3 resulted in a lack of individuals for the histology assessment. Thus, month 3 is represented graphically but was not included in the statistical analysis. Month 2B was the initial sampling, where all mussels were at 17°C, prior to raising the mussels to the desired temperature achieved by month 3 (None available (NA)). At month 15B there were no mussels left in the 24C treatment to sample (NA).

		Sampling month and date															
		2B	3	4	5	6	6B	7	8	9	10	11	11B	12	13	14	15B
		2018						2019									
		21 Aug	24 Sept	19 Oct	19 Nov	01 Dec	06 Dec	02 Jan	25 Feb	03 April	02 May	04 Jun	11 Jun	10 Jul	05 Aug	30 Sept	15 Oct
Temperature	17°C	15	1	8	8	8	10	8	8	8	8	8	10	8	8	8	18
	21°C	NA	3	8	8	8	10	8	8	8	8	8	10	8	8	8	18
	24°C	NA	0	8	8	8	10	8	8	8	8	8	10	8	8	4	NA

Tissues were removed intact from the shell and sectioned as shown in figure 5.1. The 5 mm sectioned samples (mantle, gill, kidney, digestive gland, mid-gut, muscle, and nervous tissue) were placed into histological cassettes and fixed in a 4% formalin solution (1:9 v/v, 37% formaldehyde: 0.35µm filtered seawater). The samples were left in the 4% formalin solution for 48 hours before being transferred to a 70% ethanol solution (Howard, 2004). Samples were embedded in paraffin wax, sectioned (3-5µm) using a rotary microtome and stained using routine hematoxylin and eosin (H&E) (Howard, 2004).

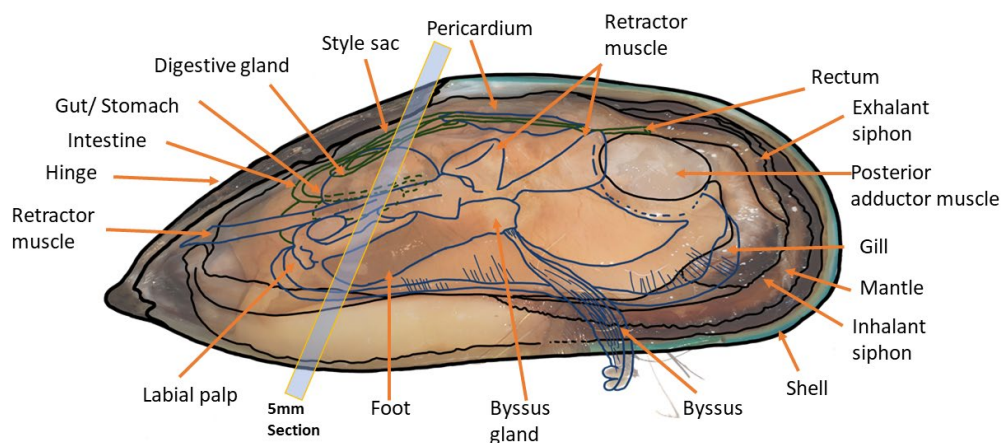


Figure 5.1 Green-lipped mussel (*Perna canaliculus*) general anatomy depiction. Rectangular window indicates the location of the 5 mm histology section. This section was selected to maximise chances of acquiring all tissue types, including midgut, digestive gland, gill, gonad (mantle) and muscle.

5.2.3.1. Tissue Analysis

Histological observation under a light microscope (Olympus BX40), at a magnification of x40 to x1000, was conducted on a range of tissues, assessing tissue-specific alterations by scoring semi-quantitatively and quantitatively as explained below in sections 2.3.2 to 2.3.4.

5.2.3.2. Gill and digestive gland scoring

The gill and the digestive gland were assessed at x200 and x400 magnification, then a score of tissue quality was devised based on structural deviations from those seen in mussels sampled on arrival (Baseline: month 2). The gill and digestive gland grading criteria were generalised and adapted from Kim et al., (2006a) and Perez-Cebrecos et al., (2022), whereby 0= normal tissue and no obvious changes, 1= ‘mild’: minor alterations, 2= ‘moderate’: up to half of the organ affected and 3= ‘severe’ alterations with marked disruption to tissue architecture. Tissues were graded at each timepoint between the three temperatures (17°C, 21 °C and 24°C) and then compared across time (16 months).

5.2.3.3. Mantle and connective tissue scoring

The mantle tissues were graded using four subjective semi-quantitative criteria, each graded from least to most severe: 1) the level of ceroid material found in the section (implicating oxidative stress or previous immune response, for this research ceroid and lipofuscin are considered together), 2) the level of focal haemocytosis (nodule or inflammatory capsule), indicative of an immune response (Table. 5.2; Fig. 5.4), 3) the level of storage cell material in the mantle, and 4) the width of the subepithelial layer between the gut and the digestive tubule tissue (Table. 5.3; Fig. 5.5). These scores were developed to assist with the identification of a stress or an immune response to increasing temperature, as well as to help standardise interpretation. The mean scores of each of the four criteria for each temperature were plotted against time in a heat map table to detect changes in each related to their respective criteria.

Table 5.2 Semi-quantitative scoring of level of ceroid material and focal haemocytosis from least severe (1) to most severe (4). Criteria are similar to the grading scale of Carella et al., (2015) and Bignell et al. (2008) and specific illustrations are located in the results section..

Score	Ceroid level criterion	Focal haemocytosis level criterion
0	No ceroid material observed	No haemocytosis alterations observed
1	Low level ceroid, focal alterations observed across tissues	Low level focal haemocytosis alterations observed across tissues
2	Moderate level of multifocal ceroid alterations observed across tissues	Moderate level multifocal haemocytosis alterations in multiple tissues
3	Severe level of multifocal ceroid alterations across tissues	Severe multifocal and haemocytosis alterations
4	Extensive diffuse ceroid accumulation in multiple tissue types	Extensive haemocytosis diffusely distributed across multiple tissue types

Table 5.3 Semi-quantitative scoring of level of storage cell material (glycogen) and gut subepithelial thickening from least severe (1) to most severe (3). A score of 3 for storage cell coverage indicates glycogen rich mantle tissue whereas a score of 1 for the gut is indicative of healthy gut performance, with low numbers of haemocytes around the gut epithelial layer.

Score	Storage cell (Glycogen) coverage criterion	Gut subepithelial layer extent criterion
0	No storage cells observed	None observed (no haemocytes observed around the epithelium).
1	Light coverage of storage granules in the mantle tissue.	Normal thickness the width of the gut epithelium \leq width of the epithelium.
2	Moderate coverage of storage granules in the mantle tissue.	Thickness greater than thickness of the gut epithelial layer \leq 2x thickness of epithelium.
3	Full coverage of storage granules in the mantle tissue	Thickness greatly increased expanding into the digestive tissue greater than thickness of gut epithelial layer (Abnormal).

5.2.3.4. Immunohistochemical detection of HSP70 in gill and gonad: A preliminary investigation

Three paraffin blocks prepared from mussel tissues before temperature exposure (month 2b) and 3 blocks after temperature acclimation (month 4) were selected for preliminary assessment of HSP70 as a potential heat stress marker. A 4 μ m section was obtained from the paraffin blocks as processed and described in section 2.3. The paraffin section was then mounted on to a microscope glass slide. This section was then dewaxed, hydrated, and processed through a heat-mediated antigen retrieval procedure for 5 minutes at 120°C. The prepared slides were stained using an indirect antibody approach with a primary monoclonal antibody reactive to HSP70 (MA3-006, Invitrogen) used at a concentration of 1:200. A complementary secondary antibody conjugated with Alexa fluor 647 (A32728, Invitrogen) was used at a concentration of 1:1000. DAPI (0.2 μ g ml⁻¹) was then used as a counter stain to highlight the cellular nuclei. Sections were mounted using an aqueous mounting media and 22x50 mm (1.5 H) cover slip.

Slides were observed under an inverted microscope (IX83, Olympus, Tokyo, Japan) equipped with a laser scanning confocal head (FV3000, Olympus, Tokyo, Japan), using a 405nm (50 mW) and a 640nm (40mW) laser line, and Fluoview FV31S-SW software (version 2.3.2, Olympus Corp.). Images of gill and gonad tissue were acquired using the UplanSApo 20x N.A. 0.75 objective and a confocal aperture of 125 μ m. These acquisition conditions were established according to Nyquist sampling criterion and acquired signals that fulfil the Rose criterion for signal-to-noise ratio in all the marker channels (Pawley, 2006). Images were collected using the following emission filter configuration for each fluorophore: DAPI (430-470nm), AF647 (650-700nm). Image visualisation and formatting was performed using ImageJ (Schindelin et al., 2012).

5.2.3.5. Reproductive staging

Gonad development scoring proceeded using the following system similar to Kennedy (1977), Alfaro et al. (2001) and Buchanan (2001) (Table. 5.4). Stage definitions were altered to include maturity of the oocytes as well as mantle coverage. Females and males were scored based on the criteria of stages and given a numerical gonad index value using microscopy (Table. 5.4). The frequency or proportion

at each stage was plotted for visual representation. The gonadal index (GIn) was then calculated based on formulae by King et al. (2009), Galinou-Mitsoudi and Sinis (1994), Buchanan (2001) and Alfaro et al. (2001), whereby GIn is determined by the mean rank, or score, of the population. A GIn of 0 is indicative that the population is closer to the resting phase and 3 the population is close to full maturity. Percent follicle coverage (FC) within the mantle tissue was estimated by eye followed by image analysis.

Area analysis was then conducted on the 25 females identified within this trial using cellSens™ software (Olympus cellsens Standard 3.1 [build 21199] on an Olympus BX53 compound) to validate the estimates. To validate FC the area of the frame was recorded then a free-form polygon was used to define the cross-sectional area of each follicle contained within the frame. The percent area coverage was then calculated. The values were then fitted to a regression and compared with the estimates. Estimates by eye were developed to be used for routine determination in a commercial aquaculture setting where image analysis is not always possible.

Table 5.4 Histological criteria of seven stages and the associated gonad index score for the reproductive condition of green-lipped mussels.

Stage	Gonad score	Description	Male	Female
Resting	0	Sex indeterminable. Resting or inactive some basal cells and/or very early precursors. Good coverage of storage reserve cells in mantle (glycogen).		
Early	1	Gametogenesis has begun and small germinal cells are present. Follicles 500µm or less in diameter.	Spermatogonia inside follicles along the wall. Some spermatozoa are visible.	Oogonia line follicle wall, oocyte nuclei large attached to wall by cytoplasmic stalk
Late	2	Follicles become larger in size; 50% of follicles equal to, or larger, than medium size and/or both sexes have the potential to spawn and produce 50% or less of their mature sperm when force spawned. Follicles 500µm or more in diameter.	Concentric layers of spermatogonia, spermatocytes and spermatids. 50:50 Precursor to mature cell ratio.	Oocytes accumulate yolk and some mature oocytes are free and/or 50% distribution of precursor cells to mature oocytes.
Ripe	3	Mantle nearly full, with at least 80% coverage of the mantle, follicles are large (1000µm or more) and/or development of gonad is as follows for males and females.	Mantle filled and follicles show <10% precursor cells and with up to 50% of follicles with mature sperm converging in the centre but still dense.	Most oocytes at maximum size and mostly free from the wall, some small loss of oocytes.
Spawning	2	Release of gametes has begun, spillage of loose gametes evident upon histological sectioning. Evidence of a reduction in gamete density within follicle. Less than 80% atresia observed.	Dense band of ripe spermatozoa; greater than 80% spermatozoa converging in the centre with some follicles showing a loss in density.	Ripe oocytes present with a reduction in density of gametes in the centre of the follicle. Very few precursor cells (<10%).
Redevelopment	1	Follicles reduced in size and do not take up all the mantle area, remaining oocytes arranged loosely with new oocytes visible.	Dense band of ripe spermatids give rise to new lamellae, with gaps still present; very few follicles with phagocytosis developing (less than 50%).	Some atresic debris as well as phagocytes, but phagocytes are not affecting the new oocytes.
Spent	0	Follicles either empty or collapsing and degenerate amoebocytes/ phagocytes attack unspawned material, autolysis. Lumen filled with debris, atresia, and phagocytosis. Residual gametes will be broken down.	Phagocytes attack unspawned sperm.	Phagocytes clearing debris and follicles display greater than 80% oocyte atresia.
Atresia		Autolysis, degradation, and reabsorption of oocytes. Includes cytoplasmic discolouration and darker staining, irregular jigsaw shape, retraction, and detachment of the cell membrane. Lysing of the cell membrane, oocyte contents spill into follicle. Can occur at any stage.		
Phagocytosis		Phagocytes clear unspawned gametes: the follicle will have cellular debris with some ceroid material visible. Can occur at any stage.		

Preliminary investigations of female gonad status and indications of presence of atresic oocytes (defined in Table. 5.4) resulted in further analysis of the oocyte condition. Three micrographs were taken of the gonad and mantle tissue for each female at 20x using an Olympus BX53 compound microscope and cellSens imaging software (Olympus cellsens Standard 3.1 [build 21199]). Oocytes in each of the micrographs were then quantitatively analysed using methods by Chérel and Beninger (2017). Quantification of the oocytes was performed using stereological counts and oocytes allocated to 3 groups, immature (I) (attached to follicle (acinal) wall; stalked), mature (M) (detached from follicle wall) and atresic (A) (Fig. 2). The three counts were then averaged and recorded to produce a single value per category for each female, and the importance of atresia was calculated using the following by Chérel and Beninger (2017):

- 1) Percent atresia (PA) = $\frac{A}{I+M+A} * 100$
- 2) Percent mature (PM) = $\frac{M}{I+M+A} * 100$
- 3) Percent immature (PI) = $\frac{I}{I+M+A} * 100$
- 4) Atresic impact (AI) = $\frac{PA}{PA+PM} * 100$

The atresic impact was determined to be the minimum impact of atresia on the oocytes whereby the fate was known (i.e., spawned as healthy oocytes and fate known). Health of immature oocytes was yet to be determined and could either develop into healthy oocytes or become atresic (Chérel and Beninger, 2017).

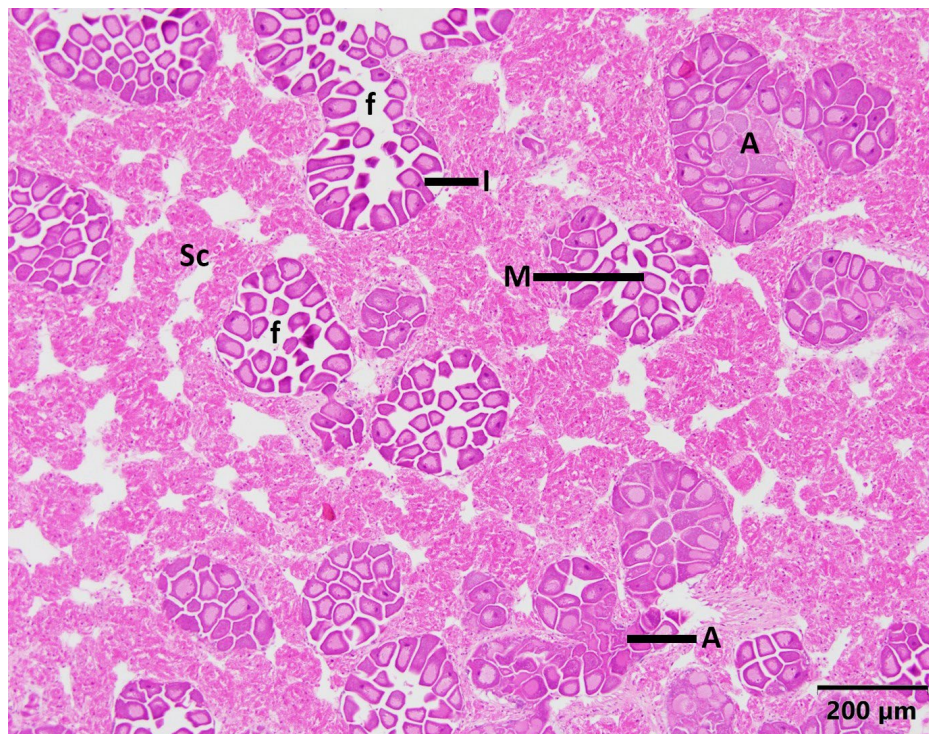


Figure 5.2 Female gonad stained with H&E indicating stages of oocytes immature (I), mature (M), atresic (A) within the follicles (f) and glycogen rich mantle storage cell (Sc).

5.2.3.6. Pathogens

Presence/absence of parasites was recorded and presented as proportion of population prevalence. The apicomplexan-X (APX) and *P. olseni* were the most prevalent and, as such, were investigated further (Fig. 5.5). The intensity of APX and *P. olseni* were scored using adapted methods from Hine (2002), Kim et al., (2006a) and Suong (2018) (Table. 5.5). The section was screened at x200 to identify cells, x400 and x1000 magnifications were then used for further identification. Following the histological identification of *P. olseni*, a selection of processed blocks was sent to the NZ Ministry for Primary Industry National Animal Health Laboratory and subjected to PCR screening using standard and specific primers to confirm diagnosis.

Table 5.5 Two parasites, APX and *Perkinsus olseni*, were scored using a 0 – 5 grading scale, where 0 indicated no parasites were observed and 5 is a severe level of parasites was observed.

Score	APX: Criterion	<i>Perkinsus olseni</i> : Criterion
0	No parasites were observed in the tissue section.	No parasites were observed in the cross-section.
1	Low: Parasite difficult to detect <10 APX zoites were present in the tissue section after extensive search.	Low: <10 <i>Perkinsus</i> cells observed in tissues after extensive searching. For the purpose of this scoring rosette- stage groups were considered as 1.
2	Moderate: APX zoites were present in the tissue section and detected in small groups. Occasionally associated with ceroid material.	Moderate: <i>Perkinsus</i> cells were observed in tissues and more easily identified.
3	High: APX zoites were more easily detected, developing multiple moderate to large lesions of APX zoites and in most cases associated with ceroid.	High: <i>Perkinsus</i> cells observed to be distributed in multiple tissues <i>Perkinsus</i> cells. No lesions observed.
4	Heavy: APX zoites abundant in most tissues developing large lesions.	Heavy: <i>Perkinsus</i> cells abundant in most tissues, developing lesions.
5	Severe: APX zoites abundant with high tissue congestion and connective tissue destruction.	Severe: <i>Perkinsus</i> cells abundant in most tissues, developing large and abundant lesions.

5.2.4. Statistical analysis

Statistical analyses were conducted using R version 4.0.3 (R Core Team, 2024) with the R studio interface (RStudio Team, 2021). Histology data were analysed using both temperature and time as explanatory factors. Quantitative data (FC and atresia) were checked for normality and homogeneity of variance using the Shapiro-Wilks and Levene's tests, followed by analysis using ANOVA. The atresia data were non-normal and unbalanced due to the lack of female representation in each category. However, ANOVA Type II sum of squares at the 0.05 level was used as the data met the requirement for homogeneity of variance (Quinn and Keough, 2012). The ANOVA was followed by the TukeyHSD post hoc test. Analysis of the semi-quantitative data (haemocytosis, ceroid material, mantle reserve cell, gut subepithelium and gonad index) was performed using a Generalised linear mixed effect model in the MCMCglmm package (Hadfield, 2010). Tank number was included as a random effect for the MCMCglmm however was tested and excluded from the other analyses. Binomial general linear models were performed on the pathogen (APX and *P. olseni*) prevalence

data. Ridge penalizers were added prior to the estimates to increase data ‘sensitivity’ if the differences between the responses were deemed as “perfect” (Cule and Frankowski, 2021). A p value < 0.05 was considered statistically significant.

5.3. Results

5.3.1. Water quality and survival

On initiation of the trial, once seawater had reached the desired temperature, the treatments were maintained at that temperature. A logistical issue with the temperature system occurred in the 21 °C and 24 °C treatments during month 10 of the experiment and the temperature dropped to 17 °C for 2 weeks (see Ericson et al., 2023). Analysis of mussel tissue alterations did not reveal obvious effects from this technical difficulty. Temperatures were slowly increased back to 21 °C and 24 °C once the system’s malfunctioning was repaired. The dissolved oxygen and pH levels remained stable through the trial (Table. 5.6).

Table 5.6 Water quality parameters (mean \pm standard error (SE)) measured throughout the experiment for further details see Ericson et al., (2023).

Water parameter	Desired temperature		
	17°C	21°C	24 °C
Temperature (recorded)	17.9 \pm 0.5°C	21.2 \pm 1.0°C	23.2 \pm 1.6°C
Dissolved oxygen	92.6 \pm 1.3%	90.5 \pm 0.3%	90.6 \pm 1.3%
pH	8.14 \pm 0.01	8.12 \pm 0.01	8.13 \pm 0.01

Survival was significantly impacted by chronic temperature exposure to 24°C, and a mortality began at month 5 of the trial until a 100% mortality was reached at month 15. At 17 °C and 21°C, survival at completion of the trial was at 94% and 90%, respectively (see complementary study presented by Ericson et al. (2023) for further details). No individuals were available for sampling from the 24 °C treatment in the final month of the trial.

5.3.2. Tissue condition

5.3.2.1. Gill and digestive gland architecture

There were statistically significant histological differences in the appearance of the digestive gland tissue (Temp*Month $p=0.008$) and the gills (Temp*Month $p=<0.001$) in mussels among the three temperatures. There was an observable histological trend towards degradation in tissue architecture in the digestive gland and the gill condition of the mussels kept at all temperatures over time. These effects were only subtly different as temperature increased. For the digestive gland, there was: 1) an increase in the intracellular spaces in the epithelium, which took on an increasingly thin and lacey appearance, 2) minor epithelial atrophy, and 3) epithelial sloughing in a few individuals, as well as an increase in the amount of interstitial space between the tubules as time progressed (Fig. 5.6a and b). For the gills, there were individuals with some minor lifting between the chitin layer and the epithelium, increased cell separation, minor haemocyte infiltration, in some cases loss of cilia and an accumulation of ceroid material as time progressed (Fig. 5.3c and d).

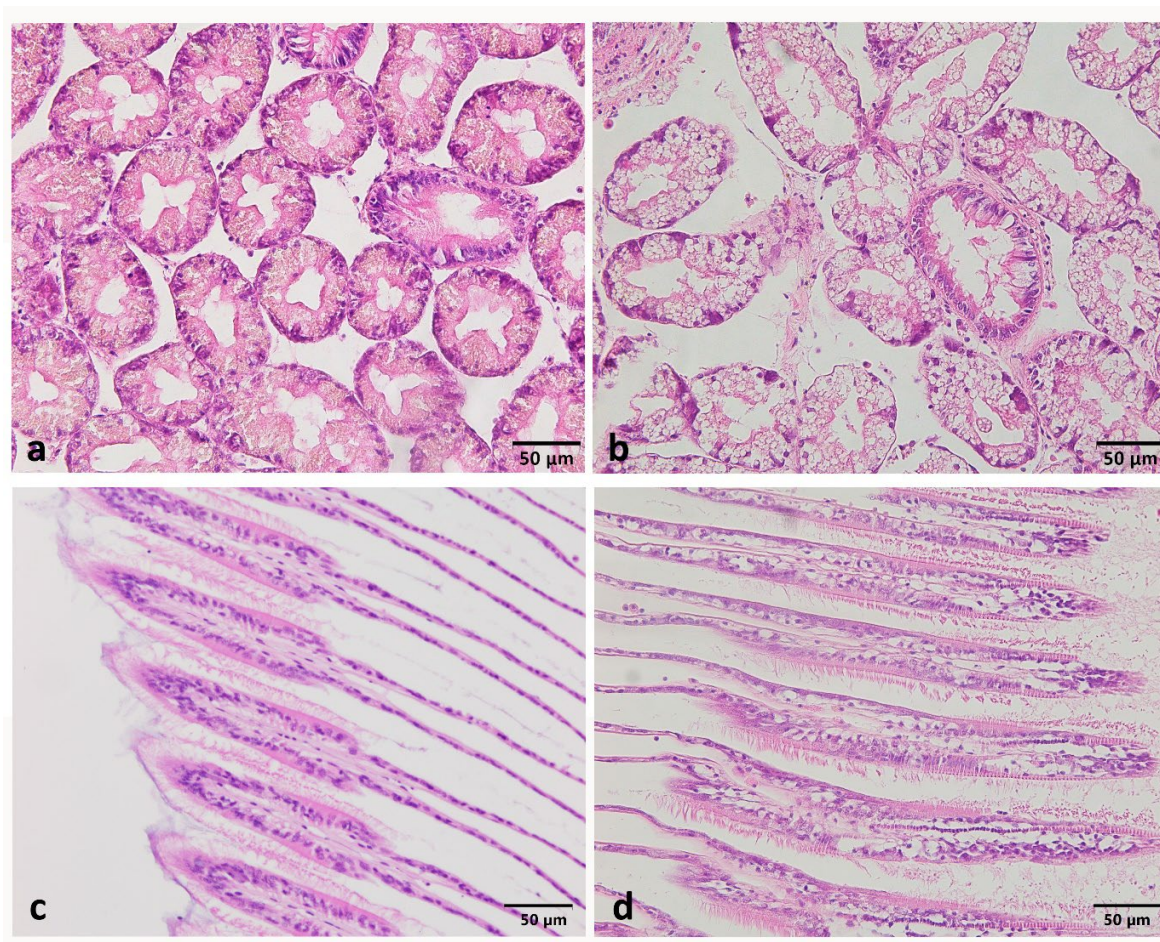


Figure 5.3 General alterations to digestive gland tissues at trial start and trial end A) normal digestive gland at trial initiation (graded as 0) B) altered digestive gland after 14 months at 24 °C with expanded intracellular spaces (graded as 2). *Perna canaliculus* gill prior to acclimation to the temperature treatments C) Healthy gill filaments (graded as 0) and D) Gill filaments after 14 months with alterations to the gill architecture and no loss of cilia as described in section 2.3.1.1. (graded as 2). Scale = 50µm.

5.3.2.2. Mantle and connective tissue

Semi-quantitative criteria of ceroid granules, focal haemocytosis, mantle storage cell coverage and the extent of the sub-epithelial layer of the gut indicate that the differences between the temperature treatments were linked to the month and were amplified over time (chronic time factor) (Table. 5.7). Ceroid material was present in the majority of individuals and increased with both temperature and time (Temp*Month $p < 0.001$). Focal haemocytosis increased in intensity ($p < 0.001$) with increasing temperature and was amplified over time (Temp*Month $p < 0.001$). There was a decrease in the coverage of the mantle storage cells which was also influenced by exposure time (Temp*Month $p < 0.001$). The subepithelial layer of the gut increased in thickness, extending into the digestive tubule tissue increasingly over time (Temp*Month $p < 0.001$) (Table. 5.7). In some individuals, the thickness was extensive and displaced the digestive tubules, resulting in the appearance of higher numbers, and increased density, of haemocytes.

Table 5.7 Heatmap of the semi-quantitative levels of ceroid material, focal haemocytosis, mantle storage cell coverage and the thickness of the subepithelial layer of the gut. Sampling month 3 had fixation issues and, as such, only had an n = 1 at 17 °C and n =3 at 21°C; no samples were available for the 24 °C treatment. Sampling months 4 to 15 had n = 8 at 17°C, n = 8 at 21 °C and n = 8 at 24 °C for each sampling month (Table. 5.1). Where no data were collected, cells are blacked out.

		<u>Impact level</u>																	
		No impact	Increasingly impacted																
		Sampling month																	
		2B	3	4	5	6	6B	7	8	9	10	11	12B	13	14	15	16B		
Ceroid granules	17°C	0.9	1.0	0.8	0.4	1.1	1.3	1.2	1.2	1.3	1.4	1.5	1.1	1.1	1.2	1.1	1.6		
	21°C		1.0	0.6	0.9	1.0	1.3	1.1	1.4	1.0	1.6	1.3	1.0	1.5	2.5	2.1	1.8		
	24°C			1.0	1.3	1.3	1.2	1.3	1.7	1.9	2.5	2.1	2.8	2.8	3.0	2.8			
Haemocytosis	17°C	0.3	0.0	0.1	0.1	0.4	0.3	0.2	0.7	0.8	0.6	0.9	0.7	0.4	0.8	0.5	0.9		
	21°C		0.0	0.0	0.1	0.3	1.0	0.3	0.7	0.3	0.6	1.0	0.9	0.9	1.4	1.5	1.3		
	24°C			0.0	0.0	0.6	0.2	1.3	1.3	1.1	2.4	2.1	2.3	2.0	2.2	2.0			
Mantle storage cell	17°C	1.9	3.0	2.3	2.1	1.9	2.4	2.3	2.2	2.0	2.9	2.3	2.8	2.6	2.2	2.0	2.7		
	21°C		2.7	2.3	2.1	2.0	2.2	2.1	2.0	2.0	2.8	1.8	2.8	2.1	1.7	0.4	1.9		
	24°C			2.1	1.9	1.9	2.5	2.0	2.0	2.0	1.7	2.1	1.3	1.4	1.8	0.5			
sub-epithelial gut layer	17°C	1.1	1.0	1.0	1.0	1.1	1.0	1.2	1.8	1.7	1.8	2.1	1.9	1.6	1.6	1.6	1.4		
	21°C		1.0	1.1	1.2	1.2	1.5	1.4	1.8	2.0	1.7	2.7	2.2	2.1	2.0	2.0	1.6		
	24°C			1.1	1.1	1.2	1.3	1.1	1.8	2.0	2.3	2.4	2.6	2.3	2.4	2.1			

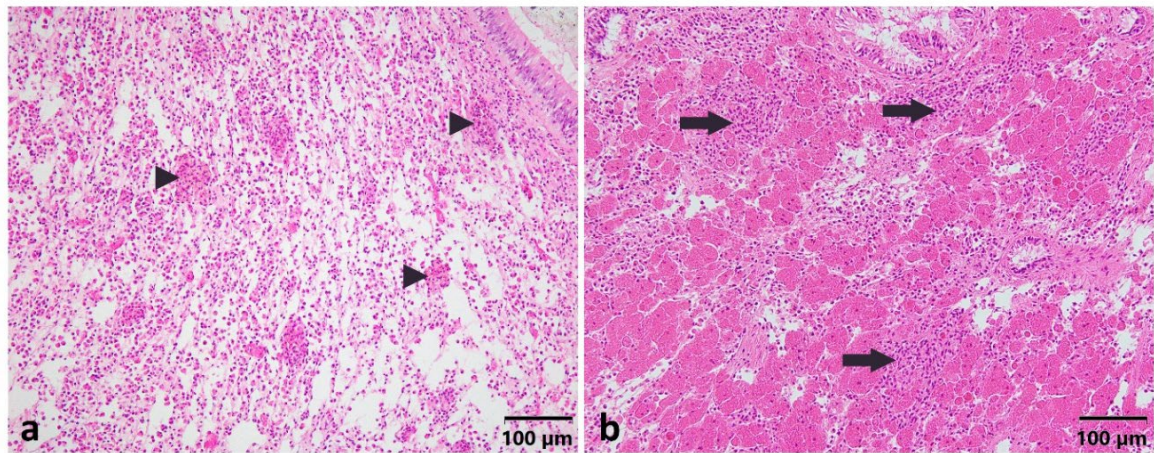


Figure 5.4 Ceroid level and the focal haemocytosis level 3. a) Severe level (score 3) of ceroid material, multiple accumulations observed (arrowhead) b) Severe level (score 3) of focal haemocytosis with multiple patches throughout the mantle tissue.

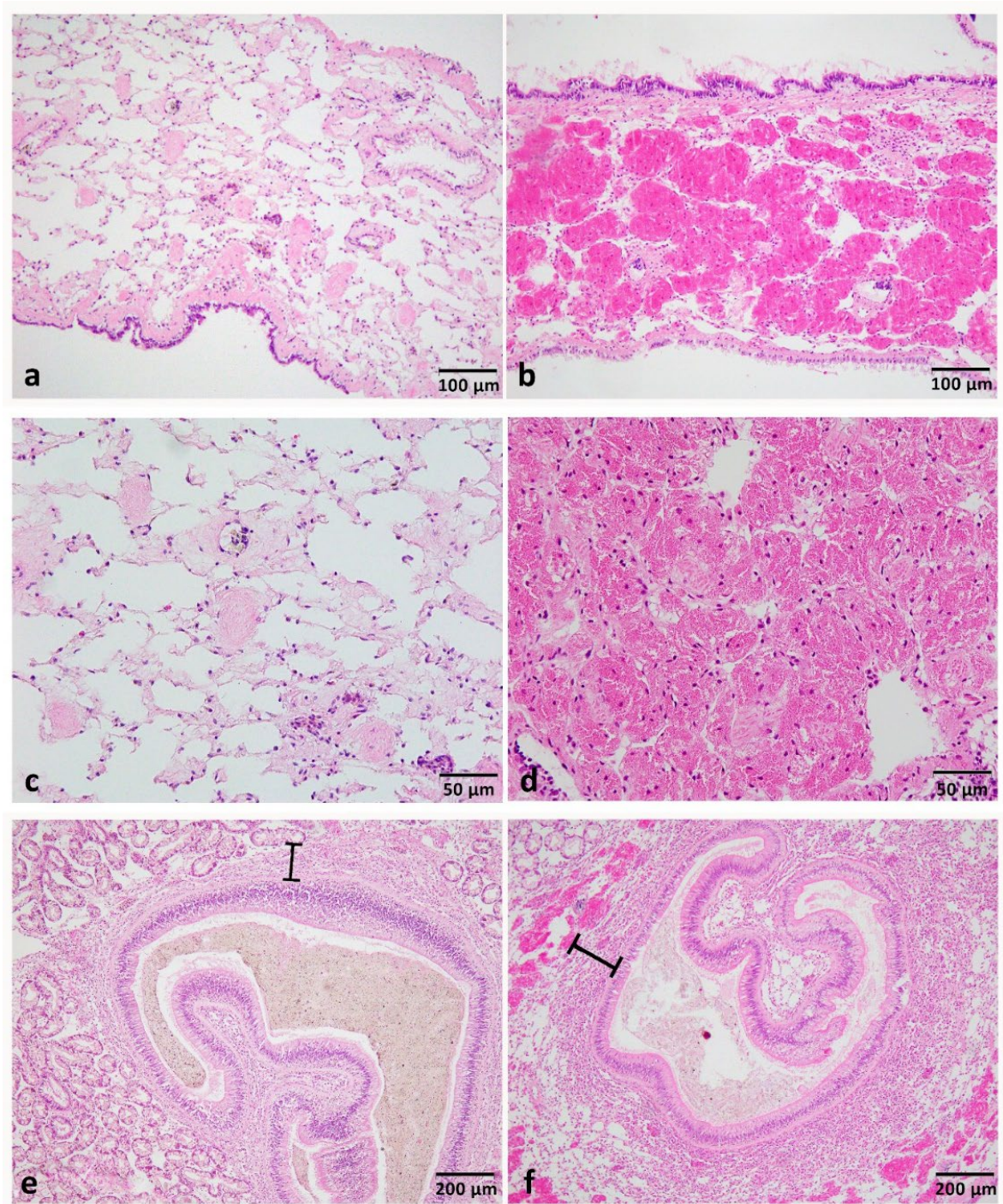


Figure 5.5 Mantle storage cell coverage and the subepithelial extent or thickness of green-lipped mussels. a) Mantle tissue with a score of 0 no glycogen cells (granules) observed higher levels of haemocytes and connective tissue visible. b) Mantle tissue with a score of 2 with some patches of no storage cell tissue. c) Zoomed in mantle tissue of image a, only connective and some musculature tissue, with no visible glycogen granules. d) Zoomed in mantle tissue of image b showing densely packed storage cells e) Subepithelial layer of the intestine score of 1, low level of haemocytes surrounding the epithelial layer of the intestine f) Subepithelial anomalous thick layer (score of 3) around the intestine extending into the digestive tubule region, indicating increased number of haemocytes surrounding the intestine Black line indicating subepithelial layer.

5.3.2.3. Immunohistochemical exploration of HSP70 in gill and gonad: A preliminary investigation.

HSP70 presence in the gills appears to be localised to the epithelial cells at the frontal lateral edge of each filament (Fig. 5.6 b, c, and d). The gill tissue suggested an increase in HSP70 protein abundance with temperature in the 'benign' and elevated one-month post-temperature acclimation. At this stage HSP70 proteins were not observed in the ambient ($17\text{ }^{\circ}\text{C} \pm 2^{\circ}\text{C}$) samples prior to the temperature increase for the experiment (Fig. 5.6 a).

HSP70 was suggested to be visible at elevated temperatures in both male and female gonads. HSP70 in males appeared to be localised to spermatogonia and spermatocytes (Fig. 6 e and f). Female oocytes were highly abundant with HSP70 some oocytes displayed dense "patches" with elevated temperatures (Fig. 5.6 g and h).

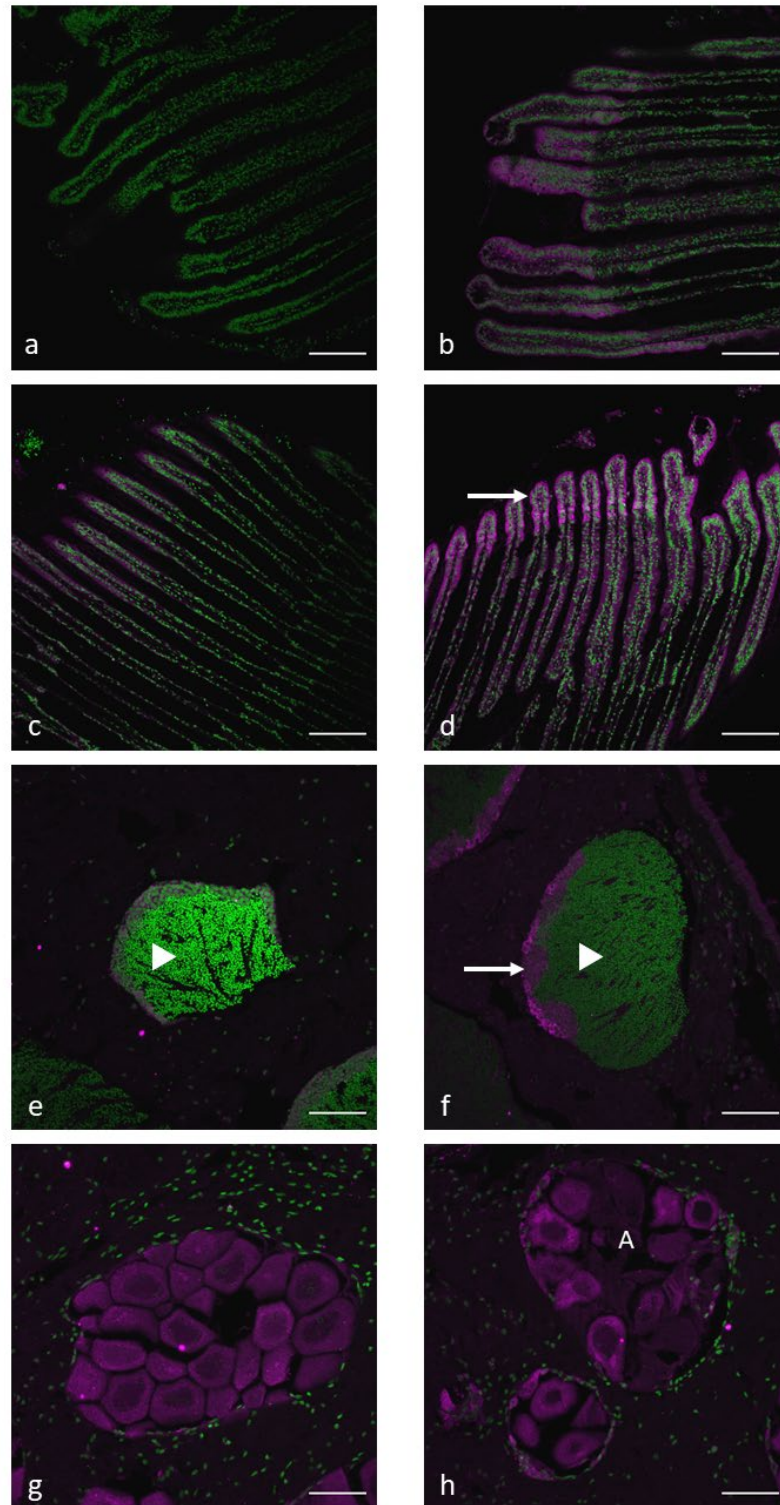


Figure 5.6 Preliminary investigations show the presence of HSP70 in gill and gonad tissue determined by immunohistochemistry. a) gill tissue in 17 °C temperature at month 2 prior to the temperature elevation. Images b, c and d correspond to mussels that had been exposed for 1 month at 17, 21 and 24°C, respectively. Male reproductive follicle HSP70 (magenta) detected to be associated to spermatogonia and spermatocytes, green is the mature sperm cell at 2 temperatures 1-month post-temperature increase e) 17 °C and f) 21°C. Female reproductive follicle at 2 temperatures 1-month post-temperature increase g) 17 °C and h) 21 °C with increased atresic oocytes (A). Magenta (arrow) is the HSP70, and green (arrowhead) is the nuclear material. Images A - D Scale bar= 100µm, Images E – H Scale bar= 50µm.

5.3.3. Reproductive tissue

Reproductive condition and gametogenesis appeared to have regressed over time, with much of the population in either the spent or resting phase of gametogenesis by month eight. Initial observational patterns suggest a natural decline (month 3 to 5 [21°C] and 6 [17°C]) from mature individuals to the rest and spent phase, but no initiation of gametogenesis after the rest phase (Fig. 5.8). There was no significant difference in gonadal development among the treatment temperatures ($p=0.87$), nor in the interaction with months ($p=0.49$) (Fig. 5.7).

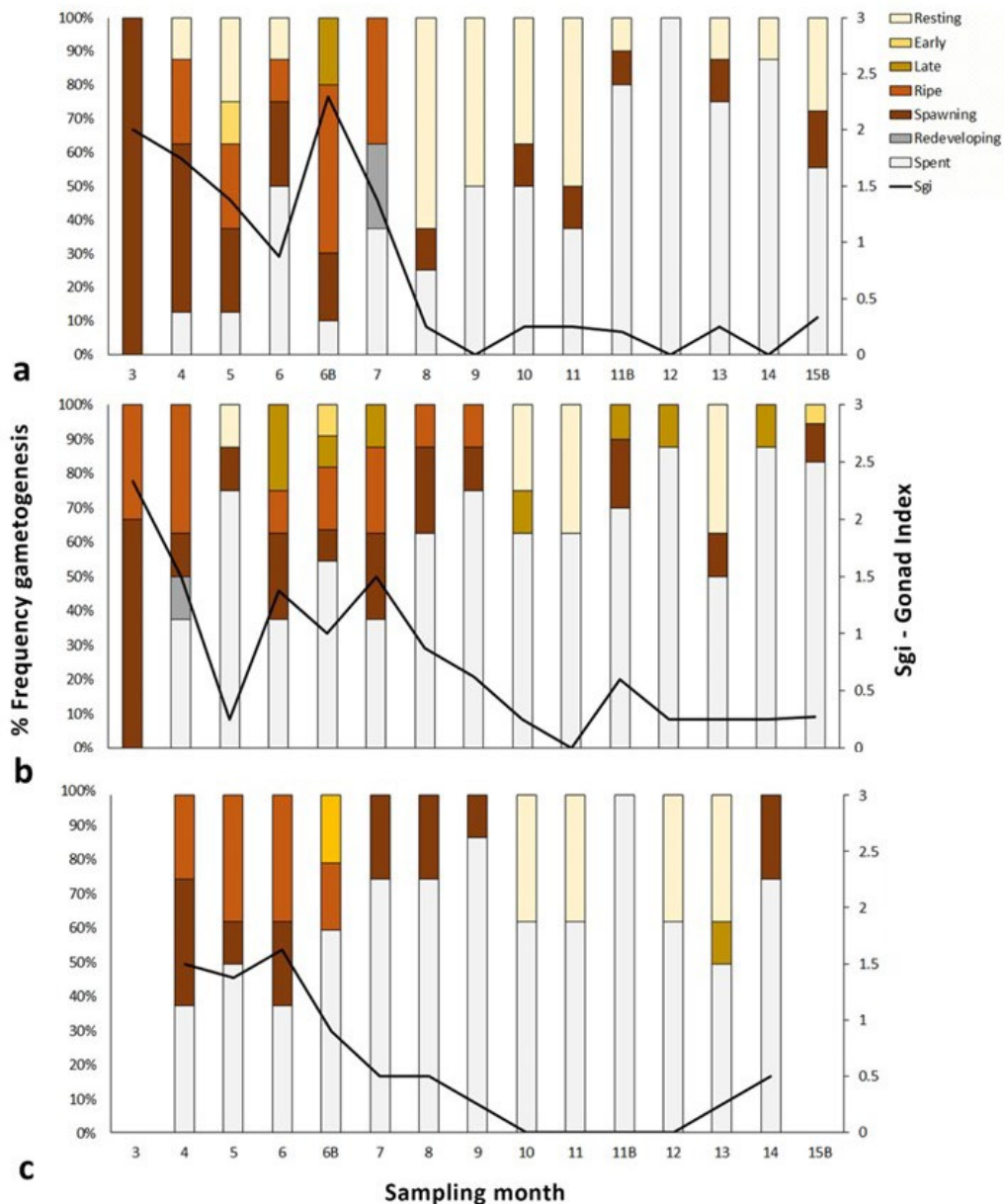


Figure 5.7 Gonad condition (proportion of sampled individuals in each development stage and overall gonad index) over 14 months exposure to a) 17°C, b) 21 °C and c) 24°C. No data were collected at month 3 or 15B for 24°C.

There was no difference in the percentage coverage of the follicles between the three temperatures ($p > 0.05$). Visual estimates of coverage correlated with objective image analysis quantification with

an R^2 value of 0.93. The female gonad tissue displayed various anomalies, particularly in the spent category; 1) dilated follicles post-spawning; 2) dilated follicles with increased levels of atresic debris; 3) increased numbers of follicles with atresic oocytes and some phagocytosis; and 4) follicle regression and atrophy (Fig. 5.8).

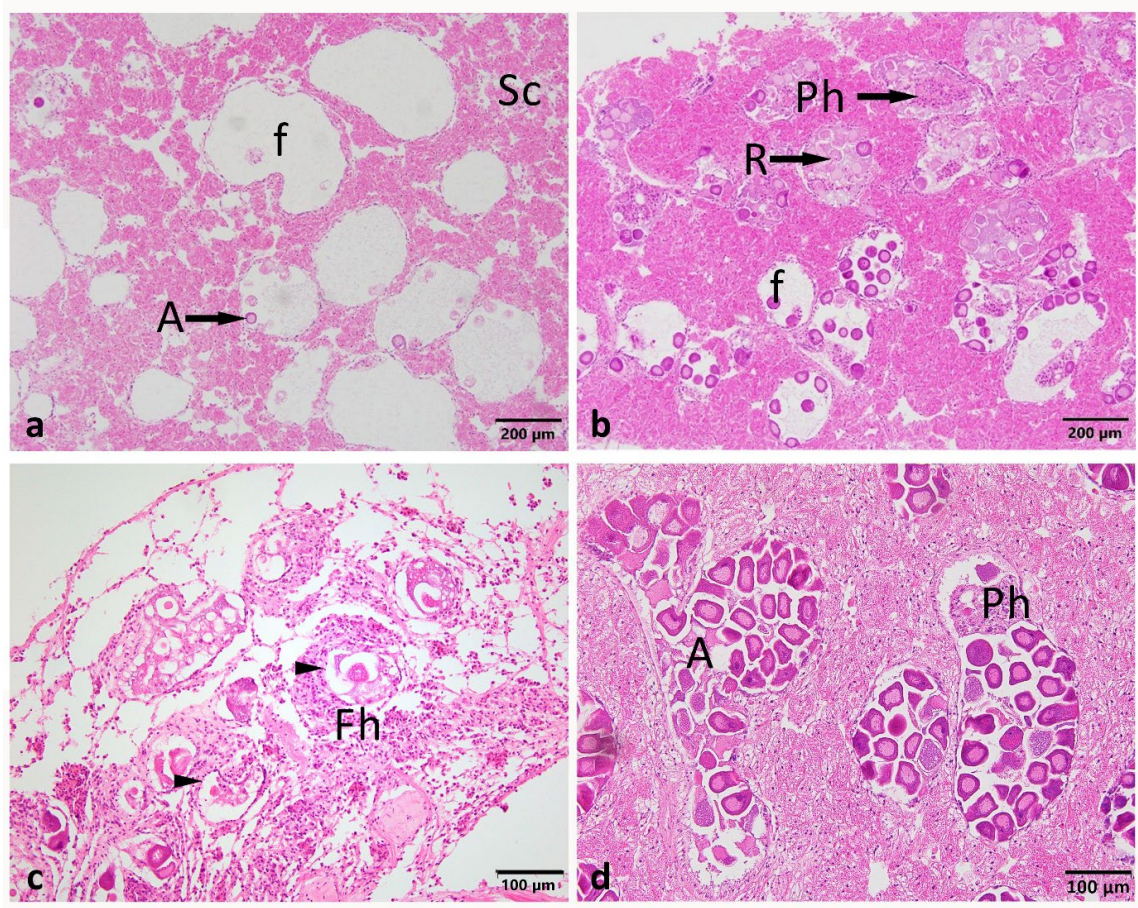


Figure 5.8 Female reproductive tissue (mantle) showing: a) anomalous dilated post-spawning follicle (f), b) dilated follicles with high levels of atresic debris, c) female mantle tissue with low levels of storage cell (glycogen (Sc)), regressing and atrophying follicles (Arrow) and focal haemocytosis (Fh) from a female in the 24 °C treatment, d) full follicles with high level of atresic oocytes (A), residual oocytes (R), and phagocytosis (Ph) within the follicle.

Due to the under-representation of females as a result of many of the sexes being indeterminate across the three temperature treatments throughout the experiment, only temperature was used as a factor, and female gonad images from each month were pooled.

No significant differences were observed among mean proportion of immature oocytes ($F_{(3, 117)} = 0.75, p = 0.53$), mature oocytes ($F_{(3, 117)} = 0.85, p = 0.47$), atresic oocytes ($F_{(3, 117)} = 0.3, p = 0.82$), and atresic impact ($F_{(2, 109)} = 0.4, p = 0.76$). The mean proportion of oocytes showing atresia, as well as overall atresic impact was observed to be high across the 17°C, 21 °C and 24 °C temperatures ($62\% \pm 4.1, 58\% \pm 4.3, 60\% \pm 5.8$ and $74\% \pm 3.3, 78\% \pm 2.9, 75\% \pm 5.2$, respectively (mean percent \pm SD)).

5.3.4. Pathogens

There were several parasites observed in the green-lipped mussel tissues. Due to the very low percent population prevalence many of these are only reported by temperature treatment category rather than temperature and month. These included various unidentifiable ciliates and copepods, as well as a low prevalence of *Paravortex* and *Endozoicomonas* (Table. 5.8). The two most significant parasites observed were APX (Fig. 5.9a) and *Perkinsus olseni* which were reported by temperature and month (Fig. 5.9b).

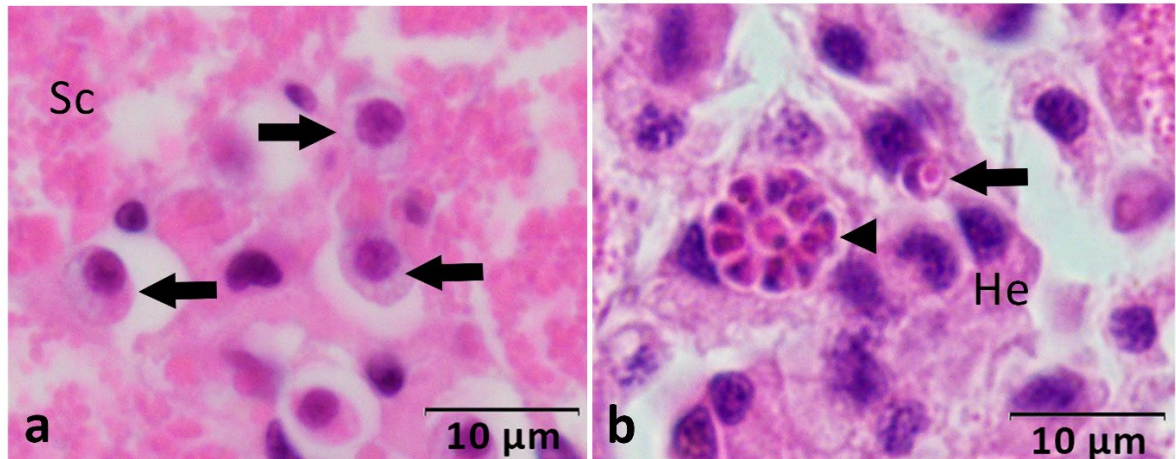


Figure 5.9 Representative microphotographs of a) APX at a score of level 2: a group of 6 APX zoites within the mantle tissue no ceroid material or haemocytosis associated, and b) *P. olseni* indicating level 3 displays different stages of the lifecycle trophozoite signet ring (arrow) and the rosette-like (arrowhead). *P. olseni* cells detectable across mantle and connective tissue of multiple tissues occasionally associated with haemocytosis.

Table 5.8 Total population percentage prevalence (%) of parasites found in the green-lipped mussels during the experiment. APX and *P. olseni* are excluded from this table and discussed in further detail below (17°C (n=142), 21°C (n=129) and 24°C (n=104)).

	Temperature		
	17°C	21°C	24°C
<i>Endozoicomonas</i>	0.0	1.6	1.9
<i>Microsporidium rapuae</i>	0.7	0.8	0.0
<i>Paravortex</i>	0.7	0.0	0.0
Copepod	2.1	1.6	2.9
Ciliates	1.4	0.0	0.0

APX was present in mussels in all three temperatures, and by month 4 of thermal exposure, APX approached 100% population prevalence. Small groups of APX were found scattered in the mantle, connective tissue of digestive glands and gut subepithelial as well as at the base of the gills and plicate organ near the kidney. Ceroid material was only associated occasionally at this level. No differences were identified among the sample time points, but a significant difference in the total population prevalence of APX was observed between mussels in the 17 °C and 24 °C temperatures with prevalence being higher in the 24 °C treatment ($t = 2.548$, $p=0.011$). *Perkinsus olseni* percent

prevalence in mussels increased with temperature between 24 °C compared to 17 °C temperatures ($t = 6.051$, $p < 0.001$), and there was an interaction between temperature and month ($t = 4.058$, $p < 0.001$). The first detection of *P. olseni* in mussels occurred in 24°C, 5 months after the start of thermal manipulation (i.e., month 7), which was 2 months earlier than detection in mussels at 21°C. *P. olseni* was detected in only 1 individual at 17 °C towards the conclusion of the trial (Table. 5.9). Focal haemocytosis (haemocytes - He) was associated to *P. olseni* cells.

Table 5.9 Population prevalence (%) of APX and *P. olseni* during 15 months of sampling at three temperatures 17°C, 21 °C and 24 °C (sample numbers available in Table. 5.1)

		Sampling month														
		2b	4	5	6	6b	7	8	9	10	11	12b	13	14	15	16b
<i>APX</i>	17°C	33	75	63	25	100	100	100	100	100	100	100	100	100	100	100
	21°C		100	75	50	80	100	100	100	100	100	100	100	100	88	100
	24°C		100	88	88	100	100	100	100	75	88	100	88	100	100	
<i>P. olseni</i>	17°C	0	0	0	0	0	0	0	0	0	0	0	0	13	0	0
	21°C		0	0	0	0	0	0	13	0	13	0	13	38	25	17
	24°C		0	0	0	0	38	25	25	50	63	50	25	50	25	

The APX intensity levels throughout this trial were quite low and, as such, only the first three semi-quantitative grades from Hine (2002) and Suong (2018) were required. The mean intensities of APX across the three temperatures were 17 °C = 1.3 ± 0.6 (n=109), 21 °C = 1.4 ± 0.5 (n=108) and 24 °C = 1.1 ± 0.4 (n=90) (mean \pm SD). The mean intensity of *P. olseni* was relatively low at 17 °C = 1 (n=1), 21 °C = 2.1 ± 0.9 (n=11) and 24 °C = 1.8 ± 0.8 (n=28) (mean \pm SD). No lesions were identified in response to APX, and minor haemocyte reactions were present on occasion with *P. olseni* (Fig. 5.9).

5.4. Discussion

Prolonged exposure to constant temperature, even at the benign 17 °C typical in summer was associated with apparently deleterious histopathological alterations in digestive gland, gill, and gonad (The artificial constancy of laboratory trials and its potential confounding effect is discussed in section 4.5). Higher temperatures and prolonged exposure were also associated with increased prevalence of the pathogen *Perkinsus olseni*, suspension of gametogenesis, and oocyte atresia (see below). Elevated temperatures, in addition, significantly impacted survival, growth and immune response as also reported by Ericson et al., (2023). The histopathological alterations associated with elevated temperature may be valuable in assessing vulnerability to environmental challenges such as those arising with climate change. Further refinement of these potential indicators would contribute to improved health assessment of green-lipped mussels and the aquaculture industry it supports.

5.4.1. *Impacts on survival and growth.*

In a complementary study, Ericson et al. (2023) demonstrated that for green-lipped mussels, prolonged exposure to elevated temperatures (21 °C and 24°C) was detrimental to both growth and survival. This detrimental effect indicates that the optimal thermal range was exceeded with consequential impacts on physiology, metabolism, immune response, and survival (Petes et al., 2007; Dame, 2016; Delorme et al., 2021b). In addition, there was a noticeable difference in the development of byssus (anecdotal observation), where mussels at 24 °C had sparse and weak byssus development compared with mussels maintained at lower temperatures. Although not part of the initial experiment this is worth noting and exploring further in the future as mussels that prioritise growth, over byssal development in the natural environment (i.e. rocky shores) risk dislodgement and increased mortality (Clarke, 1999; Sebens et al., 2018; Roberts et al., 2021). The byssus threads were clipped four times throughout the trial to weigh and measure mussels, thus, introducing a potential confounding factor in terms of energy availability for growth, survival, and immune response across all temperature treatments. The energetic cost of byssal production for reattachment therefore represented a compounding stressor for mussels within this study.

5.4.2. *Tissue abnormalities*

Chronic exposure to the three temperatures (17, 21 and 24°C) resulted in an accumulation of ceroid (lipofuscin-like pigment) during the trial. The ceroid accumulation in response to thermal stress could be the result of an initial increase in metabolic rate, which leads to increased oxygen consumption, followed by higher basal reactive oxygen species (ROS) production, faster accumulation of peroxidised material and finally loss of cell function (see Ericson et al., 2023). Therefore, the accumulation of ceroid indicates accelerated senescence and potentially the advancement of the physiological age when compared with the chronological age (Terman and Brunk, 1998; Basova et al., 2012). Typically, lipofuscin production has been associated with aging and is also known to be a temperature dependent process (Miquel et al. 1976); (e.g. in clams Lomovasky et al., 2002). Ceroid is a pigment associated to pathological conditions (Basova et al., 2012; Carella, 2015). There are several potential causes of ceroid accumulation, including immune response and oxidative stress (Zarogian and Yevich, 1993). Increases in oxidative stress were observed in mussels exposed to the same temperature treatments in the complementary study by Ericson et al. (2023). Lipofuscin and ceroid are both end-products of lipid peroxidation and the oxidation of proteins (Seehafer and Pearce, 2006; Basova et al., 2012; Carella, 2015). Both also can catalyse their own formation and drive further lipid peroxidation (Jung et al. (2007b)). Due to the characteristic histological similarities between lipofuscin and ceroid material, it is difficult to determine the difference between the two in this work. Therefore, “ceroid” was used in this study to refer to the pigmented granules. Ceroid-lipofuscin accumulation has been considered to be an outcome of inadequate intra-lysosomal digestion from the phagocytosis process. These residual ceroid granules accumulate in the cell’s cytoplasm, which can then be expelled into the connective tissue (Hendriks and Eestermans, 1986; Basova et al., 2012; Hartenstein and Martinez, 2019). In addition, accumulation may also indicate

previous and ongoing pathological conditions (i.e., APX and *Perkinsus* spp. exacerbating the accumulation).

Elevated recruitment of haemocytes to the gut region at higher temperatures may indicate defence against incoming pathogens or a response to altered gut microbiota and nutritional affects. For example, increased aggregations of haemocytes around the gut have been observed in *Crassostrea gigas* when exposed to the toxic algae *Alexandrium minutum* (Haberkorn et al., 2010). While haemocytes can function as defence cells, they also fulfil digestion and nutrient transport roles or support shell formation and tissue repair (e.g. Allam and Raftos, 2015; Rolton and Ragg, 2020), the aggregation of haemocytes referred to as haemocytosis is a response limited to tissue repair and pathogens (see section 4.3) (e.g. Haberkorn et al., 2010; Ben-Horin et al., 2015). Across bivalve tissues, circulating haemocytes encapsulate and traffic pathogens such as viral particles through the gut epithelium (Haberkorn et al., 2010; Ben-Horin et al., 2015) in a process called diapedesis. This process has been suggested to be a defence response to protect the tissues (e.g. Haberkorn et al. (2010). The digestive process, gut epithelial layer and mucosal layers provide a strong defence against the physical environment and pathogens in healthy individuals. However, during host stress, such as the thermal stress inflicted here, physiological state and immunity may be compromised, allowing the entry of viruses, bacteria and parasites through the gut tract and pallial organs (Bower, 2006; Ben-Horin et al., 2015).

In addition to minor alterations to the gill architecture there also appeared to be expression of the HSP70 protein with increasing temperature based on our preliminary observations. HSP70 is a wide spectrum heat inducible protein in the HSP family which is expressed under stress (Feder and Hofmann, 1999; Hu et al., 2022). Gills are directly exposed to the environment and therefore detection of HSP70 is expected as a “first layer of defence” response to thermal stress. The increasing HSP70 expression with increasing temperature is worth further research as production is associated with a high energetic cost (Feder and Hofmann, 1999; Tomanek, 2010; Valenzuela-Castillo et al., 2019). Possibly though HSP70 production might have been beneficial for green-lipped mussels exposed to higher temperatures, which could explain the minimal gill architectural alterations observed. The inclusion of these preliminary results is novel and promising for green-lipped mussels and worth further investigation.

5.4.3. Pathogen prevalence and influence on the host

Perkinsus olseni was observed in mussels at month 7 at 24°C, month 9 at 21 °C in the trial. The intensity of the parasite, based on the scale by Hine and Diggles, (2002) and Kim et al., (2006a) was considered to be low and therefore potentially at the initial stage of infection. In association with *P. olseni*, there was an increasing intensity of focal haemocytosis at the elevated temperatures 21 °C and 24°C. In addition, the presence of *P. olseni* was associated with decreased energy reserves and immune responses such as increased intensity of focal ceroid aggregations, focal haemocytosis, and encapsulation of parasites across different tissue types. The parasite is known to have an affinity for

waters above 20 °C which commonly occur in the North Island (Hine and Diggles, 2002), and the top of the South Island (Broekhuizen et al., 2021). This temperature (20°C) may represent a threshold of natural occurrence of *P. olsenii* whereby infective cells are present in low concentrations in the environment, with temperatures above this (e.g. 24 °C from this research) accelerating initiation of infection (Lester, 1986; Goggin and Lester, 1995). The present work corroborated this temperature effect.

Marine diseases are the result of complex host-parasite-environment interactions and there is growing evidence to suggest that, in some cases, their increased prevalence and severity may be associated with climate change (Harvell et al., 1999; Burge et al., 2014). Suboptimal environmental conditions, such as temperature stress in combination with stressed hosts can favour pathogen transmission and replication resulting in mortalities (Harvell et al., 1999). *Perkinsus* spp. host interactions exemplify this. This protist endoparasite infects several species worldwide including, green-lipped mussels, *Perna canaliculus* (Muznebin et al., 2022a), the clams *Austrovenus stutchburyi* (Dungan et al., 2007), *Paphies australis* (Ben-Horin et al., 2015), abalone *H. iris* (Hine and Diggles, 2002; Muznebin et al., 2021) and the oyster *C. gigas* (Ben-Horin et al., 2015). Climate warming has been implicated in driving increased spatial distribution of *Perkinsus* spp. and resulting disease events (Carella, 2015).

Perkinsus spp. inhibits phagocytosis and suppresses apoptosis of haemocytes in molluscs (Ordás et al., 1999; Sunila and LaBanca, 2003; Hughes et al., 2010). Phagocytic inhibition allows the parasites to infect and proliferate in circulating haemocytes, without being destroyed, and spread to other tissues (e.g. Ordás et al., 1999; Sunila and LaBanca, 2003; Hughes et al., 2010; Ben-Horin et al., 2015). Phagocytosis is one of the main mechanisms for defence and it is a temperature-dependent process (Oliver and Fisher, 1995) (Yu et al., 2009). The haemocytes in the mussels at the warmer temperatures potentially tried to ingest the *P. olsenii* cells initially, without success. This process was then followed by parasite-mediated inhibition once infection was established, with *Perkinsus* cells developing into replicative trophozoites. Partial phagocytosing could have resulted in the inadequate intra-lysosomal digestion and therefore further accumulation of ceroid material as described in the above section (Hendriks and Eestermans, 1986; Hartenstein and Martinez, 2019).

As heatwaves progress two outcomes are hypothesised, either pathogen intensity continues to increase in response to favourable conditions, or the pathogen intensity diminishes allowing for elimination during the cool winter months as previously suggested by Goggin and Lester (1995). It remains a question of how *P. olsenii* was acquired and whether development to detectable levels was facilitated primarily by stress from the suboptimal chronic conditions. In the current study, it was difficult to determine this or to establish the true extent of the *P. olsenii* infection, and whether *P. olsenii* is detrimental to green-lipped mussels and, if so, at what intensity level. The occurrence of *P. olsenii* was unexpected as it was not a pathogen-focused trial. Therefore, this research highlights the need for additional surveillance methods and diagnostic tools including PCR and histology, when

performing experiments. There is little published information regarding green-lipped mussels as a host for *P. olsenii* (Muznebin et al., 2022a) and, considering that environmental fluctuations may be exacerbated by climate change, further research is required on the disease progression and implications for the Greenshell mussel industry and wild mussel beds. This should include work on farmed and wild populations to reflect conditions that are experienced in the sea.

The decline in energy reserves (glycogen) within the mantle, based on the mantle storage cell scale, is likely to explain the decline in the green-lipped mussel weight found by Ericson et al., (2023) in response to elevated temperature (21 and 24°C). Additionally, the thermal stress and potentially the *P. olsenii* infection, in combination, are likely to have resulted in the observed decline in mantle energy reserves from month 10 onward at 24°C. However, declines in weight-based measurements, such as condition index have been observed in other mussels, such as *Mytilus edulis* (Clements et al., 2018) and green-lipped mussels (Venter et al., 2023), in response to elevated temperatures. The energy available for growth, immune response and reproduction is acquired through food assimilation and is stored as lipids and glycogen within the mantle tissues, digestive glands, and muscle. These reserves are primarily used as energy over the winter period, as well as for gametogenesis (Bayne et al., 1982; Hummel et al., 1989; Fearman et al., 2009). Accumulation and use of reserve glycogen content is likely to vary with environmental changes, such as extreme temperatures, pollution and starvation (Hummel et al., 1989). Glycogen is the primary carbohydrate used for maintenance under stressful conditions and has been used as an indicator of health (Bayne, 1976; Barber and Blake, 1981). The depletion of glycogen in storage cells is of interest and possibly related to several factors, including its allocation to processes, such as routine metabolic maintenance, shell and byssal development, phagocytosis and immune responses, as well its appropriation by pathogens (Cheng, 1983).

5.4.4. Reproductive condition

Histopathological investigations in this study have revealed that at initial sampling timepoints, green-lipped mussels were passing the ripe and spawning stage and advancing towards the post-spawning, spent stage. Prolonged experimental exposure, irrespective of temperature, was observed to have impacts on reproductive condition in the present study. Gametogenesis was suspended with increased atresia (oocyte degradation) in the majority of the mussels in all temperature treatments, including the “benign” 17°C, which may result from a) the prolonged temperature stress, b) without the quiescent winter phase, the initiation of gonadogenesis is indistinguishable, regardless of the amount of food available, c) reproduction is the first energetic process to be sacrificed when temperatures are outside the reproductive optimum and d) an undetected mussel spawning occurred post-transfer into the system prior to trial initiation.

Successful reproduction is crucial for the survival of any species. It is an energy-demanding process with its own physiological stressors. It has been found that sublethal conditions in the environment can inhibit reproduction as many species will reallocate energy from gamete production and move it

to the somatic tissues for growth, defence and repair (Michalek-Wagner and Willis, 2001; Petes et al., 2007). Heat shock proteins are one of the main defence and repair mechanisms in organisms (Feder and Hofmann, 1999; Tomanek, 2010; Valenzuela-Castillo et al., 2019). In this study, a seemingly higher HSP70 expression was observed in gonads of mussels exposed to elevated temperatures. This indicates that the mussels had activated specific mechanisms to cope with the stress, as has been shown in other marine invertebrates (e.g. Nash et al., 2019; Delorme et al., 2020a; Delorme et al., 2020b). Additionally, the HSP70 presence in gonad tissue suggests that mussels responded to the heat stress by investing in loading the gametes with HSP70 to protect their offspring against potential further increases in temperature or other stressors. As a result of the promising preliminary observations further research and targeted sampling is required to determine the mechanisms of parental investment in green-lipped mussels exposed to chronic heat stress.

The lack of noticeable spawning, and increased oocyte atresia, observed within this investigation suggests a potential strategy of green-lipped mussels to cope with prolonged stress and may indicate a method of adaptation and survival. Atresia is the degeneration and reabsorption of oocytes prior to a spawning event and is a strategy to recycle energy (Beninger, 2017; Chérel and Beninger, 2017). Atresic oocytes are determined by their histological characterisations and unusual fixation effects, such as shrunken, highly irregular shapes, cytoplasmic detachment from membrane, lysing of the membrane and increased staining affinity (Beninger, 2017; Chérel and Beninger, 2017). Atresia has been reported in a number of bivalve species, e.g. the clam *Tapes philippinarum* (Chérel and Beninger, 2017), oyster *C. gigas* (Steele and Mulcahy, 1999) and mussels *Mytilus edulis* (Pipe, 1987), *Mytilus galloprovincialis* (Ortiz-Zarragoitia et al., 2011) and *Aulacomya atra* (Pérez et al., 2013). The probable causes of increased incidence and intensities of atresia are adverse environmental conditions, including pollution, starvation, and sub-optimal temperature (Galap et al., 1997; Steele and Mulcahy, 1999; Pérez et al., 2013; Vazquez et al., 2020). Atresia is a strategy to reallocate energy reserves in order to cope with stress and energy depletion (Beninger, 2017). Observations of atresia in this study are therefore expected, particularly when green-lipped mussels exposed to sub-optimal elevated temperatures. Interestingly, the incidence of atresia prior to increasing the temperatures was higher than expected. Several questions remain. For example, was the incidence of atresia at this point representative of field conditions, or was it a consequence of energy reallocation to byssal development following stripping from the farm ropes at initial collection time? Additionally, was the atresia related to movement into the spent stage as a result of an undetected spawning. Failure to identify and determine atresia within field and the laboratory populations will result in several implications including over-estimations of fecundity and reproductive effort (Beninger, 2017).

Both reproduction and somatic growth reflect complex intrinsic and extrinsic interactions. The reproductive cycle is controlled by both endogenous factors and environment, with temperature being the driving force behind the initiation and the rate of gametogenesis (Michalek-Wagner and Willis,

2001; Petes et al., 2007). Reproductive timing, synchronicity, fertilisation, and recruitment success are influenced by temperature. Chronic stress can lead to a loss of propagules, low gamete quality and spawning of pre-mature gametes that supply the adult population (Walther et al., 2002; Philippart et al., 2003; Petes et al., 2007; Petes et al., 2008). The green-lipped mussel is a gonochoric broadcast spawning species with gonadal development and gametogenesis occurring throughout the year (Alfaro et al., 2001; Buchanan, 2001). The depletion of the glycogen content and the decline in growth (Ericson et al., 2023) in green-lipped mussels exposed to elevated temperatures during the present study suggests there is very little residual energy after increased metabolism for both growth and reproduction, as observed in other molluscan species (Fearman and Moltshaniwskyj, 2010). Present and future climate change influences on environmental stressors are of major concern for green-lipped mussels in the aquaculture industry and in the wild. In terms of reproductive capability, it is crucial to determine the true extent of oocyte atresia in green-lipped mussels and how ongoing stressors, such as marine heatwaves are likely to impact oocyte development further. Knowledge relating to interactions between the reproductive condition and health of green-lipped mussels is key for the aquaculture industry, particularly as heatwaves increase in frequency and intensity (Beninger, 2017). Such expected changes to reproduction and spawning status of mussels could impact the aquaculture industry by affecting not only their ability to plan harvesting operations, but their ability to produce economically valuable products.

5.4.5. *Research implications*

It was surprising that the unchanging conditions within this study were ultimately detrimental and 17°C, although considered as a benign temperature, does have negative effects over time. This impact on overall health in the benign treatment was also observed in the immune stress indicators in the complementary study by Ericson et al. (2023). It is yet to be determined whether these effects on the benign temperature was due to captivity stressors, including nutrition, density effects, lack of natural variation, and general holding conditions, although, a similar effect of captivity has been considered and observed in other invertebrates such as mytilids (Bayne and Thompson, 1970) and freshwater mussels (Roznere et al., 2021; Morin et al., 2022). The thermal conditions in this study were maintained to eliminate treatment variability and focus on temperature as a single stressor. Single stressor long-term studies such as the work present herein are required to isolate the compounding effects of continuous stress such as temperature elevations. While green-lipped mussels in their natural environment are unlikely to be chronically exposed to elevated temperatures for the extended durations used in this study the average sea surface temperatures are increasing. Although predictions of climate change are highly complex, impacts of increasing seawater temperatures on species phenology, distribution and physiological performance are likely (Zippay and Helmuth, 2012; Shelmerdine et al., 2017; Steeves et al., 2018). Therefore, the results of this work provide key knowledge on health at a tissue level and caution is required when extrapolating laboratory data to field conditions.

5.4.6. Conclusions

The present research identified changes in response to thermal stress and provides new insights into the host-environment-pathogen interactome for green-lipped mussels under changing environments. Additionally, this is the first study that shows immunodetection of HSP70 in green-lipped mussels. The decline in growth, loss of byssal development and suspension of gametogenesis in green-lipped mussels suggests that, with increasing temperature and loss of seasonal variability, there is insufficient energy available after metabolic maintenance and immune defense in the laboratory conditions provided. In addition, the unexpected appearance of *P. olseni* needs further investigation and could be indicative of potential range spread if average temperatures and marine heatwave frequency continue to rise. Although, the HSP 70 technique is not comprehensively studied within this research it is a novel technique for this species, the small numbers of samples that were selected for IHC, do show promising protein expression between temperature treatments in the gills and gonad and is worth future investigation. Furthermore, the aetiological causes of the mortalities during the trial are also still to be determined, with further investigations required to determine whether the mortalities were a result of exhaustion of energy reserves, phagocytosis inhibition, increased toxicity in the tissues from anaerobic metabolism, increased toxicity from the ceroid accumulation or other causes. Timely sampling at point of death before decay had set in would have provided further information for this investigation. This work highlights the potential effects of chronic thermal stress if climate change and marine heatwave frequency continues to rise. Further work using simultaneous laboratory and field studies incorporating realistic fluctuating and increased temperatures, as well as baseline ambient sampling, will help to provide further beneficial knowledge on the future impacts to green-lipped mussels in response to climate change.

CHAPTER 6. IMPLICATIONS OF FLOODING EVENTS FOR THE GREEN-LIPPED MUSSELS
(*PERNA CANALICULUS*): AN AQUATIC HEALTH PERSPECTIVE: PART A

Published in its entirety in Journal of New Zealand Marine and Freshwater science:

Copedo, J. S., Webb, S. C., Ragg, N. L. C., Alfaro, A. C., (2025) Implications of flooding events for the green-lipped mussels (Perna canaliculus): An Aquatic health perspective. Journal of New Zealand Marine and Freshwater science. 10.1080/00288330.2025.2474570.

Abstract

Flood events are increasingly impacting coastal infrastructures and marine organisms. Prominent among these organisms, the green-lipped mussel, *Perna canaliculus*, is an important marine ecosystem engineer and one of New Zealand's key aquaculture species. Although relatively robust, the species may have limited capacity to tolerate acute environmental shocks such as exposure to riverine floodwater. As flood events become more frequent, they may present serendipitous opportunities for further research. Thirty days into a temperature and starvation co-stressor experiment a storm event resulted in the staff evacuation and eventual flooding of the research facility. Additional samples for histology were opportunistically collected after the flood waters receded and the survival of the green-lipped mussels were monitored for two weeks post-event. Although no mortalities were observed post-flood exposure, histological results indicate that the event did cause the mussels to spawn. Tissue conditions, such as haemocytosis of the gill, digestive gland atrophy appeared to be correlated with the flood event, however impact to green-lipped mussel health was considered as negligible. This research highlights not only the importance of targeted research in elucidating impacts of climate-related hazards on marine species, but also the importance of opportunistically incorporating these unforeseen events into the research.

6.1. Introduction

Dynamic and productive ecosystems are essential for aquatic life in coastal marine environments (Pourmozaffar et al., 2019). Abnormal fluctuations in temperature and salinity resulting from climate change and flood events, respectively, are increasingly impacting marine organisms and ecosystems, their performance, and their ability to respond to additional and future stressors (Talbot et al., 2018; Pourmozaffar et al., 2019). Heavy rainfall and flooding along the coast can decrease salinity and expose aquatic organisms to osmotic stress, sedimentation and potential smothering, and exposure to pathogens (Coughlan et al., 2009; Peteiro et al., 2018; Pourmozaffar et al., 2019). Marine bivalves are highly abundant, productive, and economically valuable whilst also providing critical ecological services such as improving water quality through filtration (van der Schatte Olivier et al., 2020; Verdelhos et al., 2021). Bivalves in particular have adapted to tolerate a range of environmental stressors and anthropogenic inputs (Peteiro et al., 2018; Pourmozaffar et al., 2019).

In addition to the role as an ecosystem engineer, the marine bivalve, *Perna canaliculus* Gmelin 1791 (green-lipped mussel) is one of New Zealand's key aquaculture species. Although apparently robust, osmo-conforming bivalve species, such as the green-lipped mussel, often have difficulties tolerating acute environmental shocks associated with events such as riverine flood water (salinity changes, high nutrient and sediment loading) (e.g., Peteiro et al., 2018; Pourmozaffar et al., 2019; Sokolov and Sokolova, 2019). This is because osmo-conforming bivalves have very limited capacity to regulate their haemolytic fluid, which therefore tends to resemble the external salinity (Peteiro et al., 2018; Pourmozaffar et al., 2019; Sokolov and Sokolova, 2019; Tan et al., 2023). Suboptimal salinity can impair animal physiology by reducing energy acquisition when increased energy is required for cellular maintenance and mitigation of osmotic stress (Peteiro et al., 2018; Sokolov and Sokolova, 2019). However, bivalves do have adaptive strategies to protect their soft tissues including physical barriers such as shell closure and the production of mucus (Allam and Raftos, 2015; Knowles et al., 2023). As a filtering mollusc, bivalves are exposed to various suspended particles in the water column, including phytoplankton and bacteria. The retention of, and exposure to, these suspended particles, and acute or chronic exposure to environmental challenges, such as thermal and salinity stress, can increase their vulnerability to pathogen infection (Pourmozaffar et al., 2019).

Prior studies on green-lipped mussels have demonstrated increased stress or mortality at seawater temperatures $\geq 24^{\circ}\text{C}$ (Copedo et al., 2023; Ericson et al., 2023; Venter et al., 2023) (Chapter 5) and identified nutrition as a key factor influencing health (Skelton et al., 2024). Previous studies have also investigated the combined effect of bacterial infections and warming on green-lipped mussel health and found either negative synergistic effects of infection and temperature (Azizan et al., 2024), or no effect of increased temperature (Ericson et al., 2022). Such investigations on the impact of multiple stressors on the health of green-lipped mussels have been relatively limited to date, therefore further investigations are required, since environmental stressors seldom occur in isolation.

In NZ, flooding and drought events and storm damage are occurring more frequently as a result of changing precipitation patterns (Manning et al., 2014). New Zealand also has significant other assets located in coastal regions which are at risk from sea level rise and flooding (Manning et al., 2014). These assets include not only many seafood and aquaculture production facilities, which occur in coastal regions, but also marine research facilities that require access to seawater. Whilst climate hazards such as flooding are becoming more frequent, as presented in this study, they can also present serendipitous opportunities when research facilities are impacted. Despite the inferential post hoc nature of data derived from serendipitous events, such opportunities can be utilised as the effects of flood events on aquatic ecosystems and species are not well understood. Additionally, there is currently a lack of data concerning the adverse effects of flood events on aquatic health, therefore taking advantage of flooding in aquatic research facilities will help address critical knowledge gaps (Poff and Zimmerman, 2010; Peters et al., 2015; Talbot et al., 2018).

During August 2022, an ‘atmospheric river’ event (742 mm of rain over 5 days) resulted in the flooding of the research facility and disrupted the experiment. The rainfall within the Nelson, NZ region during this period was between 18% and 27% higher than the biggest future predicted events estimated for the years 2080 to 2100 (NIWA, 2017). The effects of this 1-in-100-year flood event were opportunistically included in the study plan to enhance our understanding of sediment-laden flood water impacts on the tissue condition of green-lipped mussels, as well as to consider the impacts of such events on future research and assess the utility of such serendipitous findings.

6.2. Methods

6.2.1. Experimental setup

Adult, green-lipped mussels (*Perna canaliculus*) were collected from Pelorus Sound, Marlborough, New Zealand in July 2022 (austral winter) and transported to Nelson, NZ, to be held at the Cawthron Aquaculture Park (CAP). A total of 1600 mussels were weighed, and shell lengths were measured (± 1 g and ± 1 mm respectively). Mussels were engraved with a unique identification number (Dremel 3000® with a 1.6 mm burr). The mussels were allocated to each of 16 holding tanks ($n = 100$ per tank) which were well aerated (100% dissolved oxygen level) and seawater flow-through rates of 3 L/ min (Ericson et al., 2023). After two weeks of acclimation to the system at the current winter ambient seawater temperature of 14°C, the temperature was increased by 1°C per week to the pre-determined temperature. The set up of this trial resulted in two experimental factors: temperature (benign 17°C (cool) and elevated 22°C (warm)) and feed level (high and low, defined below), and four replicate tanks per treatment), with reference mussels from the source farm collected to compare on-farm performance with mussels in the trial.

The temperature was controlled using two heat pump systems which delivered water to two primary header tanks per system. Mussels in the high food treatment were fed *ad libitum* with pond stored seawater which was then supplemented with a 50:50 cell ratio of monocultured algae (*Tisochrysis lutea* and *Chaetoceros muelleri*). The ‘low food’ treatment had access primarily to filtered, pond-stored seawater, but was also supplemented with monocultured algae at a 10% ration of the high food treatment. The 10% ration was achieved by pumping header tank seawater from the respective high food treatment at a rate of 0.5 to 1 L/ minute. Thirty days into the trial (two weeks after the initiation of temperature ramping) the treatment temperatures in the cool and warm system had reached 15 °C and 18 °C \pm 0.5 °C, respectively. The 15°C temperature was delayed due to weather conditions and an inefficient heat pump (Fig. 1). The day after the first monthly sampling timepoint (described in section 2.2) a storm system resulted in the evacuation of staff and eventual flooding of the research facility. The heavy rainfall continued for 5 days. Within this period the mussels in the system were inundated with freshwater in their tank for 24 -30 hours as well as exposed to the following; a) seawater with reduced salinity from the mixing of floodwater and seawater (salinity levels unknown due to site evacuation); b) no light, aeration or water flow due to intermittent power outages; c)

temperature decline back to winter ambient of 13-14°C; and d) high sediment loading with potential viral and bacterial exposure.

After the 24-to-30-hour inundation period the engineers were provided permission to enter the site to repair the power supply to the site and allow seawater to flow into the system. By the time the evacuation call was lifted the flood water had receded and the salinity had returned to normal (~34 ppt). The temperature differential was not re-engaged during this time to avoid compounding thermal stress. Immediately after the initial sampling (Section 2.2) the tank system was drain and cleaned to remove silt and assess mussels for signs of mortality or ill health. The shell length was measured and recorded for all mussels and survival was then monitored for two weeks post-event (Fig. 6.1)

6.2.2. Tissue sampling

Green-lipped mussels (82.2 ± 6.0 mm) were sampled for histological analysis on arrival at the Cawthron Aquaculture Park (CAP; 14 July 2022) to assess their baseline condition (n=40). After one month (16 August 2022), following initiation of food and temperature ramp treatment exposures, twenty mussels were collected from the source farm (same cohort) as a reference and four mussels per tank were removed and prepared for histological analysis (n=64). Seven days later, when the evacuation call was lifted, two mussels per tank (n=32) were sampled. Finally, after one month of post-flood recovery (i.e. the second month of tank exposure) 3 mussels per tank (n= 48, 13 September 2022) and 20 mussels were collected from the source farm (23 September 2022) were prepared for histological assessment.

To track the evolution of tissue-level changes, the sampled, green-lipped mussels were shucked, photographed, and a standard 5 mm section was taken for histological analysis (Howard, 2004; Copedo et al., 2023). The tissue sections were placed into histological cassettes and fixed in a 4% formalin: seawater solution for 48 hrs. The samples were then transferred into 70% ethanol for transportation and processing. Samples were embedded in paraffin wax, sectioned (3-5µm) using a rotary microtome and stained using routine hematoxylin and eosin (H&E) by Awanui Veterinary, Christchurch, and Medlab Central, Palmerston North (Howard, 2004). Histology preparations were observed by light microscopy using an Olympus BX35 at magnifications of x40 to x1000.

The gonad development of both males and females was scored as per Kennedy (1977) and Copedo et al., (2023) (Chapter 5), whereby gonadogenesis stages included resting, early development, late development, ripe or mature, spawning, spent, redeveloping. The frequency of these stages was plotted for visual representation. The gonad index (GIn), based on Kennedy (1977), was created by allocating each stage a score of 0 (resting or spent), 1 (early), 2 (late or spawning), or 3 (ripe mature). A range of tissue conditions were scored as present or absent across tissues including mantle, gill, digestive gland, gastro-intestinal tract, and muscle. Parasites were identified histologically and recorded as present or absent (binary as 1 or 0 respectively) and presented as percent of population prevalence.

6.2.3. Statistical analysis

Statistical analyses were conducted using R version 4.3.0 (R Core Team, 2024) with the R studio interface (RStudio Team, 2021). Histological data were analysed using the initial trial parameters, sampling month, temperature and food treatment as explanatory and interacting factors. Binomial general linear models (GLM) were performed on tissue and pathogen prevalence data using the MCMCglmm package (Hadfield, 2010). The gametogenesis rank scoring was analysed using an ordinal linear regression model followed by ANOVA employing type two sum of squares. When significant effects were detected, a pairwise comparison was performed using a TukeyHSD post hoc test. For both models a p value < 0.05 was considered statistically significant.

6.3. Results

6.3.1. Temperature and survival

Temperature was increased 0.5 °C every 3–4 days from 28th July to 24th August 2022. At the first sampling timepoint (August), the temperatures for the warm and cool treatments were 18 °C and 15 °C, respectively with each temperature fluctuating 0.5 °C around the target. Temperatures dropped to ambient during the flood period, with the warm temperature having a larger temperature drop. On the post-flood sampling day temperatures for both treatments were between 14 °C to 16 °C (Fig. 6.1). Two mortalities occurred within the first 2 weeks of the trial; however, these are likely to have been related to transport stress. There were no mortalities before the flood or during the post-flood recovery period. Note* a cold weather pattern late July resulted in a small decline in temperature for the cool temperature. This was still considered to be within the winter temperature range.

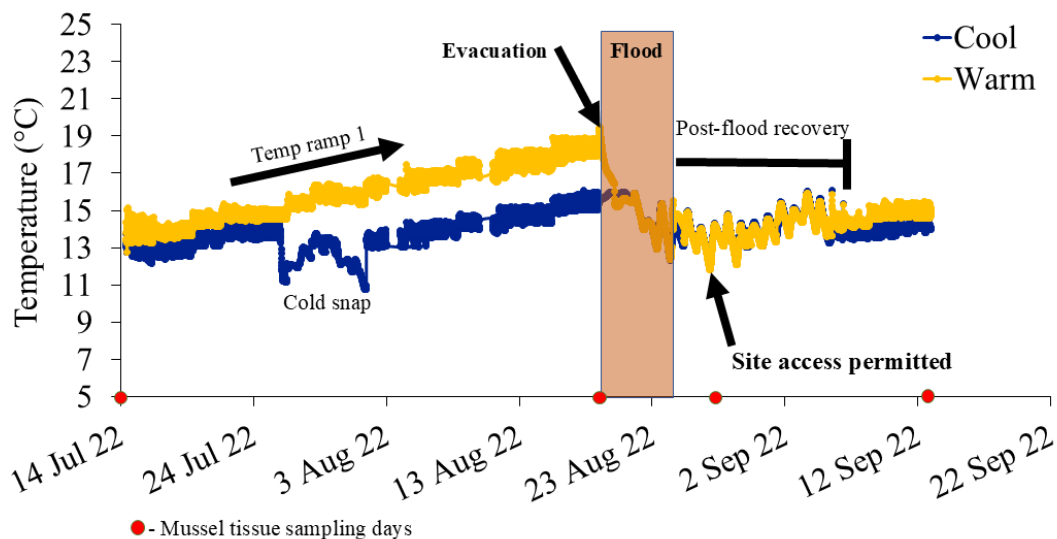


Figure 6.1 Time series of temperature between July 22nd and 13th Sept 2022. Sampling time points are indicated by the red circles: July 2022 is the baseline sampling when mussels arrived on site. The flood occurred on 17th Aug 2022 (second circle). The flood section indicates length of time (5 days) where site access was prohibited. The opportunistic post-flood collection occurred at the site access resumption point (third circle). A post-flood recovery of approximately 3½ weeks was used to

monitor survival prior to final sampling (month 2, circle four). The designation “cool” is the treatment destined to be 17°C and “warm” indicates 22°C

6.3.2. Reproductive condition

At sampling month 1 the mussels appeared to be developing in gonad condition based on the appearance of early, late and ripe developing mussels. Flood animals were associated with partial spawning, evidenced by the observation of the loss of gametes in the gonad follicles in some of the mussels (Fig. 6.2).

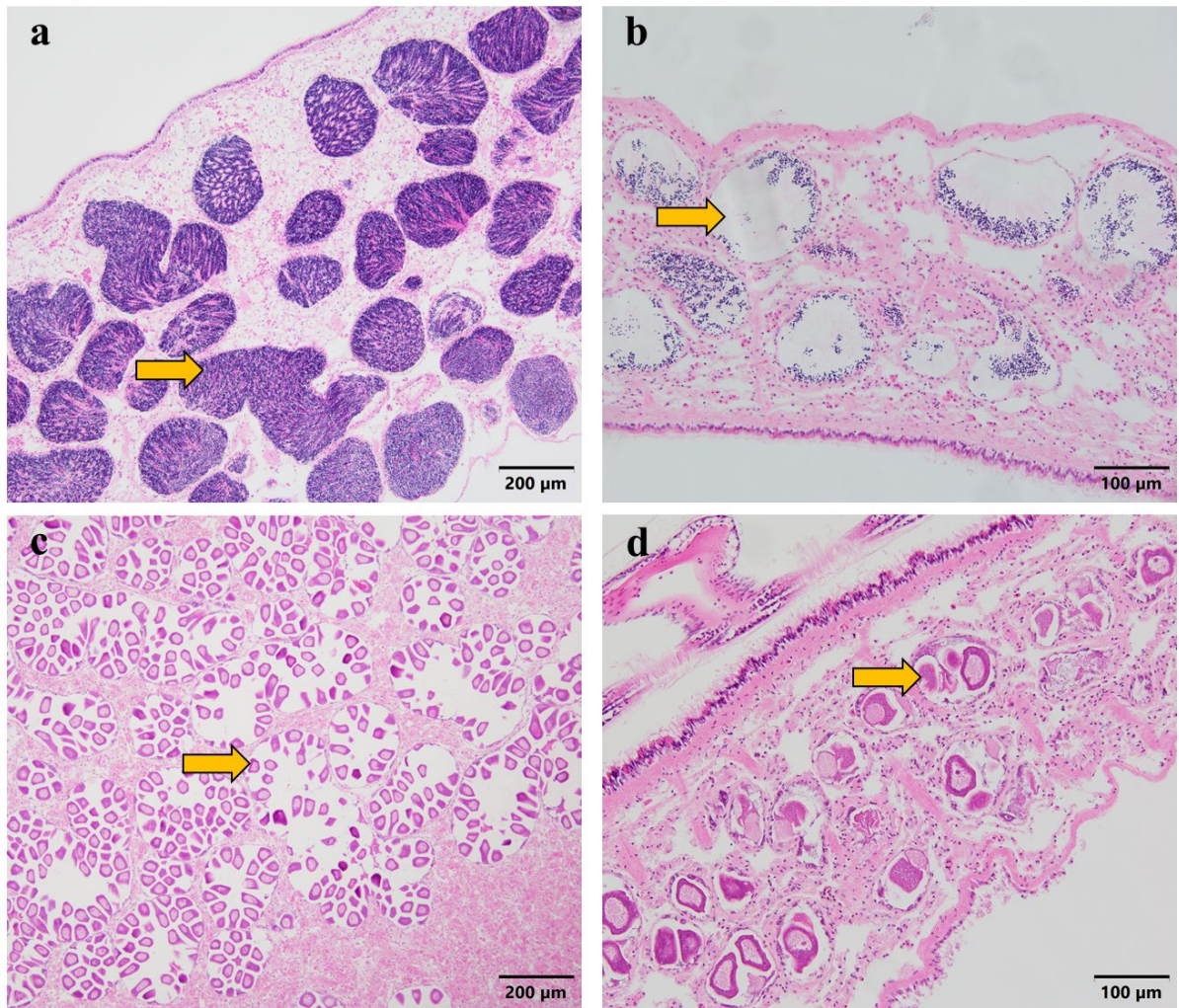


Figure 6.2 Example histology micrographs of gonad follicles in *Perna canaliculus* a) Male in ripe condition with follicles containing mature sperm cells b) Male partially spawned, c) Female spawning based on missing ripe oocytes (arrow) and atresic spent follicles (*), however many developing oocytes are still attached to the wall (arrow head) and d) female spent with small follicles and most follicles containing atresic (degenerating) oocytes.

The month 2 treatment samples appear out of phase when compared to the field samples which had spent, resting, early, and late gonads. The field mussels show a natural gametogenesis cycle which is indicated by early development starting in September 2022 (Month 2) and spawning prior to August (month 0). This resulted in a statistically significant difference between the temperature treatments for the gonad index score (GIn) ($\chi^2_{(2)} = 54.6$, $p = 0.001$ ($n =$ see table. 6.2)). However,

there were no statistical differences between the month and food treatment or interaction effects between the three factors ($\chi^2_{(1)} = 1.9, p = 0.2, \chi^2_{(2)} = 4.99, p = 0.08, \text{ and } \chi^2_{(1)} = 0.9, p = 0.3$, respectively ($n = \text{see table. 6.2}$)) (Fig. 6.3).

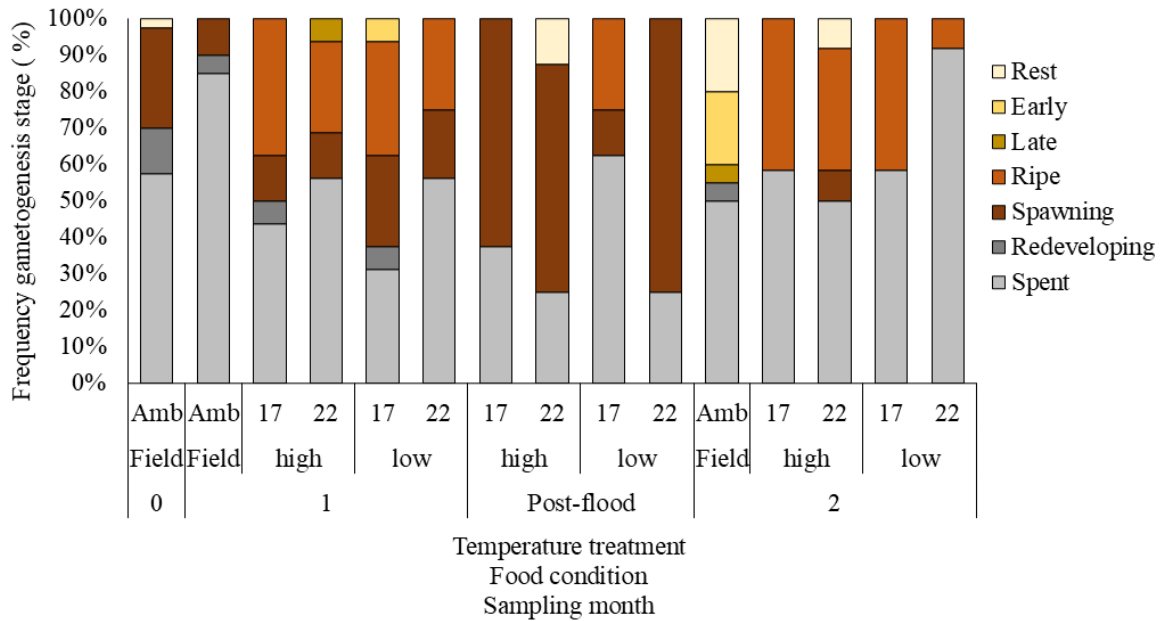


Figure 6.3 Visual representation of the reproduction condition and gametogenesis frequency stages for the mussels from the field and the laboratory experiment. The temperature treatments are grouped by the target experimental temperatures, feed treatment and sample month. For sample size per treatment see Table 6.1.

6.3.3. Tissue conditions

The conditions detected in the mussels included: presence of haemocytosis, ceroid (a brown waxy substance produced from lipid peroxidation), gastrointestinal tract haemocyte aggregations, and digestive gland atrophy. Prior to the flood event, the tissue conditions observed were detected in both the farm and the laboratory mussels. Ceroid and APX, detected in multiple tissue types, were observed in all mussels. Population prevalence of APX transitioning through the gastro-intestinal epithelium to the luminal space (Fig. 6.4) increased significantly in the low feed, cooler temperature during the post-flood sampling, while other treatments were similar to the field samples ($\chi^2_{(2)} = 9.9, p = 0.007$). Due to the low prevalence, statistical analyses were not performed on the presence of gill ciliates or *Microsporidium rapuae* detected in the sub-epithelial layer of the gastro-intestinal tract. The prevalence of *Endozoicomonas*-like organisms (ELO) detected in the gastrointestinal tract epithelium and primary digestive gland ducts (Fig. 6.4), although statistically significant, was observed to have varying prevalence between each treatment (month* food treatment*temperature treatment, $\chi^2_{(2)} = 3.0, p = 0.22$). A low prevalence of haemocyte infiltration in the gill epithelium was detected in the warmer treatment during the post-flood sampling (month* temperature treatment, $\chi^2_{(2)} = 9.1, p = 0.01$) (Fig. 6.4) (Table. 6.1 and 6.2).

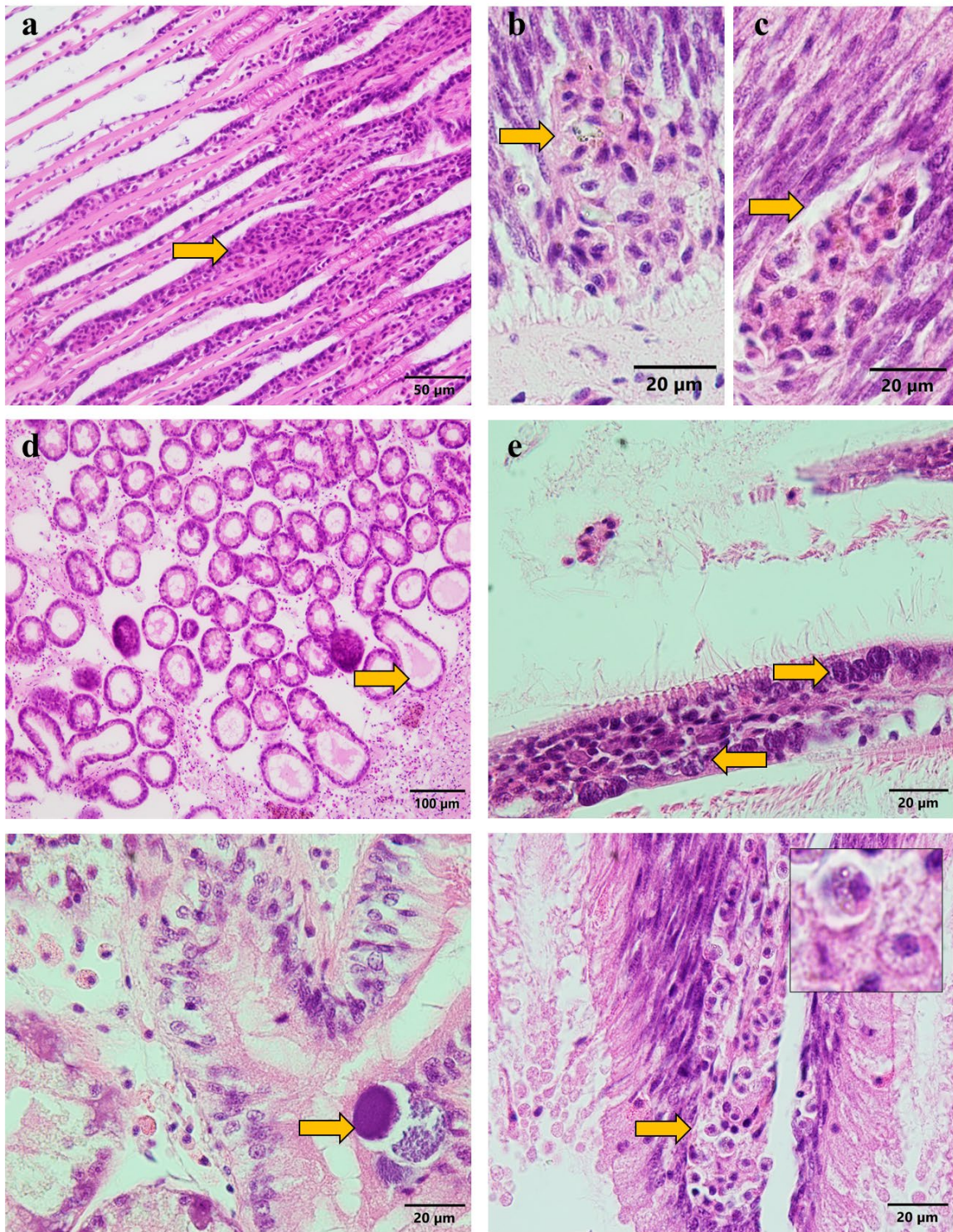


Figure 6.4 Histological micrographs of example conditions detected in adult *Perna canaliculus*, a) gill epithelium with increased haemocyte infiltration b) and c) Cluster of haemocytes, sediment, and ceroid transitioning through the gastrointestinal tract epithelium, digestive gland tubules with some displaying atrophy (arrow), e) Gill intracellular bacteria-like cells (arrow), f) ELO and shadowy to fine bacterium in the secondary duct of the digestive gland, considered as part of the gastrointestinal tract within the text and table. 6.1, g) large cluster of APX transitioning through the gastrointestinal tract epithelium.

Table 6.1 The percent prevalence of common tissue conditions and parasites observed in the green-lipped mussels during the 3-month period of sampling around the August 2022 flood: Base (Baseline), M1 (Month 1) and M2 (Month 2). The ambient (Amb) temperature samples represent mussels collected from the field (source farm) within a 5 to 10-day period after laboratory sampling. Tissue conditions include Ceroid, infiltration of haemocytes in the gill epithelium (Gill infil), and the gastrointestinal tract epithelial layer (GIT infil), digestive gland necrosis (DG nec), digestive gland wall atrophy (DG atr). Common parasites include *Endozoicomonas*-like organisms in the gastrointestinal tract and DG epithelium (GI ELO), intracellular bacterial cysts in the gills and mantle tissue (BA cyst), gill ciliates (CI), parasitic copepods in gastrointestinal tract lumen or mantle (CO), *Microsporidium rapuae*, APX in mantle and interstitial connective tissue (APX), and APX transitioning through the gastrointestinal tract wall to the luminal space (APX GI).

	Temp treat (actual)	Food	Sample n	Mean length (mm)	Ceroid	Gill infil	GIT infil	DG nec	DG atr	GI ELO	BA cyst	CI	CO	<i>M.</i> <i>rapuae</i>	APX	APX GI
Base	Amb (13 °C)	Field	40	82 ± 5.5	100	0	75	0	53	3	40	0	20	0	100	55
M 1	Cool (15 °C)	high	16	85 ± 5.9	100	0	50	0	6	13	6	0	19	0	100	69
M 1	Cool (15 °C)	low	16	81 ± 5.7	100	0	81	0	0	0	6	0	19	0	100	31
M 1	Warm (18 °C)	high	16	81 ± 5.5	100	0	63	0	25	13	0	0	6	0	100	31
M 1	Warm (18 °C)	low	16	82 ± 5.3	100	0	81	6	75	6	0	0	19	0	100	75
M 1	Amb (13 °C)	Field	20	82 ± 7.2	100	15	100	0	100	0	20	0	15	0	100	80
Flood	Cool (13 °C)	high	8	82 ± 4.6	100	0	100	0	100	13	50	0	0	0	100	75
Flood	Cool (13 °C)	low	8	78 ± 5.6	100	0	100	0	100	13	0	0	38	0	100	100
Flood	Warm (13 °C)	high	8	80 ± 7.0	100	13	63	0	100	25	38	0	0	0	100	88
Flood	Warm (13 °C)	low	8	84 ± 2.8	100	13	100	0	100	0	13	0	0	13	100	75
M 2	Cool (14 °C)	high	12	86 ± 7.7	100	0	25	0	100	0	8	8	0	0	100	42
M 2	Cool (14 °C)	low	12	81 ± 7.0	100	0	83	0	100	0	8	0	8	0	100	58
M 2	Warm (14 °C)	high	12	79 ± 5.6	100	0	58	0	100	0	8	0	8	8	100	42
M 2	Warm (14 °C)	low	12	82 ± 7.1	100	0	42	0	100	17	8	0	8	8	100	75
M 2	Amb (13 °C)	Field	20	86 ± 3.9	100	0	100	0	60	15	0	0	0	0	100	55

The prevalence of mussels with gastro-intestinal epithelium haemocyte aggregations increased in the post-flood however was similar to the month 1 field sampling which also had 100% prevalence ($\chi^2_{(2)} = 7.1, p = 0.03$). An intracellular bacterial-like cyst in the gills was detected with increased prevalence in the post-flood samples, however prevalence was also similar to the initial field samples which had a prevalence of 40% (month, $\chi^2_{(3)} = 19.6, p = 0. <0.001$). Finally, copepods in the gastro-intestinal tract were detected throughout and appeared not to be directly related to the flood event ($\chi^2_{(3)} = 8.1, p = 0.04$ for month only). Minor observations of digestive gland tubule (DG) necrosis were detected in 6% of the samples in the warm low food treatment during the first month ($\chi^2_{(2)} = 0, p = 1.0$). The prevalence of digestive gland tubule atrophy appeared to increase in the post-flood samples ($\chi^2_{(4)} = 145.9, p = <0.001$), however only a small proportion of the total number of digestive tubules were affected, differences were detected across all treatments ($\chi^2_{(1)} = 22.5, p = <0.001, \chi^2_{(1)} = 5.7, p = 0.02$) (Table. 6.1 and 6.2.) (Fig. 6.4).

Table 6.2 Trend of tissue conditions based on prevalence data presented in table. 6.1 whereby the increase in a condition (response variable) in relation to the environmental factor (explanatory variable) is indicated by an arrow up (\uparrow), no change is indicated by a dash (-), and a decrease by arrow down (\downarrow , not observed herein).

Tissue condition	Temperature	Food	Temperature x Food	Flood
Ceroid	-	-	-	-
Gill haemocytosis	\uparrow	-	-	\uparrow
GI haemocytosis	-	-	-	\uparrow
DG necrosis	-	-	-	-
DG atrophy	\uparrow	\uparrow	-	\uparrow
GI ELO	-	-	-	-
BA cyst	-	-	-	\uparrow
Copepods	-	-	-	-
APX	-	-	-	-
APX GI wall	-	-	-	\uparrow

6.4. Discussion

Given that environmental stressors rarely occur in isolation, our research aimed to fill a knowledge gap by examining the impact of thermal stress and nutritional factors on tissue changes and oocyte atresia (reabsorption). Initially, our research was designed to track the tissue-level alterations using histopathological, biochemical, and physiological techniques in response to warming and food deprivation, while also investigating the impact on gametogenesis and oocyte degeneration. Although the initial experiment was in its early phase, it was progressing well. The unforeseen flood event required reassessment of the research opportunity. The research essentially became a characterisation of the acute effects of a complex weather event stressor applied to mussels that had experienced one of four treatment histories. It is important to recognise that the reference farm population also experienced the same weather event, mitigated somewhat by their submerged offshore location. Although there was no way to determine some of the water quality parameters

such as salinity, pH, and bacteria content during the event, it was established that the main seawater intake pumps stopped earlier than the internal experiment reticulation pumps. This meant that flood waters rose above the internal supply tanks. The flood water was then pumped up to the mussel tanks during the event, inevitably introducing hyposaline water contaminated with suspended solids and potential pathogens, of both molluscs and humans.

6.4.1. *Histological observations*

The most distinct response observed in the present experiment was the spawning of the majority of the individuals that were starting to develop mature gonads in the treatment groups in the laboratory experiment. This spawning behaviour is a common response to salinity stress (Qiu et al., 2002). Gametogenesis is an energy-demanding process which is affected by salinity stress in other species, such as the mussel *Perna viridis* (Wang et al., 2012; Tan et al., 2023) and the cockle *Cerastoderma edule* (Vázquez et al., 2021; Tan et al., 2023). Fortunately for the reference sampling population on the farm the post-flood event mussels were either in the spent, resting or early development phase due to a spawning event in June (anecdotal observation). Therefore, the farm-based mussels did not appear to be impacted by the flood event. However, this flood event did occur close to the spawning season, which in the Marlborough region, NZ, has previously be reported to be late winter / early autumn (July – September) (Jeffs et al., 1999; Buchanan, 2001; Ren et al., 2019). If the event had occurred earlier in the season, or spawning was later, potential impacts may have been detected due to the consequences of salinity stress. These consequences of gamete release into low salinity environment include mortality of the oocytes and sperm, developmental abnormalities if the gametes manage to survive the fertilisation process (Santos et al., 2020; Boukadida et al., 2024) and loss of condition for harvest. The reproductive cycle is of particular relevance to the commercial harvest due to its relationship to market value and meat yield (Hickman and Illingworth, 1980; Buchanan, 2001). The meat yield and anti-inflammatory properties of green-lipped mussels makes it a desirable product for food and nutraceuticals (Azizan et al., 2023; Miller et al., 2023). Furthermore, the meat of green-lipped mussels is typically consumed whole and in good reproductive condition with plump gonads (Males: creamy white, Females pink- orange), when meat yield is greatest (Buchanan, 2001).

The impact of salinity stress on reproduction presents a potential reason to continue health monitoring of the mussels in both wild and farmed environments. For instance, Vázquez et al. (2021) found that exposure to salinity stress during early gamete development resulted in oocyte abnormalities at maturity. Spawning period mismatches, reduced recruitment and larval development, as well as increasing mortality, are also likely to occur (Tan et al., 2023). Changes to reproductive condition and reproductive output could potentially impact the next generation through recruitment failure (Shanks et al., 2020; Vázquez et al., 2021), resulting in a potential decline in wild mussel populations. Although the flood event presented here occurred in the Marlborough region these events are occurring more frequently around the country and may impact other local populations of mussels. Furthermore, bivalve fisheries are already experiencing variability in catches

due to mortality from fluctuating temperatures and salinity (Juanes et al., 2012; Morgan et al., 2013; Vázquez et al., 2021).

The high survival rate of the population within the lab, and in the field (marine farmers - personal communications) was also encouraging. Although the tissue conditions detected are not specifically associated to mortality, it is likely that if the flood persisted for longer, or at higher temperatures, respiration and feeding would have been impacted and mortalities may have ensued. For example, a similar event where oysters were exposed to freshwater flooding near a river mouth for 9 to 10 days in northeastern Tasmania, Australia, during a summer period resulted in mortalities up to 90% (e.g., Knowles et al., 2014). During the period of flooding, it is thought that the mussels remained closed during the freshwater exposure based on the survival rates and low impact on the mussel tissues. Valve closure behaviour is a typical response to suboptimal environmental conditions such as freshwater flooding, as many bivalve species close their valves to protect their soft tissues and avoid osmotic stress (Pourmozaffar et al., 2019; Delorme et al., 2021a; Tan et al., 2023). However, closure cannot be maintained for extended periods of time (Zubkoff and Ho, 1982; Knowles et al., 2014). Very few post-flood individual mussels appeared to be affected in terms of gill haemocyte infiltration, which is a typical sign of osmotic stress. Expected tissue observations would include infiltration of haemocytes into the gill haemolymph vessel and the gill epithelia (David et al., 2008; Carella, 2010). Other signs and host responses include oedema and inflammation on the gastrointestinal tract. These tissues are particularly vulnerable due to their role in respiration, ingestion, and absorption, and their close contact with the external environment (David et al., 2008; Carella, 2010; Knowles et al., 2014).

Tissue conditions detected include increased prevalence of individuals with digestive gland atrophy, haemocytosis and ELO in the epithelium of the gastrointestinal tract and intracellular bacteria-like clusters in the gill epithelium. However, these tissue conditions were minor and were repeatedly seen in the field population samples prior to the post-flood sampling, therefore considered within the range of normality.

Digestive gland atrophy only occurred in a few tubules across the total number observed. Atrophy of the digestive gland was also expected based on previous research (Langton, 1975; David et al., 2008; Carella, 2010; Knowles et al., 2014). The digestive gland tubules are typically categorised into four phases: holding, absorptive, disintegrating and reconstituting (Langton, 1975; Costa, 2018a), and alternate between these stages during the digestive processes. Often, there is lack of coordination and synchronicity whereby some tubules will be at a different stage, or some may appear thinner giving it an atrophied appearance, thereby confounding the histological analysis (Langton, 1975; Costa, 2018a). Additionally, digestive gland atrophy has also previously been associated to valve closure in response to the salinity stress (Winstead, 1995; Horodesky et al., 2019) and may represent changes due to reduced feeding (Langton, 1975).

Endozoicomonas-like organisms (ELO's) and other intracellular bacteria were regularly detected in green-lipped mussels without a host response. This likely represents the natural prevalence based on initial baseline sampling data and are therefore assumed to have negligible effects on the health of the mussels within this study. Prevalence of the gill intracellular bacteria-like clusters was 40% in the field when the mussels were first sampled (Baseline) and may represent a natural occurrence which peaked in the laboratory samples (post-flood) due to the introduction of the flood stressor. *Endozoicomonas*, for instance, is typically seen in green-lipped mussels using histological techniques, however they have also been detected using PCR during a study of the microbiome by Bennion et al. (2021) and Li et al. (2022). Interestingly, both Bennion et al. (2021) and Li et al. (2022) suggested that ELOs are a participant in the microbiome health and antimicrobial production which could play a key role in gastrointestinal health. Conversely, ELO have also been associated to mortalities (Bennion et al., 2021; Howells et al., 2021; Li et al., 2022). Further investigation of the ELO's, and intracellular bacterial-like cysts in the gills, is required particularly in response to environmental stressors and water contamination but also their impact on green-lipped mussel health.

6.4.2. *Implications of salinity stress and contamination from flooding*

The exposure to the flood water represented a confounding stressor which requires further study and understanding in the future. However, incorporating these unforeseen events into the research and reporting results can provide unique insights to future conditions that should not be ignored. Capturing these events is therefore critical in building a biological data repository, as disentangling the complex interaction of multiple stressors over time is difficult (Reid et al., 2019a), particularly with climate change-related hazards increasing in intensity and frequency in the future. The effect of climate driven flood events on the biological response of many organisms, in this case green-lipped mussels, will be difficult to tease out due to the occurrence of other environmental factors (Winsemius et al., 2015; Reid et al., 2019a). Furthermore, extrapolating a single stressor biological response to a multifactorial situation is also near impossible and requires further investigation (Riebesell and Gattuso, 2014; Reid et al., 2019a).

Should storm events become more frequent, these flood conditions may alter the coastline creating a favourable environment for not only invasive species, but novel emerging diseases (Zell et al., 2008; Okamura, 2016; Handisyde et al., 2017; Reid et al., 2019a; Reid et al., 2019b). Rivers, in particular, are known conduits for contamination from terrestrial activities which correlate to rainfall, and flooding, resulting in freshwater plumes that form along the coast (Cornelisen et al., 2011; Reid et al., 2019b). During this study, experimental mussels were potentially exposed to contaminated brackish water resulting from the freshwater flood plumes. For instance, a previous storm event for the Nelson region resulted in the increase in faecal loading in the Motueka River which spilled into the Tasman Bay. As a result of the low salinity plume during this storm, elevated Enterococci and *Escherichia coli* concentrations contaminated a major shellfish production area (Cornelisen et al., 2011; Reid et al., 2019b). Owing to their filter feeding nature the mussels used within this study may

therefore have retained bacteria, viruses, and parasites which poses a risk for human health, particularly if shellfish meat is consumed raw, or only lightly cooked (Bayne, 1976; Vásquez-García et al., 2019; Srisuphanunt et al., 2023).

Another potential pathogen with increased pathogenicity during flood events is the protozoan parasite *Cryptosporidium* which is widespread throughout New Zealand (Garcia-R and Hayman, 2023). Cryptosporidiosis is a disease that causes gastroenteritis in immunocompromised mammals and has reportedly been found in other mussels such as *Perna viridis* (Srisuphanunt et al., 2009; Garcia-R and Hayman, 2023; Srisuphanunt et al., 2023). Although none of these bacteria or parasites were observed, or specifically sought, within this study the likelihood of contamination of water and food sources is higher under these conditions (Aguirre et al., 2016; Garcia-R and Hayman, 2023). Accordingly, bivalves may serve as disease vectors following consumption, with implications for human health (Srisuphanunt et al., 2009; Garcia-R and Hayman, 2023; Srisuphanunt et al., 2023). Whilst pathogens such as, *Cryptosporidium*, *Enterococcus* and *Escherichia coli* do represent a food safety issue managing the food safety risks can be achieved through control schemes (e.g. MPI, 2024b), and monitoring such as depuration, temporary farm closure, once the event has passed (Lee et al., 2008; Rupnik et al., 2021; Tuckey et al., 2023), as well as thoroughly cooking food.

6.4.3. *Perspective: implications for research facilities, research outcomes and the utility of serendipitous findings.*

The extent, duration and impact of the flood will depend to the physical characteristics of the coastline and topography. As a result of the modified environment and the increasing frequency of storm events with deleterious consequences are more likely to occur. In many instances, coastal infrastructure development, such as urban development and agriculturalization, has resulted in the degradation and destabilisation of the coastal environment. This often manifests in the loss of coastal vegetation and wetlands, exacerbating the flooding and erosion (Arkema et al., 2013; Reid et al., 2019b). In other cases, infrastructure is built within already altered environments where the coastal barriers, rivers and land elevation have been modified. Financial projections have already suggested that global damage and economic loss as a result of flooding is expected to increase further (Winsemius et al., 2015). These economic impacts encompass various factors, including disease outbreaks (as above), loss of livestock, structural damage, higher capital costs through flood resistance engineering, increased insurance premiums and costs (Handisyde et al., 2017), and impacts to project budget costs. Many aquaculture areas and research facilities, such as the location of the current study, are often close to marine, estuary and river systems, and are therefore vulnerable to flooding (Reid et al., 2019a). Consequently, they can be exposed to river plumes that occur during flood events. Current and future development of facilities should undergo risk preparedness and mitigation procedures to reduce future damage.

In the science community, producing high quality defensible research on a 'limited budget' is already a challenge. However, as researchers, it is crucial to address and report results from unforeseen

events, such as the impact of flooding, and their implications on our current and future research activities. In addition, it not only raises concerns about the future impacts of increasing precipitation, storm events, flood events, erosion, and agricultural contamination on marine organisms, particularly those of cultural and commercial value, under a changing climate, but highlights the broader repercussions affecting the researchers and the research facility as well as the aquaculture industry. Finally, incorporating these confounding events into our research narratives is essential for acknowledging the realities of conducting science in a complex and changing environment. Occurrences such as this flood event are likely to become more frequent in the future and may pose ongoing challenges. However, they do not diminish our research, but rather provide opportunities for hypothesis development, adaptation, and resilience.

6.4.4. Conclusion

The spawning of the mussels in the post- flood samples was the most distinct result. If the field mussels had been at a similar reproductive stage, or the flood event occurred earlier in the spawning season, then this event may have had more significant impacts such as mortality of the oocytes, and sperm, and loss of condition reducing market value in subsequent harvest. Histological results indicated no significant pathologies in relation to the flooding event when comparing the experimental mussels to the field samples. Therefore, this short-term flood event appeared to have relatively negligible effects on the overall health of the mussels and was not long enough for the mussels to incur tissue-related impacts. However, contaminants relating to human health (e.g. bacteria, viruses and parasites) were not specifically sought that represents a significant food safety risk. Whilst the research provides valuable insight, larger sample sizes and molecular techniques are required to provide confidence in the findings. Further study on the salinity and contaminants should be conducted to determine impacts on reproductive and pathology particularly as climate change progresses and these storm events become more frequent. Further research will facilitate the early detection of changes to reproductive condition and tissue pathology which could impact the green-lipped mussel population and gamete production. Finally, incorporating temperature, salinity, agricultural contamination, and pathogens to future trials will provide further understanding of the impacts of flood events on green-lipped mussels which will ultimately contribute to the sustainability of the mussel industry and wild mussel beds.

CHAPTER 6. THERMAL STRESS AND FOOD LIMITATION IN ADULT MUSSEL (*PERNA CANALICULUS*)
PART B

Abstract

The green-lipped mussel is an ecologically and commercially valuable bivalve to New Zealand's coastal waters. Good reproductive condition is of major commercial, as well as ecological relevance as it is related to the meat quality and quantity, underpinning market value. It is well known that the interaction of temperature and nutrition are critical to gametogenesis which drives gonad development. However, research efforts to date regarding alternations to gametogenesis in the green-lipped mussel do not appear to consider oocyte degeneration or atresia. Therefore, temperature and nutrition were manipulated to provide a preliminary characterisation of atresia in green-lipped mussels. The chapter speculates on the advantages of atresia and discusses its relevance to aquaculture and restoration efforts. The work presented is preliminary in nature and has been provided to showcase the methods through the experimentation period. The images collected from the initial cryo-sectioning training session resulted in the detection of oocyte lipid changes in maturing mussels when compared with mussels with high atresia. Survival was not impacted by the flood event in August 2022, reported in chapter 6A, however the heat pump failures did elicit mortalities in the 22°C "low food" treatment. This indicated that compromised nutritional status and chronic elevated temperature exposure were implicated in survival when exacerbated by exposure to an acute thermal stress.

6.5. Introduction

The green-lipped mussel, *Perna canaliculus* (Gmelin 1791), is an ecologically and commercially valuable bivalve endemic to New Zealand's coastal waters (Jeffs et al., 1999; Alfaro et al., 2001). The meat yield of the green-lipped mussel is the desirable and marketable factor for commercial farming. Good gonad/ reproductive condition is of major relevance as it improves the meat quality and quantity (Hickman and Illingworth, 1980; Buchanan, 2001). Additionally, the anti-inflammatory properties of green-lipped mussel also makes it a desirable product for nutraceuticals (Azizan et al., 2023; Miller et al., 2023). It is well known that the interaction of temperature and nutrition are critical to gametogenesis and oocyte quality (Sprung, 1983; Rodhouse et al., 1984; Hickman et al., 1991; Seed, 1992; Buchanan, 2001). The interaction of temperature and nutrition also controls reproductive development and timing as well as moderating local variation in reproductive events between different populations (Sprung, 1983; Rodhouse et al., 1984; Buchanan, 2001). However, research regarding changes to reproductive condition with climate change are limited and earlier research often does not refer to oocyte degeneration or atresia when reporting reproductive condition in green-lipped mussels (Copedo et al., 2023) (Chapter 5). Whilst in other species, such as clams, the atresia research is quickly developing, particularly in scenarios where molluscs are experiencing suboptimal

environments (Chérel and Beninger, 2017; Chérel and Beninger, 2019; Beninger et al., 2021; Beninger et al., 2022).

The term ‘oocyte atresia’ includes the degradation, autolysis and resorption of normal oocytes (Le Pennec et al., 1991; Beninger and Le Pennec, 2016; Eckelbarger and Hodgson, 2021). It is a normal process, typically utilised when bivalves cannot spawn all their oocytes. However, ‘pre-spawning atresia’ is a similar process, but occurs during the gametogenic development and is often associated with sub-optimal environmental conditions (Beninger and Le Pennec, 2016). The initial aim of the present study was to assess reproductive condition, gametogenesis and oocyte atresia in green-lipped mussels in response to thermal stress and nutrient deprivation using a multi-disciplinary approach. These techniques considered physiology, histopathology and biochemistry; however, many of these have not been reported due to the confounding nature of the flood event and the additional logistical issues. One month into the trial a 1 in 100-year flood exposed the trial to brackish flood waters which caused some of the mussels to spawn. This flood event is reported in Chapter 6a. As previously described by Copedo et al. (2025b) and Chapter 6a, the field mussels experienced the same event, but the sedimentation and salinity changes were lower in comparison to the laboratory scenario, but they were exposed for a more protracted period of time. In addition to this event there were logistical issues in the form of heat pump failures which resulted in erratic in-tank temperatures, causing mortalities and in-tank spawning of mussels. Therefore, the work presented is of a preliminary nature and provided to highlight the methods through the experimentation period and some of the interesting findings. The aim of the research in its current form is to provide a preliminary characterisation of atresia in green-lipped mussels and speculate on its selective advantage, as well as discuss utility to aquaculture and restoration efforts.

6.6. Methods

6.6.1. Experimental set up

Individually labelled adult mussels were assigned to treatment tanks, as described in Chapter 6a (2x2 factorial design: 17 (Cool) or 22°C (Warm), low or high food level; 4 replicate tanks per treatment), as well as repeated sampling from the reference on-farm population. At the time of collection six temperature loggers were deployed on the farm (three at 1 m depth and three at 5 m). Four temperature loggers per temperature treatment were also deployed in the laboratory tanks. Four weeks into the trial a flood event (1 in 100-year flood) resulted in the evacuation of the research facility and exposure of the mussels to silty fresh water (see in detail in Chapter 6a). The system was repaired and the mussels observed for an additional 2 weeks for mortalities. At the end of the 2-week period the temperatures were incrementally increased as above (target: 1°C increase/week). However, further hardware issues delayed the initiation of temperature ramping in the 17°C treatment by 2 weeks. Once the desired temperatures were reached, they were maintained for 8 weeks. Three weeks after reaching the desired temperature some logistical issues occurred with the heat pump

resulting in three temperature spikes during a 1-hour period. For the warm treatment, temperatures briefly spiked at 24, 26 and 27.8°C, and for the cool treatment decreased to 10°C (Fig. 6.3).

6.6.2. *Elaboration of experimental food treatments*

Chlorophyll-*a* (chl-*a*) levels were recorded on inflow and outflow of each tank daily using a handheld fluorometer (FluoroSense; Turner Designs model 2860-000-C). Ingestion rate (mg chl-*a* mussel/day) of the tank was recorded using the following equation from Ericson et al. (2023):

$$\frac{\mu\text{g Chl } a \text{ (inflow-outflow)}}{\text{Number of animals in tank}} \times \frac{\text{Flow rate (in l/ day)}}{1000}$$

The above calculation assumes that all mussels were equally contributing to the chl-*a* reduction (Ericson et al., 2023). Weekly coulter counter samples were measured from inflow and outflows to record the total suspended cell count of the tanks. This was followed by monthly sampling to obtain particulate organic matter (POM) levels, using known volumes of water samples were collected from the inflows and outflows of all 16 tanks. The POM level was calculated using the methods of Ibarrola et al. (2017), whereby water samples were filtered on to pre-combusted and weighed GFC filters (Whatman Glass microfibre, 47 mm circle, 0.75 µm). The filters were carefully placed on to a vacuum filtration unit and samples were filtered until a blockage point, the total volume of the sample was then recorded. The samples were rinsed with ammonium formate (3.6% w/v) to remove salts and carefully removed from the vacuum filtration unit. The sample-loaded filters were dried at 105°C for 24 hours then weighed to acquire total particulate matter. After drying, the filters were then ashed in a muffle furnace at 450°C for 6 hours to obtain the particulate inorganic matter (PIM) and total particulate matter (TPM). The POM was calculated using the following equation:

$$\text{POM} = \text{TPM} - \text{PIM}$$

Percent organic content per sample was calculated as:

$$\text{Organic content (\%)} = \frac{\text{POM}}{\text{TPM}} * 100$$

The final POM values were then standardised against the total sample volume. The low food treatment was maintained to obtain an organic feed component of ~10 to 20% of the high feed treatment.

6.6.3. *Physiological measurements*

On arrival to the Cawthron Aquaculture Park (CAP) all mussels were weighed (g) and measured (mm) (Chapter 6a). Further measurement time points were conducted at either: point of sampling, mortality date or the final experimental date (22 December 22). Additionally, sixteen green-lipped mussels per treatment (n =64) were removed for sampling every 30 days (Chapter 6a). At the final timepoint, the remaining mussels were weighed and measured.

6.6.4. General physiology

Weight (g) and lengths (mm) were recorded to determine the shell growth rate (mm/ day) and the Specific Growth Rate (SGR) using the following equations from Ericson et al. (2023):

$$\text{Shell growth rate} = \frac{(l_2 - l_1)}{(t_2 - t_1)}$$

Whereby l_2 = final length, l_1 = initial length, t_2 = final date and t_1 = the initial date.

$$\text{SRG} = \frac{\ln(w_2) - \ln(w_1)}{(t_2 - t_1)} \times 100$$

Whereby w_2 = final weight, w_1 = initial weight (live mass, g) t_2 = final date and t_1 = the initial date.

6.6.5. Condition index

The green-lipped mussels were then shucked to remove the visceral mass, the flesh weight and the shell weight were then recorded to determine the wet condition index (CI) (Hickman and Illingworth, 1980). Three CI options are provided and recorded in the results:

- 1) Condition index (CI) based on meat weight and shell weight with pallial cavity fluid free:

$$\text{CI}_{\text{Adapted}} = \frac{\text{Meat weight}}{\text{Meat weight} + \text{shell weight}} * 100$$

- 2) Recommend as a simple and rapid CI for biological studies:

$$\text{CI}_{\text{Biological}} = \frac{100 * \text{dry meat weight}}{\text{Whole weight} - \text{shell weight}}$$

- 3) Recommended for use in field and/ or farming practices:

$$\text{CI}_{\text{Commercial}} = \frac{100 * \text{wet meat weight}}{\text{Whole (live) weight}}$$

Images of the visceral mass were taken for further gonad condition analysis. Gonad condition was scored on a subjective visual scale of 0 to 10, with 0 being watery and thin, with no gonad development or glycogen (Fig. 6.5a) and 10 being in full gonad condition with a thick, plump mantle (Fig. 6.5b). Scores between 0 and 10 were considered as incremental grades between these two values; for example, 5 described a developing gonad with half of the coverage of 10.

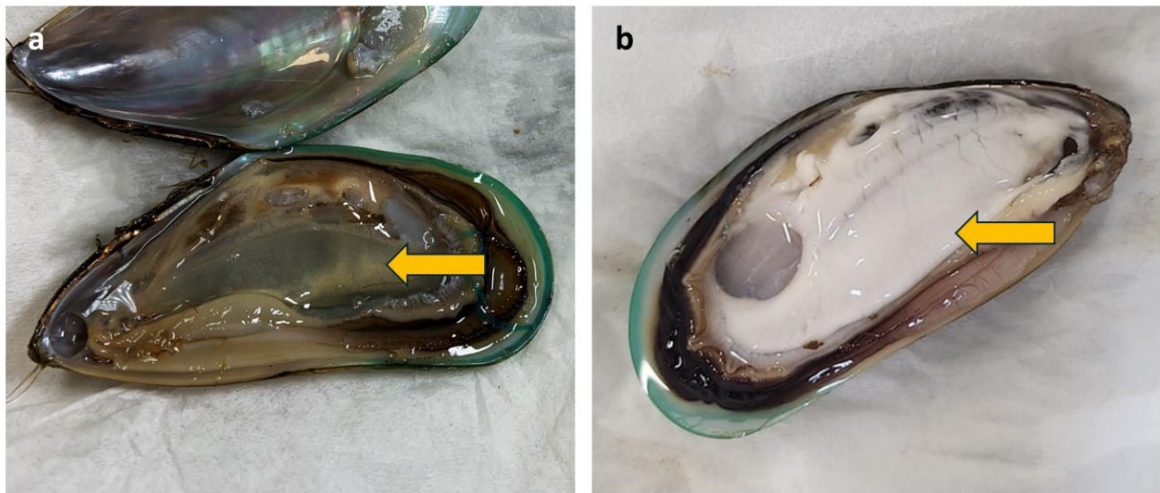


Figure 6.5 Representative images of gonad condition whereby a) is a mussel with no condition and scored as a 0 (arrow), whereas b) is gaining condition and was given a score of 8 out of 10 (arrow).

6.6.6. Histology

Green-lipped mussel tissue was removed intact, and a 5 mm steak of tissue was cut (mantle, gill, kidney, digestive gland, mid-gut, muscle, and nerve) as shown in Howard (2004) and Copedo et al. (2023) (Chapter 5). The sections were placed into cassettes and fixed in a 4% formalin solution (1:9 v/v, 37% Formaldehyde:0.35µm filtered seawater) for 48hrs then transferred to 70% ethanol for further processing (Howard, 2004). Samples were embedded in paraffin wax and sectioned (3-5µm) using a microtome. Routine processing was conducted either by Medlab central, Palmerston North, or by Awanui veterinary, Christchurch, following standard techniques and staining using hematoxylin and eosin (H&E) (Howard, 2004).

The tissues available were screened using standard histology techniques reported in (Copedo et al., 2025b) and Chapter 6a. The results for different conditions were reported on as presence/absent and glycogen storage cell density (in mantle) was scored semi-quantitatively on a scale of 1 (low to empty) to 3 (dense and fully packed) (Copedo et al., 2023) (Chapter 5) (Table. 6.8). Gonad development was staged following Kennedy, (1977) and methods in Chapter 2 and 5, whereby each mussel was identified as resting, early, late, ripe, spawning, redeveloping or spent. The percent frequency of the stages was then plotted for visual representation. Due to the preliminary nature of the cryo-sectioning method development, observations are reported but not analysed.

6.6.7. Cryo histology: preliminary investigation

As part of an exploratory method development process, an additional 5 mm histology steak was cut and transferred into a cryo-sectioning mould. The sections were embedded in a Tissue-Plus OCT (optimal cutting temperature) compound (Scigen Scientific Gardena) and frozen using a Gentle Jane® snap freezer (Fig. 2). Once frozen the block was sectioned 3-5µm using a cryostat set at -10°C. The sections were then mounted onto glass microscopy slides. The OCT compound was dissolved off the slide using RO water, half of the samples were then fixed with a 4% paraformaldehyde solution for 24hours and re-rinsed with RO water. The slide around the tissue

section was dried and a hydrophobic pen (PST liquid blocker pen, Proscitec, Australia) was used to draw around the tissue for the staining process. The samples of the slides were stained using DAPI (4',6-diamidino-2-phenylindole) to highlight nuclear material and Nile Red to stain lipids (oil droplets), to observe oocyte lipids in maturing mussels. Once complete and the slides has been cover-slipped they were examined using a confocal microscope (FV3000, Olympus, Tokyo, Japan) equipped with 405nm and 640nm lasers (Fig. 6.6). Images were collected from the Confocal microscope using Fluoview FV31S-SW software (version 2.3.2, Olympus) and were observed using image J Fiji software. Images were collected to identify if the process could identify atresic oocytes and determine the impact of fixing for 24hrs upon the H&E sections.

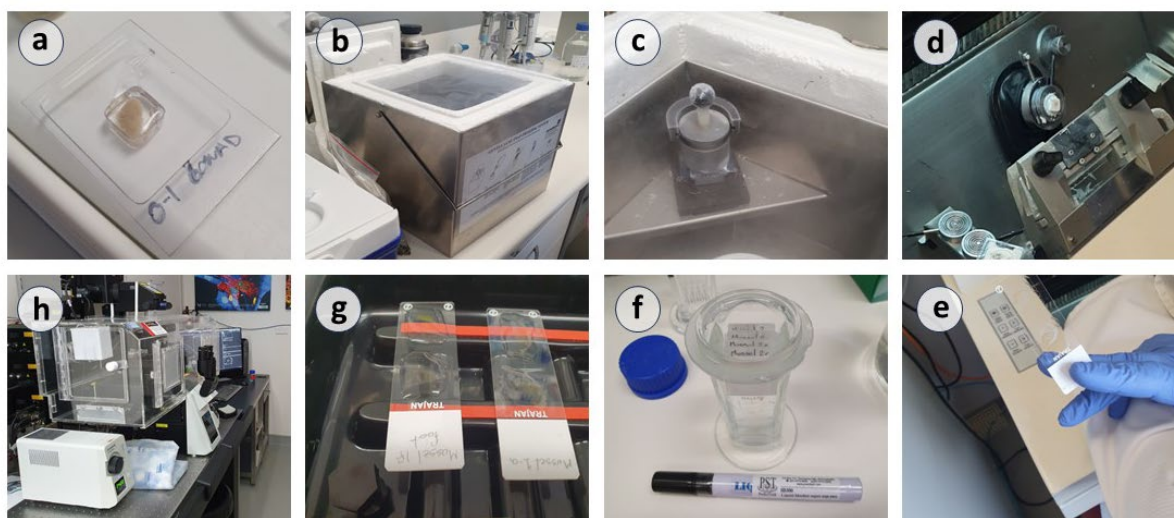


Figure 6.6 Cryosectioning and staining process completed at the Malaghan Institute; a) embedding mussel mantle tissue in OCT (optimal cutting temperature) compound in the mould. b) and c) freezing mould and tissue sample in Gentle Jane. d) Sectioning the frozen sample in a cryostat to acquire 3-5 μ m frozen sections. e) frozen section mounted on to the slide, f) OCT compound rinsed off the slide, the tissue on the slide was fixed in a paraformaldehyde solution (4%) and rinsed off with RO water, g) glass around the tissue sample was dried then a border was drawn around the section. The tissue was the stained using DAPI (4',6-diamidino-2-phenylindole) and Nile Red; once stained and rinsed the slide was mounted with a DPX Solvet containing; distyrene, a plasticizer, and xylene) cover slip medium and a coverslip, h) once samples were completed, they were examined using a confocal microscope.

6.6.8. Biochemistry

Gill and mantle were dissected and then snap frozen and stored at -80°C for biochemical analysis to quantify proteins and lipids. However, due to the flood and the heat pump issues it was decided not to progress with these samples.

6.6.9. Statistical analysis

Statistical analyses were conducted using R version 4.3.0 (R Core Team, 2024) with the R studio interface (RStudio Team, 2021). Morphometric data, such as weights and lengths were analysis using a three-way ANOVA with sampling month, temperature and food treatment used as explanatory factors. Data were checked for homogeneity of variance and normality; modest departures from normality were detected in 2 and 1 of the treatment groups, respectively. The ANOVA was still run

without transforming data due to the power of these parametric tests and the three explanatory factors (Quinn and Keough, 2012). A general linear model (GLM) with a gaussian family was used to analyse the condition index once log transformed, only 2 outliers were detected which had a minor impact on the residuals. Post hoc comparisons were conducted where appropriate using Tukey's HSD. Histological tissue and pathogen prevalence data were analysed using a binomial general linear models (GLM) using the MCMCglmm package (Hadfield, 2010). Sampling month, temperature and food treatment were used as explanatory factors for each response variable. A p value < 0.05 was considered statistically significant. A Kaplan Meyer was conducted using the "survival" package followed by a log rank test.

6.7. Results

6.7.1. Water quality parameters

With the exception of the flooding period, water quality parameters were stable at ~100% dissolved oxygen and 35ppt salinity (Table. 6.3). The mean food levels (as chl - a) throughout the trial are reported in table. 6.4. Food levels were difficult to manage and maintain due to algal growth in the external ponds. However, these external ponds provided the microalgae species diversity sufficient to support gonad development.

Table 6.3 Mean (\pm SD) water quality parameters throughout the trial period for the external seawater (SW) ponds, High food and Low food treatment for dissolved oxygen, salinity (ppt) and pH.

Treatment tank	Dissolved oxygen (%)	Salinity ppt	pH
External SW ponds	104.1 \pm 2.3 (n= 37)	34.4 \pm 2.1 (n= 35)	8.2 \pm 0.1 (n=35)
High food	99.3 \pm 2.9 (n=49)	35.2 \pm 2.8 (n=17)	NA
Low food	99.6 \pm 1.5 (n = 44)	35.2 \pm 2.8 (n=17)	NA

Table 6.4 Mean (\pm SD) Chl- a \pm of in-flow, algae consumed (in-flow minus out- flow), chl- a mussel/day, amount and the chl- a reading converted to algal cells (n=50).

Treatment tank	Chl- a μ g/ l in-flow	Chl- a μ g/ l consumed	Chl- a mg/day/ mussel	cells/ mussel	POM consumed
External SW ponds	2.7 \pm 0.6	NA	NA	1277.8 \pm 331.4	57 \pm 14.0
High food	40.7 \pm 14.0	29.1 \pm 12.8	1.1 \pm 0.5	209.5 \pm 197.1	40 \pm 10.4
Low food	1.6 \pm 1.8	0.6 \pm 1.4	0.02 \pm 0.1		

The temperature was monitored through the trial. The flood event occurred during August 2022 and resulted in a decline in temperature back down to the winter ambient of 14°C and is reported in Chapter 6a. After monitoring acute mortality, the trial was restarted. However, during November 2022 further experimental disruption in the form of several temperature peaks and troughs due to heat pump malfunctions occurred (Fig. 6.7).

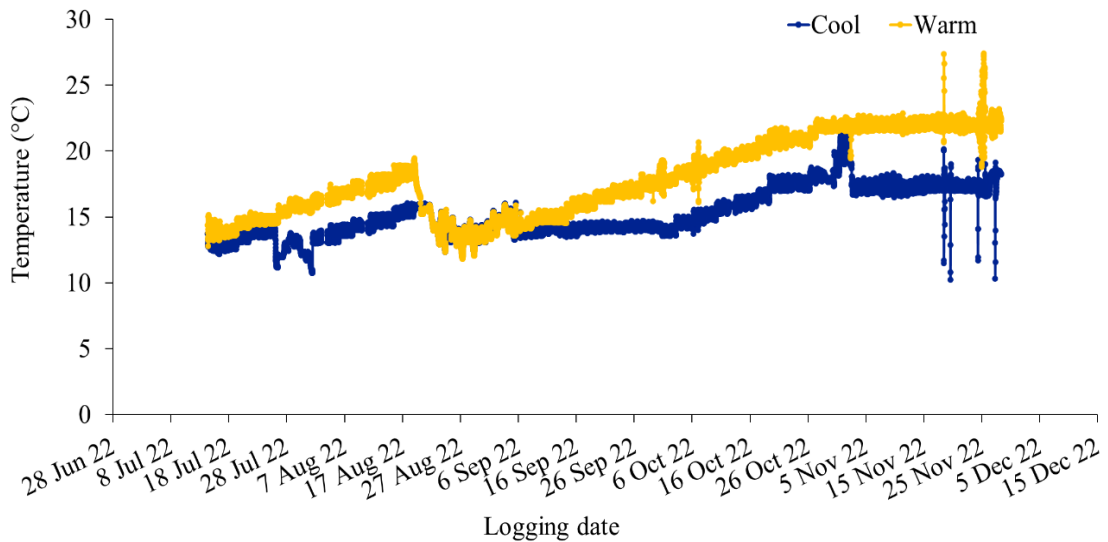


Figure 6.7 Raw temperature data of the experiment between July and December 2022. The warm (nominal 22°C) treatment temperature is in yellow and cool (nominal 17°C) treatment in dark blue. The heat pump temperature spikes occurred between November 15th and 25th.

Furthermore, the field temperatures showed that at 1-meter temperature started to deviate away from the 5-meter depth temperature around the 1st of November (Fig. 6.8). This is likely due to warming as summer approaches.

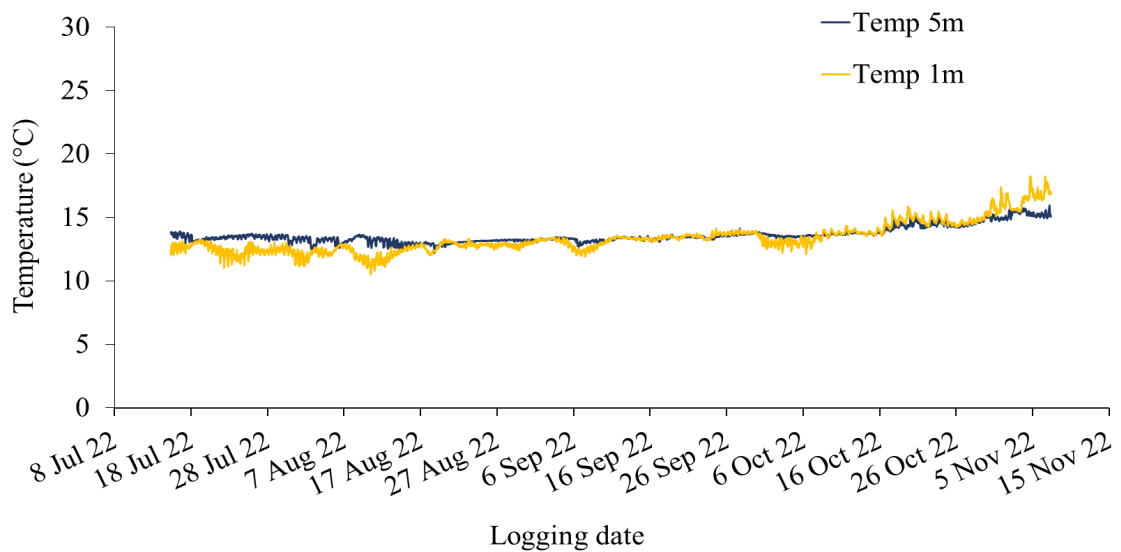


Figure 6.8 Raw temperature of the reference field population with loggers set at 1 meter and 5 meters. Data were logged every 30min. There is considerable overlap of the temperatures where they are the same.

6.7.2. *Physiology under stress*

The mean shell length was affected by sample month (duration within the trial) but, interestingly, reflected a decrease over time (Table. 6.5). There was also significant interaction (2- and 3-way) between the main effects of month, food and temperature, this is likely driven by the increase in shell length in the ambient treatment (Table. 6.6). Small differences in live weight were significantly

influenced by all the main effects of sample month, food level and temperature; significant interactions were also apparent (Table. 6.5 and 6.6). The post-hoc analysis for the length and weight data failed due to missing data in the ambient treatment. The SGRs were not analysed, or reported, due to the lack of shell growth over the trial period.

Table 6.5 Mean (\pm SD) length and weight data for each treatment at each sampling timepoint. Collection date is indicated by month with approximately 30 days between collections.

	Month	Cool		Warm		Ambient
		high	low	high	low	Field
Length mm	16 Aug	84.9 \pm 5.9	80.7 \pm 5.7	81 \pm 5.5	82 \pm 5.3	81.7 \pm 7.2
	13 Sept	85.9 \pm 7.7	81.4 \pm 7	79.1 \pm 5.6	82.4 \pm 7.1	85.7 \pm 3.9
	11 Oct	81.4 \pm 5	80.7 \pm 6.1	81.1 \pm 3.3	84 \pm 6.4	
	08 Nov	82.3 \pm 4.9	81.4 \pm 4.8	84.1 \pm 6	82.3 \pm 5	89.1 \pm 6.7
	15 Dec	78.1 \pm 6.9	79.6 \pm 8.1	80.6 \pm 5.5	79.8 \pm 4.1	

	Month	Cool		Warm		Ambient
		high	low	high	low	Field
Weight g	16 Aug	43.5 \pm 9.2	37 \pm 7.9	38.9 \pm 5.8	40 \pm 5.8	38.8 \pm 8.4
	13 Sept	44 \pm 13.5	38.4 \pm 7	37 \pm 6.6	41.4 \pm 9	45.1 \pm 6.7
	11 Oct	43.1 \pm 6.7	40.6 \pm 9	39.7 \pm 4.8	42.3 \pm 8.8	
	08 Nov	42.7 \pm 6.3	40.8 \pm 5.6	44.1 \pm 7.6	41.9 \pm 7	44.1 \pm 6.8
	15 Dec	40.3 \pm 7.2	40.9 \pm 9.6	44.2 \pm 7.6	41 \pm 5	

Table 6.6 Statistical results from length, weight and condition index ($CI_{Adapted}$) data using a GLM. A p value $<$ 0.05 was considered statistically significant and is indicated by the bold text.

	Length		Weight		$CI_{Adapted}$	
	F value	P ($>$ F)	F value	P ($>$ F)	F value	P ($>$ F)
Month	8.67 ₁	0.001	1.56 ₁	0.21	68.99	<0.001
Temperature	0.22 ₁	0.640	0.05 ₁	0.82	99.87	<0.001
Food	0.33 ₁	0.566	2.88 ₁	0.09	19.78	<0.001
Month: Temperature	0.99 ₁	0.320	1.32 ₁	0.25	8.12	0.0003
Month: Food	0.35 ₁	0.551	0.01 ₁	0.92	4.51	0.031
Temperature: Food	5.35 ₁	0.021	6.19 ₁	0.01	0.02	0.89
Month: Temperature: Food	5.11 ₁	0.024	6.83 ₁	0.01	0.28	0.595

Using the $CI_{Adapted}$ calculation there was a trend with $CI_{Adapted}$ declining over time (Table 6.6), regardless of temperature and food level treatment (Table. 6.7). There was no interaction between month, temperature treatment and food level or temperature and food. There were, however, statistically significant interactions between month and food, and month and temperature treatment driven by the field samples (Table 6.6). The post-hoc analysis for the length and weight data failed due to missing data in the ambient treatment.

Table 6.7 Mean (\pm SD) condition index ($CI_{Adapted}$) for each treatment for each sampling time point. Collection date is indicated by month with approximately 30 days between collections.

	Month	17 °C		22 °C		Amb
		high	low	high	low	Field
Condition index	16 Aug	45.7 \pm 3.1	44.2 \pm 3.5	45.6 \pm 3.1	44.1 \pm 3.7	49.4 \pm 4
	13 Sept	45.8 \pm 3.6	44.8 \pm 3	45.1 \pm 2.1	43.1 \pm 3.5	52.8 \pm 3.1
	11 Oct	41.7 \pm 2.4	40.6 \pm 2.6	41 \pm 4.4	39.6 \pm 2.6	
	08 Nov	41.6 \pm 2.8	36.1 \pm 9.2	42.1 \pm 4.6	38.1 \pm 3.2	49.4 \pm 3.3

The condition index using both the commercial and biological CI had similar patterns, whereby the high food treatments had higher CIs ($z = -8.23$, $p < 0.001$ and $z = -8.76$, $p < 0.001$) (Fig. 6.9). No differences were detected between the two temperatures using the commercial CI ($z = -1.51$, $p = 0.13$). Unlike the commercial CI there was a weak statistical interaction between temperature and food in the biological CI, hinting at a subtle synergistic interaction between treatments ($z = 2.57$, $p = 0.01$) (Fig. 6.9).

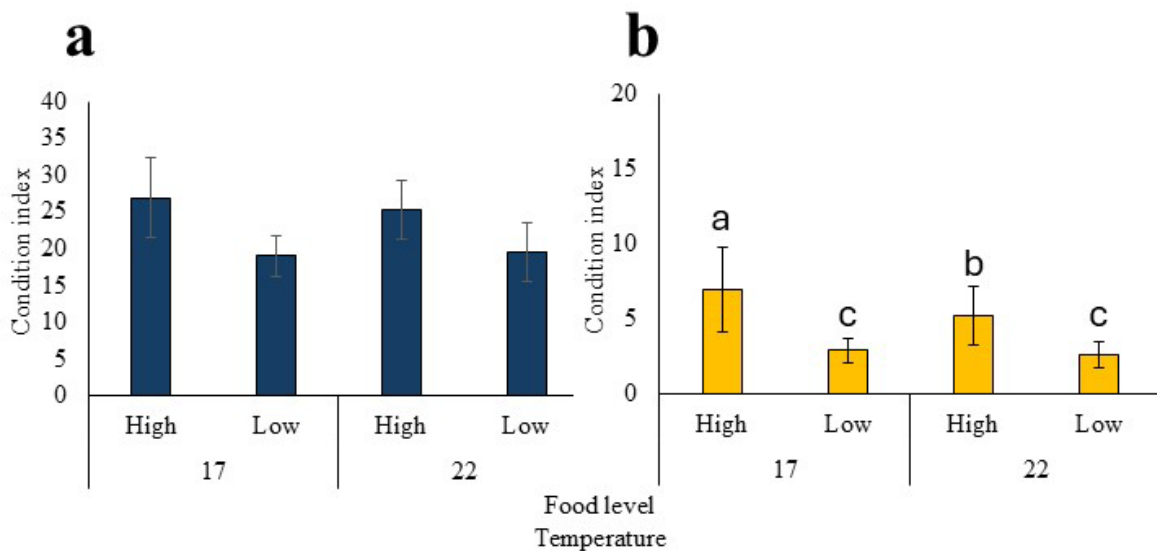


Figure 6.9 Final condition index (CI) using the a) commercial and b) biological equations of 40 mussels for each treatment (\pm standard deviation).

Visual grading of condition was not analysed using statistical packages due to the spawning that occurred during the flood event (Copedo et al., 2025b) (Chapter 6a), the lack of gonad development during the trial and the thermal shocking relating to the heat pump malfunctions. The lack of gonad development may be an impact of the laboratory environment, as well as the effect of the flood event that occurred in August 2022. Gonad condition was expected to rise to a score of 8 to 10 over the course of the experiment, however instead it remained between the 3 to 5 grades (Fig. 6.10).

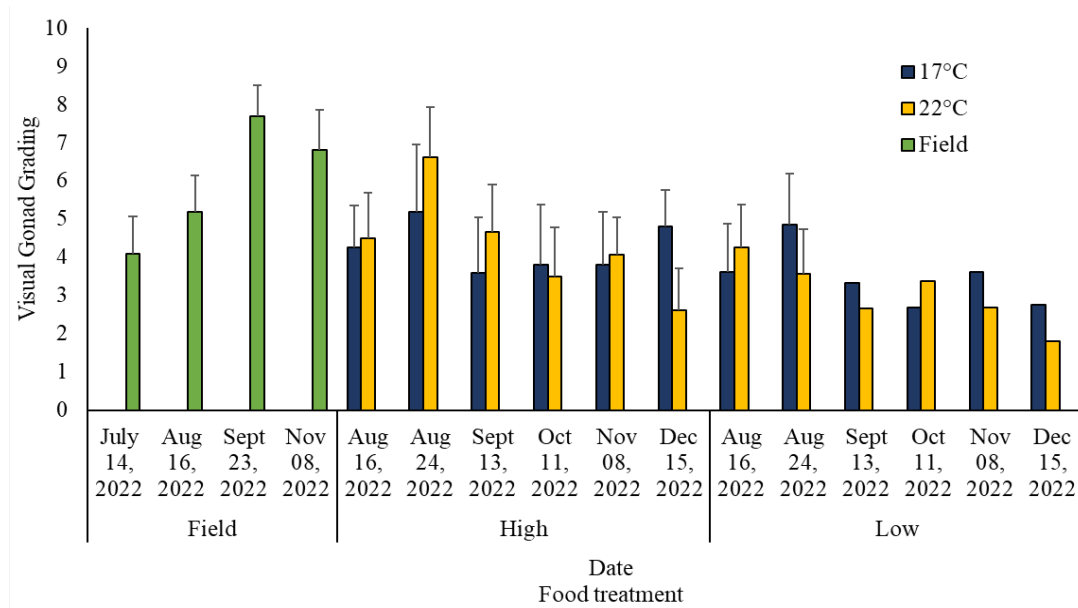


Figure 6.10 Visual grading of gonad condition for each sampling timepoint and treatment.

6.7.3. Pathological findings

The most common pathological feature in the mussels was the ceroid, digestive gland atrophy and APX (Table 6.8; Chapter 6a). Interestingly, the prevalence of APX transitioning through the gastrointestinal tract to the external environment (Chapter 6a and Copedo et al. (2025b)) increased to 100% in the 22°C low food treatment earlier than the other treatments (Table. 6.8). The digestive gland tubules in the low feed treatments were observed to have very sparse tubules with increased digestive gland atrophy. In many cases the atrophy thinning went to the basement membrane (Fig. 6.11). The interstitial space between the digestive gland tubules also increased between the initial and final sampling timepoints (Fig. 6.11).

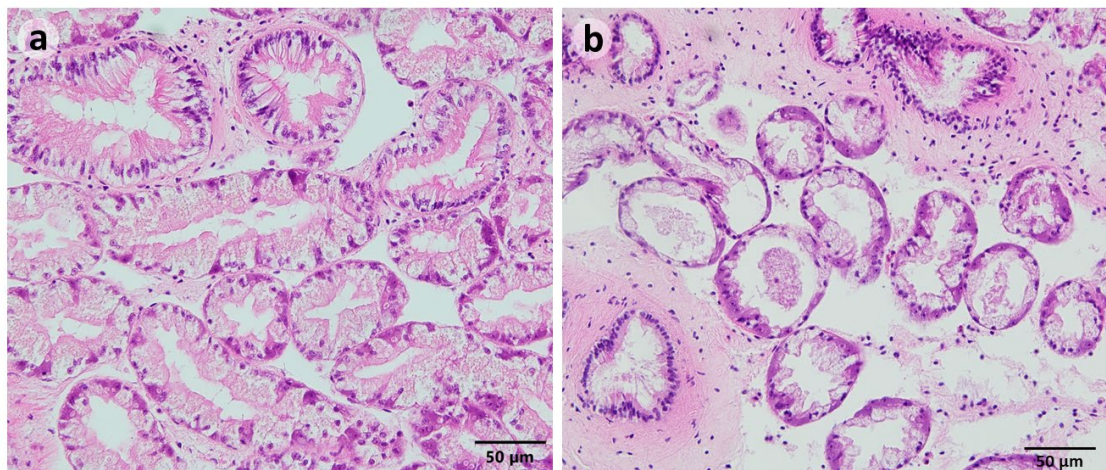


Figure 6.11 Digestive gland tubules in green-lipped mussels in a) a mussel sampled at the initial baseline, tubules have thick epithelial walls and a typical star or cross shape lumen, and b) digestive gland at final time point of a mussel in the 22°C low food treatment with sparse tubules with atrophy (thinning and attenuation of walls).

Copepods were regularly detected during August and September across all treatments. During each of the sampling sessions one of the goals was to capture the live copepods for imaging to provide more information on the species. Collection was successful and an image was taken of the *Pseudomyicola* sp., identified based on morphological features using an Olympus stereo microscope which shows the live specimen with its egg sacs intact (Fig. 6.12). Further investigation is required to confirm species (*Pseudomyicola* sp., or *Lichomolgus*).

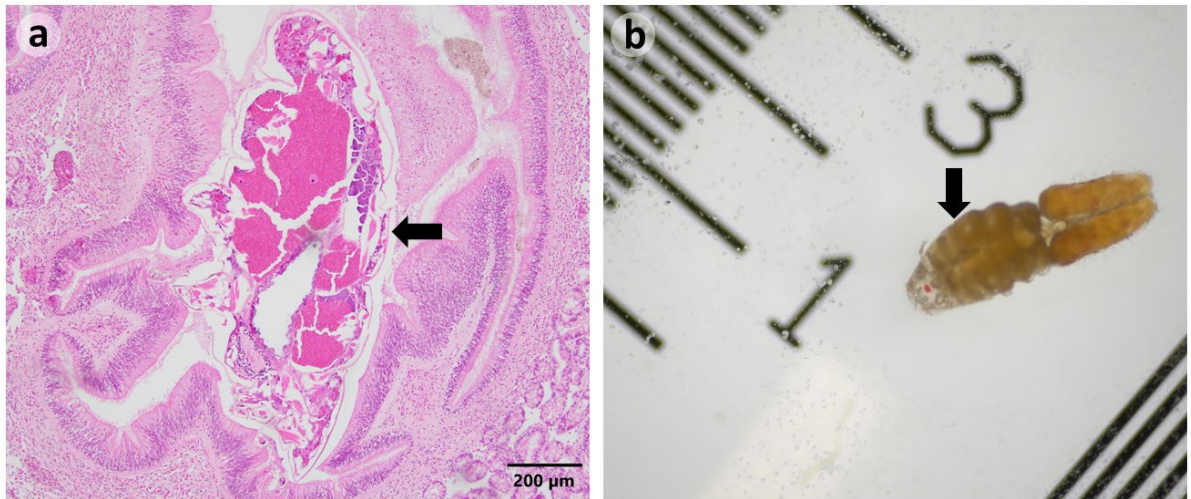


Figure 6.12 Copepod detected in green-lipped mussels a) histology micrograph stained with H&E and b) image of live specimen on a ruler.

Several other parasites were also detected, including bacterial cysts, APX, *Endozoicomonas*-like organisms (ELOs), gill ciliates, *Pseudomyicola* sp. (Copepods), *Microsporidium rapuae*, and *Paravortex* (Jones, 1975; Jones, 1976; Hine and Diggles, 2002; Suong et al., 2018; Castinel et al., 2019; Webb and Duncan, 2019; Muznebin et al., 2022a; Copedo et al., 2023) (Chapter 6a) (Table. 6.8).

Reproductive condition using the gametogenesis staging showed that most mussels were in the spawning or spent phase (Fig. 6.13). Preliminary exploration of the lipids (oil droplets) in the oocytes was of particular interest for this study. The images collected from the initial cryo-sectioning training session resulted in the detection of the oocyte lipid change in maturing mussels when compared with mussels with high atresia (Fig. 6.14). In the ripe mussels the lipids were bright red-stained and numerous, whereas there appeared to be a marked loss in lipid droplet quantity and a potential switch to phospholipids, the main component in membranes, in the mussels that had high atresia, based on the green autofluorescence (Fig. 6.14).

Table 6.8 Percent prevalence of tissue pathology and parasites detected in green-lipped mussels during the experiment. The ambient (Amb) temperature samples represent mussels collected from the field (source farm). Tissue conditions include mean score of glycogen storage cell density in the mantle and digestive gland tubules (**G-S cell**) (Copedo et al., 2023), digestive gland necrosis (**DG nec**), digestive gland wall atrophy (**DG atr**), infiltration of haemocytes in the gill epithelium (**Gill HE**), and **Ceroid**. Common parasites include intracellular bacterial cysts and *Endozoicomonas*-like organisms (ELOs) in the gills (**BA cyst**), gill ciliates, *Pseudomyicola* sp. (**Copepods**), *Microsporidium rapuae*, *Paravortex*, APX in mantle and interstitial connective tissue (**APX**), and APX transitioning through the gastrointestinal tract wall to the luminal space (**APX GI**), and ELOs in the gastrointestinal tract and DG epithelium (**GI ELO**).

	Temp	Food	DG nec	DG atr	Gill HE	Ceroid	BA cyst	Ciliates	Copepods	<i>M. rapuae</i>	Paravortex	APX	APX GI wall	GI ELO
Baseline	Amb	Field	0	53	0	100	40	0	20	0	0	100	55	3
16-Aug	17 °C	high	0	6	0	100	6	0	19	0	0	100	69	13
16-Aug	17 °C	low	0	0	0	100	6	0	19	0	0	100	31	0
16-Aug	22 °C	high	0	25	0	100	0	0	6	0	0	100	31	13
16-Aug	22 °C	low	6	75	0	100	0	0	19	0	0	100	75	6
16-Aug	Amb	Field	0	100	15	100	20	0	15	0	0	100	80	0
13-Sep	17 °C	high	0	100	8	100	8	8	0	0	0	100	42	0
13-Sep	17 °C	low	0	100	42	100	8	0	8	0	0	100	58	0
13-Sep	22 °C	high	0	100	0	100	8	0	8	8	0	100	42	0
13-Sep	22 °C	low	0	100	0	100	8	0	8	8	0	100	75	17
13-Sep	Amb	Field	0	60	20	100	0	0	0	0	0	100	55	15
08-Nov	17 °C	high	0	100	0	100	0	0	0	0	0	100	63	0
08-Nov	17 °C	low	0	100	0	100	0	13	0	0	0	100	63	13
08-Nov	22 °C	high	0	100	0	100	0	0	0	14	0	100	71	0
08-Nov	22 °C	low	0	100	0	100	0	0	0	0	0	100	100	0
08-Nov	Amb	Field	0	100	0	100	0	0	0	0	0	100	0	0
15-Dec	17 °C	high	0	100	0	100	0	0	0	13	13	100	100	0
15-Dec	17 °C	low	0	100	0	100	0	0	0	13	0	100	100	0
15-Dec	22 °C	high	0	100	0	100	0	0	13	13	0	100	100	0
15-Dec	22 °C	low	0	100	0	100	0	0	0	13	13	100	100	0

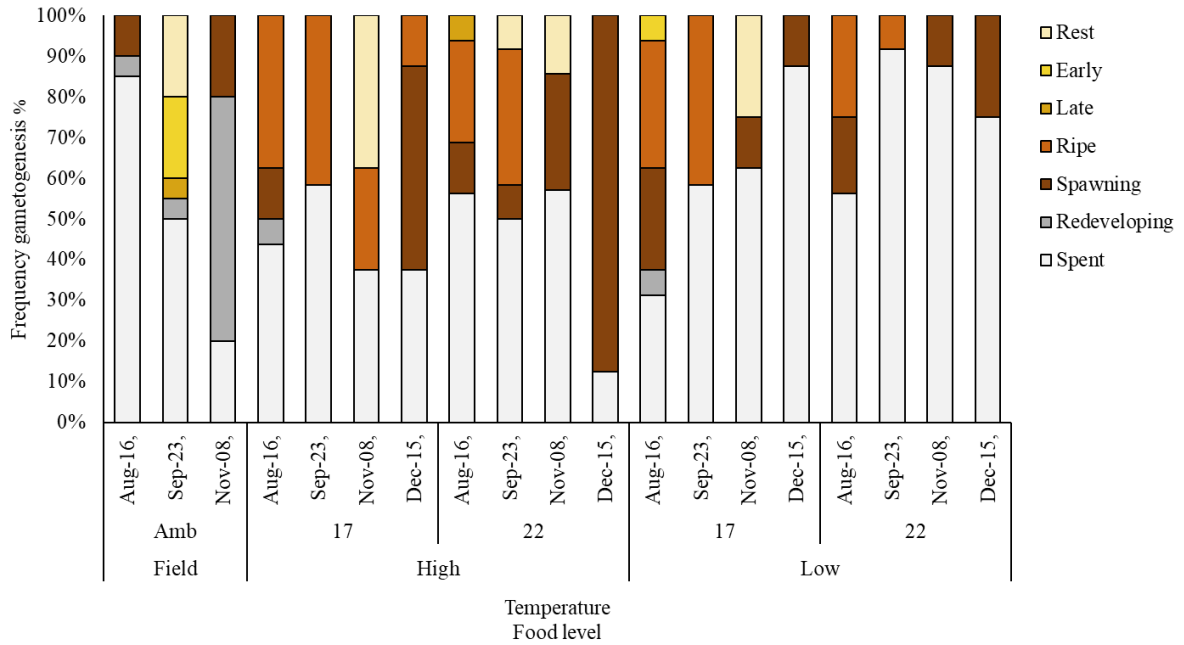


Figure 6.13 Frequency of gametogenesis stages for each sampling timepoint at each temperature (17 or 22°C) and each food level treatment (low or high).

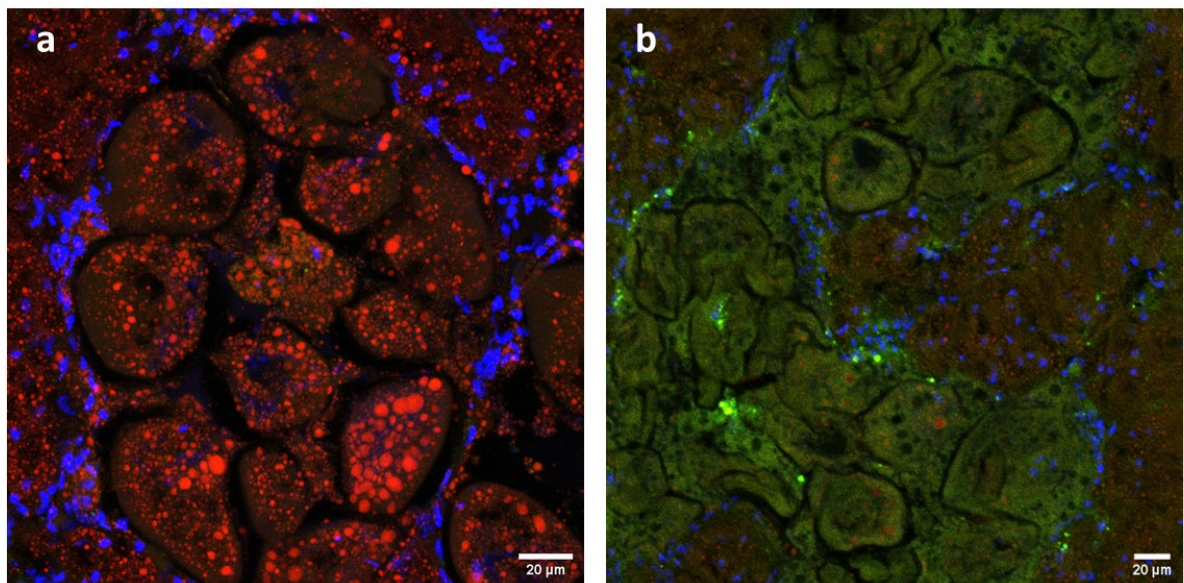


Figure 6.14 Confocal microscope imaging of the green-lipped mussels female gonad tissue showing a) lipid droplets (Red) in a ripening female and, b) Atresic oocytes in a spent female – green (autofluorescence of tissue) in colour with sparse lipid droplets. Nuclei in both stained with DAPI (blue).

Survival was not impacted by the flood event in August 2022 (day 32 to 39) (Chapter 6a) (Fig. 6.15). However, the heat pump failures did impact the 22°C low food treatment, which declined when compared with the 17°C high food, 17°C low food and 22°C high food treatments ($p < 0.001$) (Fig. 6.15).

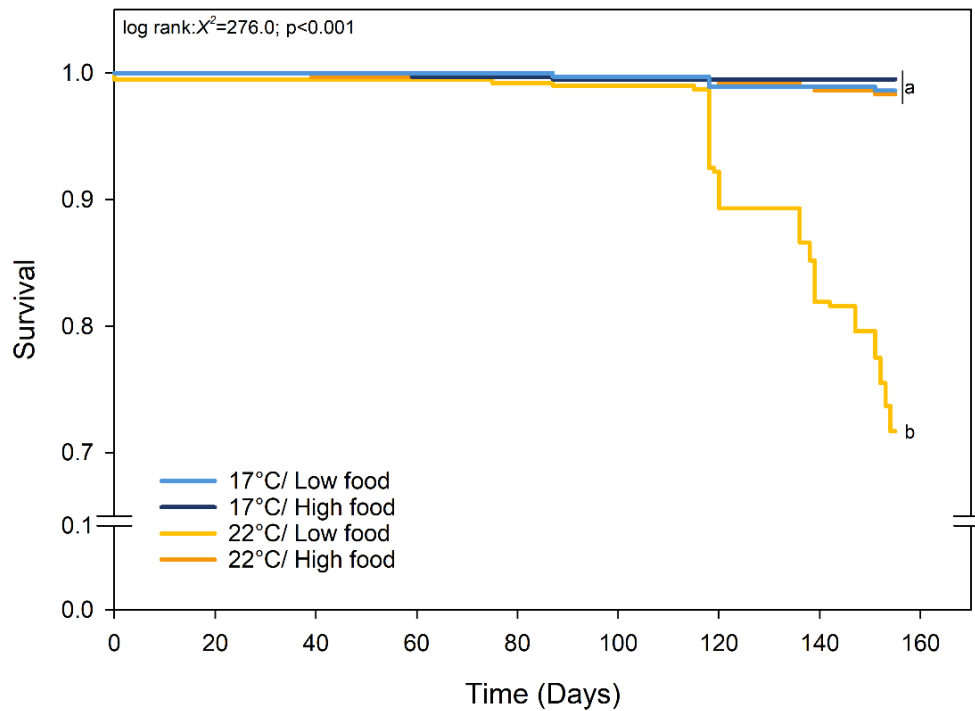


Figure 6.15 Kaplan Meyer probability curve for the 4 experimental groups. Statistical differences indicated by a and b $p = <0.05$.

6.8. Discussion

The main results and observations emerging from this compromised experiment included: 1) the spawning in relation to the flood event, 2) the lack of growth in the mussels in the laboratory scenario when compared with the field mussels, 3) the decline in digestion gland health observed as an increase in the proportion of the total tubules impacted by atrophy, 4) the increase in the prevalence of APX transitioning through the gastrointestinal epithelium to 100% in all treatments in the final sampling month (December) and 100% the month prior (November) in the low food 22°C treatment, 5) the visual changes in lipid classes in ripe typical oocytes versus atresic oocytes and 6) the low survival in the 22°C - low food treatment when exposed to the thermal shocks.

Long-term experiments such as this study are likely to experience issues, particularly with system maintenance, and now also with climate-related issues such as flood events (Chapter 6a). Approximately 1 month into the experiment, the day after the first sampling, a 1 in 100-year storm event occurred causing increased flooding, turbulent seas, increased sediment loading, as well as alterations to food availability and rapid declines in temperature (Chapter 6a). Although it was concluded that there were negligible effects on the overall health of the mussels, and it was not long enough to incur tissue-related pathology, the research did highlight the significance of incorporating these events into research narratives to acknowledge the complexity of science in a changing world (Copedo et al., 2025b) (Chapter 6a). This scenario also highlighted the impact of climate change on the coastal ecosystem and the parasites and pathogens (of human and aquatic hosts) that may be an issue in the future (Copedo et al., 2025b) (Chapter 6a). The lack of growth and gonad conditioning of the mussels and in this experiment after the flood event is also of interest.

It was expected that in the high food treatments that there would be some growth and gonad development over time, particularly in the warmer temperature. It is possible that there were impacts from the flood event that were undetectable in the histology, however more likely is the impact of the laboratory environment. Compromised performance in the laboratory has been observed in prior studies that the lack of natural variation in temperature and algal species diversity for nutrition, as well as the general constraints of captivity, influencing blue mussels (Bayne and Thompson, 1970), and green-lipped mussels as part of a chronic thermal challenge trial (Copedo et al., 2023; Ericson et al., 2023) (Chapter 5). It was also interesting that 100% of the mussels in the laboratory trial were observed to have digestive gland tubule atrophy (thinning and wall attenuation), likely resulting in reduced glycogen storage. Mussels were initially acquiring glycogen based on the storage density results, which then started to decline. The lack of available nutrients likely resulted in a reallocation of energy away from growth and reproduction to other physiological processes. Furthermore, although no quantification was conducted on the lipids in the oocytes, visual observations showed clear differences between the healthy oocytes and oocytes that were determined to be atresic.

Bivalves can store acquired nutrients as protein-bound glycogen, and occasionally lipids, prior to gametogenesis in various tissue types, including the digestive gland and mantle tissue (Wong and Alfaro, 2019; Yurchenko and Kalachev, 2019; Eckelbarger and Hodgson, 2021). These nutrients, particularly glycogen, are then employed for development of gametes and somatic maintenance (e.g. Gabbot, 1975; Bayne et al., 1982; Brokordt et al., 2019). Glycogen stored in tissues, such as mantle, is typically converted and transferred to the gonad and developing oocytes in the form of lipid droplets (Gabbot, 1975; Bayne, 1976). These lipid droplets are generally composed of triacylglycerides and polyunsaturated fatty acids (PUFAs) and accumulate in the oocyte throughout development (Gabbot, 1975; Bayne, 1976; Rodríguez-MoscOSO and Arnaiz, 1998). These lipid droplets were clear to see in the cryo-sectioned and Nile Red-stained sections of the mussels with healthy, ripe oocytes. Conversely, the oocytes that were atresic had very few lipid droplets and appeared to be showing phospholipids only, based on the green autofluorescence and lack of red oil droplets. Phospholipids such as phosphatidylcholine and phosphatidylethanolamine are key components to the structure of cell membranes and modulate intracellular exchange (Soudant et al., 1998; Hochachka and Somero, 2002; Balbi et al., 2023). It is hypothesised that the lipid droplets have been converted and reabsorbed by the follicular cells for reallocation to other tissues and physiological processes.

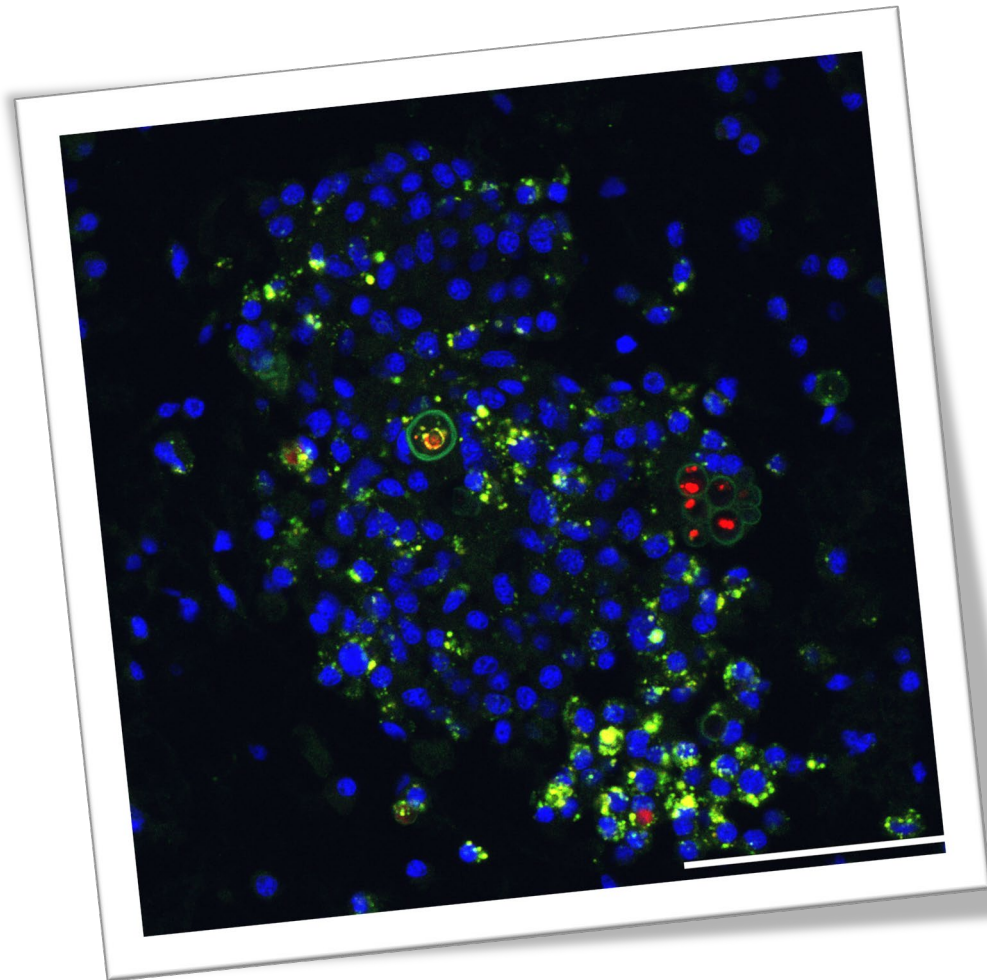
The low density of the glycogen material, the lack of gametes and the oocyte atresia in the low food/warm water treatment may have contributed to the vulnerability of the mussels, resulting in mortality when exposed to unexpected thermal spikes. These results present a potential issue for the future that is worth investigating further; for instance, increasing seawater temperature is likely to impact the mussels directly; however, temperature will also impact the algae, altering the quantity and quality of food. Furthermore, heavier rainfall and flooding are likely with increased atmospheric temperatures,

resulting in salinity changes, and sedimentation (Coughlan et al., 2009; Peteiro et al., 2018; Pourmozaffar et al., 2019).

6.9. Conclusion

Although this work was preliminary and/or qualitative in nature, it did highlight interesting results and potential research avenues. For instance, quantifying the storage cell glycogen under thermal stress, quantifying the lipids and glycogen in the oocytes, and exploring other techniques to characterise and further describe oocyte atresia and its impact on the bivalves in suboptimal environments would provide key knowledge in the energy flow between tissues. This provides further information towards elucidating whether the oocytes are reabsorbed during spawning. Furthermore, it provides other researchers and industry representatives with information which affects the reproductive condition and therefore larval quality and quantity. In addition to the poor reproductive condition, the decline in tissue health is of relevance for the aquaculture industry and its mussels in a changing environment; for example, poor condition will be reflected by mussels that are thin and watery. It would be of interest to also compare mussels with elevated levels of atresia and a mussel in good reproductive condition to see if the taste and biochemical profile changes and affects the flavour and quality of the mussels. Lastly, this trial provided the opportunity to network with other research institutes and allowed for further professional development and growth as a researcher in an emerging field. Going forward, the trial will be repeated but with a different set of questions and is therefore outside the scope of the thesis. However, it does show that the work presented expands beyond the PhD and will likely provide key information to the aquaculture industry on reproduction, and therefore meat quality, in a changing climate.

SECTION 4. DISEASE PROGRESSION OF *PERKINSUS OLSENI* IN *PERNA CANALICULUS*: A
LABORATORY STUDY



In this section:

Section 4: Preamble

Chapter 7: Progression of *Perkinsus olseni* in the Green-lipped mussel (*Perna canaliculus*).

Section 4. Preamble

The protozoan parasite *Perkinsus olsenii* is common to both *Perna canaliculus* and *Haliotis iris* around New Zealand. It is well known to be influenced by warming seawater therefore, not surprisingly, it was regularly observed in the green-lipped mussels throughout this thesis. The appearance of the parasite in the Chapter 5 “Histopathological changes in the green-lipped mussel, *Perna canaliculus*” experiment and the Chapter 2 field study “Interacting influence of changing environment on parasite assemblage and reproductive potential of a marine heatwave-affected population of mussels” highlighted the need for ongoing research into the disease progression of *P. olsenii* in green-lipped mussels.

Experiments such as this are complex and require a different type of set up. For instance, due to *P. olsenii* being an OIE notifiable disease, the work required a PC2 facility (level 2 physical containment) which adhered to MPI biosecurity standards. The experiment and eventual chapter were academically high risk and first required the successful establishment of a culture which could be sub-cultured and proliferated. Upon the successful establishment the *P. olsenii* we could then proceed with the *in vitro* method by injecting *P. olsenii* cells into adult, green-lipped mussels. Prior to developing a thermal stress and pathogen infection experiment, the methods and investigation first required validation and observation of the proliferation of cells within the host tissue under benign conditions.

The subsequent chapter is a culmination of the thesis not only in the environment/ host/pathogen interaction model but also development as a scientist. There were different methods and mentors resulting in an adjustment of analysis and writing style, which ultimately enhanced my knowledge and skills, and provided additional diversity.

CHAPTER 7. DISEASE PROGRESSION OF *PERKINSUS OLSENI* IN ADULT, GREEN-LIPPED MUSSELS, *PERNA CANALICULUS*.

To be published.

Abstract

The protozoan parasite *Perkinsus* spp. is an aetiological agent of the perkinsosis (dermo) disease. Two of these species, *Perkinsus marinus* and *P. olsenii*, are also capable of inducing mortality in several shellfish species. As sea-surface temperatures continue to rise the parasite is spreading to new regions and infecting new shellfish hosts, driving the need for understanding the disease progression. In 2014 *P. olsenii* was detected in green-lipped mussel (*Perna canaliculus*) in New Zealand. However, the knowledge around disease progression in green-lipped mussels remains limited. As such, histopathological techniques, standard and fluorescence *in situ* hybridisation (F-ISH), were used with the aim of understanding *P. olsenii* infection, associated onset, and development of disease in green-lipped mussels during an experimental *in vivo* infection challenge. For the first time, the life stages of *P. olsenii* in green-lipped mussels were reported to be similar between a natural infection and injection of cultured cells into the adductor muscle, with both scenarios also eliciting a similar host immune response. Furthermore, regardless of injection method, the *P. olsenii* migrated primarily to the mantle tissue. Lastly, F-ISH detected more *P. olsenii* cells compared to standard H&E and was an improved method for quantification and detection. This research highlights the potential risks for the green-lipped mussel farming industry, particularly if farms are established in regions where environmental conditions are optimal for *P. olsenii* proliferation. Therefore, this investigation provides a foundation for future research and a basis for disease modelling.

7.1. Introduction

Infectious diseases are emerging worldwide (Byers, 2021; Carella et al., 2023), often linked to changing climate, habitat fragmentation, and host species range shifts (Harvell et al., 1999; Okamura and Feist, 2011; Coen and Bishop, 2015; Okamura, 2016). In aquatic environments, increases in average sea surface temperature and incidence of temperature anomalies are likely to promote the frequency and severity of molluscan infectious diseases (Harvell et al., 1999; Burge et al., 2014; Guo and Ford, 2016a; Lane et al., 2023). Disease is considered as a major factor contributing to the decline of wild populations, as well as impeding aquaculture and restoration efforts (Coen and Bishop, 2015). Although pathogens and parasites are a natural part of a functioning ecosystem (Lane et al., 2020), climate change may promote conditions that increase host susceptibility and promote prolific parasite

reproduction, with increased disease risk for the host (Harvell et al., 1999; Burge et al., 2014; Guo and Ford, 2016a; Lane et al., 2023).

Perkinsus spp. are aetiological agents of the perkinsosis disease in shellfish. Members of the genus *Perkinsus* are generalist protozoan parasites infecting several gastropod and bivalve species and have been associated with host mass mortality (Goggin and Lester, 1995; Itoiz et al., 2021; Carella et al., 2023; Lane et al., 2023). There are currently seven accepted *Perkinsus* species worldwide, one of which is *Perkinsus olsenii* (Villalba et al., 2004; Soudant et al., 2013). Along with *Perkinsus marinus*, *P. olsenii* infects more than 30 molluscan species and is a World Organisation for Animal Health (WOAH) notifiable pathogen (WOAH, 2025), due the potential severity of the disease (Itoiz et al., 2021; Lane et al., 2023; Delisle et al., 2025). While *P. olsenii* has been detected in various shellfish species throughout New Zealand (*Austrovenus stutchburyi*; *Pecten novaezelandiae* and *Haliotis iris*), it has not been previously associated with mass mortality or disease in NZ (Hine and Diggles, 2002; Muznebin et al., 2021; Lane et al., 2023).

The green-lipped mussel, *Perna canaliculus*, is New Zealand's dominant aquaculture mollusc species (AQNZ, 2023). Endemic to NZ, green-lipped mussels have, historically, been considered as free from significant diseases (Castinel et al., 2019; Lane et al., 2023). However, in 2014, *P. olsenii* was detected in farmed green-lipped mussels during a routine histopathology survey (McDonald, 2014). *Perkinsus olsenii* has since been confirmed through Ray's fluid thioglycolate medium (RFTM), *in situ* hybridisation (Muznebin et al., 2022a), as well as PCR in samples from Coromandel, Waipu, Nelson Haven and Kenepuru, NZ (Lane et al., 2023). An *in vitro* *P. olsenii* culture has also been established by Delisle et al. (2025). The importance of green-lipped mussels in NZ and the emergence of *P. olsenii* has highlighted a need for further investigation on disease progression and the environmental parameters facilitating spread (Lane et al., 2023).

To date, only a few studies have examined *P. olsenii* infections in green-lipped mussels and typically as part of surveillance or distribution studies (McDonald, 2014; Muznebin et al., 2022a; Lane et al., 2023), or as incidental occurrences in experimental challenges (Copedo et al., 2023) (Chapter 5). Knowledge regarding *P. olsenii* disease progression in green-lipped mussels is limited and can currently only be inferred based on infection in other bivalve species, such as the Manila clam, *Tapes philippinarum* (see Lee et al., 2001), and the abalone, *Haliotis iris* (see Muznebin et al., 2021; Handler, 2022). Furthermore, histological screening for pathogens as small as *Perkinsus* spp. (average size 2-20 µm) relies on associated haemocyte infiltration to locate areas of interest for detection (Roberts et al., 2012; Muznebin et al., 2022a; Lane et al., 2023) and is typically biased towards the larger trophozoite or rosette life stages. The potential to not detect *P. olsenii* cells when they are present is high (false negative; type II error). As such additional techniques, including *in situ* hybridisation (ISH), PCR and RFTM (Muznebin et al., 2022a; Lane et al., 2023), and fluorescence staining (Reece and Dungan, 2006), are required to assess the extent of the disease. Moreover, *Perkinsus* spp. are generally quantified on a semi quantitative scale designed for RFTM.

These scaling criteria have then been transferred to histological assessments (e.g. Kim et al., 2006a; Muznebin et al., 2022b), without consideration to host responses, highlighting the need for an updated scaling criteria to assist with informing *P. olseni* disease progression.

Unlike other species of mollusc, macroscopically, there have been no reports of the typical external presentation of pustule-like lesions in the gross pathology of green-lipped mussels (see Goggin and Lester, 1995; Villalba et al., 2004; Lane et al., 2023; Moore, 2023). Microscopically, typical haemocyte migration and phagocytosis have been observed in green-lipped mussels in response to *P. olseni*, although detection of encapsulated cells is often rare (Muznebin et al., 2022a; Lane et al., 2023). Additionally, the presentation of the *P. olseni* cells in green-lipped mussels under histology has differed when compared to other infected species such as the abalone, *H. iris*. The mature signet ring trophozoite with its vacuoplast is much smaller (<10µm) and typically only three or fewer *P. olseni* cells are found per focal haemocyte aggregation (Muznebin et al., 2022a; Lane et al., 2023). The haemocyte aggregations are typically large indicating an overreaction of the immune response. The life cycle of *P. olseni* in the green-lipped mussel is typical and consists of four development stages (Delisle et al., 2025) (Fig 1.7). The mature trophozoites proliferate through successive cycles of karyokinesis and cytokinesis (palintomy) to produce daughter cells in the form of rosettes (Villalba et al., 2004). The membrane of the rosette then ruptures to release immature trophozoites (Villalba et al., 2004).

The development of *in vitro* cultures of *Perkinsus olseni* in New Zealand provides the opportunity to investigate disease progression in susceptible shellfish. Furthermore, it permits deeper investigation of disease kinetics and disease development while advancing the understanding of the parasite's biology (Villalba et al., 2004; Moore, 2023). An experimental *in vivo* infection challenge was conducted to understand *P. olseni* infection dynamics and disease development in green-lipped mussels. The aims of this study were to:

- a. Provide a description of *P. olseni* progression and its impact on the green-lipped mussel maintained at 20 °C (typical average summer seawater temperature in coastal NZ).
- b. Propose a new histology scoring system for *P. olseni* incorporating the semi-quantitative scale and host cellular responses to produce a scale to infer disease severity.
- c. Advance histological techniques whilst improving confidence of detection of *P. olseni* cells using standard H&E staining techniques and fluorescence in situ hybridisation (F-ISH).

7.2. Methods

7.2.1. Naturally, infected mussel population and *Perkinsus* collection

Twenty green-lipped mussels, *Perna canaliculus*, (80 to 120 mm) were sampled at two time points using histological and RFTM techniques (Section 7.2.2.3.) during the summer period (November (Time 1) and December (Time 2)) of 2021. The population was identified to be *Perkinsus olseni* positive during a prior routine histological health screening. These mussels originated from an

aquaculture farm in the South Island, New Zealand, in 2017 and were subsequently transferred to secure tank holding facilities at the Cawthron Aquaculture Park (CAP), Nelson. They were maintained in four 100 L tanks, with ambient seawater temperatures at a flow rate of 3 L/ min, aerated to maintain 6.8 to 8.2 mg/ L dissolved oxygen and fed continuously *ad libitum* on algal bloomed pond seawater (Copedo et al., 2023) (Chapter 5). Histological sampling proceeded as per section 2.2.3 and the histological slides were analysed along with the experimentally infected mussels and used for comparison.

7.2.2. Experimentally infected mussels

7.2.2.1. Experimental setup

In August 2023, 80 adult green-lipped mussels, *Perna canaliculus*, (65-80 mm) sourced from a farm in the Pelorus Sound, New Zealand, were transported to the Cawthron Aquaculture Park, Nelson. The green-lipped mussels were distributed to two 100 L flow-through tanks (n=40 per tank) which were well aerated (100% dissolved oxygen), received seawater flow rates of 3 L/ min and fed a 50:50 mix of *Tisochrysis lutea* and *Chaetoceros muelleri*. After two weeks of acclimation to ambient winter temperatures of approx. 14 °C, the water temperature was increased by 0.5 °C every 12 h to reach the desired temperature of 18 °C. The green-lipped mussels were then held at 18 °C for one week. On the 1st of September 2023, the green-lipped mussels were transferred to Te Wero Aro-anamata, Cawthron's PC2 aquatic biocontainment facility in Nelson, New Zealand, for the infection challenge. Following arrival, 5 mussels were sampled (section 2.2.3; Table. 7.1). The green-lipped mussels were randomly distributed into 15 x 8 L tanks (n = 5 per tank) pre-assigned to three treatments:

Treatment 1 - infection of mussels with *P. olsenii* zoospores (4 tanks, 20 mussels total)

Treatment 2 - infection of mussels with *P. olsenii* trophozoites (6 tanks, 30 mussels total)

Control - mussels were injected with culture media without the parasite (5 tanks, 25 mussels total).

The temperature for all tanks was increased to 20 °C and maintained by an external water bath which was connected to a recirculating freshwater heat pump (Hailea). All tanks received flow-through seawater of 260 ml/ min and survival was monitored daily. The green-lipped mussels were batch fed daily with 500ml of a 50:50 mix of *Tisochrysis lutea* and *Chaetoceros muelleri* to a chl a concentration of ~3µl/ L on outflow. Water quality parameters, including dissolved oxygen, temperature and pH, were measured daily using a YSI ProSolo handheld digital meter (Xylem Inc., Yellow Springs, OH, USA). The YSI ProSolo was calibrated weekly following manufacture instructions. Ammonia, nitrates, and nitrites were assessed using API saltwater aquarium test kits twice a week to maintain desired levels and a complete water change occurred every 2 days.

Before infection, a “baseline” health status assessment was conducted using five adult green-lipped mussels (Table. 7.1). Baseline mussels were weighed (g) and measured (mm), then sampled for histology. To assess the progression of infection over time, mussels were randomly sampled at two other timepoints, 18th October (33 days post injection) and 14th November (60 days post injection)

(sample sizes are indicated in Table. 7.1). Control mussels were always sampled first. Between sampling each mussel and treatment group the sampling area and dissection tools were cleaned and disinfected using a 600-ppm bleach (sodium hypochlorite) solution.

7.2.2.2. Pathogen source and infection

Perkinsus olsenii trophozoites were sourced from the *in vitro* culture and routinely sub cultured (Delisle et al., 2025). To improve *P. olsenii* infectivity, the culture was supplemented with 1000µg/ml green-lipped mussel plasma protein then maintained at 22 °C (Delisle et al., 2025). Prior to injection of mussels with the parasites, parasite cell concentrations were quantified and standardised to 5.45x10⁶ cells/ mL for trophozoites and 1.3 x10⁷ cells/ mL for zoospores. The control inoculation treatment contained Dulbecco's Modified Eagle Medium (DMEM)-Ham's F12 (3% Fetal Bovine Serum, 0.1% lipids mixture (1000X, Sigma Aldrich L5146)) was then prepared to imitate the propagating media without the parasite.

On 15th September 2023 (0 days post injection (dpi)), seventy-five adult mussels were injected with either 200µl of the DMEM culture media (control), 200µl of the trophozoites suspension corresponding to 1.09x10⁶ cells/ injection or 200µl of the zoospore suspension corresponding to 2.6x 10⁶/ injection. The two shells of the green-lipped mussels were gently prised open using a blunt rounded butter knife to provide enough space for the insertion of a 1ml 25 x 1.5” gauge syringe (BD PrecisionGlide™ needle). The treatments were then injected into the haemolymph sinus of the posterior adductor muscle of each mussel.

7.2.3. Sampling

The mussels were carefully shucked to half shell using a blunt butter knife. The visceral mass was then removed intact from the second half of the shell. A 5 mm thick transversal steak was cut for histology to include organs such as mantle, gill, digestive gland, gastrointestinal tract and muscle, as per Howard (2004). The adductor muscle was removed to acquire a longitudinal section, including the lesion associated with the site of injection. The tissue steak and muscle were placed in the histology cassette and fixed for 48 hours in a 10% formalin solution (1:9 v/v, 37% formaldehyde: 0.35µm filtered seawater), then transferred to 70% ethanol (Howard, 2004; Copedo et al., 2023) (Chapter 5). Half of the samples were sent to Awanui Veterinary Pathology and the other half to Medlab Central, Palmerston North, for routine histological processing and H&E staining (hematoxylin and eosin) (Howard, 2004; Copedo et al., 2023). An additional three consecutive paraffin embedded tissue sections were cut (3µm) from 25 samples for fluorescence *in situ* hybridisation (F-ISH), described in section 7.2.5.

Ray's fluid thioglycollate culture method (RFTM) was also conducted to confirm presence of *Perkinsus* spp. The RFTM test was conducted following methods in WOA (2024). In brief 5 – 10mm of gill was excised and placed in a tube containing the sterile medium supplemented with Chloramphenicol and nystatin. The medium containing the gill tissue was then incubated for 5 days

in the dark at 22°C. Once incubation was complete the tissue was then digested by centrifuging the RFTM medium with the tissue at 1500rpm for 10 min. The RFTM was then removed and replaced with 2 M NaOH, which was incubated at 60°C for 2 h (or until tissue dissolved). The NaOH solution was then removed after an additional centrifugation at 1500rpm for 10min. The remaining pellet was then washed three times in sterile seawater. After the third wash the solution was stained with Lugol's iodine. The samples were then assessed for *Perkinsus* spp. cells (WOAH, 2024). Diagnostic sensitivity and specificity (DSe) of the histology was then estimated relative to the RFTM results. True positives (TP) were those that were *Perkinsus* spp. positive in both histology and RFTM. False negatives (FN) were mussels that were negative in histology but positive in the RFTM. False positives (FP) were those that were positive in histology but negative in RFTM. True negatives (TN) were those without *Perkinsus* spp. cells in both methods.

Diagnostic sensitivity (DSe) and diagnostic specificity (DSp) was then calculated using the following equations by Heuer and Stevenson (2021):

$$DSe = \frac{TP}{TP+FN} * 100$$

$$DSp = \frac{TN}{TN+FP} * 100$$

Table 7.1 Total number of *Perna canaliculus* sampled in each treatment at each timepoint.

Sampling timepoint	Initial sampling	Control	Zoospores	Trophozoites
Naturally infected: Time 1	20	NA	NA	NA
Naturally infected: Time 2	20	NA	NA	NA
0 days post injection:	5	NA	NA	NA
33 days post injection		9	5	10
60 days post injection		15	9	18

7.2.4. Standard H&E tissue analysis

Histological observations were performed using an Olympus BX53 light microscope and cellsens™ software (Olympus cellsens Standard 3.1 [build 21,199]). Initial assessment of the slides consisted of a general health screening to identify the presence:

- Mussel sex and reproductive status e.g. resting, early, late, ripe, spawning, spent, and redeveloping (Kennedy, 1977; Copedo et al., 2023) (Chapter 5 and 6)
- Presence of parasites including:
 - *Perkinsus olsenii*, APX, *Microsporidium rapuae*, ciliates, copepods
- Digestive gland tubule atrophy (epithelial thinning) (Cuevas et al., 2015; Costa, 2018a)
- Above normal gastrointestinal tract diapedesis
- Above normal haemocyte phagocytosis ceroid (Copedo et al., 2023) (Chapter 5)

- Haemocytosis (Table. 7.2, Column 4) with or without associated pathogens
- Focal pustule-like lesions and/ or encapsulation (Handlering, 2022; Carella et al., 2023)

On completion of initial histological assessment, a deeper analysis was conducted on *P. olsenii* positive samples, including population prevalence of *P. olsenii*, cell counts, cell measurements, area analysis of haemocytosis, and recording of associated pathology of *Perkinsus olsenii* occurred using two methods on mussels identified as *P. olsenii* positive. The methods were evaluated by comparison of results with those of one independent pathologist using a subset (n = 20) of the H&E histology slides. The first method applied was a full screen and count of the *P. olsenii* cells in all the tissues available in the histology section under 1000x magnification (oil immersion) for each sample. The *P. olsenii* cells were recorded (trophozoites and rosette stages were considered as individual units for this analysis) across the whole section and allocated to pre-determined tissues (Fig. 7.1).

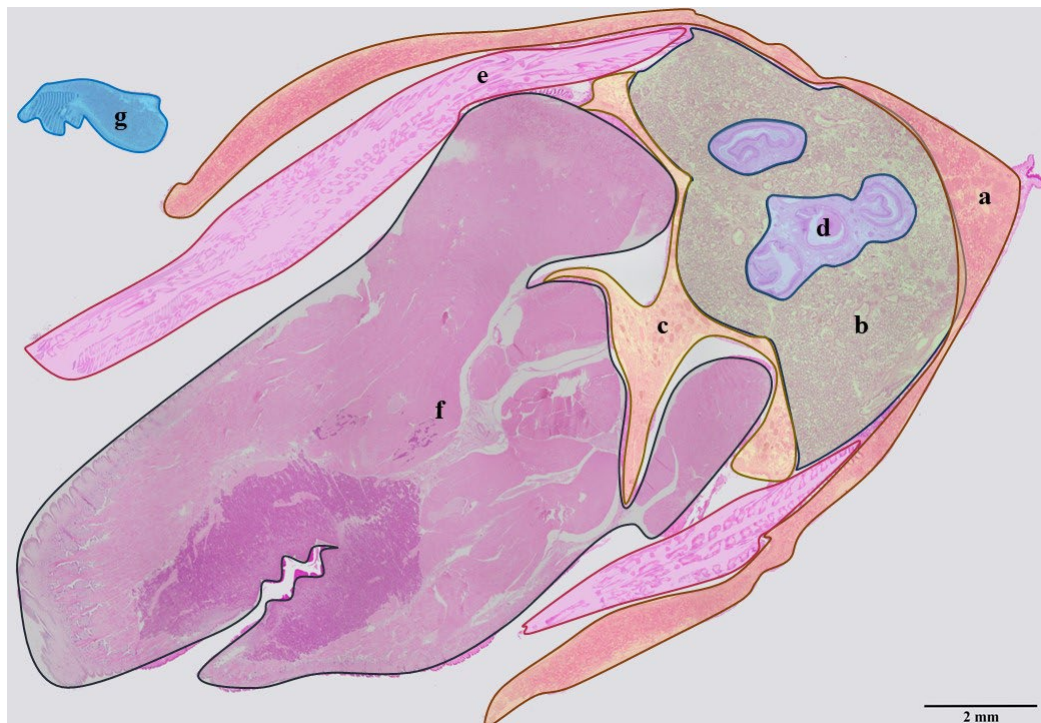



Figure 7.1 Typical, green-lipped mussel transverse histological section (~130mm²). *P. olsenii* cells detected were recorded and allocated to the following tissues: (a) mantle, where gonad was likely to develop, (b) digestive gland tissue (DG) including the interstitial space between tubules, (c) haemal space (connective tissue) between DG and foot muscle, (d) gastrointestinal tract including the subepithelial layer and the surrounding interstitial tissue gill, (e) muscle, (f) either foot or adductor (if available in section), and (g) palp

The pre-determined tissues were allocated as a proxy for the disease progression and level of systemic infection from the baseline (day 0) to day 66. The area of each of the tissues was also recorded whereby a polygon tool in the cellsensTM software was used to draw around each of the tissues, the projected area calculated and *P. olsenii* counts were standardised to cells mm².

The second method followed the criteria outlined in the proposed histological scoring system (Table 2) and was applied to individuals identified as *P. olsenii* positive during the initial screening process.

The *P. olsenii* cell count was estimated by examining 10 randomly selected suspicious haemocyte aggregations at 1000x magnification. If no haemocyte aggregations were observed, then 10 field of views at 1000x magnification were selected for analysis. Based on these counts, each individual was assigned a score from 1 to 5 in the *Perkinsus* criterion column reflecting an estimate of cell numbers across the entire transverse section. Additional scores were then allocated across three further columns. The tissue involvement score represented the number of tissues containing cells, a maximum of five tissues selected based on the most common presentation. The haemocyte aggregation score accounted for the presence of aggregations and granulomas, with higher scores indicating diffuse haemocytosis. The lesion development score incorporated the presence of various life stages of *P. olsenii* (rosettes and trophozoites), encapsulated cells potentially leading to the formation of pustules, and systemic infection indicated by the level of free-circulating cells without associated haemocyte aggregation. A score of 4 or 5 in the lesion development column, which corresponds to potential pustule development is hypothetical for green-lipped mussels as this pathology has not been previously observed (Table 3; S1). Each mussel was assigned a score of zero to five for each of the columns to produce four values. These values were then summed to produce a single composite score (Table 7.2).

Table 7.2 Proposed histopathological scoring of *Perkinsus olseni* including number of tissues affected (Fig. 1), haemocyte aggregation, and development of lesions, as well as encapsulated *P. olseni* cells and systemic presence. The score is the sum of the individual score in each column. The minimum score is 2 and must consist of detection of 1 *P. olseni* cell in 1 tissue type. A score of 20 is the maximum value and indicates a severe impact. A score of 10 is moderate and 15 is high. Values between 2 and 20 can be created by a combination of these scores. For example, a score of 15 could be created by the combination 5, 5, 5, 0 (very high cell number, 5 tissues, diffuse haemocytosis, but no pustule). Note* pustule descriptions are hypothetical, and based on clam and abalone species (Handlering, 2022). Systemic free cells have been observed in green-lipped mussels in a thermal challenge trial Chapter 5.

Score	Perkinsus criterion	Number affected tissues (Fig. 1)	Haemocytosis aggregations (Costa, 2018c)	Lesion development	Weighted host: pathogen score
0	No <i>P. olseni</i> detected	None	No haemocytosis observed	No lesions observed	Non infected
1	Very low: <5 <i>P. olseni</i> cells observed by eye in section.	1 tissue	Infrequent: Small number of focal haemocyte aggregations (associated to <i>P. olseni</i> cells) across all tissues (e.g. <10 haemocytosis aggregations)	Small pustule-like lesions developing; or low frequency of encapsulation of approximately 5 to 10 immature trophozoite <i>P. olseni</i> cells or a rosette.	<p>Mild: Score 2: Minimum obtainable score by summing columns 2 to 5. Sum of the criterion equals 2 and must include column 2 whereby <i>P. olseni</i> is detected in 1 tissue.</p>  <p>Severe: Score 20: Maximum obtainable score. Many <i>P. olseni</i> cells with extensive haemocytosis in most of the available tissues. Pustules may be detected histologically; and/or <i>P. olseni</i> cells, or pustules, are in contact with the environment; and/ or host has a systemic <i>P. olseni</i> infection. The host is compromised and at risk of secondary infection, predation and mortality.</p>
2	Low: 5 to 25 <i>P. olseni</i> cells counted and/or estimated in section	2 tissues	Medium number of focal haemocyte aggregations scattered through tissues (e.g. 10 to 30)	Small pustule-like lesions detected; or low frequency of encapsulation of 10 to 20 <i>P. olseni</i> cells (rosettes or trophozoites).	
3	Moderate: 26 to 50 <i>P. olseni</i> cells counted and/or estimated in section	3 tissues	High number of focal haemocyte aggregations scattered through tissues (e.g. 30 to 50)	Medium pustule-like lesion; or frequent encapsulation of cells >20 <i>P. olseni</i> cells lesion visible at low light microscopy and ≤ 1mm; or low occurrences of free <i>P. olseni</i> cells	
4	High: 51-100 <i>P. olseni</i> cells counted and/or estimated in section	4 tissues	Diffuse continuous (>50): High number of focal haemocyte aggregations scattered through tissues and aggregations merging	Large pustules detected macroscopically >1mm; or frequent encapsulation of between 5 and 20 <i>P. olseni</i> cells. Haemocyte debris and potential necrosis, or regular occurrences of free <i>P. olseni</i> in many tissues	
5	Very High: >100 <i>P. olseni</i> cells counted and/or estimated in section	5 or more tissues	Diffuse continuous: Extensive haemocytosis and large areas of continuous diffuse haemocytosis	Large pustule; or frequent encapsulation of >20 <i>P. olseni</i> cells. Pustules visible externally >5 mm; or high number of free <i>P. olseni</i> cells (rosettes or trophozoites).	

7.2.5. Fluorescence in situ hybridisation (F-ISH)

Fluorescent *Perkinsus olseni* probes were designed and acquired from Daicel Arbor Biosciences. The probe candidates (43-47 NTS) were designed across the full *P. olseni* genome. Candidates were then checked *in silico* against the following genomes, to identify and omit any probes that could cross-hybridise and target with potential host genomes:

Crassostrea gigas (GCF_902806645.1_cgigas_uk_roslin_v1_genomic.fna).

Haliotis rufescens (GCF_023055435.1_xgHalRufe1.0.p_genomic.fna).

Perna viridis (GCA_018327765.1_Pvar_1.0_genomic.fna).

Finally, the 27,392 probes specific to *P. olseni* that passed the specificity analysis were selected for the final design. The final probe was then conjugated with the fluorochrome ATTO 594.

Once the probes were acquired, the formalin-fixed, paraffin embedded, microscopy slide mounted, histological sections produced in section 2.4 were dewaxed and hydrated. The tissue sections were hydrated, and an antigen retrieval process was optimised and applied using eBioscience™ (00-4956-58) for 30 min at 85 °C in a water bath. Slides were cooled for 20 min at room temperature and rinsed in a phosphate buffered saline (PBS) solution for 10 min. The slides were then incubated for 15 min at room temperature in proteinase K at 20 mg/ ml (Invitrogen™, 25530049). The subsequent dehydration procedure was optimised using 70 % ethanol for 2 min and 100 % ethanol until the slide was fully dehydrated, both steps at room temperature. The whole genomic probe from Arbor Bioscience was reconstituted to a concentration of 40 µmol/ µl using hybridisation buffer (Bio Scientific, Hyb-Buffer). The hybridisation process was performed using a hotplate, 15 min at 85 °C. To prevent evaporation of the reagents a silicone ring was applied around the cover slip. Complementary slides were incubated at 37 °C for 16 hours. Once the process was complete the slides were washed in SSC 1 (0.4 X SSC Buffer (Invitrogen, AM9770) and 0.3% NP-40 (Thermo Scientific, 85124) solution at 70 °C for 2 min and rinsed in SSC 2 (2 X SSC Buffer (Invitrogen, AM9770) and 0.1 % NP-40 (Thermo Scientific, 85124) at room temperature for 1.5 min. Finally, the slides were incubated for 2 min at room temperature using True VIEW (50µl per section; Vector Laboratories, SP-8500-15). An autofluorescence quencher was applied and the slides were mounted with a DAPI mounting media for further image processing.

Images were obtained using an Olympus inverted microscope IX83 equipped with Laser Scanning Confocal Microscope head (FV3000, Tokyo, Japan) with a 405nm (50 mW), 514 nm (40 mW), 594 nm (20 mW) excitation laser lines and highly sensitive detectors configured with emission bands of 430-470 nm, 520-565 nm and 600-700 nm respectively. All the images were captured using an UPLSAPO 40X N.A. 1.4 objective, with a 170 nm pixel size in image of 10 megapixels. The collected images then underwent image analysis whereby the autofluorescence signal was subtracted from the target signal and the number of target object per power field was quantified. Images were

Section 4: Disease progression of *Perkinsus olseni*.

processed and analysed using FIJI software (Schindelin et al., 2012) and CellProfiler (Carpenter et al., 2006).

7.2.6. Standard H&E and Fluorescence in situ hybridisation (F-ISH) comparison

Once F-ISH image analysis was complete (Section 2.5) an initial ten haemocyte aggregations in one of the mussels with a high *Perkinsus* intensity score (Table. 7.1; column 2) underwent analysis. Whereby the haemocyte nuclei in the aggregations were counted and averaged. The *P. olseni* cells were then counted using FIJI software (Schindelin et al., 2012) and CellProfiler (Carpenter et al., 2006). A small subset of the completed slides then had the coverslip de-mounted and re-stained with H&E to collect images of identical haemocyte aggregations to compare *P. olseni* cells between the two methods.

After the initial slide was investigated and the ten haemocyte aggregations analysed a further twenty haemocyte aggregations in the H&E sections and F-ISH sections were randomly selected across 5 mussels for area analysis. The area of the haemocyte aggregation and the total number of cells was quantified for each method. Images for the F-ISH were collected and analysed as in section 2.5 whereby the target signals (cells (Haemocyte nuclei) and object (haemocyte aggregation)) were quantified using the FIJI software (Schindelin et al., 2012) and CellProfiler (Carpenter et al., 2006). The number of *Perkinsus olseni* cells was then targeted to acquire number per area of haemocyte aggregation and number of *P. olseni* cells to number of haemocytes. For the H&E sections the area of each aggregation was obtained by using a polygon tool in the cellsensTM software (Olympus cellsens Standard 3.1 [build 21,199]). The number of *P. olseni* cells within each of the areas was then counted and recorded. The data from both techniques was plotted and compared.

7.2.7. Statistical analysis

Statistical analyses were conducted using R version 4.0.4 (R Core Team, 2021). A general linear model (GLM) in the MCMCglmm package (Hadfield, 2010) was conducted to analyse the interaction of tissue and timepoint (dpi) on the number of *P. olseni* cells mm² for each tissue type. Four GLM models were run, Number ~ Tissue * Timepoint (family = Poisson); Number ~ Tissue + Timepoint (family = Poisson); Number ~ Tissue + Timepoint (family = Quasipoisson); and Number ~ Tissue + Timepoint (family = negative binomial). The negative binomial option was selected due to the lower AIC value (Table S11). A Kruskal-Wallis chi-squared test was also used to compare the differences in the weighted score using the proposed histology scoring criteria. A Mann-Whitney test was used to compare the size differences between the natural and injected populations due to the unbalanced sample size numbers. Lastly, a linear model was conducted on the H&E and F-ISH *P. olseni* cell count data. A *p* value < 0.05 was considered statistically significant.

7.3. Results

7.3.1. *Perkinsosis* in naturally infected mussels

Based on the initial histological assessment all mussels were observed to be in good health and condition. For instance, the mantle tissue was full of glycogen-like material, ceroid intensity was low and typically associated with APX. All reproductive stages were represented and there were 21 females, 14 males with only 5 where sex was unidentifiable. All mussels had a small number of thinning digestive gland tubules, likely associated to the digestive gland phases (Costa, 2018a) and therefore benign in terms of overall health. All the mussels associated to the naturally infected sample group also had APX, one mussel had residual copepod limbs in the mantle tissue, one had *Microsporidium rapuae* and two mussels had *Endozoicomonas*-like organisms (ELOs). Additionally, 50% of the mussels had mild focal haemocytosis in sample Time 1 and 40% in sample Time 2. The overall average focal haemocytosis grade (Table. 7.2 column 4) was low at 1.7. It is also worth noting that occasionally the haemocyte aggregations were observed to be associated to APX rather than *P. olseni*. However, this was not the focus of the current study but could represent a confounding factor in subsequent results.

The prevalence of *P. olseni* was 20% and 40% for Time 1 and Time 2 with a mean histological weighted intensity score of 6.4 and 4.75 (Fig. 7.6), respectively, with *P. olseni* cells primarily detected in the palp and mantle tissue. The DSe was 71.4% and 100% and DSp 100% and 100% respectively. Trophozoites were the main life stage detected and were on average $5.02\mu\text{m} \pm 1.7\mu\text{m}$ (n= 35). However, small rosettes and immature trophozoites were also present (Fig. 7.2 d, e, f). One mussel with a high intensity *P. olseni* score (Table. 7.2: column 2) also had *P. olseni* cells in the gills, and interstitial connective tissue of the digestive gland. This mussel was also identified to have a large cluster of encapsulated immature trophozoite of *P. olseni* cells (Fig. 7.2 e). The high intensity and encapsulated cells are likely due to the accumulation time and advanced diseased state in this individual.

The initial exploration of ten larger haemocyte aggregations using F-ISH techniques in the naturally infected mussels with medium to high *P. olseni* intensities had on average 750 haemocytes associated with 25 to 30 *P. olseni* cells. When the haemocyte aggregations on the consecutive histological sections were compared there were no differences in haemocyte nuclei numbers and associated *P. olseni* cells ($F_{1,18}=0.71$, $p = 0.41$ and $F_{1,18} = 1.34$, $p = 0.26$, respectively). Furthermore, comparison of *P. olseni* cells in same haemocyte aggregations on the same section using F-ISH then retrospectively stained with standard H&E showed many more *P. olseni* cells in the F-ISH than what could be detected in the H&E (Fig. 7.3).

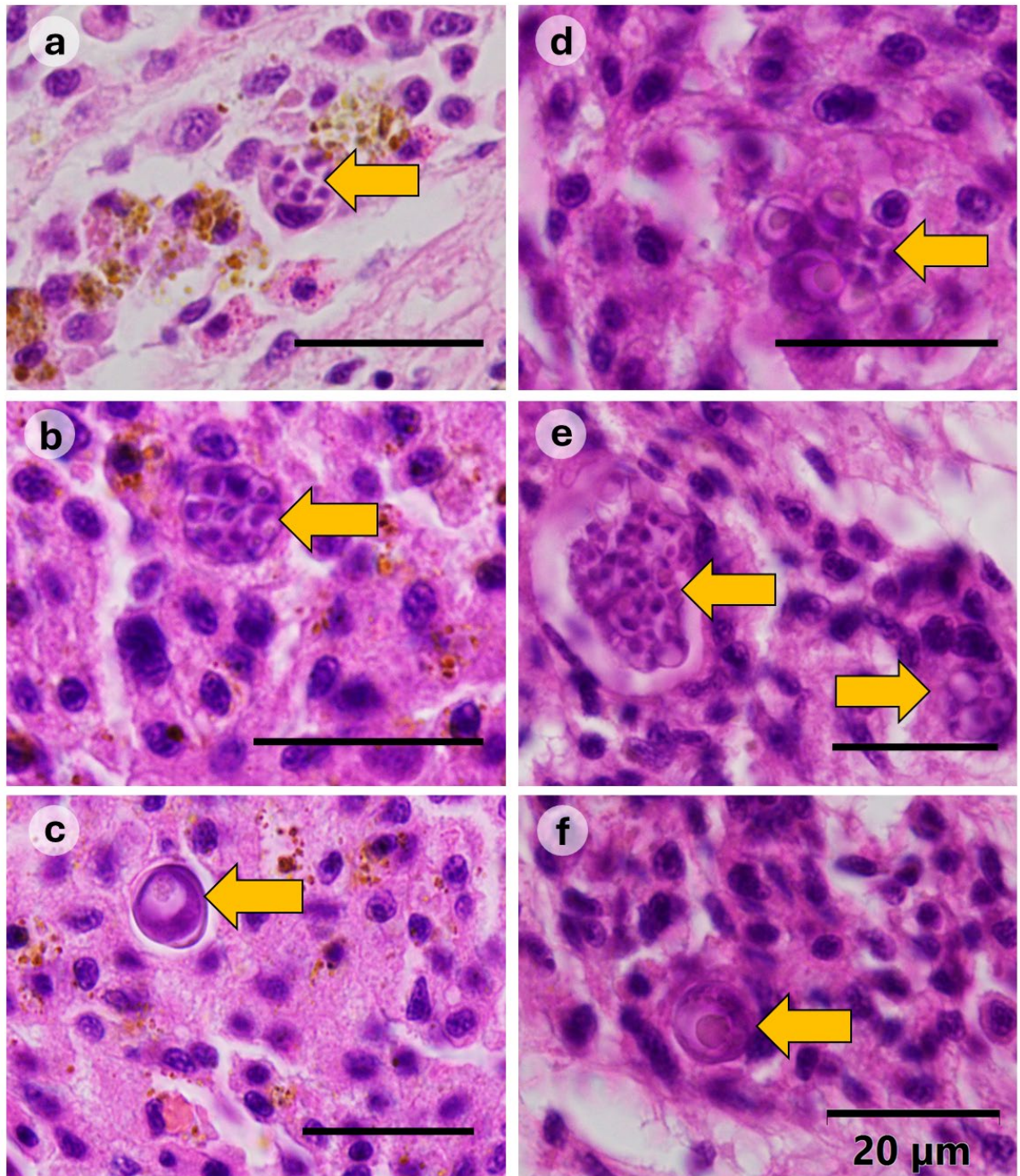


Figure 7.2 *Perkinsus olseni* life stages encountered in the injected trophozoite culture in green-lipped mussels a) small rosette stage engulfed by a haemocyte, b) small rosette cells dividing and developing into small immature trophozoites, c) large well-developed trophozoite. The *P. olseni* life stages of the naturally infected, green-lipped mussels d) small rosette with early division and 3 trophozoites nearby, e) large cluster of rosette stage cells encapsulated by haemocytes and small early developing trophozoites, a second cluster to the right with slightly larger trophozoites and f) large well-developed trophozoite. *P. olseni* cells indicated by arrows.

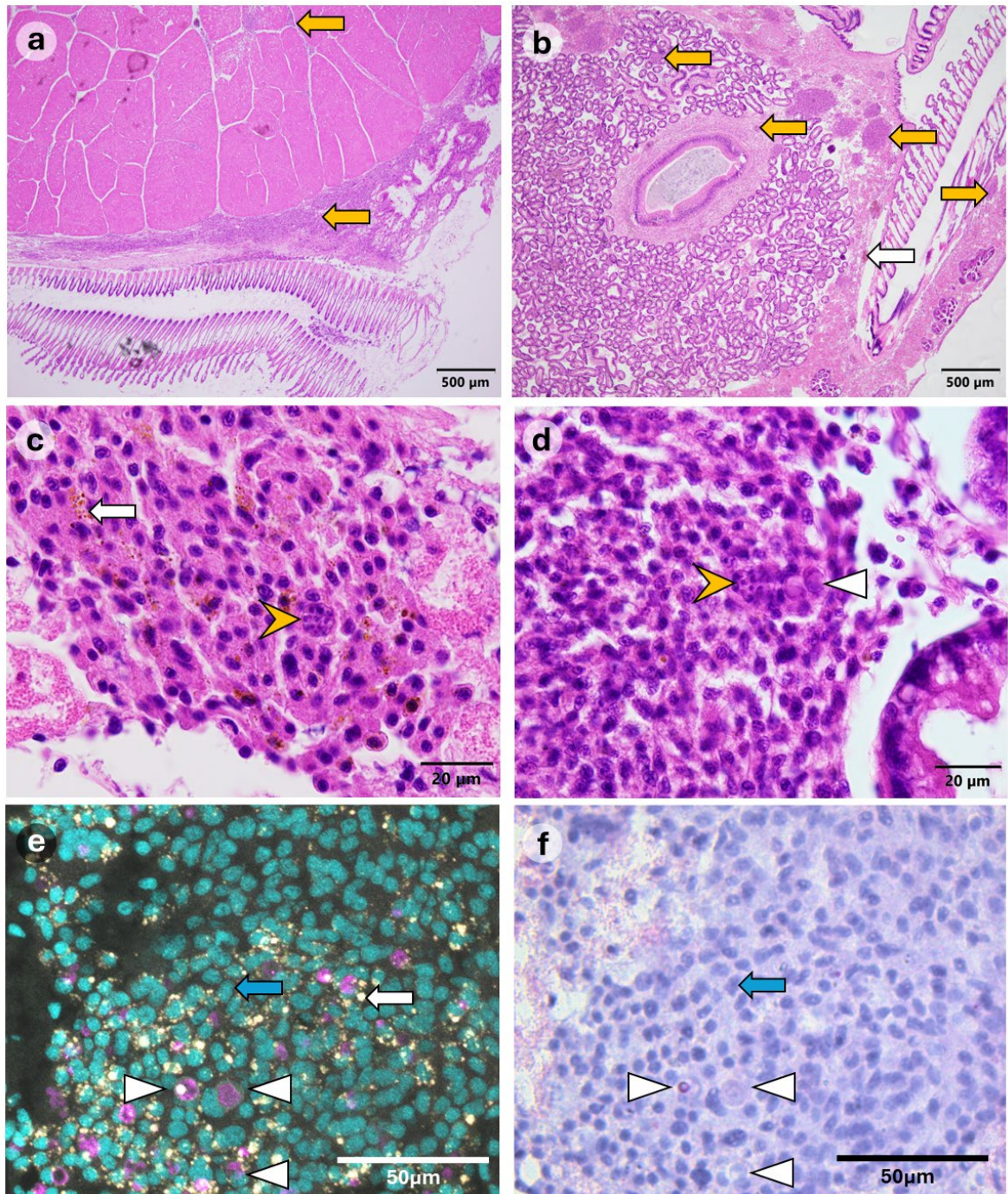


Figure 7.3 Histological (hematoxylin and eosin) micrographs of transverse tissue sections of green-lipped mussels 33 days post-injection, a) mussel with infiltration of haemocytes between the muscle fibres as a result of injection and external to adductor muscle between kidney tissue and gill (yellow arrow), b) high number of focal haemocyte aggregations associated to mantle, digestive gland, the gastrointestinal tract and the interstitial space between digestive gland and muscle, c) enlarged view of one of the focal aggregations with ceroid (white arrow) and multiplying *P. olseni* cells, at 66 dpi, d) a naturally infected mussel from the broodstock holding system with *P. olseni* trophozoite (white arrowhead) and rosette stage (yellow pointed arrowhead) cells associated with large aggregation of haemocytes. Comparison of the same microphotograph of an aggregation of haemocytes associated with *P. olseni* stained with, e) Fluorescence *in situ* hybridisation, nuclei of haemocytes are green (blue arrow) and *P. olseni* positive cells are magenta (white arrowhead), autofluorescence (yellow: white arrow) is likely to be phagocytosis, and f) traditional H&E staining, detectable *P. olseni* cells (arrow).

Section 4: Disease progression of *Perkinsus olseni*.

7.3.2. *Perkinsosis in experimentally infected mussels*

Based on the initial histological assessment, all mussels in the experimental scenario were observed to begin the trial in good health and condition. In the day 0 sampling group, and the control groups, all mussels had APX, and none were observed to have *P. olseni*. All the mussels in the *P. olseni* infected group had APX, one mussel had *Microsporidium rapuae*, a second individual had an unidentified apicomplexan and 59.5% of the group were *P. olseni* positive based on standard H&E histology.

The experimentally injected mussels displayed more population variation in glycogen-like storage material in the mantle tissue than in the naturally infected mussels. For instance, in two *P. olseni* positive mussels where intensity was considered as high, one had no storage cell material, and the other was dense and well packed. Additionally, 35% of mussels had a small number of thinning digestive gland tubules; as with the natural mussel population (section 7.3.1), this is likely to have negligible effect in terms of overall health. Ceroid was detected in all mussels, however, similarly to the naturally infected mussel population, intensity was low and also associated with APX. Most of the mussels were recorded as spawning, spent or resting. Furthermore, across all the treatments, including the baseline, there were 25 females, 25 males and 21 where sex was unidentifiable. Due to the low sample size for each treatment, it was difficult to determine if conditions such as glycogen levels and reproductive status influenced *P. olseni*.

Surprisingly, focal haemocytosis was not detected in the baseline or the control and zoospore treatment at 33 days post injection (dpi). At day 33 100% of the trophozoite treatment had focal haemocytosis and a grade of 1.2. At day 60 percent population prevalence for the controls, trophozoite treatment and zoospore treatment was 20%, 94% and 77%, and 1, 2.1 and 1 for grade of focal haemocytosis, respectively. There was an increase in the focal haemocytosis grade at day 60 in the trophozoite treatment ($\beta = 0.984$, $SE=0.356$, $p= 0.006$). Furthermore, the presence of *P. olseni* resulted in the increased likelihood of a higher focal haemocytosis grade ($\beta = 17.26$, $SE=0.36$, $p< 0.001$).

No mussels were identified as *P. olseni* positive in the zoospore treatment at day 33 or day 60 using histological techniques but 8 were positive in the RFTM at day 60. Whilst the percent prevalence of mussels with *P. olseni* trophozoites ('signet ring' cells) and schizonts (vegetative daughter cells known as rosettes) prevalence in the trophozoite treatment was 88% and 75% respectively, at day 33 and 100% and 12% at day 60. The DSe and DSp at day 33 was 87.5% and 50% and at day 60 100% and 100% respectively.

The trophozoites were the main life stage detected and were on average $4.1\mu\text{m} \pm 1.7\mu\text{m}$ ($n= 100$). The size of these trophozoites did not change between the two time points ($w=1284.5$, $p= 0.64$). However, the trophozoites were also smaller than those detected in the naturally infected population ($w=1019$, $p=<0.001$). Although the trophozoite sizes were different there were no observable

Section 4: Disease progression of *Perkinsus olseni*.

differences in the appearance of *P. olseni* life stages between the experimentally injected mussels and the naturally infected mussels (Fig. 7.2 a, b, c). The experimentally injected mussels were also observed to have clusters of rupturing schizonts and developing trophozoites (Fig. 7.2 b). The mussels at 33 dpi were considered as having low intensity, based on the *P. olseni* criterion (Table. 7.1: column 2).

There was a statistically significant difference in the *P. olseni* cell counts between time points ($z = 2.82_{(44)}$, $p = 0.005$) with a 6.75-fold increase in expected counts between 33 dpi and 60 dpi. While there were no differences in the counts between the tissue types, the intercept was significant with an expected count of 0.179. This difference indicates that the expected count in the reference tissue and time point (adductor muscle and day 33) was statistically different from zero (expected count at time 0) ($p = 0.04$). While there were no differences detected between the different tissue types there was a trend with more *P. olseni* cells observed in the mantle tissue, the interstitial connective tissue of the gastrointestinal tract (GI), and the digestive gland tubules (DG) (Fig. 7.3 and 7.4).

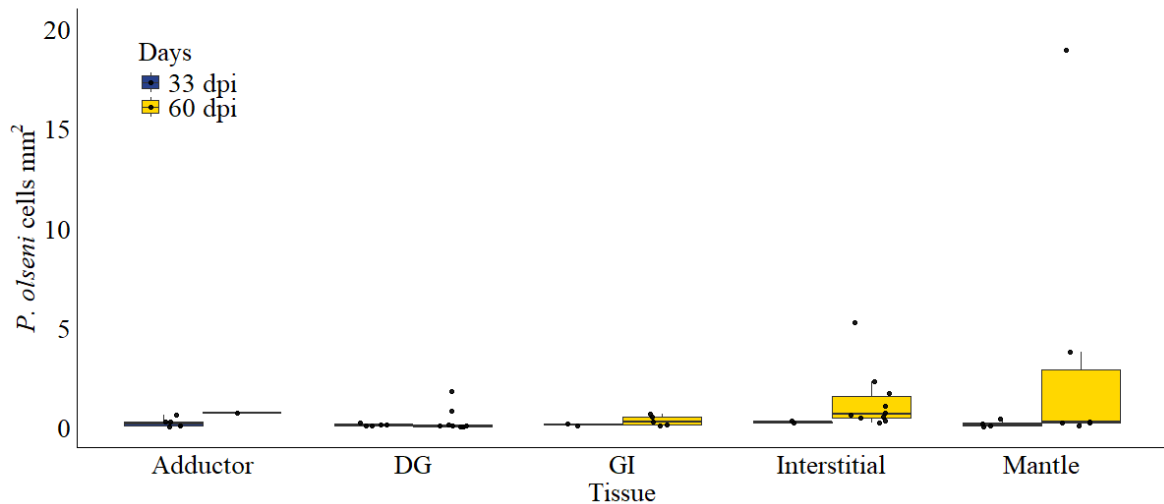


Figure 7.4 *Perkinsus olseni* cells per mm² detected in each tissue type of the mussels that were *P. olseni* positive. *Perkinsus olseni* cells were counted 33 days post injection (dpi) (Blue/Black) adductor (n = 6), DG (n = 5), Gastrointestinal tract (GI) (n = 2), Interstitial (n = 2), Mantle (n = 4), and 60 dpi (Yellow) adductor n = 1, DG n = 9, GI n = 5, Interstitial n = 10, Mantle n = 6). The outliers on the digestive gland (DG), interstitial and mantle are from one individual mussel.

Furthermore, diffuse haemocytosis was observed in two individuals of the experimentally injected group, one of which contained *P. olseni* cells within the epithelium wall that appeared to be associated with a pink substance, possibly lectin secreted by the haemocytes (Kim et al., 2006c) (Fig. 7.5). This may potentially be early development of a pustule as it appears to be affecting the epithelium layer of the mantle or displaying autolysis of the associated mantle tissue, based on the loss of column architecture of the epithelium (Fig. 7.5).

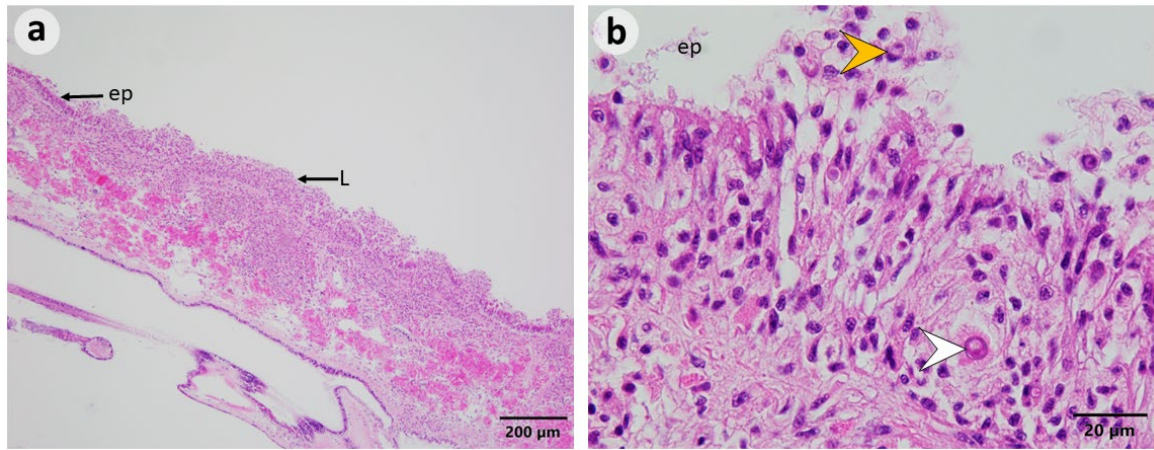


Figure 7.5 Histological (hematoxylin and eosin) micrographs of transverse tissue sections of green-lipped mussel mantle tissue two months post *P. olseni* injection (60dpi), a) very high diffuse haemocyte aggregations in the mantle on the shell edge (L) potentially disrupting the epithelial layer (ep), b) oil immersion 1000x view of the disrupted epithelium with *P. olseni* cells identified external to the epithelial layer (yellow arrowhead) and within the epithelial layer (white arrowhead).

The utilisation of the proposed *P. olseni* scheme showed that overall, the scores were low and observed to be around 5 for the experimental group and the naturally infected group. However, there were several outliers in the 66 dpi and Nov-21 group and an increase in spread of the data at 66 dpi highlighting population variation and inter-individual differences. Therefore, there were no statistical differences detected between the four sample groups ($\chi^2 = 3.4_{(3)}, p = 0.34$) or the combined natural versus the injected treatments ($\chi^2 = 2.2_{(1)}, p = 0.14$) (Fig. 7.6).

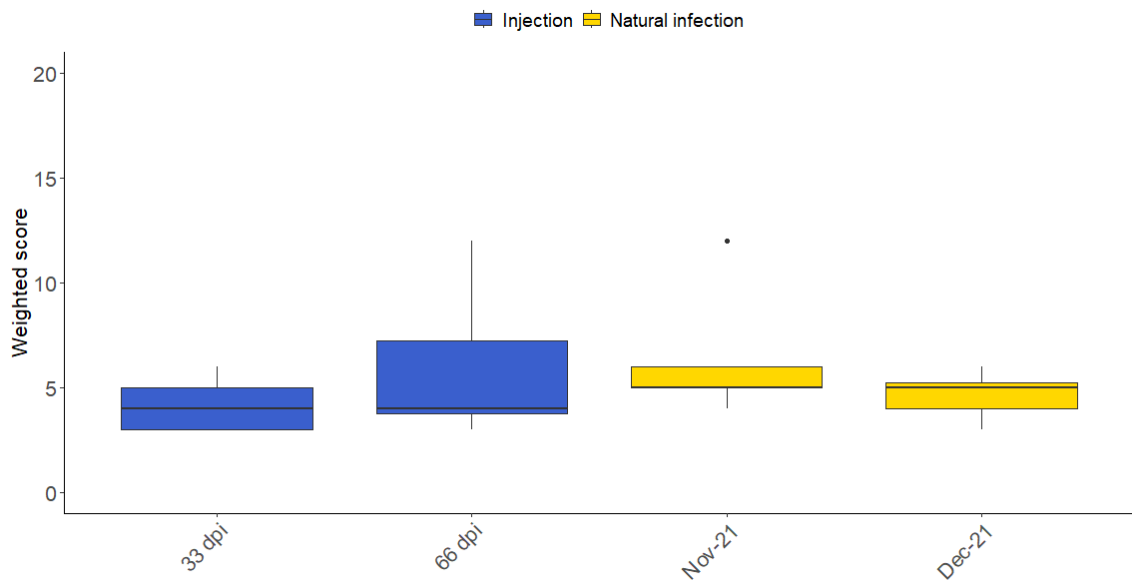


Figure 7.6 The weighted histopathological score (Table. 7.1) for the *P. olseni* injected mussels at 33 days post injection (dpi) (n = 8) and 66 dpi (n = 16) and naturally *P. olseni* infected mussels detected and collected November 2021 (n = 5) and December 2021 (n=8). The middle line of each box indicates the median.

There was a strong positive correlation between the size (mm²) of the haemocyte aggregation and the number of cells detected ($R^2 = 0.99$) (Fig. 7.7 a). Although there was a large size range of focal haemocyte aggregations overall the immune response appeared high with a high number of haemocytes associated with *P. olseni* cells in both the naturally infect and injected mussel populations (Fig. 7.2 d, e, and f). However, there was also a high variation of *P. olseni* cell numbers within haemocytes of similar sizes (Fig. 7.3). There was an increase in the number of *P. olseni* positive cells identified using the F-ISH techniques in comparison to the H&E ($F_{1,38}=101.3$, $p<0.001$). (Fig. 7.7 b).

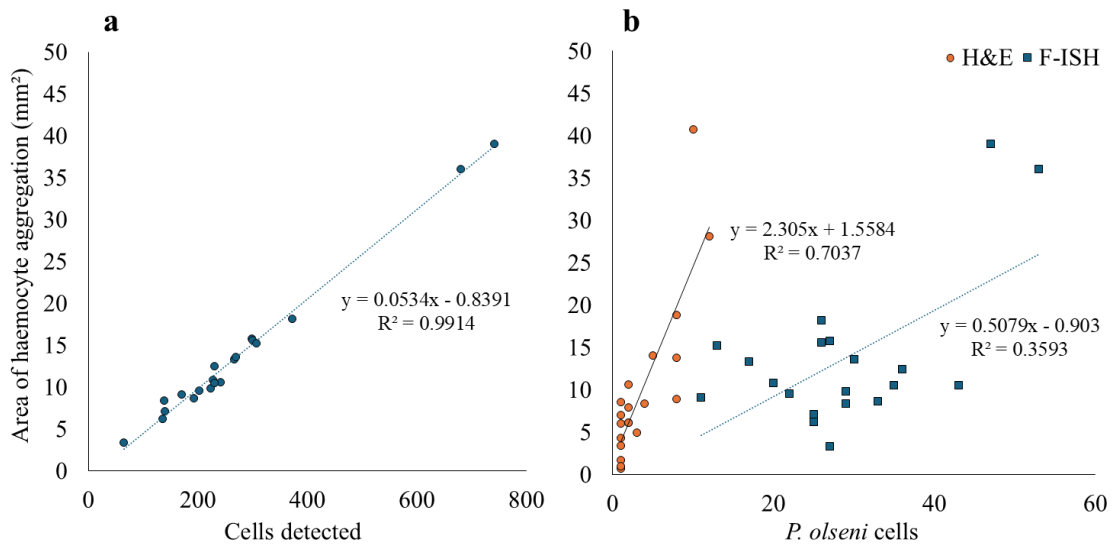


Figure 7.7 Image analysis and quantification of a) total cell number detected within the focal haemocyte aggregation, and b) the number of *P. olseni* cells within the focal haemocyte aggregation.

7.4. Discussion

This appears to be the first report investigating the disease progression of *Perkinsus olseni* in green-lipped mussels in an experimental infection study using traditional histology and fluorescence *in situ* hybridisation techniques. Based on similarities observed in the *P. olseni* cells of the subculture, the host response and *P. olseni* proliferation in the green-lipped mussel naturally infected and the culture injected mussels, the *P. olseni* cells are viable and pathogenic. The mantle tissue and the interstitial haemal space (the connective tissue between the digestive gland, pallial cavity and the muscle), appear to be the primary locations for proliferation of *P. olseni*. Encapsulation of rosette cells was detected in the naturally infected mussels (Fig. 2). Furthermore, disruption of the mantle epithelium and the first identification of very early potential pustule development was detected in a *P. olseni* culture infected mussel. The proposed histology-based scoring criterion also allowed for increased sensitivity and improved accuracy of infection intensity. Lastly, F-ISH detected more *P. olseni* cells compared to traditional H&E and was an improved method for quantification.

No *P. olseni* infections or disease were detected in the initial histological assessment of the injected Time 0 samples or the controls throughout the study. RFTM confirmed the negative status. From the onset of infection until the first sampling time point through histological investigations the *P. olseni*

Section 4: Disease progression of *Perkinsus olseni*.

cells appeared to rapidly spread through the circulatory system of the green-lipped mussel tissues such as the mantle based on the detection and injection location (adductor muscle haemolymph sinus).

The circulation of *P. olseni* cells was also based on the continuing trend at the second sampling time point, where proliferation of *P. olseni* was occurring primarily in the mantle where gonad development occurs and interstitial tissue between the digestive gland and the foot. These are the main locations of proliferation where nutritional conditions may be more favourable for the parasites. Lipids and glycogen are required for *P. olseni* development, and are typically acquired from the host mantle, digestive gland and/or muscle tissue (Lee et al., 2001; Park and Choi, 2001; Soudant et al., 2013). *Perkinsus* spp. trophozoites are therefore frequently found in the mantle, gonad, base of the gill filaments, and interstitial spaces between the digestive tubules. This has been observed in the green-lipped mussels within this study as well as previous studies (Muznebin et al., 2022a; Lane et al., 2023) and other species such as the Manila clam, *Tapes philippinarum*, (Lee et al., 2001) and the foot muscle in the abalone, *Haliotis iris* (Muznebin et al., 2021; Handler, 2022). Furthermore, the preference for certain tissue types and their biochemical components can impact the lifecycle of *Perkinsus* sp., drive expansion within the host, promote persistence and amplify transmission potential (Carella et al., 2023).

The advancement and usage of *in vitro* cultures of *Perkinsus* spp. are continuing to improve the understanding of host-pathogen interactions and disease progression (La Peyre, 1993; Soudant et al., 2013; Li et al., 2019; Carella et al., 2023). Furthermore, it allowed for observations of similarities and differences in *P. olseni* infections between green-lipped mussels and other molluscan species. The life cycle of *P. olseni* in green-lipped mussels resembled *P. olseni* in *Haliotis iris* and *P. marinus* in the oyster *Crassostrea virginica*, whereby trophozoites (signet ring), mature and recently ruptured, young trophozoites, as well as rosettes were detected. Additionally, it was initially considered that *P. olseni* cells in green-lipped mussels were smaller, with very few cells aggregating, no external lesions and very rare occurrences of encapsulated rosettes (Muznebin et al., 2022a; Lane et al., 2023). The *P. olseni* cells do tend to be smaller and no pustules or nodules have been detected when compared with other species such as abalone (Handler, 2022), scallops (Bower et al., 1998; Carella et al., 2023) and clams (Navas et al., 1992; Choi and Park, 1997; Carella et al., 2023). However, in terms of the immune response the strong response *P. olseni* elicits is reasonable as there were more cells detected using F-ISH than identified using standard histology hematoxylin and eosin staining. Furthermore, only one mussel from the naturally infected population exhibited encapsulation of *P. olseni* cells. Typically, encapsulation processes and immune responses to *P. olseni* continue to increase until pustules or abscesses become detectable in host mantle or foot tissue (Villalba et al., 2004; Soudant et al., 2013; Handler, 2022; Carella et al., 2023). These pustules are creamy white and occur in heavy infections (Villalba et al., 2004; Soudant et al., 2013; Handler, 2022; Carella et al., 2023). However, these have yet to be identified in green-lipped

Section 4: Disease progression of *Perkinsus olseni*.

mussels. It is likely that under optimal conditions the immune capabilities of green-lipped mussels can defend against *P. olseni*. However, the time scale may also not be sufficient for the infection to run its course. Therefore, further research is required to determine how long is required to induced transmission and/or mortality as well as elucidating how other stressors, such as thermal stress, will impact the host response and disease development.

Resistance to any disease depends on the development of the host immune response (Ordás et al., 2000). The increased response to *P. olseni* in green-lipped mussels indicates there is enough energy for defence capabilities. However, the two individuals that displayed areas of diffuse haemocytosis are of interest. The diffuse haemocytosis and *P. olseni* also appeared to be impacting the epithelium of the mantle at the shell edge. These haemocyte aggregations and epithelial damage could either be the beginning of a developing lesion, or pustule, or coincidental epithelial damage from the shucking process. However, in clams, *P. olseni* is known to damage basal membranes and destroy the epithelia of the digestive gland and gills, resulting in host vulnerability to secondary bacterial infections and risk of mortality (Montes et al., 1996; Soudant et al., 2013; Carella et al., 2023). Conversely, *P. olseni* in other species such as the mussel *Mytilus galloprovincialis* very rarely impacts the epithelial tissues (Carella et al., 2023). If the present observations were an artifact of sampling, a loss of the epithelial layer without a thinning or a folding would be expected, however in this study it appears to be intact, the columnar architecture is loose, indicating disruption. Future investigation is required to elucidate this impact.

Pathogens such as *P. olseni* are typically exposed to the external barriers and epithelial layers of the host tissue prior to entry. Chintala et al., (2002), and Pales Espinosa et al., (2013) have suggested that uptake of *Perkinsus* cells, e.g. *P. marinus*, may occur through diapodesis, whereby *Perkinsus* cells are transported through the epithelial layers of, primarily, pallial organs by haemocytes. However, further research is required on how the *P. olseni* evades the host's defences and traverses the epithelia. Due to the similarities between the naturally infected and the culture injected cells, and the lack of mortalities, injection of the *P. olseni* into the haemolymph through the adductor muscle appears an appropriate method for understanding disease progression in green-lipped mussels. Although there are several other methods of pathogen introduction, including gastrointestinal track intubation, shell cavity injection and feeding/ filtering, these require the parasite to cross the epithelial layer. Depending on the host resistance, these methods may be unreliable, risky and require long term (greater than 3 months) holding of mussels and increased sample numbers over time (Chintala et al., 2002). The injection method is suggested to be the most effective and accurate way of infecting individual mussels for research purposes (Chintala et al., 2002). A larger experiment using both bathing techniques and injection methods, followed by the addition of an environmental stressor, such as temperature, should be conducted in the future. This will allow for exploration of parasite shedding and entry when the host is under stress.

Section 4: Disease progression of *Perkinsus olseni*.

To investigate *P. olseni* disease progression several techniques were required. Histological observations are typically biased toward the larger trophozoites and rosette stages, highlighting the need for other supporting techniques such as fluorescence *in situ* hybridisation (F-ISH), PCR and RFTM. Traditional H&E histology was suitable for general assessment and often the most appropriate to describe disease progression. Histology is an ideal technique when quantifying *P. olseni* cells, however fluorescence *in situ* hybridisation offered improved cell detection to validate the histological analysis. F-ISH increased sensitivity and specificity, while H&E allowed for a broader view and allowed for the detection of other parasites that may elicit a host response as well, such as APX. Furthermore, other techniques, including RFTM, were effective for identifying *P. olseni* cells but had low specificity and no ability to describe impact on host tissue.

The associated time, costs and specialised equipment required for F-ISH often means that these techniques are not available, and collaborative relationships are required. Therefore, traditional H&E will continue to be the go-to technique; as such, semi-quantitative scoring systems are likely to continue to be key for assessing pathogen intensity. However, for *Perkinsus* sp., prior scoring criteria are based on RFTM methods and transferred to histological assessments or based on other parasite species, e.g. APX (Kim et al., 2006a; Suong et al., 2018; Muznebin et al., 2022a; Copedo et al., 2023) (Chapter 2 and 5). As such the proposed scoring criteria presented aimed to provide a more comprehensive grading system to improve accuracy compared with the original 0 to 5 grading scale. It is worth highlighting that there are several assumptions and limitations with the proposed scoring. The scoring systems assumes a reasonable quality section obtained using the typical histological section methods proposed by Howard (2004). It assumes at least 5 tissue types will be detected, and equal distribution within the tissues. All section used in this experiment met the first two assumptions. The assumption of equal distribution also becomes the first limitation, as the tissues can be of varying sizes and the mantle can be larger or smaller depending on nutritional status and condition. Haemocytosis can be associated with other conditions, parasites and pathogens, which needs to be taken into consideration when using the scoring. The *P. olseni* cell numbers will depend on the life stage, age and size of organism being assessed. Lastly, lesions associated with necrosis and pustules have yet to be observed in green-lipped mussels and a systemic *P. olseni* infections have only been observed and theorised in a thermal challenge trial (Chapter 5). Although there are limitations, the data collected here are considered fundamental to understanding the disease progression in green-lipped mussels.

Although speculative and not the focus of the current study, mussels with the highest *P. olseni* intensity -whether naturally infected or injected – did not appear to show noticeable impacts on growth, reproduction or survival. This suggests that the infection intensity may not be high enough to impact host condition, such as slowing gametogenesis or reducing reproductive output. Alternatively, it may indicate a current balance in host pathogen co-evolution. Reduced growth and castration of reproductive capacity with *P. olseni* infection has been observed in highly affected

oysters and clams (Villalba et al., 2004; Soudant et al., 2013). However, Dittman et al. (2001) found that this was limited to highly infected oysters during spring, when gametogenesis occurred. Casas et al. (2002) also observed reduced storage (glycogen) tissue and gametogenesis in early spring in carpet-shell clams (Villalba et al., 2004). Furthermore, although green-lipped mussels have previously been suggested to be a poor host for *P. olseni* (Lane et al., 2023), based on the development of the *P. olseni* cells and the host immune response within this research, as well as the co-evolution theory, the green-lipped mussels may become a good host in the future. It is worth noting that pathogen evolution typically occurs to optimise reproductive output, whereas the host will evolve to minimise the fitness cost related to immune defence (Perlman, 2013). Additionally, pathogens can potentially moderate host population thereby driving selection towards resilient genes in future generations. Similarly, the hosts can drive a progressive loss in mechanisms relating to immune invasion, thereby reducing infectivity (Seal et al., 2021).

Despite the advancement in knowledge of *Perkinsus* spp./ host interactions worldwide and the increasing number of techniques available, there are typically no “early clinical warning” signals (Soudant et al., 2013). The same applies to green-lipped mussels where *P. olseni* has yet to be elucidated as a pathogenic agent of mortality. This is supported by the current study, where no mortalities were observed, even with injection injury. This indicates that in adult green-lipped mussels *P. olseni* is potentially a long-term chronic disease related to accumulation and age. This has been observed in clams and the oyster, *Crassostrea virginica*, whereby the time to mortality can be up to one to two years post infection (Chong, 2022c; OIE, 2024). Thereby the status of *P. olseni* in green-lipped mussels could be considered as an enzootic disease rather than epizootic disease as there is typically a low prevalence of the parasite in the wild population (Shapiro-Ilan et al., 2012). However, with the influence of climate change, warming waters may cause an epizootic wave whereby *P. olseni* moves into an epizootic cycle and impacts a higher prevalence of the population (Shapiro-Ilan et al., 2012). Thermal and salinity stress are two of the important factors regulating perkinsosis development (Soudant et al., 2013), therefore thermal stressor and heat wave scenarios should be assessed to further our understanding of future *P. olseni* advancement and disease progression.

7.4.1. Conclusion

The *in vitro* culture research has provided a unique opportunity to enhance our understanding of green-lipped mussels - *P. olseni* relationship without additional environmental stressors, such as thermal and salinity stress. *P. olseni* was primarily detected in tissues with optimal and nutrient rich host biochemical components such as the mantle where gonad development occurs and interstitial tissue between the digestive gland and the foot. The movement and development of the *P. olseni* cells in the tissues of the experimental, green-lipped mussels when compared to the naturally infected population provided confidence in the methodology and allowed for the investigation on disease progression and overall impact on the host. The proposed histological scoring allowed for an

Section 4: Disease progression of *Perkinsus olseni*.

improved grading of *P. olseni* infections and is more transferrable to real world scenarios with reduced risk of concern of misinterpretation of high grades. The immune response detected also appears reasonable as there were many more cells detected in the F-ISH staining techniques compared with the low numbers typically detected with the H&E staining. However, many researchers may not have access to laser scanning confocal microscopy and quantitative analysis capabilities, therefore traditional H&E is still likely to be the most used technique. The research highlights the abilities of laser scanning confocal microscopy to support areas or parasites of interest in histology. The integrated histology techniques also allowed for the access of precise time points to understand the disease progression in detail. Finally, research such as that presented here allows for the understanding of host-pathogen interactions which is fundamental to predict, mitigate and manage diseases under future climate scenarios. The work presented highlights potential risks for the marine farming industry, particularly if green-lipped mussels is a vector for *P. olseni*, and farms are established in regions where environmental conditions are optimal for proliferation. Furthermore, there is a necessity to expand experimental infection research to assess the role of environmental factors such as temperature and salinity on the prevalence, proliferation and infectivity of *P. olseni* in green-lipped mussels.

SECTION 5. GENERAL DISCUSSION

In this Section:

Chapter 8: General discussion

CHAPTER 8. GENERAL DISCUSSION

8.1. Discussion*8.1.1. Overview*

The research presented in this thesis has focused significantly on the scientific field of, the effects of, environmental stress on molluscs, *Perna canaliculus* and *Haliotis iris*, and the disease progression of *P. olseni* in green-lipped mussels. The overall aim was to “**explore the environment-host-pathogen interactions in relation to heatwave-related stressors affecting two molluscan study species, *Perna canaliculus* and *Haliotis iris*, and their shared parasite *Perkinsus olseni*,**” using, primarily, histopathological techniques. As observed in both species, in the natural environment there are several environmental factors to consider in addition to elevated sea surface temperature and marine heatwaves. These include increasing sedimentation and decreasing salinity because of rainfall and flooding. Furthermore, biological factors such as growth, reproduction and parasite-disease interactions are also critical when determining optimal physiological condition of the species (Gosling, 2015b; Esposito et al., 2022). The effect of the environment on reproductive condition, pathogen diversity, disease progression and deposition of ceroid, as well as their interactions detected in both the field and the laboratory studies, are of particular interest for this research. Temperature was highlighted as the primary stressor and burgeoning issue impacting the fitness and health of molluscs, and is a key theme threaded throughout this thesis.

The following discussion outlines and integrates several key outcomes and conditions detected in relation to the initial overarching questions proposed in section 1.8 of the introduction, then delving deeper into the complexities of the host-pathogen-environment interactome, the risks to wild and farmed marine organisms, stewardship and guardianship of marine organisms, limitations to the work conducted and future recommendations as research avenues through investigation of the two model species: the bivalve, green-lipped mussels, and the gastropod, *H. iris*.

The subsequent sections aim to provide integrated discussion to the initial overarching questions:

1. What is the tissue-level impacts of marine heatwave-related stressors? And are organismic changes indicative of these stressors?

Field and laboratory studies demonstrated the impacts of thermal stress on reproductive capacity, pathogen assemblage and several pathological indicators, including ceroid, haemocytosis and digestive gland atrophy. Furthermore, it was demonstrated that increased mortality occurred in bivalves that had extended periods of food deprivation and were exposed to warmer sea water temperatures (22°C), when compared with those that had access to copious levels of food. Laboratory studies corroborated the field findings and provided insight for hypothesis development which will also be discussed in greater detail.

2. What are the implications for reproductive performance and is there evidence for resource recycling from reproductive tissues under stress?

The implications for reproduction inferred from the research include changes to gametogenesis in the form of prolonged ripening and spawning periods, with potentially smaller follicles. Importantly, increased oocyte atresia was observed and should now be expanded to consider other populations. Based on the field investigations of green-lipped mussels and *H. iris* the increased oocyte atresia indicates resource recycling, although this also requires further investigation. Experimental challenges did not allow for full completion of this question; however, the research did allow for methodology exploration and hypothesis development.

3. Do opportunistic pathogens take advantage of the host stress and exacerbate environmental effects?

The increase in parasite assemblage in the green-lipped mussels sampled in August 2019 suggests that they infect when the host is allocating more energy to physiological processes such as gametogenesis and spawning. However, peak parasite richness did not always occur at the same time and drivers should be interpreted cautiously. Furthermore, it is still unknown when *Perkinsus olseni* infects its host, but it seems likely that they would infect due to increased access to glycogen as a food source, which drives proliferation and growth of the *P. olseni*. The period when the mussel building glycogen stores for physiological activities, such as gametogenesis, may therefore be targeted. The *P. olseni* would then be detected after a period of proliferation, as observed in Chapters 2, 5 and 7. Additionally, the *in vivo* experiments using *in vitro* cultures of *P. olseni* injected into green-lipped mussels indicates these methods are powerful in investigating disease progression (Chapter 7).

8.1.2. *Effects of the environmental stressors on molluscs*

New Zealand's coastline, with its wide temperature range and high biodiversity, is increasingly being affected by a changing climate. Rising sea surface temperatures (SSTs) around the NZ coastline now frequently reach 25°C (Delorme et al., 2024), including the Coromandel region presented in Chapter 2. These warm temperatures (25 – 26°C) approach critical thermal tolerance limits for not only green-lipped mussels (Ericson et al., 2023; Benjamin et al., 2024), but also *Haliotis iris* and many other endemic marine organisms. The strongest NZ summer marine heatwave on record was the 2017/18 event (Salinger et al., 2019), however since then two others have come close; the summers of 2021/22 (Montie et al., 2023), and 23/24 (Chapter 2). Temperature is not the only stressor associated with a changing climate; increasing incidences of extreme precipitation are also leading to more flooding events (Houghton et al., 2001; Booij, 2005). Rising levels in freshwater bodies are inundating surrounding areas (Jacobs et al., 2000), sending sediment-loaded and contaminant rich water into the coastal environment. These abrupt changes resulting from warming and flooding events are

increasingly impacting marine organisms and ecosystems, their performance, and their ability to respond to additional and future stressors (Talbot et al., 2018; Pourmozaffar et al., 2019) (Chapter 6).

Histological investigations in both field and laboratory studies showed that prolonged exposure to thermal stress was associated with suspension of gametogenesis, increased prevalence and accumulation of ceroid, and increased prevalence and diversity of pathogens and parasites, including *Perkinsus olseni*, in green-lipped mussels (Chapters 2 and 5). Marine ecosystems are perpetually changing, with fluctuations often exacerbated by climate disruptions such as marine heatwaves (Chapter 2), and flood events (Chapter 6). Present and future climate change influences on preexisting environmental stressors, including rising temperature and salinity fluctuations, are of major concern for several key molluscs. These environmental changes can impact reproductive processes such as timing, synchronicity, fertilisation, and recruitment success. In particular, the combined effect of temperature and pathogen presence can lead to a loss of propagules, low gamete quality and premature spawning of under-developed gametes (Walther et al., 2002; Philippart et al., 2003; Petes et al., 2007; Petes et al., 2008). These stressors contribute to reduced survival and increased vulnerability in larvae, poor larval development, reduced settlement and a reduction in later survival through to spat and adulthood. Ultimately reducing future broodstock numbers in the wild (Walther et al., 2002; Philippart et al., 2003; Petes et al., 2007; Petes et al., 2008). Regarding reproductive capability, atresic oocytes are consistently present at each stage of the gametogenesis cycle (Chapter 2, 4, and 5). It is essential to further investigate how ongoing environmental and pathogenic stressors are likely to inhibit oocyte development and the intensity of atresia.

Elevated levels of oocyte atresia were detected when assessing the oocyte development in the field investigations of green-lipped mussels and *H. iris*. The elevation of this pathology is based on personal experience through comparisons with other archived histological slides (Chapters 2 and 4). It appears that atresia is a potential resource for energy particularly in suboptimal conditions and it can be present through all gametogenesis stages. Furthermore, it was also found that *H. iris* could potentially maintain reproductive condition and use the older oocytes through atresia as a source of energy to maintain development of the younger, potentially more viable oocytes (Chapter 4). Although, there are only a few histological investigations on gametogenesis for green-lipped mussels and *H. iris*, a better understanding of their reproductive biology is critical in not only wild populations, particularly the exploited early life stages, but also in managing populations of molluscs in fisheries and aquaculture (Chérel and Beninger, 2017).

In *H. iris* there were also other impacts and associations, including kidney stones and slow growth, which was correlated with accumulation of ceroid material (Chapter 3 and 4). The intensity of ceroid also was higher in *H. iris* compared with green-lipped mussels within this study. The proliferation of ceroid could be associated to with several factors. One possibility is suboptimal environmental

conditions, as *H. iris* likely has a narrower thermal tolerance range. For instance, Nguyen et al. (2023) found that in *H. iris* prolonged periods (weeks) of temperature above 18°C resulted in energy demand exceeding supply, increasing vulnerability to thermal stress during the summer period. Another factor could be the age of the organism, including differences between the physiological vs chronological age (e.g., Basova et al., 2012) as discussed in Chapter 3, 4, and 5, or 3) pathogens, however in this study only two parasites were detected histologically in *H. iris*, the haplosporidian-like parasite and the gill ciliates (Chapter 3 and 4). In contrast 11 were detected in *Perna canaliculus*, with three types of intracellular bacterial colonies (one *Endozoicomonas*-like), rod bacteria, *Microsporidian rapuae*, a hydroid species, *Bucephalus* sp., an unidentified multinucleate parasite (Chapter 2), APX, copepods and *Perkinsus olseni* (Chapter 2, 5 and 7).

When considering the relationship between the physiological age, the functional age, and the chronological age, life expectancy is of particular interest (e.g., Basova et al., 2012) and could provide a better explanation of the elevated presence of ceroid in the model gastropod (*H. iris*). The distinction between ceroid (pathology related) and lipofuscin in molluscan species still requires investigation. However, similarly to mammals, accumulation of lipofuscin reflects cellular wear-and-tear (Terman and Brunk, 1998; Seehafer and Pearce, 2006), while ceroid is associated to pathological conditions and immune response (Basova et al., 2012; Carella, 2015). It is well known that both ceroid and lipofuscin can catalyse their own formation and can therefore accumulate further (Jung et al. (2007a) (Chapter 2). The combination of aging, as well as the influence of environmental factors, is the most probable cause of this elevated deposition. If the ceroid is making the molluscs physiologically older than their chronological age it could complicate age assessments in long living molluscs. *Haliotis iris* reaches maturation at four years of age (60 – 100mm) (Poore, 1973) whereby green-lipped mussels reach maturation within the first year (40 – 50 mm) (Jeffs et al., 1999), meaning ceroid-lipofuscin deposition is likely to be more pronounced in slower-growing, older, molluscs such as *H. iris*.

The idea of physiological aging vs chronological aging and the higher-than-expected atresia in the females of the molluscan populations also leads to further questions such as do shellfish have reproductive biological clocks? Is there an optimal age for spawning and are gamete quality and quantity mutually exclusive? Furthermore, does the interaction of physiological age and environmental stressors influence overall fecundity and oocyte viability? It is well known that molluscs are driven by biorhythms to account for environmental oscillations (tidal, circadian, circalunar, seasonal/annual) (Tessmar-Raible et al., 2011; de la Iglesia and Johnson, 2013; Bulla et al., 2017; Tran et al., 2020). These oscillations impact timing of spawning, synchronisation, initiation of gametogenesis (de la Iglesia and Johnson, 2013), but do they also impact egg quality, optimal fecundity age, and optimal spawning or spawning age? Alternatively, are molluscs likely to spawn and reinvest energy into the development of new oocytes or recycle energy from unspawned oocytes (atresia) (Chérel and Beninger, 2017; Chérel and Beninger, 2019)? Although these questions could

not be answered in the present study they do highlight potential interesting avenues for further research, which could improve broodstock conditioning and increase overall fecundity and larval numbers (section 8.1.8).

Due to the complex nature of the marine environment, a comprehensive investigation is required to elucidate its influence on molluscan physiology, reproductive biology and pathogen diversity, through both laboratory and field studies (e.g., Ewere et al., 2021; Xu et al., 2021; Copedo et al., 2023; Ericson et al., 2023; Venter et al., 2023). Although it is difficult to extrapolate biological responses from laboratory experiments to the field, both are required when trying to understand future impacts on key species (Riebesell and Gattuso, 2014; Reid et al., 2019a). This is due to the difficulty in extrapolating biological responses from single to multiple stressors, as well as determining which is the dominant stressor, and which combination of stressors impact the biological responses of the organisms of interest in the field (Riebesell and Gattuso, 2014; Reid et al., 2019a). Furthermore, the interaction of these stressors and limited understanding can lead to misinterpretation of impacts on the biological responses (Kroeker et al., 2014; Brennan and Collins, 2015; Humphreys and Browman, 2017; Reid et al., 2019a). Comprehensive baseline monitoring on a multidisciplinary level, over relevant periods, would provide critical knowledge to assist with the understanding of reproductive anomalies, increasing atresia, ceroid as a pathological condition, and advanced senescence. This knowledge will be critical in understanding how environmental changes, along with shift in pathogen diversity and virulence, influence these biological processes.

8.1.3. *Host: pathogen interactions and coevolution.*

Pathogens and parasites are key components to a healthy ecosystem and play a fundamental role in food web interactions, one way is by regulating host populations (Lafferty et al., 2006; Lafferty and Kuris, 2009; Soudant et al., 2013; Bjorbækmo et al., 2020; Lafferty, 2020). The most well understood host pathogen interactions, such as *Perkinsus* spp. (Chapter 7), are based on those organisms which are either commercially harvested or cultivated (Coen and Bishop, 2015), for example green-lipped mussels, or species that have experienced mortality events, for instance the cockle *Austrovenus stutchburyi* (Lane et al., 2020).

Typically, the commercial organisms are grown in high densities to balance survival with growth and economic value. In addition, the high density of molluscan populations in one area (e.g. mussel farms) may increase disease intensity and prevalence through increased contact between individuals (Anderson and May, 1991; Coen and Bishop, 2015). Furthermore, as average sea surface temperatures climb and precipitation increases, encroaching on the suboptimal limits of the host molluscs, pathogens and diseases are likely to impact life history functions (growth, reproduction and survival) (e.g. Lafferty and Kuris, 2009; Coen and Bishop, 2015; Lafferty, 2020). Laboratory and field research has shown that parasites can significantly impact the life history and behaviour of the host population (e.g., Barnard and Behnke, 1990; Byers et al., 2008; Coen and

Bishop, 2015). For instance, the digenean trematode *Curtuteria australis* manipulates the burying behaviour of *A. stutchburyi* by encysting in the foot, leaving the host more vulnerable to predation, thereby allowing for completion of the parasite's lifecycle (Thomas et al., 1998; Lane et al., 2020).

In field samples, two pathogens were detected in *H. iris* and up to 12 pathogens and parasites were detected in green-lipped mussels, as listed in section 8.1.2. This difference may be due to several factors. Firstly, the number of samples assessed. A greater number (>500) of green-lipped mussel samples were collected. Secondly, histology was the primary tool used. Techniques such as metabarcoding may have provided different results. Lastly, the combination of the density of the mussels from the mussel farms when compared with wild populations of the gastropods collected and the warmer temperatures may have contributed (Coen and Bishop, 2015). The number of pathogens detected in the field samples highlights the importance of baseline sampling, of wild populations and continuous monitoring of the farmed populations. These efforts will enable early detection of abnormal tissue conditions and pathogens, which are critical for the survival of any exploited marine organism (Chapter 2).

Three pathogens of the fourteen detected were of particular interest because of their pathogenicity in other molluscs or their apparent affinities with suspected pathogens. The first was a multinucleate parasite found in the right kidney tissue of *H. iris*. This parasite was previously described in the same tissue in association with a haplosporidian-like pathogen by Diggles et al. (2002). Higher numbers of the *H. iris* multinucleate cells were detected in the adults when compared to the subadult populations, suggesting that older hosts are likely to accumulate parasites due to longer exposure time and increased likelihood of ingestion through food (Mouritsen et al., 2003; Lafferty and Kuris, 2009; Coen and Bishop, 2015). Moreover, associations between age and pathogen infection can be positive and negative. For instance, as discussed by Taskinen and Saarinen (1999), larger or older individuals are more likely to invest more energy into reproductive effort. This investment reduces energy for immune defence making them more susceptible (Taskinen and Saarinen, 1999; Coen and Bishop, 2015). However older molluscs also have had more time to develop physical defence mechanisms e.g. thicker and larger shells (Stefaniak et al., 2005; Coen and Bishop, 2015).

The two other pathogens of concern detected in green-lipped mussels were an unknown multinucleate cell and *P. olseni*. The unknown multinucleate cell in green-lipped mussels elicited an immune response in some of the mussels, however this was not associated with a mortality event. Further investigation is required to determine what this unknown cell is, and whether it is still in the population or was a short-lived, incidental, occurrence (Chapter 2). Unlike other species such as *Crassostrea virginica* and *Ruditapes philippinarum* (Villalba et al., 2004; Soudant et al., 2013), when host-pathogen interactions were considered without the influence of the thermal stress, green-lipped mussel growth and reproduction were not impacted. However, only one mussel size range (adults at

approx. 80mm) was used so further disease progression research should incorporate varied sizes and life stages as well as multi-stressor scenarios (Chapter 7).

Interestingly, although *P. olsenii* was detected in green-lipped mussels in the field study (Chapter 2), and the laboratory trial (Chapter 5), it was not detected in *H. iris* during this study (Chapter 3 and 4). However, *P. olsenii* has been previously detected in *H. iris* in other warmer New Zealand localities (Hine and Diggles, 2002; Webb and Duncan, 2019; Muznebin et al., 2021; Lane et al., 2023). *Perkinsus olsenii* is a generalist pathogen, as opposed to a specialist pathogen, and can infect a wide host range across bivalve and gastropod species (Villalba et al., 2004; Itoiz et al., 2021; Carella et al., 2023). It is therefore not surprising that *P. olsenii* is being detected in other species, as the research and surveillance of marine organisms expands. In contrast to its presentation in *H. iris* and other molluscan species, no visible pustules or abscesses were detected in green-lipped mussels, highlighting a key difference within this host species. The limited knowledge around disease progression of *P. olsenii* in green-lipped mussels, its presence in both *H. iris* and green-lipped mussels, its ability to proliferate with increasing temperature and its ability to cause mortality in other molluscan species highlighted the need for further research particularly as marine heatwaves become more intense and frequent.

For the first time disease progression of *P. olsenii* in green-lipped mussels was investigated to understand associated onset of infection and the disease development. The *P. olsenii* cells were similar between a natural infection and injection of cultured cells into the adductor muscle, and the host immune response was also reacted the same. This similarity indicated the *in vitro* techniques are viable methods to investigate proliferation of cells in host tissue. *P. olsenii* elicited a very high immune response and rare occasions of encapsulation in green-lipped mussels. This immune response suggests that development of pustules is possible as the disease progresses, and the pathogen adapts to the host's immune defences (Chapter 7). However, it is also likely that a systemic response, instead of pustule development, may occur particularly if the host no longer has enough available energy to put into localised immune defence, or temperature extends thermal optima of the green-lipped mussels (Copedo et al. 2023) (Chapter 5). To gain an initial understanding of the disease progression and to validate the methodology the environmental component, e.g. temperature, was not included. Therefore, further investigation is also required to elucidate the effects of environmental challenges such as temperature on host-pathogen interactions.

Given the complex nature of host-pathogen interactions, understanding disease progression requires examination of the immune response and consideration of the broader evolutionary context. In this regard, the concept of the evolutionary 'arms race', where hosts and pathogens continuously adapt, coevolution must be taken into consideration (Raberg et al., 2014; Coen and Bishop, 2015).

Coevolution is the net effect of selection in pathogen virulence and pathogenicity to bypass host defences to infect and survive (Coen and Bishop, 2015). As stated by May and Anderson (1979) - and Coen and Bishop (2015) population interactions and relationships must take into account evolutionary pressures on both the hosts and parasites when characterizing infectious diseases.

Parasite and pathogen evolution does not necessarily occur to have a benign or malign outcome on the host but rather to optimise pathogen reproductive output. In this aspect it may be a sound strategy to limit harm to long-standing hosts (Perlman, 2013; Coen and Bishop, 2015). In contrast to the parasite, the host will evolve to minimise the fitness cost related to immune defence (Raberg et al., 2014; Coen and Bishop, 2015). Parasites can also change rapidly in comparison to their host, particularly if an antagonistic coevolution interaction exists. The effects of this selection and coevolution will, over time, shape the outcome of the ensuing disease (Brockhurst et al., 2014; Betts et al., 2016). It is thus critical to understand host pathogen-environment interactions to determine the outcome of a disease (Chapter 7).

8.1.4. A complex interactome: environment: host: pathogen

Marine diseases are broadly categorised as either non-infectious (caused by chronic environmental conditions) or infectious. Marine infectious diseases are the result of complex host-parasite-environment interactions which are often disrupted by changing climate, including global warming and increased precipitation (Harvell et al., 1999; Okamura and Feist, 2011; Coen and Bishop, 2015; Okamura, 2016) (Fig. 8.1). As described in section 8.1.1., the host is influenced by environmental factors which drive growth and reproduction and influence physiological age and immune defence capabilities. Each of which require energy investment and can be a source of stress. For instance, reproduction is an energy-demanding process that may limit the amount of available energy to protect and defend against external stressors and pathogens (Chapter 2, 4, 5, 7). This is primarily due to the constraint in energy allocation and a trade-off is typically required (Brokordt et al., 2019). Furthermore, environmental factors also influence the pathogen pathogenicity, and proliferation. The interaction of host and pathogen is dependent on the external defence, immune system, physiology, genetics and microbiome of the host, and the ability of the pathogen to bypass these systems to establish an infection (Raberg et al., 2014; Guo and Ford, 2016a; King et al., 2019).

The environmental challenge of increasing temperature can degrade the immune system, thus increasing the vulnerability of some host species, thereby enhancing infectivity, proliferation and increased pathogenicity of the pathogen of interest, with resultant induction of infectious disease (Harvell et al., 1999; Soudant et al., 2013; Burge et al., 2014). Furthermore, the pathogen population may increase due to the ability to complete their lifecycle more rapidly (Marcogliese, 2001; Löhmus and Björklund, 2015; Costello et al., 2021; Masanja et al., 2024). It is worth noting that interactions between a host and its pathogens are not fixed and there can be winners and losers. The changing environment could change the response to the host's favour and reduce the pathogenicity of the

pathogen. Other pathogens may decline as they are pushed outside of their thermal optima (Byers, 2021), allowing the host's immune system to effectively remove them (Fig. 8.1). For instance, higher temperatures (29°C) decrease susceptibility of the Pacific oyster, *Crassostrea gigas*, to Ostreid herpesvirus type 1 (OsHV-1) (Delisle et al., 2018).

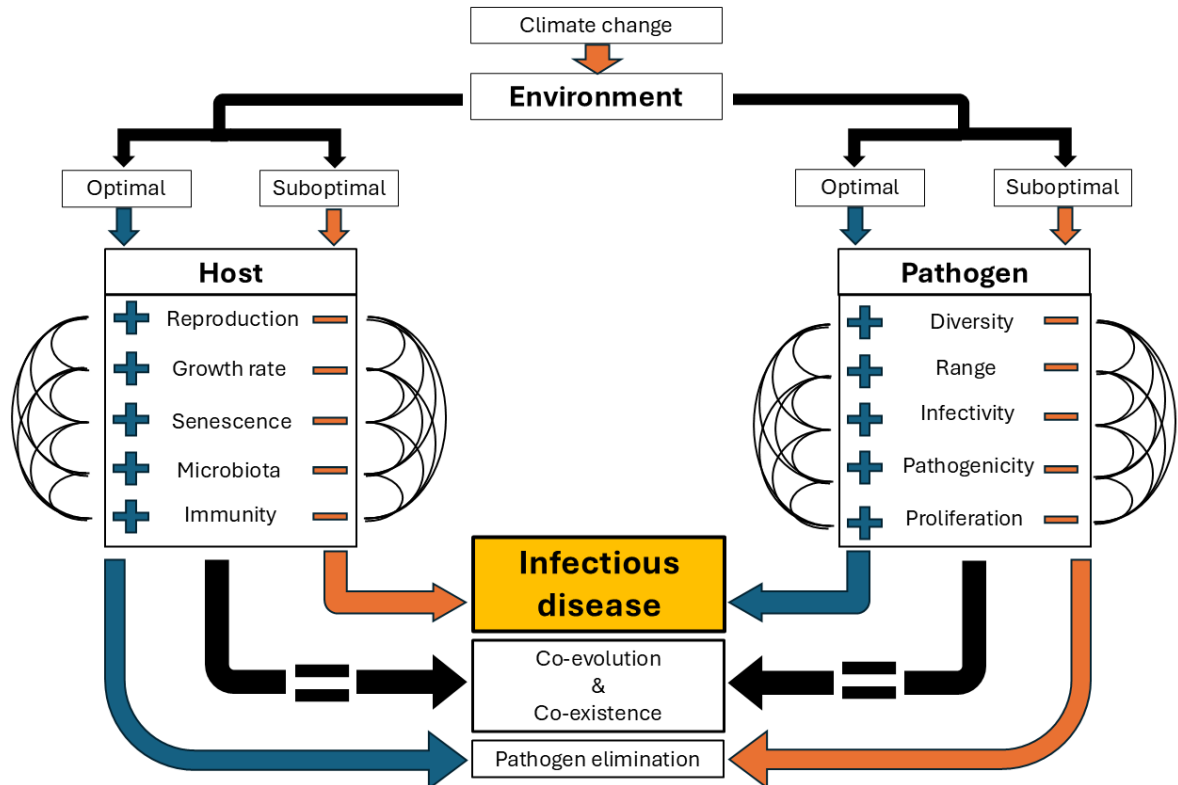


Figure 8.1 A generalised and simplified depiction of the complex nature of the host pathogen environment interactome. Changing climate can either be a stressor for the host or the pathogen, or both. Under optimal conditions the host and pathogen can either compete thereby driving co-evolution or remain in a state of coexistence. However, if the host becomes stressed either by the environment, by its own physiology (e.g. reproduction) or by the pathogen infecting the host this will drive disease. The severity of the infectious disease will be in theory moderated by the competing interactions of the environment and/or the pathogen, and the ability of the host to defend against both. In conditions which are optimal for the host and suboptimal for the pathogen disease is not likely to progress and the pathogen may be eliminated.

One such pathogen, *Perkinsus olseni*, emerged as a focus due to its appearance in the warmer temperatures during the thermal challenge trial (Chapter 5), and its disease potential in both selected molluscs. *In vitro* research of *P. olseni* from green-lipped mussels also indicates that 22°C to 24°C is the optimal temperature range for proliferation (Delisle et al., 2025). The earlier detection in the green-lipped mussels in the 24°C treatment 6 months prior to the 21°C treatment in Chapter 5 may also indicate increased proliferation and reduced green-lipped mussel immune defence (Chapter 5). The earlier detection in the 24°C could also be explained by the thermal optima of the host and pathogen. While *P. olseni* proliferated well in the 22°C *in vitro* trial, this temperature is only just reaching the transition region to the sub-optimal range for green-lipped mussels. As a result, the host's immune system may be more effective in resisting infection much longer than when

maintained at 24°C (Chapter 5) (Fig. 8.2). When the putative thermal optima of both green-lipped mussels and *H. iris* are combined with the *P. olsenii* proliferation curve there is extensive overlap (Fig. 8.2). However, for the *H. iris* the thermal tolerance range is potentially narrower, and it is hypothesised that *P. olsenii* was not detected due to the reduced population density and cooler regional temperatures.

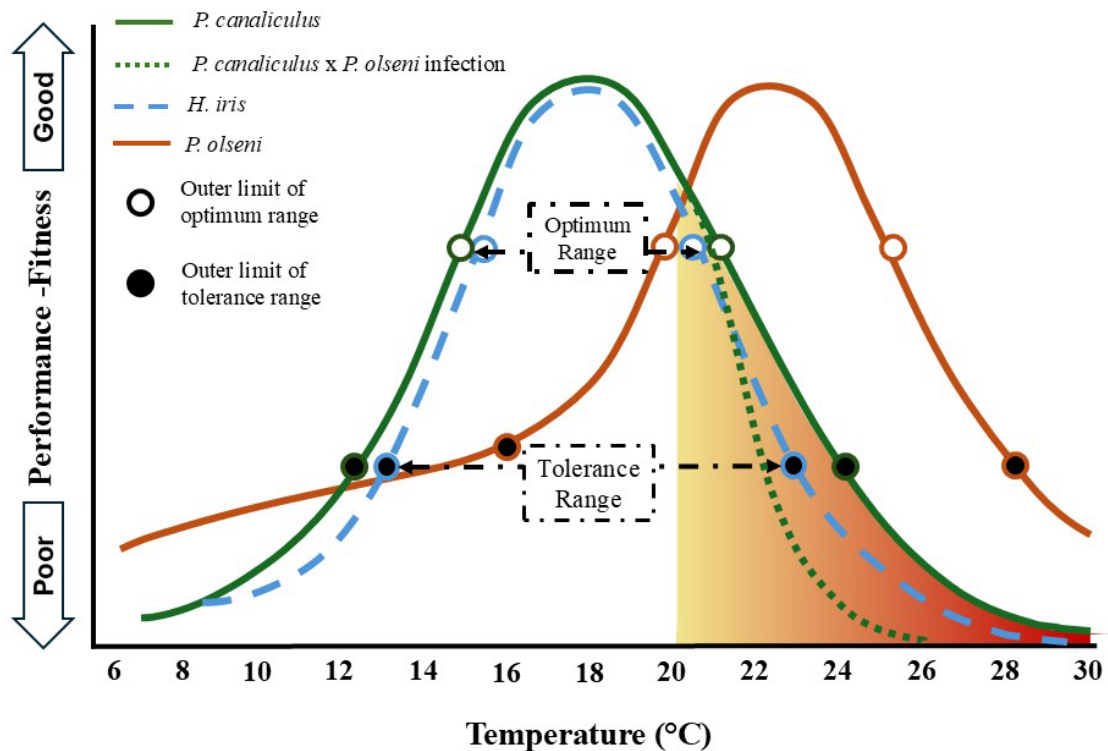


Figure 8.2 General depiction of optimum and tolerance ranges of green-lipped mussels (Copedo et al., 2023; Ericson et al., 2023; Venter et al., 2023), *H. iris* (Searle et al., 2006; Nguyen et al., 2023), and *P. olsenii* (Delisle et al., 2025) based on current knowledge/ information. Shade area (in colour yellow to red) is the region where a potential synergistic stress effect and physiological stress may increase. *Perkinsus olsenii* may induce a shift in the critical region at a lower temperature (green dotted line). The white section indicates the hypothetical region where the host immune response could maintain defence even with the parasite (*P. olsenii*) present.

Surprisingly, there is a key gap in knowledge in relation to the thermal optima of both green-lipped mussels and *H. iris*. Whilst published information on green-lipped mussels and *H. iris* thermal limits is extensive, the data for the optimal thermal environment have not been published and the putative levels presented here relied on anecdotal information. There is a considerable amount of work to be completed and compiled to provide this information and incorporate optimum conditions for growth, reproduction and immunity. Furthermore, noting that determining that these thermal optima models are complex, and the ranges are determined by several factors. As described in section 1.2.1. the optimum range can be affected by organism adaptation, acclimation, genetics, season, life stage and size (Sokolova et al., 2012). Therefore, interpretation can also be complex. For instance, in Figure

8.2 14°C is considered as sub-optimal, or in the tolerance range; however, 14°C is also a typical winter temperature in some New Zealand regions such as the Marlborough sounds (Chapter 6b). For green-lipped mussels being at this temperature during winter initiates gametogenic processes, so is broadly beneficial (Alfaro et al., 2001).

Lastly, it is well known that proliferation of *Perkinsus* sp., is influenced and exacerbated by a combination for warmer temperatures and reduced salinity (e.g., Villalba et al., 2004; Soudant et al., 2013; Moore, 2023). Therefore, further experimental research investigating interactions between thermal stress, salinity stress and the model mollusc would be beneficial, particularly as flooding events in New Zealand become more frequent on top of increasing average temperature (Chapter 2 and 6). As discussed in section 8.1.2., although extrapolating results from a laboratory experiment to the field is difficult and requires a simplified facsimile of natural conditions, they are critical in understanding underlying causes and potential threats to marine organisms. For example, should storm events become more frequent these flood conditions may alter the coastline, creating a favourable environment for other novel emerging diseases (Zell et al., 2008; Okamura, 2016; Handisyde et al., 2017; Reid et al., 2019a; Reid et al., 2019b), highlighting the need for disease preparedness and risk management.

8.1.5. *Risks to wild and industry populations*

With changing climate at the forefront of most discussions, there is a need to understand the risks for both wild and commercial populations of molluscs. As previously mentioned, most of the research on changing climate and pathogens has been conducted on species with commercial value (Lane et al., 2020). Considering that some aquaculture practices currently rely on wild-caught juveniles, such as the green-lipped mussels adults collected herein, this appears to be a risk particularly in terms of reproductive condition. It is important to determine whether the gametogenesis patterns observed can be applied to wild populations or is there a risk of missing key information on spawning patterns of wild populations. This is particularly important when there is emerging evidence that marine heatwaves and flood events could influence spawning times of molluscs. Additionally, when considering coevolution (section 8.1.3.), if summer mortalities and diseases are occurring and driving evolutionary processes then it is likely the physiological processes such as reproduction may commence earlier and at a younger age to increase chances of survival (Kochin et al., 2010).

Poor reproductive capacity and disease are considered as major factors implicated in the decline of wild populations, impeding aquaculture and restoration efforts (Coen and Bishop, 2015). Furthermore, even though it is known that expansion of aquaculture farming practices increases the risk of diseases, there appears to be very little monitoring of wild populations of molluscs (Lane et al., 2020). Considerable research, monitoring and reporting of molluscan conditions is required not only on the farmed species, but their wild counterparts to manage potential disease outbreaks (Lane et al., 2020; Suja et al., 2020), as well as changes to reproductive output. However, cultivated (aquaculture) populations may benefit from improved water quality and provision of habitat (Overton

et al., 2024). Although, when done right, the application of molluscan aquaculture can provide a range of benefits, including the support of restoration of wild populations it needs monitoring. This is particularly true when the population may harbour pathogens with a consequent of transmission to wild stocks. This is a potential risk for any translocated bivalve or gastropod species. Coen and Bishop (2015) reported that wild and farmed molluscs grown side-by-side had very different disease patterns, disease incidence was typically lower in the wild group compared to the cultivated (Wilkie et al., 2013; Coen and Bishop, 2015; Lafferty et al., 2015), unless the cultivated group was selectively bred for disease or environmental resistance. Therefore, the farmed molluscs, such as green-lipped mussels, are potentially more susceptible. Furthermore, in restoration efforts, the use of selectively bred populations can also lead to genetic dilution, as well as pathogen introduction to wild populations (Coen and Bishop, 2015; Lafferty et al., 2015). Additionally, interactions between wild and cultivated populations may alter disease prevalence as each can serve as reservoirs of disease (Coen and Bishop, 2015; Lafferty et al., 2015). For example, a wild population may carry a disease, it then infects the cultivated population and due to the high density and stressful environment may spread and cause greater issues in both populations.

8.1.6. *Guardianship versus utility in a changing world*

While conducting the research for this thesis and highlighting key components in sections 8.1.1. to 8.1.5., one question remained: *is guardianship of the environment being adequately balanced with commercial activities?* Although social values between local communities, scientists, primary industries, and government may be different, ultimate objectives such as improving species abundance, habitat quality and productivity, as well as improved social wealth, wellbeing and food security are key for the benefit of future generations (Bennett et al., 2018). Clearly, in the current paradigm, these values could potentially conflict or be held in different priority in different communities. To reconcile them, creative thinking is required; for instance: 1) the extension of criteria for commercial evaluation which incorporates the biology of the species and the habitat (Chapter 4), 2) improved adaptive management strategies that balance commercial harvest with ecosystem biodiversity, while acknowledging the complex nature of societal processes in response change, and 3) nature-based solutions such as restorative aquaculture, whereby aquaculture provides direct net-positive benefits to the ecosystem and recognises socio-economic values (Alleway et al., 2023),

In this author's opinion, balancing ecological and economic values is essential in building a thriving aquatic economy and a sustainable, healthy ecosystem. Relationship and network building are key to bridging the gap between governing bodies, science, industry, and communities to establish this balance. A successful approach to this has been observed while collaborating with the pāua industry council (Chapters 3 and 4). It was found that collaboration is underway with local communities, scientists, and fishermen working together with the aim of balancing livelihood (pāua catch) with the sustainability of the population under a regional management plan (Personal communication). For

instance, the Chatham Island pāua management area committee (PauMAC4) actively supports *H. iris* population growth by identifying new management strategies and developing collaborative partnerships with researchers (Venter et al., 2022; Van Nguyen et al., 2023). Methods employed here could provide a basis for further development in other molluscan species.

Building on this, the role of aquatic diseases also requires consideration in sustainable management. Diseases are often neglected based on the mindset “if you don’t look, you won’t find.” This leaves key organisms at risk of disease outbreaks and leaves us blind to the true number of hosts infected by generalist pathogens and potential disease threats. Whilst pathogens and parasites are a natural part of a sustainable ecosystem, recognising abnormal changes is akin to requiring a ‘doctors visit,’ which is critical in reducing and mitigating the impacts of future outbreaks. Currently, monitoring and sampling efforts (histopathology, molecular, and physiological) on aquatic diseases of economically valuable species are largely “passive” and typically conducted in response to mass mortality events, and occasionally through scientific research programmes. The Ministry of Primary Industries (MPI) NZ has a long-term pest management plan for the monitoring and diagnosis of *Bonamia ostreae*, with field surveillance being conducted in collaboration with NIWA (MPI, 2024a). However, there appear to be no other mandated surveillance programmes relevant to shellfisheries and aquaculture. Furthermore, without monitoring baseline conditions or describing pathogens and the associated diseases, it becomes difficult to distinguish between endemic, introduced or exotic and potentially an emerging disease.

Lane et al. (2020) suggested several areas of multidisciplinary research including: developing disease baselines, conducting trials to test and understand host-parasite interactions, elucidating the life cycle of parasites of interest, and implementing surveillance plans by identifying and prioritising key aquatic diseases, which are critical especially with warming oceanic waters. Finally, incorporation of community-based knowledge is also key to understanding these changes as prior generations and storytelling will often provide insight into habitat structure, changes in species diversity, loss of species and reduced recruitment, which could also indicate reproductive and disease issues. Bridging the gap and having aquatic health and disease surveillance as part of typical day-to-day (or rather month-to-month) activities will also improve education and provide a comprehensive understanding of abnormal changes, whilst supporting aquaculture and restoration efforts thereby providing good stewardship.

8.1.7. *Logistical issues, unforeseen circumstances, limitations, and biases*

This work exposed logistical issues, unforeseen circumstances, limitations, and potential biases. Devising measures for mitigation or exploration of these factors required a creative and resilient mind set. The factors and their accommodations are set out in order below.

Long term (greater than 3 months) trials are vulnerable to logistical disruption from small scale issues such as water flow stopping, aeration issues and larger issues from system failures including heat

pump malfunctions, power outages etc. However, long term trials do provide key information, regardless of outcome, and can drive facility improvement. For instance, in Chapter 5 the warmer temperatures of a 15-month trial relied on the use of heater bars to stabilise the temperature. The heater bars malfunctioned, resulting in the temperature dropping for 2 weeks. The malfunction was written into the Chapter as a confounding factor and, to our knowledge, had no effect on mortality or tissue conditions. To mitigate the issue more reliable titanium heaters were installed with water level alarm systems to reduce the risk of heat element exposure to plastic. In Chapter 6 the 3-month trial was exposed to flood water during a 1-in-100-year flood which resulted in a site-wide evacuation. This event fundamentally compromised the trial conditions; although there is no short-term solution to mitigating extreme climate events it does support long-term mitigation strategies associated with research facilities, such as land use change and facility infrastructure improvement. The flood scenario was written as its own Chapter to highlight not only general biological resilience and adaptation, but the specific effects of flood events: hyposalinity, increased sediment, and agricultural contamination on mussels exposed to preexisting stresses. Three months later this same experiment experienced heat pump malfunctions resulting in mortalities. One learning from this experience was if the mussels had access to abundant food they were less at risk of mortality in the short term. Furthermore, this also drove the improvement of the water heating systems. The laboratory scenarios were not the only studies affected by unforeseen circumstances. The emergence of Covid-19 in New Zealand resulted in the loss of several sampling timepoints during the field studies in 2020 (Chapter 2). These time points would have been informative but did not impact the overall story of the Chapter.

The histological approach, like any diagnostic technique, also has its limitations. For one it requires a significant amount of time, expertise, and learning. The tissue sections are typically small relative to the size of the mollusc, which means that there is a chance to miss pathogens or changes to tissues in unrepresented regions of the body. Additionally, changes and progression can only be inferred from timeseries sampling of the population but not changes in an individual. However, it has one major advantage when compared to other techniques and it allows us to directly observe changes and impacts on tissues, describe disease progression, gametogenesis cycles, oocyte atresia as well as providing the ability to detect new and emerging pathogens and parasites. Furthermore, histopathology can also validate molecular findings and confirm tissue-level effects, thereby bridging the gap between molecular biology, physiology and ecology. The staining types and techniques can also allow for more specificity, for example the F-ISH technique used to quantify *P. olseni* in green-lipped mussels (Chapter 7). Histopathology is also highly integrative, providing cellular and structural context, while molecular techniques such as PCR allow for improved speed, specificity, and sensitivity if a specific pathogen is of interest. However, for unknown pathogens, PCR is limited and although metabarcoding can apply a much broader lens, it can overwhelm users with substantial amounts of data for a small number of parasites of interest.

Next, the biases. Survival prejudices were the first obvious biases within the research. The lack of sampling from moribund or dead molluscs meant key information, e.g. earlier *P. olseni* detection in Chapter 5, could have been missed. Subsequent trials endeavoured to collect moribund individuals and mortalities for sampling to mitigate the bias and provide further information on the cause of death. The next were the sampling biases, for the *H. iris* and the green-lipped mussels, sampling more than 10 to 20 animals can be logistically difficult, particularly when multiple sampling time points and a large team is required. To increase the number of samples at each timepoint, logistics and budget need to be considered. For instance, a larger team may be required to collect and process more samples at a single timepoint which increases the overall cost. This cost would then need to be balanced across the project timeline. Both biases were considered through the thesis but were considered minor and did not substantially affect interpretation of the results.

There are also some aspects I would have improved. For instance, adding molecular techniques earlier on in the experimental research to provide more information. In hindsight the methods which were developed and learned in the later chapters such as the RFTM method for *P. olseni* detection, and PCR for parasite identification could have provided more information on the population prevalence of *P. olseni* in the initial 15-month thermal challenge trial, particularly the mortalities. Biochemistry techniques such as those for lipids, glycogen and proteins could also have been used in a preliminary nature to validate their potential use for investigating atresia in subsequent chapters. It would have been great to have more time to redo experiments or move them to the next stage to incorporate multi-stressors. However, it also provides the opportunity for future research and to transition from PhD candidate to researcher. Statistics will always feel like a weakness particularly in a sector of science that occupies the non-parametric world where statistical normality is a rare occurrence. However, much has been learnt from mentors who are experienced, and their knowledge and input has been invaluable to the success of the publications.

8.1.8. Future research avenues and recommendations

As mentioned throughout this discussion there are several potential avenues for research and further questions to be answered. Furthermore, priority of each of these is determined by the researcher's opinion. Some researchers may view one as higher on the priority list whilst another may consider it as low priority. The questions below are listed based on order throughout the thesis, however personal priority order is mentioned where applicable. Furthermore, several of these highlighted research avenues are also progressing beyond the scope of this thesis.

- Do we need to better understand reproductive biology in a changing world in both wild and farmed populations?

The answer is 'yes.' A better understanding of their reproductive biology is critical in not only fisheries and aquaculture species, but wild populations as well. There are only a few histological investigations on gametogenesis for green-lipped mussels and *H. iris*. It is currently unknown

whether the research conducted can be applied to wild populations. This is a critical question, particularly with the expansion of aquaculture practices and the decline of wild populations. Additionally, as discussion moves towards restorative aquaculture practices, understanding the reproductive biology, oocyte atresia and gamete survival is key to determine the true number of propagules entering the wild population.

- Do shellfish have reproductive biological clocks, and do we need to evaluate gametogenesis histologically earlier to determine the accurate age of maturation for various species?
 - As ocean warming progresses, does the age of optimal fecundity change? Are molluscs maturing earlier than we think?

Throughout this thesis the health and reproductive status of the molluscs in a naturally heatwave challenged environment was impacted by sub-optimal environmental conditions. This was inferred based on prolonged reproduction and higher than expected oocyte atresia. The next natural step for the reproduction work and understanding reproductive biology is investigating the idea of the age of optimal fecundity. Additionally, if restorative aquaculture practices continue to develop, then these aspects of reproductive biology are critical to improving larval yield and spat retention. Furthermore, investigating whether the age of maturation is starting earlier will provide more accurate information, driving reproductive capacity, growth and immune response to pathogens.

- Is the hypothesis of physiological age versus chronological age worth further exploration and what does it mean for aging methods?
 - Is the accumulation of ceroid related to advanced physiological age and is there another method we could use as a proxy?

Throughout Chapters 2, 3, 4 and 5 the idea of physiological aging versus chronological aging was hypothesised. This idea becomes key when incorporating the reproductive questions above. Although this question may be lower on the priority list, it could provide further information on the vulnerability of the mollusc to disease (infectious and non-infectious). Technical advancements may help in addressing these questions. For instance, determination of physiological age versus the chronological age: new tools (e.g. advanced DNA methylation tools) may be developed to cheaply biopsy tissue and shell to analyse the age.

- Are the impacts of the changing climate the same between farmed and wild populations?

Based on discussion in sections 8.1.4. and 8.1.5. the two populations would be expected to be different due to differences in age, population density, distribution and diversity of food access. Therefore, it is expected the changing marine environment will impact both populations differently. The research for this becomes critical particularly for restoration efforts and the spread of disease, inducing parasites. Furthermore, the investigation of the green-lipped mussel in the Coromandel region highlighted a need for sampling in other populations and molluscan species. It would be

interesting, and therefore recommended, to sample *H. iris* and wild populations of green-lipped mussels in the Coromandel region where the farmed, green-lipped mussels were sampled from and assess pathogen prevalence differences (and potential transfer) between local regions.

- What are the impacts of *P. olsenii* on green-lipped mussels in a changing climate where temperatures are rising, and frequency of flood events are increasing?
- *Perkinsus olsenii* is one pathogen that infects many molluscs; how many more host species could we be neglecting?
 - At what intensity or disease progression level will we start to see critical fitness impacts on green-lipped mussels?
 - What is the pathogen intensity and prevalence in wild populations?
 - What other pathogens could we be missing without proper surveillance programmes?

The development and establishment of the *in vitro* culture of *P. olsenii* by Delisle et al. (2025) allowed for the research conducted in Chapter 7. Chapter 7 was the first investigation of *P. olsenii* progression in green-lipped mussels and created opportunities for future work. This allowed us to address the question: **what is the disease progression of *P. olsenii* in green-lipped mussels and what are the technical barriers to undertaking this type of research?** This section of work was high risk with many associated barriers, the first being establishing a culture to produce enough cells for injection and determine the optimal proliferation temperature (Delisle et al., 2025). The next natural step would be to introduce a thermal component to investigate the impact of temperature and *P. olsenii* infection of the host species (Green-lipped mussel). Subsequent work would systematically introduce each stressor to build a bigger picture, then compare with wild and farmed populations in areas of interest to support findings. However, this type of research although critical and of high priority, is expensive and highlights another question that cannot be answered here: **How do we maximise research to consider multi-year/multi-generation effects while keeping resources and costs down.**

- Are we perpetually trying to understand the environment/host/pathogen interactome in an unstable system, or is fluctuation and instability required for evolution, adaptation, and resilience? And therefore, is stability deleterious?

The last question proposed is likely theoretical, however worth noting and keeping in mind in the future. The marine environment is constantly changing, whether exacerbated by climate change or not, and each organism is subject to evolutionary pressures. These pressures can be environmental, or parasite driven, but ultimately select for favouring traits to pass to the next generation. In a benign situation fluctuating conditions and instability are required for adaptation and are beneficial to the population; however, large-scale fluctuations can have detrimental and irreversible effects. Investigation across many generations will provide a better understanding of these benign and severe fluctuations and the impact to the species of interest, whilst improving generalisations. Every living

organism requires change, so: ‘yes,’ we are trying to understand the interactome in a perpetually unstable system, but stability is deleterious and does not allow for adaptation and resilience.

8.1.9. Conclusion

Many species of molluscs, not just green-lipped mussels and *H. iris*, are likely to be impacted by a changing environment. Mean temperatures around the New Zealand coast are continuing to rise and these temperature changes are expected for most areas, particularly the intertidal zones. Although temperature was highlighted as a key theme, other stressors such as salinity, food availability, pathogen and parasites, reproduction and growth were also discussed. Thermal stress was observed to inhibit gametogenesis, drive accumulation of ceroid and increase the diversity and presence of parasites in green-lipped mussels, whilst nutrition was hypothesised to be the primary source of stress limiting growth in *H. iris*. In terms of pathogens, *Perkinsus olseni* is one parasite of concern due to its appearance in the prolonged 24°C treatment, 6 months earlier than the 21°C treatment of the green-lipped mussel thermal challenge trial, as well as its broad host range, temperature range, pathogenicity, and documented ability to induce disease. Therefore, *P. olseni* represents a risk to the sustainability of both wild and farmed marine populations.

The histopathological investigations presented identify critical knowledge gaps, such as the processes initiating oocyte atresia, the impact of increasing sea surface temperatures on *H. iris* and influence of other pathogens of interest, such as APX, in environment-host-pathogen interactions. The tissue alterations, reproductive impacts and pathogens detected highlight a need for collaborative interdisciplinary approaches, not just for science, but incorporating local communities, aquaculture and fisheries industries and governing bodies to protect NZ’s diverse marine ecosystem.

The work presented, and the techniques used, demonstrate that the research can provide useful information on many levels and can be applied to other molluscan species. Regular monitoring will facilitate early detection of abnormal conditions, highlighting the benefits of an expanded programme or platform. Therefore, one of the key recommendations is the implementation of surveillance programmes for several key molluscs to monitor aquatic health. Continued integration of field and laboratory research will support discoveries and the effects of external and internal stressors on molluscs to provide early detection of non-infectious and infectious diseases.

“All models are wrong, but some are useful”.

George Box

REFERENCES

- Aalto, E. A., Barry, J. P., Boch, C. A., Litvin, S. Y., Micheli, F., Woodson, C. B., and De Leo, G. A. 2020. Abalone populations are most sensitive to environmental stress effects on adult individuals. *Marine Ecology Progress Series*, 643, 75-85. <https://doi.org/10.3354/meps13320>
- Abdi, H. 2007. *The Kendall rank correlation coefficient*. In S. NJ (Ed.), *Encyclopedia of measurement and statistics* (Vol. 2, pp. 508-510).
- Adema, C. M. 2021. Sticky problems: extraction of nucleic acids from molluscs. *Philosophical transactions of the Royal Society of London. Series B, Biological Sciences*, 376(1825), 20200162. <https://doi.org/10.1098/rstb.2020.0162>
- Aguirre, J., Greenwood, S. J., McClure, J. T., Davidson, J., and Sanchez, J. 2016. Effects of rain events on *Cryptosporidium* spp. levels in commercial shellfish zones in the Hillsborough River, Prince Edward Island, Canada. *Food and Waterborne Parasitology*, 5, 7-13. <https://doi.org/https://doi.org/10.1016/j.fawpar.2016.08.003>
- Alfaro, A. C., Jeffs, A. G., Hooker, S. H., 2001. Reproductive behavior of the green-lipped mussel, *Perna canaliculus*, in Northern New Zealand. *Bulletin of Marine Science*. 69, 1095-1108,
- Alfaro, A. C., Jeffs, A. G., King, N., 2014. Enabling and driving aquaculture growth in New Zealand through innovation. *New Zealand Journal of Marine and Freshwater Research*. 48, 311-313, 10.1080/00288330.2014.933115.
- Alfaro, A. C., Young, T., 2018. Showcasing metabolomic applications in aquaculture: a review. *Reviews in Aquaculture*. 10, 135-152,
- Allam, B., Raftos, D., 2015. Immune responses to infectious diseases in bivalves. *Journal of Invertebrate Pathology*. 131, 121-36, 10.1016/j.jip.2015.05.005.
- Allen, M. R., Ingram, W. J., 2002. Constraints on future changes in climate and the hydrologic cycle. *Nature*. 419, 224-32, 10.1038/nature01092.
- Allen, V. J., Marsden, I. D., Ragg, N. L. C., Giese, S., 2006. The effects of tactile stimulants on feeding, growth, behaviour, and meat quality of cultured Blackfoot abalone, *Haliotis iris*. *Aquaculture*. 257, 294-308, 10.1016/j.aquaculture.2006.02.070.
- Alleway, H. K., Waters, T. J., Brummett, R., Cai, J., Cao, L., Cayten, M. R., Costa-Pierce, B. A., Dong, Y.-W., Brandstrup Hansen, S. C., Liu, S., Liu, Q., Shelley, C., Theuerkauf, S. J., Tucker, L., Wang, Y., Jones, R. C., 2023. Global principles for restorative aquaculture to foster aquaculture practices that benefit the environment. *Conservation Science and Practice*. 5, e12982, <https://doi.org/10.1111/csp2.12982>.
- Alley, R. B., Berntsen, T., Bindoff, N. L., Chidthaisong, A., Friedlingstein, P., Gregory, J. M., Hegerl, G. C., Heimann, M., Hewitson, B., and Hoskins, B. J. 2007. IPCC, 2007: Summary for Policymakers. In: Solomon, S., D. Qin, M. Manning, Z. Chen, M. Marquis, K.B. Averyt, M. Tignor and H.L. Miller (eds.) *Climate Change 2007: The Physical Science Basis. Contribution of Working Group I to the Fourth Assessment Report of the Intergovernmental Panel on Climate Change*. Cambridge University Press, Cambridge, United Kingdom and New York, NY, USA.
- Anderson, R., May, R., 1991. *Infectious diseases of humans*. Oxford Science Publications, Great Britain, 757.
- Andrews, J. D., 1981 Pelecypoda: Ostreidae. In: Giese AC, Pearse JS, editors. *Reproduction of marine invertebrates*, volume v, molluscs: pelecypods and lesser classes. New York: Academic Press; p. 293–341
- Angilletta Jr and Angilletta, 2009. *Thermal Adaptation: A Theoretical and Empirical Synthesis*. Oxford University Press, Oxford. <https://doi.org/10.1093/acprof:oso/9780198570875.001.1>
- Apeti, D. A., Lauenstein, G., Warner, R. A., Kim, Y., and Tull, J. 2014. Occurrence of parasites and diseases in oysters and mussels of US coastal waters national status and trends, the Mussel Watch Monitoring Program. NOAA technical memorandum NOS NCCOS. National Centers for Coastal Ocean Science (U.S.) 70
- AQNZ, Aquaculture for new zealand: A sector overview with key facts and statistics for 2023. In: A. N. Zealand, (Ed.), Nelson, New Zealand, 2023.
- Aranguren, R., and Figueras, A. 2016. Moving from histopathology to molecular tools in the diagnosis of molluscs diseases of concern under EU Legislation. *Frontiers in Physiology*, 7, 538. <https://doi.org/10.3389/fphys.2016.00538>

- Arkema, K. K., Guannel, G., Verutes, G., Wood, S. A., Guerry, A., Ruckelshaus, M., Kareiva, P., Lacayo, M., and Silver, J. M. 2013. Coastal habitats shield people and property from sea-level rise and storms. *Nature Climate Change*, 3(10), 913-918. <https://doi.org/10.1038/nclimate1944>
- Arzul, I., and Carnegie, R. B. 2015. New perspective on the haplosporidian parasites of molluscs. *Journal of Invertebrate Pathology*, 131, 32-42. <https://doi.org/10.1016/j.jip.2015.07.014>
- Azizan, A., Venter, L., Alfaro, A. C., 2023. A review on green-lipped mussel, *Perna canaliculus* immunology: the drivers, virulence factors, advances, and applications. *New Zealand Journal of Marine and Freshwater Research*. 58, 319-363, 10.1080/00288330.2023.2269865.
- Azizan, A., Venter, L., Zhang, J., Young, T., Ericson, J. A., Delorme, N. J., Ragg, N. L. C., Alfaro, A. C., 2024. Interactive effects of elevated temperature and *Photobacterium swingsii* infection on the survival and immune response of marine mussels (*Perna canaliculus*): A summer mortality scenario. *Marine Environmental Research*. 196, 106392, 10.1016/j.marenvres.2024.106392.
- Baba, K., Miyazono, A., Matsuyama, K., Kohno, S., and Kubota, S. 2007. Occurrence and detrimental effects of the bivalve-inhabiting hydroid *Eutima japonica* on juveniles of the Japanese scallop *Mizuhopecten yessoensis* in Funaka Bay, Japan: relationship to juvenile massive mortality in 2003. *Marine Biology*, 151(5), 1977-1987. <https://doi.org/10.1007/s00227-007-0636-x>
- Balbi, T., Cortese, K., Ciacci, C., Bellese, G., Vezzulli, L., Pruzzo, C., and Canesi, L. 2018. Autophagic processes in *Mytilus galloprovincialis* hemocytes: Effects of *Vibrio tapetis*. *Fish and Shellfish Immunology*, 73, 66-74. <https://doi.org/10.1016/j.fsi.2017.12.003>
- Balbi, T., Trenti, F., Guella, G., Miglioli, A., Sepčić, K., Ciacci, C., and Canesi, L. 2023. Changes in phospholipid profiles in early larval stages of the marine mussel *Mytilus galloprovincialis* indicate a role of ceramides in bivalve development. *International Journal of Biochemistry and Molecular Biology*, 14(5), 87-100.
- Barber, B. J., and Blake, N. J. 1981. Energy storage and utilization in relation to gametogenesis in *Argopecten irradians concentricus* (Say). *Journal of Experimental Marine Biology and Ecology*, 52(2-3), 121-134.
- Barnard, C., and Behnke, J. 1990. *Parasitism and Host Behaviour*. (2009/04/06 ed., Vol. 102). Taylor and Francis, Cambridge University Press. <https://doi.org/10.1017/S0031182000064453>
- Barnes, R. D. 1987. *Invertebrate zoology*. Saunders College Publishing, East Sussex
- Basova, L., Begum, S., Strahl, J., Sukhotin, A., Brey, T., Philipp, E., and Abele, D. 2012. Age-dependent patterns of antioxidants in *Arctica islandica* from six regionally separate populations with different lifespans. *Aquatic Biology*, 14(2), 141-152.
- Bayne, B. 1976. *Marine mussels, their ecology and physiology*. Cambridge University Press, Cambridge.
- Bayne, B., Bubel, A., Gabbott, P., Livingstone, D., Lowe, D., and Moore, M. 1982. Glycogen utilisation and gametogenesis in *Mytilus edulis* L. *Marine Biology Letters*, 3, 89-105.
- Bayne, B. L., 2004. Phenotypic flexibility and physiological tradeoffs in the feeding and growth of marine bivalve molluscs. *Integrative and Comparative Biology*. 44, 425-32, 10.1093/icb/44.6.425.
- Bayne, B. L., Thompson, R. J., 1970. Some physiological consequences of keeping *Mytilus edulis* in the laboratory. *Helgoländer wissenschaftliche Meeresuntersuchungen*. 20, 526-552, 10.1007/bf01609927.
- Bayne, B., Wiley, M., 1976. *Estuarine processes*. Academic Press, New York.
- Bayne, B. L., Widdows, J., Newell, R. I. E., 1977 *Physiological Measurements on Estuarine Bivalve Molluscs in the Field*. In: B. F. Keegan, et al., Eds., *Biology of Benthic Organisms*. Pergamon, pp. 57-68.
- Behrens, E., Rickard, G., Rosier, S., Williams, J., Morgenstern, O., Stone, D., 2022. Projections of future marine heatwaves for the oceans around New Zealand using New Zealand's earth system model. *Frontiers in Climate*. 4, 10.3389/fclim.2022.798287.
- Bell, J. J., Smith, R. O., Micaroni, V., Strano, F., Balemi, C. A., Caiger, P. E., Miller, K. I., Spyksma, A. J. P., Shears, N. T., 2023. Marine heat waves drive bleaching and necrosis of temperate sponges. *Current Biology*. 33, 158-163 e2, 10.1016/j.cub.2022.11.013.
- Ben-Horin, T., Bidegain, G., Huey, L., Narvaez, D. A., Bushek, D., 2015. Parasite transmission through suspension feeding. *Journal of Invertebrate Pathology*. 131, 155-76, 10.1016/j.jip.2015.07.006.

- Beninger, P. G., 1987. A qualitative and quantitative study of the reproductive cycle of the giant scallop, *Placopecten magellanicus*, in the Bay of Fundy (New Brunswick, Canada). *Canadian Journal of Zoology*. 65, 495-498,
- Beninger, P. G., 2017. Caveat observator: the many faces of pre-spawning atresia in marine bivalve reproductive cycles. *Marine Biology*. 164, 163, 10.1007/s00227-017-3194-x.
- Beninger, P. G., Chérel, D., Kessler, L., 2021. Examining bivalve fecundity: oocyte viability revealed by Neutral Red vital staining. *Aquaculture International*. 29, 1219-1231, 10.1007/s10499-021-00686-6.
- Beninger, P. G., Chérel, D., Le Pennec, G., Shumway, S. E., 2022. Evolutionary and ecological insights from vital staining of bivalve oocytes: A Red Queen at the sweepstakes? *Ecosphere*. 13, e4047, 10.1002/ecs2.4047.
- Beninger, P. G., Le Pennec, M., 2016, Scallop Structure and Function. In: S. E. Shumway, G. J. Parsons, Eds.), *Scallops - Biology, Ecology, Aquaculture, and Fisheries*. Elsevier, pp. 85-159.
- Benito, D., Palecek, D., Lekube, X., Izagirre, U., Marigomez, I., Zaldibar, B., Soto, M., 2022. Variability and distribution of parasites, pathologies and their effect on wild mussels (*Mytilus* sp.) in different environments along a wide latitudinal span in the Northern Atlantic and Arctic Oceans. *Marine Environmental Research*. 176, 105585, 10.1016/j.marenvres.2022.105585.
- Benjamin, E. D., Toone, T. A., Hillman, J. R., Handley, S. J., Jeffs, A., 2024. Aerial exposure and critical temperatures limit the survival of restored intertidal mussels. *Restoration Ecology*. 32, 10.1111/rec.14105.
- Bennett, N. J., Whitty, T. S., Finkbeiner, E., Pittman, J., Bassett, H., Gelcich, S., Allison, E. H., 2018. Environmental stewardship: A conceptual review and analytical framework. *Environmental Management*. 61, 597-614, 10.1007/s00267-017-0993-2.
- Bennion, M., Ross, P., Howells, J., McDonald, I. R., Lane, H., 2021. Characterisation and distribution of the bacterial genus *Endozoicomonas* in a threatened surf clam. *Diseases of Aquatic Organisms*. 146, 91-105, 10.3354/dao03626.
- Benomar, S., Costil, K., El Filali, F., Mathieu, M., Moukrim, A., 2010. Annual dynamics of glycogen, lipids and proteins during the sexual cycle of *Perna perna* (Mollusca: Bivalvia) from south-western Morocco. *Journal of the Marine Biological Association of the United Kingdom*. 90, 335-346,
- Benson, D. A., Karsch-Mizrachi, I., Lipman, D. J., Ostell, J., Wheeler, D. L., 2008. GenBank. *Nucleic Acids Research*. 36, D25-30, 10.1093/nar/gkm929.
- Bergström, P., Lindgarth, M., 2016. Environmental influence on mussel (*Mytilus edulis*) growth – A quantile regression approach. *Estuarine, Coastal and Shelf Science*. 171, 123-132, 10.1016/j.ecss.2016.01.040.
- Berthelin, C., Kellner, K., Mathieu, M., 2000. Storage metabolism in the Pacific oyster (*Crassostrea gigas*) in relation to summer mortalities and reproductive cycle (west coast of France). *Comparative Biochemistry and Physiology Part B: Biochemistry and Molecular Biology* 125, 359-69, 10.1016/s0305-0491(99)00187-x.
- Betts, A., Rafaluk, C., King, K. C., 2016. Host and parasite evolution in a tangled bank. *Trends in Parasitology*. 32, 863-873, <https://doi.org/10.1016/j.pt.2016.08.003>.
- Bignell, J. P., Dodge, M. J., Feist, S. W., Lyons, B., Martin, P. D., Taylor, N. G. H., Stone, D., Trivalent, L., Stentiford, G. D., 2008. Mussel histopathology: effects of season, disease and species. *Aquatic Biology*. 2, 1-15, 10.3354/ab00031.
- Bjorbækmo, M. F. M., Evenstad, A., Røsæg, L. L., Krabberød, A. K., Logares, R., 2020. The planktonic protist interactome: where do we stand after a century of research? *The ISME journal*. 14, 544-559,
- Boehnert, S., Ruiz Soto, S., Fox, B. R. S., Yokoyama, Y., Hebbeln, D., 2020. Historic development of heavy metal contamination into the Firth of Thames, New Zealand. *Geo-Marine Letters*. 40, 149-165, 10.1007/s00367-019-00597-9.
- Booij, M. J., 2005. Impact of climate change on river flooding assessed with different spatial model resolutions. *Journal of Hydrology*. 303, 176-198, 10.1016/j.jhydrol.2004.07.013.
- Booth, M., Chapter Three - Climate Change and the Neglected Tropical Diseases. In: D. Rollinson, J. R. Stothard, Eds.), *Advances in Parasitology*. Academic Press, 2018, pp. 39-126.
- Borja, A., Franco, J., Pérez, V., 2000. A marine biotic index to establish the ecological quality of soft-bottom benthos within European estuarine and coastal environments. *Marine Pollution Bulletin*. 40, 1100-1114,

- Bouallegui, Y., 2019. Immunity in mussels: An overview of molecular components and mechanisms with a focus on the functional defenses. *Fish and Shellfish Immunology*. 89, 158-169, 10.1016/j.fsi.2019.03.057.
- Boukadida, K., Mlouka, R., Abelouah, M. R., Chelly, S., Romdhani, I., Conti, G. O., Ferrante, M., Cammarata, M., Parisi, M. G., AitAlla, A., Banni, M., 2024. Unraveling the interplay between environmental microplastics and salinity stress on *Mytilus galloprovincialis* larval development: A holistic exploration. *Science of the Total Environment*. 927, 172177, 10.1016/j.scitotenv.2024.172177.
- Bower, S. M., 2006 Synopsis of infectious diseases and parasites of commercially exploited shellfish: Ciliates associated with Abalone. dfo.
- Bower, S. M., Blackburn, J., Meyer, G. R., 1998. Distribution, prevalence, and pathogenicity of the protozoan *Perkinsus qugwadi* in Japanese scallops, *Patinopecten yessoensis*, cultured in British Columbia, Canada. *Canadian Journal of Zoology*. 76, 954-959,
- Bower, S. M., McGladdery, S. E., Price, I. M., 1994. Synopsis of infectious diseases and parasites of commercially exploited shellfish: *Sphenophrya*-like ciliates of clams and cockles. Dfo.
- Boyd, P. W., Lennartz, S. T., Glover, D. M., Doney, S. C., 2014. Biological ramifications of climate-change-mediated oceanic multi-stressors. *Nature Climate Change*. 5, 71-79, 10.1038/nclimate2441.
- Breen, P. A.; Adkins, B. E. 1982: Observations of abalone populations on the north coast of British Columbia, July 1980. Canadian manuscript report fisheries and aquatic science 1633: 55 p
- Brennan, G., Collins, S., 2015. Growth responses of a green alga to multiple environmental drivers. *Nature Climate Change*. 5, 892-897, 10.1038/nclimate2682.
- Britton, D., Schmid, M., Revill, A. T., Virtue, P., Nichols, P. D., Hurd, C. L., Mundy, C. N., 2020. Seasonal and site-specific variation in the nutritional quality of temperate seaweed assemblages: implications for grazing invertebrates and the commercial exploitation of seaweeds. *Journal of Applied Phycology*. 33, 603-616, 10.1007/s10811-020-02302-1.
- Britz, P. J., Hecht, T., Knauer, J., 1996. Gastric evacuation time and digestive enzyme activity in abalone *Haliotis midae* fed a formulated diet. *South African Journal of Marine Science*. 17, 297-303, 10.2989/025776196784158581.
- Brockhurst, M. A., Chapman, T., King, K. C., Mank, J. E., Paterson, S., Hurst, G. D., 2014. Running with the Red Queen: the role of biotic conflicts in evolution. *Proceedings of the Royal Society B: Biological Sciences*. 281, 20141382,
- Broekhuizen, N., Plew, D. R., Pinkerton, M. H., Gall, M. G., 2021. Sea temperature rise over the period 2002–2020 in Pelorus Sound, New Zealand – with possible implications for the aquaculture industry. *New Zealand Journal of Marine and Freshwater Research*. 55, 46-64, 10.1080/00288330.2020.1868539.
- Brokordt, K., Defranchi, Y., Esposito, I., Carcamo, C., Schmitt, P., Mercado, L., de la Fuente-Ortega, E., Rivera-Ingraham, G. A., 2019. Reproduction immunity trade-off in a mollusk: Hemocyte energy metabolism underlies cellular and molecular immune responses. *Frontiers in Physiology*. 10, 77, 10.3389/fphys.2019.00077.
- Buchanan, S., 2001. Measuring reproductive condition in the Greenshell™ mussel *Perna canaliculus*. *New Zealand Journal of Marine and Freshwater Research*. 35, 859-870, 10.1080/00288330.2001.9517048.
- Bulla, M., Oudman, T., Bijleveld, A. I., Piersma, T., Kyriacou, C. P., 2017. Marine biorhythms: bridging chronobiology and ecology. *Philosophical transactions of the Royal Society of London. Series B, Biological Sciences*. 372, 20160253, 10.1098/rstb.2016.0253.
- Burge, C. A., Mark Eakin, C., Friedman, C. S., Froelich, B., Hershberger, P. K., Hofmann, E. E., Petes, L. E., Prager, K. C., Weil, E., Willis, B. L., Ford, S. E., Harvell, C. D., 2014. Climate change influences on marine infectious diseases: implications for management and society. *Annual Review of Marine Science*. 6, 249-77, 10.1146/annurev-marine-010213-135029.
- Byers, J. E., 2021. Marine parasites and disease in the era of global climate change. *Annual Review of Marine Science*. 13, 397-420, <https://doi.org/10.1146/annurev-marine-031920-100429>.
- Byers, J. E., Blakeslee, A. M., Linder, E., Cooper, A. B., Maguire, T. J., 2008. Controls of spatial variation in the prevalence of trematode parasites infecting a marine snail. *Ecology*. 89, 439-51, 10.1890/06-1036.1.

- Callahan, B. J., McMurdie, P. J., Rosen, M. J., Han, A. W., Johnson, A. J., Holmes, S. P., 2016. DADA2: High-resolution sample inference from Illumina amplicon data. *Nature Methods*. 13, 581-3, 10.1038/nmeth.3869.
- Camacho, C., Coulouris, G., Avagyan, V., Ma, N., Papadopoulos, J., Bealer, K., Madden, T. L., 2009. BLAST+: architecture and applications. *BMC Bioinformatics*. 10, 421, 10.1186/1471-2105-10-421.
- Cano, I., Ryder, D., Webb, S. C., Jones, B. J., Brosnahan, C. L., Carrasco, N., Bodinier, B., Furones, D., Pretto, T., Carella, F., Chollet, B., Arzul, I., Cheslett, D., Collins, E., Lohrmann, K. B., Valdivia, A. L., Ward, G., Carballal, M. J., Villalba, A., Marigomez, I., Mortensen, S., Christison, K., Kevin, W. C., Bustos, E., Christie, L., Green, M., Feist, S. W., 2020. Cosmopolitan Distribution of *Endozoicomonas*-Like organisms and other intracellular microcolonies of bacteria causing infection in marine mollusks. *Frontiers in Microbiology*. 11, 577481, 10.3389/fmicb.2020.577481.
- Carella, F., 2010 Biotechnologies to evaluate the environmental status: new test organisms in ecotoxicology and histopathological and molecular biomarkers in natural population. . *Biotechnological Sciences*, Vol. PhD. University of Naples, University of Naples Federico II, Naples, Italy.
- Carella, F., Aceto, S., Mangoni, O., Mollica, M. P., Cavaliere, G., Trinchese, G., Aniello, F., De Vico, G., 2018. Assessment of the health status of mussels *Mytilus galloprovincialis* along the Campania coastal areas: A multidisciplinary approach. *Frontiers in Physiology*. 9, 683, 10.3389/fphys.2018.00683.
- Carella, F. F., S.W. Bignell, J.P. DeVico G. , 2015. Comparative pathology in bivalves: Etiological agents and disease processes. *Journal of Invertebrate Pathology* 131:107-120.
- Carella, F., Fernandez Tejedor, M., Villari, G., Andree, K. B., De Vico, G., 2023. The endoparasite *Perkinsus olseni* affecting the Mediterranean mussels (*Mytilus galloprovincialis*) in the Italian and Spanish waters: A new possible threat for mussel aquaculture and wild animal population. *Frontiers in Marine Science*. 10, 10.3389/fmars.2023.1116837.
- Carmichael, N. G., Fowler, B. A., 1981. Cadmium accumulation and toxicity in the kidney of the bay scallop *Argopecten irradians*. *Marine Biology*. 65, 35-43, 10.1007/bf00397065.
- Carmichael, N. G., Squibb, K. S., Fowler, B. A., 1979. Metals in the molluscan kidney: A comparison of two closely related bivalve species (*Argopecten*), Using X-Ray microanalysis and atomic absorption spectroscopy. *Journal of the Fisheries Research Board of Canada*. 36, 1149-1155, 10.1139/f79-162.
- Carpenter, A. E., Jones, T. R., Lamprecht, M. R., Clarke, C., Kang, I. H., Friman, O., Guertin, D. A., Chang, J. H., Lindquist, R. A., Moffat, J., Golland, P., Sabatini, D. M., 2006. CellProfiler: image analysis software for identifying and quantifying cell phenotypes. *Genome Biology*. 7, R100, 10.1186/gb-2006-7-10-r100.
- Carrier-Belleau, C., Drolet, D., McKindsey, C. W., Archambault, P., 2021. Environmental stressors, complex interactions and marine benthic communities' responses. *Scientific Reports*. 11, 4194, 10.1038/s41598-021-83533-1.
- Casas, S. M., Villalba, A., Reece, K. S., 2002. Study of perkinsosis in the carpet shell clam *Tapes decussatus* in Galicia (NW Spain). I. Identification of the aetiological agent and *in vitro* modulation of zoosporulation by temperature and salinity. *Diseases of Aquatic Organisms*. 50, 51-65, 10.3354/dao050051.
- Castinel, A., Forrest, B. M., Hopkins, G., Review of diseases of potential concern for New Zealand shellfish aquaculture: perspectives for risk management., Cawthron, 2014.
- Castinel, A., Webb, S. C., Jones, J. B., Peeler, E. J., Forrest, B. M., 2019. Disease threats to farmed green-lipped mussels *Perna canaliculus* in New Zealand: review of challenges in risk assessment and pathway analysis. *Aquaculture Environment Interactions*. 11, 291-304, <https://www.int-res.com/abstracts/aei/v11/p291-304/>
- Chagot, D., Comps, M., Boulo, V., Ruano, F., Grizel, H., 1987. Histological study of a cellular reaction in *Ruditapes decussatus* infected by a protozoan. *Aquaculture* 67 : 260-261. <https://archimer.ifremer.fr/doc/00000/3109/>
- Checa, A. G., 2018. Physical and biological determinants of the fabrication of molluscan shell microstructures. *Frontiers in Marine Science*. 5, 10.3389/fmars.2018.00353.
- Cheng, T. C., 1983. The role of lysosomes in molluscan inflammation. *American Zoologist*. 23, 129-144,

- Chérel, D., Beninger, P. G., 2017. Oocyte atresia characteristics and effect on reproductive effort of Manila clam *Tapes philippinarum* (Adams and Reeve, 1850). *Journal of Shellfish Research*. 36, 549-557, 10.2983/035.036.0302.
- Chérel, D., Beninger, P. G., 2019. Oocyte atresia and its effect on reproductive effort of the common cockle *Cerastoderma edule* (Linnaeus, 1758). *Journal of Shellfish Research*. 38, 603-609, 7, <https://doi.org/10.2983/035.038.0311>
- Chin, T. M., Vazquez-Cuervo, J., Armstrong, E. M., 2017. A multi-scale high-resolution analysis of global sea surface temperature. *Remote Sensing of Environment*. 200, 154-169, 10.1016/j.rse.2017.07.029.
- Chintala, M. M., Bushek, D., Ford, S. E., 2002. Comparison of *in vitro*-cultured and wild-type *Perkinsus marinus*. II. Dosing methods and host response. *Diseases of Aquatic Organisms*. 51, 203-16, 10.3354/dao051203.
- Choi, K.-S., Park, K.-I., 1997. Report on the occurrence of *Perkinsus* sp. in the Manila clams, *Ruditapes philippinarum* in Korean. *Journal of Aquaculture*. 10, 227-237,
- Chong, R. S.-M., 2022a, Kidney coccidiosis (scallop, abalone, mussels, oysters, and clams). In: F. S. B. Kibenge, et al., Eds., *Aquaculture Pathophysiology*. Academic Press, pp. 551-553.
- Chong, R. S.-M., 2022b, Molluscan immunology. In: F. S. B. Kibenge, et al., Eds., *Aquaculture Pathophysiology*. Academic Press, pp. 383-392.
- Chong, R. S.-M., 2022c, Perkinsosis. In: F. S. B. Kibenge, et al., Eds., *Aquaculture Pathophysiology*. Academic Press, pp. 577-582.
- Chu, F. L., Soudant, P., Lund, E. D., 2003. *Perkinsus marinus*, a protozoan parasite of the Eastern oyster (*Crassostrea virginica*): effects of temperature on the uptake and metabolism of fluorescent lipid analogs and lipase activities. *Experimental Parasitology*. 105, 121-30, 10.1016/j.exppara.2003.11.002.
- Clarke, A., 1988. Seasonality in the antarctic marine environment. *Comparative Biochemistry and Physiology Part B: Comparative Biochemistry*. 90, 461-473, 10.1016/0305-0491(88)90285-4.
- Clarke, M., 1999. The effect of food availability on byssogenesis by the zebra mussel (*Dreissena polymorpha Pallas*). *Journal of Molluscan Studies*. 65, 327-333, 10.1093/mollus/65.3.327.
- Clements, J. C., Hicks, C., Tremblay, R., Comeau, L. A., 2018. Elevated seawater temperature, not pCO₂, negatively affects post-spawning adult mussels (*Mytilus edulis*) under food limitation. *Conservation Physiology*. 6, cox078, 10.1093/conphys/cox078.
- Coates, C. J., Söderhäll, K., 2021. The stress-immunity axis in shellfish. *Journal of Invertebrate Pathology*. 186, 107492, <https://doi.org/10.1016/j.jip.2020.107492>.
- Coen, L. D., Bishop, M. J., 2015. The ecology, evolution, impacts and management of host-parasite interactions of marine molluscs. *Journal of Invertebrate Pathology*. 131, 177-211, 10.1016/j.jip.2015.08.005.
- Cohen, A. A., 2018. Aging across the tree of life: The importance of a comparative perspective for the use of animal models in aging. *Biochimica et Biophysica Acta (BBA) - Molecular Basis of Disease*. 1864, 2680-2689, 10.1016/j.bbadis.2017.05.028.
- Cook, P. A., 2014. The worldwide abalone industry. *Modern Economy*. 05, 1181-1186, 10.4236/me.2014.513110.
- Copedo, J. S., Webb, S. C., Delisle, L., Knight, B., Ragg, N. L. C., Laroche, O., Venter, L., Alfaro, A. C., 2025a. Elucidating divergent growth and climate vulnerability in abalone (*Haliotis iris*): A multi-year snapshot. *Marine Environmental Research*. 107090, 10.1016/j.marenvres.2025.107090.
- Copedo, J. S., Webb, S. C., Ragg, N. L. C., Alfaro, A. C., 2025b. Implications of flooding events for the green-lipped mussels (*Perna canaliculus*): An aquatic health perspective. *New Zealand Journal of Marine and Freshwater Research* 10.1080/00288330.2025.2474570.
- Copedo, J. S., Webb, S. C., Ragg, N. L. C., Venter, L., Alfaro, A. C., 2024. Histopathological investigation of four populations of abalone (*Haliotis iris*) exhibiting divergent growth performance. *Journal of Invertebrate Pathology*. 202, 108042, 10.1016/j.jip.2023.108042.
- Copedo, J. S., Webb, S. C., Ragg, N. L. C., Ericson, J. A., Venter, L., Schmidt, A. J., Delorme, N. J., Alfaro, A. C., 2023. Histopathological changes in the greenshell mussel, *Perna canaliculus*, in response to chronic thermal stress. *Journal of Thermal Biology*. 117, 103699, 10.1016/j.jtherbio.2023.103699.

- Cornelisen, C. D., Gillespie, P. A., Kirs, M., Young, R. G., Forrest, R. W., Barter, P. J., Knight, B. R., Harwood, V. J., 2011. Motueka River plume facilitates transport of ruminant faecal contaminants into shellfish growing waters, Tasman Bay, New Zealand. *New Zealand Journal of Marine and Freshwater Research*. 45, 477-495, 10.1080/00288330.2011.587822.
- Cossey, N. L., Dvanajscak, Z., Larsen, C. P., 2020. A diagnostician's field guide to crystalline nephropathies. *Seminars in Diagnostic Pathology*. 37, 135-142, 10.1053/j.semmdp.2020.02.002.
- Costa, P. M., 2018a, Identification of Major Histopathological Traits. In: P. M. Costa, (Ed.), *The Handbook of Histopathological Practices in Aquatic Environments*. Academic Press, London pp. 135-190.
- Costa, P. M., 2018b Introduction. In: P. M. Costa, (Ed.), *The Handbook of Histopathological Practices in Aquatic Environments*. Academic Press, London , pp. 1-20.
- Costa, P. M., 2018c, Scoring and Data Processing. In: P. M. Costa, (Ed.), *The Handbook of Histopathological Practices in Aquatic Environments*. Academic Press, London pp. 191-216.
- Costa, P. M., Carreira, S., Costa, M. H., Caeiro, S., 2013. Development of histopathological indices in a commercial marine bivalve (*Ruditapes decussatus*) to determine environmental quality. *Aquatic Toxicology*. 126, 442-54, 10.1016/j.aquatox.2012.08.013.
- Costello, K. E., Lynch, S. A., O'Riordan, R. M., McAllen, R., Culloty, S. C., 2021. The importance of marine bivalves in invasive Host-Parasite introductions. *Frontiers in Marine Science*. 8, 10.3389/fmars.2021.609248.
- Costello, M. J., Coll, M., Danovaro, R., Halpin, P., Ojaveer, H., Miloslavich, P., 2010. A census of marine biodiversity knowledge, resources, and future challenges. *PloS one*. 5, e12110, 10.1371/journal.pone.0012110.
- Coughlan, B. M., Moroney, G. A., van Pelt, F. N., O'Brien, N. M., Davenport, J., O'Halloran, J., 2009. The effects of salinity on the Manila clam (*Ruditapes philippinarum*) using the neutral red retention assay with adapted physiological saline solutions. *Marine Pollution Bulletin*. 58, 1680-4, 10.1016/j.marpolbul.2009.06.020.
- Crick, R. E., Burkart, B., Chamberlain, J. A., Mann, K. O., 2009. Chemistry of calcified portions of *Nautilus Pompilius*. *Journal of the Marine Biological Association of the United Kingdom*. 65, 415-420, 10.1017/s0025315400050517.
- Crissman, J. W., Goodman, D. G., Hildebrandt, P. K., Maronpot, R. R., Prater, D. A., Riley, J. H., Seaman, W. J., Thake, D. C., 2004. Best practices guideline: toxicologic histopathology. *Toxicologic Pathology*. 32, 126-31, 10.1080/01926230490268756.
- Cuevas, N., Zorita, I., Costa, P. M., Franco, J., Larreta, J., 2015. Development of histopathological indices in the digestive gland and gonad of mussels: integration with contamination levels and effects of confounding factors. *Aquatic Toxicology*. 162, 152-164, 10.1016/j.aquatox.2015.03.011.
- Cule, E. S., Frankowski, M. D., ridge: Ridge Regression with Automatic Selection of the Penalty Parameter. R package version 3.0, <https://CRAN.R-project.org/package=ridge>, 2021.
- Dame, R. F., 2016. *Ecology of Marine Bivalves: An Ecosystem Approach*, Second Edition (2nd ed.). CRC Press. <https://doi.org/10.1201/b11220>
- Damodaran, D., 2020. Morphological, histological and behavioural change in two species of marine bivalves in response to environmental stress. *Marine Biology*, (Masters). Victoria University of Wellington, New Zealand, pp. 130.
- Darriba, S., San Juan, F., Guerra, A., 2005. Energy storage and utilization in relation to the reproductive cycle in the razor clam *Ensis arcuatus* (Jeffreys, 1865). *ICES Journal of Marine Science*. 62, 886-896,
- David, J. A., Salaroli, R. B., Fontanetti, C. S., 2008. The significance of changes in *Mytella falcata* (Orbigny, 1842) gill filaments chronically exposed to polluted environments. *Micron*. 39, 1293-9, 10.1016/j.micron.2008.03.001.
- Dawber, C., Association, N. Z. M. F., Staff, N. Z. M. F. A., 2004. *Lines in the water: A history of greenshell mussel farming in New Zealand*. River Press.
- Day, R. W., Cook, P., 1995. Bias towards brown algae in determining diet and food preferences: The South African abalone *Haliotis midae*. *Marine and Freshwater Research*. 46, 623-627, 10.1071/mf9950623.
- Day, R.W. and Fleming, A.E. (1992) The Determinants and Measurement of Abalone Growth. In: Shepherd, S.A., Tegner, M.J. and Guzmán del Próo, S.A., Eds., *Abalone of the World: Biology, Fisheries and Culture*, Blackwell, Oxford, 141-164.

- de la Ballina, N. R., Maresca, F., Cao, A., Villalba, A., 2022. Bivalve haemocyte subpopulations: A review. *Frontiers in immunology*. 13, 826255, 10.3389/fimmu.2022.826255.
- de la Ballina, N. R., Villalba, A., Cao, A., 2020. Differences in proteomic profile between two haemocyte types, granulocytes and hyalinocytes, of the flat oyster *Ostrea edulis*. *Fish and Shellfish Immunology*. 100, 456-466, 10.1016/j.fsi.2020.03.033.
- de la Iglesia, H. O., Johnson, C. H., 2013. Biological clocks: riding the tides. *Current Biology*. 23, R921-3, 10.1016/j.cub.2013.09.006.
- de La Rocque, S., Rioux, J. A., Slingenbergh, J., 2008. Climate change: effects on animal disease systems and implications for surveillance and control. *Revue Scientifique et Technique*. 27, 339-54, <https://www.ncbi.nlm.nih.gov/pubmed/18819664>
- de Montaudouin, X., Paul-Pont, I., Lambert, C., Gonzalez, P., Raymond, N., Jude, F., Legeay, A., Baudrimont, M., Dang, C., Le Grand, F., Le Goic, N., Bourasseau, L., Paillard, C., 2010. Bivalve population health: multistress to identify hot spots. *Marine Pollution Bulletin*. 60, 1307-18, 10.1016/j.marpolbul.2010.03.011.
- De Vico, G., Carella, F., 2012. Morphological features of the inflammatory response in molluscs. *Research in Veterinary Science*. 93, 1109-15, 10.1016/j.rvsc.2012.03.014.
- de Zwaan, A., Zandee, D., 1972. Body distribution and seasonal changes in the glycogen content of the common sea mussel *Mytilus edulis*. *Comparative Biochemistry and Physiology Part A: Physiology*. 43, 53,
- Delisle, L., Bui, T., Copedo, J., Laroche, O., von Ammon, U., Lane, H. S., Hutson, K. S., 2025. Isolation, culture, and optimal growth conditions for the shellfish protozoan parasite, *Perkinsus olseni*. *International Journal of Parasitology*. 10.1016/j.ijpara.2025.04.011.
- Delisle, L., Petton, B., Burguin, J. F., Morga, B., Corporeau, C., Pernet, F., 2018. Temperature modulate disease susceptibility of the Pacific oyster *Crassostrea gigas* and virulence of the *Ostreid herpesvirus* type 1. *Fish and Shellfish Immunology*. 80, 71-79, 10.1016/j.fsi.2018.05.056.
- Delorme, N., Biessy, L., South, P., Zamora, L., Ragg, N., Burritt, D., 2020a. Stress-on-stress responses of a marine mussel, *Perna canaliculus*: food limitation reduces the ability to cope with heat stress in juveniles. *Marine Ecology Progress Series*. 644, 105-117,
- Delorme, N. J., 2017, Thermal biology of the New Zealand sea urchin. School of Biological science, (Doctoral dissertation) University of Auckland, Auckland, New Zealandpp. 160.
- Delorme, N. J., Burritt, D. J., Ragg, N. L. C., South, P. M., 2021a. Emersion and Relative Humidity Modulate Stress Response and Recovery Dynamics in Juvenile Mussels (*Perna canaliculus*). *Metabolites*. 11, 580, 10.3390/metabo11090580.
- Delorme, N. J., Frost, E. J., Sewell, M. A., 2020b. Effect of acclimation on thermal limits and hsp70 gene expression of the New Zealand sea urchin *Evechinus chloroticus*. *Comparative Biochemistry and Physiology Part A: Molecular and Integrative Physiology*. 250, 110806, 10.1016/j.cbpa.2020.110806.
- Delorme, N. J., King, N., Cervantes-Loreto, A., South, P. M., Baettig, C. G., Zamora, L. N., Knight, B. R., Ericson, J. A., Smith, K. F., Ragg, N. L. C., 2024. Genetics and ontogeny are key factors influencing thermal resilience in a culturally and economically important bivalve. *Scientific Reports*. 14, 19130, 10.1038/s41598-024-70034-0.
- Delorme, N. J., Venter, L., Rolton, A., Ericson, J. A., 2021b. Integrating animal health and stress assessment tools using the green-lipped mussel *Perna canaliculus* as a case study. *Journal of Shellfish Research*. 40, 93-112,
- Di Lorenzo, E., Mantua, N., 2016. Multi-year persistence of the 2014/15 North Pacific marine heatwave. *Nature Climate Change*. 6, 1042-1047,
- Diggles, B. K., Nichol, J., Hin, P. M., Wakefield, S., Cochenne-Laureau, N., Roberts, R. D., Friedman, C. S., 2002. Pathology of cultured paua *Haliotis iris* infected with a novel haplosporidian parasite, with some observations on the course of disease. *Diseases of Aquatic Organisms*. 50, 219-31, 10.3354/dao050219.
- Diggles, B. K., Oliver, M., 2005. Diseases of cultured paua (*Haliotis iris*) in New Zealand. In: Walker, P.J., R.G. Lester, M.G. Bondad-Reantaso (eds.) *Diseases in Asian Aquaculture V. Proceedings of the 5th Symposium on Diseases in Asian Aquaculture*. Fish Health Section, Asian Fisheries Society, Manila. pp. 275-287.
- Dittman, D., Ford, S., Padilla, D., 2001. Effects of *Perkinsus marinus* on reproduction and condition of the eastern oyster, *Crassostrea virginica*, depend on timing. *Journal of Shellfish Research*. 20, 1025-1034,

- Dolman, C. L., MacLeod, P. M., Lipofuscin and its Relation to Aging. In: S. Fedoroff, L. Hertz, (Eds.), *Advances in Cellular Neurobiology*. Elsevier, 1981, pp. 205-247.
- Doney, S. C., Ruckelshaus, M., Duffy, J. E., Barry, J. P., Chan, F., English, C. A., Galindo, H. M., Grebmeier, J. M., Hollowed, A. B., Knowlton, N., Polovina, J., Rabalais, N. N., Sydeman, W. J., Talley, L. D., 2012a. Climate change impacts on marine ecosystems. *Annual Review of Marine Science*. 4, 11-37, 10.1146/annurev-marine-041911-111611.
- Doney, S. C., Ruckelshaus, M., Emmett Duffy, J., Barry, J. P., Chan, F., English, C. A., Galindo, H. M., Grebmeier, J. M., Hollowed, A. B., Knowlton, N., 2012b. Climate change impacts on marine ecosystems. *Annual Review of Marine Science*. 4, 11-37,
- Doyle, L. J., Blake, N. J., Woo, C. C., Yevich, P., 1978. Recent biogenic phosphorite: concretions in mollusk kidneys. *Science*. 199, 1431-3, 10.1126/science.199.4336.1431.
- Dungan, C. F., Reece, K. S., Moss, J. A., Hamilton, R. M., Diggles, B. K., 2007. *Perkinsus olseni* in vitro isolates from the New Zealand clam *Austrovenus stutchburyi*. *Journal of Eukaryotic Microbiology*. 54, 263-70, 10.1111/j.1550-7408.2007.00265.x.
- Dunphy, B. J., Ragg, N. L., Collings, M. G., 2013. Latitudinal comparison of thermotolerance and HSP70 production in F2 larvae of the greenshell mussel (*Perna canaliculus*). *Journal of Experimental Biology*. 216, 1202-9, 10.1242/jeb.076729.
- Dunphy, B. J., Ruggiero, K., Zamora, L. N., Ragg, N. L. C., 2018. Metabolomic analysis of heat-hardening in adult green-lipped mussel (*Perna canaliculus*): A key role for succinic acid and the GABAergic synapse pathway. *Journal of Thermal Biology*. 74, 37-46, <https://doi.org/10.1016/j.jtherbio.2018.03.006>.
- Dunphy, B. J., Watts, E., Ragg, N. L. C., 2015. Identifying thermally-stressed adult green-lipped mussels (*Perna canaliculus* Gmelin, 1791) via metabolomic profiling. *American Malacological Bulletin*. 33, 127-135, 9, <https://doi.org/10.4003/006.033.0110>
- Eckelbarger, K. J., Hodgson, A. N., 2021. Invertebrate oogenesis – a review and synthesis: comparative ovarian morphology, accessory cell function and the origins of yolk precursors. *Invertebrate Reproduction and Development*. 65, 71-140, 10.1080/07924259.2021.1927861.
- Elbrecht, V., Peinert, B., Leese, F., 2017. Sorting things out: Assessing effects of unequal specimen biomass on DNA metabarcoding. *Ecology and Evolution*. 7, 6918-6926, 10.1002/ece3.3192.
- Elmore, S. A., Dixon, D., Hailey, J. R., Harada, T., Herbert, R. A., Maronpot, R. R., Nolte, T., Rehg, J. E., Rittinghausen, S., Rosol, T. J., Satoh, H., Vidal, J. D., Willard-Mack, C. L., Creasy, D. M., 2016. Recommendations from the INHAND Apoptosis/Necrosis Working Group. *Toxicologic Pathology*. 44, 173-88, 10.1177/0192623315625859.
- Ericson, J. A., Venter, L., Copedo, J. S., Nguyen, V. T., Alfaro, A. C., Ragg, N. L. C., 2023. Chronic heat stress as a predisposing factor in summer mortality of mussels, *Perna canaliculus*. *Aquaculture*. 564, 10.1016/j.aquaculture.2022.738986.
- Ericson, J. A., Venter, L., Welford, M. R., Kumanan, K., Alfaro, A. C., Ragg, N. L., 2022. Effects of seawater temperature and acute *Vibrio sp.* challenge on the haemolymph immune and metabolic responses of adult mussels (*Perna canaliculus*). *Fish and Shellfish Immunology*. 128, 664-675,
- Esposito, G., Pastorino, P., Prearo, M., 2022. Environmental stressors and pathology of marine molluscs. *Journal of Marine Science and Engineering*. 10, 313, <https://www.mdpi.com/2077-1312/10/3/313>
- Euripidou, E., Murray, V., 2004. Public health impacts of floods and chemical contamination. *Journal of Public Health (Oxf)*. 26, 376-83, 10.1093/pubmed/fdh163.
- Ewere, E. E., Rosic, N., Bayer, P. E., Ngangbam, A., Edwards, D., Kelaher, B. P., Mamo, L. T., Benkendorff, K., 2021. Marine heatwaves have minimal influence on the quality of adult Sydney rock oyster flesh. *Science of the Total Environment*. 795, 148846, 10.1016/j.scitotenv.2021.148846.
- Fearman, J.-A., Bolch, C. J. S., Moltschaniwskyj, N. A., 2009. Energy storage and reproduction in mussels, *Mytilus galloprovincialis*: The influence of diet quality. *Journal of Shellfish Research*. 28, 305-312, 8, <https://doi.org/10.2983/035.028.0212>
- Fearman, J., Moltschaniwskyj, N., 2010. Warmer temperatures reduce rates of gametogenesis in temperate mussels, *Mytilus galloprovincialis*. *Aquaculture*. 305, 20-25,
- Feder, M. E., Hofmann, G. E., 1999. Heat-shock proteins, molecular chaperones, and the stress response: evolutionary and ecological physiology. *Annual Review of Physiology*. 61, 243-82, 10.1146/annurev.physiol.61.1.243.

- Filgueira, R., Guyondet, T., Comeau, L. A., Tremblay, R., 2016. Bivalve aquaculture-environment interactions in the context of climate change. *Global Change Biology*. 22, 3901-3913, 10.1111/gcb.13346.
- Foale, S., Day, R., 1992. Recognizability of algae ingested by abalone. *Marine and Freshwater Research*. 43, 1331-1338, <https://doi.org/10.1071/MF9921331>.
- Folt, C. L., Chen, C. Y., Moore, M. V., Burnaford, J., 1999. Synergism and antagonism among multiple stressors. *Limnology and Oceanography*. 44, 864-877, 10.4319/lo.1999.44.3_part_2.0864.
- Fraga, N., Benito, D., Briaudeau, T., Izagirre, U., Ruiz, P., 2022. Toxicopathic effects of lithium in mussels. *Chemosphere*. 307, 136022, 10.1016/j.chemosphere.2022.136022.
- Fraser, C., White, R., Snelder, T., Stoffels, R., New Zealand Coastal Water Quality Assessment. In: NIWA, (Ed.), Prepared for the Ministry for the Environment., 2021.
- Froehlich, H. E., Koehn, J. Z., Holsman, K. K., Halpern, B. S., 2022. Emerging trends in science and news of climate change threats to and adaptation of aquaculture. *Aquaculture*. 549, 737812, 10.1016/j.aquaculture.2021.737812.
- Fukazawa, H., Takami, H., Kawamura, T., Watanabe, Y., 2005. The effect of egg quality on larval period and postlarval survival of an abalone *Haliotis discus hannai*. *Journal of Shellfish Research*. 24, 1141-1147,
- Fulda, S., Gorman, A. M., Hori, O., Samali, A., 2010. Cellular stress responses: cell survival and cell death. *International Journal of Cell Biology*. 2010, 214074, 10.1155/2010/214074.
- Gabbot, P., 1975, Storage cycles in marine bivalve molluscs: A hypothesis concerning the relationship between glycogen metabolism and gametogenesis, in. *Proceeding of the 9th European Marine Biology Symposium*. Aberdeen University Press, pp. 191-211.
- Gabbott, P. A., Bayne, B. L., 2009. Biochemical effects of temperature and nutritive stress on *Mytilus Edulis* L. *Journal of the Marine Biological Association of the United Kingdom*. 53, 269-286, 10.1017/s0025315400022268.
- Gagnaire, B., Gay, M., Huvet, A., Daniel, J. Y., Saulnier, D., Renault, T., 2007. Combination of a pesticide exposure and a bacterial challenge: *in vivo* effects on immune response of Pacific oyster, *Crassostrea gigas* (Thunberg). *Aquatic Toxicology*. 84, 92-102, 10.1016/j.aquatox.2007.06.002.
- Galap, C., Leboulenger, F., Grillot, J. P., 1997. Seasonal variations in biochemical constituents during the reproductive cycle of the female dog cockle *Glycymeris glycymeris*. *Marine Biology*. 129, 625-634, 10.1007/s002270050205.
- Galinou-Mitsoudi, S., Sinis, A. I., 1994. Reproductive cycle and fecundity of the date mussel *Lithophaga Lithophaga* (Bivalvia: Mytilidae). *Journal of Molluscan Studies*. 60, 371-385, 10.1093/mollus/60.4.371.
- Galtsoff, P. S., 1964. *The American oyster, Crassostrea virginica* gmelin. US Government Printing Office, Washington.
- Garcia-R, J. C., Hayman, D. T. S., 2023. A review and analysis of cryptosporidiosis outbreaks in New Zealand. *Parasitology*. 150, 606-611, 10.1017/S0031182023000288.
- Garrabou, J., Coma, R., Bensoussan, N., Bally, M., Chevaldonn É, P., Cigliano, M., Diaz, D., Harmelin, J. G., Gambi, M. C., Kersting, D. K., Ledoux, J. B., Lejeusne, C., Linares, C., Marschal, C., Perez, T., Ribes, M., Romano, J. C., Serrano, E., Teixido, N., Torrents, O., Zabala, M., Zuberer, F., Cerrano, C., 2009. Mass mortality in North-western Mediterranean rocky benthic communities: effects of the 2003 heat wave. *Global Change Biology*. 15, 1090-1103, 10.1111/j.1365-2486.2008.01823.x.
- Geider, S., Dussol, B., Nitsche, S., Veesler, S., Berthezene, P., Dupuy, P., Astier, J. P., Boistelle, R., Berland, Y., Dagorn, J. C., Verdier, J. M., 1996. Calcium carbonate crystals promote calcium oxalate crystallization by heterogeneous or epitaxial nucleation: possible involvement in the control of urinary lithogenesis. *Calcified Tissue International*. 59, 33-7, 10.1007/s002239900082.
- Geiger, D. L., 1999. Distribution and biogeography of the recent Haliotidae world-wide: (Gastropoda: Vetigastropoda). *Bollettino Malacologico*. 35, 57-118,
- Geraghty, R., Wood, K., Sayer, J. A., 2020. Calcium oxalate crystal deposition in the kidney: identification, causes and consequences. *Urolithiasis*. 48, 377-384, 10.1007/s00240-020-01202-w.
- Gibson-Corley, K. N., Olivier, A. K., Meyerholz, D. K., 2013. Principles for valid histopathologic scoring in research. *Veterinary Pathology*. 50, 1007-15, 10.1177/0300985813485099.

- Gibson, R., Atkinson, R., 2003. The effects of sedimentation on rocky coast assemblages. *Oceanography and Marine Biology*. 41, 161-236,
- Giese, A. C., Pearse, J. S., 1974. *Reproduction of marine invertebrates: I. Acoelomate and Pseudocoelomate Metazoans*. Academic Press: New York. 546 pp. <https://dx.doi.org/10.1016/C2013-0-10718-0>
- Gignoux-Wolfsohn, S. A., Newcomb, M. S. R., Ruiz, G. M., Pagenkopp Lohan, K. M., 2021. Environmental factors drive the release of *Perkinsus marinus* from infected oysters. *Parasitology*. 148, 532-538, [10.1017/S0031182020002383](https://doi.org/10.1017/S0031182020002383).
- Gnanalingam, G., Pritchard, D. W., Richards, D. K., Subritzky, P., Flack, B., Hepburn, C. D., 2021. Local management to support local fisheries: Rāhui (temporary closure) and bag limits for blackfoot abalone (*Haliotis iris*) in southern New Zealand. *Aquatic Conservation: Marine and Freshwater Ecosystems*. 31, 2320-2333, [10.1002/aqc.3662](https://doi.org/10.1002/aqc.3662).
- Goggin, C., Lester, R., 1995. *Perkinsus*, a protistan parasite of abalone in Australia: a review. *Marine and Freshwater Research*. 46, 639-646,
- Golstein, P., Kroemer, G., 2007. Cell death by necrosis: towards a molecular definition. *Trends in Biochemical Sciences*. 32, 37-43, [10.1016/j.tibs.2006.11.001](https://doi.org/10.1016/j.tibs.2006.11.001).
- Gordon, H. R., Cook, P. A., 2004. World abalone fisheries and aquaculture update: supply and market dynamics. *Journal of Shellfish Research*. 23, 935-940,
- Gosling, E., 2008. *An Introduction to Bivalves*. In. *Bivalve molluscs: biology, ecology and culture*. John Wiley and Sons. Blackwell Publishing, Oxford pp. 1-6
- Gosling, E., 2015a *Diseases and parasites*. In. *Marine Bivalve Molluscs*, John Wiley and Sons. Oxford pp. 429-477.
- Gosling, E., 2015b *Reproduction, settlement and recruitment*. In. *Marine Bivalve Molluscs*, John Wiley and Sons. Oxford pp. 157-202.
- Govekar, P. D., Griffin, C., Beggs, H., 2022. Multi-sensor sea surface temperature products from the Australian bureau of meteorology. *Remote Sensing*. 14, 3785, <https://www.mdpi.com/2072-4292/14/15/3785>
- Grandiosa, R., 2019. *Investigation of the Pathophysiology of the New Zealand Black-Footed Abalone (Haliotis iris)* (Doctoral dissertation), Auckland University of Technology, New Zealand.
- Gruber, N., Clement, D., Carter, B. R., Feely, R. A., van Heuven, S., Hoppema, M., Ishii, M., Key, R. M., Kozyr, A., Lauvset, S. K., Lo Monaco, C., Mathis, J. T., Murata, A., Olsen, A., Perez, F. F., Sabine, C. L., Tanhua, T., Wanninkhof, R., 2019. The oceanic sink for anthropogenic CO₂ from 1994 to 2007. *Science*. 363, 1193-1199, [10.1126/science.aau5153](https://doi.org/10.1126/science.aau5153).
- Gunderson, A. R., Armstrong, E. J., Stillman, J. H., 2016. Multiple stressors in a changing world: The need for an improved perspective on physiological responses to the dynamic marine environment. *Annual Review of Marine Science*. 8, 357-78, [10.1146/annurev-marine-122414-033953](https://doi.org/10.1146/annurev-marine-122414-033953).
- Guo, X., Ford, S. E., 2016a. Infectious diseases of marine molluscs and host responses as revealed by genomic tools. *Philosophical transactions of the Royal Society of London. Series B, Biological sciences*. 371, [10.1098/rstb.2015.0206](https://doi.org/10.1098/rstb.2015.0206).
- Guo, X., Ford, S. E., 2016b. Infectious diseases of marine molluscs and host responses as revealed by genomic tools. *Philosophical Transactions of the Royal Society B: Biological Sciences*. 371, 20150206,
- Guo, X., He, Y., Zhang, L., Lelong, C., Jouaux, A., 2015. Immune and stress responses in oysters with insights on adaptation. *Fish and Shellfish Immunology*. 46, 107-19, [10.1016/j.fsi.2015.05.018](https://doi.org/10.1016/j.fsi.2015.05.018).
- Haberkorn, H., Lambert, C., Le Goïc, N., Moal, J., Suquet, M., Guéguen, M., Sunila, I., Soudant, P., 2010. Effects of *Alexandrium minutum* exposure on nutrition-related processes and reproductive output in oysters *Crassostrea gigas*. *Harmful Algae*. 9, 427-439, [10.1016/j.hal.2010.01.003](https://doi.org/10.1016/j.hal.2010.01.003).
- Hadfield, J. D., 2010. MCMC Methods for multi-response generalized linear mixed models: The MCMCglmm R Package. *Journal of Statistical Software*. 33, 1 - 22, [10.18637/jss.v033.i02](https://doi.org/10.18637/jss.v033.i02).
- Halpern, B. S., Frazier, M., Verstaen, J., Rayner, P.-E., Clawson, G., Blanchard, J. L., Cottrell, R. S., Froehlich, H. E., Gephart, J. A., Jacobsen, N. S., Kuempel, C. D., McIntyre, P. B., Metian, M., Moran, D., Nash, K. L., Többen, J., Williams, D. R., 2022. The environmental footprint of global food production. *Nature Sustainability*. 5, 1027-1039, [10.1038/s41893-022-00965-x](https://doi.org/10.1038/s41893-022-00965-x).
- Halpern, B. S., Walbridge, S., Selkoe, K. A., Kappel, C. V., Micheli, F., D'Agrosa, C., Bruno, J. F., Casey, K. S., Ebert, C., Fox, H. E., Fujita, R., Heinemann, D., Lenihan, H. S., Madin, E. M.,

- Perry, M. T., Selig, E. R., Spalding, M., Steneck, R., Watson, R., 2008. A global map of human impact on marine ecosystems. *Science*. 319, 948-52, 10.1126/science.1149345.
- Handisyde, N., Telfer, T. C., Ross, L. G., 2017. Vulnerability of aquaculture-related livelihoods to changing climate at the global scale. *Fish and Fisheries*. 18, 466-488,
- Handler, J., 2022, General pathology and diseases of abalone. In: F. S. B. Kibenge, et al., Eds., *Aquaculture Pathophysiology*. Academic Press, Elsevier Inc. pp. 405-447.
- Handler, J., Bastianello, S., Callinan, R., Carson, J., Creeper, J., Deveney, M., Forsyth, W., Freeman, K., Hooper, C., Jones, B., 2002. Abalone aquaculture subprogram: A national survey of diseases of commercially exploited abalone species to support trade and translocation issues and the development of health surveillance programs. FRDC project Report. 201,
- Harris, J., Burke, C., Maguire, G., 1998. Characterisation of the digestive tract of greenlip abalone, *Haliotis laevis* Donovan. I. morphology and histology. *Journal of Shellfish Research*. 17, 979-988,
- Hartenstein, V., Martinez, P., 2019. Phagocytosis in cellular defense and nutrition: a food-centered approach to the evolution of macrophages. *Cell Tissue Research*. 377, 527-547, 10.1007/s00441-019-03096-6.
- Hartmann, D. L., Pendergrass, A. G., 2014. The atmospheric energy constraint on global-mean precipitation change. *Journal of Climate*. 27, 757-768, 10.1175/jcli-d-13-00163.1.
- Harvell, C. D., Kim, K., Burkholder, J. M., Colwell, R. R., Epstein, P. R., Grimes, D. J., Hofmann, E. E., Lipp, E. K., Osterhaus, A. D., Overstreet, R. M., Porter, J. W., Smith, G. W., Vasta, G. R., 1999. Emerging marine diseases - climate links and anthropogenic factors. *Science*. 285, 1505-10, 10.1126/science.285.5433.1505.
- Harvell, C. D., Mitchell, C. E., Ward, J. R., Altizer, S., Dobson, A. P., Ostfeld, R. S., Samuel, M. D., 2002. Climate warming and disease risks for terrestrial and marine biota. *Science*. 296, 2158-62, 10.1126/science.1063699.
- Hasani, E., Schallner, J., von der Hagen, M., Falkenburger, B., Sobottka, S. B., Eyupoglu, I., Schackert, G., Polanski, W. H., 2023. Deep brain stimulation in a patient with TSPOAP1-Biallelic variant of autosomal-recessive dystonia. *Movement Disorders*. 38, 2139-2140, 10.1002/mds.29618.
- Hassan, M. M., Qin, J. G., Li, X., 2018. Gametogenesis, sex ratio and energy metabolism in *Ostrea angasi*: implications for the reproductive strategy of spermcasting marine bivalves. *Journal of Molluscan Studies*. 84, 38-45, 10.1093/mollus/eyx041.
- Hawkins, A. J. S., Bayne, B. L., 1985. Seasonal variation in the relative utilization of carbon and nitrogen by the mussel *Mytilus edulis*: budgets, conversion efficiencies and maintenance requirements. *Marine Ecology Progress Series*. 25, 181-188, <http://www.jstor.org/stable/24817328>
- Hawks, B. S., Michael Aust, W., Chad Bolding, M., Barrett, S. M., Schilling, E. B., Prisley, S. P., 2022. Increased levels of forestry best management practices reduce sediment delivery from middle and lower coastal plain clearcut harvests and access features, southeastern states, USA. *Forest Ecology and Management*. 519, 120323, 10.1016/j.foreco.2022.120323.
- Hay, M. E., 1996. Defensive synergisms? reply to Pennings. *Ecology*. 77, 1950-1952, 10.2307/2265800.
- Healy, J. M., 2001, The mollusca. In: D. T. Anderson, (Ed.), *Invertebrate zoology*. Oxford University, Oxford, pp. 453.
- Heidemann, H., Ribbe, J., 2019. Marine heat waves and the influence of El Niño off southeast Queensland, Australia. *Frontiers in Marine Science*. 6.
- Hendriks, H. R., Eestermans, I. L., 1986. Phagocytosis and lipofuscin accumulation in lymph node macrophages. *Mechanisms of Ageing and Development*. 35, 161-7, 10.1016/0047-6374(86)90006-0.
- Hettiarachchi, S., Wasko, C., Sharma, A., 2018. Increase in flood risk resulting from climate change in a developed urban watershed – the role of storm temporal patterns. *Hydrology and Earth System Sciences*. 22, 2041-2056, 10.5194/hess-22-2041-2018.
- Heuer C, Stevenson MA. (2021) Diagnostic test validation studies when there is a perfect reference standard. *Revue scientifique et technique*.;40(1):261-270. doi: 10.20506/rst.40.1.3223. PMID: 34140725.
- Hickman, R. W., Illingworth, J., 1980. Condition cycle of the green-lipped mussel *Perna canaliculus* in New Zealand. *Marine Biology*. 60, 27-38,

- Hickman, R. W., Waite, R. P., Illingworth, J., Meredyth-Young, J. L., Payne, G., 1991. The relationship between farmed mussels, *Perna canaliculus*, and available food in Pelorus-Keneperu Sound, New Zealand, 1983–1985. *Aquaculture*. 99, 49-68, [https://doi.org/10.1016/0044-8486\(91\)90287-H](https://doi.org/10.1016/0044-8486(91)90287-H).
- Hill, K. M., Stokes, N. A., Webb, S. C., Hine, P. M., Kroeck, M. A., Moore, J. D., Morley, M. S., Reece, K. S., Burrenson, E. M., Carnegie, R. B., 2014. Phylogenetics of *Bonamia* parasites based on small subunit and internal transcribed spacer region ribosomal DNA sequence data. *Diseases of Aquatic Organisms*. 110, 33-54, 10.3354/dao02738.
- Hine, M., Diggles, B., 2002. The distribution of *Perkinsus olseni* in New Zealand bivalve molluscs. *Surveillance (Wellington)*. 29, 8-1.
- Hine, P. M., 1997. Health status of commercially important molluscs in New Zealand. Ministry for Primary Industries.
- Hine, P. M., 2002. Severe apicomplexan infection in the oyster *Ostrea chilensis*: a possible predisposing factor in bonamiosis. *Diseases of Aquatic Organisms*. 51, 49-60, 10.3354/dao051049.
- Hine, P. M., 2020. Haplosporidian host:parasite interactions. *Fish and Shellfish Immunology*. 103, 190-199, 10.1016/j.fsi.2020.05.004.
- Hine, P. M., Wakefield, S., Diggles, B. K., Webb, V. L., Maas, E. W., 2002. Ultrastructure of a haplosporidian containing Rickettsiae, associated with mortalities among cultured paua *Haliotis iris*. *Diseases of Aquatic Organisms*. 49, 207-19, 10.3354/dao049207.
- Hobday, A. J., Alexander, L. V., Perkins, S. E., Smale, D. A., Straub, S. C., Oliver, E. C. J., Benthuyssen, J. A., Burrows, M. T., Donat, M. G., Feng, M., Holbrook, N. J., Moore, P. J., Scannell, H. A., Sen Gupta, A., Wernberg, T., 2016. A hierarchical approach to defining marine heatwaves. *Progress in Oceanography*. 141, 227-238, 10.1016/j.pocean.2015.12.014.
- Hochachka, P. W., Somero, G. N., 2002. *Biochemical adaptation: mechanism and process in physiological evolution*. Online edn, Oxford University Press, New York. <https://doi.org/10.1093/oso/9780195117028.001.0001>.
- Hole, L. M., Moore, M. N., Bellamy, D., 1995. Age-related cellular and physiological reactions to hypoxia and hyperthermia in marine mussels. *Marine Ecology Progress Series*. 122, 173-178, <https://ezproxy.aut.ac.nz/login?url=https://search.ebscohost.com/login.aspx?direct=true&site=eds-live&db=edsjsrandAN=edsjsr.24852267>
- Hooker, S. H., Creese, R. G., 1995. Reproduction of paua, *Haliotis iris* Gmelin 1791 (Mollusca: Gastropoda), in north-eastern New Zealand. *Marine and Freshwater Research*. 46, 617-622, 10.1071/mf9950617.
- Hooper, C., Day, R., Slocombe, R., Benkendorff, K., Handlinger, J., Goulias, J., 2014. Effects of severe heat stress on immune function, biochemistry and histopathology in farmed Australian abalone (hybrid *Haliotis laevis* × *Haliotis rubra*). *Aquaculture*. 432, 26-37, 10.1016/j.aquaculture.2014.03.032.
- Horodesky, A., Castilho-Westphal, G., Cozer, N., Rossi, V., Ostrensky, A., 2019. Effects of salinity on the survival and histology of oysters *Crassostrea gasar* (Adanson, 1757). *Bioscience Journal*. 35, 586-597, 10.14393/BJ-v35n2a2019-42099.
- Houghton, J., 2009. *Global warming: the complete briefing*. Cambridge University press, Cambridge. 1-238, <https://doi.org/10.1017/CBO9780511841590>
- Houghton, J. E. T., Ding, Y., Griggs, D., Noguer, M., van der Linden, P., Dai, X., Maskell, M., Johnson, C., Climate Change 2001: The Scientific Basis: Contribution of Working Group I to the Third Assessment Report of the Intergovernmental Panel on Climate Change (IPCC). Cambridge University Press, pp. 881.
- Houghton, J. T., Jenkins, G. J., Ephraums, J. J., 1990. Climate change: the IPCC scientific assessment. *American Scientist*, United States. 80,
- Howard, D. W., 2004. *Histological techniques for marine bivalve mollusks and crustaceans*. NOAA, National Ocean Service, National Centers for Coastal Ocean Service, Center for Coastal Environmental Health and Biomolecular Research, Cooperative Oxford Laboratory.
- Howells, J., Jaramillo, D., Brosnahan, C. L., Pande, A., Lane, H. S., 2021. Intracellular bacteria in New Zealand shellfish are identified as *Endozoicomonas* species. *Diseases of Aquatic Organisms*. 143, 27-37, 10.3354/dao03547.
- Hu, Z., Song, H., Feng, J., Zhou, C., Yang, M.-J., Shi, P., Yu, Z.-L., Li, Y.-R., Guo, Y.-J., Li, H.-Z., Zhang, T., 2022. Massive heat shock protein 70 genes expansion and transcriptional signatures

- uncover hard clam adaptations to heat and hypoxia. *Frontiers in Marine Science*. 9, 10.3389/fmars.2022.898669.
- Hughes, F. M., Foster, B., Grewal, S., Sokolova, I. M., 2010. Apoptosis as a host defense mechanism in *Crassostrea virginica* and its modulation by *Perkinsus marinus*. *Fish and Shellfish Immunology*. 29, 247-57, 10.1016/j.fsi.2010.03.003.
- Hummel, H., de Wolf, L., Zurburg, W., Apon, L., Bogaards, R. H., van Ruitenburg, M., 1989. The glycogen content in stressed marine bivalves: The initial absence of a decrease. *Comparative Biochemistry and Physiology Part B: Comparative Biochemistry*. 94, 729-733, 10.1016/0305-0491(89)90157-0.
- Humphreys, M. P., Browman, H., 2017. Climate sensitivity and the rate of ocean acidification: future impacts, and implications for experimental design. *ICES Journal of Marine Science*. 74, 934-940, 10.1093/icesjms/fsw189.
- Ibarrola, I., Hilton, Z., Ragg, N. L. C., 2017. Physiological basis of inter-population, inter-familial and intra-familial differences in growth rate in the green-lipped mussel *Perna canaliculus*. *Aquaculture*. 479, 544-555, 10.1016/j.aquaculture.2017.06.031.
- Itoiz, S., Metz, S., Derelle, E., Rene, A., Garces, E., Bass, D., Soudant, P., Chambouvet, A., 2021. Emerging parasitic protists: The Ccse of Perkinsia. *Frontiers in Microbiology*. 12, 735815, 10.3389/fmicb.2021.735815.
- Jacobs, P., Blom, G., van der Linden, T., 2000. Climatological changes in storm surges and river discharges: the impact on flood protection and salt intrusion in the Rhine-Meuse Delta. In: ECLAT-2 KNMI Workshop Report No. 3. 35.
- Jeffs, A. G., Holland, R. C., Hooker, S. H., Hayden, B. J., 1999. Overview and bibliography of research on the Greenshell mussel, *Perna canaliculus*, from New Zealand waters. *Journal of Shellfish Research*. 18, 347-360,
- Jones, J. B., Studies on animals closely associated with some New Zealand shellfish. (Doctoral dissertation) Te Herenga Waka—Victoria University of Wellington, Te Herenga Waka—Victoria University of Wellington, 1975.
- Jones, J. B., 1976. *Lichomolgus uncus* sp. (Copepoda: Cyclopoida) An associate of the mussel *Perna canaliculus* Gmelin. *Journal of the Royal Society of New Zealand*. 6, 301-305, 10.1080/03036758.1976.10421478.
- Jones, J. B., 2016. Aquaculture: exotic diseases and surveillance. *Microbiology Australia*. 37, 124-125, 10.1071/ma16042.
- JPL, GHRSSST Level 4 MUR Global Foundation Sea Surface Temperature Analysis. In: PO.DAAC, (Ed.), JPL MUR MEaSURES Project., CA, USA, 2015.
- Juanes, J. A., Bidegain, G., Echavarri-Erasun, B., Puente, A., García, A., García, A., Bárcena, J. F., Álvarez, C., García-Castillo, G., 2012. Differential distribution pattern of native *Ruditapes decussatus* and introduced *Ruditapes philippinarum* clam populations in the Bay of Santander (Gulf of Biscay): Considerations for fisheries management. *Ocean and Coastal Management*. 69, 316-326,
- Jung, T., Bader, N., Grune, T., 2007a. Lipofuscin: formation, distribution, and metabolic consequences. *Annals of the New York Academy of Sciences*. 1119, 97-111, 10.1196/annals.1404.008.
- Jung, T., Bader, N., Grune, T., 2007b. Lipofuscin: formation, distribution, and metabolic consequences. *Ann N Y Acad Sci*. 1119, 97-111, 10.1196/annals.1404.008.
- Kalachev, A. V., Yurchenko, O. V., 2019. Autophagy in nutrient storage cells of the Pacific oyster, *Crassostrea gigas*. *Tissue Cell*. 61, 30-34, 10.1016/j.tice.2019.08.007.
- Kang, D.-H., Chu, F.-L. E., Yang, H.-S., Lee, C.-H., Koh, H.-B., Choi, K.-S., 2010. Growth, reproductive condition, and digestive tubule atrophy of Pacific Oyster *Crassostrea gigas* in Gamakman Bay off the southern coast of Korea. *Journal of Shellfish Research*. 29, 839-845, 10.2983/035.029.0418.
- Karapanagiotidis, I. T., Mente, E., Berillis, P., Rotllant, G., 2015. Measurement of the feed consumption of *Nephrops norvegicus* feeding on different diets and its effect on body nutrient composition and digestive gland histology. *Journal of Crustacean Biology*. 35, 11-19,
- Karray, S., Smaoui-Damak, W., Rebai, T., Hamza-Chaffai, A., 2015. The reproductive cycle, condition index, and glycogen reserves of the cockles *Cerastoderma glaucum* from the Gulf of Gabes (Tunisia). *Environmental Science and Pollution Research*. 22, 17317-29, 10.1007/s11356-015-4337-6.

- Ke, Q., Li, Q., 2013. Annual dynamics of glycogen, lipids, and proteins during the reproductive cycle of the surf clam *Macra veneriformis* from the north coast of Shandong Peninsular, China. *Invertebrate Reproduction and Development*. 57, 49-60, 10.1080/07924259.2012.664174.
- Kennedy, V. S., 1977. Reproduction in *Mytilus edulis aoteanus* and *Aulacomya maoriana* (Mollusca: Bivalvia) from Taylors Mistake, New Zealand. *New Zealand Journal of Marine and Freshwater Research*. 11, 255-267, <https://doi.org/10.1080/00288330.1977.9515676>.
- Kent, M. L., Benda, S., St-Hilaire, S., Schreck, C. B., 2013. Sensitivity and specificity of histology for diagnoses of four common pathogens and detection of nontarget pathogens in adult Chinook salmon (*Oncorhynchus tshawytscha*) in fresh water. *Journal of Veterinary Diagnostic Investigation*. 25, 341-51, 10.1177/1040638713482124.
- Kesarcodi-Watson, A., Kaspar, H., Lategan, M. J., Gibson, L., 2009. Screening for probiotics of Greenshell™ mussel larvae, *Perna canaliculus*, using a larval challenge bioassay. *Aquaculture*. 296, 159-164, 10.1016/j.aquaculture.2009.08.008.
- Kim, H., Kim, B. H., Son, M. H., Jeon, M. A., Lee, Y. G., Lee, J. S., 2016. Gonadal development and reproductive cycle of cultured abalone, *Haliotis discus hannai*, (Gastropoda: Haliotidae) in Korea: Implications for Seed Production. *Journal of Shellfish Research*. 35, 653-659, 7, <https://doi.org/10.2983/035.035.0311>
- Kim, Y., Ashton-Alcox, K. A., Powell, E. N., 2006a. Histological techniques for marine bivalve molluscs: update. Vol. 27. NOAA/National Centers for Coastal Ocean Science, Silver Spring,.
- Kim, Y., Powell, E., Ashton-Alcox, K., 2006b. Histopathology analysis. Histological techniques for marine bivalve molluscs: Update. NOAA Tech. Mem. NOS NCCOS. 27, 19-52,
- Kim, Y. M., Park, K.-I., Choi, K.-S., Alvarez, R. A., Cummings, R. D., Cho, M., 2006c. Lectin from the Manila Clam *Ruditapes philippinarum* is induced upon infection with the protozoan parasite *Perkinsus olseni*. *Journal of Biological Chemistry*. 281, 26854-26864, <https://doi.org/10.1074/jbc.M601251200>.
- King, P. A., McGrath, D., Gosling, E. M., 2009. Reproduction and settlement of *Mytilus Edulis* on an exposed rocky shore in Galway Bay, West Coast of Ireland. *Journal of the Marine Biological Association of the United Kingdom*. 69, 355-365, 10.1017/s0025315400029465.
- King, W. L., Jenkins, C., Seymour, J. R., Labbate, M., 2019. Oyster disease in a changing environment: Decrypting the link between pathogen, microbiome and environment. *Marine Environmental Research*. 143, 124-140, 10.1016/j.marenvres.2018.11.007.
- Klobucar, G. I., Lajtner, J., Erben, R., 2001. Increase in number and size of kidney concretions as a result of PCP exposure in the freshwater snail *Planorbarius corneus* (Gastropoda, Pulmonata). *Diseases of Aquatic Organisms*. 44, 149-54, 10.3354/dao044149.
- Knowles, G., Handlinger, J., Jones, B., Moltschaniwskyj, N., 2014. Hemolymph chemistry and histopathological changes in Pacific oysters (*Crassostrea gigas*) in response to low salinity stress. *Journal of Invertebrate Pathology*. 121, 78-84, 10.1016/j.jip.2014.06.013.
- Knowles, S., Dennis, M., McElwain, A., Leis, E., Richard, J., 2023. Pathology and infectious agents of unionid mussels: A primer for pathologists in disease surveillance and investigation of mortality events. *Veterinary Pathology*. 60, 510-528, 10.1177/03009858231171666.
- Koch, R., 2018, Die Ätiologie der Tuberkulose 1882. In: Robert Koch . *Klassische Texte der Wissenschaft*. Springer Spektrum, Berlin, Heidelberg. pp. 113-131.
- Kochin, B. F., Bull, J. J., Antia, R., 2010. Parasite evolution and life history theory. *PLoS Biology*. 8, e1000524,
- Kooijman, B., Kooijman, S., 2010. *Dynamic energy budget theory for metabolic organisation*. Cambridge University Press, Amsterdam.
- Koolhaas, J. M., Bartolomucci, A., Buwalda, B., de Boer, S. F., Flugge, G., Korte, S. M., Meerlo, P., Murison, R., Olivier, B., Palanza, P., Richter-Levin, G., Sgoifo, A., Steimer, T., Stiedl, O., van Dijk, G., Wöhr, M., Fuchs, E., 2011. Stress revisited: a critical evaluation of the stress concept. *Neuroscience and Biobehavioral Reviews*. 35, 1291-301, 10.1016/j.neubiorev.2011.02.003.
- Kroeker, K. J., Gaylord, B., Hill, T. M., Hofelt, J. D., Miller, S. H., Sanford, E., 2014. The role of temperature in determining species' vulnerability to ocean acidification: a case study using *Mytilus galloprovincialis*. *PloS one*. 9, e100353, 10.1371/journal.pone.0100353.
- Kroemer, G., Galluzzi, L., Vandenabeele, P., Abrams, J., Alnemri, E. S., Baehrecke, E. H., Blagosklonny, M. V., El-Deiry, W. S., Golstein, P., Green, D. R., Hengartner, M., Knight, R. A., Kumar, S., Lipton, S. A., Malorni, W., Nunez, G., Peter, M. E., Tschopp, J., Yuan, J., Piacentini, M., Zhivotovsky, B., Melino, G., 2009. Classification of cell death: recommendations of the

- Nomenclature Committee on Cell Death Cell Death and Differentiation. 16, 3-11, 10.1038/cdd.2008.150.
- Kubota, S., 1992. Four bivalve-inhabiting hydrozoans in Japan differing in range and host preference. *Scientia Marina*. 56, 149-159,
- La Peyre, J. F., 1993. Studies on the oyster pathogen *Perkinsus marinus* (Apicomplexa): Interactions with host defenses of *Crassostrea virginica* and *Crassostrea gigas*, and *in vitro* propagation. The College of William and Mary.
- La Peyre, M., Casas, S., La Peyre, J., 2006. Salinity effects on viability, metabolic activity and proliferation of three *Perkinsus* species. *Diseases of Aquatic Organisms*. 71, 59-74,
- Laferriere, A. A. M., Examining the ecological complexities of blackfoot paua demography and habitat requirements in the scope of marine reserve protection. Vol. Doctorate. Victoria University of Wellington, Victoria University of Wellington, 2016.
- Lafferty, K. D., 2020. *Marine disease ecology*. Oxford University Press, USA.
- Lafferty, K. D., Dobson, A. P., Kuris, A. M., 2006. Parasites dominate food web links. *Proceedings of the National Academy of Sciences*. 103, 11211-11216,
- Lafferty, K. D., Harvell, C. D., Conrad, J. M., Friedman, C. S., Kent, M. L., Kuris, A. M., Powell, E. N., Rondeau, D., Saksida, S. M., 2015. Infectious diseases affect marine fisheries and aquaculture economics. *Annual Review of Marine Science*. 7, 471-96, 10.1146/annurev-marine-010814-015646.
- Lafferty, K. D., Kuris, A. M., 2009. Parasitic castration: the evolution and ecology of body snatchers. *Trends in Parasitology*. 25, 564-72, 10.1016/j.pt.2009.09.003.
- Lane, H. S., Brosnahan, C. L., Poulin, R., 2020. Aquatic disease in New Zealand: synthesis and future directions. *New Zealand Journal of Marine and Freshwater Research*. 56, 1-42, 10.1080/00288330.2020.1848887.
- Lane, H. S., Jaramillo, D., Sharma, M., 2023. *Perkinsus olseni* in green-lipped mussels *Perna canaliculus*: diagnostic evaluation, prevalence, and distribution. *Diseases of Aquatic Organisms*. 155, 175-185, 10.3354/dao03750.
- Langton, R. W., 1975. Synchrony in the digestive diverticula of *Mytilus edulis* L. *Journal of the Marine Biological Association of the United Kingdom*. 55, 221-229, 10.1017/S0025315400015861.
- Laroche, O., 2024. biohelper: Bioinformatics and data analysis helper functions (0.0.11.000). <https://rdr.io/github/olar785/biohelper/>.
- Law, C. S., Rickard, G. J., Mikaloff-Fletcher, S. E., Pinkerton, M. H., Behrens, E., Chiswell, S. M., Currie, K., 2017. Climate change projections for the surface ocean around New Zealand. *New Zealand Journal of Marine and Freshwater Research*. 52, 309-335, 10.1080/00288330.2017.1390772.
- Le Pennec, G., Le Pennec, M., Beninger, G., 2001. Seasonal digestive gland dynamics of the scallop *Pecten maximus* in the Bay of Brest (France). *Marine Biological Association of the United Kingdom*. 81, 663,
- Le Pennec, M., Beninger, P. G., Dorange, G., Paulet, Y. M., 1991. Trophic sources and pathways to the developing gametes of *Pecten maximus* (Bivalvia: Pectinidae). *Journal of the Marine Biological Association of the United Kingdom*. 71, 451-463,
- Le, T. C., Kang, H. S., Hong, H. K., Park, K. J., Choi, K. S., 2015. First report of *Urosporidium* sp., a haplosporidian hyperparasite infecting digenean trematode *Parvatrema duboisj* in Manila clam, *Ruditapes philippinarum* on the west coast of Korea. *Journal of Invertebrate Pathology*. 130, 141-6, 10.1016/j.jip.2015.08.004.
- Le Treut, H., Sommerville, R., Cubasch, U., Ding, Y., Mauritzen, C., Mokssit, A., Peterson, T., Prather, M., Widmann, M., Historical overview of climate change science. IPCC 4RG, 2006.
- Lee, M.-K., Cho, B.-Y., Lee, S.-J., Kang, J.-Y., Jeong, H. D., Huh, S. H., Huh, M.-D., 2001. Histopathological lesions of Manila clam, *Tapes philippinarum*, from Hadong and Namhae coastal areas of Korea. *Aquaculture*. 201, 199-209, [https://doi.org/10.1016/S0044-8486\(01\)00648-2](https://doi.org/10.1016/S0044-8486(01)00648-2).
- Lee, R., Lovatelli, A., Ababouch, L., 2008. Bivalve depuration: fundamental and practical aspects. *FAO Fisheries Technical Paper*. No. 511. Rome, FAO. 139p.
- Lenth, R. V., 2021. emmeans: Estimated Marginal Means, aka Least-Squares Means. <https://CRAN.R-project.org/package=emmeans>.
- Lester, R., 1986. Abalone die-back caused by protozoan infection? *Australian Fisheries*. 45, 26-27,

- Li, S., Alfaro, A. C., Nguyen, T. V., Young, T., Lulijwa, R., 2020. An integrated omics approach to investigate summer mortality of New Zealand Greenshell™ mussels. *Metabolomics*. 16, 1-16,
- Li, S., Ruan, Z., Yang, X., Li, M., Yang, D., 2019. Immune recognition, antimicrobial and opsonic activities mediated by a sialic acid binding lectin from *Ruditapes philippinarum*. *Fish and Shellfish Immunology*. 93, 66-72, <https://doi.org/10.1016/j.fsi.2019.07.027>.
- Li, S., Young, T., Archer, S., Lee, K., Sharma, S., Alfaro, A. C., 2022. Mapping the green-lipped mussel (*Perna canaliculus*) microbiome: A multi-tissue analysis of bacterial and fungal diversity. *Current Microbiology*. 79, 76, 10.1007/s00284-021-02758-5.
- Lima, F. P., Wetthey, D. S., 2012. Three decades of high-resolution coastal sea surface temperatures reveal more than warming. *Nature Communications*. 3, 704, 10.1038/ncomms1713.
- Liu, G., Heron, S. F., Eakin, C. M., Muller-Karger, F. E., Vega-Rodriguez, M., Guild, L. S., De La Cour, J. L., Geiger, E. F., Skirving, W. J., Burgess, T. F. R., Strong, A. E., Harris, A., Maturi, E., Ignatov, A., Sapper, J., Li, J., Lynds, S., 2014. Reef-Scale Thermal Stress Monitoring of Coral Ecosystems: New 5-km Global Products from NOAA Coral Reef Watch. *Remote Sensing*. 6, 11579-11606, <https://www.mdpi.com/2072-4292/6/11/11579>
- Leonart, M., A gonad conditioning study of the greenlip abalone (*Haliotis laevis*). Vol. Masters. University of Tasmania, 1992, pp. 162.
- Löhmus, M., Björklund, M., 2015. Climate change: what will it do to fish—parasite interactions? *Biological Journal of the Linnean Society*. 116, 397-411,
- Lomovasky, B. J., Morriconi, E., Brey, T., Calvo, J., 2002. Individual age and connective tissue lipofuscin in the hard clam *Eurhomalea exalbida*. *Journal of Experimental Marine Biology and Ecology*. 276, 83-94, 10.1016/s0022-0981(02)00240-x.
- Lotze, H. K., Lenihan, H. S., Bourque, B. J., Bradbury, R. H., Cooke, R. G., Kay, M. C., Kidwell, S. M., Kirby, M. X., Peterson, C. H., Jackson, J. B., 2006. Depletion, degradation, and recovery potential of estuaries and coastal seas. *Science*. 312, 1806-9, 10.1126/science.1128035.
- Lubchenco, J., Navarette, S., Tissot, B., Castilla, J. C., Lubchenco, J. L., S. A. Navarette, B. N. Tissot, and J. C. Castilla. 1993. Possible ecological responses to global climate change: nearshore benthic biota of northeastern Pacific coastal ecosystems. Chapter 12 In: H. A. Mooney, E. R. Fuentes, and B. I. Kronberg. eds. *Earth System Responses to Global Change: Contrasts between North and South America*. Academic Press, San Diego.
- Lynch, S. A., Rowley, A. F., Longshaw, M., Malham, S. K., Culloty, S. C., 2022, Diseases of molluscs. In: A. F. Rowley, et al., Eds., *Invertebrate Pathology*. Oxford University Press, pp. 171-216.
- MacDonald, B., Thompson, R., 1986. Influence of temperature and food availability on the ecological energetics of the giant scallop *Placopecten magellanicus*: III. Physiological ecology, the gametogenic cycle and scope for growth. *Marine Biology*. 93, 37-48,
- Mackin, J. G., Boswell, J. L., 1955. The life cycle and relationships of *Dermocystidium marinum*. *Proceedings of the National Shellfisheries Association*. 46, 112-115,
- Mai, K., Mercer, J. P., Donlon, J., 1995. Comparative studies on the nutrition of two species of abalone, *Haliotis tuberculata* L. and *Haliotis discus hannai* Ino. III. response of abalone to various levels of dietary lipid. *Aquaculture*. 134, 65-80, 10.1016/0044-8486(95)00043-2.
- Malagoli, D., Franchi, N., Sacchi, S., 2023. The eco-immunological relevance of the anti-oxidant response in invasive molluscs. *Antioxidants (Basel)*. 12, 1266, 10.3390/antiox12061266.
- Manduzio, H., Rocher, B., Durand, F., Galap, C., Leboulenger, F., 2005. The point about oxidative stress in molluscs. *Invertebrate Survival Journal*. 2, 91-104,
- Manning, M., Lawrence, J., King, D. N., Chapman, R., 2014. Dealing with changing risks: a New Zealand perspective on climate change adaptation. *Regional Environmental Change*. 15, 581-594, 10.1007/s10113-014-0673-1.
- Marcogliese, D. J., 2001. Implications of climate change for parasitism of animals in the aquatic environment. *Canadian Journal of Zoology*. 79, 1331-1352,
- Marigomez, I., Mugica, M., Izagirre, U., Sokolova, I. M., 2017. Chronic environmental stress enhances tolerance to seasonal gradual warming in marine mussels. *PloS one*. 12, e0174359, 10.1371/journal.pone.0174359.
- Marigomez, I., Soto, M., Cajaraville, M. P., Angulo, E., Giamberini, L., 2002. Cellular and subcellular distribution of metals in molluscs. *Microscopy Research and Technique*. 56, 358-92, 10.1002/jemt.10040.

- Martin, M., 2011. Cutadapt removes adapter sequences from high-throughput sequencing reads. European Molecular Biology network (EMBNET). 17, 3, 10.14806/ej.17.1.200.
- Martin, R. J., Bergey, E. A., 2013. Growth plasticity with changing diet in the land snail *Patera appressa* (Polygyridae). Journal of Molluscan Studies. 79, 364-368, 10.1093/mollus/eyt033.
- Masanja, F., Luo, X., Jiang, X., Xu, Y., Mkuye, R., Zhao, L., 2024. Environmental and social framework to protect marine bivalves under extreme weather events. Science of the Total Environment. 946, 174471, 10.1016/j.scitotenv.2024.174471.
- Massapina, C., Joaquim, S., Matias, D., Devauchelle, N., 1999. Oocyte and embryo quality in *Crassostrea gigas* (Portuguese strain) during a spawning period in Algarve, South Portugal. Aquatic Living Resources. 12, 327-333,
- Mauri, M., Orlando, E., 1982. Experimental study on renal concretions in the wedge shell *Donax trunculus* L. Journal of Experimental Marine Biology and Ecology. 63, 47-57, 10.1016/0022-0981(82)90049-1.
- McAvaney, L. A., Day, R. W., Dixon, C. D., Huchette, S. M., 2004. Gonad development in seeded *Haliotis laevigata*: growth environment determines initial reproductive investment. Journal of Shellfish Research. 23, 1213-1218.
- McDonald, W., 2014, Animal Health Laboratory. Surveillance, Vol. 41, pp. 12- 17.
- McLeod, I. M., Parsons, D. M., Morrison, M. A., Van Dijken, S. G., Taylor, R. B., 2014. Mussel reefs on soft sediments: a severely reduced but important habitat for macroinvertebrates and fishes in New Zealand. New Zealand Journal of Marine and Freshwater Research. 48, 48-59, 10.1080/00288330.2013.834831.
- McShane, P. E., Naylor, J. R., 1995. Small-scale spatial variation in growth, size at maturity, and yield- and egg-per-recruit relations in the New Zealand abalone *Haliotis iris*. New Zealand Journal of Marine and Freshwater Research. 29, 603-612, 10.1080/00288330.1995.9516691.
- McShane, P. E., Schiel, D. R., Mercer, S. F., Murray, T., 1994. Morphometric variation in *Haliotis iris* (Mollusca: Gastropoda): analysis of 61 populations. New Zealand Journal of Marine and Freshwater Research. 28, 357-364.
- Meyerholz, D. K., Beck, A. P., 2018. Fundamental concepts for semiquantitative tissue scoring in translational research. ILAR J. 59, 13-17, 10.1093/ilar/ily025.
- Michalek-Wagner, K., Willis, B. L., 2001. Impacts of bleaching on the soft coral *Lobophytum compactum*. I. Fecundity, fertilization and offspring viability. Coral Reefs. 19, 231-239, 10.1007/s003380170003.
- Miller, M.A., & Zachary, J.F. 2017. Mechanisms and morphology of cellular injury, adaptation, and death. *Pathologic Basis of Veterinary Disease*, 2 - 43.e19.
- Miller, M. R., Abshirini, M., Wolber, F. M., Tuterangiwhiu, T. R., Kruger, M. C., 2023. Greenshell mussel products: A comprehensive review of sustainability, traditional use, and efficacy. Sustainability. 15, 3912, <https://www.mdpi.com/2071-1050/15/5/3912>
- Milliman, J. D., Mei-e, R., 2021. River flux to the sea: impact of human intervention on river systems and adjacent coastal areas. In: Elsma, D. *Climate Change Impact on Coastal Habitation*. CRC press, pp. 57-83.
- Miquel, J., Lundgren, P. R., Bensch, K. G., Atlan, H., 1976. Effects of temperature on the life span, vitality and fine structure of *Drosophila melanogaster*. Mechanisms of Ageing and Development. 5, 347-70, 10.1016/0047-6374(76)90034-8.
- Mitta, G., Vandenbulcke, F., Roch, P., 2000. Original involvement of antimicrobial peptides in mussel innate immunity. FEBS Letter. 486, 185-90, 10.1016/s0014-5793(00)02192-x.
- Mladineo, I., Petrić, M., Hrabar, J., Bočina, I., Peharda, M., 2012. Reaction of the mussel *Mytilus galloprovincialis* (Bivalvia) to *Eugymnanthea inquilina* (Cnidaria) and *Urastoma cyprinae* (Turbellaria) concurrent infestation. Journal of Invertebrate Pathology. 110, 118-125, <https://doi.org/10.1016/j.jip.2012.03.001>.
- Montes, J., Del Rio, J., Durfort, M., Garcia-Valero, J., 1997. The protozoan parasite *Perkinsus atlanticus* elicits a unique defensive response in the clam *Tapes semidecussatus*. Parasitology. 114, 339-349,
- Montes, J. F., Durfort, M., Garcia-Valero, J., 1996. When the venerid clam *Tapes decussatus* is parasitized by the protozoan *Perkinsus* sp. it synthesizes a defensive polypeptide that is closely related to p225. Diseases of Aquatic Organisms. 26, 149-157,
- Montie, S., Thorat, F., Smith, R. O., Cook, F., Tait, L. W., Pinkerton, M. H., Schiel, D. R., Thomsen, M. S., 2023. Seasonal trends in marine heatwaves highlight vulnerable coastal ecoregions and

- historic change points in New Zealand. *New Zealand Journal of Marine and Freshwater Research*. 58, 274-299, 10.1080/00288330.2023.2218102.
- Mooney, H., Larigauderie, A., Cesario, M., Elmquist, T., Hoegh-Guldberg, O., Lavorel, S., Mace, G. M., Palmer, M., Scholes, R., Yahara, T., 2009. Biodiversity, climate change, and ecosystem services. *Current Opinion in Environmental Sustainability*. 1, 46-54, 10.1016/j.cosust.2009.07.006.
- Moore, J. D., 2023 Disease and potential disease agents in wild and cultured abalone. In: P. A. Cook, S. E. Shumway, Eds., *Abalone: Biology, Ecology, Aquaculture and Fisheries*. Elsevier, pp. 189-250.
- Moore, M. N., Allen, J. I., McVeigh, A., Shaw, J., 2006a. Lysosomal and autophagic reactions as predictive indicators of environmental impact in aquatic animals. *Autophagy*. 2, 217-20, 10.4161/auto.2663.
- Moore, M. N., Allen, J. I., Somerfield, P. J., 2006b. Autophagy: role in surviving environmental stress. *Marine Environmental Research*. 62 Suppl, S420-5, 10.1016/j.marenvres.2006.04.055.
- Morash, A. J., Alter, K., 2016. Effects of environmental and farm stress on abalone physiology: perspectives for abalone aquaculture in the face of global climate change. *Reviews in Aquaculture*. 8, 342-368, 10.1111/raq.12097.
- Morgan, E., O'Riordan, R., Culloty, S., 2013. Climate change impacts on potential recruitment in an ecosystem engineer. *Ecology and Evolution*. 3, 581-594, doi.org/10.1002/ece3.419.
- Morin, M., Jönsson, M., Wang, C. K., Craik, D. J., Degnan, S. M., Degnan, B. M., 2022. Crown-of-thorns starfish in captivity experience sustained large-scale changes in gene expression. *bioRxiv*. 2022.07.21.501052, 10.1101/2022.07.21.501052.
- Moss, G. A., 1998. Effect of temperature on the breeding cycle and spawning success of the New Zealand abalone, *Haliotis australis*. *New Zealand Journal of Marine and Freshwater Research*. 32, 139-146, 10.1080/00288330.1998.9516813.
- Motavkine, P., Varaksine, A., 1983. *Histophysiologie du système nerveux et régulation de la reproduction chez les mollusques bivalves*. Sciences, Moscow. 208.
- Mouritsen, K. N., McKechnie, S., Meenken, E., Toynbee, J. L., Poulin, R., 2003. Spatial heterogeneity in parasite loads in the New Zealand cockle: the importance of host condition and density. *Journal of the Marine Biological Association of the United Kingdom*. 83, 307-310, 10.1017/S0025315403007124h.
- MPI, M. f. P. I., 2023a. Pāua status and information. 2023, <https://www.mpi.govt.nz/fishing-aquaculture/recreational-fishing/information-on-popular-fish-in-nz/paua-status-and-information/>.
- MPI, M. f. P. I., 2023b. Recreational daily pāua limits reduced for lower and central North Island. 2023, <https://www.mpi.govt.nz/news/media-releases/recreational-daily-paua-limits-reduced-for-lower-and-central-north-island/#:~:text=The%20daily%20limit%20for%20recreationally,effect%20on%20%20September%202023.>
- MPI, M. f. P. I., 2024a. Long-term biosecurity management programmes. 2024, <https://www.mpi.govt.nz/biosecurity/exotic-pests-and-diseases-in-new-zealand/long-term-biosecurity-management-programmes/>.
- MPI, M. f. P. I., 2024b. Regulated Control Scheme -Bivalve Molluscan Shellfish for Human Consumption. Animal products notice. 2025,
- Muznebin, F., Alfaro, A. C., Webb, S. C., 2021. Occurrence of *Perkinsus olseni* and other parasites in New Zealand black-footed abalone (*Haliotis iris*). *New Zealand Journal of Marine and Freshwater Research*. 57, 261-281, 10.1080/00288330.2021.1984950.
- Muznebin, F., Alfaro, A. C., Webb, S. C., 2022a. *Perkinsus olseni* and other parasites and abnormal tissue structures in New Zealand Greenshell™ mussels (*Perna canaliculus*) across different seasons. *Aquaculture International*. 31, 547-582, 10.1007/s10499-022-00991-8.
- Muznebin, F., Alfaro, A. C., Webb, S. C., Merien, F., 2022b. Characterization of mussel (*Perna canaliculus*) haemocytes and their phagocytic activity across seasons. *Aquaculture Research*. 53, 4288-4303, 10.1111/are.15926.
- Muznebin, F., Van Nguyen, T., Webb, S. C., Alfaro, A. C., 2024. Histological examination of *Perna canaliculus* mussels during a summer mortality event in New Zealand. *Aquaculture Research*. 2024, 6679103, <https://doi.org/10.1155/2024/6679103>.

- Nash, S., Johnstone, J., Rahman, M. S., 2019. Elevated temperature attenuates ovarian functions and induces apoptosis and oxidative stress in the American oyster, *Crassostrea virginica*: potential mechanisms and signaling pathways. *Cell Stress Chaperones*. 24, 957-967, 10.1007/s12192-019-01023-w.
- Navas, J., Castillo, M., Vera, P., Ruiz-Rico, M., 1992. Principal parasites observed in clams, *Ruditapes decussatus* (L.), *Ruditapes philippinarum* (Adams et Reeve), *Venerupis pullastra* (Montagu) and *Venerupis aureus* (Gmelin), from the Huelva coast (SW Spain). *Aquaculture*. 107, 193-199,
- Naylor, J. R., Andrew, N., 2004. Productivity and response to fishing of stunted paua stocks. New Zealand Fisheries Assessment Report 2004/31. 17 p.
- Naylor, J. R., Andrew, N. L., Kim, S. W., 2006. Demographic variation in the New Zealand abalone *Haliotis iris*. *Marine and Freshwater Research*. 57, 215-224,
- Naylor, J. R., Manighetti, B. M., Neil, H. L., Kim, S. W., 2007. Validated estimation of growth and age in the New Zealand abalone *Haliotis iris* using stable oxygen isotopes. *Marine and Freshwater Research*. 58, 354-362,
- Naylor, R. L., Hardy, R. W., Buschmann, A. H., Bush, S. R., Cao, L., Klinger, D. H., Little, D. C., Lubchenco, J., Shumway, S. E., Troell, M., 2021. A 20-year retrospective review of global aquaculture. *Nature*. 591, 551-563, 10.1038/s41586-021-03308-6.
- Nguyen, T. T., Marsden, I. D., Davison, W., Pirker, J., 2023. Effects of acclimation temperature and exposure time on the scope for growth of the blackfoot Pāua (*Haliotis iris*). *Marine and Freshwater Research*. 74, 1465-1477,
- Nguyen, T. V., Alfaro, A., Frost, E., Chen, D., Beale, D. J., Mundy, C., 2021. Investigating the biochemical effects of heat stress and sample quenching approach on the metabolic profiling of abalone (*Haliotis iris*). *Metabolomics*. 18, 7, 10.1007/s11306-021-01862-8.
- Nguyen, T. V., Alfaro, A. C., 2020. Metabolomics investigation of summer mortality in New Zealand Greenshell mussels (*Perna canaliculus*). *Fish and Shellfish Immunology*. 106, 783-791, 10.1016/j.fsi.2020.08.022.
- NIWA, 2024. High Intensity Rainfall Design System V4. <https://hirds.niwa.co.nz/>.
- OIE, 2024. Infection with *Perkinsus marinus* in manual of diagnostic tests for aquatic animals. https://www.woah.org/fileadmin/Home/eng/Health_standards/aahm/current/chapitre_perkinsus_marinus.pdf.
- Okamura, B., 2016. Hidden infections and changing environments. *Integrative and Comparative Biology*. 56, 620-9, 10.1093/icb/icw008.
- Okamura, B., Feist, S. W., 2011. Emerging diseases in freshwater systems. *Freshwater Biology*. 56, 627-637, 10.1111/j.1365-2427.2011.02578.x.
- Oliver, E. C. J., Benthuyzen, J. A., Bindoff, N. L., Hobday, A. J., Holbrook, N. J., Mundy, C. N., Perkins-Kirkpatrick, S. E., 2017. The unprecedented 2015/16 Tasman Sea marine heatwave. *Nature Communications*. 8, 16101, 10.1038/ncomms16101.
- Oliver, E. C. J., Donat, M. G., Burrows, M. T., Moore, P. J., Smale, D. A., Alexander, L. V., Benthuyzen, J. A., Feng, M., Sen Gupta, A., Hobday, A. J., Holbrook, N. J., Perkins-Kirkpatrick, S. E., Scannell, H. A., Straub, S. C., Wernberg, T., 2018. Longer and more frequent marine heatwaves over the past century. *Nature Communications*. 9, 1324, 10.1038/s41467-018-03732-9.
- Oliver, L., Fisher, W., 1995. Comparative form and function of oyster *Crassostrea virginica* hemocytes from Chesapeake Bay (Virginia) and Apalachicola Bay (Florida). *Diseases of Aquatic Organisms*. 22, 217-225,
- Ordás, M. C., Novoa, B., Figueras, A., 1999. Phagocytosis inhibition of clam and mussel haemocytes by *Perkinsus atlanticus* secretion products. *Fish and Shellfish Immunology*. 9, 491-503, 10.1006/fsim.1999.0208.
- Ordás, M. C., Ordás, A., Beloso, C., Figueras, A., 2000. Immune parameters in carpet shell clams naturally infected with *Perkinsus atlanticus*. *Fish and Shellfish Immunology*. 10, 597-609, 10.1006/fsim.2000.0274.
- Ortiz-Zarragoitia, M., Garmendia, L., Barbero, M. C., Serrano, T., Marigomez, I., Cajaraville, M. P., 2011. Effects of the fuel oil spilled by the Prestige tanker on reproduction parameters of wild mussel populations. *Journal of Environmental Monitoring*. 13, 84-94, 10.1039/c0em00102c.

- Overton, K., Dempster, T., Swearer, S. E., Morris, R. L., Barrett, L. T., 2024. Achieving conservation and restoration outcomes through ecologically beneficial aquaculture. *Conservation Biology*. 38, e14065,
- Oyarzún, P. A., Toro, J. E., Garcés-Vargas, J., Alvarado, C., Guiñez, R., Jaramillo, R., Briones, C., Campos, B., 2016. Reproductive patterns of mussel *Perumytilus purpuratus* (Bivalvia: Mytilidae), along the Chilean coast: effects caused by climate change? *Journal of the Marine Biological Association of the United Kingdom*. 98, 375-385, 10.1017/s0025315416001223.
- Pachauri, R., Meyer, L., 2014. AR5 Synthesis Report: Climate Change 2014—IPCC. Climate Change 2014: Synthesis Report. Contribution of Working Groups I, II and III to the Fifth Assessment Report of the Intergovernmental Panel on Climate Change.
- Pales Espinosa, E., Winnicki, S., Allam, B., 2013. Early host-pathogen interactions in a marine bivalve: *Crassostrea virginica* pallial mucus modulates *Perkinsus marinus* growth and virulence. *Diseases of Aquatic Organisms*. 104, 237-47, 10.3354/dao02599.
- Pandian, T. J., 2018. *Reproduction and development in mollusca*. In: *Series on reproduction and development in aquatic invertebrates* CRC Press. Taylor and Francis, London. 3-24
- Park, K.-I., Choi, K.-S., 2001. Spatial distribution of the protozoan parasite *Perkinsus* sp. found in the Manila clams, *Ruditapes philippinarum*, in Korea. *Aquaculture*. 203, 9-22, [https://doi.org/10.1016/S0044-8486\(01\)00619-6](https://doi.org/10.1016/S0044-8486(01)00619-6).
- Parmesan, C., Yohe, G., 2003. A globally coherent fingerprint of climate change impacts across natural systems. *Nature*. 421, 37-42, 10.1038/nature01286.
- Pāua Industry Council, 2023. Markets and Exports. 2023, <https://www.paua.org.nz/markets-export>.
- Paul, L. J., A history of the Firth of Thames dredge fishery for mussels: use and abuse of a coastal resource. In: NIWA, (Ed.). *New Zealand Aquatic Environment and Biodiversity*, Ministry of Agriculture and Forestry, 2012, pp. 27.
- Pawley, J., 2006. *Handbook of biological confocal microscopy*. Springer Science and Business Media. New York and London, 232.
- Perdue, J., Beattie, J., Chew, K., 1981. Some relationships between gametogenic cycle and summer mortality phenomenon in the Pacific oyster (*Crassostrea gigas*) in Washington State. *Journal of Shellfish Research*. 30, 8-21
- Perez-Cebrecos, M., Prieto, D., Blanco-Rayon, E., Izagirre, U., Ibarrola, I., 2022. Differential tissue development compromising the growth rate and physiological performances of mussel. *Marine Environmental Research*. 180, 105725, 10.1016/j.marenvres.2022.105725.
- Pérez, A. F., Boy, C. C., Curelovich, J. N., Pérez Barros, P., Calcagno, J. Á., 2013. Relationship between energy allocation and gametogenesis in *Aulacomya atra* (Bivalvia: Mytilidae) in a sub-Antarctic environment. *Revista de Biología Marina y Oceanografía* 48, 459-469,
- Perkins, S. E., Alexander, L. V., 2013. On the measurement of heat waves. *Journal of Climate*. 26, 4500-4517,
- Perlman, R. L., 2013 *Host–pathogen coevolution*. *Evolution and Medicine*. Oxford University Press, pp. 77-90.
- Peteiro, L. G., Woodin, S. A., Wetthey, D. S., Costas-Costas, D., Martinez-Casal, A., Olabarria, C., Vazquez, E., 2018. Responses to salinity stress in bivalves: Evidence of ontogenetic changes in energetic physiology on *Cerastoderma edule*. *Scientific Reports*. 8, 8329, 10.1038/s41598-018-26706-9.
- Peters, D. L., Caissie, D., Monk, W. A., Rood, S. B., St-Hilaire, A., 2015. An ecological perspective on floods in Canada. *Canadian Water Resources Journal / Revue canadienne des ressources hydriques*. 41, 288-306, 10.1080/07011784.2015.1070694.
- Petes, L. E., Menge, B. A., Murphy, G. D., 2007. Environmental stress decreases survival, growth, and reproduction in New Zealand mussels. *Journal of Experimental Marine Biology and Ecology*. 351, 83-91,
- Petes, L. E., Mouchka, M. E., Milston-Clements, R. H., Momoda, T. S., Menge, B. A., 2008. Effects of environmental stress on intertidal mussels and their sea star predators. *Oecologia*. 156, 671-80, 10.1007/s00442-008-1018-x.
- Petton, B., Destoumieux-Garzon, D., Pernet, F., Toulza, E., de Lorgeril, J., Degremont, L., Mitta, G., 2021. The Pacific Oyster mortality syndrome, a polymicrobial and multifactorial disease: State of knowledge and future directions. *Frontiers in Immunology*. 12, 630343, 10.3389/fimmu.2021.630343.

- Philipp, E., Brey, T., Portner, H. O., Abele, D., 2005. Chronological and physiological ageing in a polar and a temperate mud clam. *Mechanisms of Ageing and Development*. 126, 598-609, 10.1016/j.mad.2004.12.003.
- Philippart, C. J., van Aken, H. M., Beukema, J. J., Bos, O. G., Cadée, G. C., Dekker, R., 2003. Climate-related changes in recruitment of the bivalve *Macoma balthica*. *Limnology and Oceanography*. 48, 2171-2185,
- Pinheiro, J., Bates, D., 2023. nlme: Linear and Nonlinear Mixed Effects Models., <https://CRAN.R-project.org/package=nlme>.
- Pipe, R. K., 1987. Ultrastructural and cytochemical study on interactions between nutrient storage cells and gametogenesis in the mussel *Mytilus edulis*. *Marine Biology*. 96, 519-528, 10.1007/bf00397969.
- Piraino, S., Todaro, C., Geraci, S., Boero, F., 1994. Ecology of the bivalve-inhabiting hydroid *Eugymnanthea inquilina* in the coastal sounds of Taranto (Ionian Sea, SE Italy). *Marine Biology*. 118, 695-703,
- Poff, N. L., 2002. Ecological response to and management of increased flooding caused by climate change. *Philosophical Transactions: Mathematical, Physical and Engineering Sciences*. 360, 1497-510, 10.1098/rsta.2002.1012.
- Poff, N. L., Zimmerman, J. K., 2010. Ecological responses to altered flow regimes: a literature review to inform the science and management of environmental flows. *Freshwater Biology*. 55, 194-205,
- Poore, G. C. B., 1972. Ecology of New Zealand abalones, *Haliotis* species (Mollusca: Gastropoda). *New Zealand Journal of Marine and Freshwater Research*. 6, 11-22, 10.1080/00288330.1977.9515407.
- Poore, G. C. B., 1973. Ecology of New Zealand abalones, *Haliotis* species (Mollusca: Gastropoda). *New Zealand Journal of Marine and Freshwater Research*. 7, 67-84, 10.1080/00288330.1973.9515456.
- Portner, H. O., 2002. Climate variations and the physiological basis of temperature dependent biogeography: systemic to molecular hierarchy of thermal tolerance in animals. *Comparative Biochemistry and Physiology Part A: Molecular and Integrative Physiology*. 132, 739-61, 10.1016/s1095-6433(02)00045-4.
- Portner, H. O., Farrell, A. P., 2008. Ecology. Physiology and climate change. *Science*. 322, 690-2, 10.1126/science.1163156.
- Pourmozaffar, S., Tamadoni Jahromi, S., Rameshi, H., Sadeghi, A., Bagheri, T., Behzadi, S., Gozari, M., Zahedi, M. R., Abrari Lazarjani, S., 2019. The role of salinity in physiological responses of bivalves. *Reviews in Aquaculture*. 12, 1548-1566, 10.1111/raq.12397.
- Proctor, R., Roberts, K., Ward, B. J., 2010. A data delivery system for IMOS, the Australian Integrated Marine Observing System. *Advances in Geosciences*. 28, 11-16, 10.5194/adgeo-28-11-2010.
- Purcell, J. E., 2005. Climate effects on formation of jellyfish and ctenophore blooms: a review. *Journal of the Marine Biological Association of the United Kingdom*. 85, 461-476, 10.1017/S0025315405011409.
- Qiu, J.-W., Tremblay, R., Bourget, E., 2002. Ontogenetic changes in hyposaline tolerance in the mussels *Mytilus edulis* and *M. trossulus*: implications for distribution. *Marine Ecology Progress Series*. 228, 143-152,
- Quast, C., Pruesse, E., Yilmaz, P., Gerken, J., Schweer, T., Yarza, P., Peplies, J., Glockner, F. O., 2013. The SILVA ribosomal RNA gene database project: improved data processing and web-based tools. *Nucleic Acids Research*. 41, D590-6, 10.1093/nar/gks1219.
- Quinn, G. P., Keough, M. J., 2012. *Experimental Design and Data Analysis for Biologists*. Cambridge University Press, Cambridge.
- R Core Team, 2021. R: A language and environment for statistical computing. R Foundation for Statistical Computing. <https://www.R-project.org/>.
- R Core Team, 2024. R: A language and environment for statistical computing. R Foundation for Statistical Computing. <https://www.R-project.org/>.
- RStudio Team, 2021. RStudio: Integrated Development Environment for R. RStudio, PBC, <https://www.R-project.org/>.
- Raberg, L., Alacid, E., Garcés, E., Figueroa, R., 2014. The potential for arms race and Red Queen coevolution in a protist host–parasite system. *Ecology and Evolution*. 4, 4775-4785,

- Ragg, N. L. C., 2023, Physiology: Energetics, metabolism, and gas exchange. In: P. A. Cook, S. E. Shumway, (Eds.), *Abalone: Biology, Ecology, Aquaculture and Fisheries*. Elsevier, pp. 119-160.
- Rahman, M. A., Henderson, S., Miller-Ezzy, P., Li, X. X., Qin, J. G., 2019. Immune response to temperature stress in three bivalve species: Pacific oyster *Crassostrea gigas*, Mediterranean mussel *Mytilus galloprovincialis* and mud cockle *Katylsia rhytiphora*. *Fish and Shellfish Immunology*. 86, 868-874, 10.1016/j.fsi.2018.12.017.
- Rajapandi, T., 2020. Apicomplexan lineage-specific polytopic membrane proteins in *Cryptosporidium parvum*. *Journal of Parasitic Diseases*. 44, 467-471, 10.1007/s12639-020-01209-5.
- Rebello Mde, F., Figueiredo Ede, S., Mariante, R. M., Nobrega, A., de Barros, C. M., Allodi, S., 2013. New insights from the oyster *Crassostrea rhizophorae* on bivalve circulating hemocytes. *PloS one*. 8, e57384, 10.1371/journal.pone.0057384.
- Reece, K. S., Dungan, C. F., 2006 *Perkinsus* sp. infections of marine molluscs., American Fisheries Society-Fish Health Section (AFS-FHS) Blue Book: suggested procedures for the detection and identification of certain finfish and shellfish pathogens, Bethesda, Maryland.
- Reece, K. S., Stokes, N. A., 2003. Molecular analysis of a haplosporidian parasite from cultured New Zealand abalone *Haliotis iris*. *Diseases of Aquatic Organisms*. 53, 61-6, 10.3354/dao053061.
- Reid, G. K., Filgueira, R., Garber, A., 2015. Revisiting temperature effects on aquaculture in light of pending climate change. *Aquaculture Canada 2014 Proceedings of Contributed Papers*. 85-92.
- Reid, G. K., Gurney-Smith, H. J., Flaherty, M., Garber, A. F., Forster, I., Brewer-Dalton, K., Knowler, D., Marcogliese, D. J., Chopin, T., Moccia, R. D., Smith, C. T., De Silva, S., 2019a. Climate change and aquaculture: considering adaptation potential. *Aquaculture Environment Interactions*. 11, 603-624, <https://www.int-res.com/abstracts/aei/v11/p603-624/>
- Reid, G. K., Gurney-Smith, H. J., Marcogliese, D. J., Knowler, D., Benfey, T., Garber, A. F., Forster, I., Chopin, T., Brewer-Dalton, K., Moccia, R. D., Flaherty, M., Smith, C. T., De Silva, S., 2019b. Climate change and aquaculture: considering biological response and resources. *Aquaculture Environment Interactions*. 11, 569-602, <https://www.int-res.com/abstracts/aei/v11/p569-602/>
- Ren, J. S., Fox, S. P., Howard-Williams, C., Zhang, J., Schiel, D. R., 2019. Effects of stock origin and environment on growth and reproduction of the green-lipped mussel *Perna canaliculus*. *Aquaculture*. 505, 502-509, 10.1016/j.aquaculture.2019.03.011.
- Ren, J. S., Ragg, N. L. C., Cummings, V. J., Zhang, J., 2020. Ocean acidification and dynamic energy budget models: Parameterisation and simulations for the green-lipped mussel. *Ecological Modelling*. 426, 109069, 10.1016/j.ecolmodel.2020.109069.
- Ren, J. S., Ross, A. H., 2005. Environmental influence on mussel growth: A dynamic energy budget model and its application to the greenshell mussel *Perna canaliculus*. *Ecological Modelling*. 189, 347-362, 10.1016/j.ecolmodel.2005.04.005.
- Rhein, M., Rintoul, S., Aoki, S., Campos, E., Chambers, D., Feely, R., Gulev, S., Johnson, G., Josey, S., Kostianoy, A., 2013. Observations: Ocean in Climate Change 2013: The Physical Science Basis. Contribution of Working Group I to the Fifth Assessment Report of the Intergovernmental Panel on Climate Change. Fifth assessment report of the Intergovernmental Panel on Climate Change. 255-316,
- Riebesell, U., Gattuso, J.-P., 2014. Lessons learned from ocean acidification research. *Nature Climate Change*. 5, 12-14, 10.1038/nclimate2456.
- Roberts, E. A., Newcomb, L. A., McCartha, M. M., Harrington, K. J., LaFramboise, S. A., Carrington, E., Sebens, K. P., 2021. Resource allocation to a structural biomaterial: Induced production of byssal threads decreases growth of a marine mussel. *Functional Ecology*. 35, 1222-1239,
- Roberts, S. B., Sunila, I., Wikfors, G. H., 2012. Immune response and mechanical stress susceptibility in diseased oysters, *Crassostrea virginica*. *Journal of Comparative Physiology B*. 182, 41-48, 10.1007/s00360-011-0605-z.
- Rodhouse, P. G., Roden, C. M., Burnell, G. M., Hensey, M. P., McMahon, T., Ottway, B., Ryan, T. H., 1984. Food resource, gametogenesis and growth of *Mytilus edulis* on the shore and in suspended culture: Killary Harbour, Ireland. *Journal of the Marine Biological Association of the United Kingdom*. 64, 513-529, 10.1017/S0025315400030204.
- Rodríguez-MoscOSO, E., Arnaiz, R., 1998. Gametogenesis and energy storage in a population of the grooved carpet-shell clam, *Tapes decussatus* (Linné, 1787), in northwest Spain. *Aquaculture*. 162, 125-139, [https://doi.org/10.1016/S0044-8486\(98\)00170-7](https://doi.org/10.1016/S0044-8486(98)00170-7).

- Rogers-Bennett, L., Catton, C. A., 2019. Marine heat wave and multiple stressors tip bull kelp forest to sea urchin barrens. *Scientific Reports*. 9, 15050, 10.1038/s41598-019-51114-y.
- Rogers-Bennett, L., Dondanville, R. F., Moore, J. D., Vilchis, L. I., 2010. Response of red abalone reproduction to warm water, starvation, and disease stressors: Implications of ocean warming. *Journal of Shellfish Research*. 29, 599-611, 13, <https://doi.org/10.2983/035.029.0308>
- Rogers-Bennett, L., Klamt, R., Catton, C. A., 2021. Survivors of climate driven abalone mass mortality exhibit declines in health and reproduction following kelp forest collapse. *Frontiers in Marine Science*. 8, 10.3389/fmars.2021.725134.
- Rolton, A., Ragg, N. L. C., 2020. Green-lipped mussel (*Perna canaliculus*) hemocytes: A flow cytometric study of sampling effects, sub-populations and immune-related functions. *Fish and Shellfish Immunology*. 103, 181-189, 10.1016/j.fsi.2020.05.019.
- Rothig, T., Trevathan-Tackett, S. M., Voolstra, C. R., Ross, C., Chaffron, S., Durack, P. J., Warmuth, L. M., Sweet, M., 2023. Human-induced salinity changes impact marine organisms and ecosystems. *Global Change Biology*. 29, 4731-4749, 10.1111/gcb.16859.
- Roussel, S., Huchette, S., Gaillard, F., Servili, A., Malet, L., Di Giglio, S., Richard, N., Coheleach, M., Badou, A., Dubois, P., Martin, S., Auzoux-Bordenave, S., Avignon, S., Norkko, J., 2020. An integrated investigation of the effects of ocean acidification on adult abalone (*Haliotis tuberculata*). *ICES Journal of Marine Science*. 77, 757-772, 10.1093/icesjms/fsz257.
- Roznere, I., Sinn, B. T., Daly, M., Watters, G. T., 2021. Freshwater mussels (Unionidae) brought into captivity exhibit up-regulation of genes involved in stress and energy metabolism. *Scientific Reports*. 11, 2241, 10.1038/s41598-021-81856-7.
- RStudio Team, 2021. RStudio: Integrated Development Environment for R. <http://www.rstudio.com/>.
- Rubio-Portillo, E., Izquierdo-Munoz, A., Gago, J. F., Rossello-Mora, R., Anton, J., Ramos-Espla, A. A., 2016. Effects of the 2015 heat wave on benthic invertebrates in the Tabarca Marine Protected Area (southeast Spain). *Marine Environmental Research*. 122, 135-142, 10.1016/j.marenvres.2016.10.004.
- Rupnik, A., Doré, W., Devilly, L., Fahy, J., Fitzpatrick, A., Schmidt, W., Hunt, K., Butler, F., Keaveney, S., 2021. Evaluation of norovirus reduction in environmentally contaminated Pacific oysters during laboratory controlled and commercial depuration. *Food and Environmental Virology*. 13, 229-240, 10.1007/s12560-021-09464-2.
- Sainsbury, K. J., 2010. Population dynamics and fishery management of the paua, *Haliotis iris*. Population structure, growth, reproduction, and mortality. *New Zealand Journal of Marine and Freshwater Research*. 16, 147-161, 10.1080/00288330.1982.9515958.
- Salinger, M. J., Diamond, H. J., Behrens, E., Fernandez, D., Fitzharris, B. B., Herold, N., Johnstone, P., Kerckhoffs, H., Mullan, A. B., Parker, A. K., 2020a. Unparalleled coupled ocean-atmosphere summer heatwaves in the New Zealand region: drivers, mechanisms and impacts. *Climatic Change*. 162, 485-506,
- Salinger, M. J., Diamond, H. J., Behrens, E., Fernandez, D., Fitzharris, B. B., Herold, N., Johnstone, P., Kerckhoffs, H., Mullan, A. B., Parker, A. K., Renwick, J., Scofield, C., Siano, A., Smith, R. O., South, P. M., Sutton, P. J., Teixeira, E., Thomsen, M. S., Trought, M. C. T., 2020b. Unparalleled coupled ocean-atmosphere summer heatwaves in the New Zealand region: drivers, mechanisms and impacts. *Climatic Change*. 162, 485-506, 10.1007/s10584-020-02730-5.
- Salinger, M. J., Renwick, J., Behrens, E., Mullan, A. B., Diamond, H. J., Sirguy, P., Smith, R. O., Trought, M. C. T., Alexander, L., Cullen, N. J., Fitzharris, B. B., Hepburn, C. D., Parker, A. K., Sutton, P. J., 2019. The unprecedented coupled ocean-atmosphere summer heatwave in the New Zealand region 2017/18: drivers, mechanisms and impacts. *Environmental Research Letters*. 14, 044023, 10.1088/1748-9326/ab012a.
- Santana-Falcón, Y., Séférian, R., 2022. Climate change impacts the vertical structure of marine ecosystem thermal ranges. *Nature Climate Change*. 12, 935-942, 10.1038/s41558-022-01476-5.
- Santos, J. J. S., Bernardes, J. P., Ramirez, J. R. B., Gomes, C., Romano, L. A., 2020. Effect of salinity on embryo-larval development of yellow clam *Mesodesma mactroides* (Reeve, 1854) in laboratory. *Anais da Academia Brasileira de Ciências*. 92 Suppl 1, e20190169, 10.1590/0001-3765202020190169.
- Saulsbury, J., Moss, D. K., Ivany, L. C., Kowalewski, M., Lindberg, D. R., Gillooly, J. F., Heim, N. A., McClain, C. R., Payne, J. L., Roopnarine, P. D., Schöne, B. R., Goodwin, D., Finnegan, S.,

2019. Evaluating the influences of temperature, primary production, and evolutionary history on bivalve growth rates. *Paleobiology*. 45, 405-420, 10.1017/pab.2019.20.
- Saunders, T., Mayfield, S., Hogg, A., 2009a. Using a simple morphometric marker to identify spatial units for abalone fishery management. *ICES Journal of Marine Science*. 66, 305-314, 10.1093/icesjms/fsn212.
- Saunders, T. M., Connell, S. D., Mayfield, S., 2009b. Differences in abalone growth and morphology between locations with high and low food availability: morphologically fixed or plastic traits? *Marine Biology*. 156, 1255-1263,
- Saunders, T. M., Mayfield, S., Hogg, A. A., 2008. A simple, cost-effective, morphometric marker for characterising abalone populations at multiple spatial scales. *Marine and Freshwater Research*. 59, 32-40, 10.1071/mf07150.
- Schiel, D. R., 1993. Experimental evaluation of commercial-scale enhancement of abalone *Haliotis iris* populations in New Zealand. *Marine Ecology Progress Series*. 97, 167-181, <https://ezproxy.aut.ac.nz/login?url=https://search.ebscohost.com/login.aspx?direct=true&site=eds-live&db=edsjsr&AN=edsjsr.24833613>
- Schiel, D. R., Andrew, N. L., Foster, M. S., 1995. The structure of subtidal algal and invertebrate assemblages at the Chatham Islands, New Zealand. *Marine Biology*. 123, 355-367,
- Schiel, D. R., Lilley, S. A., South, P. M., 2018. Ecological tipping points for an invasive kelp in rocky reef algal communities. *Marine Ecology Progress Series*. 587, 93-104,
- Schiel, D. R., Wood, S. A., Dunmore, R. A., Taylor, D. I., 2006. Sediment on rocky intertidal reefs: Effects on early post-settlement stages of habitat-forming seaweeds. *Journal of Experimental Marine Biology and Ecology*. 331, 158-172, 10.1016/j.jembe.2005.10.015.
- Schindelin, J., Arganda-Carreras, I., Frise, E., Kaynig, V., Longair, M., Pietzsch, T., Preibisch, S., Rueden, C., Saalfeld, S., Schmid, B., Tinevez, J. Y., White, D. J., Hartenstein, V., Eliceiri, K., Tomancak, P., Cardona, A., 2012. Fiji: an open-source platform for biological-image analysis. *Nature Methods*. 9, 676-82, 10.1038/nmeth.2019.
- Schoch, C. L., Ciufu, S., Domrachev, M., Hotton, C. L., Kannan, S., Khovanskaya, R., Leipe, D., McVeigh, R., O'Neill, K., Robbertse, B., Sharma, S., Soussov, V., Sullivan, J. P., Sun, L., Turner, S., Karsch-Mizrachi, I., 2020. NCBI Taxonomy: a comprehensive update on curation, resources and tools. *Database (Oxford)*. 2020, 10.1093/database/baaa062.
- Seal, S., Dharmarajan, G., Khan, I., 2021. Evolution of pathogen tolerance and emerging infections: A missing experimental paradigm. *Elife*. 10, 10.7554/eLife.68874.
- Searle, T., Roberts, R. D., Lokman, P. M., 2006. Effects of temperature on growth of juvenile blackfoot abalone, *Haliotis iris* Gmelin. *Aquaculture Research*. 37, 1441-1449,
- Sebens, K. P., Sara, G., Carrington, E., 2018. Estimation of fitness from energetics and life-history data: An example using mussels. *Ecology and Evolution*. 8, 5279-5290, 10.1002/ece3.4004.
- Seed, R., 1969. The ecology of *Mytilus edulis* L. (Lamellibranchiata) on exposed rocky shores : I. Breeding and settlement. *Oecologia*. 3, 277-316, 10.1007/BF00390380.
- Seed, R. a. S., T.H., 1992, Population and community ecology of *Mytilus*. In: E. Gosling, (Ed.), *The Mussel Mytilus: Ecology, Physiology, Genetics and Culture*. Elsevier, London, pp. 87 - 169.
- Seehafer, S. S., Pearce, D. A., 2006. You say lipofuscin, we say ceroid: defining autofluorescent storage material. *Neurobiology of Aging*. 27, 576-88, 10.1016/j.neurobiolaging.2005.12.006.
- Seuront, L., Nicastro, K. R., Zardi, G. I., Goberville, E., 2019. Decreased thermal tolerance under recurrent heat stress conditions explains summer mass mortality of the blue mussel *Mytilus edulis*. *Scientific Reports*. 9, 17498, 10.1038/s41598-019-53580-w.
- Shackelford, C., Long, G., Wolf, J., Okerberg, C., Herbert, R., 2002. Qualitative and quantitative analysis of nonneoplastic lesions in toxicology studies. *Toxicologic Pathology*. 30, 93-6, 10.1080/01926230252824761.
- Shanks, A. L., Rasmuson, L. K., Valley, J. R., Jarvis, M. A., Salant, C., Sutherland, D. A., Lamont, E. I., Hainey, M. A., Emler, R. B., 2020. Marine heat waves, climate change, and failed spawning by coastal invertebrates. *Limnology and Oceanography*. 65, 627-636,
- Shapiro-Ilan, D. I., Bruck, D. J., Lacey, L. A., 2012, Principles of Epizootiology and Microbial Control. In: F. E. Vega, H. K. Kaya, Eds., *Insect Pathology*. Academic Press, San Diego, pp. 29-72.
- Shaw, J. P., Moore, M. N., Readman, J. W., Mou, Z., Langston, W. J., Lowe, D. M., Frickers, P. E., Al-Moosawi, L., Pascoe, C., Beesley, A., 2019. Oxidative stress, lysosomal damage and

- dysfunctional autophagy in molluscan hepatopancreas (digestive gland) induced by chemical contaminants. *Marine Environmental Research*. 152, 104825, 10.1016/j.marenvres.2019.104825.
- Shelmerdine, R. L., Mouat, B., Shucksmith, R. J., 2017. The most northerly record of feral Pacific oyster *Crassostrea gigas* (Thunberg, 1793) in the British Isles. *BioInvasions Records*. 6, 57-60,
- Shepherd, S., Hearn, W., 1983. Studies on Southern Australian abalone (genus *Haliotis*). IV. Growth of *H. laevigata* and *H. ruber*. *Marine and freshwater research*. 34, 461–475.
- Shin, S. R., Kim, H. J., Lee, D. H., Kim, H., Sohn, Y. C., Kim, J. W., Lee, J. S., 2020. Gonadal maturation and main spawning period of *Haliotis gigantea* (Gastropoda: Haliotidae). *Development and Reproduction*. 24, 79-88, 10.12717/DR.2020.24.2.79.
- Shumway, S. E., Parsons, G. J., 2011. *Scallops: biology, ecology and aquaculture*. Elsevier. Amsterdam- Oxford-New York-Tokyo. 1095
- Skelton, B. M., Múgica, M., Zamora, L. N., Delorme, N. J., Stanley, J. A., Jeffs, A. G., 2024. Nutritional condition of wild and hatchery-reared, green-lipped mussel (*Perna canaliculus*) spat used for aquaculture. *Aquaculture, Fish and Fisheries*. 4, 1-13,
- Skirving, W., Marsh, B., De La Cour, J., Liu, G., Harris, A., Maturi, E., Geiger, E., Eakin, C. M., 2020. CoralTemp and the coral reef watch coral bleaching heat stress product suite Version 3.1. *Remote Sensing*. 12, 3856, <https://www.mdpi.com/2072-4292/12/23/3856>
- Smale, D. A., Wernberg, T., Oliver, E. C. J., Thomsen, M., Harvey, B. P., Straub, S. C., Burrows, M. T., Alexander, L. V., Benthuisen, J. A., Donat, M. G., Feng, M., Hobday, A. J., Holbrook, N. J., Perkins-Kirkpatrick, S. E., Scannell, H. A., Sen Gupta, A., Payne, B. L., Moore, P. J., 2019. Marine heatwaves threaten global biodiversity and the provision of ecosystem services. *Nature Climate Change*. 9, 306-312, 10.1038/s41558-019-0412-1.
- Sokolov, E. P., Sokolova, I. M., 2019. Compatible osmolytes modulate mitochondrial function in a marine osmoconformer *Crassostrea gigas* (Thunberg, 1793). *Mitochondrion*. 45, 29-37, 10.1016/j.mito.2018.02.002.
- Sokolova, I., 2009. Apoptosis in molluscan immune defense. *Invertebrate Survival Journal*. 6, 49-58.
- Sokolova, I. M., Frederich, M., Bagwe, R., Lannig, G., Sukhotin, A. A., 2012. Energy homeostasis as an integrative tool for assessing limits of environmental stress tolerance in aquatic invertebrates. *Marine Environmental Research*. 79, 1-15, 10.1016/j.marenvres.2012.04.003.
- Solan, M., Whiteley, N., 2016. *Stressors in the marine environment: physiological and ecological responses; societal implications*. Oxford, online edn, Oxford Academic. United Kingdom.
- Soon, T. K., Ransangan, J., 2019. Extrinsic factors and marine bivalve mass mortalities: An overview. *Journal of Shellfish Research*. 38, 223-232, 10, <https://doi.org/10.2983/035.038.0202>
- Sorensen, R. E., Minchella, D. J., 2001. Snail-trematode life history interactions: past trends and future directions. *Parasitology*. 123 Suppl, S3-18, 10.1017/s0031182001007843.
- Soudant, P., FL, E. C., Volety, A., 2013. Host-parasite interactions: Marine bivalve molluscs and protozoan parasites, *Perkinsus* species. *Journal of Invertebrate Pathology*. 114, 196-216, 10.1016/j.jip.2013.06.001.
- Soudant, P., Marty, Y., Moal, J., Masski, H., Jean François, S., 1998. Fatty acid composition of polar lipid classes during larval development of scallop *Pecten maximus* (L.). *Comparative Biochemistry and Physiology Part A: Molecular and Integrative Physiology*. 121, 279-288, [https://doi.org/10.1016/S1095-6433\(98\)10130-7](https://doi.org/10.1016/S1095-6433(98)10130-7).
- Spann, N., Harper, E. M., Aldridge, D. C., 2010. The unusual mineral vaterite in shells of the freshwater bivalve *Corbicula fluminea* from the UK. *Naturwissenschaften*. 97, 743-51, 10.1007/s00114-010-0692-9.
- Sprung, M., 1983. Reproduction and fecundity of the mussel *Mytilus edulis* at Helgoland (North sea). *Helgoländer Meeresuntersuchungen*. 36, 243-255, 10.1007/BF01983629.
- Srisuphanunt, M., Wilairatana, P., Koolthead, N., Damrongwatanapokin, T., Karanis, P., 2023. Occurrence of *Cryptosporidium* oocysts in commercial oysters in southern Thailand. *Food Waterborne Parasitology*. 32, e00205, 10.1016/j.fawpar.2023.e00205.
- Srisuphanunt, M., Wiwanitkit, V., Saksirisampant, W., Karanis, P., 2009. Detection of *Cryptosporidium* oocysts in green mussels (*Perna viridis*) from shell-fish markets of Thailand. *Parasite*. 16, 235-9, 10.1051/parasite/2009163235.
- Steele, S., Mulcahy, M., 1999. Gametogenesis of the oyster *Crassostrea gigas* in southern Ireland. *Journal of the Marine Biological Association of the United Kingdom*. 79, 673-686.

- Steeves, L., Filgueira, R., Guyondet, T., Chassé, J., Comeau, L., 2018. Past, present, and future: Performance of two bivalve species under changing environmental conditions. *Frontiers in Marine Science*. 5, 184, 10.3389/fmars.2018.00184.
- Stefaniak, L. M., McAtee, J., Shulman, M. J., 2005. The costs of being bored: effects of a clionid sponge on the gastropod *Littorina littorea* (L). *Journal of Experimental Marine Biology and Ecology*. 327, 103-114,
- Steffani, C. N., Branch, G. M., 2003. Growth rate, condition, and shell shape of *Mytilus galloprovincialis*: responses to wave exposure. *Marine Ecology Progress Series*. 246, 197-209, 10.3354/meps246197.
- Stenton-Dozey, J. M. E., Heath, P., Ren, J. S., Zamora, L. N., 2020. New Zealand aquaculture industry: research, opportunities and constraints for integrative multitrophic farming. *New Zealand Journal of Marine and Freshwater Research*. 55, 265-285, 10.1080/00288330.2020.1752266.
- Steyaert, M., Priestley, V., Osborne, O., Herraiz, A., Arnold, R., Savolainen, V., Paiva, V., 2020. Advances in metabarcoding techniques bring us closer to reliable monitoring of the marine benthos. *Journal of Applied Ecology*. 57, 2234-2245, 10.1111/1365-2664.13729.
- Stuart, M. D., Brown, M. T., 1994. Growth and diet of cultivated black-footed abalone, *Haliotis iris* (Martyn). *Aquaculture*. 127, 329-337, 10.1016/0044-8486(94)90235-6.
- Subritzky, P., The identification of juvenile *Haliotis iris* habitat within the East Otago Taiāpure. University of Otago, 2013.
- Suja, G., Lijo, J., Kripa, V., Mohamed, K. S., Vijayan, K. K., Sanil, N. K., 2020. A comparison of parasites, pathological conditions and condition index of wild and farmed populations of *Magallana bilineata* (Roding, 1798) from Vembanad Lake, west coast of India. *Aquaculture*. 515, 734548, 10.1016/j.aquaculture.2019.734548.
- Sunday, J. M., Pecl, G. T., Frusher, S., Hobday, A. J., Hill, N., Holbrook, N. J., Edgar, G. J., Stuart-Smith, R., Barrett, N., Wernberg, T., Watson, R. A., Smale, D. A., Fulton, E. A., Slawinski, D., Feng, M., Radford, B. T., Thompson, P. A., Bates, A. E., 2015. Species traits and climate velocity explain geographic range shifts in an ocean-warming hotspot. *Ecology Letters*. 18, 944-53, 10.1111/ele.12474.
- Sunila, I., LaBanca, J., 2003. Apoptosis in the pathogenesis of infectious diseases of the eastern oyster *Crassostrea virginica*. *Diseases of Aquatic Organisms*. 56, 163-70, 10.3354/dao056163.
- Suong, N. T., Banks, J. C., Webb, S. C., Jeffs, A., Wakeman, K. C., Fidler, A., 2018. PCR test to specifically detect the apicomplexan 'X' (APX) parasite found in flat oysters *Ostrea chilensis* in New Zealand. *Diseases of Aquatic Organisms*. 129, 199-205, 10.3354/dao03244.
- Sutton, P. J. H., Bowen, M., 2019. Ocean temperature change around New Zealand over the last 36 years. *New Zealand Journal of Marine and Freshwater Research*. 53, 305-326, 10.1080/00288330.2018.1562945.
- Swales, A., Gibbs, M. M., Handley, S., Olsen, G. M., Ovenden, R., Wadhwa, S., Brown, J., 2021. Sources of fine sediment and contribution to sedimentation in the inner Pelorus Sound/ Te Hoiere. NIWA.
- Tacon, A. G., 2020. Trends in global aquaculture and aquafeed production: 2000–2017. *Reviews in Fisheries Science and Aquaculture*. 28, 43-56,
- Talbot, C. J., Bennett, E. M., Cassell, K., Hanes, D. M., Minor, E. C., Paerl, H., Raymond, P. A., Vargas, R., Vidon, P. G., Wollheim, W., Xenopoulos, M. A., 2018. The impact of flooding on aquatic ecosystem services. *Biogeochemistry*. 141, 439-461, 10.1007/s10533-018-0449-7.
- Tan, K., Yan, X., Julian, R., Lim, L., Peng, X., Fazhan, H., Kwan, K. Y., 2023. Effects of climate change induced hyposalinity stress on marine bivalves. *Estuarine, Coastal and Shelf Science*. 294, 108539, 10.1016/j.ecss.2023.108539.
- Taskinen, J., Saarinen, M., 1999. Increased parasite abundance associated with reproductive maturity of the clam *Anodonta piscinalis*. *Journal of Parasitology*. 85, 588-91, <https://www.ncbi.nlm.nih.gov/pubmed/10386464>
- Taylor, D. I., Schiel, D. R., 2003. Wave-related mortality in zygotes of habitat-forming algae from different exposures in southern New Zealand: the importance of 'stickability'. *Journal of Experimental Marine Biology and Ecology*. 290, 229-245,
- Terman, A., Brunk, U. T., 1998. Lipofuscin: mechanisms of formation and increase with age. *Apmis*. 106, 265-76, 10.1111/j.1699-0463.1998.tb01346.x.

- Tessmar-Raible, K., Raible, F., Arboleda, E., 2011. Another place, another timer: Marine species and the rhythms of life. *Bioessays*. 33, 165-72, 10.1002/bies.201000096.
- Thomas, C. D., Cameron, A., Green, R. E., Bakkenes, M., Beaumont, L. J., Collingham, Y. C., Erasmus, B. F., De Siqueira, M. F., Grainger, A., Hannah, L., Hughes, L., Huntley, B., Van Jaarsveld, A. S., Midgley, G. F., Miles, L., Ortega-Huerta, M. A., Peterson, A. T., Phillips, O. L., Williams, S. E., 2004. Extinction risk from climate change. *Nature*. 427, 145-8, 10.1038/nature02121.
- Thomas, F., Renaud, F., de Meeûs, T., Poulin, R., 1998. Manipulation of host behaviour by parasites: ecosystem engineering in the intertidal zone? *Proceedings of the Royal Society of London. Series B: Biological Sciences*. 265, 1091-1096, 10.1098/rspb.1998.0403.
- Thomas, L. J., Milotic, M., Vaux, F., Poulin, R., 2022. Lurking in the water: testing eDNA metabarcoding as a tool for ecosystem-wide parasite detection. *Parasitology*. 149, 261-269, 10.1017/S0031182021001840.
- Thompson, K. J., Inglis, S. D., Stokesbury, K. D., 2014. Identifying spawning events of the sea scallop *Placopecten magellanicus* on Georges Bank. *Journal of Shellfish Research*. 33, 77-87,
- Thomsen, M. S., Mondardini, L., Alestra, T., Gerrity, S., Tait, L., South, P. M., Lilley, S. A., Schiel, D. R., 2019. Local extinction of bull kelp (*Durvillaea* spp.) due to a marine heatwave. *Frontiers in Marine Science*. 6, 10.3389/fmars.2019.00084.
- Thomson, J. D., Pirie, B. J., George, S. G., 1985. Cellular metal distribution in the Pacific oyster, *Crassostrea gigas* (Thun.) determined by quantitative X-ray microprobe analysis. *Journal of Experimental Marine Biology and Ecology*. 85, 37-45,
- Thorarinsdóttir, G. G., Gunnarsson, K., 2003. Reproductive cycles of *Mytilus edulis* L. on the west and east coasts of Iceland. *Polar Research*. 22, 217-223,
- Tiffany, W. J., 3rd, Luer, W. H., Watkins, M. A., 1980. Intracellular and intraluminal aspects of renal calculosis in the marine mollusc *Macrocallista nimbosa*. *Investigative Urology*. 18, 139-43, <https://www.ncbi.nlm.nih.gov/pubmed/7410025>
- Todgham, A. E., Stillman, J. H., 2013. Physiological responses to shifts in multiple environmental stressors: relevance in a changing world. *Integrative and Comparative Biology*. 53, 539-44, 10.1093/icb/ict086.
- Tomanek, L., 2010. Variation in the heat shock response and its implication for predicting the effect of global climate change on species' biogeographical distribution ranges and metabolic costs. *Journal of Experimental Biology*. 213, 971-9, 10.1242/jeb.038034.
- Tran, D., Perrigault, M., Ciret, P., Payton, L., 2020. Bivalve mollusc circadian clock genes can run at tidal frequency. *Proceedings: Biological Sciences*. 287, 20192440, 10.1098/rspb.2019.2440.
- Trenberth, K. E., 2011. Changes in precipitation with climate change. *Climate Research*. 47, 123-138, <https://www.int-res.com/abstracts/cr/v47/n1-2/p123-138>
- Trump, B. F., Berezsky, I. K., Chang, S. H., Phelps, P. C., 1997. The pathways of cell death: oncosis, apoptosis, and necrosis. *Toxicologic Pathology*. 25, 82-8, 10.1177/019262339702500116.
- Trussell, G. C., 1996. Phenotypic plasticity in an intertidal snail: The role of a common crab predator. *Evolution*. 50, 448-454, 10.1111/j.1558-5646.1996.tb04507.x.
- Tuckett, C. A., de Bettignies, T., Fromont, J., Wernberg, T., 2017. Expansion of corals on temperate reefs: direct and indirect effects of marine heatwaves. *Coral Reefs*. 36, 947-956, 10.1007/s00338-017-1586-5.
- Tuckey, N. P. L., Timms, B. A., Fletcher, G. C., Summers, G., Delorme, N. J., Ericson, J. A., Ragg, N. L. C., Miller, P., Wibisono, R., Taylor, R., Adams, S. L., Zamora, L. N., 2023. Examination of the potential of refrigerated seawater to improve live transport of the mussel *Perna canaliculus*: Physiological responses, meat quality and safety implications under different chilled storage conditions. *Aquaculture*. 575, 739794, <https://doi.org/10.1016/j.aquaculture.2023.739794>.
- Uzaki, N., Kai, M., Aoyama, H., Suzuki, T., 2003. Changes in mortality rate and glycogen content of the Manila clam *Ruditapes philippinarum* during the development of oxygen-deficient waters. *Fisheries science*. 69, 936-943,
- Valenzuela-Castillo, A., Sánchez-Paz, A., Castro-Longoria, R., López-Torres, M. A., Grijalva-Chon, J. M., 2019. Hsp70 function and polymorphism, its implications for mollusk aquaculture: a review. *Latin American Journal of Aquatic Research*. 47, 224-231,
- van der Schatte Olivier, A., Jones, L., Vay, L. L., Christie, M., Wilson, J., Malham, S. K., 2020. A global review of the ecosystem services provided by bivalve aquaculture. *Reviews in Aquaculture*. 12, 3-25,

- Van Nguyen, T., Alfaro, A. C., Venter, L., Ericson, J. A., Ragg, N. L. C., McCowan, T., Mundy, C., 2023. Metabolomics approach reveals size-specific variations of blackfoot abalone (*Haliotis iris*) in Chatham Islands, New Zealand. *Fisheries Research*. 262, 106645, 10.1016/j.fishres.2023.106645.
- Vásquez-García, A., Oliveira, A. P. S. C. d., Mejia-Ballesteros, J. E., Godoy, S. H. S. d., Barbieri, E., Sousa, R. L. M. d., Fernandes, A. M., 2019. *Escherichia coli* detection and identification in shellfish from southeastern Brazil. *Aquaculture*. 504, 158-163, <https://doi.org/10.1016/j.aquaculture.2019.01.062>.
- Vázquez, E., Woodin, S. A., Wetthey, D. S., Peteiro, L. G., Olabarria, C., 2021. Reproduction under stress: Acute effect of low salinities and heat waves on reproductive cycle of four ecologically and commercially important bivalves. *Frontiers in Marine Science*. 8, 10.3389/fmars.2021.685282.
- Vazquez, N., Frizzera, A., Cremonte, F., 2020. Diseases and parasites of wild and cultivated mussels along the Patagonian coast of Argentina, southwest Atlantic Ocean. *Diseases of Aquatic Organisms*. 139, 139-152, 10.3354/dao03467.
- Vázquez, N., Ituarte, C., Cremonte, F., 2015. A histopathological study of the geoduck clam *Panopea abbreviata* from San José Gulf, North Patagonia, Argentina. *Journal of the Marine Biological Association of the United Kingdom*. 95, 1173-1181, 10.1017/s0025315415000144.
- Vélez-Arellano, N., García-Domínguez, F. A., Lluch-Cota, D. B., Gutiérrez-González, J. L., Sánchez-Cárdenas, R., 2015. Histological validation of morphochromatically-defined gonadal maturation stages of green abalone (*Haliotis fulgens*) Philippi, 1845 and Pink Abalone (*Haliotis corrugata*) Wood, 1828. *International Journal of Morphology*. 33, 1054-1059, 10.4067/s0717-95022015000300039.
- Venables, B., Ripley, B., 2002. Modern applied statistics With S. In. *Statistics and computing*. Springer. New York, 496.
- Venegas, R. M., Acevedo, J., Treml, E. A., 2023. Three decades of ocean warming impacts on marine ecosystems: A review and perspective. *Deep Sea Research Part II: Topical Studies in Oceanography*. 212, 105318, 10.1016/j.dsr2.2023.105318.
- Venter, L., Alfaro, A. C., Ragg, N. L. C., Delorme, N. J., Ericson, J. A., 2023. The effect of simulated marine heatwaves on green-lipped mussels, *Perna canaliculus*: A near-natural experimental approach. *Journal of Thermal Biology*. 117, 103702, 10.1016/j.jtherbio.2023.103702.
- Venter, L., Alfaro, A. C., Van Nguyen, T., Lindeque, J. Z., 2022. Metabolite profiling of abalone (*Haliotis iris*) energy metabolism: a Chatham Islands case study. *Metabolomics*. 18, 52, 10.1007/s11306-022-01907-6.
- Verdelhos, T., Verissimo, H., Marques, J. C., Anastácio, P., 2021. Behavioural responses of *Cerastoderma edule* as indicators of potential survival strategies in the face of flooding events. *Applied Sciences*. 11, 6436, <https://www.mdpi.com/2076-3417/11/14/6436>
- Viera, M. P., de Vicose, G. C., Gómez-Pinchetti, J. L., Bilbao, A., Fernandez-Palacios, H., Izquierdo, M. S., 2011. Comparative performances of juvenile abalone (*Haliotis tuberculata coccinea* Reeve) fed enriched vs non-enriched macroalgae: Effect on growth and body composition. *Aquaculture*. 319, 423-429, 10.1016/j.aquaculture.2011.07.024.
- Villalba, A., Reece, K. S., Camino Ordás, M., Casas, S. M., Figueras, A., 2004. Perkinsosis in molluscs: A review. *Aquatic Living Resources*. 17, 411-432, 10.1051/alr:2004050.
- Vitt, L. J., Caldwell, J. P., 2014, Reproduction and life histories. In: L. J. Vitt, J. P. Caldwell, Eds., *Herpetology*. Academic Press, San Diego, pp. 117-155.
- Walther, G. R., Post, E., Convey, P., Menzel, A., Parmesan, C., Beebee, T. J., Fromentin, J. M., Hoegh-Guldberg, O., Bairlein, F., 2002. Ecological responses to recent climate change. *Nature*. 416, 389-95, 10.1038/416389a.
- Wang, Q., Garrity, G. M., Tiedje, J. M., Cole, J. R., 2007. Naive Bayesian classifier for rapid assignment of rRNA sequences into the new bacterial taxonomy. *Applied and Environmental Microbiology*. 73, 5261-7, 10.1128/AEM.00062-07.
- Wang, Y., Hu, M., Cheung, S. G., Shin, P. K., Lu, W., Li, J., 2012. Chronic hypoxia and low salinity impair anti-predatory responses of the green-lipped mussel *Perna viridis*. *Marine Environmental Research*. 77, 84-9, 10.1016/j.marenvres.2012.02.006.
- Webb, S. C., Aspects of stress with particular reference to mytilid mussels and their parasites. University of Cape Town, 1999. Unpublished PhD Thesis, University of Cape Town

- Webb, S. C., 2020. Fixative artefacts in histology: Mitigation and interpretation. Cawthron Report No. 3502. 37.
- Webb, S. C., Duncan, J., 2019. New Zealand shellfish health monitoring 2007 to 2017: insights and projections. Cawthron Report No. 2568. 67.
- Webber, H., Giese, A., 1969. Reproductive cycle and gametogenesis in the black abalone *Haliotis cracheroidii* (Gastropoda: Prosobranchiata). *Marine Biology*. 4, 152-159,
- Wells, F. E., Mulvay, P., 1995. Good and bad fishing areas for *Haliotis laevis*: A comparison of population parameters. *Marine and Freshwater Research*. 46, 591-598, 10.1071/mf9950591.
- Wendling, C. C., Wegner, K. M., 2013. Relative contribution of reproductive investment, thermal stress and *Vibrio* infection to summer mortality phenomena in Pacific oysters. *Aquaculture*. 412-413, 88-96, <https://doi.org/10.1016/j.aquaculture.2013.07.009>.
- Wernberg, T., Smale, D. A., Tuya, F., Thomsen, M. S., Langlois, T. J., De Bettignies, T., Bennett, S., Rousseaux, C. S., 2013. An extreme climatic event alters marine ecosystem structure in a global biodiversity hotspot. *Nature Climate Change*. 3, 78-82,
- Wilcox, M. D., 2007. Observations on seaweeds at the Chatham Islands. *Auckland Botanical Society Journal*. 61, 27-28,
- Wilkie, E. M., Bishop, M. J., O'Connor, W. A., McPherson, R. G., 2013. Status of the Sydney rock oyster in a disease-afflicted estuary: persistence of wild populations despite severe impacts on cultured counterparts. *Marine and Freshwater Research*. 64, 267-276,
- Wilson, N. H. F., Schiel, D. R., 1995. Reproduction on two species of abalone (*Haliotis iris* and *H. australis*) in southern New Zealand. *Marine and Freshwater Research*. 46, 629-637, 10.1071/mf9950629.
- Winsemius, H. C., Aerts, Jeroen C. J. H., van Beek, Ludovicus P. H., Bierkens, Marc F. P., Bouwman, A., Jongman, B., Kwadijk, Jaap C. J., Ligtoet, W., Lucas, Paul L., van Vuuren, Detlef P., Ward, Philip J., 2015. Global drivers of future river flood risk. *Nature Climate Change*. 6, 381-385, 10.1038/nclimate2893.
- Winstead, J. T., 1995. Digestive tubule atrophy in eastern oysters, *Crassostrea virginica* (Gmelin, 1791), exposed to salinity and starvation stress. *Journal of Shellfish Research*. 14, 105-112,
- WOAH, 2015. Chapter 1.4. OIE Aquatic Animal Health Surveillance. *Aquatic Animal Health Code*. https://www.woah.org/fileadmin/Home/eng/Health_standards/aahc/2010/en_chapitre_aqua_animal_surveillance.htm.
- WOAH, 2024. Chapter 2.4.5. Infection with *Perkinsus marinus*. In: *WOAH Aquatic Manual*. https://www.woah.org/fileadmin/Home/fr/Health_standards/aahm/current/2.4.05_P_MARINUS.pdf
- WOAH, 2025. Animal diseases. World organisation of animal health. https://www.woah.org/en/what-we-do/animal-health-and-welfare/animal-diseases/?tax_animal=aquatics%2Cmolluscs. Accessed September 2025
- Wolf, J. C., Baumgartner, W. A., Blazer, V. S., Camus, A. C., Engelhardt, J. A., Fournie, J. W., Frasca, S., Jr., Groman, D. B., Kent, M. L., Khoo, L. H., Law, J. M., Lombardini, E. D., Ruehl-Fehlert, C., Segner, H. E., Smith, S. A., Spitsbergen, J. M., Weber, K., Wolfe, M. J., 2015. Nonlesions, misdiagnoses, missed diagnoses, and other interpretive challenges in fish histopathology studies: a guide for investigators, authors, reviewers, and readers. *Toxicologic Pathology*. 43, 297-325, 10.1177/0192623314540229.
- Wong, K. L. C., Alfaro, A. C., 2019. Nutrient storage and utilization in relation to reproductive condition of the New Zealand scallop *Pecten novaezelandiae*. *Marine Ecology Progress Series*. 632, 101-122,
- Wu, Y., Kaiser, H., Jones, C. L. W., 2018. A first study on the effect of dietary soya levels and crystalline isoflavones on growth, gonad development and gonad histology of farmed abalone, *Haliotis midae*. *Aquaculture International*. 27, 167-193, 10.1007/s10499-018-0315-6.
- Xu, Y., Zhang, Y., Liang, J., He, G., Liu, X., Zheng, Z., Le, D. Q., Deng, Y., Zhao, L., 2021. Impacts of marine heatwaves on pearl oysters are alleviated following repeated exposure. *Marine Pollution Bulletin*. 173, 112932, 10.1016/j.marpolbul.2021.112932.
- Yang, S., Rothman, R. E., 2004. PCR-based diagnostics for infectious diseases: uses, limitations, and future applications in acute-care settings. *Lancet Infectious Diseases*. 4, 337-48, 10.1016/S1473-3099(04)01044-8.

- Yu, J. H., Song, J. H., Choi, M. C., Park, S. W., 2009. Effects of water temperature change on immune function in surf clams, *Mactra veneriformis* (Bivalvia: Mactridae). *Journal of Invertebrate Pathology*. 102, 30-5, 10.1016/j.jip.2009.06.002.
- Yurchenko, O. V., Kalachev, A. V., 2019. Morphology of nutrient storage cells in the gonadal area of the Pacific oyster, *Crassostrea gigas* (Thunberg, 1793). *Tissue and Cell*. 56, 7-13, <https://doi.org/10.1016/j.tice.2018.11.004>.
- Zannella, C., Mosca, F., Mariani, F., Franci, G., Folliero, V., Galdiero, M., Tiscar, P. G., Galdiero, M., 2017. Microbial diseases of bivalve mollusks: Infections, immunology and antimicrobial defense. *Marine Drugs*. 15, 182, 10.3390/md15060182.
- Zarogian, G., Yevich, P., 1993. Cytology and biochemistry of brown cells in *Crassostrea virginica* collected at clean and contaminated stations. *Environmental Pollution*. 79, 191-7, 10.1016/0269-7491(93)90069-z.
- Zell, R., Krumbholz, A., Wutzler, P., 2008. Impact of global warming on viral diseases: what is the evidence? *Current Opinion in Biotechnology*. 19, 652-60, 10.1016/j.copbio.2008.10.009.
- Zhan, A., Hulák, M., Sylvester, F., Huang, X., Adebayo, A. A., Abbott, C. L., Adamowicz, S. J., Heath, D. D., Cristescu, M. E., MacIsaac, H. J., 2013. High sensitivity of 454 pyrosequencing for detection of rare species in aquatic communities. *Methods in Ecology and Evolution*. 4, 558-565.
- Zhu, H., Zhang, H., Xu, Y., Lassakova, S., Korabecna, M., Neuzil, P., 2020. PCR past, present and future. *BioTechniques*. 69, 317-325, 10.2144/btn-2020-0057.
- Zippay, M. L., Helmuth, B., 2012. Effects of temperature change on mussel, *Mytilus*. *Integrative Zoology*. 7, 312-327, 10.1111/j.1749-4877.2012.00310.x.
- Zubkoff, P. L., Ho, M.-S., 1982. Krebs cycle intermediates of the oyster, *Crassostrea virginica* and the mussel, *Geukensia demissa*. *Comparative Biochemistry and Physiology Part B: Comparative Biochemistry*. 72, 577-580.

APPENDIX

9.1. Appendix: Research outputs*9.1.1. Peer reviewed published papers.*

Copedo, J. S., Webb, S. C., Ragg, N. L. C., Venter, L., Alfaro, A. C., (2023). Histopathological investigation of four populations of abalone (*Haliotis iris*) exhibiting divergent growth performance. *Journal of Invertebrate Pathology*. Vol, 202.

<https://doi.org/10.1016/j.jip.2023.108042>

Copedo, J. S., Webb, S. C., Ragg, N. L. C., Ericson, J. A., Venter, L., Schmidt, A. J., Delorme, N. J., Alfaro, A. C., (2023). Histopathological changes in the greenshell mussel, *Perna canaliculus*, in response to chronic thermal stress. *Journal of Thermal Biology*. Vol, 117. DOI: <https://doi.org/10.1016/j.jtherbio.2023.103699>

Copedo, J. S., Webb, S. C., Delisle, L., Knight, B., Ragg, N. L. C., Laroche, O., Venter, L., Alfaro, A. C., (2025). Elucidating divergent growth and climate vulnerability in abalone (*Haliotis iris*): A multi-year snapshot. *Marine Environmental Research*. 107090, [10.1016/j.marenvres.2025.107090](https://doi.org/10.1016/j.marenvres.2025.107090).

Copedo, J. S., Webb, S. C., Ragg, N. L. C., Alfaro, A. C., (2025) Implications of flooding events for the green-lipped mussels (*Perna canaliculus*): An aquatic health perspective. *New Zealand Journal of Marine and Freshwater Research* [10.1080/00288330.2025.2474570](https://doi.org/10.1080/00288330.2025.2474570).

9.1.2. Peer reviewed co-authored papers (During PhD program)

Ericson, J.A., Venter, L., **Copedo, J.S.**, Nguyen, V.T., Alfaro, A.C., Ragg, N.L.C. **2023**. Chronic heat stress as a predisposing factor in summer mortality of mussels, *Perna canaliculus*. *Aquaculture*. DOI: <https://doi.org/10.1016/j.aquaculture.2022.738986>

Bullon, N., Alfaro, A.C., Guo, J., **Copedo, J.S.**, Nguyen, V.T., Seyfoddin, A. **2023**. Expanding the menu for New Zealand farmed abalone: dietary inclusion of insect meal and grape marc (effects on gastrointestinal microbiome, digestive morphology, and muscle metabolome). *New Zealand Journal of Marine and Freshwater Research*. DOI: <https://doi.org/10.1080/00288330.2023.2272592>

Elvines, D.M., Hopkins, G.A., MacLeod, C.K., Ross, D.J., Ericson, J. A., Ragg, N. L. C., **Copedo, J. S.**, White, C.A. **2024** Assimilation of fish farm wastes by the ecosystem engineering bivalve *Atrina zelandica*. *Aquaculture Environmental Interactions* 16:115-131. DOI: <https://doi.org/10.3354/aei00475>

Hale, R., Muetzel, L., Ericson, J., **Copedo, J. S.**, Cummings, V., Ragg, N. L. C., McGraw, C., Currie, K., Rodgers, K., and Sewell. M. A., (2025) Future actions for the ocean acidification research community to support marine industries and coastal communities of Aotearoa New Zealand. *New Zealand Journal of Marine and Freshwater Research*. DOI:

<https://doi.org/10.1080/00288330.2025.2460574>

Delisle, L., Bui, T., **Copedo, J.S.**, Laroche, O., von Ammon, U., Lane, H.S., Hutson, K.S. (2025). Isolation, culture, and optimal growth conditions for the shellfish protozoan parasite, *Perkinsus olseni*. *International Journal of Parasitology*. 10.1016/j.ijpara.2025.04.011.

9.1.3. *Book chapters*

Plouviez, M; **Copedo, J.S**; Ingebrigtsen, R (submitted 2025) Chapter 7: Pathogens and predators in large-scale microalgal cultures. In. E. Jacob-Lopes, M.M. Maroneze, M.I. Queiroz, and L.Q. Zepka *Handbook of Microalgae-Based Processes and Products*. Second edition, Elsevier

9.1.4. *Conference poster presentations*

Joanna Copedo, Andrea Alfaro, Norman Ragg, Steve Webb, Leonie Venter, and Jess Ericson (2021). Thermal stress in mussels: A histopathological perspective Physiomar Poster 2021, 7-9 September Nelson New Zealand. (First place student poster).

Joanna Copedo, Steve Webb, Norman Ragg, Andrea Alfaro (2022) Climate hazards and Greenshell mussels (*Perna canaliculus*): From unexpected flooding to opportunistic research. NZMSS Poster, 22-24 November, Auckland New Zealand.

Joanna S. Copedo, Stephen C. Webb, Norman L. C. Ragg, Leonie Venter, Andrea C. Alfaro (2023). Histopathological investigation of four populations of abalone (*Haliotis iris*) exhibiting divergent growth performance. IAS 27/02/23 -01/03/23 Auckland New Zealand.

9.1.5. *Conference oral presentations*

Joanna Copedo, Steve Webb, Norman Ragg, Andrea Alfaro, and Leonie Venter (2021). Histopathological assessment of *Haliotis iris* populations exhibiting divergent growth performance: A baseline study Physiomar Oral 2021, 7-9 September Nelson New Zealand.

Joanna S. Copedo, Stephen C. Webb, Norman L. C. Ragg, Leonie Venter, Andrea C. Alfaro (2023). Influence of summer heatwaves on slow and fast-growing populations of pāua. IAS 27/02/23 - 01/03/23 Auckland New Zealand.

Joanna S. Copedo, Stephen C. Webb, Lizenn Delisle, Ben Knight, Norman L. C. Ragg, Olivier Laroche, Leonie Venter, Andrea C. Alfaro (2024). Elucidating climate vulnerability in *Haliotis iris*: A histological investigation Mini abalone Symposium 11 Sept- 13 Sept, Online Hobart.

Joanna Copedo, Steve Webb (2023) Histology- Greenshell mussels. SpatNZ, Nelson, New Zealand

Joanna Copedo, Steve Webb (2023) Aquaculture pathology activities in NZ and Cawthron. Given to 5th year veterinary students Massey University, 2023, Nelson, NZ

Joanna Copedo (2024) Aquaculture pathology activities in NZ and Cawthron. Given to 5th year veterinary students Massey University, 2024, Nelson, NZ

9.2. Appendix: unique outputs

Appendix 2: Establishment of the Oceania Aquatic Histopathology Network.



Oceania Aquatic Histopathology Network

We are inviting expressions of interest for involvement in an Oceania Aquatic Histopathology Network.

A network of aquatic histopathologists and regular fora will allow greater connection and interaction. The fora will provide a place to discuss case studies across a wide range of marine and freshwater species including interesting cases, general research and new applications or technologies.

The network will consist of bi-monthly or quarterly meetings online to connect experts and histopathologists in training.

To register your interest please contact:
Joanna Copedo
Joanna.copedo@cawthron.org.nz
Phone: +64 3 668 7753

 **CAWTHRON**

cawthron.org.nz

Appendix 3: Chair and Co-chair of the 2023 New Zealand Ocean Acidification Conference and Climate change Resilience in Aquaculture symposium.

**2023 New Zealand Ocean
Acidification Conference & Climate
Change Resilience in Aquaculture
Symposium**

**17th - 18th of August
Tides Hotel, Nelson**

NZOAC
NZ Ocean Acidification Community

CAWTHRON

9.3. Appendix: supplementary tables.

Post hoc analysis data from the statistical analysis for the following:

Table S1: Post-hoc statistical analysis for the weights of pāua from four sites: Site 1: Ascots, Site 2: Owenga harbour, Site 3: Durham, and Site 4: Wharekauri Harbour, around the Chatham Islands.

	contrast	estimate	SE	df	t. ratio	p.value
Adults	Site 1 - Site 2	152.2	16.3	72	9.334	<.0001
	Site 1 - Site 3	-20.4	16.3	72	-1.251	0.5967
	Site 1 - Site 4	-85.7	16.3	72	-5.256	<.0001
	Site 2 - Site 3	-172.6	16.3	72	-10.585	<.0001
	Site 2 - Site 4	-237.9	16.3	72	-14.59	<.0001
	Site 3 - Site 4	-65.3	16.3	72	-4.005	0.0008
Sub-adults	Site 1 - Site 2	-14.1	16.3	72	-0.865	0.8229
	Site 1 - Site 3	-42.9	16.3	72	-2.631	0.0499
	Site 1 - Site 4	-40.6	16.3	72	-2.49	0.07
	Site 2 - Site 3	-28.8	16.3	72	-1.766	0.2979
	Site 2 - Site 4	-26.5	16.3	72	-1.625	0.3711
	Site 3 - Site 4	2.3	16.3	72	0.141	0.999

Table S2: Post-hoc statistical analysis for the shell length of pāua from four sites: Site 1: Ascots, Site 2: Owenga harbour, Site 3: Durham, and Site 4: Wharekauri Harbour, around the Chatham Islands.

	contrast	estimate	SE	df	t. ratio	p.value
Adults	Site 1 - Site 2	14.45	2.5	72	5.788	<.0001
	Site 1 - Site 3	0.05	2.5	72	0.02	1
	Site 1 - Site 4	-11.77	2.5	72	-4.715	0.0001
	Site 2 - Site 3	-14.4	2.5	72	-5.768	<.0001
	Site 2 - Site 4	-26.2	2.5	72	-10.503	<.0001
	Site 3 - Site 4	-11.82	2.5	72	-4.735	0.0001
Sub-adults	Site 1 - Site 2	-4.7	2.5	72	-1.883	0.2445
	Site 1 - Site 3	-9.7	2.5	72	-3.886	0.0013
	Site 1 - Site 4	-12.23	2.5	72	-4.899	<.0001
	Site 2 - Site 3	-5	2.5	72	-2.003	0.1965
	Site 2 - Site 4	-7.53	2.5	72	-3.016	0.0181
	Site 3 - Site 4	-2.53	2.5	72	-1.013	0.7421

Table S3: Post-hoc statistical analysis for the shell width of pāua from four sites: Site 1: Ascots, Site 2: Owenga harbour, Site 3: Durham, and Site 4: Wharekauri Harbour, around the Chatham Islands.

	contrast	estimate	SE	df	t. ratio	p.value
Adults	Site 1 - Site 2	10.71	2.61	58	4.102	0.0007
	Site 1 - Site 3	2.25	2.69	58	0.838	0.8364
	Site 1 - Site 4	-7.2	2.78	58	-2.588	0.0574
	Site 2 - Site 3	-8.46	2.61	58	-3.24	0.0104
	Site 2 - Site 4	-17.9	2.71	58	-6.613	<.0001
	Site 3 - Site 4	-9.45	2.78	58	-3.397	0.0066
Sub-adults	Site 1 - Site 2	1	2.53	58	0.395	0.9789
	Site 1 - Site 3	-3.6	2.47	58	-1.458	0.469
	Site 1 - Site 4	-7.5	2.83	58	-2.649	0.0496
	Site 2 - Site 3	-4.6	2.47	58	-1.863	0.2551
	Site 2 - Site 4	-8.5	2.83	58	-3.002	0.0201
	Site 3 - Site 4	-3.9	2.77	58	-1.406	0.501

Table S4: Post-hoc statistical analysis for the shell height of pāua from four sites: Site 1: Ascots, Site 2: Owenga harbour, Site 3: Durham, and Site 4: Wharekauri Harbour, around the Chatham Islands.

	contrast	estimate	SE	df	t. ratio	p.value
Adults	Site 1 - Site 2	14.45	2.5	72	5.788	<.0001
	Site 1 - Site 3	0.05	2.5	72	0.02	1
	Site 1 - Site 4	-11.77	2.5	72	-4.715	0.0001
	Site 2 - Site 3	-14.4	2.5	72	-5.768	<.0001
	Site 2 - Site 4	-26.22	2.5	72	-10.503	<.0001
	Site 3 - Site 4	-11.82	2.5	72	-4.735	0.0001
Sub-adults	Site 1 - Site 2	-4.7	2.5	72	-1.883	0.2445
	Site 1 - Site 3	-9.7	2.5	72	-3.886	0.0013
	Site 1 - Site 4	-12.23	2.5	72	-4.899	<.0001
	Site 2 - Site 3	-5	2.5	72	-2.003	0.1965
	Site 2 - Site 4	-7.53	2.5	72	-3.016	0.0181
	Site 3 - Site 4	-2.53	2.5	72	-1.013	0.7421

Table S5: Post-hoc statistical analysis for the algal quality within the stomach/crop region of pāua from four sites: Site 1: Ascots, Site 2: Owenga harbour, Site 3: Durham, and Site 4: Wharekauri Harbour, around the Chatham Islands.

contrast	estimate	SE	z. ratio	p.value
Site 1 - Site 2	-7.977	1.206	-6.616	<.0001
Site 1 - Site 3	-2.396	0.733	-3.267	0.006
Site 1 - Site 4	-2.997	0.728	-4.118	0.0002
Site 2 - Site 3	5.581	1.114	5.011	<.0001
Site 2 - Site 4	4.979	1.077	4.625	<.0001
Site 3 - Site 4	-0.602	0.621	-0.969	0.7672

Table S6: Post-hoc statistical analysis for the ceroid located in the subepithelial layer of the intestinal tract of pāua from four sites: Site 1: Ascots, Site 2: Owenga harbour, Site 3: Durham, and Site 4: Wharekauri Harbour, around the Chatham Islands. The perfect separation of the values at the sites resulted in a warning: **glm.fit: fitted probabilities numerically 0 or 1 occurred** and as such statistical analysis was compromised.

contrast	estimate	SE	df	z. ratio	p.value
Site 1 - Site 2	-36.3	69.8768	Inf	-0.52	0.9543
Site 1 - Site 3	-15.8	85.6923	Inf	-0.184	0.9978
Site 1 - Site 4	0	0.0136	Inf	0	1
Site 2 - Site 3	20.5	131.9377	Inf	0.156	0.9987
Site 2 - Site 4	36.3	69.8667	Inf	0.52	0.9543
Site 3 - Site 4	15.8	85.6884	Inf	0.184	0.9978

Table S7: Post-hoc statistical analysis for the digestive gland tubule detachment coverage from four sites: Site 1: Ascots, Site 2: Owenga harbour, Site 3: Durham, and Site 4: Wharekauri Harbour, around the Chatham Islands.

contrast	estimate	SE	df	z. ratio	p.value
Site 1 - Site 2	-1.5939	0.66	Inf	-2.415	0.0742
Site 1 - Site 3	-1.5427	0.658	Inf	-2.345	0.088
Site 1 - Site 4	-0.2722	0.806	Inf	-0.338	0.9867
Site 2 - Site 3	0.0512	0.593	Inf	0.086	0.9998
Site 2 - Site 4	1.3216	0.8	Inf	1.651	0.3499
Site 3 - Site 4	1.2704	0.799	Inf	1.589	0.3847

Table S8: Post-hoc statistical analysis for the extent of detachment around the digestive gland tubules from four sites: Site 1: Ascots, Site 2: Owenga harbour, Site 3: Durham, and Site 4: Wharekauri Harbour, around the Chatham Islands.

	contrast	estimate	SE	df	t. ratio	p.value
Adults	Site 1 - Site 2	-4.293	1.111	Inf	-3.862	0.0006
	Site 1 - Site 3	-2.673	1.019	Inf	-2.622	0.0433
	Site 1 - Site 4	-2.06	1.392	Inf	-1.479	0.4501
	Site 2 - Site 3	1.62	0.976	Inf	1.66	0.3449
	Site 2 - Site 4	2.233	1.361	Inf	1.641	0.3557
	Site 3 - Site 4	0.613	1.322	Inf	0.464	0.9669
Sub-adults	Site 1 - Site 2	-0.282	0.851	Inf	-0.332	0.9874
	Site 1 - Site 3	-0.799	0.827	Inf	-0.966	0.7689
	Site 1 - Site 4	0.508	0.835	Inf	0.608	0.9295
	Site 2 - Site 3	-0.516	0.825	Inf	-0.626	0.9238
	Site 2 - Site 4	0.79	0.843	Inf	0.937	0.7847

	Site 3 - Site 4	1.306	0.824	Inf	1.586	0.3867
--	-----------------	-------	-------	-----	-------	--------

Table S9: Post-hoc statistical analysis for the ceroid score in the interstitial space of the digestive gland from four sites: Site 1: Ascots, Site 2: Owenga harbour, Site 3: Durham, and Site 4: Wharekauri Harbour, around the Chatham Islands.

	contrast	estimate	SE	df	t. ratio	p.value
Adults	Site 1 - Site 2	-17.388	0.448	Inf	-38.838	<.0001
	Site 1 - Site 3	1.037	1.09	Inf	0.952	0.7769
	Site 1 - Site 4	19.642	0.438	Inf	44.867	<.0001
	Site 2 - Site 3	18.425	1.187	Inf	15.517	<.0001
	Site 2 - Site 4	37.029	0.451	Inf	82.112	<.0001
	Site 3 - Site 4	18.604	1.166	Inf	15.953	<.0001
Sub-adults	Site 1 - Site 2	-0.651	0.895	Inf	-0.727	0.8862
	Site 1 - Site 3	0.812	0.855	Inf	0.951	0.7773
	Site 1 - Site 4	0.935	0.876	Inf	1.067	0.7094
	Site 2 - Site 3	1.464	0.88	Inf	1.663	0.3433
	Site 2 - Site 4	1.586	0.902	Inf	1.758	0.2936
	Site 3 - Site 4	0.122	0.827	Inf	0.148	0.9989

Table S10: Post-hoc statistical analysis for the ciliates attached to the gills of pāua from four sites: Site 1: Ascots, Site 2: Owenga harbour, Site 3: Durham, and Site 4: Wharekauri Harbour, around the Chatham Islands.

contrast	estimate	SE	df	z. ratio	p.value
Site 1 - Site 2	-0.0309	0.0886	68	-0.349	0.9853
Site 1 - Site 3	0.2089	0.0871	68	2.398	0.0871
Site 1 - Site 4	0.1227	0.0871	68	1.409	0.4983
Site 2 - Site 3	0.2398	0.0897	68	2.672	0.0454
Site 2 - Site 4	0.1536	0.0897	68	1.712	0.3254
Site 3 - Site 4	-0.0862	0.0883	68	-0.976	0.7636

Table S11 GLM models and associated AIC results for figure 7.4

GLM model	Family	df	AIC
Number ~ Tissue * Timepoint	Poisson	7	249.6
Number ~ Tissue + Timepoint	Poisson	11	254.4
Number ~ Tissue + Timepoint	Quasipoisson	7	NA
Number ~ Tissue + Timepoint	Negative binomial	7	120.4